

# **Evaluating the late gas potential of source rocks stemming from different sedimentary environments**

vorgelegt von  
Diplom-Geowissenschaftler  
Nicolaj L. Mahlstedt  
aus Lahn-Gießen

Von der Fakultät VI – Planen, Bauen, Umwelt  
der Technischen Universität Berlin  
zur Erlangung des akademischen Grades  
Doktor der Naturwissenschaften  
Dr. rer. nat.

## **genehmigte Dissertation**

Promotionsausschuss:

Vorsitzender: Prof. Dr. Wilhelm Dominik

Berichter: Prof. Dr. Brian Horsfield

Berichter: Prof. Dr. Jan Schwarzbauer

Tag der wissenschaftlichen Aussprache: 18.07.2012

**Berlin 2012**

**D83**



I dedicate this thesis to my father  
Prof. Dr. med. Jörg Mahlstedt (25.02.1943 – 12.11.2011).

It is an easy job to say that an elephant, however good, is not a good warthog.

*Ford Madox Ford*



## ACKNOWLEDGEMENTS

First of all I want to thank Brian Horsfield for providing and supervising this study as well as for giving the space to develop and realise my own ideas. Without his scientific and personal support the present thesis would not have been possible. I also owe Dr. Jan Schwarzbauer (RWTH, Aachen) a dept of gratitude for taking charge of the expert testimony. I wish to express my gratitude to Volker Dieckmann (Shell) who somehow managed, with his enthusiasm and attitude, to spark my deeper interest in the field of Organic Geochemistry and its applications.

Shell, Maersk, Petrobras, Eni, Total, Wintershall, and Devon Energy are gratefully acknowledged here for the funding of this study and for providing sample material.

I would like to thank Prof. Dr. Andreas Pöpl and Dipl.-Ing. Joachim Hoentsch (Physikalisches Institut der Universität Leipzig, Abteilung Struktur der Materie) for their help and the possibility to conduct ESR measurements, as well as Per Erling Johansen (APT) for the always rapid and flawless performance of Rock-Eval analyses.

Special thanks go out to all people of the technical staff of the organic geochemistry group at GFZ, especially to the lord of the pyrolysis lab, Ferdinand Perssen. Without his considerable assistance and creativity execution of experiments would have been impossible. I want to thank Michael Gabriel for the performance of the isotope analyses. Cornelia Karger and Anke Kaminsky shall be acknowledged here separately for their always happy faces when asked for unfindable laboratory equipment. Life at GFZ would not be the same without Claudia Röhl.

I would like to express my gratitude to all former and recent colleagues at the Institute for providing a great working atmosphere. Eric Lehne, Matthias Keym, and Volkmar Neumann shall be thanked for getting me started during the first time, and Stefanie Pötz and An-Ka Scherf for always providing food (kiosk) besides scientific support and friendship. Last but not least at all and as a heartfelt wish I would like to thank my “Doctor-sisters and -brothers” Alex Vetter, Katja Theuerkorn, Clemens Glombitza, and Philipp Kuhn for sharing all the good and all the bad times as well as the one or the other beverage.

I want to thank my parents for their love, constant encouragement and invaluable support in any situation, as well as my friends outside GFZ for being around whenever I needed them.

Words alone do not suffice to thank Verena Ezerski, my love is all yours.



## ABSTRACT/KURZFASSUNG

### ABSTRACT

The assessment of timing, i.e. kinetics, and amount of thermally driven, metagenetic methane generation from deeply buried, mature kerogen in petroleum source rocks of different geographical and depositional origin was the overall goal of the work. Mechanisms involved in this late stage gas formation were constrained on the basis of a large sample set comprising immature source rocks, natural and artificial maturity series, and synthetic source rocks as well as extracted versus unextracted source rocks using open- and closed-system pyrolysis experiments.

The major outcome is that, based on a variety of natural and artificial maturity series investigated by a novel, rapid MSSV-pyrolysis screening method spanning the main stage of late gas generation, a late gas potential of at least ~40 mg/g TOC seems to exist for every type of source rock at maturities around 2.0%  $R_o$ . During natural and artificial maturation, chain shortening reactions via  $\beta$ -scission related to hydrocarbon generation within the oil window as well as simple concentration of refractory organic matter related to the release of labile compounds lead to an enrichment of methyl-aromatics and hence late gas precursor structures within the residual organic matter. Predicted absolute late gas amounts for a large series of immature source rocks (65 samples), shales and coals covering all main kerogen types and depositional environments, are therefore underestimates. Nevertheless, assigned low, high, or intermediate late gas potentials are meaningful as the absolute generated amount of high temperature methane is strongly coupled to the TOC content of the respective source rock. Homogeneous, aliphatic Type I and Type II organic matter of aquatic lacustrine and marine origin exhibit low late gas potentials as they are good expeller during natural maturation and “loose” great amounts of their initial carbon content. In contrast, more heterogeneous aromatic and/or phenolic marine or mixed marine-terrestrial to terrestrial source rocks could be assigned intermediate to high late gas potentials as retention of  $C_{6+}$  compounds within the residual organic matter leads to preservation of TOC.

Based on closed-system MSSV-pyrolysis at three different heating rates and using an immature coal sample, the late methane forming reaction itself can be kinetically described by a single activation energy  $E_a$  of ~56 kcal/mol and a surprisingly low frequency factor  $A$  of only ~5.00E+09 1/s. Those kinetic parameters seem to be characteristic for high temperature methane formation by a final demethylation of residual aromatic nuclei within spent organic matter via  $\alpha$ -cleavage mechanisms involving condensation reactions of aromatic clusters.

Extrapolation to a linear geologic heating rate of 3°C/ma revealed onset temperatures of ~220°C for a calculated  $R_o$  of ~2.5% and a geologic  $T_{max}$  of ~240°C at 3.1%  $R_o$ . Those timing predictions are in accordance with the observation that late gas potentials of naturally matured source rocks start to decrease for vitrinite reflectances exceeding 2.0%  $R_o$  which directly confirms that previous (Erdmann and Horsfield, 2006) and present kinetic parameters are meaningful and that high temperature methane generation under geologic conditions is most likely reality and not a laboratory artefact. As kinetics of late stage methane generation from immature samples satisfactorily describe natural trends late dry gas formation is demonstrated to be kinetically unaffected of possible second-order recombination/stabilisation reactions occurring at earlier natural maturation stages between first formed bitumen and residual organic matter, a process previously thought to be a prerequisite for high temperature methane generation. The latter reactions might nevertheless influence the composition of primary and secondary cracking products as well as the maximum amount of late gas to be generated as they were shown to lead to the retention of organic matter.

The existence of such a late gas potential (~40 mg/g TOC), which is overlooked when only routinely used open-system pyrolysis methods are applied, has profound implications for conventional and unconventional petroleum systems, in that significant additional charges of dry gas can be expected at high maturity levels. The importance for gas-in place calculation when evaluating shale gas plays is obvious as late methane is sure to be formed from a thermally stable moiety within the residual organic matter and not by degradation of retained  $C_{6+}$  compounds which might as well have left the source kitchen prior to cracking.

The implementation of late gas amount and kinetic parameters into basin modelling software packages allows the regional simulation of generation (as well as migration if migrated) and fate of that late dry gas charge and can be applied to any geological setting or source rock type. As a matter of fact, evaluation of the unconventional gas potential of Silurian Shales in Poland was already performed by industry using, among other parameters, the here assessed late methane generation characteristics. Retention/recombination-reactions of first formed petroleum with residual organic matter leading to the preservation of refractory kerogen and to potentially higher absolute late gas yields depend on the kerogen type and should be accounted for in mass balance calculations individually for a respective petroleum prospect. This, sadly, was out of the scope of this thesis.



## KURZFASSUNG

Das übergeordnete Ziel der Arbeit war, sowohl die metagenetische Bildung von Methan aus weit abgeteufem und reifem Kerogen in Erdöl- bzw. Erdgasmuttergesteinen unterschiedlichen geographischen Ursprungs und Ablagerungsmilieus zu beschreiben, als auch dessen Menge und Bildungsgeschwindigkeit zu verifizieren. Die der späten Gasgenese zugrunde liegenden Mechanismen konnten, basierend auf Pyrolyseexperimenten im offenen und geschlossenem System und der Benutzung einer statistisch signifikanten Menge an Proben ( $> 100$ ), bestehend aus unreifen Muttergesteine, natürlich und künstlich gereiften Muttergesteinsserien, synthetischen Muttergesteinen und extrahierten vs. unextrahierten Muttergesteinen, abgeschätzt werden.

Basierend auf einer Reihe unterschiedlicher natürlicher und künstlicher Reifeserien, die im Rahmen der Doktorarbeit mit einer neu entwickelten „Screening“-Technik unter Verwendung von MSSV-Pyrolyse untersucht wurden, ist das Hauptergebnis, dass für jeden Muttergesteinstypus zu Beginn der Metagenese (Vitrinit Reflektion  $R_o \sim 2.0\%$ ; geologische Temperatur  $\sim 200^\circ\text{C}$ ) ein spätes Gasgenesepotential von ca. 40 mg/g TOC zu existieren scheint. Während der natürlichen und künstlichen Reifung von organischem Material führen Kettenverkürzungsreaktionen durch  $\beta$ -Spaltung sowohl zur Bildung von Kohlenwasserstoffen im „Ölfenster“ als auch zur Bildung von Methyl-Aromaten im aufkonzentrierten refraktorischen Material, welche als chemische Vorläuferstrukturen des später zu generierenden Gases agieren. Die für eine Reihe unreifer Muttergesteine (65 Proben) vorhergesagten späten Gasmengen sind daher zu niedrig. Da die absolute Methanausbeute bei hohen Reifen stark von dem TOC Gehalt eines jeweiligen Muttergesteins abhängt, sind die den Schiefern und Kohlen zugeordneten niedrigen, mittleren und hohen „Späte Gaspotentiale“ dennoch aussagekräftig. Homogenes, aliphatisches Typ I und Typ II organisches Material aquatischen Ursprungs besitzt ein niedriges „Spätes Gaspotential, weil es große Mengen des ursprünglich vorhandenen organischen Kohlenstoffs im Zuge der natürlichen Reifung und primären Migration verliert. Im Gegensatz dazu kann heterogeneres, aromatisch und/oder phenolisches organisches Material marinen oder gemischt marin-terrestrischen bis terrestrischen Ursprungs Teile der primär gebildeten  $C_{6+}$  Komponenten durch Rekombinationsreaktionen zurückhalten, wodurch mehr von der ursprünglich vorhandenen organischen Kohlenstoffmenge bewahrt wird, was zu mittleren bis hohen „Späten Gaspotentialen“ führt.

Die Reaktion, die der späten Methangenese zu Grunde liegt, kann durch eine einzelne Aktivierungsenergie  $E_a$  von  $\sim 56$  kcal/mol und einen erstaunlich niedrigen Frequenzfaktor  $A$

von lediglich  $5.00 \times 10^9$  1/s kinetisch beschrieben werden. Die kinetischen Parameter wurden für eine unreife Kohleprobe durch MSSV-Pyrolyse bei drei verschiedenen Heizraten ermittelt und scheinen charakteristisch für die Bildung von Methan bei hohen Temperaturen durch eine finale Demethylierung von residualem, aromatischen organischen Material zu sein. Die Reaktion verläuft hierbei höchstwahrscheinlich über  $\alpha$ -Spaltungsmechanismen, die Kondensationsreaktionen von aromatischen Clustern beinhalten. Für eine lineare geologische Heizrate von  $3^\circ\text{C}/\text{ma}$  kann der Beginn der Methanbildung für Temperaturen um die  $220^\circ\text{C}$  ( $R_o \sim 2.5\%$ ) erwartet werden, wohingegen der  $T_{\max}$  bei  $240^\circ\text{C}$  ( $R_o \sim 3.1\%$ ) liegt. Diese zeitlichen Vorhersagen sowie die zeitliche Vorhersagen von Erdmann and Horsfield (2006) werden durch die Beobachtung verifiziert, dass die „Späten Gaspotentiale“ von Muttergesteinen mit  $R_o > 2\%$  anfangen zu sinken. Weil die Kinetik der späten Methangene aus einem unreifen Muttergestein die natürlichen Reifetrends exzellent beschreibt, kann gesagt werden, dass die Bildung von diesem Gas kinetisch nicht durch Rekombinations/Stabilisierungs-Reaktionen zweiter Ordnung zwischen Bitumen und residualem organischen Material bei früheren natürlichen Reifestadien gestört wird; ein Prozess, der zuvor als Grundvoraussetzung für die Bildung eines „späten Gaspotentials“ angesehen wurde (Erdmann and Horsfield, 2006). Diese bimolekularen Reaktionen können trotz allem sowohl die Zusammensetzung primärer oder sekundärer Cracking-Produkte beeinflussen als auch die maximal zu erwartende, absolute „späte“ Gasmenge (TOC Gehalt).

Die Existenz dieses „Späten Gaspotentials“ ( $40 \text{ mg/g TOC}$ ), welches übersehen wird, wenn nur Routineuntersuchungen basierend auf Pyrolyse im offenen System (z.B. Rock-Eval) durchgeführt werden, hat tief greifende Auswirkungen auf die Bewertung von konventionellen oder unkonventionellen Petroleumsystemen, da eine nicht zu unterschätzende, zusätzliche Menge Gas bei hohen Reifestadien erwartet werden kann. Die Bedeutung für „Gas-in-Place“-Kalkulationen bei der Beurteilung von z.B. unkonventionellen Gaslagerstätten (Shale Gas) ist augenscheinlich, da „spätes“ Methan direkt aus einer thermisch stabilen Vorläuferstruktur im residualen organischen Material gebildet wird und nicht durch sekundäres „Cracken“ von  $C_{6+}$ -Komponenten, die womöglich vor ihrer Degradation das Muttergestein schon verlassen haben.

Die Implementierung von „späten“ Gas Mengen und kinetischen Parametern in Beckenmodellierungsprogrammen erlaubt die regionale Simulation der Bildung und des Verbleibs des metagenetischen Methans und kann auf jedes geologische Setting sowie Muttergesteinstypen angewendet werden. Zur Abschätzung des unkonventionellen Gaspotentials von Silurischen Schiefern in Polen wurden, neben anderen Parametern, die hier

erarbeiteten „späten“ Methanbildungs-Charakteristika von der Industrie schon eingesetzt. Da Retentions- oder Rekombinations-Reaktionen zwischen Bitumen und residualem organischen Material abhängig vom Kerogentyp sind, aber zur Erhaltung von organischem Material und somit zu potentiell höheren absoluten Gasmengen im Muttergestein führen, sollten diese in Massenbilanzierungsberechnungen individuell für ein jeweiliges Erkundungsgebiet berücksichtigt werden. Die Durchführung dieser Berechnung lag außerhalb des Rahmens der Doktorarbeit.



# CONTENTS

ACKNOWLEDGEMENTS .....	I
ABSTRACT/KURZFASSUNG .....	III
CONTENTS .....	IX
INDEX OF FIGURES .....	XV
INDEX OF TABLES .....	XXI
LIST OF COMMON ABBREVIATIONS .....	XXIII
<b>1 INTRODUCTION .....</b>	<b>1</b>
<b>1.1 Natural Gas Generation from Sedimentary Organic Matter .....</b>	<b>1</b>
1.1.1 General Geochemistry of Natural Gas .....	1
1.1.2 Stable Isotopic Signature of Natural Gas .....	3
Isotope Distributions in Natural Gas Accumulations .....	3
Isotopic Fractionation during Biogenic Gas Generation .....	4
Isotopic Fractionation during Thermogenic Gas Generation .....	4
1.1.3 Classification of Organic Matter focusing on Kerogen .....	5
Definition of Kerogen .....	5
Main Formation Pathways of Kerogen .....	5
Classification of Kerogen .....	6
1.1.4 Bulk Mechanisms of Petroleum Formation .....	8
The“Cooles model” .....	8
Limitations of the”Cooles model” .....	9
1.1.5 Major Cracking Mechanisms of Petroleum Formation .....	10
Thermal Cracking via Free Radicals .....	10
Acidic Catalysed Cracking via Carbonium Intermediates .....	12
Catalytically Mediated Cleavage of Carbon-Carbon Bonds .....	13
1.1.6 Predicting the Timing of Thermal Gas Genesis .....	14
Timing of primary and secondary thermal gas formation .....	14
Basics of Kinetics – the parallel reaction model .....	15
Limitations of the parallel reaction model .....	19
1.1.7 Predicting the Composition of Petroleum .....	20
Heating rate dependency .....	20
Second-order recombination reactions in shales .....	22
Second-order recombination reactions in coals .....	23

<b>1.2</b>	<b>Research Perspectives and Objectives.....</b>	<b>25</b>
1.2.1	Overall Goal: Constrain Mechanisms of Late Gas Generation.....	25
	Status Quo - Late Gas Generation.....	25
1.2.2	Inherent fundamental questions .....	29
<b>1.3</b>	<b>Detailed Approach.....</b>	<b>30</b>
	Suitability of Pyrolysis for Petroleum Generation Simulation.....	30
	Open-System Pyrolysis GC-FID as a Kerogen Typing Tool.....	31
	Closed-System Pyrolysis Methods: Hydrous vs. Anhydrous.....	33
	Convenience and Suitability of Confined MSSV-Pyrolysis .....	35
	Detailed Approach to Answer “Inherent fundamental questions” .....	36
<b>1.4</b>	<b>Structure of Dissertation.....</b>	<b>38</b>
<b>2</b>	<b>SAMPLES AND METHODOLOGY.....</b>	<b>39</b>
<b>2.1</b>	<b>Sample Set.....</b>	<b>39</b>
2.1.1	Immature source rocks .....	39
	Lacustrine source rocks .....	39
	Marine source rocks .....	40
	Fluvio deltaic - terrestrial source rocks .....	42
2.1.2	Natural maturity series .....	42
	Cenozoic Coals, New Zealand .....	42
	Ruhr Area Coals, Germany .....	44
	Wealden Coals, Germany.....	44
	Exshaw Formation, Canada.....	44
	Barnett Shale, USA .....	44
<b>2.2</b>	<b>Analytical Program .....</b>	<b>45</b>
2.2.1	Geochemical Characterisation.....	46
	TOC determination and Rock-Eval pyrolysis .....	46
	Bulk Kinetics.....	47
	Open pyrolysis-gas chromatography-FID (Py-GC-FID) .....	48
	Infrared Spectroscopy (IR).....	49
	Mineralogy (ATR-IR) .....	49
2.2.2	Artificial maturation: products .....	50
	Stepwise Open-Pyrolysis Gas Chromatography-FID (Py-GC-FID) .....	50
	Closed-Pyrolysis Gas-Chromatography-FID (MSSV-Py-GC-FID) .....	50
	Kinetic modelling.....	52
	Isotopic gas composition of MSSV-pyrollysates .....	53

2.2.3	Artificial maturation: residues.....	54
	Preparative pyrolysis – closed versus open system.....	54
	Thermovaporisation gas chromatography-FID (Tvap-GC-FID).....	55
	ESR-measurements .....	56
<b>3</b>	<b>GEOCHEMICAL CHARACTERISATION.....</b>	<b>59</b>
<b>3.1</b>	<b>Bulk Organic Geochemical Characterisation (TOC/Rock-Eval) .....</b>	<b>59</b>
3.1.1	Organic Matter Richness - TOC Content.....	59
3.1.2	Rock-Eval - Immature source rock samples .....	61
	Source Rock Quality – Genetic Potential.....	62
	Maturity (PI, T <sub>max</sub> ).....	66
3.1.3	Rock-Eval - Natural maturity series.....	67
<b>3.2</b>	<b>Detailed Kerogen Composition (Open Py-GC).....</b>	<b>71</b>
3.2.1	Immature source rock samples.....	71
	Kerogen Classification based on Chain Length Distribution - Petroleum Type Organofacies.....	71
	Kerogen Classification based on aliphatic, aromatic, oxygen- and sulphur-bearing compounds – Depositional Environment.....	80
3.2.2	Natural maturity series .....	85
<b>3.3</b>	<b>Bulk Hydrocarbon Generation (SRA-Kinetics) .....</b>	<b>89</b>
3.3.1	Immature source rock samples.....	89
3.3.2	Natural maturity series .....	97
<b>3.4</b>	<b>Mineralogy (ATR-IR) .....</b>	<b>103</b>
<b>4</b>	<b>EVALUATING THE LATE GAS POTENTIAL OF IMMATURE SOURCE ROCKS FROM DIFFERENT DEPOSITIONAL ENVIRONMENTS.....</b>	<b>107</b>
<b>4.1</b>	<b>Detailed Investigation on the Late Gas Generation Behaviour of a Small Sample Set using Open- and Closed-System Pyrolysis Methods .....</b>	<b>107</b>
4.1.1	Sample Set.....	107
4.1.2	Evolution of Boiling Ranges during Stepwise Open-System Pyrolysis .....	108
4.1.3	Evolution of Boiling Ranges during MSSV Pyrolysis.....	109
4.1.4	Calculation of Primary and Secondary Gas Formation.....	111
	The conservative evaluation approach .....	112
	The refined evaluation approach .....	113
	Comparison of the conservative and refined evaluation approaches .....	114
	Considering a “direct” open-versus-closed pyrolysis approach.....	117
	Recalculation of the conversion factor f <sub>c</sub> .....	120

4.1.5	Kinetics of late Secondary Gas Formation.....	122
	Fitting of Spline Curves .....	122
	Determination of Kinetic Parameters .....	124
	Extrapolation to Geological Heating Rates .....	127
<b>4.2</b>	<b>Late Gas Potential Evaluation for a large Sample Set.....</b>	<b>129</b>
4.2.1	Screening Method .....	129
4.2.2	Late Gas Generation Behaviour (MSSV Py-GC) .....	130
4.2.3	Secondary Gas Yields .....	135
4.2.4	Impact of Kerogen Type and Structure .....	138
	Chain Length Distribution - Petroleum Type Organofacies .....	139
	Influence of Oxygen-bearing Compounds on the Late Gas Potential.....	141
	Influence of Kerogen-aromaticity on the Late Gas Potential.....	142
	Influence of Sulphur-bearing Compounds on the Late Gas Potential.....	143
	Influence of Kerogen-Type as defined by Rock-Eval Pyrolysis.....	145
<b>4.3</b>	<b>Conclusion .....</b>	<b>146</b>
<b>5</b>	<b>EVOLUTION OF LATE GAS POTENTIAL WITH MATURITY ....</b>	<b>149</b>
<b>5.1</b>	<b>Natural Maturity series.....</b>	<b>149</b>
5.1.1	Late Gas Generation Behaviour (MSSV Py-GC) .....	149
5.1.2	Product Amounts.....	150
5.1.3	Relation of Late Gas Generation Behaviour to the Evolution of Kerogen/Coal Structure.....	156
	Late Gas Potential loss during early maturation stages.....	158
	Late Gas Potential increase during Catagenesis.....	162
	Late Gas Potential loss during Metagenesis.....	165
<b>5.2</b>	<b>Artificial Maturation: Simulating organic matter evolution .....</b>	<b>168</b>
5.2.1	Detailed Kerogen Composition of the Residues (Open Py).....	169
	Closed-System Maturation .....	169
	Open-System Maturation .....	172
5.2.2	Late Gas Generation Behaviour of the Residues (MSSV Py-GC).....	175
	Closed-System Maturation .....	176
	Open-System Maturation .....	177
5.2.3	Product Amounts.....	178
	Closed-System Maturation .....	178
	Open-System Maturation .....	179
	Weight loss correction for late secondary gas (B) yields.....	181



5.3	Conclusion .....	184
6	<b>FURTHER COMPOSITIONAL CONSIDERATIONS.....</b>	<b>187</b>
6.1	<b>Stable carbon isotopes of Gas (MSSV-Pyrolysis) .....</b>	<b>187</b>
6.1.1	Evolution of $\delta^{13}\text{C}$ Compositions of Individual Gas Compounds .....	187
6.1.2	Evolution of $\delta^{13}\text{C}$ Compositions of Methane .....	189
	Temperature Interval 300 – 450°C .....	189
	Temperature Interval 450 - 780°C .....	190
6.1.3	Isotopic Reversals (Rollover) in Shale Gases .....	192
6.2	<b>Second order reactions and their effect on Late Gas Generation - Synthetic Source Rock Mixture (Type I/III).....</b>	<b>194</b>
6.2.1	Open-System Pyrolysis .....	194
	TOC/Rock-Eval.....	194
	Open-system Pyrolysis GC-FID.....	195
	Stepwise Open-System Pyrolysis (GC-FID).....	197
6.2.2	Closed-System Pyrolysis.....	200
	(Stepwise) MSSV-Yields .....	200
	Stable Carbon Isotopes.....	205
6.2.3	Closed-System Artificial Maturation: Residues.....	207
	Residual Organic Matter Composition (Open-Py).....	207
	Late Gas Generation Behaviour and Amount (MSSV-Py GC).....	210
6.3	<b>ESR-Measurements (Residues Are Fm. Coal).....</b>	<b>212</b>
6.3.1	Evolution of the Free Radical Concentration .....	212
6.3.2	Evolution of the Peak-to-Peak Line-Width .....	214
6.4	<b>Conclusion .....</b>	<b>215</b>
7	<b>CONCLUSION AND PERSPECTIVES.....</b>	<b>217</b>
7.1	<b>Major Conclusions .....</b>	<b>217</b>
7.2	<b>Perspectives.....</b>	<b>220</b>
	REFERENCES.....	225
	INDEX OF APPENDIX.....	247
	APPENDIX .....	248



## INDEX OF FIGURES

Figure 1.1: Bulk hydrocarbon reaction rate curves for samples of increasing natural maturation (given in % vitrinite reflectance) for laboratory and geologic heating rates; Toarcian Shale and Westphalian Coals. Modified after Schenk and Horsfield (1998).....	20
Figure 2.1: Flowchart showing the analytical program and employed methods .....	45
Figure 3.1: Total Organic Carbon (TOC) contents of a) all Industry and GFZ provided samples and b) source rocks containing less than 5% TOC.....	60
Figure 3.2: TOC and Rock-Eval data for immature source rocks – Kerogen type (a-e) and maturity (e-f).....	63
Figure 3.3: Evolution of TOC content and Rock-Eval parameter with maturity – natural maturity sequences ....	69
Figure 3.4: Open-pyrolysis GC-FID data for immature source rocks and unextracted New Zealand Coals – Kerogen typing (Petroleum type organofacies) on a molecular basis applying the alkyl-chain length distribution classification established by Horsfield (1989) and modified by Horsfield (1997). For data see Tab. 3-1. Original chromatograms of numbered samples typifying the different organofacies are displayed in Fig. 3.5.....	72
Figure 3.5: Seven open-pyrolysis gas-chromatograms (fingerprints) of immature source rocks typifying different organic matter qualities and petroleum type organofacies. The positions of some components playing important roles as geomarker or input parameters for kerogen classification diagrams are highlighted.....	73
Figure 3.6: The relationship between depositional environment and molecular kerogen structure displayed using three ternary diagrams of a) Horsfield (1989), b) Larter (1984), and c) Eglinton <i>et al.</i> (1990).....	81
Figure 3.7: Evolution of the kerogen composition during natural maturation displayed in ternary diagrams of a) Horsfield (1989) and b) Larter (1984). Arrows indicate the evolution pathway. ....	85
Figure 3.8: Frequency factors and activation energy distribution of homogeneous alginites, fluvio deltaic – terrestrial, and mixed marine – terrestrial source rocks based on non-isothermal bulk pyrolysis using the source rock analyzer (SRA).....	90
Figure 3.9: Transformation Ratio (TR) curves for the investigated immature sample set assuming a constant geological heating rate of 3°C/Ma.....	92
Figure 3.10: Transformation Ratio (TR) curves for the investigated immature sample set at a laboratory heating rate of 2°C/min .....	96
Figure 3.11: Frequency factors and activation energy distribution of extracted and unextracted New Zealand Coals based on non-isothermal bulk pyrolysis using the source rock analyzer (SRA).....	98
Figure 3.12: Frequency factors and activation energy distribution of a) Carboniferous German Coals. (Data taken from Schenk and Horsfield (1998) with the exception of sample G000721) and b) Cretaceous Wealden Coals from Germany .....	99
Figure 3.13: Bulk hydrocarbon formation rate curves for natural maturity series (given in % vitrinite reflectance) for laboratory and geologic heating rates; New Zealand Coals (determined within this thesis) and Westphalian Coals (taken from Schenk and Horsfield (1998)). ....	101
Figure 3.14: Bulk hydrocarbon formation rate curves for Exshaw Fm. samples of different maturities (given in calculated $R_o = T_{max} * 0.018 - 7.16$ ) for laboratory and geologic heating rates and the discrete activation energy distribution with a single free frequency factor. ....	102
Figure 3.15: Mineralogical composition of 32 investigated source rocks based on ATR-IR spectroscopy displayed in a ternary diagram comparing fractions of clay, quartz + feldspar, and carbonate.....	104

Figure 4.1: Stepwise open-pyrolysis at 1°C/min: cumulative yield curves of boiling fractions methane, C <sub>2-5</sub> , C <sub>6-14</sub> , C <sub>15+</sub> and Totals for the Åre Fm., Spekk Fm., Green River Shale (GRS), and synthetic mixture I/III .....	108
Figure 4.2: MSSV-pyrolysis at 1°C/min: cumulative yield curves for total products and boiling fractions methane, C <sub>2-5</sub> , C <sub>6-14</sub> , C <sub>15+</sub> for the Åre Fm., Spekk Fm., Green River Shale (GRS), and synthetic mixture I/III .....	110
Figure 4.3: „Conservative approach“-model (Dieckmann <i>et al.</i> , 1998) for the calculation of secondary gas formation from the decrease of MSSV-pyrolysis C <sub>6+</sub> compounds and “Refined Approach”-model (Erdmann, 1999) for the calculation of secondary gas formation from the difference between open- and closed-system pyrolysis C <sub>6+</sub> compound yields .....	111
Figure 4.4: Cumulative yield curves for boiling fractions C <sub>1-5</sub> and C <sub>6+</sub> measured under open- and closed-system pyrolysis conditions and calculated primary and secondary gas input using the „Conservative approach“ (left side) or “Refined Approach” (right side) for the Åre Fm., Spekk Fm., Green River Shale (GRS), and synthetic mixture I/III .....	114
Figure 4.5: Comparison of measured primary gas yields (open pyrolysis) and calculated primary gas yields using “conservative” and “refined” approach models for the Åre Fm., Spekk Fm., Green River Shale (GRS), and synthetic mixture I/III .....	115
Figure 4.6: Calculation of late gas yields, i.e. secondary gas (B) yields based on calculated primary gas evolution curves .....	117
Figure 4.7: Evolution curves of calculated secondary gas (Equation 16), calculated secondary gas (B) (Equation 17), and directly measured open- and closed-system pyrolysis total gas yields for the Åre Fm., Spekk Fm., Green River Shale (GRS), and synthetic mixture I/III .....	118
Figure 4.8: Evolution of GOR (C <sub>1-5</sub> /C <sub>6+</sub> ) under open- and closed-system pyrolysis conditions for the Åre Fm., Spekk Fm., Green River Shale (GRS), and synthetic mixture I/III .....	118
Figure 4.9: Evolution of gas wetness (C <sub>2-5</sub> /C <sub>1-5</sub> ) under open- and closed-system pyrolysis conditions for the Åre Fm., Spekk Fm., Green River Shale (GRS), and synthetic mixture I/III .....	119
Figure 4.10: Evolution of H/C ratios and aromaticity of the MSSV C <sub>6+</sub> boiling range fraction for the Åre Fm., Spekk Fm., Green River Shale (GRS), and synthetic mixture I/III. The H/C ratio is defined as the sum of all components H/C ratios weighted by their abundance. The aromaticity is defined as the ratio of the sum of all identified aromatic and phenolic compounds over the sum of all identified C <sub>6+</sub> compounds. ....	121
Figure 4.11: Normalised C <sub>1+</sub> , C <sub>1-5</sub> , and C <sub>6+</sub> boiling fractions as well as calculated cumulative secondary gas (B) yields and manually fitted spline curves for MSSV-pyrolysis at three heating rates 0.1, 0.7, and 1.0°C/min. ....	122
Figure 4.12: Differentiated spline curves (points) and calculated generation rate curves (lines) for secondary gas (B) generation at heating rates a) 0.1, 0.7, and 1.0°C/min and b) 0.1 and 1.0°C/min as well as respective kinetic parameters.....	125
Figure 4.13: T <sub>max</sub> as an expression of kinetic parameters and heating rate for secondary gas (B) and bulk hydrocarbon generation from Åre Fm. Sample G001965 at heating rates of a) 0.1, 0.7, and 1.0°C/min and b) 0.1 and 1.0°C/min. ....	126
Figure 4.14: Laboratory (right) and predicted geological (left) generation rate curves of secondary gas (B) formation derived from MSSV-pyrolysis and bulk product formation rate curves derived from open-system (SRA)-pyrolysis.....	128
Figure 4.15: MSSV-pyrolysis end temperatures (red shaded area) used for the late gas potential screening: complete cumulative yield curves for boiling fractions C <sub>1-5</sub> and C <sub>6+</sub> of Åre Fm., Spekk Fm., Green River Shale (GRS), and synthetic mixture I/III sample during MSSV-pyrolysis at 1°C/min. ....	129
Figure 4.16: MSSV-pyrolysis yields at the three (two) screening end-temperatures .....	130

Figure 4.17: Comparison of late gas ratio 1 (LGR1) to a) the late gas amount generated between the second (for most samples 560°C) and third temperature (for most samples 700°C) and to b) the absolute gas amount at the third temperature (for most samples 700°C). Data is provided in Tab. 4-4.....	132
Figure 4.18: Comparison of late gas ratio 1 (LGR1) to a) the late secondary gas (A) amount generated between the second (for most samples 560°C) and third temperature (for most samples 700°C) by cracking of C <sub>6+</sub> compounds and to b) the secondary gas (B) amount generated between the second (for most samples 560°C) and third temperature (for most samples 700°C). Data is provided in Tab. 4-4.....	133
Figure 4.19: Discrimination of source rocks exhibiting low, high, and intermediate late gas potentials using the two Late Gas Ratios LGR1 and LGR2.....	134
Figure 4.20: Late secondary gas (B) amounts: a) Late Gas Potential classification based on LGR1 and LGR2 as well as on bubble sizes expressing additional late secondary gas (B) input as percent of the total initial primary petroleum potential (Rock-Eval HI), whereas smallest bubble = 0% and biggest bubble = 51%; .b) Calculated late secondary gas (B) yield correlated to LGR1 .....	136
Figure 4.21: Comparison of open-system pyrolysis based alkyl chain length distribution classification and closed-system (MSSV)-pyrolysis based Late Gas Potential classification.....	138
Figure 4.22: Merged Closed-System MSSV-Pyrolysis and Open-System Pyrolysis data – Alkyl chain length distribution: a) Late Gas Potential assignments in relation to organic matter structure and depositional environment in the ternary diagram of Horsfield (1989); b) Comparison of LGR1 and open-system pyrolysis GOR; c) Comparison of LGR1 and open-system pyrolysis gas wetness .....	139
Figure 4.23: Merged Closed-System MSSV-Pyrolysis and Open-System Pyrolysis data – Phenol content: a) Late Gas Potential assignments in relation to organic matter structure and depositional environment in the ternary diagram of Larter (1984); b) Comparison of LGR1 and the percentage of phenolic compounds on all identified C <sub>6+</sub> compounds (open-system pyrolysis).....	141
Figure 4.24: Comparison of LGR1 to a) aromaticity of open-system pyrolysis C <sub>6+</sub> compounds as expressed by the sum of identified aromatic and phenolic compounds divided by the sum of all identified C <sub>6+</sub> compounds and to b) aliphaticity of open-system pyrolysis C <sub>6+</sub> compounds as expressed by the weighted H/C ratio of all identified C <sub>6+</sub> compounds.....	142
Figure 4.25: Merged Closed-System MSSV-Pyrolysis and Open-System Pyrolysis data – Organic sulphur content: a) Late Gas Potential assignments in relation to organic matter structure and depositional environment in the ternary diagram of Eglinton <i>et al.</i> (1990); b) Comparison of LGR1 and the ratio of thiophenic compounds over all identified C <sub>6+</sub> compounds (open-system pyrolysis); c) Comparison of LGR1 and the ratio of thiophenic compounds over mono-aromatic compounds (open-system pyrolysis).....	144
Figure 4.26: Merged Closed-System MSSV-Pyrolysis and Open-System Pyrolysis data – Rock-Eval Bulk Parameter: Late Gas Potential assignments in relation to a) TOC <i>versus</i> S <sub>2</sub> , to b) the same as in a) in a smaller resolution, to c) OI <i>versus</i> HI, and d) T <sub>max</sub> <i>versus</i> HI .....	145
Figure 5.1: Late Gas Potentials Classification using MSSV-pyrolysis based LGR1 and LGR2 for investigated natural maturity series samples.....	150
Figure 5.2: Exponential function describing the position of all investigated maturity series samples in the LGR1 – LGR2 plot.....	151
Figure 5.3: Comparison of LGR1 and total late gas generated between MSSV end temperatures 560° and 700°C for a) Barnett Shales and shales of the Exshaw Fm. as well as coals of the German Wealden and b) for German Carboniferous and unextracted and extracted New Zealand Coals.....	151
Figure 5.4: Relation of LGR1 to the percentage of late secondary gas (B) on the total late gas generated between 560° and 700°C. ....	152
Figure 5.5: Relation of measured (German Carboniferous Coals, New Zealand Coals) or calculated Vitrinite Reflectance (% R <sub>o</sub> ) to a) LGR1 and b) secondary gas (B) yield.....	154

Figure 5.6: Evolution of late secondary gas (B) yields (MSSV-pyrolysis) and organic matter structure, as revealed by open-system pyrolysis HI, OI (Rock Eval) as well as GOR, gas wetness, aromaticity, and phenol content (GC-FID), in the course of maturation (vitrinite reflectance) for all maturity series. ....	157
Figure 5.7: Evolution of late secondary gas (B) yields (MSSV-pyrolysis) and organic matter structure, as revealed by a) infrared spectroscopic analytical results and b) open-system pyrolytical yields, in the course of maturation (vitrinite reflectance) for New Zealand and German Carboniferous Coals.....	158
Figure 5.8: Aromatic ring condensation during metagenesis stage as evidenced by a) EPR and b) dark field imaging. Pictures are taken from Marchand and Conard (1980) and Oberlin <i>et al.</i> (1980).....	166
Figure 5.9: Evolution of the residue composition during closed-system artificial maturation displayed in ternary diagrams of a) Horsfield (1989) and b) Larter (1984). Arrows indicate the evolution pathway. ....	170
Figure 5.10: Evolution of the residue composition during closed-system artificial maturation as defined by Aromaticity and Gas Wetness (Open-Pyrolysis) .....	171
Figure 5.11: Evolution of the residue composition during open- vs. closed-system artificial maturation displayed in ternary diagrams of a) Horsfield (1989) and b) Larter (1984). Arrows indicate the evolution pathway. ....	173
Figure 5.12: Evolution of open pyrolysis yields and composition of the residues during open- vs. closed-system artificial maturation as defined by Aromaticity and Gas Wetness (Open-Pyrolysis) for a) Åre Fm. sample G001965 and b) Westphalian Coal sample G000721.....	174
Figure 5.13: Late Gas Potentials Classification using MSSV-pyrolysis based LGR1 and LGR2 for closed-system artificially prepared residues of a) Åre Fm sample G001965, b) Westphalian Coal sample G000721, c) Green River Shale sample G004750, Spekk Fm sample G001955, and e) the synthetic Type I/III source rock mixture; in f) exponential functions describing the positions of residues in the LGR1 – LGR2 plot are compared to the exponential function describing the position of all investigated natural maturity series samples. ....	176
Figure 5.14: Late Gas Potentials Classification using MSSV-pyrolysis based LGR1 and LGR2 for open-versus-closed-system artificially prepared residues of a) Åre Fm sample G001965 and b) Westphalian Coal sample G000721; in c) exponential functions describing the positions of open-system residues in the LGR1 – LGR2 plot are compared to the exponential function describing the position of all investigated natural maturity series samples.....	177
Figure 5.15: Late secondary gas (B) yields: a) LGR1 and late secondary gas (B) yields of all original samples and their related residues matured under closed-system conditions; b) Comparison of naturally matured and artificially matured Type II (Barnett vs. Spekk) and Type III (natural Westph. Coal series versus Westph. Coal and Åre Fm.) source rocks. ....	178
Figure 5.16: Late secondary gas (B) yields: a) LGR1 and late secondary gas (B) yields of Åre Fm sample G001965 and Westphalian Coal sample G000721 and their related residues matured under open- vs. closed-system conditions; b) Comparison of naturally matured Westphalian Coal series and under open- vs. closed-system artificially matured Åre Fm sample G001965 and Westphalian Coal sample G000721. ....	180
Figure 5.17: Calculated Vitrinite Reflectance values for open- and closed-system residues of Westphalian Coals sample G000721 based on a) LGR1 ratios and a linear fit through data points of the natural maturity coal series from Germany between 0.99 and 2.09% $R_o$ ; b) evolution of secondary gas (B) yields with artificial and natural maturation ( $R_o$ ). ....	181
Figure 5.18: Measured, theoretical, and normalised late secondary gas yields of Åre Fm sample G001965, and Westphalian Coal sample G000721, as well as their respective open-system residues.....	183
Figure 6.1: Stepwise MSSV-pyrolysis at 1°C/min: Cumulative stable carbon isotope ratio curves of $C_{1-4}$ alkanes as well as cumulative MSSV-pyrolysis yield curves of $C_{1-3}$ alkanes for the Åre Fm. sample G001965, the Spekk Fm. sample G001955, the Green River Shale sample G004750, and the synthetic Mix type I/III sample G0047501965.....	188

Figure 6.2: TOC/Rock-Eval screening data for the synthetic Type I/III source rock mixture and its parent material; a) TOC, S1, S2, S3; b) $T_{max}$ , HI, OI.....	195
Figure 6.3: Open-Pyrolysis (300-600°C) yields of Åre Fm sample G001965, Green River Shale sample G004750, a physical 50:50 source rock mixture of the latter two samples (synthetic Type I/III MIX) and a theoretical 50:50 source rock mixture of those samples.....	196
Figure 6.4: Composition of open-system pyrolysates of Åre Fm sample G001965, Green River Shale sample G004750, the physical 50:50 source rock mixture of the latter two samples (synthetic Type I/III MIX) and a theoretical 50:50 source rock mixture of those samples displayed in ternary diagrams of a) Horsfield (1989), b) Larter (1984), and c) Eglinton <i>et al.</i> (1990).....	196
Figure 6.5: Stepwise open-pyrolysis at 1°C/min: cumulative yield curves of boiling fractions methane, $C_{2-5}$ , $C_{6-14}$ , $C_{15+}$ and totals for the Åre Fm., Green River Shale (GRS), as well as measured and calculated synthetic mixture I/III .....	198
Figure 6.6: Stepwise open-pyrolysis at 1°C/min: cumulative yield curves of single compound fractions phenolic compounds, aromatic compounds, thiophenic compounds and aliphatic compounds $n-C_{6-14}$ and $n-C_{15+}$ for the Åre Fm., Green River Shale, as well as measured and calculated synthetic mixture I/III .....	199
Figure 6.7: Stepwise MSSV-pyrolysis at 1°C/min: cumulative yield curves of boiling fractions methane, $C_{2-5}$ , $C_{6-14}$ , $C_{15+}$ and totals for the Åre Fm., Green River Shale, as well as measured and calculated synthetic mixture I/III .....	202
Figure 6.8: Stepwise MSSV-pyrolysis at 1°C/min: cumulative yield curves of single compound fractions phenolic compounds, aromatic compounds, thiophenic compounds and aliphatic compounds $n-C_{6-14}$ and $n-C_{15+}$ for the Åre Fm., Green River Shale, as well as measured and calculated synthetic mixture I/III.....	203
Figure 6.9: Stepwise MSSV-pyrolysis at 1°C/min: cumulative yield curves of di- and mono-aromatic compound fractions as well as Naphthalene and 1M-Naphthalene for the Åre Fm., Green River Shale, as well as measured and calculated synthetic mixture I/III.....	204
Figure 6.10: Stepwise MSSV-pyrolysis at 1°C/min: methane, ethane, and propane isotopic carbon composition for the Åre Fm., Green River Shale, as well as measured and calculated synthetic mixture I/III .....	206
Figure 6.11: Open-Pyrolysis GC-FID: Evolution of the measured and calculated residue composition of synthetic Type I/III source rock mixture during closed-system artificial maturation displayed in ternary diagrams of a) Horsfield (1989) and b) Larter (1984) as well as expressed in c) gas wetness, GOR, and aromaticity. Arrows indicate the evolution pathway.....	208
Figure 6.12: Open-Pyrolysis GC-FID: Evolution of the measured and calculated residue yields of the synthetic Type I/III source rock mixture for boiling fractions methane, $C_{2-5}$ , $C_{6-14}$ , and $C_{15+}$ as well as for single compound fractions phenolic compounds, aromatic compounds, thiophenic compounds and aliphatic compounds $n-C_{6-14}$ and $n-C_{15+}$ .....	209
Figure 6.13: closed-system MSSV-Pyrolysis: Comparison of a) Late Gas Potential (LGR1-LGR2 plot) and b) late secondary gas (B) yield for measured and calculated closed-system artificially prepared residues of the synthetic Type I/III source rock mixture.....	210
Figure 6.14: ESR Spectra of Åre Fm. Coal sample G001965 and seven corresponding residues artificially matured under close-system pyrolysis conditions to end temperatures between 300 and 600°C.....	212
Figure 6.15: Closed-system maturation end temperature versus ESR-parameter absolute free radical concentration $C_{abs}$ , peak-to-peak line-width $\Delta B$ , as well as late secondary gas (B) yields for investigated Åre Fm. sample and corresponding residues.....	213
Figure 7.1: Additional Late Gas Input in Tcf/km <sup>3</sup> , Sm <sup>3</sup> /m <sup>3</sup> , and scf/ton as a function of TOC.....	221





# INDEX OF TABLES

Table 2-1: Provenance of immature source rocks .....	41
Table 2-2: Provenance of natural maturity series samples .....	43
Table 3-1: Normalised single compound yields as input parameters for determination of kerogen quality and structure using ternary diagrams of Horsfield (1989), Larter (1984), and Eglinton <i>et al.</i> (1990),.....	83
Table 3-2: Organic matter evolution – natural maturity series: Normalised single compound yields as input parameters for ternary diagrams of Horsfield (1989) and Larter (1984) as well as routinely used ratios such as GOR and Gas Wetness.....	86
Table 3-3: Kinetic Parameters - calculated, variable frequency factors, geologic $T_{max}$ , and transformation ratios 10%, 50%, and 90% for an applied geologic heating rate of 3°C/Ma. ....	94
Table 3-4: Mineralogical composition of 32 investigated source rocks based on ATR-IR spectroscopy comparing normalised fractions of clay, quartz + feldspar, and carbonate. ....	103
Table 4-1: Normalised $C_{1+}$ , $C_{1-5}$ , methane, $C_{6+}$ MSSV-pyrolysis yields as well as calculated cumulative secondary gas (B) and (A) yields for the three heating rates 0.1, 0.7, and 1.0°C/min. The red labelled late secondary gas (B) value indicates the factor the manually fitted spline curve was multiplied with.....	123
Table 4-2: Calculated, variable frequency factors, geologic $T_{max}$ , and transformation ratios 10%, 50%, and 90% in °C and % vitrinite reflectance for an applied geologic heating rate of 3°C/Ma for secondary gas (B) generation (MSSV-pyrolysis) and bulk hydrocarbon generation (SRA). ....	127
Table 4-3: $C_{1-5}$ and $C_{6+}$ yields at three (two) screening end-temperatures during MSSV-pyrolysis. The exactly used end-temperatures as well as heating rates are given in Table A 7. ....	131
Table 4-4: Calculated total late gas, late secondary gas (A), and late secondary gas (B) yields as well as late gas ratios LGR1 and LGR2 for all samples based on products generated between MSSV end temperatures 560°C and 700°C.....	137
Table 5-1: Calculated late gas, secondary gas (A) and (B) yields as well as LGR1 and LGR2 for natural maturity series samples based on products generated between MSSV end temperatures 560°C and 700°C.....	153
Table 5-2: Integrated infrared absorption (cm/mg TOC) in selected spectral ranges of New Zealand Coals (extracted coals) and non-extracted German coals (table taken from Vu, 2008 (Table 6-1); data of Schenk & Richter, 1995 and Vu, 2008) .....	159
Table 5-3: Evolution of organic matter artificially matured under open- or closed-system conditions – Open pyrolysis of residues: Normalised single compound yields as input parameters for ternary diagrams of Horsfield (1989) and Larter (1984) as well as routinely used ratios such as GOR, Gas Wetness and Aromaticity.....	168
Table 5-4: Calculated late gas, secondary gas (A), and secondary gas (B) yields as well as LGR1 and LGR2 ratios for residues artificially prepared under open- or closed-system conditions based on products generated between MSSV end temperatures 560°C and 700°C. ....	175
Table 5-5: The effect of weight loss occurring during open-system artificial maturation using a SRA on Late secondary gas (B) yields of open-system residues of Åre Fm sample G001965 and Westphalian Coal sample G000721. Measured, theoretical (based on secondary gas (B) yield of the original sample and weight loss), and normalised (measured secondary gas (B) yields are normalised to original sample weight) yields are given.....	182



## LIST OF COMMON ABBREVIATIONS

A	Frequency factor
ATR	Attenuated total reflection
Ea	Activation energy
FID	Flame Ionization Detector
Fig.	Figure
GC	Gas Chromatography
GIP	Gas in Place
GOR	Gas to Oil Ratio
HC	Hydrocarbon
HI	Hydrogen Index
IR	infrared spectroscopy
IRM-GC-MS	Isotope Ratio Monitoring - Gas Chromatography - Mass Spectrometry
Ma	Million years
min.	minute
MSSV	Micro Scaled Sealed Vessel
NSO's	high molecular weight polar compounds containing N, S, and O
OI	Oxygen Index
PI	Production Index
Py	Pyrolysis
S1	Amount of Volatized Hydrocarbons at Rock Eval
S2	Amount of Generated Hydrocarbons during Pyrolysis at Rock Eval
S3	Amount of Carbon Dioxide generated during Pyrolysis at Rock Eval
scf	standard cubic feet
SRA	Source rock analyzer
Tab.	Table
Tcf	Trillion cubic feet
T <sub>max</sub>	Temperature of maximum Pyrolysis Yield
TOC	Total Organic Carbon
TR	Transformation Ratio
Tvap	Thermovaporisation Gas Chromatography
(V)R <sub>o</sub>	Vitrinite Reflection – oil emulsion
wt.-%	Weight-%
vol.-%	Volume-%



# 1 INTRODUCTION

Natural gas plays a key role as an energy source for electrical and heating applications in the industrial, commercial, and residential sectors throughout all nations (EIA, 2009, International Energy Outlook 2009, pp. 35-47). According to the Energy Information Administration (EIA, 2009), worldwide, total natural gas consumption will increase by an average of 1.6% per year from 104 trillion cubic feet (tcf) in 2006 to 153 tcf in 2030. In the U.S. natural gas, coal and oil supply about 85 percent (%) of the nation's energy, with natural gas supplying about 22% of the total today and most likely for the next 20 years (USDOE, 2009). In addition, and meeting demands to reduce greenhouse gas emissions, natural gas will be featured at the expense of coal and liquid petroleum due to its relatively high fuel efficiency, low carbon dioxide yield upon combustion and comparatively low price.

Hence, the petroleum industry is exploring new natural gas plays, either conventional or unconventional such as tight gas, coal bed natural gas or shale gas. Increasingly deeper parts of sedimentary basins move into the focus of interest as natural gas can be formed at high temperatures by the breakdown of oil in reservoirs or source rocks or by the degradation of overmature kerogen. The extent and timing of this thermally driven late hydrocarbon generation are, besides reservoir characteristics and thermal history of a sedimentary basin, crucial parameters for predictive purposes in petroleum exploration prior to drilling, and is the topic of this thesis. For a reliable, universally valid kinetic evaluation of late gas generation, key questions have to be solved concerning firstly, potentially different gas-forming mechanisms for organic matter from different depositional environments with different starting compositions, and secondly, the effect of maturity-related molecular compositional changes of initial kerogen structure and early formed bitumen on the stability of gas precursor structures. By comparison, gas formation by oil cracking in reservoirs is better understood and no longer the focus of research.

## ***1.1 Natural Gas Generation from Sedimentary Organic Matter***

### **1.1.1 General Geochemistry of Natural Gas**

Natural petroleum gas usually consists mainly of methane  $\text{CH}_4$  with varying amounts of heavier hydrocarbons in the  $\text{C}_2$ - $\text{C}_5$  range such as ethane  $\text{C}_2\text{H}_6$ , propane  $\text{C}_3\text{H}_8$ , and butane  $\text{C}_4\text{H}_{10}$  and non-hydrocarbons such as carbon dioxide  $\text{CO}_2$ , hydrogen sulphide  $\text{H}_2\text{S}$ , and nitrogen  $\text{N}_2$  (Tissot and Welte, 1984; Hunt, 1995). Compounds with more than five carbon

atoms are liquid under standard temperature and pressure (STP), though they may exist in the vapour phase under subsurface conditions.

Commercial accumulations of hydrocarbon gases almost exclusively originate from the bacterial or thermal degradation of sedimentary organic matter (Philippi, 1965; Schoell, 1980; Schoell, 1983; Tissot and Welte, 1984) and thus, are of biogenic origin (Schoell, 1988; Hunt, 1995). Only minor seeps of *abiogenic methane* formed by inorganic reactions in the deeper crust or upper mantle (Abrajano *et al.*, 1988; Welhan, 1988) are occasionally reported (Schoell, 1988) and distinguishable from *biogenic methane* by a higher relative content of  $^{13}\text{C}$ . However, the term *biogenic gas* usually refers to bacterial and microbial related, “early” dry gas generation by both fermentation and  $\text{CO}_2$  reduction (Schoell, 1988; Faber *et al.*, 1992; Whiticar, 1994) in anoxic environments at temperatures below  $80^\circ\text{C}$  (Rice and Claypool, 1981). By contrast, *organic thermal gas* generation refers to the thermochemical degradation of higher molecular weight organic matter, either kerogen or oil, during diagenesis, catagenesis and metagenesis in the so-called early-mature, mature and overmature zones (Tissot and Welte, 1984) at temperatures exceeding  $70^\circ\text{C}$  (Dieckmann *et al.*, 1998; Dieckmann, 2005; Horsfield *et al.*, 2006).

According to Rice and Claypool (1981), *biogenic gas* accounts for as much as 20% of the total world gas reserves. Nevertheless, knowing whether a natural gas show is *biogenic* or *thermogenic* in origin can have critical implications as to the presence of liquid hydrocarbons in a basin as processes leading to *biogenic* gas are decoupled from those that form *thermogenic* petroleum. If a gas seep or show is bacterial in origin, then the presence of the gas says nothing about the likelihood of an underlying petroleum system being present. In contrast, if a gas show is found to be thermogenic in origin, the possibility exists that the gas derives from a gas cap overlying a down-dip oil leg. The genetic origin of accumulated hydrocarbon gas can be easily recognised by its geochemistry, i.e. its composition and stable isotopic signature.

It is commonly said (Hunt, 1979; Tissot and Welte, 1984) that dry gas, i.e. methane with a very low content of higher hydrocarbons ( $\text{C}_1/\sum\text{C}_n > 0.97$ ), forms at shallow depth in the early diagenesis zone as a result of microbial activity, and in deeper parts of basins in the late catagenesis and early metagenesis zones by degradation of overmature kerogen or the secondary cracking of expelled or unexpelled oil in the temperature range of  $150\text{--}220^\circ\text{C}$  (Cooles *et al.*, 1986; Quigley and Mackenzie, 1988; Clayton, 1991). In contrast, wet gas (i.e.  $\text{C}_1/\sum\text{C}_n < 0.98$ ) is thermally generated co-genetically with oil from kerogen beginning during catagenesis and continuing up to temperatures of  $150^\circ\text{C}$  and probably beyond.

### 1.1.2 Stable Isotopic Signature of Natural Gas

#### *Isotope Distributions in Natural Gas Accumulations*

The isotopic fractionation is usually reported in the  $\delta$ -notation (Equation 1)

$$\delta = \frac{R_{\text{sample}} - R_{\text{standard}}}{R_{\text{standard}}} \times 1000(\text{‰}), \quad (1)$$

where  $R$  is either the ratio of  $^{13}\text{C}/^{12}\text{C}$  or  $\text{D}/\text{H}$ .  $\delta\text{D}$  is given relative to the Standard Mean Ocean Water (SMOW) standard (Craig, 1961) and  $\delta^{13}\text{C}$  relative to the Pee Dee Belemnite (PDB) standard (Craig, 1957). The  $\delta^{13}\text{C}$  value of early *biogenic* methane ranges from -90 to -55‰, whereas the  $\delta^{13}\text{C}$  ratio of late, metagenetic methane ranges from -40 to -20‰ (Stahl and Carey Jr., 1975; Galimov, 1980; Schoell, 1980; Tissot and Welte, 1984; Hunt, 1995). The methane in catagenetic wet gas shows intermediate  $\delta^{13}\text{C}$  values between -55 and -30‰. Additional information can be provided by the  $\delta\text{D}$  of methane. Schoell (1980) could show that most reservoired *biogenic* gases of economic interest originate from methanogenesis by  $\text{CO}_2$  reduction in marine environments below the zone of sulphate reduction (Rice and Claypool, 1981) leading to  $\delta\text{D}_{\text{CH}_4}$  values between -180 and 280‰. In contrast, fermentation of methylated substrates, e.g. acetate, generates deuterium depleted methane with  $\delta\text{D}$  values between -250 and -400‰ only observable in recent freshwater environments and swamps. *Thermogenic gas* formed during catagenesis together with oil exhibits  $\text{D}/\text{H}$  ratios from -260 to -150‰ with deuterium contents tending to increase with decreasing gas wetness. Dry *thermogenic gas* from the metagenesis zone is more enriched in deuterium (-180 to -130‰) and shows an increase in deuterium with increasing maturity of the related source rock as it is similarly observed for  $^{13}\text{C}_1$  (Sackett *et al.*, 1970; Schoell, 1980; Whiticar *et al.*, 1986; Schoell, 1988). Nevertheless, anomalous values occur under geologic conditions outside these ranges because of variable sources of  $^{13}\text{C}$  and  $\text{D}$ . Additionally, the extensive mixing of gases caused by vertical migration can lead to mixed gases obscuring the primary isotopic signature and composition (Berner and Faber, 1988; Faber *et al.*, 1992).

The dissimilarity or large range in isotope distributions of *biogenic* and *thermogenic gas* accumulations is related to several factors including precursor compounds, the difference in type and magnitude of the kinetic isotope effect (KIE) involved, and the difference in temperature regime in which gas-forming reactions proceed (Whiticar, 1999). A review of biological fractionation mechanisms in organisms which controls the initial isotopic

composition of gas precursors was given by Degens (1989). Generally it can be said that the lipid fraction of an organism is enriched in the  $^{12}\text{C}$  isotope relative to the whole organism. Consequently  $^{13}\text{C}$  is more abundant in e.g. terrestrial derived organic matter which contains low amounts of lipids.

### ***Isotopic Fractionation during Biogenic Gas Generation***

*Biogenic* methane generated in the diagenesis zone is an ultimate dissimilation product of microbial mediated reactions of low molecular weight organic matter which accumulates in anoxic sediments with coexisting dissolved  $\text{CO}_2$  and formation water. The  $^{13}\text{C}/^{12}\text{C}$  ratios of dissolved  $\text{CO}_2$  in interstitial waters are controlled by a combination of equilibrium and kinetic isotope effects related to atmospheric exchange, precipitation-dissolution, organic matter decomposition, and other diagenetic reactions inducing an initial possible range of isotopic values (Whiticar *et al.*, 1986). In spite of this, the magnitude of isotope separation is distinctive for the related methanogenic pathways involved, acetate-type fermentation or  $\text{CO}_2$  reduction by hydrogen. For example, methane formed by the transfer of a methyl group is more depleted in deuterium than methane formed by reduction of  $\text{CO}_2$  because all the hydrogen for the latter is incorporated directly from the formation water with a constant fractionation. In contrast, during acetate fermentation only  $\frac{1}{4}$  of the hydrogen is derived from the formation water, probably via an intermediate  $\text{H}_2\text{O}-\text{H}_2$  dissociation step (Whiticar *et al.*, 1986). The distribution of carbon isotopes during uptake and metabolism of carbon compounds is, besides the isotope signature of the source material, controlled by the KIE which is related to the phenomenon that, for particular compounds, the molecules with the lower isotopic mass diffuse and react more rapidly and thus are utilized more frequently by bacteria than the isotopically heavier species. This effect causes the depletion in  $^{13}\text{C}$  of  $\text{CH}_4$  relative to the precursor substrate leading to an isotope fractionation with different magnitudes for different pathways, whereas highest fractionations are seen for methanogenesis by carbonate reduction (Schoell, 1980; Whiticar, 1999).

### ***Isotopic Fractionation during Thermogenic Gas Generation***

The increase in deuterium and  $^{13}\text{C}_1$  with increasing maturity of related source rocks during *thermogenic gas* generation can also be explained by a kinetic isotope effect (Sackett *et al.*, 1970; Schoell, 1980).  $^{12}\text{C}$  forms slightly weaker chemical bonds than does  $^{13}\text{C}$  and thus, there are small differences in the reaction rates of molecules containing a terminal  $^{13}\text{C}$  molecule compared to molecules containing  $^{12}\text{C}$  when thermally degraded. Silverman (1967) and Sackett *et al.* (1970) demonstrated that C-C bonds of different isotope combinations result



in different bond strengths with  $^{12}\text{C}$ - $^{12}\text{C}$  being the weakest and  $^{13}\text{C}$ - $^{13}\text{C}$  the strongest bonds. The gas produced in early stages of maturation would therefore be enriched in  $^{12}\text{C}$ , isotopically lighter, and the remaining source material, kerogen, coal or oil, would become correspondingly enriched in  $^{13}\text{C}$ , isotopically heavy. Hence, there is a corresponding progressive  $^{13}\text{C}$  enrichment in gas that is subsequently formed at higher temperatures (Clayton, 1991; Whiticar, 1999) until the increasingly “heavy” gas precursor structure is depleted or turned into gas which, in a closed system, would now inherit the isotopic ratio of the original precursor structure. This carbon isotope mass balance is commonly described by the distillation functions of Rayleigh (1896) which are used to model the  $\delta^{13}\text{C}$  of a hydrocarbon gas as a function of  $\delta^{13}\text{C}$  of the gas precursor, the maturity related extent of gas generation or conversion of gas precursor, and a kinetic isotope fractionation factor of the distinct reaction (Clayton, 1991). Nevertheless, knowing the exact potential gas precursor structure within organic matter alone is not an easy task as the organic source material itself is highly heterogeneous and constantly changed chemically and structurally in the course of maturation.

### 1.1.3 Classification of Organic Matter focusing on Kerogen

#### *Definition of Kerogen*

Kerogen, the word was first coined by A. Crum-Brown (personal communication to Carruthers *et al.*, 1912, p.143) to name the organic matter of the oil shale of the Lothians (Scotland) that produces a waxy oil upon distillation (the Greek *keros* means wax), is by modern definition described as the proportion of organic matter in sedimentary rocks which is insoluble in usual organic solvents (Robinson *et al.*, 1953; Forsman and Hunt, 1958; Durand, 1980) in contrast to the soluble proportion, defined as bitumen. Asphaltenes are considered intermediates between kerogen and bitumen, i.e. they are entities soluble in polar organic solvents but structurally closely related to kerogen (Tissot, 1969; Behar and Pelet, 1985; Pelet *et al.*, 1986).

#### *Main Formation Pathways of Kerogen*

Kerogen can form via two main pathways. The first one is the “degradation–recondensation” pathway where organic constituents from living organisms (biopolymers) such as proteins, polysaccharides and lignin are biodegraded into smaller products (biomonomers) like amino acids, sugars and phenols, a portion of which may recondense randomly to form a geopolymer called humin or “protokerogen” (Nissenbaum and Kaplan,

1972; Huc and Durand, 1974; Stevenson, 1974; Welte, 1974; Stuermer *et al.*, 1978; Huc, 1980). The second pathway is the “selective preservation” of protective, often morphologically structured biopolymeric macromolecules such as spores, pollen, cuticles and degraded cellular debris, which are resistant to microbial enzymes and selectively enriched relative to other, bioavailable, constituents (Philp and Calvin, 1976; Stach *et al.*, 1982; Largeau *et al.*, 1984; Tegelaar *et al.*, 1989a; Rullkötter and Michaelis, 1990; Largeau and Derenne, 1993; Vandenbroucke and Largeau, 2007). While the respective contribution of these processes to kerogen preservation is probably controlled by environmental conditions and the nature of the starting material (Horsfield, 1997), degradation-recondensation is probably always involved to some extent, in contrast to selective preservation (Vandenbroucke and Largeau, 2007). It should be stated here, that selective preservation can lead to the formation of very homogeneous kerogens with very high oil potentials as the preserved outer cell walls of some microalgae are highly aliphatic, e.g. for *Botryococcus braunii* (Torbanites; boghead coals)(Berkaloff *et al.*, 1983; Largeau *et al.*, 1984; Largeau *et al.*, 1986) or *Tetraedron minimum* (Messel Oil shale)(Goth *et al.*, 1988).

### ***Classification of Kerogen***

Kerogens are most often and conveniently classified by elemental analysis and Rock-Eval pyrolysis (Espitalié *et al.*, 1977) as Types I, II, III (Tissot *et al.*, 1974) which are defined at low maturities by their atomic H/C and O/C ratios, or Hydrogen Index HI and Oxygen Index OI respectively. This classification is closely related to the work of Van Krevelen *et al.* (1951) and Van Krevelen (1961) who had earlier distinguished the coal macerals alginite, exinite and vitrinite in the order of decreasing H/C ratios. Terrestrial humic coals can be viewed as a form of Type III organic matter (Durand *et al.*, 1977b) whereas aquatic sapropelic coals correlate to kerogen Type I (Boghead Coals) and Type II (Cannel Coals). Mixing of various components/macerals during organic matter deposition can of course lead to “intermediate” H/C - O/C ratios or Rock-Eval Indices causing kerogen classifications such as Type I/II or Type II/III. Very low H/Cs or HIs can be observed for Type IV source rocks containing e.g. fusain which is derived from the combustion of woody material (Scott, 1989).

Using the aforementioned methods kerogen classification becomes more and more difficult with increasing natural maturation, as loss of first oxygen and then hydrogen relative to carbon during early maturation and catagenesis means that all kerogen types move along certain pathways towards the point where O/C or OI and H/C or HI are zero and eventually become indistinguishable.

The discrimination of kerogens within source rocks according to hydrogen availability and thus genetic potential helps the explorationist to determine the source rock quality in a most basic way. Concepts were established already early on (Forsman and Hunt, 1958; Philippi, 1965; Tissot *et al.*, 1974) stating that the hydrogen-rich kerogen types I and II form liquid-rich, gas-poor petroleum during maturation, whereas hydrogen-poor kerogens and humic coals tend to generate gas. Expressed in other words, immature, marine or lacustrine oil-prone source rocks exhibiting high hydrogen indices and low oxygen indices were expected to initially generate products showing low gas-oil ratios (GOR). In contrast immature, gas-prone coals and terrestrially influenced shales having lower hydrogen indices and higher oxygen indices were expected to initially generate products showing high GORs. The main cause for this are the biopolymers forming the organic matter in specific depositional environments with hydrogen-rich kerogens comprising mainly algal-derived aliphatic cell membranes and lipid components (Cane and Albion, 1973; Tegelaar *et al.*, 1989a) and with originally hydrogen-poor kerogens containing high proportions of altered lignocellulosic, land plant-derived materials whose aliphatic constituents consist of alicyclic moieties and short alkyl chains (Given, 1960). This generalised understanding led to the formulation of organic facies concepts where petroleum composition strongly correlates with sedimentary facies (e.g. Jones, 1987).

As described earlier, kerogens become indistinguishable with maturity on an elemental level. The same is true for GOR values which are high for all source rocks at more extreme levels of maturity (Tissot and Welte, 1984; England and Mackenzie, 1989) because the primary methane-forming moieties in heterogeneous kerogens are thermally stable and the last to crack (Mackenzie and Quigley, 1988; Horsfield, 1989; Krooss *et al.*, 1995), and because secondary gas might be generated from unexpelled oil (Tissot and Welte, 1984; Monin *et al.*, 1990; Dieckmann *et al.*, 1998; Dieckmann *et al.*, 2000b; Jarvie *et al.*, 2007).

Nevertheless, care should be taken when using kerogen classifications discriminating solely according to hydrogen availability defined by H/C ratios or Hydrogen Indices. Masses of expellable petroleum generated in source rock kitchens might be predicted correctly but not the petroleum composition such as gas vs. oil potential or the timing of generation (Horsfield, 1997)(see also Chapter 1.1.7 and 1.1.6 respectively).

For instance, it is now clear that Type III organic matter, defined by a rather low H/C ratio or Hydrogen Index, is not only gas prone but can expel oil under geologic conditions as evidenced for certain humic coals, e.g. New Zealand Coals, Australian Coals, Indonesian

Coals, etc. (Smith and Cook, 1984; Thompson *et al.*, 1985; Horsfield *et al.*, 1988; Isaksen *et al.*, 1998; Wilkins and George, 2002). The gas vs. oil potential of Type III kerogen results from the variable respective amounts of two main constituents within the kerogen structure; firstly, ligneous debris containing aromatic H and short aliphatic chains ( $<C_{18}$ ) generating mainly gas and secondly, aliphatic protective coatings with a paraffinic oil potential (Killops *et al.*, 1998 and ref. therein). However, petroleum composition is not necessarily related to maceral composition, e.g. liptinite content, as perhydrous vitrinite, for example, contains a noticeable oil prone aliphatic component (Powell *et al.*, 1991) probably induced by the remains of bacteria feeding on humic substances during early diagenesis (Wilkins and George, 2002).

Additionally and as shown by Horsfield *et al.* (1992a) for the Alum shale and by Muscio and Horsfield. (1996) for the Bakken shale, not every Type II source rock is predominantly oil prone but may generate high amounts of gas or condensate under geological conditions due to aromatisation of the kerogen structure related to the presence of unusual precursor biota and/or the effects of alpha-ray bombardment (Dahl *et al.*, 1988; Lewan and Burchardt, 1989; Horsfield *et al.*, 1992a).

#### **1.1.4 Bulk Mechanisms of Petroleum Formation**

##### ***The “Cooles model”***

Using the previously described, simplified classification scheme for kerogens and Rock-Eval data of immature and naturally matured source rocks Cooles *et al.* (1986) introduced an algebraic model for kerogen degradation into gaseous and liquid petroleum on the basis of a bulk concept which accounts only for educts and products without considering single chemical reactions. Here, kerogen can be divided into three parts, inert kerogen which has no petroleum forming capacity but undergoes internal rearrangements, and labile and refractory kerogen as the reactive part of kerogen which is able to generate petroleum at different levels of thermal stress. Labile kerogen generates both oil and minor amounts of wet gas in the catagenesis zone (as stated above) and is ascribed to be the main precursor for oil-prone, “sapropelic” homogeneous organic matter, whereas refractory kerogen generates dry gas at higher maturities at the end of catagenesis and early metagenesis zones and is ascribed to be the main precursor for gas-prone, “humic” heterogeneous organic matter. Expelled or unexpelled oil, generated from the labile proportion of kerogen, can subsequently be degraded to secondary gas.

***Limitations of the “Cooles model”***

The “Cooles model” was a major breakthrough, in that simple input parameter could be used to calculate elementary important parameters in petroleum exploration, namely extent of generation and expulsion efficiency. Its fundamental weakness, and the same applies to its data source, open-system pyrolysis, is the assumed static behaviour of inert, labile and refractory kerogen fractions, inherited directly from the biological precursors, when it comes to prediction of kerogen conversion with maturation of the evaluated immature source rock.

For instance, for terrigenous organic material (coal, Type III kerogen) it is known that during natural maturation, aromatisation and polycondensation reactions take place as well as decomposition reactions (Stach *et al.*, 1982; Solomon *et al.*, 1988; Hatcher *et al.*, 1992; Horsfield, 1997; Payne and Ortoleva, 2001; Wilkins and George, 2002). Some moieties within the C<sub>6+</sub> liquids which are formed by thermal cracking upon pyrolysis (Espitalié *et al.*, 1988; Forbes *et al.*, 1991) are retained or recombined into the macromolecular structure during natural coalification (Schenk and Horsfield, 1998). Based on mass balance calculations of natural maturity series of marine source rocks such as the Alum shale and the Bakken shale, Horsfield *et al.* (1992a) and Muscio and Horsfield (1996) proposed, that some dead carbon (inert kerogen) in the “Cooles model” is formed from labile kerogen in the course of maturation. Horsfield (1997) concludes that during coalification naphthenoaromatic, phenolic and cross-linked structures (Type III or mixed Type II/III coals and kerogens) are likely to be incorporated into dead carbon in nature and not released as volatile products. Furthermore, Erdmann and Horsfield (2006) and Dieckmann *et al.* (2006) could show for mixed marine-terrigenous Type III kerogens, a Heather Formation sample respectively a Taglu Formation sample, and using a combination of open and closed pyrolysis experiments, that not only dead carbon is formed but that second order recombination reactions between first formed products and residual kerogen lead to the neoformation of an insoluble, refractory macromolecular structure (char/coke) at low thermal maturation levels. This recombination residue is said to generate high amounts of methane at high levels of thermal stress and thus, labile kerogen, assumed to be oil-prone, is lost and converted into a gas-prone refractory kerogen fraction. All of these second-order reactions have an effect on the distribution of inert, labile, and refractory kerogen fractions predefined by the initial biological precursor structure, and thus have an impact on not only the masses and composition of generated products but also on the kinetics of gas generation.

As an aside and to avoid misunderstandings, carbon residues are long known to be formed under pyrolysis conditions and are usually termed char or coke (Burnham and Happe,

1984). Coke is formed by second-order reactions from a fluid intermediate that undergoes polymerization and condensation reactions whereas char could be viewed as the inert kerogen fraction which is left over after the loss of minor fragments previously described as reactive kerogen. Thus, most pyrolysis residues are mixtures of char and coke.

### 1.1.5 Major Cracking Mechanisms of Petroleum Formation

For the cracking of organic matter to smaller fragments two major mechanisms might be responsible which are discussed in Greensfelder *et al.* (1949). The first concept is the cleavage of the organic matrix by thermal cracking via free-radicals; the second alternative mechanism is the acidic catalysed cracking with carbonium intermediates.

#### *Thermal Cracking via Free Radicals*

The thermal cracking concept is based on the Rice free radical theory (Rice, 1933) which was modified by Kossiakoff and Rice (1943) and proposed by Ungerer (1990) to explain the thermal degradation behaviour of isolated kerogens. Based on the cracking behaviour of normal paraffins the so-called Rice-Herzfeld or Rice-Kossiakoff mechanism is a chain reaction consisting of initiation, chain propagation and termination reaction steps.

The chain reaction is initiated by the formation of a radical when a normal paraffin molecule loses a hydrogen atom by collision and reaction with a small free hydrocarbon radical or a free hydrogen atom.

Subsequent propagation reactions include the cracking of this radical by  $\beta$ -scission and also possible radical isomerisation by the change of the position of a hydrogen atom to stabilize the radical prior to cracking.  $\beta$ -scission is the cracking of a C – C bond located in the beta-position to the carbon atom lacking one hydrogen atom (radical centre) and leads in the case of a non-isomerised radical to the formation of an alpha olefin and a primary radical (lacking one hydrogen atom on a primary carbon atom) which may immediately recrack at the beta bond to give ethylene and another primary radical. By successive cracking, if kept in the reaction zone in a closed-system, the radicals ultimately are reduced to methyl or ethyl fragments, which then react with feed stock molecules to produce new free radicals and are themselves converted to methane and ethane. Thus, cracking is propagated as a chain reaction.

Termination of chain reactions works by radical recombination/addition and by disproportionation.

The free-radical chain reaction mechanism was used in an initial mechanistic formulation of coal reactivity (Wiser, 1968; Poutsma, 1990) who postulated that thermally

stimulated, homolytic breaking of covalent bonds in the network structure generates reactive free radicals. If these then abstracted hydrogen from a donor solvent, H<sub>2</sub>, or coal itself, they would be “capped”. Given the breaking of enough bonds, stable fragments would thus be formed that were volatile and/or soluble. However, if a reactive source of hydrogen were not immediately available, these radicals would undergo “condensation” with themselves or other parts of the coal to form stable new bonds, and the result would be char and/or coke. The transfer of hydrogen was demonstrated impressively by Hoering (1984) who pyrolysed shale in the presence of heavy water and could show that deuterium was incorporated into the products.

The detection of free radicals in kerogens and coals using the ESR technique and the observation that free radicals are being formed (increasing spin densities) associated with bond cleavage within the “classic oil window” followed by decreasing free radical concentrations due to the gradual conversion of kerogen to a graphite-like structure (condensation) at maturity levels  $R_o > 2\%$  (Ishiwatari *et al.*, 1976; Ishiwatari *et al.*, 1977; Marchand and Conard, 1980; Bakr *et al.*, 1988; Bakr *et al.*, 1990; Bakr *et al.*, 1991) support the significance of chain reactions via free radicals in natural systems. Furthermore, and because of the occurrence of olefins during open system pyrolysis, it is often assumed that thermal cracking via free radicals is the main process in nature for the formation of primary gas (Jurg and Eisma, 1964) as olefins should be continuously produced due to successive beta cracking of the resultant primary or isomerised radical (Greensfelder *et al.*, 1949).

The initiation of the chain reaction is a random process leading to a distribution of *n*-alkanes, in which the product amounts increase smoothly with increasing carbon number. Kissin (1987) observed an exponential distribution of molar quantities of C<sub>7+</sub> *n*-alkanes in petroleum which was also demonstrated for products from several pyrolysis experiments (Thompson, 2002 and references therein) using mainly kerogen Type II containing organic matter, whereas the slope of this exponential distribution increases with increasing maturity. Thompson reported two exponential series from which the C<sub>2-5</sub> slope is invariably steeper than the C<sub>6+</sub> slope confirming stability and reaction mechanism. Nevertheless, it should be mentioned here, that *n*-alkanes in natural crude oils are not necessarily exponentially distributed, but that e.g. high wax crude oils can often display strong bimodal distributions or odd-carbon number preferences (Horsfield, 1989; Tegelaar *et al.*, 1989b), especially when sourced from Type I organic matter formed by selective preservation of certain resistant biopolymers with a characteristic aliphatic structure (Tegelaar *et al.*, 1989a). E.g. Reed *et al.* (1986) had detected a strong odd-carbon predominance in the C<sub>9-19</sub> range of Ordovician oils

from the Michigan Basin whereas Tegelaar *et al* (1989b) detected an odd-carbon predominance in the C<sub>25-35</sub> range in closed-system pyrolysates of cutan from *Agave Americana* which resembled those occurring in pyrolysates of an Indonesian crude oil.

It was found that pure naphthenes and isoalkanes crack very differently compared to *n*-alkanes by ring-dehydrogenation respectively ring-closure to aromatics. The main product is methane instead of ethane (Voge and Good, 1949). Thermal cracking of substituted aromatic rings is mainly confined to the beta cracking of attached carbon chains and results in primarily substituted aromatic rings as there is a considerable reluctance to crack at the bond next to the ring. Thus e.g., thermal cracking of *n*-propyl-benzene gives chiefly toluene.

### ***Acidic Catalysed Cracking via Carbonium Intermediates***

The nowadays overlooked acid catalysed mechanism comprises similar reactions whereas the reactive intermediates are positively charged carbonium ions rather than free radicals. Acid catalysed hydrocarbon reactions include the attack on the hydrocarbon, the production of carbonium ion and the behaviour of carbonium ions according to specific rules (Greensfelder *et al.*, 1949 and references therein).

Carbonium ions are generated by proton additions to olefins at Brønsted acid centers (proton donor centers) or by hydride removal from paraffin molecules at Lewis acid centers (electron-deficient centers) whereas olefins crack much faster than saturates. The high reactivity of olefins in catalytic cracking and other acid-catalysed systems can be ascribed to the high attraction of the ethylenic double bond ( $\pi$  electrons) for a proton, which results in the rapid formation of reactive carbonium ions. Both Brønsted and Lewis acid centers are abundant in clay minerals and the acid sites existing on mineral surfaces are active to promote the formation of carbonium ions from kerogen. Fitting into this context and related to high temperature, catalytical cracking effects, Horsfield and Douglas (1980) and Espitalie *et al.* (1980) could show for source rocks containing clays or for synthetic clay-kerogen mixtures that the composition of pyrolysate depends on the type of minerals within a rock's matrix; i.e. in the case of carbonate matrix the pyrolysate composition may be similar to the pyrolysate composition of the respective isolated kerogen, whereas for montmorillonitic sediments it will be enriched in gaseous and aromatic hydrocarbons.

Main products during acid-catalysed cracking are branched hydrocarbons because hydrogen shift or methyl shift are more common than for radical supported mechanisms. Kissin (1987) for example could show that olefins produced during thermocracking are catalytically transformed in the presence of acidic clay minerals into complex mixtures of isoalkanes. Thus, not all branched hydrocarbons occurring in nature or experiments can be



tracked back to precursor structures within the organic matter structure (Ungerer, 1990) but may be related to the contribution of the ionic mechanism. Additionally, acidic aluminosilicate catalysts are widely used in the petroleum refining industry in order to promote hydrocarbon branching.

It should be stated here that cracking catalysts are available for either type of reaction mechanism; those which accelerate free radical type reactions are non-acidic, and those which accelerate carbonium ion-type reactions are acidic. Commercial acid-treated clay and synthetic silica-alumina cracking catalysts belong, as stated above, to the latter class. Activated carbon (charcoal) has no proton availability and therefore is a highly active, non-acidic catalyst. Cracking of hexadecane (Greensfelder *et al.*, 1949) over activated charcoal can be explained as a quenched free radical type of cracking and gives a unique product distribution with very little branching and more paraffins than olefins to be observed.

### ***Catalytically Mediated Cleavage of Carbon-Carbon Bonds***

A number of papers have been published suggesting a third concept in which thermal natural gas generation proceeds over a catalytically mediated cleavage of carbon-carbon bonds with the catalyst being one or more transition metals (Mango, 1992b; Mango, 1992a; Mango *et al.*, 1994; Mango, 1997; Mango and Hightower, 1997; Mango and Elrod, 1999; Mango, 2000). Deduced from molecular compound ratios, Mango has inferred that transition metal complexes like nickel or etioporphyrin III have catalytic properties, which might take part in natural gas generation reactions influencing the composition of the light end fraction.

One argument is that the chemical composition of natural gas derived through simple thermal decomposition (cracking or cleavage of carbon-carbon bonds) during laboratory experiments is too wet than that of natural observed products in reservoirs; whereas the compound distribution derived from activated catalytic cleavage of oil in the laboratory is similar to the observed geological distribution.

In contrast, Snowdon (2001) found that the distribution of compounds within cuttings gas is consistent with simple, non-catalytic cracking. The compound distribution within reservoired gases is less likely to be representative of the generation process itself than *in situ* gases from cuttings, because the former has been affected by a higher number of geological processes resulting in fractionation such as migration, accumulation, and (selective) preservation or biodegradation. Earlier work by Evans *et al.* (1971) already demonstrated that reservoir gases are typically enriched in methane relative to the gas composition in fine grained rocks which have not been subjected to migration. Similar results generated by

Snowdon (1971) and used by Hunt (1979), Monnier et al (1983), Tissot and Welte (1984) also show that the composition of natural gas in the subsurface that has not migrated into a reservoir is commonly not dominated by methane, but rather by wet gases. In this context Vandenbroucke and Largeau (2007) rule out a catalytic influence of minerals or metal complexes in general at least on primary cracking, as primary cracking occurs mainly within the organic network of kerogen where minerals are absent. Furthermore they state, that studies on Type III organic matter at any maturity stage have never shown any difference between massive coals and dispersed kerogen (Huc *et al.*, 1986) although detrital minerals predominating in the latter exhibit especially high catalytically activity if dehydrated. Similarity of kinetic parameters of source rocks (various organic matter types) from the same formation but with widely different TOC values is another indication for the importance of non-catalytic cracking over catalytic cracking during primary generation.

Thus, catalysed cracking is most likely responsible for the rearrangement of components subsequent to thermal cracking reactions as e.g. Mangos model (Mango, 1992a) is the only model so far that takes account of the observation of regularities in light end hydrocarbon compositional patterns which can hardly be explained by simple cracking of irregular precursor structures (Erdmann, 1999).

### **1.1.6 Predicting the Timing of Thermal Gas Genesis**

#### ***Timing of primary and secondary thermal gas formation***

Predicting timing and amount of oil and gas generation in sedimentary basins is of paramount importance for petroleum exploration but not a simple task. Three distinct processes are already documented as resulting in the formation of thermogenic gas (Tissot, 1969; Braun and Rothman, 1975; Ungerer, 1990) and thus, are conventionally incorporated into evaluation schemes (Jarvie *et al.*, 2007):

Primary gas is generated by decomposition of kerogen to a highly polar bitumen and gas (1) followed by decomposition of this bitumen to oil and gas (2); decomposition of oil leads to secondary gas besides a carbon-rich coke or pyrobitumen (3).

Based on kinetic parameters calculated from laboratory pyrolysis data and assuming a fixed number of parallel first-order pseudo-reactions (or Gaussian distributions), kerogen cracking can be expected to begin at geologic temperatures exceeding 70°C where progressive subsidence has occurred (e.g. Quigley and Mackenzie, 1988; Burnham and Braun, 1990; Behar *et al.*, 1991a; Tegelaar and Noble, 1994; Jarvie and Lundell, 2001;

Dieckmann, 2005), whereas secondary cracking of unexpelled oil to gas has been suggested to begin at about 150°C and  $R_o \sim 1.2\%$  for organic-rich marine Type II source rocks (Schenk *et al.*, 1997b; Dieckmann *et al.*, 1998; Jarvie *et al.*, 2004). These findings are directly confirmed by the observation that production of unconventional gas from the Barnett Shale is only successful at maturity levels above  $R_o \sim 1.1\%$  because pore-occluding petroleum is secondarily cracked into gas and condensate (Jarvie *et al.*, 2004). It should be added here that secondary cracking of unexpelled oil is also often associated with leaner source rocks (<10 mg HC/g rock) in which oil expulsion efficiencies are low (Cooles *et al.*, 1986; Pepper and Dodd, 1995). Additionally, the close contact of retained petroleum with kerogen and source rock mineralogy may be a critical factor for gas generation kinetics, because cracking rates of crude oil in conventional siliciclastic and carbonate reservoirs were calculated to be much slower with secondary gas formation starting at higher maturity levels between  $R_o = 1.6\%$  (Waples, 2000) and  $R_o = 2.0\%$  (Horsfield *et al.*, 1992b; Schenk *et al.*, 1997a).

### ***Basics of Kinetics – the parallel reaction model***

The subsequent paragraphs closely follow the review of Schenk *et al.* (1997b) on the basic principles of kinetics of petroleum formation and cracking.

The authors state that the prerequisite for reasonable predictions from laboratory to geologic conditions is the accepted fact that in both systems generation of hydrocarbons from macromolecular organic matter is primarily related to so-called “cracking” reactions via the free radical mechanism (Rice, 1933; Kossiakoff and Rice, 1943; Greensfelder *et al.*, 1949)(see also Chapter 1.1.5). This transformation of organic matter is a time and temperature dependent process which can also be described in terms of reaction velocities or reaction rates. The determination of rate laws for the change of product and educt concentration is the task of kinetic considerations which are thought to be applicable for gas generation since Tissot (1969).

The kinetic principles represent a simplification of processes occurring under artificial or natural conditions and are based in the simplest case on the assumption that hydrocarbon generation proceeds via a unknown number of quasi-irreversible, parallel reactions identically for both systems (Tissot *et al.*, 1971). In the “defunctionalisation model”, which is mechanistically closely related to the “Cooles model”, the thermal degradation of macromolecular kerogen by the rupture of increasingly stronger bonds leads to primary, hydrogen-rich products of lower molecular weight and to a hydrogen-poor residue of increasing degree of condensation (Tissot *et al.*, 1971; Espitalié *et al.*, 1988; Mackenzie and Quigley, 1988; Schenk *et al.*, 1997b). With rising temperature primary products can be

reduced to even smaller molecules by secondary cracking processes giving gas and pyrobitumen (coke) as final products.

Since the breakdown of kerogen or oil proceeds via an unknown but very large number of single reactions, “bulk” kinetic concepts are used (reviewed by Ungerer, 1990; Schenk *et al.*, 1997b). From the parallel reaction model follows that petroleum generation can be described as a first order reaction (Pepper and Corvi, 1995a), which is the decay of one molecule (A) into two or more molecules (B+C+...) where A is the educt kerogen, oil or bitumen and B, C, etc. are products. According to the first-order rate law the rate of generation of product (conversion rate  $dm/dt$ ) is proportional to the remaining amount of educt ( $M - m$ ), where  $m$  is the mass of product generated from the initial mass  $M$  of educt at a given time  $t$ :

$$dm/dt = k (M - m) \quad (2)$$

To quantify the strong temperature dependence of the reaction rate  $k$ , the semi-empirical Arrhenius law is applied which involves an activation energy or potential barrier between educt and product compounds that must be overcome during a chemical reaction (Schenk *et al.*, 1997b):

$$k(T) = A * e^{-E/(RT)} \quad (3)$$

Here,  $T$  is the absolute temperature in Kelvin;  $E$  is the activation energy of the reaction (J/mol or cal/mol; kcal/mol is used in the thesis for comparison with values from literature), and  $R$  is the gas constant (in  $J\ mol^{-1}\ K^{-1}$  or  $cal\ mol^{-1}\ K^{-1}$ ). In a reaction following a first-order kinetic rate law, as considered here, the pre exponential factor  $A$  has the dimension of a frequency ( $s^{-1}$ ) and is therefore termed frequency factor. A further development is the determination of the temperature dependence of the frequency factor  $A$  in the transition state theory, but, for the case of petroleum formation, pyrolysis based measurements are not accurate enough for such evaluations (Schenk *et al.*, 1997b).  $A$  and  $E$  are properties of a specific reactant and can be related to the degree of the vibration frequency of an “activated complex” (Polanyi and Wigner, 1928), an intermediate molecular species formed in the transition of the reaction, which in return describes the strength of a molecular bond, at least for a theoretical treatment of homogeneous gases. In view of the very complex reaction kinetics during pyrolysis Schaefer *et al.* (1990) believed that this factor is merely a mathematical optimisation parameter without a direct relation to molecular vibration frequencies. The factor  $RT$  is a

measure of the thermal energy of the system at a given temperature  $T$ . Thus, a rate constant  $k$  will be small, i.e. the reaction will proceed slowly, if the temperature is low and the activation energy high.

To investigate the temperature dependence of reaction rates for geological predictions, kinetic experiments can be performed isothermally at different temperatures or non-isothermally at a constant heating rate ( $r = dT/dt$ ). The advantage of the non-isothermal approach is that it comprises a better similarity to gradual heating of source rocks during subsidence in sedimentary basins (Schenk *et al.*, 1997b) and that a single experiment with a linear heating rate yields the activation energy and frequency factor of a given reaction. Conventionally, however, three heating rates differing by one or two orders of magnitude are used for geochemical characterisations because a reasonable starting value of  $A$  can be derived from the shift of peak generation temperatures for discrete models using only one single frequency factor for the “bulk”-reaction during generation of hydrocarbons (van Heek and Jüntgen, 1968; Ungerer and Pelet, 1987; Burnham *et al.*, 1988; Schaefer *et al.*, 1990). The generation rate as a function of temperature (generation curve) is:

$$dm/dT = dm/dt * dt/dT = dm/dt * 1/r \quad (4)$$

Combination of equations (2), (3), and (4) yields the generation rate at a given time  $t$ :

$$dm/dT = A/r * e^{-E/(RT)} * (M - m) \quad (5)$$

Upon integration one obtains the function for a non-isothermal generation curve for a first-order reaction:

$$\begin{aligned} \frac{dm}{dT} &= M \frac{A}{r} \exp\left(-\frac{E}{RT} - \frac{A}{r} J\right) \\ J &= \int_{T_0}^T \exp\left(-\frac{E}{RT}\right) dT \end{aligned} \quad (6)$$

As previously mentioned, the transformation of kerogen into petroleum cannot be exactly described in terms of individual precursor (kerogen) – product (petroleum) relationships on a molecular level, as both entities are far from chemically well-defined and highly complex (Burlingame *et al.*, 1969; Yen, 1974; Oberlin *et al.*, 1980; Behar and

Vandenbroucke, 1987). Thus, single molecular precursors for liquid and gaseous compounds are replaced by co-called bulk petroleum or “gross” hydrocarbon potentials  $M_i$  which are fractions of total product yields (Tissot and Espitalié, 1975). It is assumed that during natural and artificial maturation these potentials are more or less simultaneously transformed into the product petroleum by a certain number of  $n$  parallel “pseudo-reactions” kinetically defined by a reaction order and a rate constant  $k_i$ . Although the continuous Gaussian model involves less free parameters, the discrete model (Tissot and Espitalié, 1975) is generally preferred, at least for Type III kerogens that require a dissymmetric distribution of activation energies (Schenk *et al.*, 1997b). The assumption that all of these reactions can be described by first-order kinetics (van Krevelen *et al.*, 1951; Pitt, 1961; Jüntgen, 1964; Jüntgen and Klein, 1975; Jüntgen, 1984) is another simplification only by taking into account that organic material cracks by a chain reaction mechanism via free radicals including initiation, propagation and termination, all reactions with different reaction-orders (Ungerer, 1990). Nevertheless, it could be shown that hydrocarbon generation in sedimentary basins can be satisfactorily described as a unimolecular decay of organic matter (Tissot, 1969; Tissot *et al.*, 1971; Quigley *et al.*, 1987; Ungerer and Pelet, 1987) and is therefore characterised by first-order kinetics. Thus the rate  $dM/dt$  of bulk petroleum generation is:

$$\frac{dm}{dT} = \sum_{i=1}^n k_i \cdot (M_i - m_i) \quad (7)$$

with  $m_i$  being the fraction of partial bulk petroleum potential  $M_i$  which is already transformed into petroleum at time  $t$ . Assuming a linear heating rate ( $r = dT/dt$ ) and for practical computing reasons a single pre exponential factor  $A$  for all parallel reactions, the integration of equation (7) yields the temperature-related rate  $dM/dt$  of bulk petroleum generation as a function of temperature  $T$ :

$$\begin{aligned} \frac{dM}{dT} &= \sum_{i=1}^n M_i \frac{A}{r} \exp\left(-\frac{E_i}{RT} - \frac{A}{r} J_i\right) \\ J_i &= \int_0^T \exp\left(-\frac{E_i}{RT}\right) dT \end{aligned} \quad (8).$$

### ***Limitations of the parallel reaction model***

The main disadvantage of the parallel model is of course its simplistic approach by assuming that, besides a separation of at least 9 orders of magnitude in heating rates, high-temperature, and short-time artificially induced maturation reactions follow the same parallel model than low temperature, long-time natural maturation reactions. Two main aspects of natural organic matter evolution are not covered by applying the kinetics of a parallel reaction model. The first one is the difference in bulk composition of products generated under laboratory and natural conditions (Larter and Horsfield, 1993; Horsfield, 1997), and the second one is, in close analogy to the limitations of the “Cooles model” (Chapter 1.1.4), the occurrence of retrogressive, i.e., second-order coupling reactions often observed during natural maturation of heterogeneous, terrigenous Type III coal (Stach *et al.*, 1982; Solomon *et al.*, 1988; Hatcher *et al.*, 1992; Horsfield, 1997; Schenk and Horsfield, 1998; Payne and Ortoleva, 2001; Wilkins and George, 2002; McMillen and Malhotra, 2006).

The first aspect is related to the observation that the thermal decomposition of organic matter does not proceed via a parallel defunctionalisation but rather via successive depolymerisation. Here kerogen first cracks to highly polar bitumen ( $K \rightarrow B$ ) which then cracks to yield hydrocarbon-rich oil ( $B \rightarrow O$ ). The  $K \rightarrow B$  reaction is rate limiting at geologic heating rates (Braun and Rothman, 1975) whereas the  $B \rightarrow O$  reaction is rate limiting under laboratory heating rates (Larter and Horsfield, 1993; Horsfield, 1997). Thus and irrespective of kerogen type, natural petroleum is rich in hydrocarbons and laboratory pyrolysates are rich in polar compounds, bitumen. Nevertheless, the kinetic parameters describing these two thermal degradation reactions were shown to be closely similar using a parallel reaction model, at least in the case of rather homogeneous, marine organic matter and related petroleum systems (Quigley *et al.*, 1987; Ungerer and Pelet, 1987; Braun and Burnham, 1992; Larter and Horsfield, 1993; Pepper and Corvi, 1995b; Schenk and Horsfield, 1998). Thus, implications are more extensive for the prediction of petroleum composition than for the determination of „bulk” kinetic parameters (therefore discussion in Sub-Chapter 1.1.7).

Concerning the second aspect of short-comings of the parallel reaction model, Schenk and Horsfield (1998) outlined that extrapolation of petroleum formation to geologic heating conditions using laboratory-derived kinetic parameters is not valid for all types of kerogens. They demonstrated using non-isothermal, Rock-Eval like pyrolysis that generation rate curves of naturally and artificially matured marine Type II Toarcian shales remained always within the original envelope defined by the least mature sample (Fig. 1.1). A constant decrease in generation potentials and an increase in  $T_{\max}$ -values with increasing maturity indicated that

both natural and artificial maturation proceed through the release of hydrocarbons by the homolytic cracking of first weak and then stronger bonded labile kerogen. In contrast, formation rate curves of a natural Carboniferous coal series were shown to not follow the previously described concept by extending beyond the envelope defined by the least mature sample (Fig. 1.1). Therefore, natural maturation must have led to stabilisation of the macromolecular network by formation of new potentials with higher activation energies, which was attributed to solid-state aromatisation reactions competing with product generation during natural coalification. This reaction mechanism could not be simulated for low rank samples under open nor closed artificial maturation conditions, therefore marking kinetic predictions of petroleum generation from vitrinitic coals not reliable.

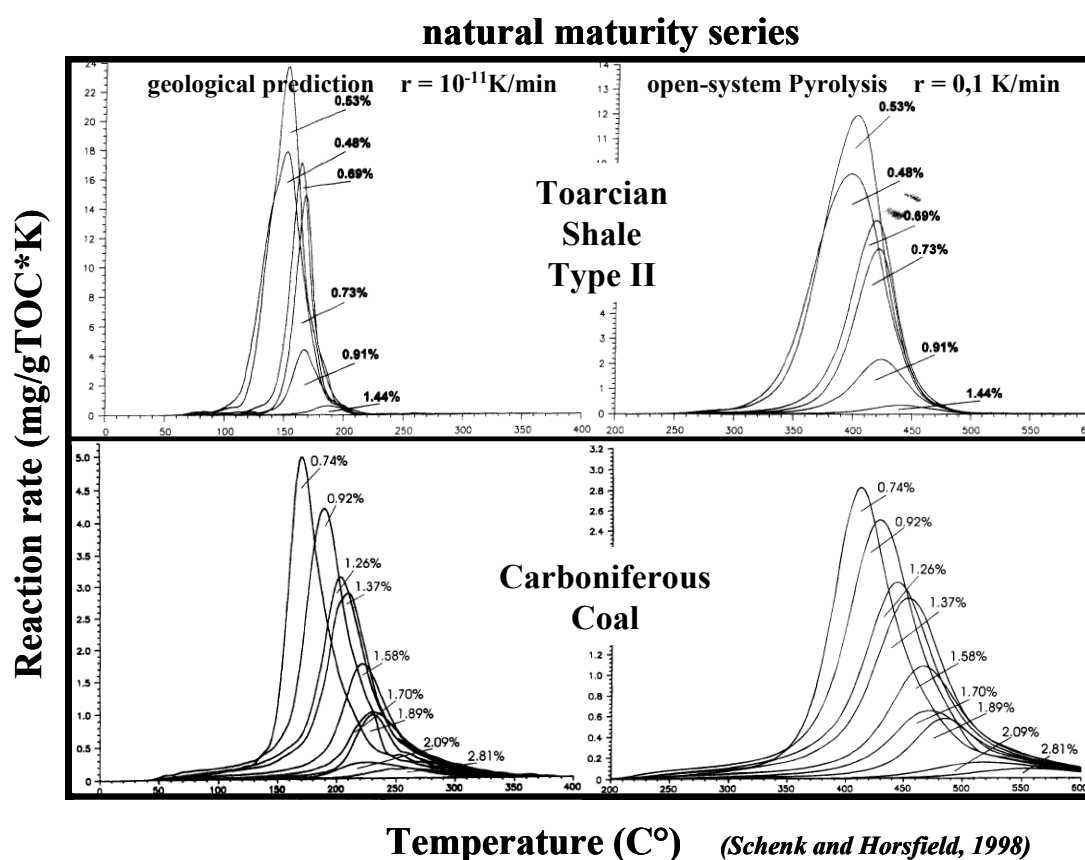


Figure 1.1: Bulk hydrocarbon reaction rate curves for samples of increasing natural maturation (given in % vitrinite reflectance) for laboratory and geologic heating rates; Toarcian Shale and Westphalian Coals. Modified after Schenk and Horsfield (1998)

### 1.1.7 Predicting the Composition of Petroleum

#### *Heating rate dependency*

Besides the determination of petroleum masses generated throughout geologic history of a sedimentary basin, it is fundamental for an explorationist to define petroleum



composition (GOR, gas wetness) for the prediction of saturation pressure  $P_{\text{sat}}$  and hence phase behaviour during petroleum generation and migration (di Primio and Skeie, 2004; di Primio and Horsfield, 2006). Sadly, this is made difficult by the difference in bulk composition of products generated under high-temperature laboratory and low-temperature natural conditions induced by a heating rate dependency of the involved reactions. The bulk composition of unaltered natural petroleum is fundamentally different to that of kerogen pyrolysate irrespective of crude oil class, kerogen type or analytical configuration (Larter and Horsfield, 1993; Horsfield, 1997). Crude oils are hydrocarbon-rich systems whereas pyrolysates from either hydrous or anhydrous open and closed systems contain a much higher proportion of polar compounds (Urov, 1980; Castelli *et al.*, 1990), which are heteroatomic compounds of high molecular weight, also called NSO's. Additionally, a systematic difference in detailed gas composition, i.e. too high ethane and propane contents and simultaneously rather low methane contents (too high gas wetness) of closed-system pyrolysates compared to natural fluids (Javaid, 2000), could be evidenced (di Primio and Skeie, 2004; di Primio and Horsfield, 2006), even though GORs correlate very well with natural fluid GORs during artificial closed-system (MSSV) maturation (Dueppenbecker and Horsfield, 1990; Erdmann, 1999; Santamaria-Orozco and Horsfield, 2004).

Lewan (1985; 1993) suggested that under hydrous pyrolysis conditions kerogen first decomposes into “tarry soluble bitumen” which is subsequently cracked into hydrocarbon rich oil. His interpretation only confirms previous models of Fitzgerald and Van Krevelen (1959) for coal, and Tissot (1969) and Ishiwatari *et al.* (1977) for kerogen, in which the NSO's (mesophase in Fitzgerald and Van Krevelen (1959)) are primary products of kerogen decomposition and the hydrocarbons are generated from cracking of these. Nevertheless, it should be noted that this two step concept was already observed in the oil shale retorting experiments of the early 1900s (McKee and Lyder, 1921; Franks and Goodier, 1922; Maier and Zimmerly, 1924) through the mid-1900s (Hubbard *et al.*, 1948; Cummins and Robinson, 1972). Such a successive reaction scheme valid for oil and gas generation can, after Ungerer (1990), be termed “depolymerisation model”, in contrast to the “defunctionalisation model”, in which oil and gas are released by rupture of increasingly tighter bonds corresponding to kinetic models with parallel independent reactions (Pitt, 1961; Jüntgen and Klein, 1975; Tissot and Espitalié, 1975; Braun and Burnham, 1987 *etc.*) or algebraic schemes as proposed by Cooles *et al.* (1986). The heating rate dependency of this two step concept ( $K \rightarrow B$ ,  $B \rightarrow O$ ) leads to the difference in natural vs. artificial product compositions.

In close relation, Burnham and Happe (1984) published a fundamental advance in understanding pyrolysis mechanisms and linked their observations mainly to the applied laboratory heating rates. Slow heating rates caused heteroaromatic compounds in the oil to be converted to coke. Pyrolysis of Green River Oil shale in a self-generated atmosphere yielded less oil and more gas and carbonaceous residue for decreasing heating rates and increasing pressure. Additionally, the oil became more paraffinic and less aromatic and olefinic. The pyrolysis mechanism proposed by Fausett and Miknis (1981) who considered kerogen pyrolysis simply to be a conversion of most of the aliphatic carbon to oil and a conversion of most of the aromatic carbon to carbon residue or only in minor amounts to aromatic oil which gives rise to coke, was therefore demonstrated to be too simple. Furthermore, Burnham and Happe (1984) found that in the absence of high-pressure hydrogen, the total amount of aromatic carbon in the products (oil and retorted shale) is nearly twice as high as in the raw shale, thus additional aromatic carbon is formed under most pyrolysis conditions which is accumulated preferentially in the carbonaceous residue (coke) with decreasing heating rates. In high-pressure hydrogen (Hershkowitz *et al.*, 1983), there is only a slight net increase in the total amount of aromatic carbon during pyrolysis, and most of the aromatic carbon of the products is in the oil. These results imply that hydrogen pressure inhibits both the formation of additional aromatic carbon during pyrolysis and the coking of aromatic oil. Variations of heating rate and the presence or absence of hydrogen therefore affect the distribution of aromatic carbon between oil and carbonaceous residue.

### ***Second-order recombination reactions in shales***

The difference between natural and artificial product compositions can also be induced by retention or recombination reactions only occurring under geological maturation conditions. For instance, certain C<sub>6+</sub> liquid components or bitumen from the previously discussed depolymerisation process are incorporated into the macromolecular structure during natural coalification (Schenk and Horsfield, 1998) but are detected as cracking products (bitumen) upon pyrolysis (Espitalié *et al.*, 1988; Forbes *et al.*, 1991).

The molecular composition of the bitumen intermediate might dictate whether the cracking pathway prevails, as proposed for most marine Type II source rocks, or whether the recombination reactions pathway predominates, as proposed for many terrestrial derived source rocks explaining regularly encountered problems when predicting petroleum composition as well as timing of product generation from heterogeneous Type III shales and coals. E.g., Erdmann and Horsfield (2006) and Dieckmann *et al.* (2006) demonstrated for mixed marine-terrestrial Type III kerogens that second-order recombination reactions

between first formed bitumen and residual kerogen lead to the neoformation of a refractory, insoluble solid bitumen or recombination structure at low thermal maturation levels. This could not be demonstrated for homogeneous Type I and Type II kerogens of aquatic origin which are predominantly aliphatic in composition. The authors stated that for the latter degradation proceeds most likely over one of successive cracking reactions in nature which is possible to simulate by standard laboratory pyrolysis. In contrast and because terrigenous influenced kerogen is more aromatic and phenolic in character (Larter and Senftle, 1985; Horsfield, 1989), its transformation pathway may involve more recombination reactions which might not be completely simulatable under the same laboratory conditions, marking kinetic evaluations and compositional predictions based on immature sample equivalents as invalid.

In a related context and indicating the importance of oxygen compounds for recombination reactions, Monin *et al.* (1980 and references therein) already noticed that as the initial material becomes more oxygen-rich (Type III organic matter of terrestrial and humic origin) the artificial behaviour of solid residue is less and less comparable to natural behaviour. In such a case, the H/C atomic ratios of the solid residues decrease too early, and the O/C atomic ratios stay abnormally high.

Michels *et al.* (1996) also hinted to the importance of the composition of bitumen which should not be viewed as a simple intermediate between kerogen and hydrocarbons during oil generation, but as an active participant to the chemical reactions involved in maturation. During the main stage of bitumen generation, a great part of the initial oil potential is transferred to the polars (Michels *et al.*, 2000). The polars, which are a source of hydronaphthalenics e.g. in Dammar Resin in the case of Mahakam Coal, appear to be a significant source of hydrogen available to organic reactions inhibiting cross-linking of the coal structure and formation of gas at later maturity stages. The importance of naphthenic structures should not be underestimated as their aromatization is a way of hydrogen transfer to other structures, through hydrogen-donor reactions (Behar and Pelet, 1988).

### ***Second-order recombination reactions in coals***

In coals, recombination or retrograde reactions between bitumen and residual organic matter are already known for a long time.

According to Levine (1993), in part based on earlier articles of Given (1984), the organic matter or non-mineral constituents of coal can be conceptually divided into two categories comparable to the terms kerogen and bitumen. He defines a macromolecular matrix fraction, comprised of a complex, three dimensional, cross-linked, aromatic carbon-rich

network structure, and a molecular fraction (mobile phase in e.g. Given, 1984; Lin *et al.*, 1986; Mansuy *et al.*, 1995; Michels *et al.*, 2000; Vu *et al.*, 2008) comprised of lower molecular weight constituents that are either loosely bonded or physically entrapped within the coal structure. The molecular fraction represents a compositional continuum, ranging from H<sub>2</sub>O, CH<sub>4</sub> and CO<sub>2</sub> at the light end to high molecular weight asphaltic materials at the heavy end that are similar in composition and structure to the matrix.

The important concept in Levine's model (Levine, 1993) is that not all the molecular products formed by depolymerisation of the macromolecular fraction escape from the coal structure, either as first-formed products or secondary lower molecular weight cracking products, but partly repolymerise with the matrix component by second order reactions via recombination or condensation reactions. Moreover, all processes (depolymerisation, cracking of molecular fraction, repolymerisation) can directly form small, relatively mobile, volatile and thus expellable by-products, e.g. H<sub>2</sub>O, CO<sub>2</sub>, CH<sub>4</sub>, during coalification. One interesting observation is that, during the classic oil window up to R<sub>o</sub> ~ 1.0%, depolymerisation leads to an enrichment of the molecular fraction within the coal structure. Increasing HI and BI values also occur throughout high volatile bituminous coal ranks of e.g. New Zealand Coals (Sykes and Snowdon, 2002). Hence, oil-like substances are formed but do not leave the coal since the H/C ratio stays relatively constant in contrast to a decreasing O/C ratio, meaning that during depolymerisation or bituminisation stage mainly gaseous, oxygenated compounds are expelled (first maturation stage in Durand and Monin, 1980). From now on molecular products are destroyed by cracking or polymerisation reactions (debituminisation) and the newly formed mobile products are partly expelled as mirrored by a decrease in the H/C ratios during end of high volatile bituminous coal ranks through medium and low volatile bituminous coal ranks. At the transition from bituminisation to debituminisation many physicochemical properties of coal pass through maximum or minimum values. Maximised values can be seen in the case of solvent extract yields (Teichmüller, 1989; Haenel, 1992; Van Krevelen, 1993; Stout and Emsbo-Mattingly, 2008), mean molecular weight of pyridine extracts, Rock-Eval S1 and S2 yields, liquefaction yields, fluidity on melting, intensity of secondary vitrinite fluorescence, volume-% of secondary fluorescent macerals. Minimal values are reached for the internal surface area, porosity, and density of the coal. Levine (1993) further states that the molecular fraction may participate actively in coalification reactions as free hydrocarbons or water could deactivate free radicals formed by the proposed depolymerisation, cracking and repolymerisation reactions.

## ***1.2 Research Perspectives and Objectives***

### **1.2.1 Overall Goal: Constrain Mechanisms of Late Gas Generation**

The main topic of this thesis is the thermally driven generation of methane from deeply buried, mature kerogen in petroleum source rocks of different geographical and depositional origin. The assessment of timing, i.e. kinetics, and amount of this late dry gas formation is the overall goal of the work as related mechanisms are still only poorly constrained. The main problem is that kitchen areas, where the late gas is formed, are seldomly drilled inhibiting the direct quantification of gas generated. Thus, predictions rely on artificial maturation experiments in the laboratory under either open or closed pyrolysis conditions, or, based on analytical data, on structural modelling with which kerogen degradation and product yields can be calculated using mechanistic numerical models (e.g. chemical structure-chemical yield modelling published in Freund *et al.*, 2007; Walters *et al.*, 2007). Published pyrolysis data with the focus on late gas generation, i.e. methane, is scarce and results vary strongly concerning temperature limits, amounts, kerogen types and pyrolytic set-ups.

#### ***Status Quo - Late Gas Generation***

Applying the “defunctionalisation model” of Cooles *et al.* (1986), Quigley *et al.* (1987) and Quigley and Mackenzie (1988) calculated that late gas is formed by the breakdown of refractory organic matter in the temperature range 150 – 220°C for geological heating rates between 1 and 10°C/ma, using immature North-West European Type III Westphalian Coals as a refractory kerogen calibrant and bulk-flow pyrolysis at a single heating rate. For modeling they assumed a set of first-order parallel reactions, whereas for each reaction, the gas potential was a function of the activation energy, following a Gaussian distribution law. For the natural maturity series itself, Cooles *et al.* (1986) assessed petroleum generation (gas from refractory organic matter) to take place between 180 and 250°C. These authors considered late methane mostly as a specific product of the thermal decomposition of Type III coals.

Other open-pyrolysis based artificial maturation experiments performed on an immature Type I Green River Shale (Campbell *et al.*, 1980; Huss and Burnham, 1982; Burnham and Happe, 1984) clearly showed that 55-86% of the total generated methane stemmed from mature kerogen hinting to the existence of late gas potentials even for source rocks exclusively composed of “labile” organic matter. However, although using the similar

reaction network model as Quigley and Mackenzie (1988), obtained kinetic parameters were rather different leading to vastly diverging kerogen conversion temperatures and rates under laboratory and geological conditions. For geologic conditions late methane generation would start at unrealistic temperatures well below the classic oil window ( $< 80^{\circ}\text{C}$ ) and come to an end around  $240^{\circ}\text{C}$ .

Behar *et al.* (1992; Behar *et al.*, 1995; Behar *et al.*, 1997) qualitatively confirmed the existence of a late gas potential for source material other than of Type III origin and calculated, using a mass balance approach and a single first-order reaction for kinetic modelling, that similar absolute quantities of methane,  $\sim 50$  mg/g TOC, can be expected to be generated late from residual organic matter at high geologic temperatures between  $200$  and  $230^{\circ}\text{C}$ . Immature kerogens of Type I, II, II-S, and III, exhibiting diagenetic levels corresponding to the beginning of the oil window, were artificially matured under open and confined pyrolysis conditions. They observed a systematic underestimation of late production of methane in compositional Rock-Eval type pyrolysis compared to closed system pyrolysis and concluded that this underestimation is partly due to a too low final temperature but also to competitive formation of methane and molecular hydrogen, as shown by previous comparisons with TG-FTIR results (Behar *et al.*, 1995). Even though differences in  $\text{C}_{2+}$  production were also observed and explained by re-condensation via cross-linking in the closed system of asphaltene-like structures, which would be flushed away in the open-system, this process was not considered to be crucial for the underestimation of late methane under open pyrolysis conditions.

In contrast, Erdmann and Horsfield (2006) claimed recombination reactions between these first formed high molecular weight compounds and residual organic matter, only detectable during non-isothermal closed-system pyrolysis, to be responsible for the formation of a thermally stabilised macromolecular moiety whose late gas precursor structures are cracked via the  $\alpha$  cleavage of methyl groups for geological heating rates at very high temperatures well in excess of  $200^{\circ}\text{C}$  ( $T_{\text{max}}$  approx.  $250^{\circ}\text{C}$ ). Erdmann (1999) calculated for this secondary late gas generation a maximum amount of  $13$  mg/g sample which equals  $\sim 40$  mg/g TOC. Nevertheless, the corresponding late gas forming mechanism was only found to be detectable for an immature mixed marine–terrigeneous Type III kerogen Heather Fm. sample but not for an immature liptinitic Type II kerogen Draupne Fm. sample. Thus, the chemical characteristic of the bitumen-intermediate, influenced by the starting composition of the organic matter type, was thought to have an effect on the late gas potential formation. Recombination of previously formed hydrocarbons with residual kerogen or coal through

aromatisation or polycondensation reactions was also used as a best explanation for the late gas potential formation of an immature sample from the Type III Taglu Sequence (Canada, Mackenzie Delta) during closed-system (MSSV)-pyrolysis in a study of Dieckmann *et al.* (2006). The gas formed from this type of rearranged organic matter shifts the bottom of the late gas window to extreme temperatures which are  $\sim 90^{\circ}\text{C}$  higher than those proposed from open system maturation, i.e.  $325^{\circ}\text{C}$  instead of  $230^{\circ}\text{C}$  for a geological heating rate of  $3.3^{\circ}\text{C/ma}$ .

To minimize the uncertainties concerning oil compound secondary cracking or the previously discussed bitumen interaction effects within confined conditions on the kinetic evaluation of late methane generation, Lorant and Behar (2002) performed open- and closed-system pyrolysis experiments on naturally matured Type II and Type III organic matter at the transition between the catagenesis and the metagenesis zones ( $R_o > 1.3\%$ ;  $\text{H/C} < 0.65$ ). Late methane production was calculated to proceed after conditions of peak oil generation, between  $160^{\circ}\text{C}$  and up to  $240^{\circ}\text{C}$ , by degradation of mature kerogen firstly by decomposition of short chain alkylated polyaromatics and diarenylalkanes together with wet gas and secondly by demethylation. Each reaction was modelled independently using a first-order rate law. However, differences in the generation of methane were observed for the Type II and Type III kerogen samples, as well as for closed vs. open pyrolysis conditions. The Type III sample generated globally more methane than the Type II sample, and the bulk rate of methane formation was higher in the Type II compared to the Type III mature kerogen. This was interpreted in terms of structural disparities between these two samples. Coal possesses more alkylated precursors than Type II, although similar bulk analytical fingerprints (e.g.,  $R_o$ ,  $\text{H/C}$  and  $\text{O/C}$  ratios,  $T_{\text{max}}$ ,  $f_a$ ) pointed to a similar maturity stage. It should be noted here though that  $\text{HI}$  was about three times higher for the Brent Coal sample ( $122 \text{ mg HC/g TOC}$ ) than for the Toarcian shale from the Hils syncline ( $44 \text{ mg HC/g TOC}$ ). Differences between the two chosen pyrolysis conditions were that the amount of methane recovered in open-system experiments was 2 to 3 times lower compared to closed-system experiments. Moreover, the kinetic model calibrated on closed-system data did not account for the rate of methane generation in the open system. These discrepancies were explained to be related to the modes of oxygen and hydrogen consumption during early pyrolysis stages of these mature kerogen;  $\text{H}_2\text{O}$  production under open-system conditions vs.  $\text{CO}_2$  production under closed-system conditions.

Another important observation in the experiments of Lorant and Behar (2002) was that ongoing methane generation at isothermal pyrolysis temperatures exceeding  $500^{\circ}\text{C}$  was

advocated to autohydrogenation of the remaining pyrolysis residue through ring opening of the aromatic network due to increasingly high H<sub>2</sub> partial pressure within the sealed gold tubes. Such a mechanism was previously suggested by Lorant *et al.* (2000) who pyrolysed methylated aromatic model compounds, and has also been invoked earlier in kerogen maturation studies, for example Fitzgerald and Van Krevelen (1959). Generation of this very late methane under geological conditions was thought to be unlikely, as geologic temperatures are not high enough to allow for significant H<sub>2</sub> generation. Moreover, the diffusion capacity of hydrogen being high, it is unlikely to remain in contact with the sedimentary organic matter long enough to interact with it. On the other hand, Sackett (1995) stated that the permeability of quartz glass, which was used for the high temperature MSSV pyrolysis experiments within the present study as well as in the studies of Erdmann and Horsfield (2006) and Dieckmann *et al.* (2006), needs to be considered, as hydrogen diffuses through the quartz glass as fast as it is formed and H<sub>2</sub> partial pressure might not increase enough to allow for autohydrogenation.

Therefore, mechanisms of late gas/methane generation as well as the kinetic parameters describing the formation process are not yet constrained. It is not fully clear, i.e. results vary, which source rocks generate late gas and which do not, and if they do, why and when. The overall goal of this thesis is to at least shed some light on these topics.



### 1.2.2 Inherent fundamental questions

For a reliable, valid kinetic evaluation of late gas generation, key questions have to be solved. The first key question is:

- “Which types of source rocks possess a late gas potential in general?” It is not clear yet, which source rocks generate late gas and which do not. Erdmann and Horsfield (2006) and Dieckmann *et al.* (2006) could evidence for only 2 single heterogeneous-aromatic/phenolic source rocks a late gas potential whereas e.g. Behar (Behar *et al.*, 1992; Behar *et al.*, 1995; Behar *et al.*, 1997) claimed, as well using only single samples, a late gas potential to be present for all kerogen types (discussed in Sub-Chapter 1.2.1).

The second key question is:

- “Which molecular compositional changes of initial kerogen structure and early formed bitumen might be involved?” As Erdmann and Horsfield (2006) and Dieckmann *et al.* (2006) demonstrated, second-order reactions between first formed bitumen and residual organic matter might be involved or might even be a prerequisite for the development of a late gas potential during natural and artificial maturation. Here, the chemical and structural composition of the initial organic matter and therefore of the generated bitumen intermediate is claimed to be the key controlling factor. Nevertheless, the initial organic matter composition alone could be ascribed a limiting role when thinking of the “defunctionalisation model” and the concept of a refractory kerogen moiety according to Cooles *et al.* (1986), Quigley *et al.* (1987) and Quigley and Mackenzie (1988)(discussed in Sub-Chapter 1.2.1). Therefore, this key question includes the question “What is the late gas generation mechanism?”

The third key question is:

- “How are these changes manifested in kinetic parameters and stable isotopic compositions?” This question is pretty much self-evident and related to the concern that kinetic or isotopic data, assessed using immature source rock equivalents under laboratory conditions, might be invalid for the prediction of hydrocarbon generation or composition under geologic conditions and higher maturities as demonstrated for naturally and artificially matured Carboniferous coals (Schenk and Horsfield, 1998).

### ***1.3 Detailed Approach***

The detailed approach for unravelling mechanisms of late gas generation and its kinetic and isotopic parameters is described in the following and orientated on the inherent fundamental questions (Sub-Chapter 1.2.2) to be solved. In general, open-system pyrolysis is applied within this work to gain basic information on the kerogen type, structure and maturity of organic matter within source rocks (Horsfield *et al.*, 1983; Larter, 1984; Horsfield, 1989; Eglinton *et al.*, 1990). Closed-system Micro-Scale-Sealed-Vessel (MSSV)-pyrolysis (Horsfield *et al.*, 1989) is used to simulate natural maturation and petroleum formation as well as to allow for secondary cracking or second-order recombination reactions to occur. Kinetic parameters of late gas generation and isotopic gas composition are determined using MSSV-pyrolysis.

First of all, there will be a short discussion on the general choice of experimental method, i.e. the suitability of pyrolysis for petroleum generation simulation. Furthermore, the usage of MSSV-pyrolysis instead of other pyrolytic set-ups will be justified.

#### ***Suitability of Pyrolysis for Petroleum Generation Simulation***

In natural systems it is never possible to quantify directly the amount of gas generated with increasing depth of burial because either the volatile compounds have already migrated or loss of gas may occur when sampling (Price, 1989; Horsfield, 1997). Thus, the only way to follow the complete generation of both gas and oil for sedimentary organic matter is to perform artificial maturation experiments in the laboratory under either open or closed pyrolysis conditions (Espitalié *et al.*, 1985; Espitalié *et al.*, 1988; Ungerer *et al.*, 1988; Horsfield, 1989; Horsfield *et al.*, 1989; Ungerer, 1990; Lewan, 1994).

The term pyrolysis has been defined as “a chemical degradation reaction that is induced by energy alone” (Ericsson and Lattimer, 1989). Here, open-system pyrolysis simulates a source rock from which the degradation products are immediately expelled and closed-system pyrolysis is expected to simulate a source rock that does not expel hydrocarbons (Ungerer *et al.*, 1988). MSSV-pyrolysis can be viewed as simulating a source rock expelling volatiles into a vapour phase, which nevertheless remain in a quasi-closed system (Carr *et al.*, 2009). In geological conditions, natural source rocks are likely to be closed or quasi-closed systems for the following reasons: the very low motion rates of fluids through sediments, a possible saturation threshold before hydrocarbon expulsion and the possible retention of a part of the mobile phase either on the minerals or inside the kerogen

network (Behar *et al.*, 1995). Furthermore and caused by saturation of free radicals within first-formed products by hydrogen abstraction and transfer from the kerogen structure in closed-systems, closed-system pyrolysis products resemble natural crude oils more closely than open-system pyrolysis products in that *n*-alkenes are not major constituents.

One should keep in mind though that a completely accurate simulation of molecular processes occurring under geologic conditions will not be possible using pyrolysis methods as reactions taking place at temperatures from ~250 to 650°C in the laboratory are extrapolated to ~100 to 170°C, spanning rates that differ by ~14 orders of magnitude. Walters *et al.* (2007) state that reactions in both temperature regimes are known which are not identical. Furthermore, and even though closed-system pyrolysis can be viewed as the better „simulation” method as metastable products which might undergo secondary cracking are not flushed away, it is often very difficult to resolve whether the measured products evolve directly from kerogen decomposition or from the thermal cracking of confined products that are not normally retained in a natural environment. All laboratory simulations fail to account accurately for the true retention and removal of products as kerogen matures under geologic conditions. To overcome this problem, recently very sophisticated, statistically relevant chemical structure models are build based on advanced solid state analysis with which kerogen degradation and product yields can be calculated for a wide range of temperatures and rates using mechanistic numerical models (e.g. chemical structure-chemical yield modelling published in Freund *et al.*, 2007; Walters *et al.*, 2007). Based on first principles the amounts and composition of products resulting from the thermal decomposition of a solid complex carbonaceous material can be modelled. Nevertheless, and although these models already captured a significant portion of the thermal reaction mechanisms and pathways (primarily free radical reaction mechanism pathways) that occur under laboratory as well as natural conditions, these models are only statistical approximations and have to be calibrated against laboratory pyrolysis data. As high temperature pyrolysis data (600 – 800°C at slow heating rates usually <5°C/min) generally is very scarce, the present thesis will not only help to gain a better understanding of the late gas generation process itself but also to fix a “data hole”.

### ***Open-System Pyrolysis GC-FID as a Kerogen Typing Tool***

Even though open-system pyrolysis simulates natural maturation of organic matter less closely than closed-system pyrolysis, it is a great tool to gain general information on the kerogen type, structure and maturity (Horsfield *et al.*, 1983; Larter, 1984; Horsfield, 1989; Eglinton *et al.*, 1990). Horsfield (1997) stated in a review article that the overall pyrolysate

composition is qualitatively similar to the parent kerogen structure and that this composition in turn determines the amount of hydrocarbons likely to be expelled under natural conditions, as chain length or boiling point distributions of the products govern the physical state of the petroleum. This strongly refines the simple Rock-Eval (S2) bulk hydrocarbon generation potential evaluation approach (Horsfield *et al.*, 1983). On the premise that kerogen composition directly controls the types and yields of volatile products generated during natural maturation, it can be further concluded that the abundance and distribution of resolved pyrolysis products give information about the bulk compositions of natural petroleum, such as paraffinicity and aromaticity (Horsfield, 1997).

The most commonly occurring major identifiable compounds formed by thermal degradation of certain precursors in the kerogen structure and seen by pyrolysis-GC are aliphatic hydrocarbons such as normal alk-1-enes and alkanes, aromatic hydrocarbons such as alkylbenzenes and alkylnaphthalenes, and other aromatic compounds such as alkylphenols as well as alkylthiophenes (Horsfield, 1997). A remarkable overlap of atomic H/C ratios versus aromaticity determined using  $^{13}\text{C}$  NMR spectroscopy and aromaticity determined using relative proportions of major aromatic and aliphatic compounds in high temperature pyrolysates (Horsfield, 1989) provides firm evidence that structural information of the kerogen *in toto* is contained within the readily identifiable, GC-amenable pyrolysis products. In addition, Larter and Horsfield (1993) have demonstrated that the alkylphenol content of Carboniferous coal pyrolysates in the United States is directly proportional to the hydroxyl oxygen content determined by wet chemical methods (Yarab *et al.*, 1979; Senftle *et al.*, 1986), pointing to phenolic structures in pyrolysates being proportionally representative of oxygen-substituted benzoid structures in kerogens. Similarly, Eglinton *et al.* (1990) have shown that the relative abundance of alkylthiophenes versus aromatic plus aliphatic hydrocarbons were proportional to the atomic S/C ratio, suggesting that pyrolytic sulphur species are proportionally representative of kerogen-bond-sulphur molecules. However, it should be mentioned here that the specific alkylthiophenes identified in the pyrolysate do not occur in natural petroleum systems and might rather be released as long-chain thiophenes due to lower temperatures and longer reaction times under geological conditions (Sinninghe Damsté *et al.*, 1990; Dieckmann *et al.*, 2000a). The presence of sulphur-containing groups also has a strong impact on hydrocarbon generation profile characteristics (Tegelaar and Noble, 1994). Sulphur, if part of the kerogen structure is thought to decrease the thermal stability of the macromolecular matter (Orr, 1986), which leads, in extreme cases, to early

generation of a low API gravity, sulphur- and asphaltene-rich heavy crude oil (Baskin and Peters, 1992).

### ***Closed-System Pyrolysis Methods: Hydrous vs. Anhydrous***

Various closed-system pyrolysis methods exist with which different potential chemical or physical influences on petroleum generation, besides thermal stress, can be taken into account or controlled. Those are the presence or absence of water and the influence of elevated pressure. Open-pyrolysis systems operate close to atmospheric pressure in which an inert gas is passed over the heated sample and generated products are flushed away. In closed-system pyrolysis such as MSSV, the vapour pressure increases during heating and gas formation, although the pressure inside the vessel is generally thought to be below 10 MPa at operating temperatures (Erdmann and Horsfield, 2006). Sealed gold bags represent another closed-system or confined analytical set-up, which can be heated and additionally pressurized by an external fluid to any desired pressure. Here, the products are kept more closely to the reaction site potentially modifying the reaction mechanism. To test the influence of water on reaction mechanisms, both systems, MSSV and gold bag, theoretically can be run with extra-amounts of added water. Nevertheless, the term hydrous pyrolysis is usually used for analytical set-ups, in which a closed vessel (or reactor) contains, beside chunks of source rock, a water phase and an inert gas phase. The closed nature of experiment leads to the presence of both, liquid and vapour phases of water at the reaction temperature and to the expulsion of products from its source. Therefore, the chemical role of water on reaction mechanisms is favoured instead of pressure. An alternative involves filling the vessel completely with source rock and water, thereby leaving no vapour space (Carr *et al.*, 2009). Here, the water itself acts as the pressure medium and both, chemical and physical influences can be investigated. The authors claimed that this analytical set-up resembles natural conditions in sedimentary basins most closely of all pyrolysis methods, as the pore spaces in rocks are saturated with water. Nevertheless, this is not necessarily always the case and effects of lithostatic or effective stress, which are also potentially important influences, are unaccounted for (Vandenbroucke and Largeau, 2007). Additionally, the water saturation especially within the organic matter, if water is present at all, is not known for certain.

It is claimed that significant differences in pyrolysate yields and composition as well as for extrapolations to geologic histories are observed whether the reactions are conducted under hydrous or anhydrous conditions (Lewan, 1993). This is mainly related to water which has two important effects on organic matter conversion under geologic or laboratory conditions, a chemical and a physical (i.e. pressure).

### *The chemical role of water*

The chemical role of water has been evaluated by the addition of water during laboratory pyrolysis which leads to increases in hydrocarbon yields and decreases in the production of unsaturated hydrocarbons, suggesting that water may participate in or catalyse the reactions in some manner (Durand *et al.*, 1977b; Lewan *et al.*, 1979; Hoering, 1984; Lewan, 1994). Possible roles of water include serving as a hydrogen transfer medium or a hydrogen and oxygen donor (Evans and Felbeck Jr., 1983; Lewan, 1992b) and water may as well enhance or facilitate hydrocarbon expulsion (Lewan, 1992a). Kinetic parameters determined by Rock-Eval pyrolysis and hydrous pyrolysis are different, whereas for the former kinetics result in oil generation at significant lower temperatures and over a broader temperature range than for kinetics determined by hydrous pyrolysis (Lewan, 1985; Burnham *et al.*, 1987; Lewan and Ruble, 2002).

On the other hand, e.g. Monthioux *et al.* (1985) have found similar results for pyrolysis with and without water, provided that other (hydrocarbon) products were allowed to remain entrapped in the closed system. In addition, Michels *et al.* (1994) could show that excess water is not necessarily needed in a closed-system pyrolysis apparatus as kerogen is self-sufficient and can provide enough protons to saturate the generated hydrocarbons, because during early maturation enough water is generated by de-oxygenation. At higher temperatures, aromatisation reactions are the principle hydrogen source. These observations suggest that within the fluid phase the roles of hydrocarbons and water to promote hydrogen transfer and thereby inhibiting recombination reactions are more or less interchangeable, but Mansuy and Landais (1995) could show that water cannot completely substitute for the hydrocarbons and removal of the latter from the reaction medium leads to a more rapid and irreversible condensation and polymerisation of the solid residue.

Water also inhibits clay induced catalytic effects during hydrous pyrolysis (e.g. Huizinga *et al.*, 1987; Weres *et al.*, 1988) by shifting the cracking process from a carbon ion towards a free radical mechanism (Tannenbaum and Kaplan, 1985).

Water might play another important chemical role under geological condition for the formation of late methane by hydrolytic disproportionation (Seewald, 1994; Price, 2001). Hydrogenation of “spent”, deeply buried, high rank, post-mature kerogen, could subsequently lead to the generation of significant amounts of deep-basin high-rank methane-rich gas and CO<sub>2</sub>. A similar mechanism involving a Fischer-Tropsch like process was recently ascribed to cause isotope “rollovers” encountered in high-productivity gas shale wells in the U.S. (Tang

and Xia, 2011)(discussed in greater detail in Chapter 6.1). However, the reaction pathway is still under discussion and not really predictable by laboratory experiments due to uncertainties in the existing geologic conditions, e.g. the flow rate of water through the organic matter fraction.

### *The physical role of water (pressure)*

Pressure increase has been shown to retard kerogen cracking in hydrous pyrolysis experiments in which pressure is transmitted by a largely incompressible liquid water phase (Michels *et al.*, 1995; Carr *et al.*, 2009), whereas such a delay is hardly observable with confined hydrous or non-hydrous (MSSV or Gold Bag with or without added water) experiments in which a compressible vapour phase is present in the reaction space. Most studies using gold bags have found that pressure either does not have any effect on hydrocarbon generation (Monthioux *et al.*, 1985; Monthioux *et al.*, 1986) or has a very minor effect on oil cracking (Al Darouich *et al.*, 2006) or retards the reaction (Domine, 1991; Price and Wenger, 1992; Michels *et al.*, 1994; Michels *et al.*, 1995; Knauss *et al.*, 1997). Wang *et al.* (2006) could document a retardation of hydrocarbon generation for dry, high temperature (400-700°C) gold bag experiments at pressures (1000-3000 bar) exceeding those observed in petroleum basins, which are typically in the range 1 – 1000 bar.

Carr *et al.* (2009) concluded that maturation or hydrocarbon generation as an endothermic, volume expanding reaction is enhanced under low pressure, hydrous conditions (part liquid, part steam) due to the chemical effect of water, but is retarded if vapour is completely replaced by pressurized liquid water, which is consistent with Le Chatelier's Principle (Atkins and de Paula, 2002). Using thermal energy for the mechanical work of water displacement to accommodate generated hydrocarbons means that less thermal energy is available to overcome the activation energy barrier, thus reactions are retarded compared to "vapour" systems. Pressure also modifies some reaction pathways and favours aromatisation (Price, 1981), because free radical reactions take place much more slowly at high pressures related to cage effects inhibiting the diffusion step of radical formation (Costa Neto, 1991; Mallinson *et al.*, 1992; Hill *et al.*, 1996). Nevertheless, Hill *et al.* (1996) have shown that the effect of pressure under geologic conditions is secondary compared to temperature despite a significant effect of pressure on isotopic fractionation of gaseous hydrocarbons.

### ***Convenience and Suitability of Confined MSSV-Pyrolysis***

The previous discussion shows that the role of water and pressure is still controversially discussed and that the different pyrolysis set-ups cannot be assigned a final

“right or wrong method”-label as none of them is able to reproduce natural hydrocarbon generation accurately due to the difference in temperature regimes. Furthermore, the generally accepted view is that their contribution to especially gas formation is small compared to temperature (Erdmann, 1999). Another aspect is that it is difficult to estimate the real pressure applied to kerogen in source rocks under geologic conditions ranging from hydrostatic to lithostatic (Vandenbroucke and Largeau, 2007) and the water saturation especially within the organic matter, if water is present at all, is not known for certain. Therefore, MSSV-pyrolysis, being by far the most convenient and budget-priced alternative of all closed-system pyrolysis methods that even allows very small sample amounts to be used, is chosen as the artificial maturation simulation technique for the scope of this thesis. Furthermore and using MSSV-pyrolysis, an excellent reconstruction of natural fluid composition was demonstrated in several case studies, e.g. Sonda de Campeche, Mexico (Santamaria-Orozco and Horsfield, 2004), Snorre Field, North Sea Viking Graben (Erdmann, 1999; di Primio and Skeie, 2004), or Reconcavo Basin, Brazil (di Primio and Horsfield, 2006), in that GORs of MSSV-pyrolysates correlated very well with natural fluid GORs in the related petroleum systems at similar transformation ratios TR (see also Dueppenbecker and Horsfield, 1990; or Horsfield, 1997). The systematic and problematic difference in detailed gas composition, i.e. too high ethane and propane contents and simultaneously rather low methane contents (too high gas wetness) compared to natural fluids (Javaid, 2000), with its inherent implications for the prediction of saturation pressure  $P_{\text{sat}}$  and hence phase behaviour during petroleum generation and migration (di Primio and Skeie, 2004; di Primio and Horsfield, 2006), is also common to other closed-system pyrolysis approaches and can be overcome by calibrating kinetic, compositional model predictions to a natural fluid data base (di Primio and Skeie, 2004) or by adjusting gas compositions empirically (di Primio *et al.*, 1998; di Primio and Horsfield, 2006).

### ***Detailed Approach to Answer “Inherent fundamental questions”***

*“Which types of source rocks possess a late gas potential in general?”*

To answer the first key question a large series of immature source rocks (65 samples), shales and coals covering all main kerogen types and depositional environments, is investigated using both, open- and closed-system pyrolysis. Open-system pyrolysis is applied to characterise the organic matter itself on a bulk and molecular chemical level, closed-system pyrolysis is applied to characterise the late gas generation behaviour of each sample. This puts the relationship of initial organic matter structure and late gas potential on a statistically more powerful basis than the analysis of only single source rock samples.



*“Which molecular compositional changes of initial kerogen structure and early formed bitumen might be involved?”*

To answer the second key question different approaches are applied. Natural maturity sequences as well as under both, open- and closed conditions artificially matured sample sequences from different depositional environments are investigated, again using open- and closed-pyrolysis to monitor possible changes in late gas generation behaviour in correlation to the organic matter evolution. If e.g. early-formed bitumen plays a major role for the development of a thermally stabilised moiety, which yields late gas only at elevated temperature stages, maturation of an immature source rock under open-system pyrolysis conditions should cause an elimination of responsible compounds from the reaction zone inhibiting the formation of a late gas potential. A similar idea represents the approach to investigate extracted and unextracted source rocks. In the present thesis the late gas potentials of extracted and unextracted “immature” New Zealand Coals are compared. Additionally, natural maturity sequences help to calibrate findings based on immature sample analysis and help to clarify which artificial maturation method more closely simulates natural processes.

*“How are these changes manifested in kinetic parameters and stable isotopic compositions?”*

The third key question already implies that second-order recombination reactions effect on kinetic parameters and isotopic compositions, which might not be necessarily true with respect to late gas generation itself. This aspect will be clarified using open- and closed-system pyrolytic methods on natural and artificial maturity sequences.

### ***1.4 Structure of Dissertation***

The thesis is organised as follows:

CHAPTER 2 describes the investigated sample set consisting of immature source rocks and natural maturity sequences. Sample provenances and depositional environments are introduced as well as organic-geochemical techniques that have been applied for the scope of this dissertation.

CHAPTER 3 geochemically characterises all investigated source rocks using both bulk and molecular characteristics. The purpose of this chapter is to gather information on the type, initial structure and maturity of organic matter within source rocks as well as alterations of bulk and molecular parameters brought about by natural maturation. The inorganic matter fraction is also evaluated for a part of the sample set.

CHAPTER 4 comprises the late gas potential evaluation of immature source rocks based on open- and closed-system pyrolysis methods. Here, late gas generation behaviour is linked to the initial organic matter structure, which depends on the depositional environment, first in detail for a small sample set consisting of 4 different source rocks and then for a larger sample set (65 samples) using a more rapid closed-system screening method. Additionally, the determination of kinetic parameters of late gas generation is discussed.

CHAPTER 5 describes the evolution of late gas generative properties related to structural and chemical changes within the organic matter during natural maturation and artificial maturation under open- and closed-system pyrolysis conditions. 5 maturity series (39 samples) comprising various kerogen types are investigated and 5 different immature source rocks are artificially matured and tested.

In CHAPTER 6 additional experiments are discussed shedding some more light on compositional changes of organic matter during pyrolysis. Here especially the role of second order reactions, i.e. interaction between bitumen and residual kerogen, during maturation and their effect on late gas generation are considered applying open- and closed-system pyrolysis methods to a synthetic source rock mixture (Type I/III). Furthermore ESR measurements on coal residues yield information on changes within the residual organic matter during artificial maturation. Additionally, the gas isotopic composition at high-temperature closed-system pyrolysis conditions is described.

CHAPTER 7 sums-up the obtained results and gives some perspectives on the applicability of the findings.

## 2 SAMPLES AND METHODOLOGY

### 2.1 *Sample Set*

To consider to what extent late stage gas generation is a function of depositional environment and organic matter evolution a large world wide sample set of immature source rocks (65 sample) and natural maturity series (5 series, 39 samples) was investigated. Samples were provided by the funding companies (Shell, Maersk, Petrobras, Eni, Total, Wintershall, Devon Energy) or taken from the GFZ in-house sample base. As the sample set was repeatedly extended during the project, related to new entry of sponsors etc., the determination of e.g. late gas generation behaviour could be optimised leading on the other hand to a slightly varied methodology (heating rates, end temperatures). Variations are explained in Chapter 2.2. The final sample set, i.e. provenance, geologic age and depositional environment is listed in Tab. 2-1 (immature source rocks) and Tab. 2-2 (natural maturity series) and shortly described in the following.

Data provided by the funding companies was mainly restricted to general background information such as formation name and in some cases TOC/Rock-Eval data, which is given in Table A 1 (Appendix).

#### 2.1.1 Immature source rocks

Sixty-five well-known, organic-rich, high-quality source rocks, shales and coals from all over the world, were used and represent a wide range of depositional settings and geologic ages (Cambrian through Miocene)(Tab. 2-1). All samples are immature to early mature with respect to petroleum generation and exhibit calculated  $R_o < 1.0\%$  (Jarvie et al., 2001) (Table A 1). They include lacustrine, marine and fluvio-deltaic – terrestrial shales and coals as well as mixtures of the like. Depositional environment assignments were made based on literature review and geochemical characterisation using different pyrolysis methods, which is discussed in detail in Chapter 3.

##### *Lacustrine source rocks*

Lacustrine sediments may be deposited under oxic through anoxic conditions and within saline through freshwater lake environments comprising a stable stratified water column (Horsfield, 1997). Ten samples originate from aquatic, lacustrine environments (Tab. 2-1) and contain homogeneous, algal derived biopolymeric organic matter in high abundance. They include eight shales; six from the Cretaceous Wealden of the North West German Basin provided by Wintershall, one Tertiary Green River Shale from the Uinta Basin, USA, and one

Eocene Messel Oil Shale from Germany. Two sapropelic coals, one Pennsylvanian Boghead Coal from the USA and one Cretaceous Cannel Coal, can also be ascribed a lacustrine origin. Nevertheless, the Messel Oil Shale and the Cannel coal contain some higher land plant material and were assigned mixed lacustrine – terrestrial depositional settings. The same applies to the synthetic kerogen Type I/III sample, a technical admixture of 50 wt.-% Green River shale (G004750) and 50 wt.-% Åre Fm. Coal (G001965).

### ***Marine source rocks***

Prolific petroleum source rocks comprise autochthonous organic matter mainly derived from algal and bacterial inputs and form in silled basins and on stagnant shelves where reducing conditions exist at or above the sediment-water interface (Horsfield, 1997). Allochthonous terrigenous macerals from higher land plants such as vitrinite, sporinite or inertinite are common but essentially absent in early Paleozoic source rocks. Twenty-eight immature marine black shales and carbonates exhibiting no to only low terrestrial contributions were investigated. The oldest ones are two Cambrian Alum Shales from Sweden described in detail by Horsfield *et al.* (Horsfield *et al.*, 1992a). Four Silurian Hot Shales from the Middle East were provided by Shell, three Silurian Hot Shales from the Murzuq and Ghadames Basin in Libya were provided by Eni. Devonian through Mississippian strata is very prominent in many basins of North America and presents a major source of petroleum. The investigated sample set includes two Woodford Shales, a Caney Shale, and a New Albany Shale provided by Devon Energy as well as another Woodford Shale, Chattanooga Shale and Bakken Shale taken from the GFZ in-house sample base. One Devonian sample originates from the Domanik Fm., which is located in the Volga-Ural Province in Russia (Eni). The youngest Paleozoic marine source rock sample is of Permian age and stems from the Brazilian Irati Fm. deposited in a marine influenced part of the Paraná Basin (Petrobras).

Mesozoic through Cenozoic marine shales are comprised of mainly European hydrocarbon source rocks taken from the GFZ sample base, with the exception of two Jurassic Toarcian Shales from the Paris Basin, France, which were provided by Total. They include a Triassic Botneheia Shale from Norway, an Upper Jurassic Spekk Fm. sample from the Haltenbanken area of Mid-Norway, a Jurassic Autun Oil Shale from France, and three Tertiary Fischschiefer from the Schöneck Fm. of the Austrian Molasse Basin. Depositional settings of the latter three samples are described in detail in Schulz *et al.* (2002). Additional marine source rocks, for which TOC/Rock-Eval and bulk kinetic parameters were already present (di Primio and Horsfield, 2006), are the Late Cretaceous sulphur-rich Brown



### ***Fluvio deltaic - terrestrial source rocks***

Here, fluvio deltaic – terrestrial source rocks comprise eighteen coals and shales deposited in continental/deltaic settings such as in swamps on lake margins or on the delta plain, but also in lower delta plain and inner shelf environments. GFZ supplied samples include six Tertiary coals, two from the Canadian Mackenzie Delta (Kugmallit Fm - lignite., Taglu Fm.) as well as three coals from the deltaic member of the Talang Akar Fm. and one Arang Coal from the Ardjuna Basin of NW Java/Indonesia (Horsfield *et al.*, 1988). Furthermore, a Jet Rock from the United Kingdom (di Primio and Horsfield, 2006) and an Åre Fm. coal from the Haltenbanken area of Mid-Norway are present within the sample set. Both are Lower Jurassic in age.

Wintershall provided a set of six fluvio-deltaic coals of the Cretaceous Wealden from the N.W. German Basin. Total supplied two Cenozoic shales from the Mahakam Delta in Indonesia and two Cretaceous shales from the Douala Basin in Cameroon.

Eight samples were assigned a mixed-marine terrestrial depositional environment, i.e. the samples contain a higher proportion of autochthonous organic matter with variable contributions of terrestrial debris. They comprise shales from the Late Cretaceous to Paleocene Akata Fm. deposited in the Gulf of Guinea offshore Nigeria (Shell), two Jurassic Hekkingen Fm. shales from the Norwegian Barents Sea (Eni) and five Upper Jurassic shales from the Farsund Fm. in the Danish Central Graben (Maersk).

### **2.1.2 Natural maturity series**

Five natural maturity series spanning different maturity ranges and organic matter types were investigated to evaluate the relation of late gas generation behaviour to organic matter evolution and depositional environment. Provenances of the used samples are given in Tab. 2-2, calculated measured vitrinite reflectance together with Rock-Eval data in Table A 1. For compilation of a continuous kerogen Type III natural maturity sequence three samples series comprising humic coals were selected. Two natural maturity series comprising kerogen Type II source rocks were used to represent Paleozoic marine organic matter.

### ***Cenozoic Coals, New Zealand***

Ten unextracted and extracted Cenozoic New Zealand coals represent an immature Type III maturity sequence with respect to oil generation (Sykes and Snowdon, 2002) and cover sub-bituminous to high volatile bituminous coal ranks (0.40% - 0.80% R<sub>o</sub>). Vitrinite, TOC, Rock-Eval, open-pyrolysis GC and IR-data was already present and described in Vu

## 2 SAMPLES AND METHODOLOGY

(2008). The coals originate from three different basins. Five samples from the Waikato Basin are of sub-bituminous in coal ranks, whereas three samples from coal pits at the West Coast and two samples from the Taranaki basin are of high volatile bituminous in coal ranks. Extracted samples were investigated to test the impact of possible second-order recombination reactions between first-formed bitumen and residual coal on the evolution or build-up of a late gas potential.

**Table 2-2: Provenance of natural maturity series samples**

Company	Company Code Wells	GFZ Code	Formation	Basin	Country	Age	Depositional Environment	
Shell	FPC_271538	G006385	Exshaw Fm.	WCSB West Canadian Sedimentary Basin	Canada	Devonian	marine	
	FPC_826949	G006387						
	FPC_271536	G006384						
	FPC_378121	G006386						
Wintershall	Rheden-18-SP-845	G006533	Wealden	NW German Basin	Germany	Cretaceous	fluvio-deltaic terrestrial	
	Rheden-29-SP-865	G006548						
	Rheden-19-SP-890	G006538						
	Bahrenborstel-Z-2-SP-285	G006552						
GFZ natural maturity series	Quarry South of San Saba, Tx	G007249	Barnett Shale	Fort Worth Basin	USA Texas	late Mississippian	marine	
	Ron Cheek #1	G007247						
	W.C.Young-2	G007250						
	Mitchell T P Sims-2	G007257						
	Oliver-1	G007219	Carboniferous Coals	Ruhr Basin Rhenish Massif	Germany	Carboniferous	fluvio-deltaic terrestrial	
	Sandbochum-1 1106 m	G000721						
	Wlastedde 1245 m	G001088						
	Dickebank-2	G001083						
	Verden-1 4695 m	G001086						
	Siedenburg Z-1 3813 m	G001092						
	Granterath-1 801 m	G001096						
	Maramarua	G001983	Waikato Coal Measures	Waikato Basin	New Zealand	Eocene-Oligocene		
	Rotowaro	G001982						
	Huntly	G001984						
	Rotowaro	G001981						
	Rotowaro	G001980	Brunner Coal Measures	West Coast		Eocene		
	Reefton	G001997				Eocene		
	Reefton	G001996				Late Cretaceous		
	Greymouth	G001990				Late Cretaceous		
		G001994	Rakopi	Taranaki Basin		Eocene		
	G001991	Mangahewa	Eocene					
Extracted Coal		G001983K	Waikato Coal Measures	Waikato Basin	New Zealand	Eocene-Oligocene		
		G001982K						
		G001984K						
		G001981K						
		G001980K	Brunner Coal Measures	West Coast		Eocene		
		G001997K				Eocene		
		G001996K				Late Cretaceous		
		G001990K				Late Cretaceous		
		G001994K	Rakopi	Taranaki Basin		Eocene		
	G001991K	Mangahewa	Eocene					

### ***Ruhr Area Coals, Germany***

Six Carboniferous German Coals from different wells in the Ruhr area cover the maturity range from end of high volatile bituminous coal ranks over medium and low volatile bituminous coal ranks to anthracite (0.99% - 2.81%  $R_o$ ). Vitrinite, TOC, open-pyrolysis GC, IR, and bulk kinetic data was taken from Horsfield and Schenk (1995) and Schenk and Horsfield (1998). Rock-Eval parameters were re-determined within this study for all samples (APT), as well as bulk kinetic parameter for sample G000721 from well Sandbochum-1.

### ***Wealden Coals, Germany***

Four Cretaceous Wealden Coals from Germany (Wintershall) with calculated  $R_o$  (Jarvie et al., 2001) between 0.56 and 1.37% (Table A 1) span high to medium volatile bituminous coal ranks filling the maturity gap between New Zealand and Carboniferous German Coals as well as supplying additional material from another geologic age. The three coals from the Rheden-well are immature to early mature ( $R_o < 1.0\%$ ) and also part of the immature sample set (Chapter 2.1.1). Only sample G006552 from Bahrenborstel is of higher maturity.

### ***Exshaw Formation, Canada***

Shell contributed four Devonian Exshaw Fm shale samples from the West Canadian Sedimentary Basin (0.76 - 3.33%  $R_o$  based on Jarvie *et al.*, 2001) representing Type II marine organic matter, which is early mature (range of peak oil generation) to over mature (0.76 - 3.33%  $R_o$  based on Jarvie *et al.*, 2001). Rock-Eval parameter of the least mature Exshaw Fm. Shale G006385 had to be estimated due to only low amounts of sample material.

### ***Barnett Shale, USA***

Five Late Mississippian Barnett Shale samples from the Fort Worth Basin, Texas represent a complete maturity sequence (0.40 - 3.21%  $R_o$ ) of typically Type II marine, initially oil prone organic matter, which is the source of the north-central Texas unconventional shale-gas system (Jarvie *et al.*, 2007). Rock-Eval data for the samples originating from different wells and outcrops throughout the Fort Worth basin was supplied by Dan Jarvie.



## 2.2 Analytical Program

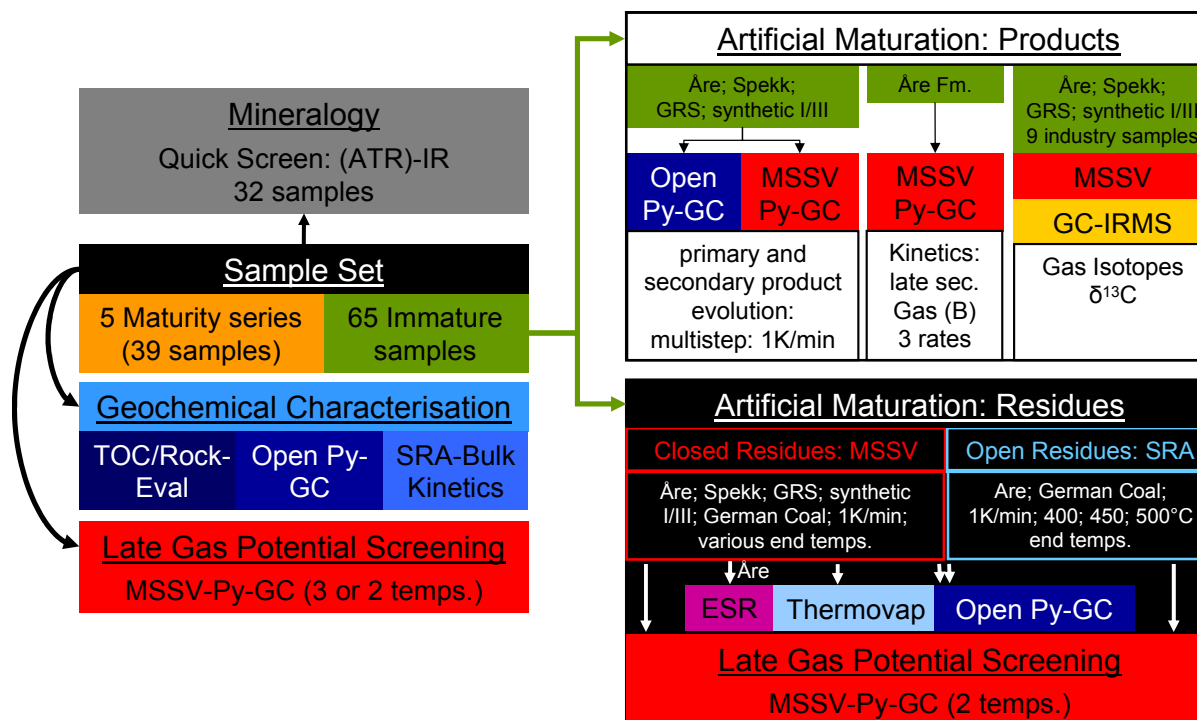


Figure 2.1: Flowchart showing the analytical program and employed methods

The flow chart in Fig. 2.1 gives an overview of the different employed methods which are described in more detail in the following sub chapters. All analyses were performed using manually crushed samples, which were already available at GFZ or delivered by the industry partners whether as powder, cuttings, cores or hand pieces from outcrops. Consolidated samples were crushed into small pieces with a hammer and subsequently ground to fine powder in a hand mill (e.g. to pass 200 mesh). The flow chart discriminates between three main stages. The first one is called geochemical characterisation and includes standard organic-geochemical techniques such as total organic carbon determination (TOC), Rock-Eval pyrolysis (RE), open-system pyrolysis gas chromatography (Py-GC), and determination of bulk kinetics using a Source Rock Analyzer (SRA) which provided basic information about kerogen quality, maturity, type, structure (depositional environment), and bulk petroleum formation properties for all investigated samples. Using a closed-system micro-scale-sealed-vessel pyrolysis gas chromatography (MSSV-Py-GC) screening method, the late gas potential of every sample was evaluated. Additionally, a novel approach, i.e. a quick mineralogy screen based on attenuated total reflection infrared spectroscopy (ATR-IR), was conducted for 32 samples, mainly shale. The second part comprises multistep open- (Py-GC) and closed-system (MSSV-Py-GC) artificial maturation experiments with the focus on compositional details of product genesis of four immature source rocks from the Åre Fm., Spekk Fm., Green River

Shale and one synthetic Type I/III source rock. Here, kinetic parameters and  $\delta^{13}\text{C}$ -isotopic compositions (MSSV-GC-IRMS) of late secondary gas (B) formation were tried to be elucidated. A third part concentrates on the characterisation of kerogen residues from artificial maturation experiments mainly using Open-Py-GC and the MSSV-Py-GC screening methods to compare results with results obtained for naturally matured organic matter. Open-system pyrolysis residues (SRA) of an Åre Fm. and an immature German Coal sample were prepared, as well as closed-system pyrolysis (MSSV) residues of Åre Fm., Spekk Fm., Green River Shale, synthetic Type I/III, and German Coal samples. Closed-system residues were investigated using thermovaporisation (Tvap-GC) to measure the concentration of free volatile organic species still present in the kerogen residues after preparation, and Åre Fm. residues additionally using electron-spin-resonance spectroscopy (ESR) to measure the development of the free radical concentration within the organic matter giving insights into the structural evolution of kerogen during artificial maturation.

## 2.2.1 Geochemical Characterisation

### *TOC determination and Rock-Eval pyrolysis*

TOC content and Rock-Eval pyrolysis is used to characterise the type and maturity of organic matter and to detect petroleum potential in sedimentary rocks. Total organic carbon concentrations (TOC) in whole rock samples (LECO) as well as Rock-Eval data (S1, S2, S3, HI, OI, PI, Tmax) were determined by the sub contractor Applied Petroleum Technology (APT) A/S, Norway for investigated source rocks for which data was not available or not provided by the industry partners (Table A 1). All procedures followed NIGOGA, 4<sup>th</sup> edition (Weiss *et al.*, 2000). Jet-Rock 1 was run as every tenth sample as an external standard and checked against the acceptable range given in NIGOGA.

For TOC analysis a Leco SC-632 was used. Finely crushed rock samples were treated with diluted HCl (1:9 HCl:Water) at 60°C to remove inorganic carbon. If no more reactions between minerals and HCl took place when adding a small amount of HCl (1:1 HCl: water), the samples were rinsed to remove HCl and dried. Rock powder was then introduced into the Leco combustion oven operating at 1350°C during analysis. To ensure full conversion to CO<sub>2</sub>, oxygen is purged into the oven. The amount of total organic carbon in weight-percent of the rock was then calculated using carbon dioxide concentrations measured by an infrared detector.

Rock-Eval pyrolysis was developed by Espitalié *et al.* (1977) on the basis of organic geochemical changes during maturation. A Rock-Eval 6 instrument (Behar *et al.*, 2001) is

used with a programmed temperature heating starting isothermally at 300°C for 3 minutes and subsequently increase temperatures to 650°C at a non-isothermal heating rate of 25°C/min. Related to TOC content up to 120 mg of grounded sample material was thermally treated and generated bulk hydrocarbons immediately transported to a flame ionisation detector in a helium gas flow. Two well-defined peaks are recorded; S1 represents the extractable product amount at 300°C which are free hydrocarbons formed up to the present maturity stage of the organic matter and still remain within the source rock, S2 represents the phase of volatilization of the very heavy hydrocarbons compounds (>C<sub>40</sub>) as well as the remaining hydrocarbon potential generated by cracking of the organic matter during the non-isothermal heating period. T<sub>max</sub> is the temperature at which S2 reaches its maximum and depends on the nature and maturity of the analysed kerogen, with higher maximum temperatures for higher maturity stages. In addition, CO<sub>2</sub> issued from the cracking of oxygen containing functional groups in the organic matter is trapped in the 300°-390°C range, then released and detected by thermal conductivity detection (TCD) during the cooling of the pyrolysis oven producing the S3 peak which can be used as a measure for the oxygen richness of the kerogen. S1, S2 and S3 are together with TOC input parameters for the calculation of HI-Hydrogen Index, OI-Oxygen Index, and PI-Production Index.

### ***Bulk Kinetics***

Whole rock samples were subjected to this Rock-Eval-like open-system, non-isothermal pyrolysis system at four different linear heating rates (0.7, 2, 5, 15°C/min) using a Source Rock Analyser SRA (Humble). The main reason to use this method was to characterise the kinetic of the kerogen to petroleum conversion process in general. Depending on the chosen heating rate and organic matter richness, between 200 and 10 mg of crushed sample material was weighed into small vessels and heated according to the temperature program from 250°C to ~600°C. Generated bulk products were transported to the FID in a constant helium flow of 50 mL/min. The discrete activation-energy (E<sub>a</sub>) distribution optimisation with a single, variable frequency factor (A) was performed using the KINETICS05 and KMOD® programs (Burnham *et al.*, 1987). Slow heating rates ≤5°C/min were used to avoid problems related to temperature transfer within the sample material if heated to fast (Burnham *et al.*, 1988; Schenk and Dieckmann, 2004). The heating rates vary enough to ensure the correct iteration of the mathematical model and the calculation of the frequency factors via the T<sub>max</sub>-shift model (van Heek and Jüntgen, 1968). Kinetic parameters of all investigated source rocks can be found in Table A 3 and further information on kinetic modelling in Chapter 3.

### ***Open pyrolysis-gas chromatography-FID (Py-GC-FID)***

Non-isothermal open-system pyrolysis was employed to characterise the macromolecular structure of the kerogen by qualification and quantification of generated primary organic compounds and totals. The analyses were performed on all samples listed in Table A 2 in which heating rates etc. are given.

30 mm long glass capillary tubes with an internal diameter of ~1.5 mm with both ends open were used. Depending on organic matter richness between 3 to 40 mg of crushed whole rock sample material was positioned in the tubes with glass-wool which was thermally pre-cleaned at 600°C in air for >1h. The glass tubes were inserted in the sample holder of the programmable furnace and flushed for 5 minutes with Helium at the start temperature to get rid of volatile constituents and pollutions. In the course of the first 6 month of investigation the temperature program of the pyrolysis oven unit (Quantum MSSV-2 Thermal Analyzer) interfaced with an Agilent GC 6890A gas chromatograph started at 200°C in order to also get information about free hydrocarbons within the organic matter which could play a role in closed system pyrolysis experiments. As maturity of the source rocks was generally low, the volatile hydrocarbon content, corresponding to Rock-Eval S1, could be expected to only play an inferior role. Pyrolysis was carried out to temperatures of 550°C for the heating rate 1°C/min, 560°C for the 2°C/min heating rate and 580°C for the 5°C/min heating rate (corresponding to MSSV end temperatures and rates). Accelerating analytical procedures, later analysed samples were thermally extracted at 300°C for 5 minutes and then heated to 600°C at 50°C/min. The final temperature was maintained for 2 min as described by Muscio and Horsfield (1996). Generated products were collected in a liquid nitrogen cooled cryogenic trap from which they were liberated by ballistic heating to 300°C into an Agilent GC 6890A gas chromatograph equipped with a HP-Ultra 1 column of 50 m length, 0.32 mm internal diameter and 0.52 µm thickness and a Flame Ionisation Detector (FID). The GC oven temperature was programmed from 30°C to 320°C at 5°C/per min. Helium was used as a carrier gas with a flow rate of 30 mL/min. Quantification of individual compounds and totals was conducted by external standardisation with n-butane. Prominent hydrocarbon peaks were identified by reference chromatograms. Reproducibility of measured product concentration is generally better than 4% (Schenk et al., 1997). Because of the lower response factor of methane compared to the heavier gases the methane content was multiplied with 1.1.

### ***Infrared Spectroscopy (IR)***

Infrared spectroscopy is a non-destructive spectroscopic method in which electromagnetic waves (infrared light) directly interact with the rotation and vibration of molecules, atoms and atom groups in molecules. It can be used to identify or quantify functional groups in the organic matter structure. Previously reported data on New Zealand Coals (Vu, 2008) and German Coals (Horsfield and Schenk, 1995; Schenk and Richter, 1995) was compared to late gas generation data of the same samples in the present PhD-thesis (see Fig. 5.7).

16 immature New Zealand Coals samples covering a maturity range from 0.27 to 0.81% vitrinite reflectance (extracted samples) and 8 German Coal samples covering a maturity range from 0.75 to 2.81% vitrinite reflectance (non-extracted) were analysed at the Institute of Petroleum and Organic Geochemistry, Forschungszentrum Jülich. Experimental procedure and parameters basically followed configurations described by Schenk *et al.* (1986). 1- 2 mg of finely ground sample material was dried in vacuum for 24 hours, mixed with 200g of KBr, milled for 3 minutes and pressed into a pellet in an evacuated 13 mm die at 8 tons/cm<sup>2</sup> pressure in duplicate. A Perkin-Elmer 783 dispersive spectrophotometer coupled to a Spectrafile IR plus-2.00 data station was used to record infrared spectra, Spectrafile software to calculate baselines and band areas. Integrated infrared absorptions (K in cm/mg TOC) are measures of the concentrations of functional groups in the sample and are listed in Table 5-2 for the following selected spectral ranges (wave number 1/cm, vibration mode, functional group) of main interest.

3000 - 2700 cm <sup>-1</sup> :	C-H stretching vibrations of aliphatic CH <sub>2</sub> and CH <sub>3</sub> groups
1520 - 1390 cm <sup>-1</sup> :	asymmetric bending vibrations of aliphatic CH <sub>2</sub> and CH <sub>3</sub> groups
1390 - 1340 cm <sup>-1</sup> :	symmetric bending vibration of aliphatic CH <sub>3</sub> groups
900 - 700 cm <sup>-1</sup> :	out- of- plane vibrations of aromatic CH groups

### ***Mineralogy (ATR-IR)***

Attenuated total reflection infrared spectroscopy (ATR-IR) was carried out to roughly characterise the mineralogical composition of the inorganic matter within the rock, which effects adsorption capacity and fracability. 32 finely crushed samples, mainly shale, were sent to Newcastle University and analysed there in the group of A.C. Aplin. Detailed results are given in Table A 4 and are discussed in Chapter 3.4.

An attenuated total reflection accessory (multiple reflection ATR system) operates by measuring the changes that occur in a totally internally reflected infrared beam when the beam comes into contact with a small amount of sample (a few milligrams). The spectrum collection typically takes only 30 seconds per sample leading to a very high sample throughput. The recorded spectrum is evaluated using a least squares calibration model based on the spectra of mixtures of mineral standards. This model is then used to determine the bulk mineralogy of the investigated sample. A total of 87 clastic and carbonates mixtures were designed from five mineral standards based on mineral combinations common to many sedimentary environments. Quartz, illite-smectite (70:30), kaolinite, calcite and dolomite make up the calibration mixtures. Each mineral in the mixture set was distributed within concentration ranges typically encountered in shales.

### **2.2.2 Artificial maturation: products**

#### ***Stepwise Open-Pyrolysis Gas Chromatography-FID (Py-GC-FID)***

In order to gain a better understanding about the evolution of exclusively primary gas and oil, and to compare results to closed-system experiments in which secondary and primary gas input is hard to differentiate, a stepwise open pyrolysis GC approach was employed for four samples stemming from different depositional environments. The terrigenous Åre Fm. sample G001965, the marine Spekk Fm. sample G001955, the lacustrine Green River Shale sample G004750, and the synthetic Mix Type I/III sample G0047501965 were pyrolysed at a heating rate of 1°C/min, starting at 250°C and ending at various end temperatures between 300 and 600°C. Temperatures higher than 600°C could not be investigated as the heating cartridge performance of the pyrolysis oven unit (Quantum MSSV-2 Thermal Analyzer) is not laid out for those temperatures regimes. The equipment and procedure used is the same as previously described under Open pyrolysis-gas chromatography-FID (PY-GC-FID). The only difference is the need for manual refilling liquid nitrogen into the cryogenic trap every 10 minutes until the desired end temperature is reached and the trap removed to release products onto the gas-chromatographic -column. The results are given in Table A 5 and are discussed in Chapter 4.1.4.

#### ***Closed-Pyrolysis Gas-Chromatography-FID (MSSV-Py-GC-FID)***

Non-isothermal closed-system pyrolysis was employed as thermally (primary) generated hydrocarbons are retained within the hot reaction zone and can be cracked to yield secondary gas (secondary gas (A)). Additionally, second order recombination reactions of

first formed products with residual organic matter possibly take place (Dieckmann *et al.*, 2006; Erdmann and Horsfield, 2006) leading to the formation of a thermally stabilised recombination structure acting as a precursor for extra amounts of secondary gas (late secondary gas (B)) at elevated temperatures.

The closed-system approach was applied firstly to define primary and secondary gas evolution curves of the same four samples which were used for stepwise open-pyrolysis (Chapter 4.1.4.) acting as a tool to investigate which source rocks possess a late gas potential in general and as a prerequisite to determine kinetic parameters for late secondary gas (B) generation (Table A 6). Kinetic parameters for high temperature methane generation were determined for the Åre Fm coal sample G001965 using MSSV pyrolysis at three different heating rates 0.1, 0.7, and 1°C/min. Secondly, non-isothermal closed-system pyrolysis was employed as a screening tool for the late gas generation behaviour of all investigated coals and shales (Table A 7).

For non-isothermal closed-system micro-scale sealed vessel (MSSV) pyrolysis (Horsfield *et al.*, 1989) between 1 and 20 mg of finely ground sample was weighed into glass capillaries which were then sealed by an H<sub>2</sub>-flame after reducing the internal volume of the tube from ca. 40 µL to ca. 15 µL with pre-cleaned quartz sand. Using such small sample amounts has got the advantage that the temperature of the aliquot is likely to match precisely the temperature detected by the thermocouple. For temperatures exceeding 600°C quartz-glass tubes had to be used due to a lower melting point of glass tubes. For this reason an H<sub>2</sub>/O<sub>2</sub>-flame was necessary to seal quartz-tubes. Pyrolysis was performed off-line, using an external high performance oven consisting of a massive cylindrical metal block acting as a circular sample holder enclosing a central heating cartridge which provided a very homogeneous temperature field throughout the core. Excellent temperature control was guaranteed by a thermocouple introduced directly into one sample holder. Up to 10 samples at a time in the high temperature pyrolysis oven (>600°C) and up to 25 samples in the normal pyrolysis oven (<600°C) could be heated at different heating rates and removed one by one at specific desired end temperatures. A heating rate of 1°C/min was used for the terrigenous Åre Fm. sample G001965, the marine Spekk Fm. sample G001955, the lacustrine Green River Shale sample G004750, and the synthetic Mix Type I/III sample G0047501965 with a programmed start temperature of 250°C and end temperatures spaced by ~50°C between 300 and 780°C to calculate primary and secondary gas evolution curves and compare results to stepwise open pyrolysis. Three different heating rates 0.1, 0.7, and 1°C/min with different end temperatures in the high temperature range were applied for the calculation of kinetic

parameters for the late secondary gas (B) generation of the Åre Fm. coal sample. Slow heating rates had to be chosen as late gas generation would shift to exceedingly high temperatures with faster heating rates. For the late gas potential screening of source rocks a heating rate of 2°C/min was used in most cases and vessels were heated up from 200°C to 460°C (end of cumulative C<sub>6+</sub> generation), 560°C (end of primary and secondary gas (A) generation), and 700°C (main stage of secondary gas (B) generation). At the beginning of analytical procedures a 5.0°C/min was chosen to speed up the screening (samples G005762, G005763, G004563, G004564, G005812, G000206) with the desired end temperatures being 480°C, 580°C, and 720°C. As the heating cartridge performance was not sufficient for this heating rate, only 690°C could be reached instead of 720°C. Thus 2°C/min was established as the main “screening” rate with previously described end temperatures. Accelerating analytical procedures, later analysed samples were only heated up to 560°C and 700°C as late secondary gas (B) generation could be evaluated within this temperature interval sufficiently.

After removal from the pyrolysis oven, the samples were introduced into an Agilent GC 6890A apparatus (described above). The tubes were purged 5 minutes at 300°C to remobilise generated products and then cracked open by a piston device to transfer generated products from within the vessel by a helium carrier into a liquid nitrogen-cooled trap. The trapped hydrocarbons were released by ballistic heating of the trap to 300°C and subsequently analysed by gas chromatography as described for open Py-GC-FID. Results for the different analyses such as total products, resolved products and single compound yields are listed in Table A 7- A 8.

### ***Kinetic modelling***

Kinetic parameters were derived using a parallel reaction model. The reactions of this kinetic scheme are considered to follow first-order kinetics and the Arrhenius law (van Krevelen *et al.*, 1951; Jüntgen and Van Heek, 1968; Tissot, 1969; Jüntgen, 1984; Schenk *et al.*, 1997b). Thus, hydrocarbon generation kinetic parameters consist of a series of activation energies and a single frequency factor. “Bulk kinetic parameters” are derived from non-isothermal open-system, Rock-Eval-like pyrolysis using the Source Rock Analyzer (SRA) at four different linear heating rates and describe the kerogen to primary petroleum conversion process as a whole without differentiating between single compounds or boiling fractions. To determine these “compositional kinetic parameters” non-isothermal closed-system MSSV-pyrolysis at three different linear heating rates had to be applied with the possibility to calculate specific frequency factors and activation energies for the generation of individual compounds, compound groups, boiling fractions, and most importantly for the present thesis



secondary gas species (cracking gas, late gas, etc.). The used mathematical routine for these determinations is based on non-isothermal kinetics (Jüntgen, 1964; van Heek and Jüntgen, 1968) and is published by Schaefer *et al.* (1990) who further indicated that specific frequency factors should be considered as mathematical optimisation parameter.

The procedure to determine kinetic parameters for late secondary gas (B) generation from MSSV-pyrolysis yields can be described as follows. Spline curves were approximated to the calculated cumulative gaseous hydrocarbon formation curves for the three linear heating rates. In a second step the spline functions had to be numerically differentiated to obtain generation rate versus temperature curves from which kinetic parameters, assuming twenty-five first order parallel reactions with activation energies regularly spaced by 1 kcal/mol and a single pre exponential factor, could be calculated according to Schenk and Horsfield (1993) using KINETICS05 and KMOD® programs (Burnham *et al.*, 1987). The draw back exists that heating rates of 0.1, 0.7 and 1.0°C/min might not be sufficiently different to ensure accuracy for the determination of a start-frequency factor (van Heek and Jüntgen, 1968) but had to be chosen as late gas generation would have shifted to exceedingly high temperatures with faster heating rates. Nevertheless, promising results were obtain which are in accordance with previously published data for late gas generation (Erdmann and Horsfield, 2006). Linear and non-linear least square iteration procedures allowed to find an optimised parameter set of activation energy distribution and frequency factor, which results in a best-fit for calculated curves and measured curves. Calculations were performed several times by carefully checking the cumulative plateaus, different spline function approximations and resulting first deviations as this method is very sensitive due to the number of calculation steps.

### ***Isotopic gas composition of MSSV-pyrollysates***

Stable carbon isotope compositions of C<sub>1-4</sub> gases were determined in triplicate for MSSV pyrollysates of the Åre Fm. sample G001965, the Spekk Fm. sample G001955, the Green River Shale sample G004750, and the synthetic Mix Type I/III sample G0047501965 prepared by applying identical heating rate (1°C/min) and end temperatures (11) as used during the previously described MSSV pyrolysis for calculation of primary and secondary gas evolution curves. In addition, stable carbon isotope compositions of C<sub>1-4</sub> gases were determined for the three MSSV- screening-pyrollysates prepared by using heating rates and end temperatures given in Table A 13 of the following 10 samples: Akata shale G005935, Mahakam Delta Shale G006207, Irati Fm. shale G005812, Hekkingen Fm. shale G005763, Murzuq Basin shale G004564, Toarcian shale G006208, New Albany shale G006156, Caney shale G006155, Bakken shale G005298, Fischschiefer G004070.

Each MSSV tube was placed into a 2 ml vial. The tube was cracked when crimping the vial with aluminium caps containing Teflon-coated septa. Cracking was forced by placing 1 – 2 small glass balls ( $\varnothing$  4-6 mm) on top of the tubing and below the cap. Gas volumes between 30 and 400  $\mu$ l have been sampled using gas-tight syringes. Each cracked MSSV tubing was taken just for one measurement. To guarantee the quality of the isotope data MSSV tubes have been produced in triplicate. The standard deviation of three similar samples was below  $\leq 0.5$  ‰ for all compounds.

The carbon isotopic composition of the generated hydrocarbon gases was measured by GC-C-IRMS (gas chromatography/combustion/isotope-ratio mass spectrometry). The GC-C-IRMS system consisted of a GC unit (6890N, Agilent Technology, USA) connected to a GC-C/TC III combustion device coupled via open split to a MAT 253 mass spectrometer (ThermoFisher Scientific, Germany). The organic substances of the GC effluent stream were oxidised to CO<sub>2</sub> in the combustion furnace held at 940°C on a CuO/Ni/Pt catalyst. CO<sub>2</sub> was transferred on line to the mass spectrometer to determine carbon isotope ratios. The gas samples were injected to the programmable temperature vaporisation inlet (PTV, Agilent Technology, USA) with a septumless head, working in split/splitless mode. The injector was held at a split ratio of 1:1 and an initial temperature of 40°C. With injection, the injector was heated to 230°C at a programmed rate of 700°C/min and held at this temperature for the rest of the analysis time. The saturated fractions were separated on a PoraPlot column (CP-PoraPlotQ, 25 m x 0.32 mm x 10  $\mu$ m, Varian). The temperature program started at 30°C, held for 10 min, and was then increased at a rate of 6°C/min to 200°C, held for 5 minutes. Helium, set to a flow rate of 1.0 mL/min, was used as carrier gas. The quality of the carbon isotope measurements was checked daily by measuring *n*-alkane gas standard (*n*-C<sub>1</sub> to *n*-C<sub>6</sub>).

### **2.2.3 Artificial maturation: residues**

#### ***Preparative pyrolysis – closed versus open system***

Pyrolysis residues were prepared by applying non-isothermal open- and closed-system pyrolysis in order to simulate natural maturation and to investigate if secondary reactions between first formed primary products and residual kerogen play a role for the development of a late gas potential of source rocks during artificial maturation. If yes, residues prepared in the open-system should not exhibit late methane generation features as primary products are transported out of the hot reaction zone. The approach was to further analyse open- and closed-residues by open-system pyrolysis to gain information on structural changes within the residual macromolecular organic matter, and by the closed-system MSSV-pyrolysis late gas

potential screening method (two end temperatures) to investigate the impact of those structural changes on the high temperature methane generation. The results for these analyses are listed in Table A 9 – A 12.

Closed-system residues were prepared for the Åre Fm. sample G001965, the Spekk Fm. sample G001955, the Green River Shale sample G004750, the synthetic Mix Type I/III sample G0047501965, and one Westphalian Coal sample G000721 (for comparison with a German coals natural maturity sequence) using MSSV-tubes and the off-line pyrolysis oven device explained earlier. A start temperature of 250°C, a heating rate of 1°C/min and end temperatures between 300 and 550°C were chosen in accordance with previously applied analytical parameters. For the Åre Fm. sample G001965 residues were prepared for maturation stages up to 300, 350, 400, 450, 500, and 550°C, for the Spekk Fm. sample G001955, the Green River Shale sample G004750, and the synthetic Mix Type I/III sample G0047501965 residues were prepared for maturation stages up to 350, 400, 450, and 500°C. Only three residues, 400, 450, and 500°C, were made for the Westphalian Coal G000721. At least 100 mg of residue for further analyses was needed for each residue. Thus, up to 20 MSSV-tubes per residue were filled with grounded untreated sample material as described for closed-pyrolysis. The filling weight depended on the end temperatures, with lower weight for higher temperatures, as at higher thermal stress the tubes tended to explode due to gas pressure increase. Regular MSSV-tube were used to keep the “preparation”-pressure within the vessels as similar as possible to the pressure the organic material experienced throughout previous analytical set-ups. After removal from the pyrolysis oven sample residues still remaining in the centre of the vessel had to be isolated from the MSSV glass capillary. One tube at a time was quenched in liquid nitrogen immediately before cracking it open manually and the residue picked and stored in a vial.

Open-system residues were prepared for the Åre Fm. sample G001965 and the Westphalian Coal sample G000721 for the maturation stages 400, 450, and 500°C with a heating rate of 1°C/min and a start temperature 250°C using the Source Rock Analyser SRA (Humble). One residue of 100 mg could be gained in a single run as the used sample vessel is bigger and no pressure problems occur due to the open-system with immediate removal of primary products by the carrier gas.

### ***Thermovaporisation gas chromatography-FID (Tvap-GC-FID)***

Closed-system residues were investigated using thermovaporisation (Tvap-GC) to measure the concentration of free volatile organic species still present in the kerogen residues after preparation. The analytical procedure is mainly the one described for closed-system

MSSV pyrolysis-gas chromatography-FID in the last paragraph. Simply, up to 10 mg of coarsely crushed residue material was weighted into previously described MSSV glass capillary tubes (Horsfield *et al.*, 1989), sealed by an H<sub>2</sub>-flame after reducing the internal volume of the tube from ca. 40  $\mu$ L to ca. 15  $\mu$ L with pre-cleaned quartz sand, and then introduced into an Agilent GC 6890A apparatus (details given in sub chapter (Py-GC-FID)).

### ***ESR-measurements***

The process of kerogen maturation/transformation respectively petroleum generation proceeds via free radical reactions involving formation and recombination of free radicals (Bakr *et al.*, 1988; Bakr *et al.*, 1991) For this reason free radical concentrations within the original Åre Fm. sample G001965 and its closed-system residues were determined by ESR measurements at Physikalisches Institut der Univerität Leipzig, Abteilung Struktur der Materie.

Free electrons are aligned at random, but in the presence of an external magnetic field they can occur in a lower or in a higher energy state. A higher energy state exists when the electrons line up with the magnetic field, a lower energy state exists, when the electrons line up opposing to the magnetic field. The difference in energy between those two states ( $\Delta E$ ) is proportional to the applied field (B). Therefore one can write

$$\Delta E = g\beta B$$

with g being the constant of proportionality called the spectroscopic splitting factor and  $\beta$  being the magnetic moment of the electron called the Bohr magneton. The energy required for the transition of an electron from one state to another will be for a given applied field

$$\Delta E = h\nu = g\beta B,$$

where  $\nu$  is the frequency of the applied electromagnetic radiation. The area, beneath an ESR absorption curve is an expression of intensity (I) of absorption and is proportional to the number of unpaired spins in the sample. Nevertheless, ERS-spectra are usually recorded as the first derivative of the absorption spectrum (Fig. 6.14) instead of absorption itself for instrumental purposes and improved resolution. The peak-to-peak line-width ( $\Delta B$ ) is the distance of the first derivative curve and represents the width of the absorption curve at the level of maximum slope.

The measurements were performed with a Varian E 112 spectrometer working in X-band. About 20 mg of sample material was fitted into 200 mm long quartz tubes with a diameter of 4 mm and an internal volume 500 mm<sup>3</sup>. They were measured alternating to a standard reference sample comprising a known concentration of free radicals (Ultramarine with  $C_{\text{abs}} = 1.42 \cdot 10^{19}$  spins/g sample). ESR spectra were recorded at room temperatures with

modulation frequencies of 100 kHz, modulation amplitude of 2, and different receiver gain. Radiation frequencies in the microwave region 9.5409 GHz at 2 mW were applied. The absorption signal was recorded (4000 points) at ~3405 G (centre field) using a sweep width of 200 G.

An easy way to interpret the ESR spectrum, i.e. to calculate the concentration ( $C_{rel}$ ) of free radicals in the investigated sample relative to the concentration of free radicals in the ultramarine reference sample (UM), can be approached by using

$$C_{rel} = (I * \Delta B^2 * gain_{UM}) / (I_{UM} * \Delta B_{UM}^2 * gain * m)$$

The absolute concentration ( $C_{abs}$ ) of radicals within the sample would then be:

$$C_{abs} = C_{absUM} * C_{rel}$$

Recorded ESR spectra for the analysed artificial maturity sequence are shown in Fig. 6.14 in which necessary parameter for the calculation of radical concentrations are explained.



### 3 GEOCHEMICAL CHARACTERISATION

The purpose of this chapter is to gather information on the type, structure and maturity of organic matter within source rocks from which late hydrocarbon gas might be generated using both bulk and molecular characteristics. Total organic carbon determination and Rock-Eval pyrolysis as a screening tool provide basic information about organic matter richness, genetic richness, quality/type and maturity of a sample. Open-system pyrolysis gas chromatography reveals structural differences between organic matters from various depositional environments or changes of the initial kerogen composition with temperature and time during natural or artificial maturation. This is of high interest for the present thesis as the chemical structure of the kerogens under investigation may primarily dictate the late gas generation behaviour. The determination of bulk kinetics using a Source Rock Analyser (SRA) provides additional information on the kerogen structure or compositional changes during maturation as bulk petroleum formation properties are influenced by the degradable major bond-types within the macromolecular organic matter.

#### ***3.1 Bulk Organic Geochemical Characterisation (TOC/Rock-Eval)***

##### **3.1.1 Organic Matter Richness - TOC Content**

TOC contents of the samples for which data was not already available or provided by the industry partners were investigated using a Leco SC-632, whereas any inorganic carbon, e.g. carbonate, was removed prior to analysis adding HCl to the crushed rock samples. In Fig. 3.1a it can be seen that most immature and natural maturity series samples exhibit high TOC contents exceeding 5% spanning the range from organic rich shales to coals.

The total organic carbon (TOC) content provides basic information about source rock richness, i.e. the quantity of organic matter present within a source rock and hence, indirectly its possible petroleum potential. Nevertheless, high TOC values alone are not always indicative of a source rock's quality because the carbon in the organic matter can be related to a number of major chemical component groups with very different petroleum potential and carbon content. This depends on both the maturity of the organic matter as well as the initial chemical structure of the bio macromolecules acting as kerogen, and therefore petroleum precursors. For example anthracite, as a highly mature equivalent of humic coal, or fusain, which is believed to derive from combustion of woody material (Scott, 1989), has a very high TOC content but very low petroleum potential. In contrast, TOC values < 0.5% can always be considered to indicate very poor potential because source rocks require a certain saturation

threshold quantity of hydrocarbons to be generated to overcome absorption and/or to fill pores before expulsion can occur (Sandvik *et al.*, 1992; Pepper and Corvi, 1995b).

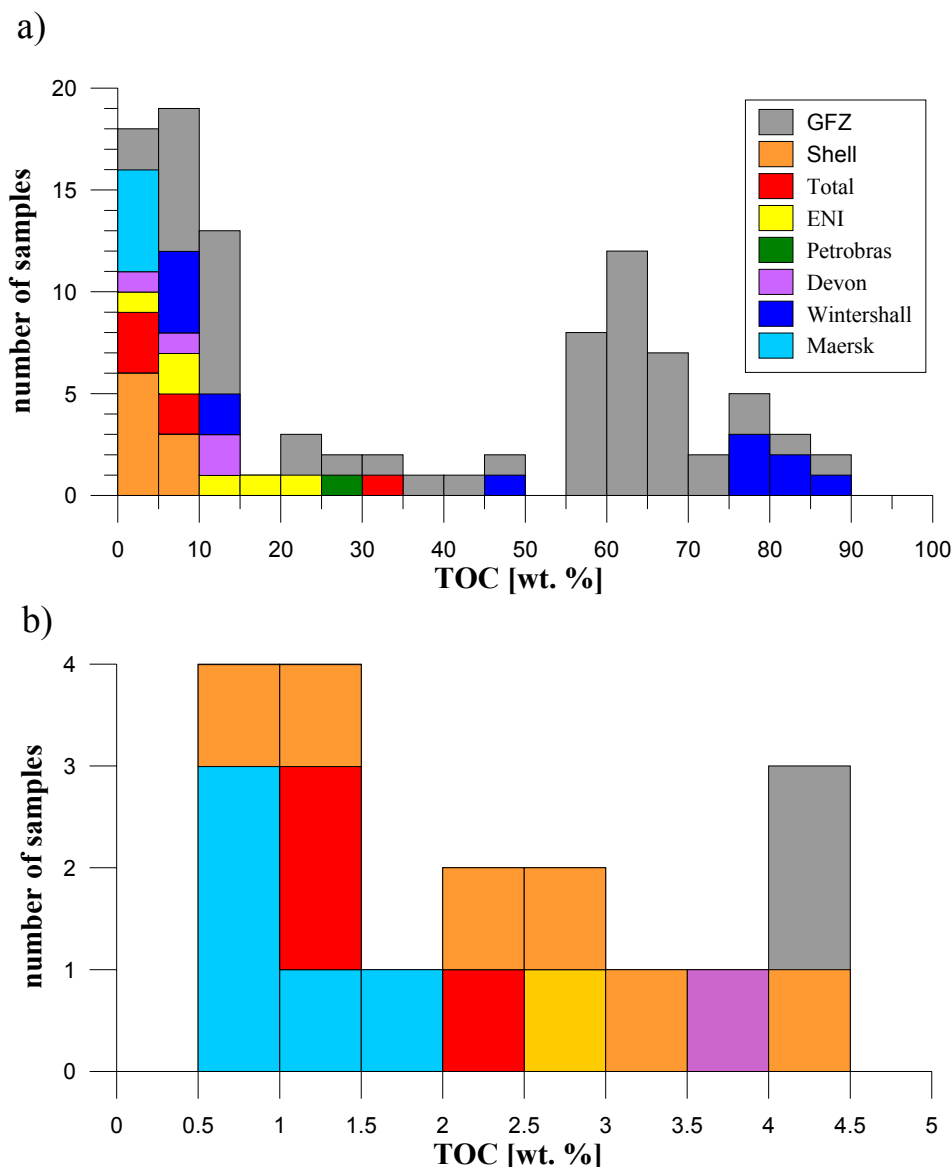


Figure 3.1: Total Organic Carbon (TOC) contents of a) all Industry and GFZ provided samples and b) source rocks containing less than 5% TOC

Source rocks with TOC contents  $>5\%$  were initially requested, firstly to avoid any concentration procedure as the kerogen isolation may alter the kerogen structure itself (Reynolds and Burnham, 1995; Erdmann, 1999), and secondly, as will be explained in the following paragraphs in more detail, to minimize mineral-induced retention or high temperature, catalytical cracking effects on petroleum composition and genetic potential which are not likely in lower temperature natural systems.

Primary pyrolysate from whole rock samples may be trapped at mineral surfaces or interlayers (Henderson *et al.*, 1968; Eisma and Jurg, 1969) and subsequently disproportionate



into secondary pyrolysate and coke (Espitalié *et al.*, 1980). This would lead to a too high  $T_{\max}$  temperature as well as a reduced genetic potential indicated by low S<sub>2</sub>-values and hence Hydrogen Indices, respectively. Using synthetic mixtures of kerogens and minerals, kaolinite was found to reduce the yield by between 0 and 30%, gypsum or calcite by up to 15%, smectite by between 25 and 50%, and illite by 85% at organic carbon concentrations of 0.9% and below (Espitalié *et al.*, 1980). Only for organic carbon concentration above 10% the amount of generated pyrolysate was sufficient to deactivate mineral reaction sites and to overcome retention effects. One has to keep in mind that retention effects may be less pronounced in actual whole rocks but were shown to be significant in sediments with TOC contents of less than 2.0% during Rock-Eval pyrolysis (Espitalié *et al.*, 1980; Katz, 1983; Dembicki, 2009).

The composition of pyrolysate additionally depends on the type of minerals within a rock's matrix. Horsfield and Douglas (1980) and Espitalié *et al.* (1980) could show that in the case of carbonate matrix the composition of the resultant pyrolysate may be similar to the pyrolysate of the respective isolated kerogen, whereas for montmorillonitic sediments it will be enriched in gaseous and aromatic hydrocarbons. In contrast, S<sub>3</sub> or OI data can be strongly influenced by the mineral composition with carbonates having the most significant impact on additional CO<sub>2</sub> generation (Katz, 1981), even though the temperature range over which CO<sub>2</sub> is collected lies below that in which carbonate minerals normally break down (Espitalié *et al.*, 1977). The organic carbon itself was shown to catalyse the thermal breakdown of CO<sub>2</sub> precursors of different mineral phases, e.g. HCO<sub>3</sub><sup>-</sup> and CO<sub>3</sub><sup>2-</sup> species in the crystal lattice of clay minerals (Horsfield *et al.*, 1983).

TOC contents of 18 investigated samples exhibit values below 5.0% (Fig. 3.1b) thus and owed to previously described aspects, complicating geochemical characterisation of especially those immature samples which contain less than 2% organic carbon,. Nevertheless, low TOC contents for highly mature shales, which is the case for investigated Exshaw Fm. samples provided by Shell and GFZ Barnett Shale samples, have to be expected and are hardly avoidable related to expulsion of generated hydrocarbons and thus loss of organic carbon during natural maturation.

### **3.1.2 Rock-Eval - Immature source rock samples**

Rock-Eval (Espitalié *et al.*, 1977) is widely used as a rapid screening technique to characterise the hydrocarbon generative potential as well as maturity of source rock samples. Analytical details are described in Chapter 2.2.1. The concentration of hydrocarbon-like

materials and CO<sub>2</sub> released during non-isothermal open-system pyrolysis as S2 and S3, respectively, are termed hydrogen index HI and oxygen index OI when normalised to the total organic carbon TOC concentration of the source rock (Espitalié *et al.*, 1977). These indices were shown to be analogous to the atomic H/C and O/C ratios of kerogens, and therefore allow kerogen type and hence source quality to be determined (Forsman and Hunt, 1958; Tissot *et al.*, 1974; Horsfield *et al.*, 1983).

### ***Source Rock Quality – Genetic Potential***

TOC and Rock-Eval data for immature source rocks provided by Shell (6), Total (6), Eni (6), Petrobras (1), Devon (4), Wintershall (12), and GFZ (26) are presented in Table A 1 (Appendix) and in Fig. 3.2. It can be said that all important kerogen types from hydrogen-rich Type I over Type II to hydrogen-poorer Type III as well as mixtures of those are covered providing the basis to gain a general understanding of the relationship between organic matter structure and late gas generation behaviour. All of the organic rich samples are of high quality exhibiting excellent hydrocarbon generation potentials (Fig. 3.2a+b). Type I and Type II source rocks with HI's exceeding 350 mg HC/g TOC are said to be mainly oil prone, Type III source rocks with HI's below 100 mg HC/g TOC are solely gas prone. Values in between indicate oil and gas generative potentials (Baskin, 1997).

#### *Organic leaner source rocks*

Interestingly, organic leaner source rocks (Fig. 3.2c) with TOC contents below 2.5%, e.g. 5 Farsund Fm. samples provided by Maersk (G0007162, G0007163, G0007164, G0007165, G0007166) or 1 Mahakam Delta (G0006206) and 2 Douala Basin (G0006204, G0006205) samples provided by Total, feature a kerogen Type III composition, which might be due to the previously discussed mineral matrix effects leading to an underestimation of pyrolysis yield (Espitalié *et al.*, 1980). At least those effects are apparent for the two Silurian Hot shales G005936 (TOC 0.93%) and G006948 (TOC 3.14%) provided by Shell which exhibit low HI's around 50 mg HC/g TOC but very high OI's, 91 and 198 mg CO<sub>2</sub>/g TOC respectively, even though terrestrial higher land plant derived lignin can be excluded as CO<sub>2</sub> precursor structures for reasons of geologic age. The same applies to sample G007161 from the Ghadames Basin (Eni), even though HI is a little bit higher and OI somewhat lower. The Silurian sample G005937 (TOC 4.29%) provided by Shell has a very poor petroleum generative potential with a S2 values of 0.5 mg HC/g rock paralleled by an extremely low T<sub>max</sub> of 285°C but high PI of 0.38 (Fig. 3.2f). High S1 or S1/(S1+S2) (Production index PI) values may indicate on the one hand non-indigenous hydrocarbons such as organic drill mud additives, and on the other hand

### 3 GEOCHEMICAL CHARACTERISATION

oil or gas-shows and seeps, as migrated hydrocarbon species are primarily detected in the lower temperature S1 peak (Horsfield *et al.*, 1983).

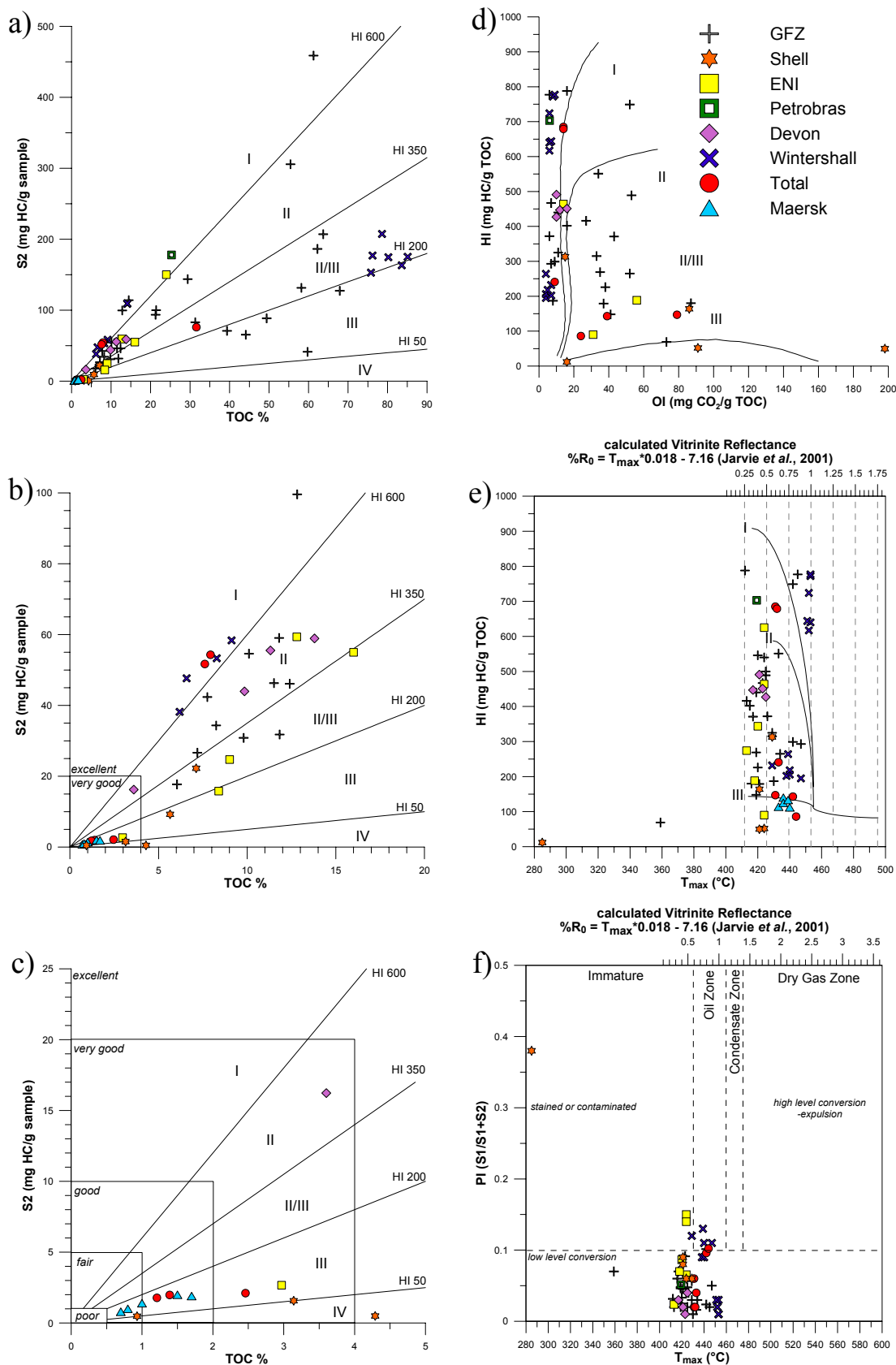


Figure 3.2: TOC and Rock-Eval data for immature source rocks – Kerogen type (a-e) and maturity (e-f)

#### *Kerogen Type I*

Type I kerogen composition based on HI's exceeding 600 mg HC/g TOC can be ascribed to the GFZ samples Alaskan Tasmanite G000693, Green River Shale G004750, and Brown Limestone G000731, to the Petrobras sample from the Irati Fm. G005812 and the Eni sample from the Domanik Fm. G004563 as well as to the two Toarcian Shale samples G006208 and G006209 provided by Total and 6 Cretaceous Wealden Shales from Germany provided by Wintershall (G006535, G006536, G006540, G006547, G006553, G006554).

Nevertheless, and deduced from open-pyrolysis GC fingerprinting (see next Chapter 3.2.1), kerogens within many of those source rocks, with the exception of the Green River Shale and Wealden Shale samples, can be described as being of a rather marine origin, whereas Type I kerogens are often said to be derived from anoxic lacustrine depositional environments. In the case of the Irati Fm., the specific source rock sample was indeed taken from a marine influenced compartment of the basin (E. Santos Neto, pers. comm.).

#### *Kerogen Type II*

Classic oil prone anoxic marine shales are often comprised of Type II organic matter exhibiting HI's between 350 and 600 mg HC/g TOC at immature stages. The Woodford Shales (G006153, G006154), Caney Shale sample G006155 and New Albany Shale sample G006156 (all Devon Energy) as well as the Domanik Fm. sample G004563 and Murzuq Basin samples G004564 and G007160 (all Eni), all of paleozoic age, contain this type of kerogen.

Based on HI values the following Paleozoic source rocks (GFZ) can also be described as being comprised of Type II kerogen: Woodford Shale G000690, Chattanooga Shale G000692, Alum Shale G000753, and Bakken Shale G005298, as well as the Boghead Coal G000697, which, however, is not a marine anoxic shale but a sapropelic Type I coal of lacustrine, algal origin. Mesozoic or younger Type II source rocks are Jet Rock G000696, Messel Oil Shale G000859, Spekk Fm G001955, and 3 Fischschiefer samples (G004070, G004071, G004072).

#### *Kerogen Type II/III*

Type II/III kerogens, defined based on HI's between 350 and 200 mg HC/g TOC, might not necessarily be mixtures of marine Type II and terrestrial Type III kerogen, but could as well be mixtures of Type I and Type III organic matter, which is most likely the case in deltaic settings with lignin derived Type III precursors and plant leaf wax/cutan derived Type I precursors being abundant (Dembicki, 2009). This effect can be demonstrated for the

synthetic Type I/III mixture (G00047501065; HI = 265 mg HC/g TOC), which is comprised of 50% Åre Fm. sample G001965 and 50% Green River Shale sample G004750, even though the latter is of algal origin. Thus, the Type II/III description should be taken as a general hydrocarbon potential estimate only.

Investigated source rocks provided by industry partners and falling into this category are Akata Shale G005935 (Shell), the Mahakam Delta sample G006207 (Total) and two Hekkingen Fm. samples G005762 and G005763 (ENI), even though an HI of 189 mg HC/g TOC for sample G005763 hints to higher amounts of Type III organic matter within the organic matter structure. Nevertheless, chromatograms (Table A 2) reveal a mixed marine terrigenous depositional environment for both samples by the abundance of alkylthiophenes, phenolic compounds, alkylbenzenes, alkyl-naphthalenes and n-alkane/alkene doublets as will be discussed later (Chapter 3.2.1).

Cretaceous Wealden Coals from Germany (Wintershall; G006533, G006538, G006542, G006544, G006548, G006550), with HI values ranging from 195 to 264 mg HC/g TOC clearly exhibit Rock-Eval Type II/III kerogen composition but are more likely of terrestrial Type III origin. Besides the overall terrestrial chromatographic fingerprint (Table A 2), Killops *et al.* (1998) found that maxima of ca. 250 mg HC/g TOC prior to the effective oil window (Sykes and Snowdon, 2002) appear to be characteristic of all coals and Type-III kerogens in the range  $R_m$  ca. 0.65-0.8% (Durand and Paratte, 1983; Teichmüller and Durand, 1983; Suggate and Boudou, 1993; Bostick and Daws, 1994), which fits the theoretical maturity calculated for the Wealden coal samples (see later). Other kerogen types do not exhibit such distinctive maxima during organic matter evolution. GFZ provided humic coal samples with similar high HI's are the Arang Coal sample G000950 and 2 Talang Akar Coal samples G000670 and G000726.

Shales exhibiting Rock-Eval based kerogen Type II/III compositions are the Jurassic Autun Oil Shale G000883 as well as the Paleozoic Botneheia Shale G000689 and Alum Shale G000758.

### *Kerogen Type III*

Typical Type III humic coals, exhibiting HI's between 200 and 50 mg HC/g TOC, provided by GFZ are samples of the Kugmallit Fm. G000206, Åre Fm. sample G001965, Taglu Fm. sample SN6750, and the Talang Akar Coal sample G000899. Interestingly, the Cannel Coal G000698 as well falls into this category, notwithstanding cannel coal being a reference for aquatic sapropelic Type II organic matter. Relative high amounts of phenolic compounds

within the pyrolysate (Table A 2) indicate enrichment of terrestrial derived material (spores) within this specific sample explaining lower bulk pyrolysis yields. The marine Silurian Hot-shale sample G006949 (Shell) features also a Type III composition. Other industry provided Type III samples are organic leaner with TOC < 5% and were discussed earlier under the aspect of potential mineral matrix effects.

### ***Maturity (PI, $T_{max}$ )***

The maturity of a given source rock can be roughly assessed from its  $T_{max}$  temperature, which represents the thermal energy required to break the most abundant chemical bonds in kerogen associated with generation of the S2 pyrolysate.

A general immature signature with respect to petroleum generation can be ascribed to the investigated sample set with more than half of the source rocks exhibiting PI's below 0.1 and  $T_{max}$  values below or around 431°C (Fig. 3.2e+f). For source rocks containing Type II and Type III organic matter, a  $T_{max}$  of 435°C is often interpreted as the beginning of catagenesis corresponding to the beginning of petroleum formation and thus to the beginning of decreasing Hydrogen Indices (Espitalié *et al.*, 1985; Espitalié and Bordenave, 1993). As weaker bonds are stripped away first during natural maturation, the  $T_{max}$  is shifted to higher temperatures for the remaining, more mature kerogen (Jüntgen, 1964). From that it can be inferred that  $T_{max}$  is a chemical indicator for thermal maturity and kinetically controlled just like vitrinite reflectance (Tissot *et al.*, 1987). Based on this assumption Jarvie *et al.* (2001) calculated vitrinite reflectances of a large suite of naturally matured Barnett Shales containing Type II organic matter applying an empirical formula ( $R_o = 0.0180 * T_{max} - 7.16$  (%)) and Rock-Eval HI- $T_{max}$  evolution pathways. Using this formula,  $T_{max}$  values measured within the current thesis (431°C) equal a calculated Vitrinite Reflectance  $R_o$  of 0.6% indicating maturity stages before the onset of hydrocarbon generation under geologic conditions (Baskin, 1997).

Elevated  $T_{max}$  values observed for the Type I source rocks Alaskan Tasmanite (G000693) and Green River Shale (G004750) as well as for 6 Type I German Wealden shales provided by Wintershall are caused by the higher stability of very homogenous Type I organic matter made up of selectively preserved lipids featuring mainly strong C-C bonds, a phenomenon previously described in many case studies, e.g. by Tissot *et al.* (1978) for the Green River Formation in the Uinta Basin. As Type I kerogen transformation can be described by one single activation energy in most of the cases, a sign for the homogeneity of the organic matter, correlation between calculated (here ~1%  $R_o$ ) and real maturity is poor, especially at immature stages (Jarvie *et al.*, 2001) with systematically higher  $T_{max}$  values seen for Type I source rocks compared to  $T_{max}$  values seen for Type II source rocks at similar

maturity levels. Low PI values of the discussed Type I samples indicate low-level kerogen conversion, and thus immaturity with respect to hydrocarbon generation.

Higher  $T_{\max}$  values observed for Talang Akar Coal sample G000670 ( $T_{\max}$  442°C) and Botneheia shale sample G000689 ( $T_{\max}$  447°C) as well as for the German Wealden Coal samples provided by Wintershall and the 2 Douala Basin samples provided by Total hint in conjunction with PI's up to 0.15 to an early oil window maturity range (Baskin, 1997). The same is true for the 5 Farsund Fm. samples provided by Maersk, even though retention of pyrolysate by the mineral matrix in these organic lean source rocks might lead to an elevation of  $T_{\max}$  values. Measured Vitrinite Reflectance (done by Maersk; 0.67 – 0.92%  $R_o$ ) supports calculated  $R_o$  data and the postulated early maturity of the samples.

### 3.1.3 Rock-Eval - Natural maturity series

Five natural maturity series spanning different maturity ranges and organic matter types were investigated to evaluate the evolution of late gas generation behaviour with maturity as a function of depositional environment. TOC/Rock-Eval data is given in Table A 2 (Appendix).

For compilation of a continuous Type III natural maturity sequence nine unextracted and extracted immature Cenozoic New Zealand coals were used, covering sub-bituminous to high volatile bituminous coal ranks (0.40% - 0.80%  $R_o$ ), as well as six Carboniferous German Coal samples (0.99% - 2.81%  $R_o$ ), covering the maturity range from end of high volatile bituminous coal ranks over medium and low volatile bituminous coal ranks to anthracite. Four Cretaceous Wealden Coals from Germany (Wintershall) with calculated  $R_o$  between 0.56 and 1.37% span high to medium volatile bituminous coal ranks filling the maturity gap between New Zealand and Carboniferous German Coals as well as supplying additional material from another geologic age. Interestingly, Wealden coal samples fit into the overall Rock-Eval maturity trend predefined by New Zealand and Carboniferous German Coals (Fig. 3.3a-d), besides exhibiting slightly lower HI's.

Five Carboniferous Barnett Shale samples from the Fort Worth Basin, Texas (0.40 - 3.21%  $R_o$ ) and four Devonian Exshaw Fm samples from Canada (0.76 - 3.33%  $R_o$ ) are investigated as examples for Type II to Type II/III organic matter evolution.

#### *Type III natural maturity sequences*

TOC and Rock-Eval data for the Type III New Zealand coals was taken from Vu (2008) and display (Fig. 3.3b+c) for unextracted samples the usual trend of rising HI values with maturity

( $R_o = 0.40\%$  to  $0.80\%$ ;  $T_{max} = 418^\circ\text{C}$  to  $436^\circ\text{C}$ ) from 161 to 267 mg HC/g TOC as well as an increase in TOC content from 58% to 75% (Fig. 3.3a), which appears, in addition to the well documented preferential loss of various oxygen functionalities through the diagenesis stage (Durand and Monin, 1980; Boudou *et al.*, 1984; Suggate and Boudou, 1993; Killops *et al.*, 1998), to be partly related to the loss of moisture (Vu *et al.*, 2009). The increase in HI prior to oil expulsion can be generally observed for New Zealand Coals (Sykes and Snowdon, 2002) and was explained by structural rearrangements of the coal macromolecular matrix during catagenesis following earlier published results of Schenk and Horsfield (1998). In contrast, Vandenbroucke and Largeau (2007) claimed that during diagenesis, the loss of O-containing molecules results in a concentration of potential hydrocarbon generating structures, and hence an increase in HI and decrease in OI, both features observable in Fig. 3.3b with OI's decreasing from 49 to 5 mg  $\text{CO}_2/\text{g TOC}$ . The simple release of large amounts of  $\text{CO}_2$ , CO and other oxygen functionalised groups was also used by Vu (2008) as an explanation for the observed trend.

The relative immaturity of unextracted New Zealand coal samples is, besides measured vitrinite reflectance, indicated by low PI's  $< 0.10$  (Fig. 3.3d), even though New Zealand coals (samples used for this study) show high azetropic solvent extraction yields between 51 and 108 mg/g TOC. Nevertheless, the extracted bitumen is enriched in heavy ends, asphaltenes and resins (NSO's)(Vu, 2008), components which do not necessarily appear in the S1 peak but contribute considerably to the S2 yield owed to their relative non-volatility for pyrolysis temperatures below  $350^\circ\text{C}$  (Clementz, 1979; Orr, 1983; Tarafa *et al.*, 1983; Tarafa *et al.*, 1988; Wilhelms *et al.*, 1991). The loss of these  $\text{C}_{6+}$ -compounds during extraction explains lower HI's for the extracted coal samples (Fig. 3.3b+c). Rock-Eval parameters of extracted New Zealand Coal samples generally follow the same trends as those for unextracted samples besides elevated PI's, which can be tracked back to solvent residue remaining in the coal after extraction (Vu, 2008).

TOC data for the unextracted Type III humic German Coals was taken from Horsfield and Schenk (1995), Rock-Eval parameters were rechecked within this study by the subcontractor APT. HI values decrease from 208 mg HC/g TOC for the least mature sample G000721 ( $T_{max} = 438^\circ\text{C}$ ;  $0.99\% R_o$ ) down to 10 mg HC/g TOC for the most mature sample G001096 ( $T_{max} = 596^\circ\text{C}$ ;  $2.81\% R_o$ ) (Fig. 3.3a-c), which can be explained by petroleum generation and expulsion or partly by the incorporation of aliphatic structures via aromatisation into the refractory residual organic matter under natural conditions in the course



of maturation from high volatile bituminous ranks to anthracite (Horsfield and Schenk, 1995; Schenk and Horsfield, 1998). PI's (Fig. 3.3d) and OI's (Fig. 3.3b) are generally low as oxygen containing precursor structures already evolved at earlier maturation stages.

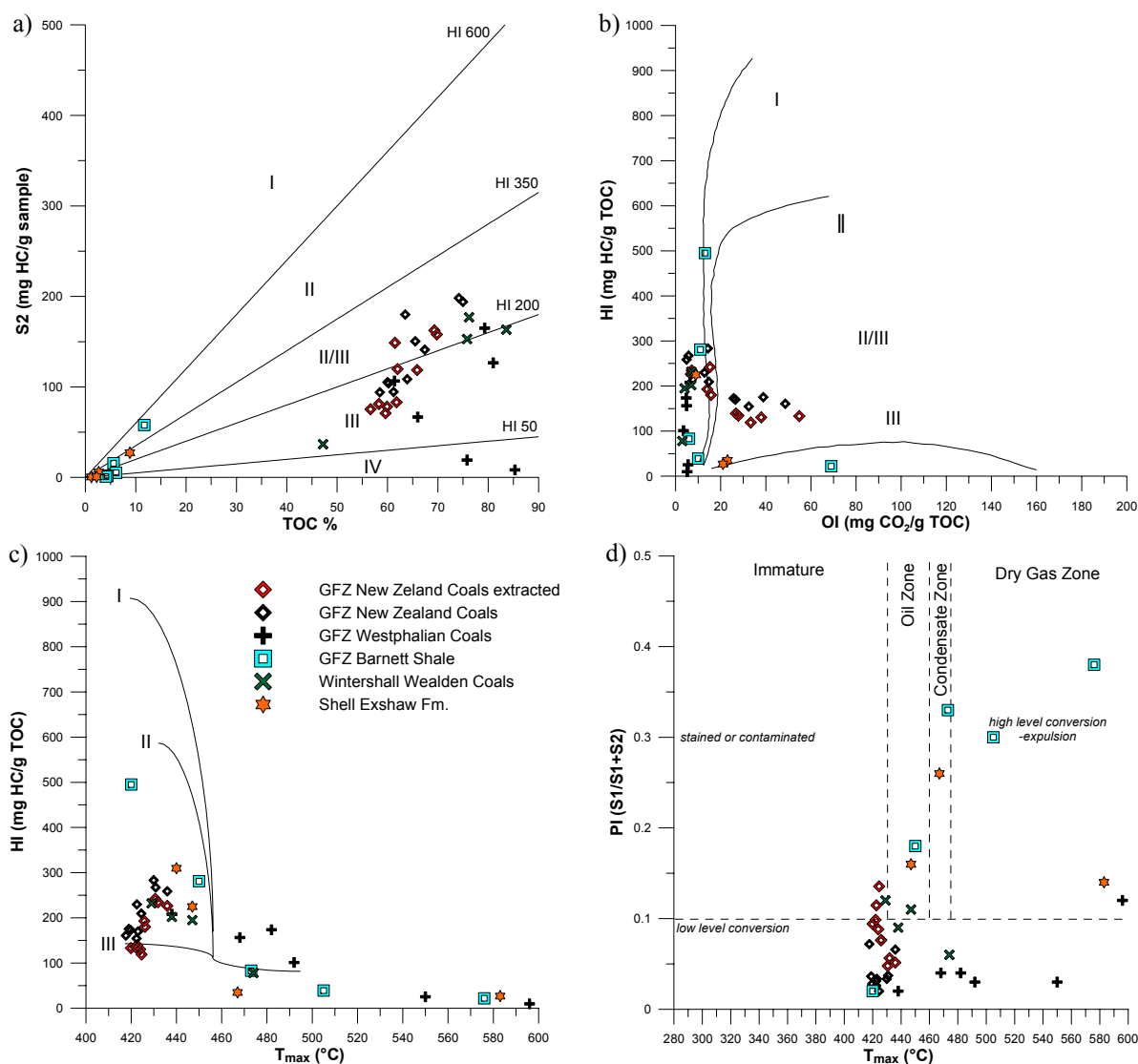


**Figure 3.3: Evolution of TOC content and Rock-Eval parameter with maturity – natural maturity sequences**

### *Type II natural maturity sequences*

Rock-Eval parameters of the least mature Exshaw Fm. Shale sample G006385 had to be estimated from bulk kinetics ( $T_{\max} \sim 440^\circ\text{C}$ ) and open-system pyrolysis GC experiments ( $S_2 \sim 27.36$  mg HC/g sample) as available sample material was not present in sufficient amounts. The TOC was measured in duplicate at GFZ. A calculated HI of 310 mg HC/g TOC indicates a Type II/III kerogen composition. Nevertheless, and related to an already advanced maturity state already well within the range of peak oil generation ( $0.76\%$   $R_o$ ), higher hydrocarbon potentials, and thus Type II kerogen can be expected for more immature equivalents.

In contrast, the least mature Barnett Shale sample exhibits an HI of 495 mg HC/g TOC with a  $T_{\max}$  of 420°C (0.40%  $R_o$ ) and is representative of a typical immature Type II marine oil prone source rock of the north-central Texas unconventional shale-gas system (Jarvie *et al.*, 2007).

For the Barnett Shale samples (Data supplied by Dan Jarvie) as well as for the Exshaw Formation samples similar TOC/Rock-Eval parameter trends with maturity can be observed (Fig. 3.3a-d). Decreasing HI's in conjunction with decreasing TOC contents indicate petroleum generation and expulsion during catagenetic stages. Increasing OI's at highest maturity levels for both sample series (Fig. 3.3b) can be tracked back to previously discussed mineral matrix effects regularly seen for organic lean source rocks (Espitalié *et al.*, 1980) as oxygen containing functional groups should have been already degraded. In addition, immature sample equivalents exhibit only low initial OI's typically observed for organic matter deposited in a marine anoxic environment.

PI's increase uniformly with maturity to values above 0.10 in the oil and condensate zone and slightly decreases in the high level conversion-expulsion zone as secondary oil cracking sets in and gas is formed, which is harder to retain by the source rock than higher molecular weight material. An unusual high PI of 0.38 for the most mature Barnett Shale sample might hint to adsorbed gas in place (GIP).

### ***3.2 Detailed Kerogen Composition (Open Py-GC)***

For further characterisation of the source rock quality, i.e. molecular kerogen type and not only genetic potential as measured by Rock-Eval pyrolysis, open-system-pyrolysis-GC was used, which provides detailed insights into the macromolecular organic matter in terms of its structural moieties (Horsfield *et al.*, 1983; Larter, 1984; Horsfield, 1989; Eglinton *et al.*, 1990). The major chemical building blocks of kerogen are determined by their biological precursors and the modifications brought about during diagenesis and catagenesis allowing for determination of depositional environments as well as prediction of bulk petroleum compositions. To what extent late gas generation is governed by these original building blocks, or petroleum type organofacies, is one of the key questions to be solved within this thesis.

#### **3.2.1 Immature source rock samples**

In this thesis, open pyrolysis-GC is used to characterise the organic matter within the worldwide sample set of immature source rocks in terms of kerogen structure and petroleum type organofacies. All chromatograms, petroleum type organofacies ternaries, as well as identified compounds and quantitative data for the single samples can be found in Table A 2 (Appendix). The data, i.e. ratios and ternaries, is later used (Chapter 4.2.4) to relate late gas generation behaviour (Chapter 4.2.2) to kerogen type and structure.

#### ***Kerogen Classification based on Chain Length Distribution - Petroleum Type Organofacies***

Fig. 3.4 shows the kerogen classification established by Horsfield (1989) and newly calibrated in Horsfield (1997), which employs the aliphatic fraction, i.e. *n*-alkyl-chain-length distribution versus total gas C<sub>1-5</sub>, from open-system pyrolysis experiments in a ternary diagram. As a first result, it should be noted that pyrolysate compositions of the different investigated source rocks plot in all predefined petroleum type organofacies fields indicating a good coverage of the main molecular organic matter types within this study. Horsfield (1989) has demonstrated that this ternary diagram allows organic matter typing as well as the typing of petroleum inferred to be formed from the studied source rocks and is build onto the basis that reactions leading to the formation of *n*-alkanes and *n*-alkenes under laboratory conditions are comparable to those leading to the formation of *n*-alkanes under geological conditions (Horsfield, 1997; Schenk and Horsfield, 1998). The relative abundance of each homologue is

controlled to variable degrees by the chain length of the linear aliphatic precursor moiety in the kerogen and therefore represents a minimum value, as second-order reactions are not prevalent under open-system pyrolysis conditions. Thus, Horsfield (1989) defined petroleum type organofacies fields based on the observation that source kerogens of high wax oils have a high proportion of long-chain *n*-alkanes and *n*-alkenes in their pyrolysates, whereas major sources of gas are characterised by very short average *n*-alkyl chain length. Intermediate chain lengths were found to characterise anoxic marine shales, which generate low-wax crude oils in nature, etc.

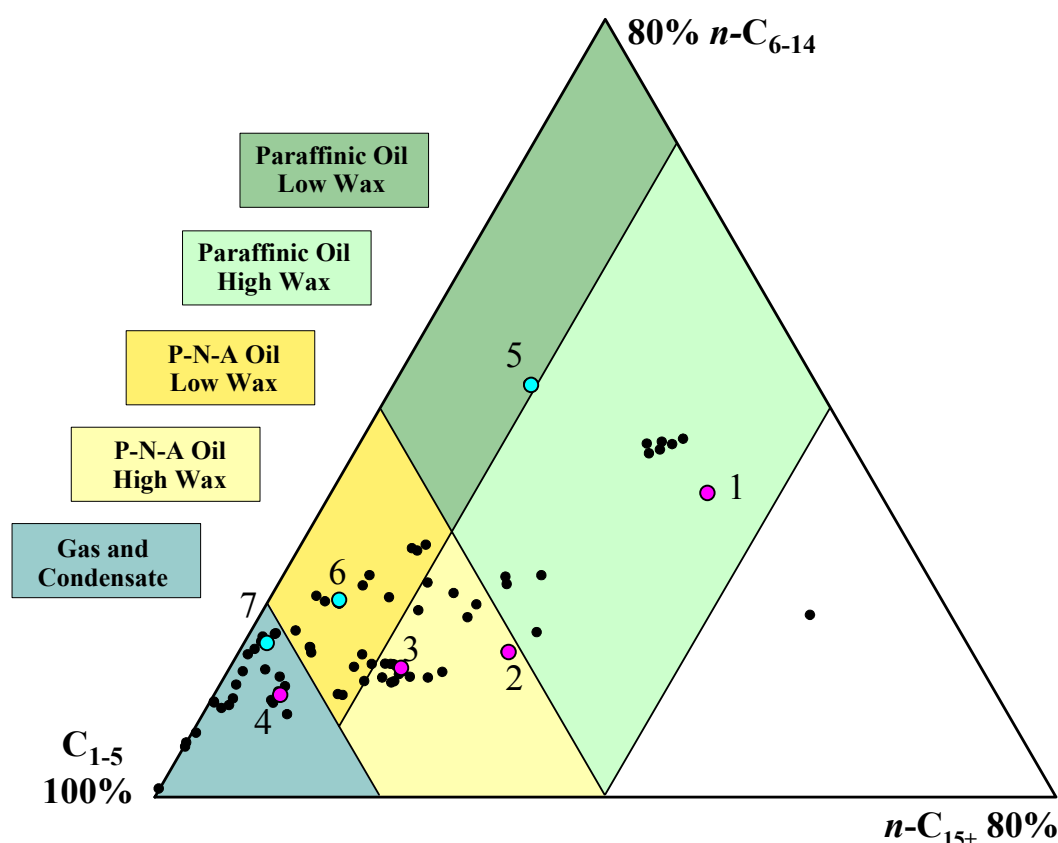


Figure 3.4: Open-pyrolysis GC-FID data for immature source rocks and unextracted New Zealand Coals – Kerogen typing (Petroleum type organofacies) on a molecular basis applying the alkyl-chain length distribution classification established by Horsfield (1989) and modified by Horsfield (1997). For data see Tab. 3-1. Original chromatograms of numbered samples typifying the different organofacies are displayed in Fig. 3.5.

In Fig. 3.5 seven pyrograms typify the different organic matter qualities and petroleum type organofacies encountered for the investigated sample set:

*Paraffinic, High-Wax petroleum type*

The homogenous Type I Green River Shale sample G004750 is dominated by long and short *n*-alkane/*n*-alk-1-ene alkyl chains with mono- and di-aromatic compounds being present in

comparable low relative abundance (Fig. 3.5) and plots, not entirely surprisingly, in the paraffinic, high-wax petroleum type organofacies field (number 1 in Fig. 3.4). Horsfield (1989) named this field after the composition of Uinta Basin oils (Tissot *et al.*, 1978) charged by the lacustrine Green River Formation, and used pyrolysates of the like, consistent in composition with the crude oils, to define it.

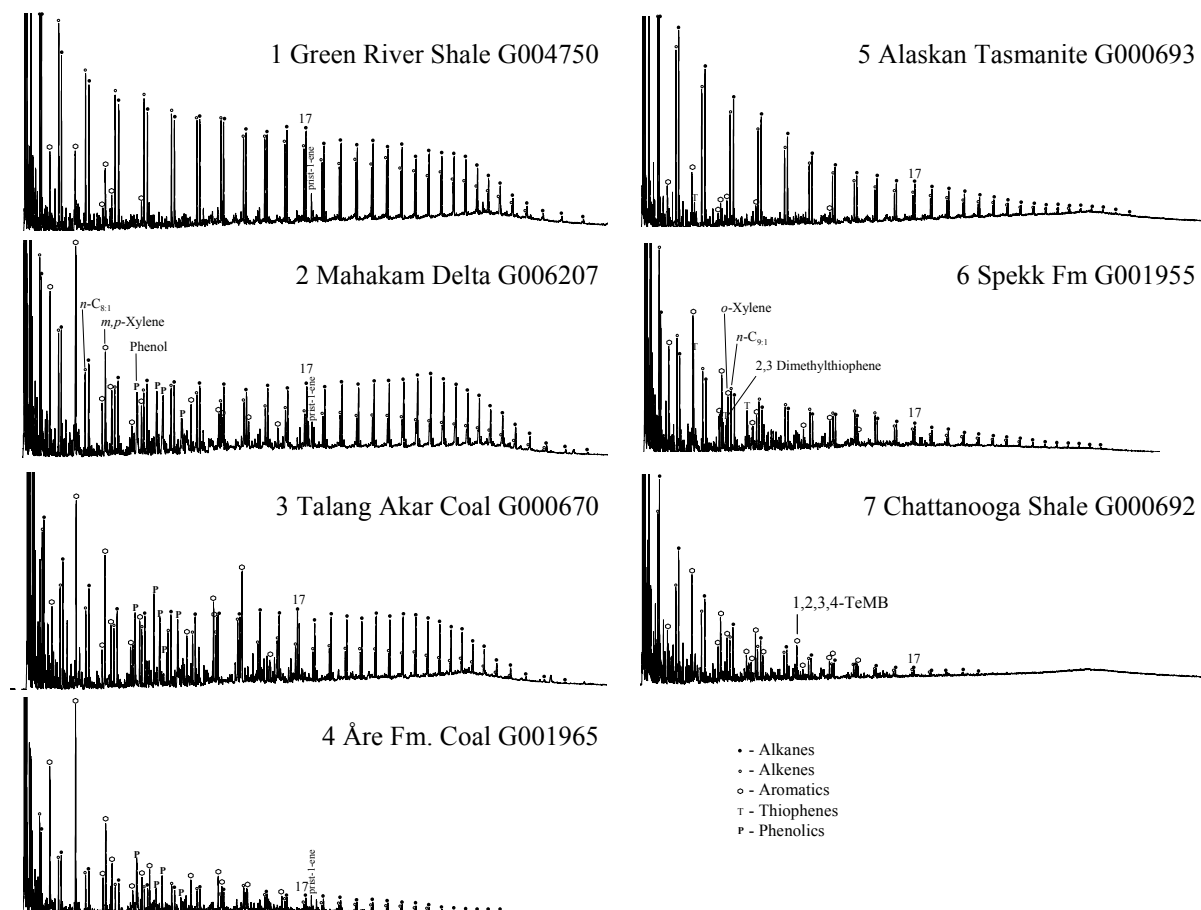


**Figure 3.5:** Seven open-pyrolysis gas-chromatograms (fingerprints) of immature source rocks typifying different organic matter qualities and petroleum type organofacies. The positions of some components playing important roles as geomarker or input parameters for kerogen classification diagrams are highlighted.

The molecular structure of kerogens yielding this type of pyrolysates are strongly related to the selective preservation of the outer cell walls of microalgae, which are highly aliphatic (Berkaloff *et al.*, 1983), e.g. remains of *Botryococcus braunii* in the case of Green River Shale or Boghead coal (in this study sample G000697). Six Type I German Wealden Shale samples provided by Wintershall (Data in Table A 2) seem to consist of similar organic matter deposited in a lacustrine, anoxic environment. The pyrolysate of the synthetic Type I/III kerogen mix (G0047501965 – 50% Green River Shale and 50% Åre Fm. Coal) is also dominated by long *n*-alkyl-chains up to  $>C_{30}$  but exhibits a composition much closer to the

border of the high wax, paraffinic-naphthenic-aromatic (P-N-A) crude oil generating facies. Due to the fraction of terrigenous derived Åre Formation Coal in the mixture, which represents humic material generating gas and condensates upon natural and artificial maturation (see later), phenolic compounds are very abundant and low molecular weight aliphatics are of greater importance compared to the original Green River Shale sample G004750.

Other samples exhibiting a paraffinic, high-wax composition grading into and intercalating with the high- to low-wax P-N-A crude oil generating facies are the Type II Fischeischiefer samples from the Schöneck Fm (G004070, G004071, G004072), which were deposited during lower Oligocene time in a shallow marine environment on the northern, upper paleo-slope of the Austrian Molasse Basin, after the first isolation of the western Central Paratethys (Schulz *et al.*, 2002). They are mostly derived from autochthonous hydrogen-rich organic matter (alginite, liptodetrinite). The extend of change in chain length distribution has been earlier described by Sachsenhofer (1994), with lowest wax contents for anoxic marine deposition and highest wax content for non-marine environments.

#### *Paraffinic, Low-Wax petroleum type*

The domination of intermediate chain lengths, i.e. low wax content, is a common feature in pyrograms of marine derived source rocks. This is best seen for the very homogeneous Type I Alaskan Tasmanite sample G000693 originating from selective preservation of the remains of the prasinophyte alga *Tasmanites* (Fig. 3.4 and Fig. 3.5) with pyrolysates exhibiting low amounts of aromatic compounds but a strong enrichment in normal paraffinic moieties up to  $n\text{-C}_{21}$ . The chain length distribution closely corresponds to the lipid fraction of the extant algal biota, deposited in a marine system under conditions of persistent anoxia (Jones, 1987; Horsfield, 1989 and references therein). This facies is relatively rare (thus only one sample in the sample set) and named low wax, paraffinic crude oil generating facies after the composition of Ordovician oils in the Michigan Basin (Horsfield, 1989) sourced from algal kerogen.

#### *Paraffinic-Naphthenic-Aromatic (P-N-A), Low-Wax petroleum type*

Most other marine source rocks such as black shales and carbonates of high petroleum potential display, besides a domination of intermediate normal alkyl-chains, an enrichment in aromatic compounds such as alkylbenzenes and alkylnaphthalenes, as well as sulphur containing compounds such as alkylthiophenes in their pyrograms (e.g. Spekk Fm. sample

G001955 in Fig. 3.5). Their organic matter is derived from algal and bacterial inputs containing autochthonous material in abundance, as well as terrigenous debris. Most dominant aromatic hydrocarbons are toluene and xylenes, with amounts equalling or exceeding those of *n*-hydrocarbons in the same boiling range. Aromatic compounds have been described as products from the non-condensed aromatic structure of Type II kerogen, like carotenoids (Behar and Vandenbroucke, 1987; Hartgers *et al.*, 1994b), which are released in the form of labile moieties during artificial and natural maturation (Horsfield, 1997). Alkylthiophenes are formed during early diagenesis by intermolecular sulphur incorporation reactions involving functionalised lipids and hydrogen sulphide (Brassell *et al.*, 1986; Sinninghe Damsté and De Leeuw, 1990), and are released preferentially by thermal degradation of polysulphide bonded linear C<sub>5</sub>-C<sub>7</sub> skeletons (Sinninghe Damsté *et al.*, 1998).

Upon open pyrolysis most marine derived organic matter yield pyrolysates plotting in the P-N-A, low-wax petroleum type organofacies field (Horsfield, 1989). The upper Jurassic marine Type II Spekk Fm. sample G001955 (Fig. 3.5) exemplifies this low wax, P-N-A crude oil generating facies in Fig. 3.4, which was defined using Mississippian-Devonian Woodford Shale and Jurassic Toarcian Shale pyrolysates in accordance with the composition of their related oils in the mid-continental U.S.A and Paris Basin, respectively (Horsfield, 1989; Horsfield, 1997). Pyrolysates of Toarcian Shales (in the present study samples G006208 and G006209 provided by Total) thereby tend to plot near the low wax paraffinic petroleum type organofacies field whilst pyrolysates of Woodford Shale tend to grade into the gas and condensate petroleum type organofacies field, which can be also observed e.g., for pyrolysates of the Devonian Duvernay Fm. from Canada *versus* the Jurassic (Lias ε) Toarcian Shale (Posidonienschiefer) from the Hils Syncline, NW-Germany (Dieckmann, 1999).

Further investigated source rocks yielding this type of pyrolysate are the marine Permian Irati Fm. sample G005812 (Petrobras), the marine Devonian Domanik Fm. sample G004563 as well as the two mixed marine-terrestrial Jurassic Hekkingen Fm. samples G005762 and G005763 (Eni), the Carboniferous Caney Shale G006155 (Devon), one of five upper marine Jurassic Farsund Fm. sample provided by Maersk (G007166 – sample with highest TOC content of 1.7%), the Silurian sample G005937 provided by Shell representing most likely migrated oil ( $T_{\max}$  = 285°C; PI of 0.38), and four GFZ provided samples, as there are Triassic marine Botneheia Shale G000689, Devonian marine Woodford Shale G000690, Mississippian marine Bakken Shale G005298, and lacustrine Jurassic Autun Oil Shale G000883, which grades into the high wax P-N-A petroleum type organofacies. Additionally, and discussed a little later, some fluvio-deltaic coals grading from the Gas and Condensate

field through the high wax P-N-A field to the high wax paraffinic field also plot in the low wax P-N-A petroleum organofacies field depending on the individual maceral composition again depending on the depositional region in the fluvio-deltaic system.

The observation that pyrolysates of many of the investigated Paleozoic marine shales (Cambrian Alum Shales G000753 and G000758; Silurian Hot Shales from the Middle-East G006949, Murzuq Basin samples G004564 and G007160, Ghadames Basin sample G007161; Woodford Shale samples G006153 and G006154, New Albany Shale G006156, Domanik Fm. G004563; Carboniferous Caney Shale G006155 and Bakken Shale G005298) tend to grade into the gas and condensate facies, which was initially defined by vitrinite and sporinite pyrolysates (Horsfield, 1989) shall be discussed now. The pyrogram of a Devonian Chattanooga Shale (G000692), a major source of petroleum in the eastern U.S.A., is displayed as an example in Fig. 3.5, in which a predominance of  $C_{1-10}$  aliphatics and mono- plus dialkylaromatics can be observed. Despite being classified as typical hydrogen-rich kerogen from bulk chemistry Rock-Eval pyrolysis, those source rocks have a molecular structure which generates pyrolysates plotting mostly in the gas and condensate field, previously seen for certain organic-rich alginitic Type II marine shales, namely the Alum shale, the Bakken Shale, and the Keg River Formation (Horsfield *et al.*, 1992a; Muscio *et al.*, 1994; Clegg *et al.*, 1997). The authors linked this behaviour to the intrinsic aromatic nature of the immature kerogen macromolecule and/or specific biological precursor material as shown for the Bakken Shale and the occurrence of 1,2,3,4-tetramethylbenzene (TeMB) by Muscio *et al.* (1994). TeMB is indeed a very prominent aromatic component in the pyrolysates of the investigated Paleozoic marine source rocks, appears in natural products, and can be traced back to the  $\beta$ -cleavage of diaromatic carotenoid moieties (Requejo *et al.*, 1992; Hartgers *et al.*, 1994a; Hartgers *et al.*, 1994b; Clegg *et al.*, 1997). The biological precursor is related to a specific green sulphur bacteria (Chlorobiaceae), living under conditions of photic zone anoxia and known to reproduce only in sulphate and hydrogen sulphide-rich water bodies (Abella *et al.*, 1980; Summons, 1993). Since this biogenic related alkylbenzene is abundant in pyrolysis products, as well as in natural products such as crude oils, bitumen and asphaltenes therein, it has use as a geomarker (Lehne and Dieckmann, 2007). The intrinsic aromatic nature of those immature kerogens or possible aromatisation reactions of the biologic precursor material during closed-system artificial or natural maturation leading to the formation of “dead” carbon (Horsfield *et al.*, 1992a; Muscio and Horsfield, 1996) raises the question, if relevant source rocks might also show an enhanced late gas generation potential.



*Gas and Condensate type*

The gas chromatographic fingerprint of the lower Jurassic Åre Fm. Coal sample G001965 (Fig. 3.5) represents the group of vitrinite-rich humic coals, shales and siltstones, which were deposited in continental/deltaic settings such as swamps on lake margins or on the lower delta plain (Horsfield, 1997). As previously mentioned, the gas and condensate field (Fig. 3.4) was defined using pyrolysates of vitrinites and sporinites in accordance with the mainly Type III gas-prone nature of northwest European Carboniferous coals, which are rich in vitrinite and whose major liptinite maceral is sporinite (Stach *et al.*, 1982; Horsfield, 1989).

The German Carboniferous Coal sample G000721 (0.99%  $R_o$ ) (Fig. 3.5) represents this group in the present sample set. The GC-amenable fraction of pyrolysates displays a chain length distribution, which is rich in low molecular weight components with alkylbenzenes, alkyl-naphthalenes as well as phenolic compounds in high abundance. These products originate from the pyrolytic degradation of lignin, sporopollenin and polycarboxylic acids (Stout and Boon, 1994). The very immature Kugmallit Fm. sample G000206 from Canada ( $T_{max}$  359°C – lignite) reveals besides benzene and toluene almost exclusively very high contents of phenolic compounds including most likely methoxyphenols (cf. van de Meent *et al.*, 1980) in its pyrogram (Table A 2), which indicates, due to the pyrolysate composition in the lower left 100% gas corner of the chain length distribution ternary of Horsfield (1989), some lignin end member-character. The chromatogram of the Pennsylvanian Jet Rock sample G000696, supposedly fossilised wood, as well features such extreme phenolic predominance with a somewhat higher abundance of straight chain aliphatics up to at least  $n$ -C<sub>11</sub> (Table A 2). The sapropelic Type III Cannel Coal sample G000698 reveals a higher abundance of longer chains but an enrichment of phenolic compounds indicates an organic matter derived from spores. Talang Akar Coal sample G000899 (Table A 2) also has a kerogen structure yielding pyrolysates plotting in the gas and condensate generating facies. Besides the usual suite of phenolic and aromatic compounds derived from vitrinite, longer chain  $n$ -alkanes/ $n$ -alk-1-enes and increasing amounts of alkyl-naphthalenes complement the gas chromatographic fingerprint. This sample can be taken as an immature end member for the coals of the Deltaic Member of the Talang Akar Formation, which is the source of waxy oil as well as gas and condensate in the Ardjuna Basin.

Based on the relative abundance of low molecular weight and aromatic compounds over heavy and aliphatic compounds within the pyrolysate, the quality of the organic lean source rocks, as there are the Silurian Hot shales from the Middle East (G005936, G006948)

and Ghadames Basin (G007161), 3 samples from the Douala Basin (G0006204, G0006205) and Mahakam Delta (G0006206), as well as 4 Farsund Fm. samples provided by Maersk (G0007162, G0007163, G0007164, G0007165) (Table A 2), can also be described as gas-prone (Horsfield *et al.*, 1983). They are organic lean with respect to open-system pyrolysis ( $S_2 < 3$  mg HC/g TOC), and thus inferred petroleum type is somewhat uncertain related to mineral matrix effects (Dahl *et al.*, 2004). For Paleozoic source rocks it was shown, that Gas and Condensate classification is not unusual. Nevertheless pyrolysates of the relevant Silurian Hot shales seem to be overly gas prone indicating some influence of mineral matrix effects, which also applies to the other samples. Nevertheless a mixed marine – terrestrial organic matter composition for Douala Basin and Mahakam Delta source rocks as well as for the Farsund Fm. shales cannot be ruled out, even though it is well established that the latter was deposited in a fully marine, low-energy environment (Ineson *et al.*, 2003). Generally oil-prone, the lower part of the Farsund Fm. is poorer in organic carbon and terrigenous organic matter is abundant, leading to a mixed gas-/oil-prone kerogen type (Damtoft *et al.*, 1992).

*Paraffinic-Naphthenic-Aromatic (P-N-A), High-Wax petroleum type*

Horsfield (1989) used pyrolysates and petroleum of coals from the Ardjuna Basin to define boundaries of the high wax P-N-A petroleum type organofacies, which usually occurs in lower delta plain and inner shelf environments and commonly grades into and intercalates with the high wax, paraffinic crude oil facies described above (New Zealand Coal sample G001994). Talang Akar coal sample G000670 exemplifies the centre of gravity for these kinds of source rocks, whereas the Mahakam Delta sample G006207 (Total) represents the longer chain dominated part of the sample set (Fig. 3.4 and Fig. 3.5). Chromatographic fingerprints of these coals vary according to maceral composition, with  $n$ -C<sub>5+</sub> chain hydrocarbons concentration correlating with percent “matrix liptinite” (Horsfield *et al.*, 1988). The kerogen consists of vitrinite, cutinite, liptodetrinite, and resinite in variable proportions, and is derived in part from lignocellulosic materials, preserved and partially degraded cuticular tissue and plant resins, which give, upon analytical pyrolysis, phenolic compounds, long chain  $n$ -alkanes and naphthenoaromatic compounds, respectively (Chromatograms 2 and 3 in Fig. 3.5).

Many Tertiary Coals of Southeast Asia and Australia containing higher plant material were shown to fall into this category (Horsfield, 1997 and references therein), which can be confirmed by investigated immature samples from New Zealand (G001983, G001982, G001984, G001981, G001980, G001997, G001996, G001990, G001991) and extended to

German Cretaceous Wealden Coals (G006533, G006538, G006542, G006544, G006548, G006550; Table A 2). One difference between Wealden Coals and Southeast Asian coals (including New Zealand coals) are lower amounts of alkyl-naphthalenic compounds in the pyrolysate of the former and a different shape of the hump fraction, indicating a lower concentration of plant resins such as “Dammar Resin” within the organic matter structure, which was shown to be abundant in Southeast Asian Coals (Horsfield, 1989; Van Aarssen *et al.*, 1990; van Aarssen *et al.*, 1991; van Aarssen *et al.*, 1992; Horsfield, 1997). As maceral abundances in the fluvio-deltaic system are thought to be influenced strongly by the actions of meandering river channels and tidal currents, which erode peat deposits and segregate the macerals (Thompson *et al.*, 1985), some coals can be relatively depleted in cuticular tissues and intercalate into the low wax P-N-A petroleum type organofacies as well as into the gas and condensate field (Talang Akar Fm. sample G000899). Talang Akar Fm. Coal G000726, Taglu Fm. Coal SN6750, Arang Coal G000950, as well as some New Zealand and German Wealden Coals are examples for fluvio-deltaic organic matter with an inferred low wax P-N-A crude oil generating character.

Other source rocks, i.e. shales, exhibiting a high wax P-N-A petroleum composition, tend to plot more towards the top of the organofacies type field. The Akata shale sample G005935 (Table A 2) resembles gas chromatographic fingerprints of previously described coals deposited in lower delta plain and inner shelf environments. In fact, the Akata Formation, which is the source of most of the petroleum in the Tertiary Niger Delta petroleum system, is of marine origin and was formed during low stands when terrestrial organic matter and clays were transported to deep water areas characterized by low energy conditions and oxygen deficiency (Short and Stäuble, 1965; Stacher, 1995).

In contrast, the pyrolysate of the sulphur-rich marine Brown Limestone G000731 from Jordan, which generates low API, high-sulphur heavy crude oils at early maturity stages under natural conditions (Orr, 1986; di Primio and Horsfield, 1996), plots at the border to the low wax P-N-A petroleum type field and displays high amounts of alkylthiophenes, a typical domination of intermediate *n*-alkyl chains and phenolic compounds in only very low abundance. The lacustrine alginitic Messel Oil Shale sample G000859, even though derived from the algae *Tetradron minimum* (Goth *et al.*, 1988) generates, besides long *n*-alkane/*n*-alk-1-ene alkyl chains up to C<sub>30</sub>, additional amounts of short chain homologues and prominent phenolic compounds indicating input of terrigenous material such as spores or the like. Sulphur containing compounds are scarce confirming lacustrine depositional environment.

### ***Kerogen Classification based on aliphatic, aromatic, oxygen- and sulphur-bearing compounds – Depositional Environment***

As mentioned previously, a small, GC-amenable proportion of low-polarity pyrolysis products is representative of the petroleum precursor structural moieties in the parent kerogen as a whole (Horsfield, 1989; Eglinton *et al.*, 1990; Larter and Horsfield, 1993). The immature source rocks under investigation can be further characterised using, besides the ternary diagram established by Horsfield (1989), two ternary diagrams, in which readily identifiable aliphatic, aromatic, oxygen- and sulphur-bearing compounds are employed (Fig. 3.6, Tab. 3-1). In the ternary diagram of Larter (1984)(Fig. 3.6b), which was originally implemented to distinguish between phenol-rich and phenol-poor Type III source rocks, the amount of kerogen representing land plant derived moieties can be inferred by relative proportions of phenol, *n*-octene and *m,p*-xylene in the pyrolysate. As pyrolytic thiophenes were shown to be proportionally representative of kerogen-bond-sulphur molecules (Eglinton *et al.*, 1990), the use of 2,3-dimethylthiophene and *o*-xylene and *n*-C<sub>9:1</sub> in a ternary diagram (Fig. 3.6c)(as proposed by Eglinton *et al.*, 1990) allows the discrimination of source rocks deposited in marine or hypersaline sedimentary environments and those deposited in freshwater lacustrine or terrestrial environments.

#### *Homogeneous Alginites – lacustrine and marine depositional environments*

Homogeneous, lacustrine algal kerogens (Green River Shale, Wealden Shales, Boghead Coal) were previously shown to be characterised by pyrolysates enriched in long and intermediate alkylchains compared to gas compounds, which infers paraffinic high wax oil generation in nature (Fig. 3.6a). Aromaticity, i.e. the sum of identified aromatic and phenolic compounds divided by the sum of all identified C<sub>6+</sub> compounds (Tab. 3-1), as well as phenol (Fig. 3.6b) and sulphur contents (Fig. 3.6c) are very low. The latter features can be as well noticed for the homogeneous marine Type I alginite Alaskan Tasmanite (G000693), whose pyrolysate is strongly enriched in normal aliphatic moieties up to *n*-C<sub>21</sub> yielding a paraffinic low wax petroleum type.

#### *Mixed lacustrine – terrestrial to fluvio deltaic depositional environments*

As observed for the Messel Oil Shale (G000859), Cannel Coal (G000698) and the synthetic Type I/III kerogen mixture, input of higher plant material into an aquatic lacustrine system leads to an overprint of the algal signature, which is illustrated by higher proportions of

phenolic and aromatic compounds relative to aliphatic compounds (Fig. 3.6b and c) as well as a shorter chain length distribution (Fig. 3.6a). Sulphur content is still low (Fig. 3.6c).

The latter is also a general feature of fluvio deltaic – terrestrial derived organic matter, which gives, upon analytical pyrolysis, mainly phenolic and aromatic compounds (Fig. 3.6b), as well as varying amounts of long chain  $n\text{-C}_{15+}$  moieties depending on the present maceral composition (Horsfield, 1997). Vitrinite- and sporinite-rich shales and coals generate gas and condensates, whereas humic source rocks containing higher amounts of long straight-chain aliphatic precursor material generate pyrolysates inferring a PNA low wax through PNA high wax to Paraffinic high wax (New Zealand Coal G001994) petroleum type (Fig. 3.6a; Tab. 3-1).

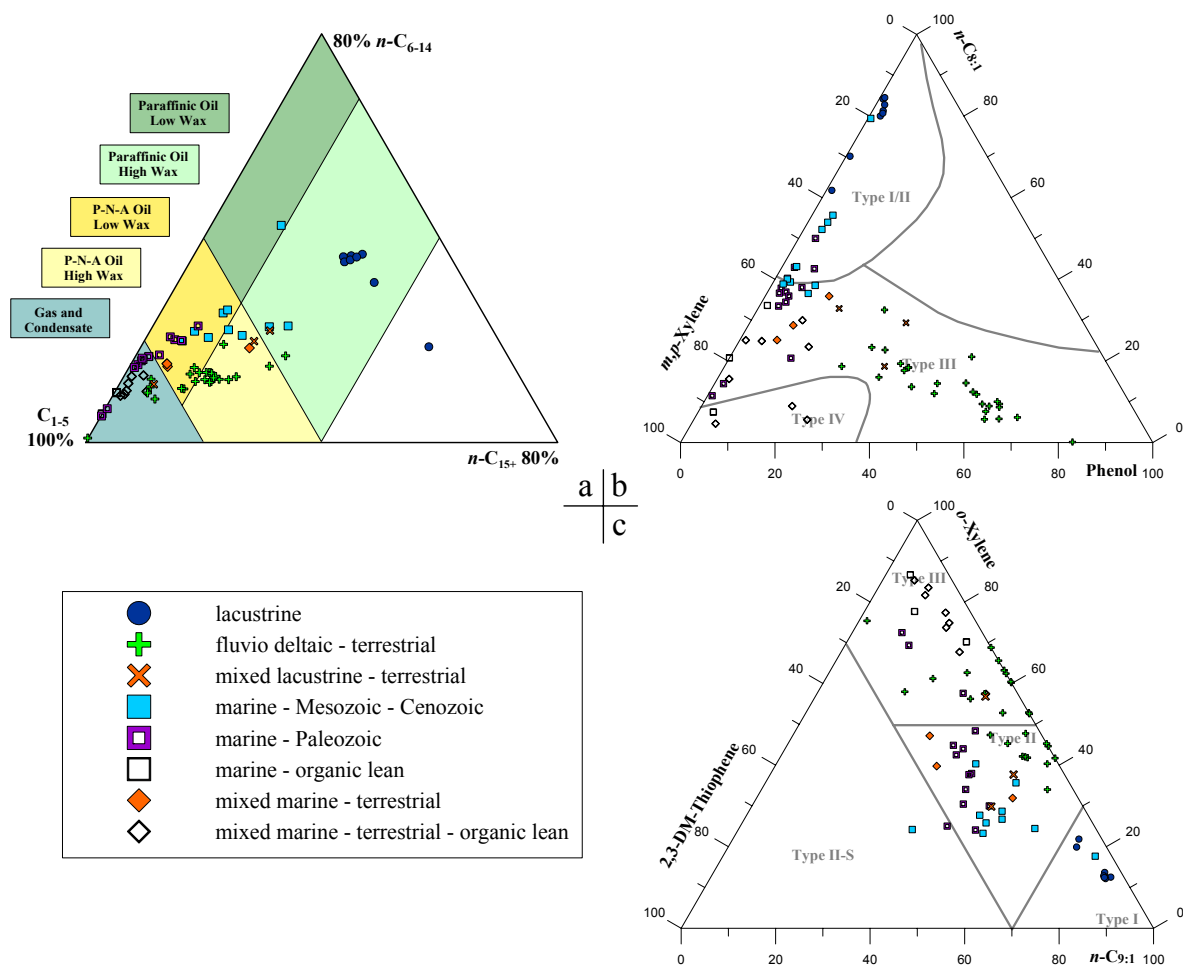


**Figure 3.6:** The relationship between depositional environment and molecular kerogen structure displayed using three ternary diagrams of a) Horsfield (1989), b) Larter (1984), and c) Eglinton *et al.* (1990)

#### *Marine depositional environments*

Pyrolysis products of typical algal/bacterial derived anoxic marine source rocks mostly display, besides a domination of intermediate normal alkyl chains (Horsfield, 1989) high relative amounts of sulphur compounds, such as 2,3-dimethylthiophene (Fig. 3.6c), and low

relative amounts of non-land plant derived phenolic compounds, such as phenol (Fig. 3.6b). The dominance of aliphatic over aromatic compounds like alkylbenzenes and alkylnaphthalenes varies strongly as illustrated by very different ratios of *m,p*-xylene over octene (Fig. 3.6b) and *o*-xylene over nonene (Fig. 3.6c).

Higher aromaticity is, as previously discussed, observed for Paleozoic marine shales, which tend to grade from the PNA low wax organofacies field into the gas and condensate field, whereas investigated Mesozoic to Cenozoic source rocks display a lower aromaticity with pyrolysate compositions grading from the PNA low wax field through the PNA high wax into the Paraffinic high wax field (Fig. 3.6a-c). The carbonate source rock, Brown Limestone from Jordan (G000731), plots on the border of the PNA high to low wax organofacies field and is the overall sulphur-richest sample of the sample set (Fig. 3.6a and c).

#### *Mixed marine – terrestrial and marine - deltaic depositional environments*

Samples deposited in a mixed marine – terrestrial or marine - deltaic environment contain, besides algal and bacterial inputs yielding intermediate *n*-alkyl moieties upon pyrolysis (Fig. 3.6a), variable amounts of allochthonous terrestrial debris of differing composition and maturity. Source rocks of the Hekkingen Fm. (G005762, G005763) e.g. generate pyrolysates rather enriched in sulphur (marine input Fig. 3.6c) and aromatic compounds (Fig. 3.6c and Tab. 3-1), inferring a PNA low wax petroleum type grading into the gas and condensate facies (Fig. 3.6a), whereas the Akata Shale sample (G005935) generates pyrolysates enriched in long alkyl chains with higher amounts of phenolic compounds, (Fig. 3.6b) inferring a PNA high wax petroleum type. The pyrolysate composition of Hekkingen Fm. samples suggest terrestrial input of resinite or early mature vitrinitic material due to relative low amounts of phenolic compounds but high aromaticity, whereas the pyrolysate composition of Akata Shale suggests higher proportions of terrestrial derived cutinite and/or liptodetrinite besides vitrinite.

#### *Organic leaner source rocks*

The gas and condensate classified, organic lean samples (Fig. 3.6a), as there are the Silurian Hot shales from the Middle East (G005936, G006948) and Ghadames Basin (G007161), 3 samples from the Douala Basin (G0006204, G0006205) and Mahakam Delta (G0006206), as well as 4 Farsund Fm. samples provided by Maersk (G0007162, G0007163, G0007164, G0007165)(Table A 2), are all characterised by an unusually high aromaticity as well as low sulphur contents (Fig. 3.6b+c) indicating mineral matrix effects (Horsfield and Douglas, 1980). Pyrolysate compositions of Farsund Fm. samples G007165 and G007166 allows

### 3 GEOCHEMICAL CHARACTERISATION

organic matter to be typified as mixed marine – terrestrial related to somewhat enhanced phenol contents.

**Table 3-1: Normalised single compound yields as input parameters for determination of kerogen quality and structure using ternary diagrams of Horsfield (1989), Larter (1984), and Eglinton *et al.* (1990),**

GFZ Code	Formation/ Basin	Age	Petroleum Type Organofacies	Depositional Environment	Horsfield (1989) Chain Length Distribution normalised yields		
					Total C <sub>1-5</sub>	<i>n</i> -C <sub>6-14</sub>	<i>n</i> -C <sub>15+</sub>
G004750	Green River Shale	Tertiary	P highwax	lacustrine	35.47	31.23	33.30
G006535	Wealden Shales	Cretaceous	P highwax		36.75	36.47	26.78
G006536	Wealden Shales	Cretaceous	P highwax		34.71	36.77	28.52
G006540	Wealden Shales	Cretaceous	P highwax		38.17	36.28	25.54
G006547	Wealden Shales	Cretaceous	P highwax		38.49	35.27	26.24
G006553	Wealden Shales	Cretaceous	P highwax		37.32	35.66	27.02
G006554	Wealden Shales	Cretaceous	P highwax		35.96	36.22	27.82
G000697	Boghead Coal	Pennsylvanian	P highwax		32.52	18.62	48.86
G0047501965	Mix type I/III		P highwax	mixed lacustrine- terrestrial	57.86	21.79	20.35
G000859	Messel Oil Shale	Eocene	PNA highwax		61.59	19.70	18.71
G000698	Cannel Coal	Cretaceous	Gas + Cond.		82.80	11.27	5.94
G000693	Alaskan Tasmantite	Jurassic	P lowwax	marine	45.62	42.44	11.94
G000731	Brown Limestone	Late Cretaceous	PNA highwax		64.80	21.96	13.24
G006208	Toarcian Shale	Jurassic	PNA lowwax		64.07	25.25	10.68
G006209	Toarcian Shale	Jurassic	PNA lowwax		63.01	25.85	11.14
G004072	Schöneck Fm.	Eocene-Oligocene	PNA highwax		63.03	20.87	16.10
G004070	Schöneck Fm.	Eocene-Oligocene	P highwax		54.32	22.70	22.98
G004071	Schöneck Fm.	Eocene-Oligocene	P highwax		57.58	22.56	19.86
G000883	Autun Oil Shale	Jurassic	PNA lowwax		68.98	20.44	10.59
G001955	Spekk Fm.	Upper Jurassic	PNA lowwax		73.74	19.76	6.50
G000689	Botneheia Shale	Triassic	PNA lowwax		70.71	21.65	7.65
G005812	Irati Fm.	Permian	PNA lowwax	marine	69.58	22.71	7.71
G004563	Domanik Fm.	Devonian	PNA lowwax		74.87	20.02	5.11
G000690	Woodford Shale	Devonian	PNA lowwax		75.36	20.58	4.06
G006153	Woodford Shale	Devonian	Gas + Cond.		80.89	16.73	2.38
G006154	Woodford Shale	Devonian	Gas + Cond.		81.00	16.66	2.33
G006156	New Albany Shale	Devonian	Gas + Cond.		82.62	15.87	1.52
G006155	Caney Shale	Carboniferous	PNA lowwax		78.99	17.01	4.01
G005298	Bakken Shale	Mississippian	PNA lowwax		73.82	19.85	6.33
G000692	Chattanooga Shale	Devonian	Gas + Cond.		82.21	16.10	1.69
G004564	Murzuq Basin	Silurian	Gas + Cond.		83.57	15.11	1.32
G007160	Murzuq Basin	Silurian	Gas + Cond.		84.45	14.56	0.99
G006949	Middle East	Silurian	Gas + Cond.		82.22	16.39	1.40
G000753	Alum Shale	Cambrian	Gas + Cond.		94.79	5.04	0.18
G000758	Alum Shale	Cambrian	Gas + Cond.		93.09	6.47	0.43
G005936	Middle East	Silurian	Gas + Cond.	org. lean marine	89.90	9.68	0.41
G006948	Middle East	Silurian	Gas + Cond.		94.46	5.47	0.07
G007161	Ghadames Basin	Silurian	Gas + Cond.		89.93	9.59	0.47
G005935	Akata Shale	Paleogene	PNA highwax	mixed marine- terrestrial	63.05	18.38	18.58
G005762	Hekkingen Fm.	Jurassic	PNA lowwax		78.73	14.74	6.53
G005763	Hekkingen Fm.	Jurassic	PNA lowwax		78.55	15.29	6.16
G006204	Douala Basin	Cretaceous	Gas + Cond.	org. lean mixed marine- terrestrial	88.74	9.32	1.94
G006205	Douala Basin	Cretaceous	Gas + Cond.		89.57	9.02	1.41
G006206	Mahakam Delta		Gas + Cond.		84.74	9.84	5.43
G007162	Farsund Fm.	upper Jurassic	Gas + Cond.		85.78	12.81	1.42
G007163	Farsund Fm.	upper Jurassic	Gas + Cond.		87.05	11.44	1.51
G007164	Farsund Fm.	upper Jurassic	Gas + Cond.		88.05	10.01	1.95
G007165	Farsund Fm.	upper Jurassic	Gas + Cond.		83.69	13.00	3.31
G007166	Farsund Fm.	upper Jurassic	PNA Low Wax		78.59	15.30	6.11
G000206	Kugmallit Fm.	Oligocene	Gas + Cond.	fluvio-deltaic terrestrial	99.28	0.72	0.00
G000721	Westphalian Coals	Carboniferous	Gas + Cond.		83.67	10.73	5.60
G001965	Are Fm.	Lower Jurassic	Gas + Cond.		84.71	9.56	5.73
G000696	Jet Rock	Lower Jurassic	Gas + Cond.		82.77	12.25	4.98
G006207	Mahakam Delta		PNA highwax		61.44	14.82	23.74
G006533	Wealden Coals	Cretaceous	PNA Low Wax		73.96	13.56	12.49
G006538	Wealden Coals	Cretaceous	PNA Low Wax		74.30	14.55	11.15
G006542	Wealden Coals	Cretaceous	PNA highwax		67.05	19.10	13.85
G006544	Wealden Coals	Cretaceous	PNA highwax		72.02	13.53	14.45
G006548	Wealden Coals	Cretaceous	PNA highwax		72.27	13.56	14.17
G006550	Wealden Coals	Cretaceous	PNA highwax		72.75	13.58	13.66
G000899	Talang Akar Coal	Eocene-Oligocene	Gas + Cond.		84.06	8.38	7.56
G000726	Talang Akar Coal	Eocene-Oligocene	PNA lowwax		78.15	10.36	11.49
G000670	Talang Akar Coal	Eocene-Oligocene	PNA highwax		71.22	12.24	16.53
G000950	Arang Coal	Miocene	PNA lowwax		75.50	11.79	12.70
SN6750	Taglu Fm.	Eocene	PNA lowwax		78.52	10.45	11.04
G001994	New Zealand Coal	Late Cretaceous	P highwax		57.68	16.84	25.49
G001997	New Zealand Coal	Eocene	PNA highwax		71.91	13.40	14.69
G001996	New Zealand Coal	Eocene	PNA highwax		71.54	12.82	15.64
G001991	New Zealand Coal	Eocene	PNA highwax		75.67	13.27	11.06
G001990	New Zealand Coal	Late Cretaceous	PNA highwax		68.10	12.74	19.16
G001980	New Zealand Coal	Eocene-Oligocene	PNA highwax		72.85	11.78	15.37
G001982	New Zealand Coal	Eocene-Oligocene	PNA highwax		69.67	12.15	18.18
G001981	New Zealand Coal	Eocene-Oligocene	PNA highwax		72.05	12.52	15.43
G001984	New Zealand Coal	Eocene-Oligocene	PNA highwax		73.18	11.65	15.17
G001983	New Zealand Coal	Eocene-Oligocene	PNA lowwax		73.73	12.16	14.11
G005937	Middle East	Silurian	PNA lowwax	migrated oil	64.42	25.49	10.09

### 3 GEOCHEMICAL CHARACTERISATION

**Table 3-1 continued**

GFZ Code	Formation/ Basin	Larter (1984) Terrestrial Input normalised yields			Eglinton <i>et al.</i> (1990) Marine Input normalised yields		
		<i>n</i> -C <sub>8:1</sub>	<i>m,p</i> -Xylene	Phenol	2,3 DM-Thiophen	<i>o</i> -Xylene	<i>n</i> -C <sub>9:1</sub>
G004750	Green River Shale	61.79	37.06	1.15		6.33	19.91
G006535	Wealden Shales	84.20	15.01	0.79		3.89	12.53
G006536	Wealden Shales	84.50	14.50	1.00		2.79	12.55
G006540	Wealden Shales	80.01	17.68	2.32		3.50	13.69
G006547	Wealden Shales	81.29	16.44	2.27		4.12	12.86
G006553	Wealden Shales	82.77	15.38	1.85		4.06	12.19
G006554	Wealden Shales	80.68	16.82	2.49		4.19	12.46
G000697	Boghead Coal	70.15	29.03	0.82		4.88	21.86
G0047501965	Mix type I/III	29.33	37.58	33.08		19.41	29.86
G000859	Messel Oil Shale	32.86	49.97	17.17		10.80	37.69
G000698	Cannel Coal	18.67	47.47	33.86		7.18	56.80
G000693	Alaskan Tasmanite	79.40	20.01	0.59		3.51	17.67
G000731	Brown Limestone	36.53	54.70	8.77		38.98	24.20
G006208	Toarcian Shale	52.21	43.95	3.84		24.46	23.29
G006209	Toarcian Shale	53.97	41.82	4.20		22.53	25.84
G004072	Schöneck Fm.	38.50	52.23	9.27		17.73	28.71
G004070	Schöneck Fm.	43.11	53.85	3.03		18.69	26.73
G004071	Schöneck Fm.	39.33	57.06	3.60		22.93	27.73
G000883	Autun Oil Shale	40.07	57.35	2.58		11.31	35.65
G001955	Spekk Fm.	38.83	58.86	2.31		17.48	40.31
G000689	Botneheia Shale	55.70	39.86	4.44		12.88	24.47
G005812	Irati Fm.	37.98	55.29	6.73		25.65	24.09
G004563	Domanik Fm.	42.60	50.36	7.04		31.15	25.05
G000690	Woodford Shale	50.02	46.40	3.58		19.79	29.99
G006153	Woodford Shale	37.82	59.78	2.41		19.56	37.92
G006154	Woodford Shale	42.91	54.41	2.68		20.25	37.67
G006156	New Albany Shale	36.88	59.24	3.88		19.96	44.85
G006155	Caney Shale	40.25	57.21	2.54		22.74	34.04
G005298	Bakken Shale	36.60	60.77	2.63		25.04	30.45
G000692	Chattanooga Shale	35.92	59.09	5.00		20.53	42.50
G004564	Murzuq Basin	33.45	62.50	4.05		18.31	43.99
G007160	Murzuq Basin	34.41	60.48	5.11		13.54	48.38
G006949	Middle East	20.69	66.27	13.04		11.50	57.61
G000753	Alum Shale	11.47	87.55	0.98		17.03	72.48
G000758	Alum Shale	14.44	83.66	1.90		17.11	69.36
G005936	Middle East	20.74	79.26	0.00		11.76	77.66
G006948	Middle East	7.49	89.29	3.22		8.17	86.64
G007161	Ghadames Basin	33.58	64.81	1.61		4.51	70.21
G005935	Akata Shale	35.85	50.59	13.55		13.87	31.93
G005762	Hekkingen Fm.	28.71	61.76	9.53		26.02	39.76
G005763	Hekkingen Fm.	25.11	67.00	7.89		23.79	47.19
G006204	Douala Basin	5.59	70.38	24.03		7.51	81.64
G006205	Douala Basin	4.62	90.25	5.13		7.97	85.28
G006206	Mahakam Delta	8.93	71.86	19.21		7.04	73.71
G007162	Farsund Fm.	24.87	70.37	4.76		5.34	77.35
G007163	Farsund Fm.	15.59	81.89	2.52		5.91	83.48
G007164	Farsund Fm.	25.07	73.63	1.31		5.81	74.85
G007165	Farsund Fm.	23.46	61.11	15.42		7.20	67.72
G007166	Farsund Fm.	29.97	59.18	10.86		6.73	57.47
G000206	Kugmallit Fm.	0.14	16.93	82.94		22.97	75.37
G000721	Westphalian Coals	16.01	49.98	34.01		5.51	52.81
G001965	Are Fm.	7.63	31.55	60.83		8.14	62.64
G000696	Jet Rock	5.80	29.67	64.53		23.66	57.97
G006207	Mahakam Delta	23.32	47.82	28.86		8.25	45.27
G006533	Wealden Coals	17.65	43.81	38.54		3.20	47.76
G006538	Wealden Coals	22.69	45.34	31.97		2.34	40.31
G006542	Wealden Coals	32.50	40.56	26.94		5.45	34.02
G006544	Wealden Coals	18.40	42.46	39.14		5.77	41.82
G006548	Wealden Coals	18.32	42.61	39.07		6.69	42.15
G006550	Wealden Coals	19.34	43.73	36.93		6.17	42.01
G000899	Talang Akar Coal	5.70	32.78	61.52		16.09	61.19
G000726	Talang Akar Coal	13.67	44.24	42.09		10.64	56.24
G000670	Talang Akar Coal	18.66	56.53	24.81		10.89	47.37
G000950	Arang Coal	12.00	40.27	47.73		7.04	57.48
SN6750	Taglu Fm.	6.15	25.59	68.26		0.00	68.82
G001994	New Zealand Coal	21.01	27.83	51.16		0.00	41.70
G001997	New Zealand Coal	11.81	31.38	56.81		0.00	52.86
G001996	New Zealand Coal	12.40	31.87	55.73		0.00	52.57
G001991	New Zealand Coal	14.47	38.37	47.16		0.00	44.66
G001990	New Zealand Coal	14.58	32.25	53.17		0.00	45.27
G001980	New Zealand Coal	9.47	27.74	62.79		0.00	60.20
G001982	New Zealand Coal	9.45	31.39	59.17		0.00	65.61
G001981	New Zealand Coal	10.00	27.92	62.09		0.00	60.41
G001984	New Zealand Coal	8.92	30.18	60.89		0.00	63.24
G001983	New Zealand Coal	8.65	28.18	63.17		0.00	62.42
G005937	Middle East	6.56	67.99	25.45		31.82	58.24



### 3.2.2 Natural maturity series

As pyrolysis-GC provides detailed insights into kerogen structure it has been employed to study the evolution of the kerogen composition during natural maturation of organic matter. Results such as the chain length distribution and phenol content are displayed in the ternary diagrams of Horsfield and Larter (Fig. 3.7), normalised yields of single compounds of the latter as well as GOR and gas wetness are given in Tab. 3-2.

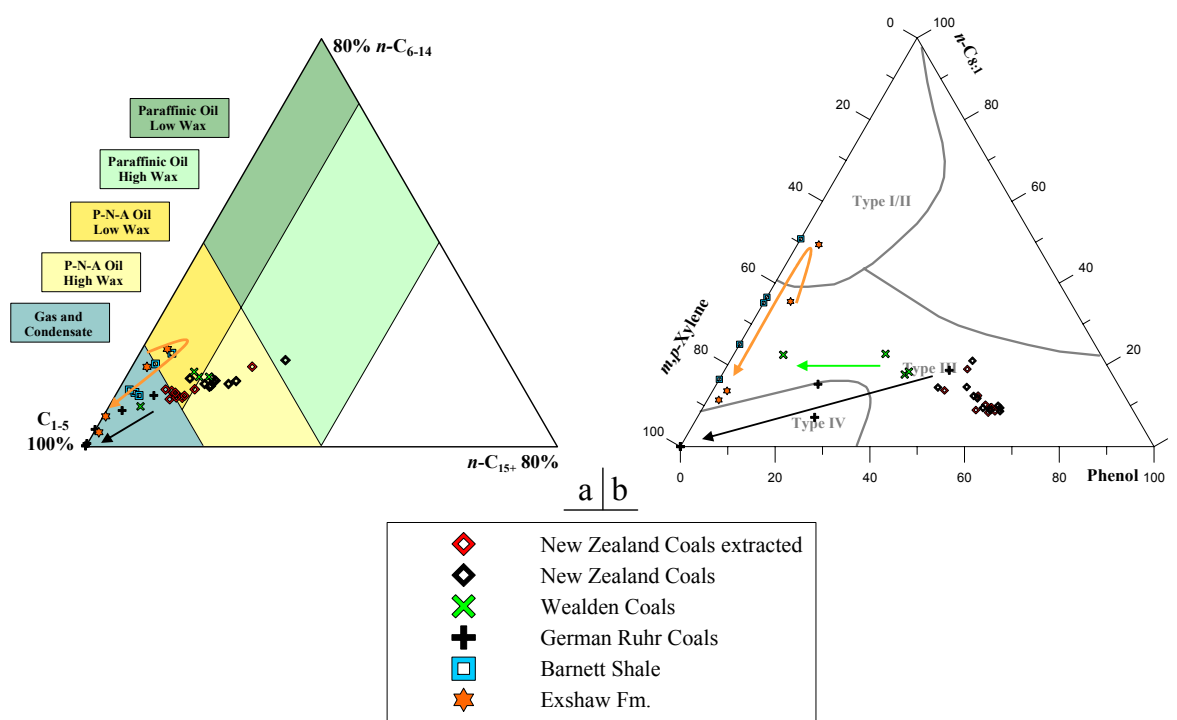


Figure 3.7: Evolution of the kerogen composition during natural maturation displayed in ternary diagrams of a) Horsfield (1989) and b) Larter (1984). Arrows indicate the evolution pathway.

#### *Humic coals*

Open-system pyrolysis results for the extracted and unextracted New Zealand Coals maturity series (Vitrinite reflectance 0.40%-0.80%) have been presented earlier by Vu (2008), and those for the German Carboniferous Coals ( $R_o$  0.99% to 2.81%) by Horsfield and Schenk (1995) and Schenk and Horsfield (1998).

Pyrolysate composition of unextracted New Zealand Coals was already discussed in the previous chapter and is dominated by long alkyl chains and aromatic compounds such as alkylbenzenes, alkylnaphthalenes and phenols typical of source rocks deposited in lower delta plain and inner shelf environments where source rocks generate high wax PNA oils (Fig. 3.6). Extraction of bitumen from the New Zealand Coals leads to the loss of long aliphatic chains

### 3 GEOCHEMICAL CHARACTERISATION

within the organic matter shifting the petroleum composition into the low wax PNA crude oil and gas/condensate generating facies (Fig. 3.7a).

**Table 3-2: Organic matter evolution – natural maturity series: Normalised single compound yields as input parameters for ternary diagrams of Horsfield (1989) and Larter (1984) as well as routinely used ratios such as GOR and Gas Wetness**

Company	GFZ Code	Formation	R <sub>0</sub>	GOR	Gas wetness	Horsfield (1989) Chain Length Distribution			Larter (1984) Terrestrial Input		
						Total C <sub>1-5</sub>	<i>n</i> -C <sub>6-14</sub>	<i>n</i> -C <sub>15+</sub>	<i>n</i> -C <sub>8:1</sub>	<i>m,p</i> -Xylene	Phenol
						Normalised yields			Normalised yields		
Shell	G006385	Exshaw Fm Shale.	0.76	0.39	0.72	81.81	15.54	2.65	35.50	58.99	5.51
	G006387		0.89	0.49	0.70	76.62	19.04	4.34	49.42	46.07	4.52
	G006384		1.25	0.63	0.65	93.68	5.82	0.51	13.65	83.33	3.02
	G006386		3.33	0.48	0.49	96.39	2.68	0.93	11.41	86.20	2.39
Wintershall	G006533	Wealden Coals	0.56	0.37	0.59	73.96	13.56	12.49	17.65	43.81	38.54
	G006548		0.72	0.37	0.55	72.27	13.56	14.17	18.32	42.61	39.07
	G006538		0.89	0.46	0.53	74.30	14.55	11.15	22.69	45.34	31.97
	G006552		1.37	0.88	0.46	86.81	7.76	5.43	22.47	67.04	10.50
GFZ natural maturity series	G007249	Barnett Shale	0.40	0.26	0.77	80.07	16.11	3.82	36.52	63.48	0.00
	G007247		0.94	0.32	0.72	76.26	18.20	5.54	50.84	49.16	0.00
	G007250		1.35	0.38	0.68	86.37	10.50	3.14	25.02	74.98	0.00
	G007257		1.93	0.30	0.68	85.96	9.90	4.14	16.46	83.54	0.00
	G007219		3.21	0.23	0.71	87.07	11.01	1.92	35.18	64.82	0.00
	G000721	Carboniferous Coals	0.99	1.30	0.41	83.47	9.90	6.63	18.67	33.90	47.43
	G001088		1.26	1.82	0.33	90.33	6.95	2.72	15.26	63.32	21.42
	G001083		1.37	2.35	0.33	96.77	3.23	0.00	7.17	68.07	24.77
	G001086		1.58	2.78	0.30	99.54	0.46	0.00	0.00	100.00	0.00
	G001092		2.09	4.73	0.17	100.00	0.00	0.00	0.00	100.00	0.00
	G001096		2.81	6.65	0.09	100.00	0.00	0.00	0.00	100.00	0.00
	G001983	New Zealand Coals	0.41	0.32	0.56	73.73	12.16	14.11	8.65	28.18	63.17
	G001982		0.40	0.30	0.55	69.67	12.15	18.18	9.45	31.39	59.17
	G001984		0.45	0.32	0.54	73.18	11.65	15.17	8.92	30.18	60.89
	G001981		0.45	0.35	0.54	72.05	12.52	15.43	10.00	27.92	62.09
	G001980		0.44	0.34	0.54	72.85	11.78	15.37	9.47	27.74	62.79
	G001997		0.52	0.32	0.55	71.91	13.40	14.69	11.81	31.38	56.81
	G001996		0.52	0.30	0.55	71.54	12.82	15.64	12.40	31.87	55.73
	G001990		0.71	0.32	0.54	68.10	12.74	19.16	14.58	32.25	53.17
	G001994		0.61	0.28	0.58	57.68	16.84	25.49	21.01	27.83	51.16
	G001991		0.80	0.37	0.53	75.67	13.27	11.06	14.47	38.37	47.16
	G001983K	New Zealand Coals extracted	0.41	0.44	0.53	79.59	10.27	10.14	8.98	29.84	61.18
	G001982K		0.40	0.51	0.51	78.88	9.45	11.67	8.92	33.16	57.92
	G001984K		0.45	0.52	0.50	81.15	9.17	9.68	8.34	30.85	60.81
	G001981K		0.45	0.54	0.51	79.85	9.53	10.62	8.62	29.28	62.10
	G001980K		0.44	0.50	0.51	78.30	9.83	11.87	9.60	29.71	60.69
	G001997K		0.52	0.49	0.55	79.98	10.80	9.22	9.62	29.47	60.91
	G001996K		0.52	0.48	0.56	79.58	10.43	9.99	10.25	30.45	59.30
	G001990K		0.71	0.50	0.55	75.92	11.12	12.95	12.47	30.92	56.61
	G001994K		0.61	0.37	0.58	63.96	15.55	20.49	18.96	29.93	51.10
	G001991K		0.80	0.57	0.54	80.89	11.07	8.05	13.74	37.37	48.89

By further natural maturation from high volatile bituminous rank to anthracite (German Coals:  $R_o$  0.99% to 2.81%) long and short alkyl chains are generated or incorporated into the residual organic matter (Schenk and Horsfield, 1998), progressively shifting the pyrolysate composition through the gas/condensate field into the corner, where source rocks mainly yield low molecular weight components and mono aromatic compounds (from  $R_o$  1.58% to 2.81%). Phenol compounds progressively decrease and vanish at 1.58%  $R_o$  (Fig. 3.7a; Tab. 3-2) whereas the main part of these compounds are most likely not released as free flowing oil during natural maturation, but are retained within the residual organic matter (Horsfield, 1997). The same trend, a chain shortening shift into the gas and condensate petroleum type field as well as a phenol decrease (Fig. 3.7a+b), can be observed for the small Wealden Coal series when going from high to medium volatile bituminous coal ranks.

For the three coal series GOR and gas wetness are relatively stable at  $R_o < 1.0\%$  and then strongly increase (GOR) respectively decrease (gas wetness) from high volatile bituminous coal ranks to anthracite (Tab. 3-2) indicating the depletion of  $C_{6+}$  precursor material and a relative increase of methylated to longer chain alkylated aromatic ring systems.

#### *Marine shales*

Pyrolysate composition of Exshaw Formation samples provided by Shell as well as Barnett Shale samples are displayed in Fig. 3.7a+b and Tab. 3-2. The two most immature samples G006385 (Exshaw Fm.,  $R_o \sim 0.76\%$ ) and G007249 (Barnett Shale.,  $R_o \sim 0.40\%$ ) are characterised by a series of n-alkane/n-alk-1-ene doublets up to  $n-C_{27}$  with a domination of intermediate chain lengths typical for marine source rock. Nevertheless, they also show a high abundance of alkylated mono and diaromatic compounds as well as low molecular weight compounds yielding pyrolysates of a gas and condensate composition in the Horsfield ternary (Fig. 3.7a) and Type III organic matter composition in the Larter ternary (Fig. 3.7b). Those features were previously described for immature Paleozoic source rocks (Chapter 3.2.1). 1,2,3,4 TeMB is again a prominent aromatic peak in both cases but of higher significance for the less mature Barnett Shale sample. Alkylthiophenes and phenols are of subordinate importance.

Interestingly, natural maturation leads for both series to a lower aromaticity (Fig. 3.7b) and a relative enrichment in intermediate alkyl chains lengths, which results in an inferred PNA low wax petroleum type (Fig. 3.7a) and a Type II organic matter composition classification (Fig. 3.7b). Concomitantly, the abundance of 1,2,3,4-TeMB reaches very low levels for the Exshaw Fm. sample G006387 and Barnett Shale G007247 at maturities around

0.9%.  $R_o$ . It might be coincidence but the same trend was observed for a natural maturity series of Bakken Shales investigated by Muscio *et al.* (1994). Here, the kerogen structure loses diaromatic components, which are the precursors of 1,2,3,4-TeMB inherited from green sulphur photosynthetic bacteria, during early catagenesis ( $R_o = 0.3 - 0.7\%$ ) whether by generation and migration and/or cross-linking and condensation. The pyrolysate composition is as well shifted from the gas condensate field into the PNA low wax field. Nevertheless, the respective maturity interval is poorly covered in the present project and observed trends could be related to organic matter heterogeneities.

The high maturity samples of the Exshaw Formation and Barnett Shales ( $R_o > 1.2\%$ ) all fall in the gas and condensate field with pyrolysates being comprised of mainly low molecular weight compounds as well as the major aromatic compounds benzene, toluene, *m,p,o*-benzene and minor amounts of alkylnaphthalenes. This indicates the removal of longer chain aliphatics from the kerogen structure during oil generation. With increasing maturity, pyrolysate compositions are progressively shifted to the lower left gas and higher aromaticity corner in the diagrams of Horsfield (1989) and Larter (1984)(Fig. 3.7a+b).

### 3.3 Bulk Hydrocarbon Generation (SRA-Kinetics)

The discrete bulk petroleum potential versus activation energy distribution model used for the evaluation of kinetic parameters within the present thesis is based on equation (8) and the calculation method of Schaefer *et al.* (1990), and presumes twenty-five parallel first order reactions with activation energies regularly spaced by 1 kcal/mol and a single frequency factor. The advantage of using only one pre-exponential factor is that all parallel reactions proceed in the order of increasing activation energy with increasing temperature (Tissot and Espitalié, 1975; Ungerer, 1990). At least three different heating rates were used for non-isothermal open- and closed-system experiments to approximate a reasonable starting value of A (van Heek and Jüntgen, 1968). Optimisation of kinetic parameters was ensured by the “least square iteration” method. Here, calculated and measured generation rates are compared at different temperatures (200 per heating rate) until the error function for calculated and measured curves reaches a minima, best fit. By variation of the parameter heating rate  $r$  in the equation (8), it is now possible to transfer directly measured, pyrolysis-derived generation rate curves to time-temperature conditions found in geologic systems.

#### 3.3.1 Immature source rock samples

Immature whole rock samples were subjected to open-system, non-isothermal pyrolysis at four different linear heating rates (0.7, 2, 5, 15°C/min) using a Source Rock Analyser SRA (Humble) in order to provide information, i.e., kerogen to petroleum conversion in general, supplementary to the standard geochemical characterisation. Another aspect is the possibility to investigate if late gas generation observed under closed-system conditions is detected here in the respective temperature interval. Covering all kerogen types and depositional environments, bulk kinetic parameters were determined for a variety of industry provided samples, and GFZ-samples Carboniferous Coal G00721, Fische Schiefer samples from the Schöneck Fm. (G004070, G004071, G004072) Åre Fm. G001965, Spekk Fm. G001955, Green River Shale G004750, and synthetic Mix Type I/III G0047501965. Data for samples from the Taglu Fm. (SN6750), Kugmallit Fm. (G000206), Woodford Shale (G000690), Alaskan Tasmanite (G000693), Boghead Coal (G000697), Brown Limestone (G000731), and Arang Coal (G000950) was taken from the GFZ in-house data base. The best fit between experimental and calculated formation rates were obtained with the activation energy distribution ( $E_a$ ) and single pre-exponential factors (A) displayed in Table A 3 (Appendix) and Fig. 3.8.

### 3 GEOCHEMICAL CHARACTERISATION

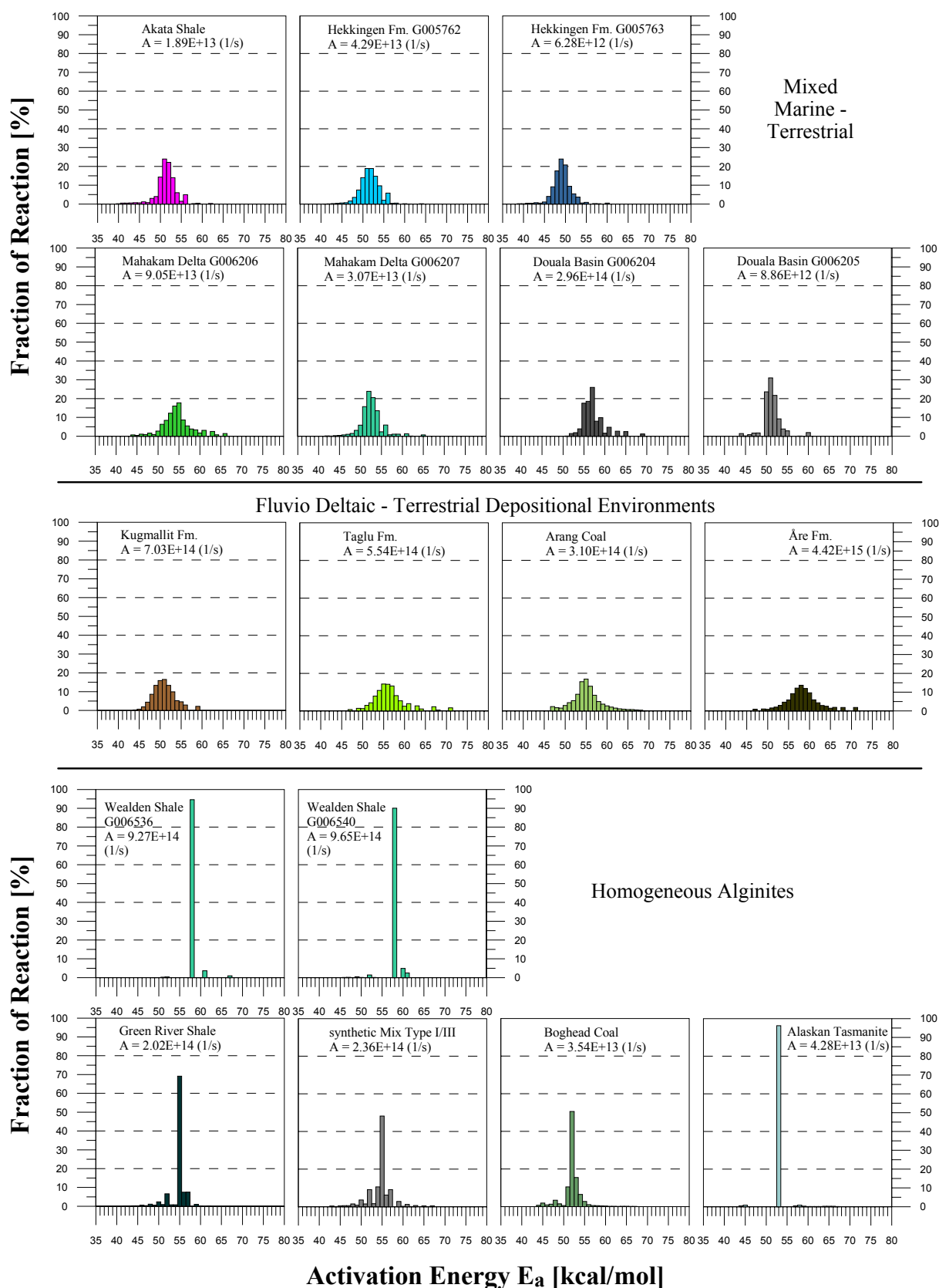
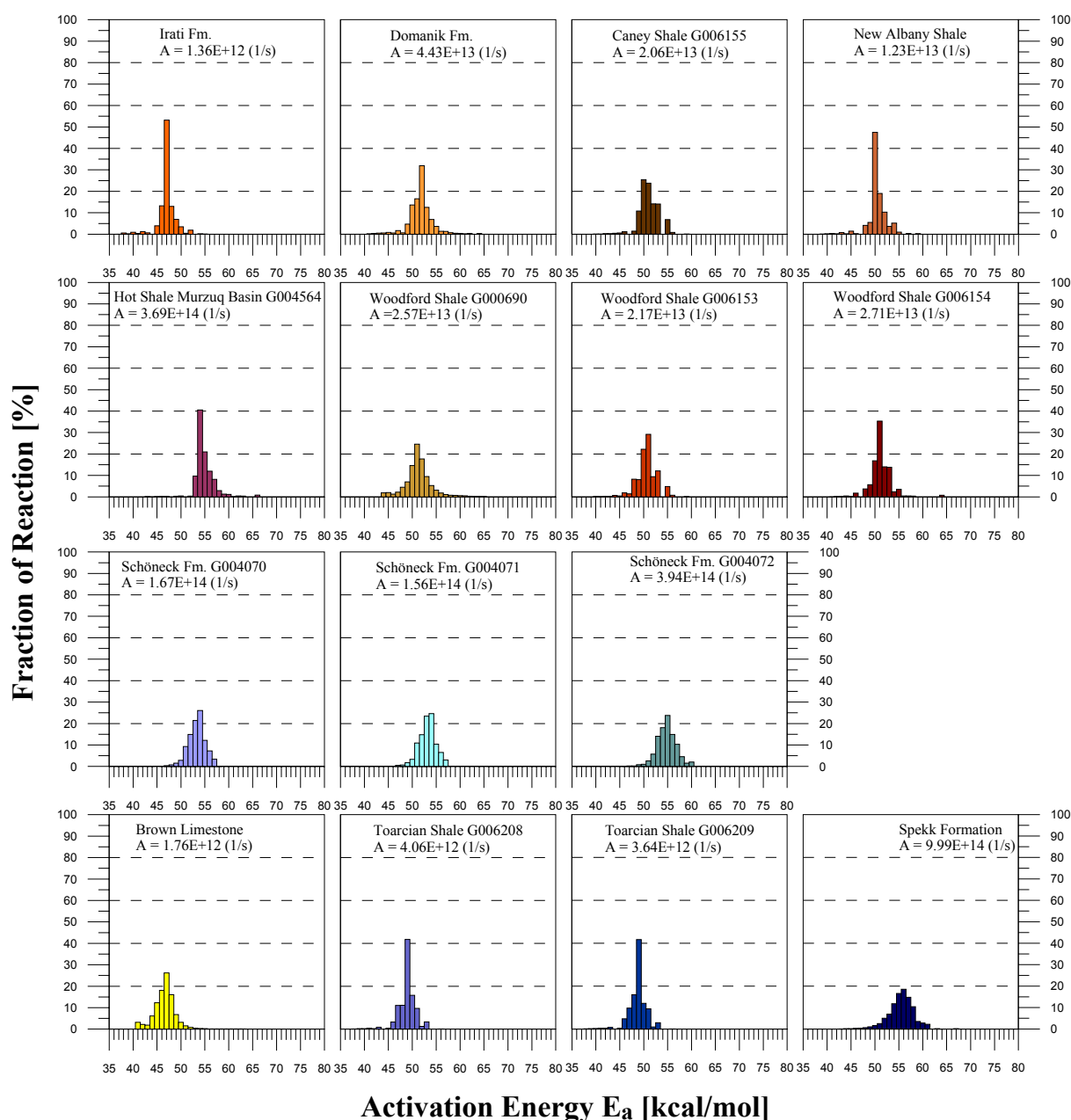


Figure 3.8: Frequency factors and activation energy distribution of homogeneous alginites, fluvio deltaic – terrestrial, and mixed marine – terrestrial source rocks based on non-isothermal bulk pyrolysis using the source rock analyzer (SRA)

### 3 GEOCHEMICAL CHARACTERISATION



**Figure 3.8 continued: Frequency factors and activation energy distribution of marine source rocks**

It should be stated here that the reaction rate constant  $k$  is dependent on both the pre-exponential factor and the activation energy solution, marking a direct comparison of numerical data for various samples difficult (Tegelaar and Noble, 1994). For a better graphical comparison of the kinetic behaviour of the organic matter, transformation rate *versus* temperature curves are given for the investigated samples in Fig. 3.9 assuming a hypothetical burial history with a constant heating rate of  $3^{\circ}\text{C}/\text{Ma}$ , which corresponds to average geologic heating rates in sedimentary basins (Schenk *et al.*, 1997b). The temperatures for the onset (10% transformation), middle (50% transformation), end (90% transformation) and maximum (geological  $T_{\text{max}}$ ) of petroleum generation can be found in Tab. 3-3.

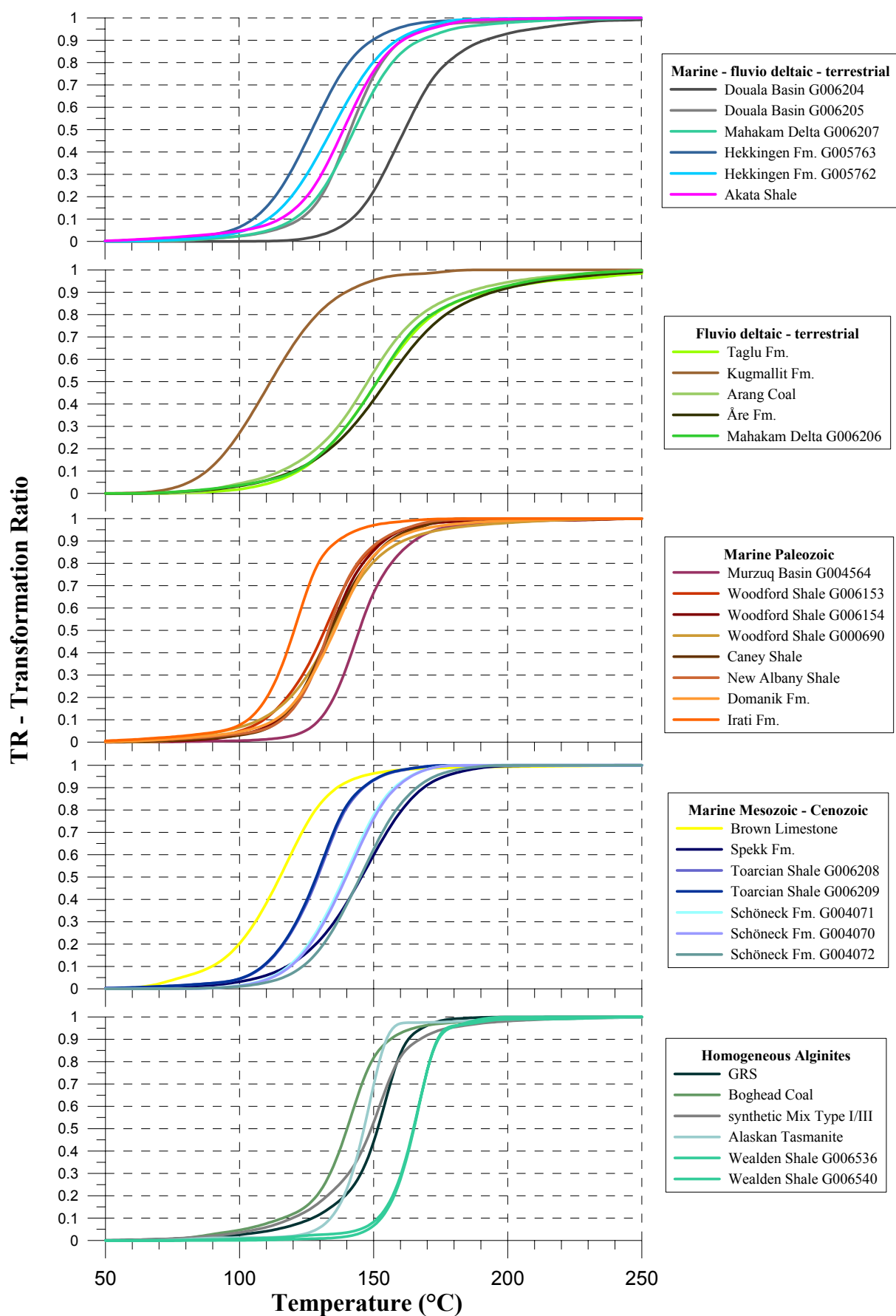


Figure 3.9: Transformation Ratio (TR) curves for the investigated immature sample set assuming a constant geological heating rate of 3°C/Ma



*Homogeneous Alginites – lacustrine and marine depositional environments*

Kinetic parameters of source rocks derived from selectively preserved algal biopolymer occurring in the cell walls of various aquatic algae, deposited in lacustrine (Green River Shale, Boghead Coal,) or marine (Alaskan Tasmanite) environments, are dominated by a single activation energy or are characterised by very narrow activation energy distributions (Fig. 3.8). A frequency factor of  $2.02\text{E}+14$  (1/s) and mean  $E_a$  of 55 (kcal/mol) for e.g. the Green River Shale sample is very similar to published data of Tegelaar and Noble (1994) and Braun *et al.* (1991) for this type of organic matter, even though a Gaussian distribution model is usually preferred in cases of single activation energy distributions (Braun *et al.*, 1991; Tegelaar and Noble, 1994). The dominant activation energy describes at least 50% of the total kerogen conversion (Boghead Coal; synthetic kerogen Type I/III) and accounts for up to 96% of kerogen conversion in the case of Alaskan Tasmanite and the two Wealden Shale samples. This is related to the limited range of chemical bonds which crack to yield mainly aliphatic normal hydrocarbons with increasing thermal stress mirroring the homogeneous character of the precursor material, which is relatively stable and cracks at later stages than other alkyl moieties containing organic matter (Burnham *et al.*, 1988; Schenk *et al.*, 1997b; Dieckmann, 2005). The latter finds its expression in relatively steep (narrow) transformation ratio curves and high onset and peak petroleum generation temperatures (Fig. 3.9; Tab. 3-3).

*Fluvio deltaic - terrestrial depositional environments*

In stark contrast, a very broad activation energy distribution spanning 25 energies (45-70 kcal/mol) in most cases can be observed for heterogeneous terrestrial organic matter derived from higher land plants (Fig. 3.8). Examples are Kugmallit Fm. lignite, Taglu Fm. Coal, Arang Coal, and Åre Fm. Coal as well as extracted and unextracted immature New Zealand Coals (Fig. 3.11) and high volatile bituminous Cretaceous Wealden Coals from Germany (Fig. 3.12). Here only an average of four pseudo-reactions account for more than 10% kerogen conversion each with mean activation energies ( $E_{\text{mean}}$ ) ranging between 55 and 63 kcal/mol for frequency factors ranging between  $3.1\text{E}+14$  (1/s) and  $1.99\text{E}+16$  (1/s). These kinetic parameters are typical for immature humic coals (Ungerer and Pelet, 1987; Reynolds and Burnham, 1993; Schenk *et al.*, 1997b). In Fig 3.9 it is shown that terrestrial organic matter generates hydrocarbons over a very broad temperature range ( $\sim 70^\circ\text{C}$ ; Tab. 3-3) and up to temperatures exceeding those of other kerogen types. Peak generation temperatures around  $150^\circ\text{C}$  and temperatures around  $190^\circ\text{C}$  for 90% kerogen transformation (Tab. 3-3) confirm the refractory nature of humic coals (Quigley *et al.*, 1987; Tegelaar and Noble, 1994). The

Kugmallit Fm. lignite represents an exception exhibiting mean activation energies between 49 and 52 kcal/mol and the lowest onset and peak generation temperature of the entire sample set (Tab. 3-3; Fig. 3.9) owed to its very immature state prior to completion of diagenesis. This case illustrates that one has to be very careful when using very immature, heteroelement-rich organic matter when assessing hydrocarbon generation under geologic conditions, especially for Type III organic matter (Schenk and Horsfield, 1998).

**Table 3-3: Kinetic Parameters - calculated, variable frequency factors, geologic  $T_{\max}$ , and transformation ratios 10%, 50%, and 90% for an applied geologic heating rate of 3°C/Ma.**

GFZ Code	Formation/Basin	Frequency				geologic
		factor A	10%	50%	90%	$T_{\max}$
		1/s	TR °C	TR °C	TR °C	°C
G004750	Green River Shale	2.02E+14	127.1	151.5	162.9	154.3
G0047501965	Mix type I/III	2.36E+14	119.6	149.1	167.2	152.3
G000697	Boghead Coal	3.54E+13	116.0	140.1	156.2	141.8
G000693	Alaskan Tasmanite	4.28E+13	133.9	146.3	154.7	148.4
G006536	Wealden Shale	9.27E+14	152.8	165.0	173.8	166.9
G006540	Wealden Shale	9.65E+14	151.5	164.8	174.1	166.7
G000731	Brown Limestone	1.76E+12	89.6	115.0	136.4	117.6
G006208	Toarcian Shale	4.06E+12	108.8	129.1	146.3	131.8
G006209	Toarcian Shale	3.64E+12	108.5	128.6	145.9	131.2
G004072	Fischschiefer	3.94E+14	123.4	145.0	166.0	146.4
G004070	Fischschiefer	1.67E+14	118.9	139.7	158.4	142.5
G004071	Fischschiefer	1.56E+14	118.1	139.0	157.6	141.7
G001955	Spekk Fm.	9.99E+14	117.6	145.5	168.6	147.8
G005812	Irati Fm.	1.36E+12	103.1	120.4	136.5	121.9
G004563	Domanik Fm.	4.43E+13	113.2	135.5	156.7	138.3
G000690	Woodford Shale	2.57E+13	107.5	134.5	161.0	135.2
G006153	Woodford Shale	2.17E+13	109.0	131.7	153.1	132.9
G006154	Woodford Shale	2.71E+13	114.1	133.9	153.9	134.3
G006156	New Albany Shale	1.23E+13	115.8	133.2	152.3	133.6
G006155	Caney Shale	2.06E+13	115.3	133.9	156.0	132.1
G004564	Murzuq Basin	3.69E+14	129.8	144.6	165.0	143.5
G005935	Akata Shale	1.89E+13	115.1	138.9	161.0	139.3
G005762	Hekkingen Fm.	4.29E+13	110.7	134.5	158.8	135.1
G005763	Hekkingen Fm.	6.28E+12	105.2	127.1	149.7	127.1
G006204	Douala Basin	2.96E+14	141.8	161.8	191.5	158.9
G006205	Douala Basin	8.86E+12	122.6	141.4	160.7	140.0
G006207	Mahakam Delta	3.07E+13	120.3	142.9	167.5	142.5
G006206	Mahakam Delta	9.05E+13	120.8	151.2	190.5	152.1
G000206	Kugmallit Fm.	7.03E+14	87.7	111.6	139.5	111.5
G001965	Åre Fm.	4.42E+15	120.1	154.8	194.3	154.4
G000950	Arang Coal	3.10E+14	115.3	147.8	184.5	147.5
SN6750	Taglu Fm.	5.54E+14	121.9	151.3	191.6	150.5

#### *Marine depositional environments*

Paleozoic through Cenozoic marine source rocks are characterised by kinetic parameters, which reflect on the one hand higher organic matter heterogeneity compared to organic matter exclusively derived from selective preservation and on the other hand a less complex structure than terrestrial coals. Organic matter transformation is described by a less broader distribution of activation energies spanning ten to fifteen energies ranging mainly between 45 and 60 kcal/mol for frequency factors between  $1.36\text{E}+12\text{ s}^{-1}$  (Irati Fm.) and  $9.99\text{E}+14\text{ s}^{-1}$  (Spekk Fm.)(Fig. 3.8). The mean activation energies are situated between 50 and 55 kcal/mol in most cases and account for 20 to up to 50% of kerogen conversion. Overall, those determined kinetic values are in a similar range of magnitude with other published data. In close accordance with kinetic results of Tegelaar and Noble (1994) for sulphur-rich marine source rocks, the sulphur-rich Brown Limestone (Type II-S in Eglinton ternary) and the slightly sulphur enriched Toarcian Shales (G006208, G006209) and Irati Fm. samples possess lowest frequency factors and mean activation energies of 47, 49, 49, and 47 kcal/mol respectively leading to a relatively low kerogen stability when applying geological heating rates (Fig. 3.10). Nevertheless, the sulphur richest source rock Brown Limestone from Jordan is the most unstable and already starts to generate petroleum at temperatures below 100°C with peak generation at 117°C (Fig. 3.9; Tab. 3-3), which is owed to the weaker bond strength of sulphur-sulphur and sulphur-carbon bonds compared to carbon-carbon bonds (Klomp and Wright, 1990). All other marine source rocks exhibit transformation ratio curve shapes (Fig. 3.9; Tab. 3-3) and stabilities resembling those of medium- to low-sulphur marine shales reported by Tegelaar and Noble (1994).

#### *Mixed marine – terrestrial or marine -lacustrine depositional environments*

Kinetic parameters of mixed marine – terrestrial or fluvio deltaic shales are very similar to those of marine shales with the exception of the Mahakam Delta sample G006206, which rather resembles very heterogeneous terrestrial organic matter kinetic features (Fig. 3.8; 3.9; Tab. 3-3). The “marine” signature therefore seems to overprint the “terrestrial” signature possibly related to the much higher hydrocarbon potential of H-rich algal/bacterial derived organic matter compared to H-poorer higher land plant derived organic matter. The same feature can be observed for the synthetic Type I/III kerogen mix (1:1) between Green River Shale and Åre Fm sample, for which kinetic parameters are alike those of the Green River Shale parent material and the main activation energy still accounts for 50% of total kerogen

transformation. This is again owed to a much higher hydrocarbon potential (S2) of lacustrine precursor material.

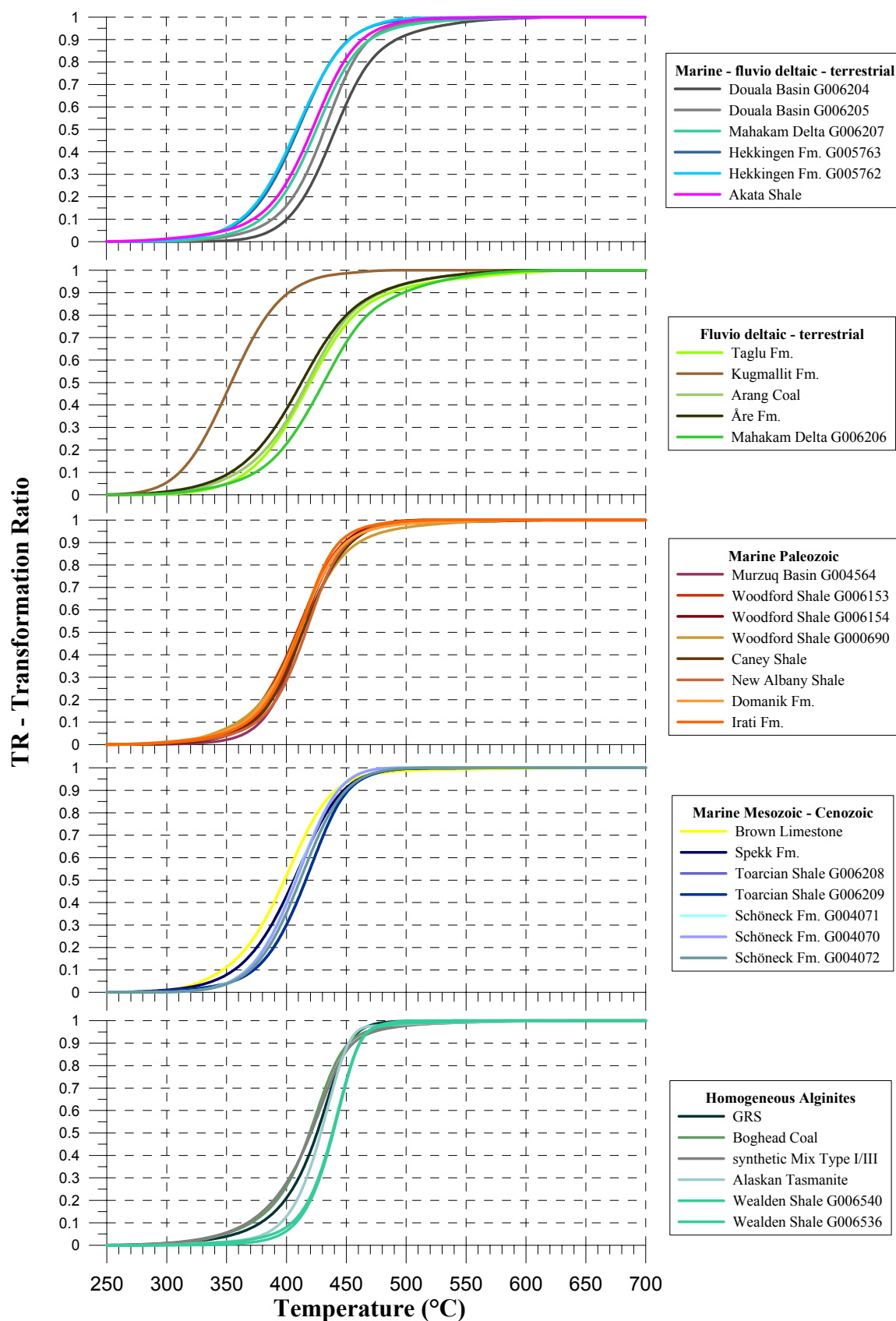


Figure 3.10: Transformation Ratio (TR) curves for the investigated immature sample set at a laboratory heating rate of 2°C/min

*Late gas generation*

Assuming a constant laboratory heating rate of 2°C/min and plotting transformation ratio curves *versus* temperature (Fig. 3.10) one can easily recognise that the end of kerogen conversion (90% TR) is reached at 500°C for all immature investigated samples. Minor amounts of primary gas might be generated between 500 and 600°C from fluvio deltaic – terrestrial organic matter but significant amounts of late gas are not observable under routinely used open-system pyrolysis conditions. Therefore, primary late gas input can be ruled out for temperatures between 600 and 700°C and should be rather ascribed to the secondary cracking of a thermally stabilised moiety, if observed under closed-system pyrolysis conditions at similar heating rates (2°C/min).

**3.3.2 Natural maturity series**

Bulk kinetic parameters were determined for samples of the Exshaw Fm. natural maturity series, for four humic coal samples from the Cretaceous Wealden and for unextracted and extracted New Zealand Coals to supplement already available kinetic data on the natural German Coal series. The best fit between experimental and calculated formation rates were obtained with the activation energy distribution and pre-exponential factors displayed in Table A 3 (Appendix) and Fig. 3.11, 3.12b, 3.14. The previously published (Schenk and Horsfield, 1998) activation energy distributions of Carboniferous German coals are given together with the newly determined activation energy distribution of the Carboniferous Coal sample G000721 ( $R_o = 0.99\%$ ) for completeness in Fig. 3.12. Kinetic parameters of the most mature Exshaw Fm sample G006386 (calculated  $R_o = 3.33\%$ ) could not be assessed because the remaining hydrocarbon potential is too low to produce well defined generation rate curves for the applied laboratory heating rates.

*Cenozoic Coals, New Zealand*

In Fig 3.11 activation energy distributions and frequency factors of extracted and unextracted New Zealand Coals are shown and graphically compared to each other. The shape of the  $E_a$  distribution as well as frequency factors of the extracted coals are very similar to those of their unextracted counterparts confirming results of Reynolds and Burnham (1993) and Schenk and Horsfield (1998) who reported that extraction has no significant influence on kinetic parameters. Thus, interestingly, the removal of high molecular weight bitumen, which contributes substantially to the S<sub>2</sub>-peak of unextracted coals (also see Chapter 3.1.2), has no major effect on bulk kinetic parameters even though Vu (2008) could demonstrate that

compositional differences (higher GOR's for extracted coals) are not neglectable and related to second-order recombination-reactions within the extracted macromolecular organic matter component during open-system pyrolysis.

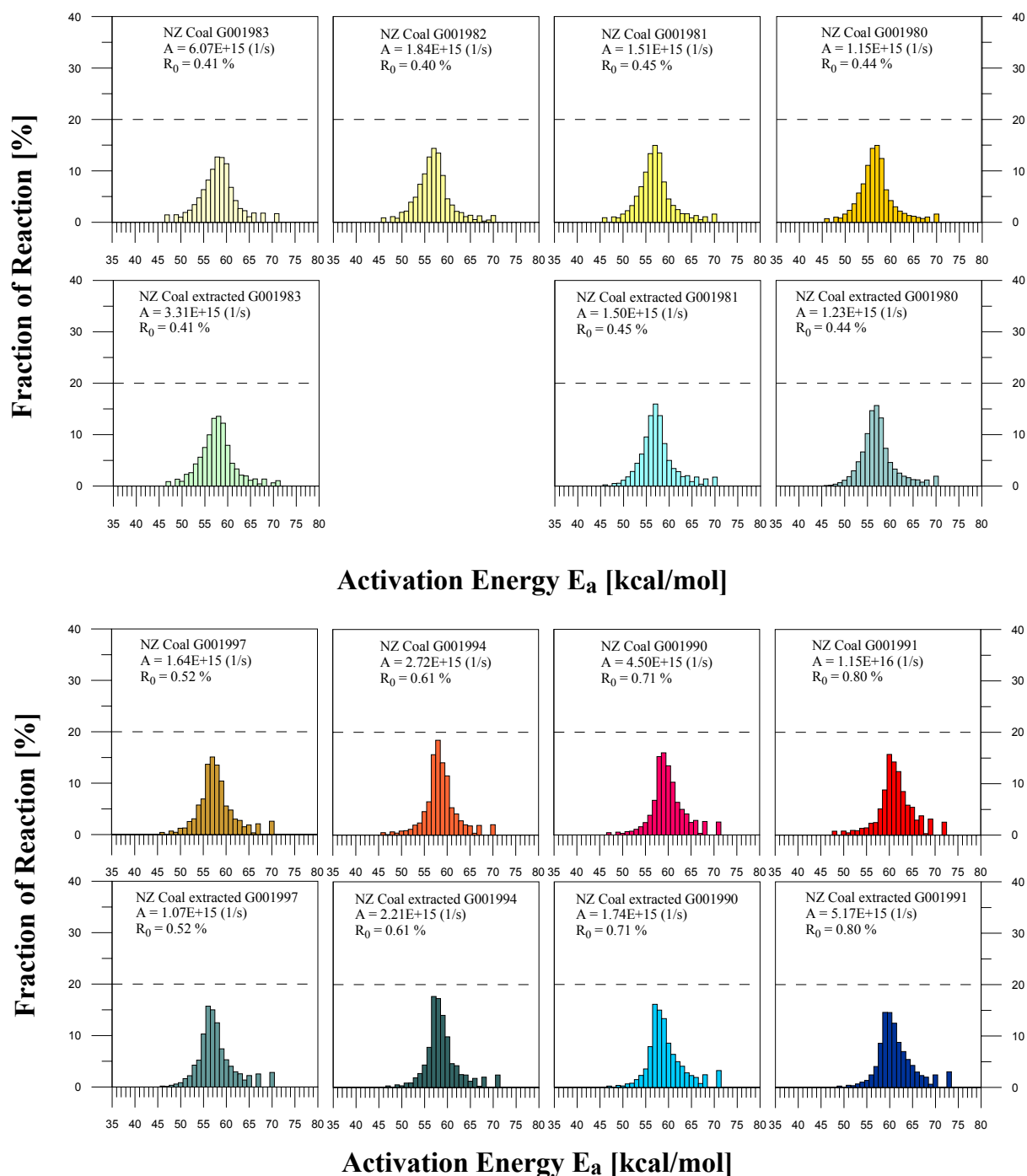


**Figure 3.11: Frequency factors and activation energy distribution of extracted and unextracted New Zealand Coals based on non-isothermal bulk pyrolysis using the source rock analyzer (SRA)**

### 3 GEOCHEMICAL CHARACTERISATION

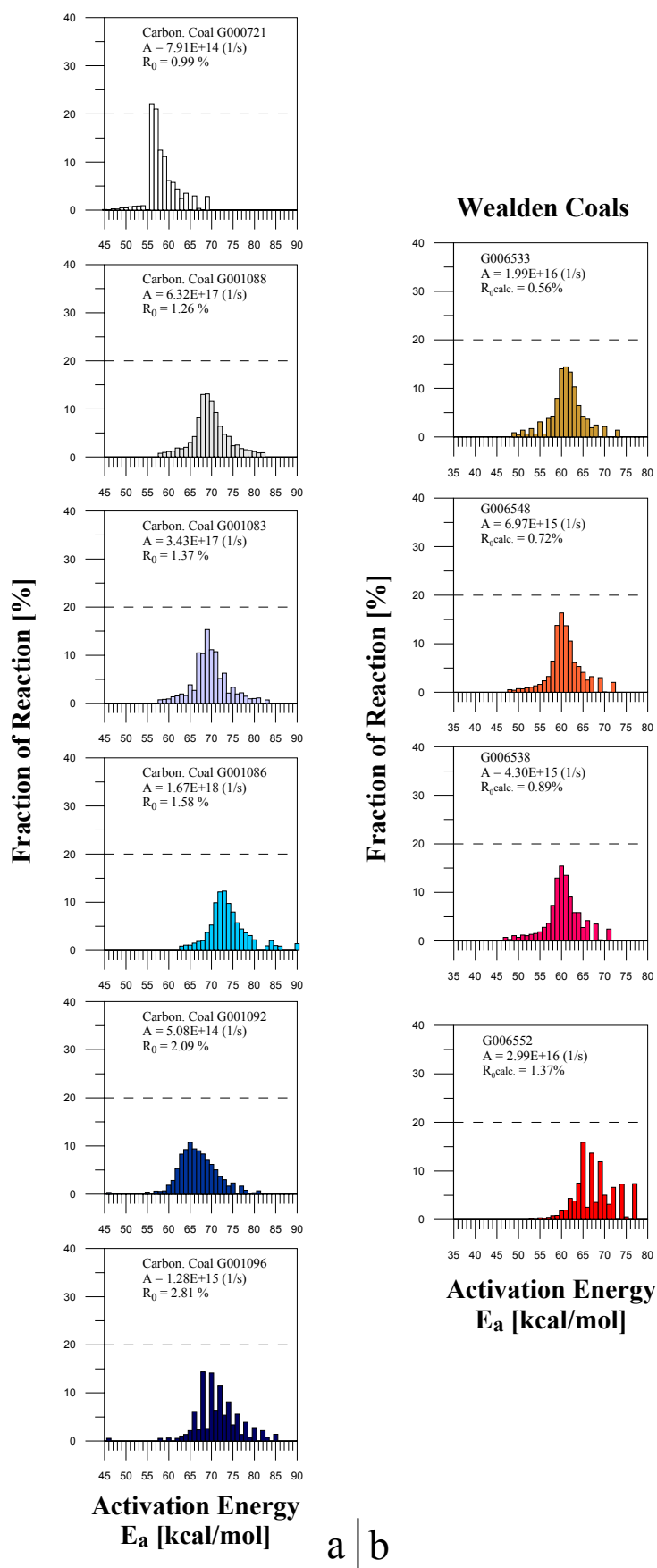


Figure 3.12: Frequency factors and activation energy distribution of a) Carboniferous German Coals. (Data taken from Schenk and Horsfield (1998) with the exception of sample G000721) and b) Cretaceous Wealden Coals from Germany

Structural rearrangement of the organic matter during natural maturation leading to a stabilisation of petroleum precursors can be evidenced by an increase of frequency factors by one order from  $1.15\text{E}+15$  (1/s) for the least stable sample G001980 ( $R_o = 0.44\%$ ) to  $1.15\text{E}+16$  (1/s) for the most stable and most mature sample G001991 ( $R_o = 0.80\%$ ). In addition, the mean activation energy is shifted from 57 kcal/mol to 60 kcal/mol. The heights of the normalised mean activation energies are more or less constant which shows that less stable precursor structures are not just stripped away but that more stable precursor structures are concomitantly formed during natural maturation. It might be an artefact, but there is an obvious shift of the symmetry of the activation energy distribution from left to right, i.e. the fraction of reaction increases slowly for low activation energies and decreases strongly for high activation energies at low maturity stages, whereas the fraction of reaction increases strongly for low activation energies and decreases slowly for high activation energies of samples at elevated maturity stages. Those features can be explained by the preferential loss of oxygen functionalities during diagenesis and early catagenesis, which leads to the formation of new and more stable moieties within the macromolecular matrix (Schenk and Horsfield, 1998; Sykes and Snowdon, 2002) and possibly to a concentration of potential hydrocarbon generating structures (Vandenbroucke and Largeau, 2007) indicated by increasing HI's and decreasing OI's (discussed in Chapter 3.1.2).

This increase in organic matter stability and product yield also has a pronounced effect on bulk petroleum formation rate curves (mg/g TOC), which are displayed in Fig. 3.13 for geologic and laboratory heating rates. In both scenarios, curves of coals exhibiting a higher maturity do not fit within the curve envelope defined by less mature samples but are shifted to higher temperatures marking hydrocarbon generation predictions using sub-bituminous coals as not reliable.

#### *German Coals, Ruhr Area*

The same “envelope shift” feature is observable for formation rate curves of Carboniferous German Coals (Fig. 3.13) up to  $R_o = 1.58\%$  for which maturation is characterised by formation of more stable petroleum potentials, presumably via solid state aromatisation reactions (Schenk and Richter, 1995; Schenk and Horsfield, 1998). Decreasing hydrocarbon potentials are therefore not only related to cracking and generation but also to the incorporation of potential petroleum precursor structures into the residual macromolecular matrix with the responsible reaction pathway not being simulatable by open-system pyrolysis methods. Formation rate curves of the more mature coal samples G001092 ( $R_o = 2.09\%$ ) and



G001096 ( $R_o = 2.81\%$ ) plot within the envelope of the more immature sample G001086 ( $R_o = 1.58\%$ ), which was explained by ring condensation during pyrolysis in the course of which hindering methyl groups are eliminated as methane (Landais and Gerard, 1996; Schenk and Horsfield, 1998). Such polycondensation reactions cause decreasing frequency factors and a simultaneous decrease of dominant activation energies (Fig. 3.12) for the relevant samples. After an increase from  $A = 7.91E+14$  (1/s) at  $R_o = 0.99\%$  to  $A = 1.67E+18$  (1/s) at  $R_o = 1.58\%$  with a shift of the mean activation energy from 56 to 73 kcal/mol due to solid state aromatisation/cyclisation-reactions in the course of natural maturation, frequency factors decrease again to lower values;  $5.08E+14$  (1/s) at  $R_o = 2.09\%$  and  $1.28E+15$  at  $R_o = 2.81\%$ . A similar decrease of kinetic parameters in going from medium- to low-volatile bituminous coals has been previously reported by Burnham *et al.* (1989).

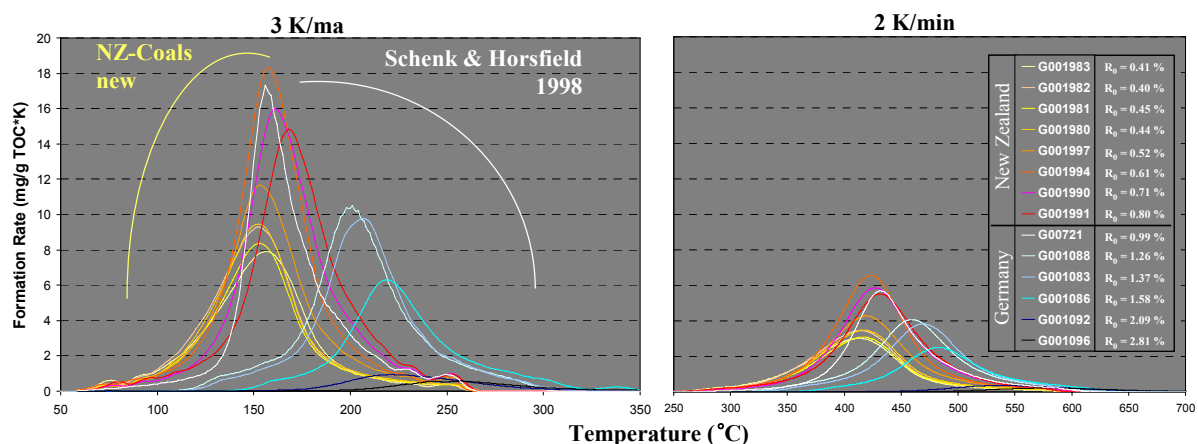


**Figure 3.13:** Bulk hydrocarbon formation rate curves for natural maturity series (given in % vitrinite reflectance) for laboratory and geologic heating rates; New Zealand Coals (determined within this thesis) and Westphalian Coals (taken from Schenk and Horsfield (1998)).

#### *Wealden Coals, Germany*

In Fig 3.12 activation energy distributions of three high ( $R_{o,calc} < 1.15\%$ ) and one medium ( $R_{o,calc} > 1.15\%$ ) volatile bituminous Wealden coal samples are displayed. Vitrinite reflectances are not measured but approximated using the empirical formula employed by Jarvie *et al.* (Jarvie *et al.*, 2001) which is not, as previously discussed, perfectly suited for Type III organic matter. Thus, the shape of the activation energy distribution, a mean activation energy of  $\sim 60$  kcal/mol as well as the frequency factors between  $4.30E+15$  and  $1.99E+16$  (1/s) of the three high volatile bituminous Wealden Coals resemble very closely those of the high volatile bituminous New Zealand Coal samples exhibiting a measured  $R_o$  between 0.71 and 0.80% (Fig. 3.11 - G001990, G001991). For the more mature Wealden Coal sample G006552 mean activation energies are shifted to values above 65 kcal/mol with a

single frequency factor at  $2.99\text{E}+16$  (1/s) again indicating, as expected for Type III organic matter, a stabilisation of the organic matter structure by formation of more stable petroleum potentials, presumably via solid state aromatisation reactions (Schenk and Richter, 1995; Schenk and Horsfield, 1998).

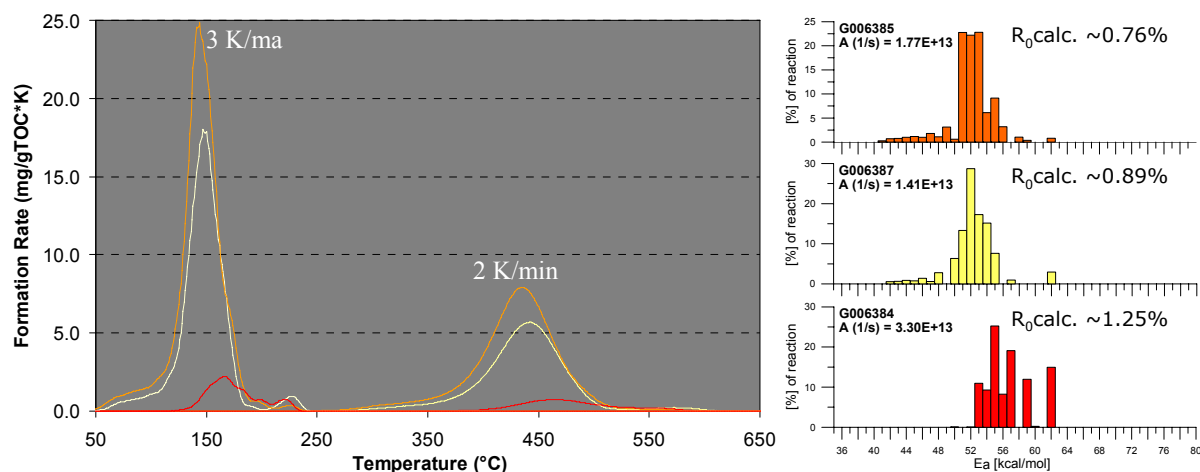


**Figure 3.14: Bulk hydrocarbon formation rate curves for Exshaw Fm. samples of different maturities (given in calculated  $R_0 = T_{\max} * 0.018 - 7.16$ ) for laboratory and geologic heating rates and the discrete activation energy distribution with a single free frequency factor.**

#### *Exshaw Formation, Canada*

In Fig. 3.14 activation energy distributions and frequency factors of Exshaw Fm samples spanning a maturity range between 0.76 and 1.25%  $R_0$  (calculated using the equation given in Jarvie *et al.*, 2001) are displayed together with geologic and laboratory formation rate curves. The frequency factors exhibit values between  $1.41\text{E}+13$  (1/s) and  $3.30\text{E}+13$  (1/s), which resembles values of other Devonian-Mississippian shales from North-America investigated within this thesis (Fig. 3.9; Tab. 3-3). The activation energy distribution of the two more immature samples is, as previously discussed, typical for marine shales with mean activation energies ranging around 52 kcal/mol. For sample G006384 low activation energies are “stripped” away and  $E_a$ ’s are centred on the higher values with the distribution shape being very unsteady related to the low hydrocarbon rest potential at those elevated maturity stages. Thus, and in contrast to the New-Zealand – German Coal maturity sequence, formation rate curves of Exshaw Fm samples remain within the envelope of the least mature sample G006385 (Fig. 3.14) indicating that during natural maturation homolytic cracking or condensation reactions prevail over cross-linking/aromatisation reactions. Here, laboratory kinetic parameters of the most immature sample could be used to predict the timing of at least primary petroleum generation under geologic conditions.

### 3.4 Mineralogy (ATR-IR)

32 samples, mainly shales (Tab. 3-4), were submitted to Attenuated Total Reflection IR Spectroscopy (ATR-IR), which was recently developed in Newcastle as a rapid tool to generate semi-quantitative information on the mineralogy of major phases within source rocks. ATR-IR can be viewed as a mineralogy screening technique or “Rock Eval for minerals” enabling key heterogeneities to be identified quickly as input to reservoir characterisation (e.g. of shale gas plays). Quantitative methods such as XRD are more costly and time consuming limiting sample throughput.

**Table 3-4: Mineralogical composition of 32 investigated source rocks based on ATR-IR spectroscopy comparing normalised fractions of clay, quartz + feldspar, and carbonate.**

GFZ Code	Formation/ Basin	Depositional Environment	Quartz+ Feldspar (%)	Calcite + Dolomite (%)	Clay (%)
G004750	Green River Shale	lacustrine	31	7	62
G006536	Wealden Shales		15	7	78
G0047501965	Mix type I/III		25	12	63
G006208	Toarcian Shale	Marine	27	25	47
G001955	Spekk Fm.	Mesozoic - Cenozoic	24	6	70
G000689	Botneheia Shale		46	9	45
G005812	Irati Fm.	Marine Paleozoic	43	3	54
G006153	Woodford Shale		77	5	18
G006154	Woodford Shale		80	3	17
G006156	New Albany Shale		37	5	59
G006155	Caney Shale		62	6	32
G005298	Bakken Shale		42	3	55
G000692	Chattanooga Shale		37	4	59
G004564	Murzuq Basin		23	5	72
G007160	Murzuq Basin		14	5	81
G006949	Middle East		15	4	81
G000753	Alum Shale		54	3	43
G000758	Alum Shale		62	4	34
G006948	Middle East		22	4	74
G007161	Ghadames Basin		48	9	43
G005935	Akata Shale		26	12	62
G005763	Hekkingen Fm.	marine - terrestrial	42	7	52
G006205	Douala Basin	org. lean mixed mar - ter	4	6	90
G007165	Farsund Fm.		26	8	66
G007166	Farsund Fm.		27	12	61
G000721	Westphalian Coals	fluvio-deltaic - terrestrial	49	23	28
G001965	Åre Fm.		22	17	61
G006207	Mahakam Delta		31	6	63
SN6750	Taglu Fm.		51	14	35
G006385	Exshaw Fm.	Marine - maturity sequence	47	5	49
G006387	Exshaw Fm.		71	23	6
G006384	Exshaw Fm.		43	14	43

In a ternary diagram (Fig. 3.15), the clay content of investigated samples is compared to its quartz + feldspar as well as carbonate content. Normalised values are displayed in Tab. 3-4. The original data set with values for all mineral phases can be found in Table A 4. Carbonates comprise calcite and dolomite, whereas clay comprises illite-smectite as well as kaolinite and chlorite.

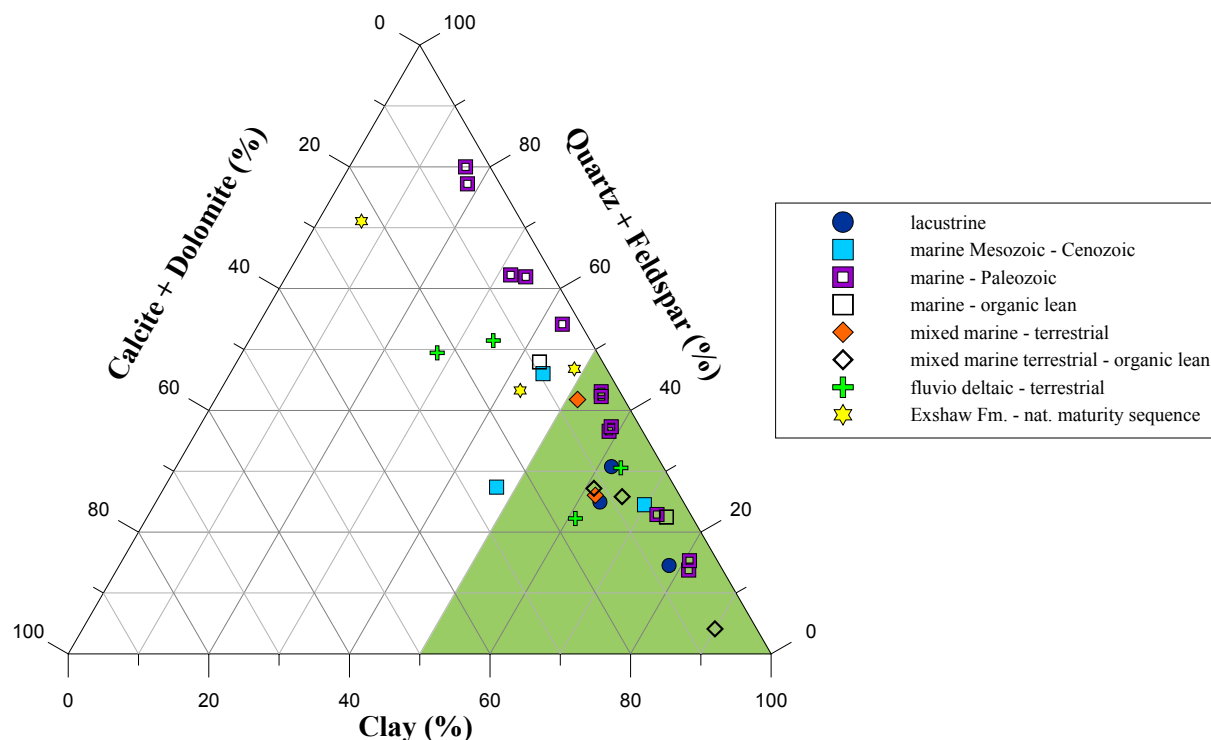


**Figure 3.15: Mineralogical composition of 32 investigated source rocks based on ATR-IR spectroscopy displayed in a ternary diagram comparing fractions of clay, quartz + feldspar, and carbonate.**

Generally it can be said, that all investigated samples are depleted in carbonates marking them as siliciclastic source rocks, in most cases shales. This is not true for the Westphalian Coal as well as for the coaly samples from the Åre Fm., Taglu Fm., and Mahakam Delta. The clay *versus* quartz content varies strongly for the investigated source rocks, which bears some practical information if considered under the aspect of gas in unconventional petroleum systems.

For the successfulness of a shale gas play, two major variables are of uppermost importance, these being the gas in place (GIP) and the fracability of the rock (Bowker, 2007; Jarvie *et al.*, 2007; Ross and Bustin, 2009). For GIP, mainly organic matter content, type, and maturity are relevant parameter effecting the total amount of gas generated, sorption capacity, and overall porosity, whereas the fracability is determined by the mineral matter composition. Although clay minerals might enhance the methane sorption capacity of a rock due to a high

internal surface area (microporosity) also featuring higher sorption energies than larger pores (Dubinin, 1975; Ross and Bustin, 2009), the non-brittle behaviour of clays upon fracturing exercises a negative impact on gas flow rates (Jarvie *et al.*, 2007). It is said that 50% brittle material like quartz or carbonate should be present keeping in mind that carbonate cement within formerly open fractures has a lowering effect on porosity (and also permeability) and therefore on the amount of free gas in place. Nevertheless, this carbonate cement also keeps generated gas within the matrix porosity and prevents its escape through an open pore fracture network which would result in mainly adsorbed gas in place releasable by pressure decrease only (Bowker, 2007). The same author formulates the straight forward advice (concerning the Barnett Shale in the Newark East Field) that “the explorationist should not look for fractured, gas-saturated shales, but instead for gas-saturated shales that can be fractured”.

Therefore, shales exhibiting clay contents much higher than 50% (empirical cut-off value) should be treated with caution if evaluated for shale gas production. In Fig. 3.15, relevant source rocks of the investigated sample set plot within the green triangle. Investigated shales with less than 50% clay content are the Jurassic Toarcian Shale and Triassic Botneheia Shale, the Paleozoic Woodford Shale (G006153, G006154), the Caney Shale, two Cambrian Alum Shales, the organic lean Silurian Hot Shale from the Ghadames Basin as well as the samples from the Exshaw Fm. representing a small natural maturity sequence. Nevertheless, it should be kept in mind that single samples are not representative of the whole source rock package due to possibly strong horizontal and lateral compositional variations of organic and inorganic matter.



## **4 EVALUATING THE LATE GAS POTENTIAL OF IMMATURE SOURCE ROCKS FROM DIFFERENT DEPOSITIONAL ENVIRONMENTS**

The purpose of this chapter is to delineate how late gas generation can be evidenced under laboratory conditions in general and to what extent the initial organic matter structure, depositional environment or precursor biota is responsible for the occurrence of late gas generation.

Almost all of the open- and closed-system pyrolysis based approaches used to monitor overall conversion of organic matter to primary and secondary petroleum (e.g. Dieckmann *et al.* (2006), Erdmann and Horsfield (2006) or Hill *et al.* (2007)), show incomplete methane generation profiles due to too low final temperatures rarely exceeding 600°C. This prevents the accurate determination of kinetic parameters for late gas generation. Here, complete, regularly spaced temperature *versus* methane generation profiles were recorded for 4 immature source rocks covering different depositional environments under closed-system pyrolysis conditions up to 780°C (maxima reached at earlier temperatures) at a single heating rate of 1°C/min. Those were then used in comparison to open-system pyrolysis profiles (only up to 600°C) to discriminate between primary and secondary gas input at high temperatures. For one sample (Åre Fm. G001965) which showed a distinct late gas potential, kinetic parameters of late gas generation could be determined using 3 different heating rates. Results are described in detail in Chapter 4.1.

In Chapter 4.2 follows the description of the relationship between late gas potential and kerogen type and structure, which could be assessed using a larger samples set, i.e. previously discussed (Chapter 3) immature source rocks covering the main kerogen types and organofacies, and a less time consuming two- to three-step closed-system pyrolysis method. The latter consisted of heating crushed whole rock samples in MSSV-tubes to two or three different end temperatures with focus on the main stage of late dry gas generation.

### ***4.1 Detailed Investigation on the Late Gas Generation Behaviour of a Small Sample Set using Open- and Closed-System Pyrolysis Methods***

#### **4.1.1 Sample Set**

Four source rocks stemming from different depositional environments were used to study primary and secondary gas generation mechanisms in detail and to assess the kinetics of high temperature gas generation if observed. The sample set comprises two source rocks from

the Haltenbanken area of Mid Norway, those being fluvio deltaic-terrestrial Type III coal from the Åre Fm (G001965) and marine Type II shale from the Spekk Fm. (G001955), as well as the lacustrine Type I Green River Shale (G004750) and a synthetic Type I/III source rock (G0047501965), which is a synthetic admixture of 50 wt.-% Green River shale (G004750) and 50 wt.-% Åre Fm. Coal (G001965). The geochemical characterisation (TOC, Rock-Eval, open-pyrolysis GC, SRA bulk kinetics, IR Mineralogy) of the specific samples can be found together with 61 other immature source rocks in Chapter 3.

#### 4.1.2 Evolution of Boiling Ranges during Stepwise Open-System Pyrolysis

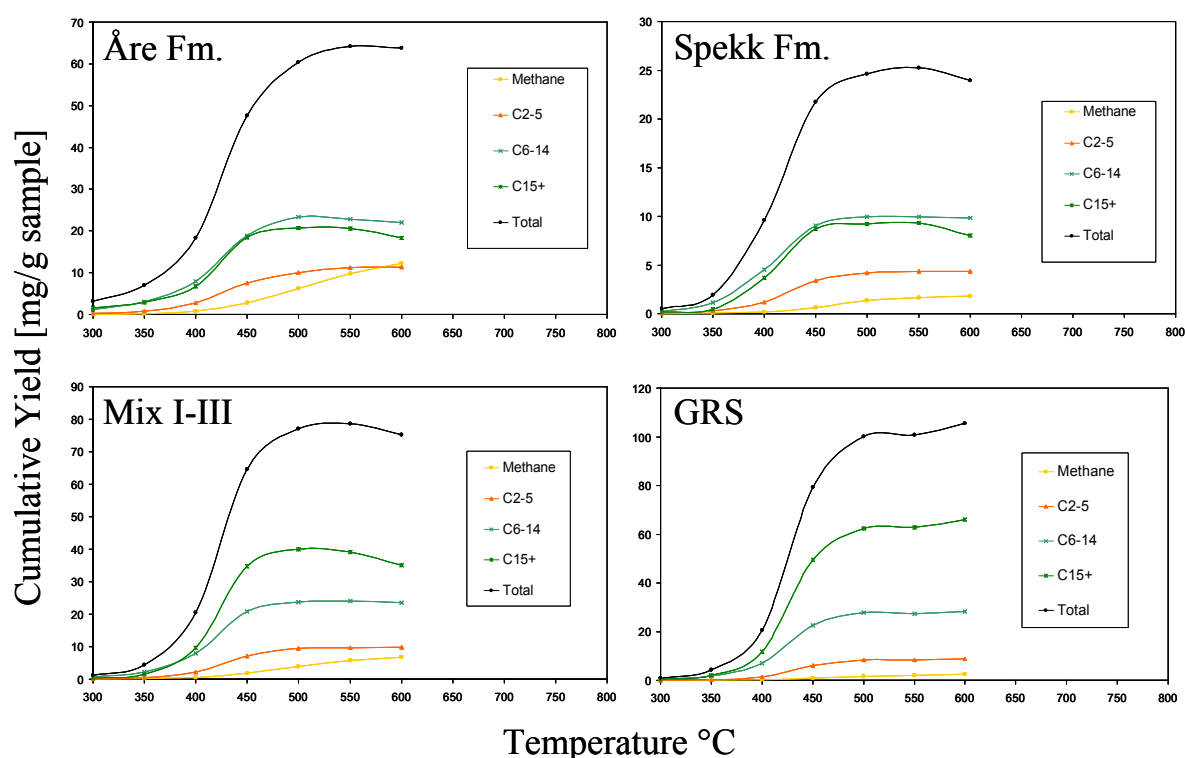


**Figure 4.1:** Stepwise open-pyrolysis at 1°C/min: cumulative yield curves of boiling fractions methane, C<sub>2-5</sub>, C<sub>6-14</sub>, C<sub>15+</sub> and Totals for the Åre Fm., Spekk Fm., Green River Shale (GRS), and synthetic mixture I/III

In order to gain a better understanding about the evolution of exclusively primary gas a stepwise open pyrolysis GC approach was employed. The Åre Fm. sample G001965, the Spekk Fm. sample G001955, the Green River Shale sample G004750, and the synthetic Mix Type I/III sample G0047501965 were pyrolysed at a heating rate of 1°C/min, starting at 200°C and ending at various end temperatures between 300 and 600°C. The results for the different boiling fractions methane (C<sub>1</sub>), C<sub>2-5</sub>, C<sub>6-14</sub>, and C<sub>15+</sub> are summarised in Fig. 4.1 (and Table A 5) as cumulative yield curves, in which displayed data points represent the sum of all products up to the temperature of each data point. Primary gas formation covers a broader



temperature interval than does  $C_{6+}$  generation which is completed at about 500°C for all source rocks, as cumulative yield curves reach a plateau. Wet gases reach a plateau somewhat later at 550°C indicating the end of  $C_{2-5}$  primary generation. Interestingly, primary methane is still being generated in significant amounts at the highest temperature 600°C from the terrigenous derived Åre Fm. sample G001965 and the synthetic mix Type I/III sample G0047501965. Thus, a different pool of precursor structures seems to be the most likely source of this late, refractory methane, linked to this organic matter type.

### 4.1.3 Evolution of Boiling Ranges during MSSV Pyrolysis

Different gas forming modes like primary and secondary generation, mechanisms and related reaction kinetics can be deduced from closed-system MSSV pyrolysis. Fig. 4.2 shows the cumulative evolution of total GC-detectable products and the different boiling fractions methane ( $C_1$ ),  $C_{2-5}$ ,  $C_{6-14}$ , and  $C_{15+}$  for the Åre Fm. sample G001965, the Spekk Fm. sample G001955, the Green River Shale sample G004750, and the synthetic mix Type I/III sample G0047501965, which were pyrolysed at a heating rate of 1°C/min to end temperatures between 300 and 780°C. Single compound yields for the specific end temperatures are given in Table A 6.

The high temperature range (>600°C) is necessary to be able to qualify and quantify late gas production and its kinetics. In previous studies (Erdmann, 1999; Dieckmann *et al.*, 2006; Erdmann and Horsfield, 2006) sufficient thermal stress was not applied and a product plateau for heterogeneous, mixed marine-terrigenous Type II/III source rocks from the Heather Fm., Norway, and the Taglu Fm., Canada, could not be reached for the highest temperature, indicating that late methane generation was not completed and calculation of kinetic parameters somewhat speculative. Here, gas and oil, as well as total product yields of all four investigated immature source rocks display a plateau or a maximum at different temperature stages.

The overall  $C_{1+}$  products reach a maximum at slightly higher temperatures than the  $C_{6+}$  compounds (>450°C) because primary gas is still being generated (see stepwise open pyrolysis) at faster rates than  $C_{6+}$  compounds are being cracked to gas and coke. Exact temperatures for maximal yields cannot be given, as individual end temperatures are separated too widely.  $C_{1+}$  products subsequently decrease, which was observed previously for various experimental set-ups, most likely due to the formation of coke (Horsfield *et al.*, 1992b) or possibly related to the neoformation of a stable moiety yielding gas at later stages of thermal stress. The latter could be only true for the synthetic mix Type I/III sample G0047501965 and

the Åre Fm. sample G001965, for which total products and  $C_{1-5}$  start to rise again at temperatures exceeding 650°C respectively 600°C. This formation of significant amounts of late methane is related to the degradation of an at least thermally stable kerogen- or pyrobitumen-like precursor structure (if not neoformed), as  $C_{6+}$  compounds are already almost completely depleted. Interestingly,  $C_{1+}$  products decrease at higher temperatures (>740°C) also for the Åre Fm. sample and synthetic mix Type I/III sample, indicating thermal decomposition of methane, which is the only GC-detectable pyrolysis product at those temperature stages. A study on the thermal decomposition of methane from 700 to 1000°C was conducted by Sackett (1995) who demonstrated that pure methane possesses half lives of 108, 34, and 4h for 800, 900, and 1000°C respectively. The products of the decomposition reaction were clearly amorphous carbon and hydrogen gas. Decomposition of methane might even start at lower temperatures if pyrolysed in an “impure” system together with its carbon-rich source rock as is the case for the present analytical set-up.

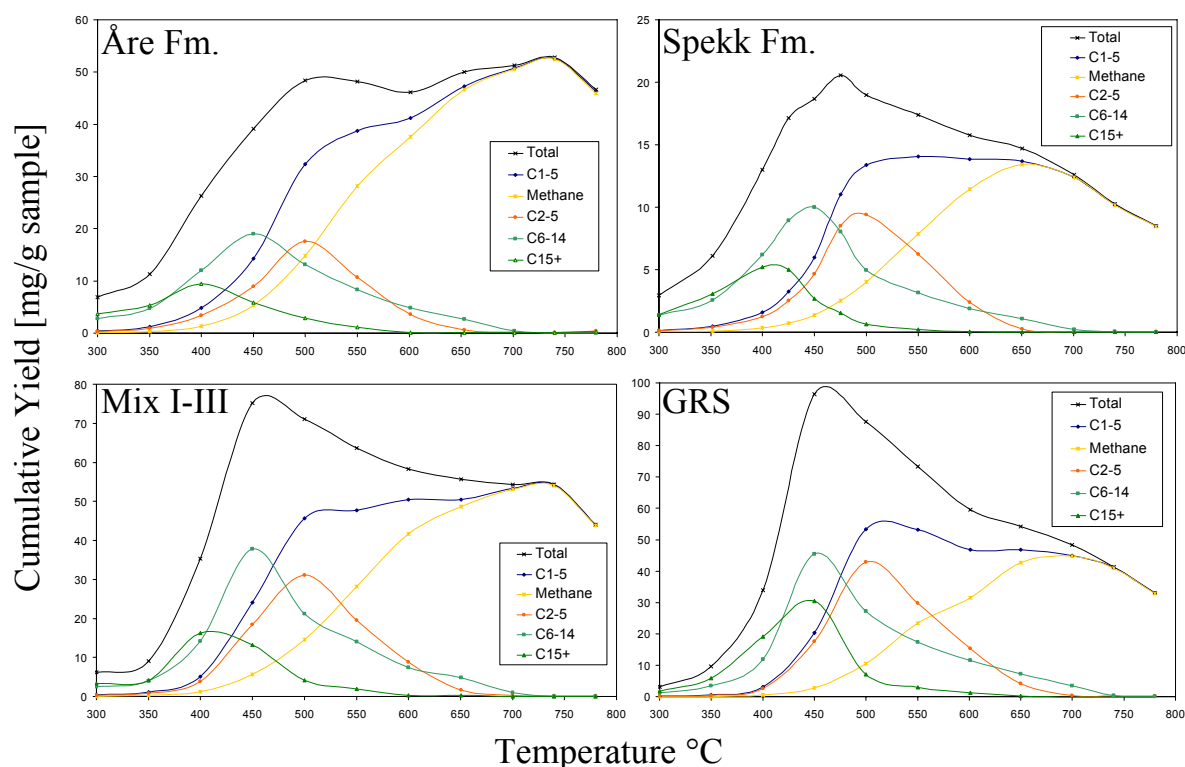


**Figure 4.2: MSSV-pyrolysis at 1°C/min: cumulative yield curves for total products and boiling fractions methane,  $C_{2-5}$ ,  $C_{6-14}$ ,  $C_{15+}$  for the Åre Fm., Spekk Fm., Green River Shale (GRS), and synthetic mixture I/III**

The  $C_{6+}$  compounds reach a maximum at 450°C (see also Fig. 4.4) for all source rocks and decrease at higher temperatures due to secondary cracking and thus formation of secondary gas and coke.  $C_{15+}$  evolution curves reach their apex already at earlier temperature

stages and are most likely cracked to  $C_{6-14}$  compounds and in minor amounts to early secondary gas. The slopes of the evolution curves decreasing parts are subdivided into a first steeper part up to 500°C and a second shallower part up to ~700°C, where  $C_{6+}$  compounds are completely depleted.

The secondary gas formation leads to a difference between  $C_{1-5}$  and  $C_{6+}$  maxima of at least 50°C for all source rocks, with wet gas components  $C_{2-5}$  decreasing at temperatures in excess of 500°C related to their decomposition to secondary methane and coke. Thus, methane is still being generated up to higher temperatures, but up to different temperature stages depending on the organic matter and its late gas potential. For the Spekk Fm. sample G001955 and the Green River Shale sample G004750 methane formation already comes to an end, simultaneously with the depletion of GC-amenable  $C_{2+}$ -compounds, at about 650°C. In contrast, methane yields keep on increasing until 740°C for the synthetic Mix Type I/III sample G0047501965 and the Åre Fm. sample G001965, indicating “true” or high temperature late gas generation from a thermally stable, kerogen-like precursor structure and not by the secondary cracking of primary products.

#### 4.1.4 Calculation of Primary and Secondary Gas Formation

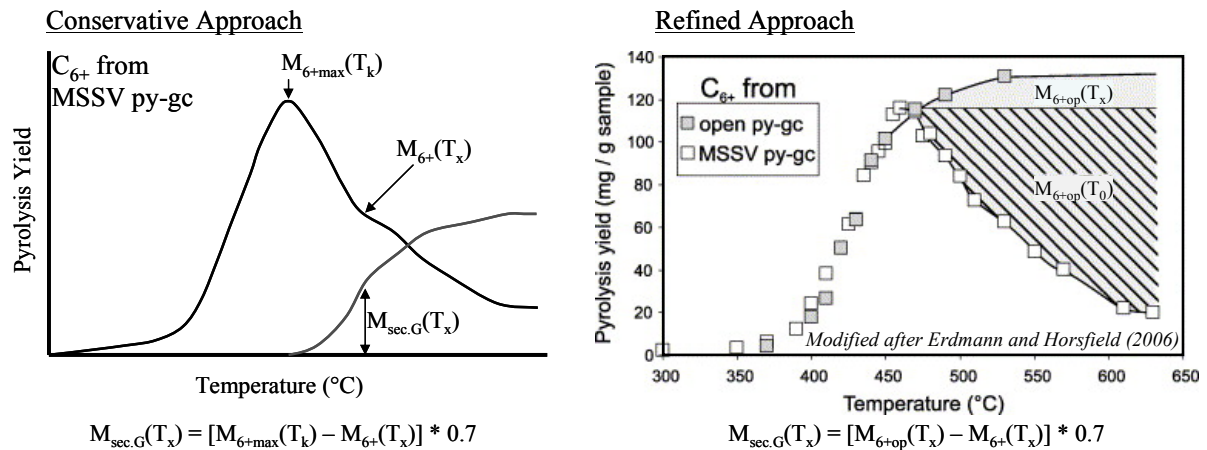


**Figure 4.3:** „Conservative approach“-model (Dieckmann *et al.*, 1998) for the calculation of secondary gas formation from the decrease of MSSV-pyrolysis  $C_{6+}$  compounds and “Refined Approach“-model (Erdmann, 1999) for the calculation of secondary gas formation from the difference between open- and closed-system pyrolysis  $C_{6+}$  compound yields

In order to enable the determination of kinetic parameters of primary, secondary and late secondary gas formation, the respective cumulative generation curves need to be unravelled first. Stepwise open-system pyrolysis can be used for the direct measurement of primary product evolution which helps to find the appropriate evaluation method for the closed-system pyrolysis based calculation of secondary and primary product evolution curves.

Two evaluation methods were previously applied and described by Dieckmann *et al.* (1998) and by Erdmann (1999), called the *conservative* and the *refined evaluation* respectively (Fig. 4.3). The choice of one of the methods has later a strong impact on the results of timing and amount predictions for gas generation under geological heating conditions.

### ***The conservative evaluation approach***

The *conservative evaluation* approach (left side of Fig. 4.3) is based on closed-system pyrolysis data alone and the assumption that secondary cracking of oil to gas starts when cumulative yields of the C<sub>6+</sub> boiling range fraction reach their apex (Sweeney *et al.*, 1987; Schaefer *et al.*, 1990; Horsfield *et al.*, 1992b). The amount of secondary gas generated within the closed system is directly related to the decrease of C<sub>6+</sub> compounds and represents additionally to primary gas an important fraction of the measured total gas C<sub>1-5</sub>. Assuming that for reasons of hydrogen balance only ~70% of cracked C<sub>6+</sub> compounds are converted in the simplest case into gas and ~30% into pyrobitumen (Coke) (Sweeney *et al.*, 1987; Braun and Burnham, 1992), cumulative secondary gas yields at a certain temperature can be calculated from the decrease of “oil” compounds according to equation (9):

$$M_{\text{sec.G}}(T_x) = [M_{6+\text{max}}(T_k) - M_{6+}(T_x)] * 0.7 \quad (9)$$

In this equation, M<sub>6+max</sub> represents the maximum of the C<sub>6+</sub> evolution curve at temperature T<sub>k</sub>, M<sub>6+</sub> is the residual amount of liquid hydrocarbons at elevated temperatures T<sub>x</sub>, while M<sub>sec.G</sub> corresponds to the resulting amount of secondary gas at temperature T<sub>x</sub>. The average conversion factor of ~0.7 is assessed from



where  $n$  = average H/C-ratio of C<sub>6+</sub> compounds;  $m$  = average H/C-ratio of secondary gas;

$u$  = average H/C ratio of pyrobitumen, which yields

$$x = (n - u)/(m - u) \quad (11)$$

and a conversion factor of

$$f_c = x(12 + m)/(12 + n) \quad (12)$$

Assuming  $n = 2.2$  (average of hexane and triacontane),  $m = 3.2$  (average of methane and pentane),  $u = 0.2$  (Behar *et al.*, 1991b; Behar *et al.*, 1992), the conversion factor is assessed to be  $f_c = 0.7$ . The assumed average compositions are hypothetical and could be adapted to different scenarios where  $f_c = 0.7$  might be too optimistic, for instance if the degradable “oil” is more aromatic or the secondary gas very dry.

Thus, the amount of primary gas  $M_{\text{prim.G}}$  at a defined temperature  $T_x$  can be easily assessed using equation (13) by subtracting calculated secondary gas yields from the measured total amount of gas  $M_{\text{tot.G}}$ .

$$M_{\text{prim.G}}(T_x) = M_{\text{tot.G}}(T_x) - M_{\text{sec.G}}(T_x) \quad (13)$$

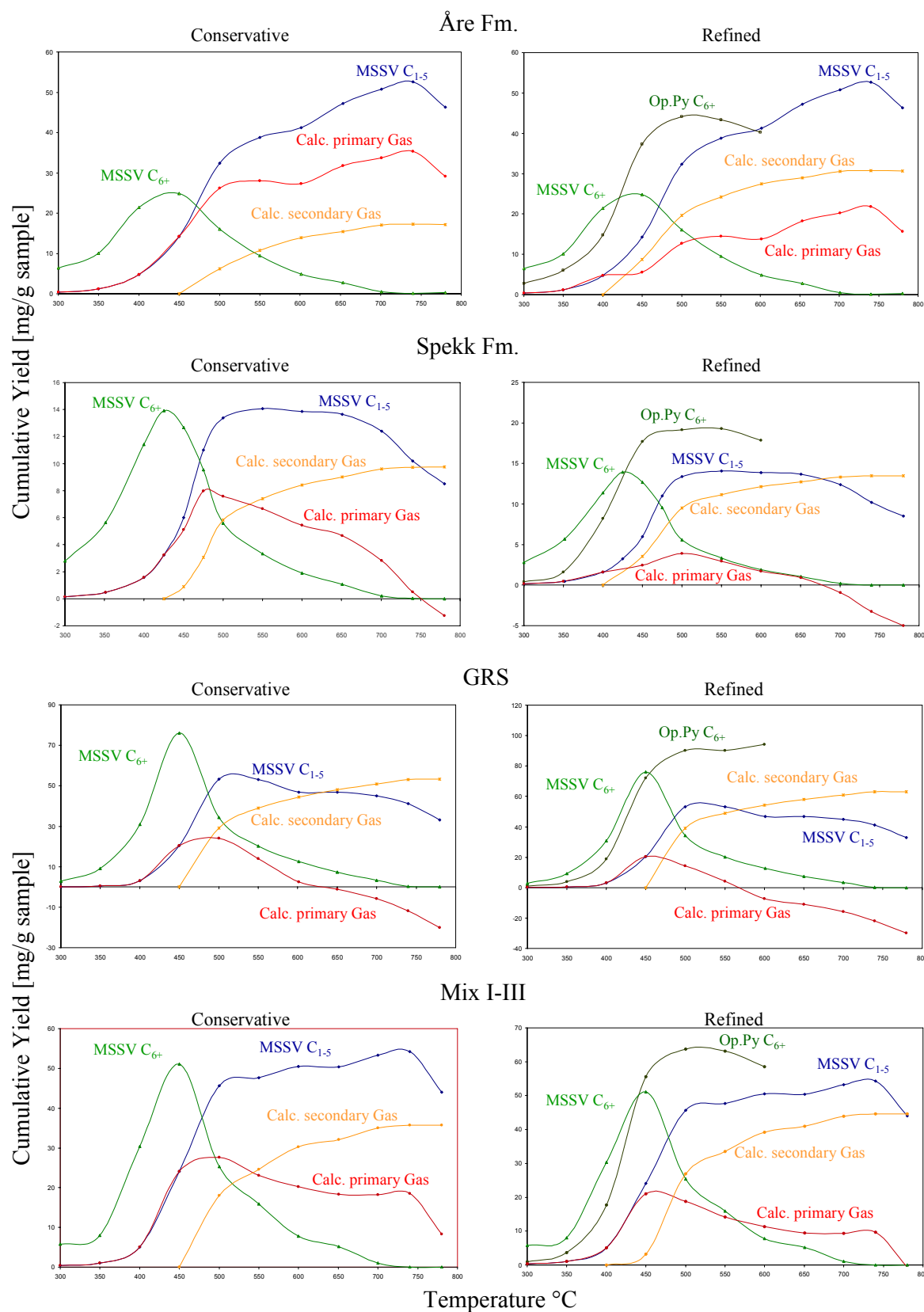
With this conservative approach using equation (9) and (13) Dieckmann *et al.* (1998) successfully calculated kinetic parameters for secondary gas generation of a Type II Toarcian Shale where the remaining gas in the closed system was confirmed to be of primary origin by direct comparison of gas yield curves from multistep-open system and closed-system pyrolysis.

### ***The refined evaluation approach***

Erdmann (1999) *refined* the conservative approach for a Draupne Formation sample containing kerogen Type II as he noticed that secondary cracking overcompensates primary cracking when comparing open- and closed-  $C_{6+}$  pyrolysis yields (right side of Fig. 4.3). Primary “oil” generation had not come to an end in the open system while under closed-system condition cumulative liquid boiling range fraction yields already decreased, thus, amounts of secondary gas would have been underestimated by ~8% using the *conservative* evaluation method alone. The *refined* amount of  $C_{6+}$  available for the cracking to secondary gas is the difference between the open and closed pyrolysis yields and as a consequence equation (9) was modified to equation (14) by replacing the amount of  $C_{6+}$  products at the cumulative maximum  $M_{6+\text{max}}(T_k)$  with the amount of observed primary  $C_{6+}$  products  $M_{6+\text{op}}$  for any temperature  $T_x$  greater than  $T_k$ .

$$M_{\text{sec.G}}(T_x) = [M_{6+\text{op}}(T_x) - M_{6+}(T_x)] * 0.7 \quad (14)$$

Primary gas content in the closed system can be calculated again using equation (13). Erdmann (1999) could show that comparing calculated primary gas and measured primary gas evolution curves results are in good agreement with regard to onset, increase and end of generation although the calculated primary gas curve shows somewhat higher yields than observed by open-system pyrolysis. This indicates that secondary gas yields might still be slightly underestimated probably due to secondary gas generation starting before the  $C_{6+}$  maximum is reached in closed pyrolysis.

*Comparison of the conservative and refined evaluation approaches*

**Figure 4.4:** Cumulative yield curves for boiling fractions C<sub>1-5</sub> and C<sub>6+</sub> measured under open- and closed-system pyrolysis conditions and calculated primary and secondary gas input using the „Conservative approach“ (left side) or “Refined Approach” (right side) for the Åre Fm., Spekk Fm., Green River Shale (GRS), and synthetic mixture I/III

In Fig. 4.4 calculated primary and secondary gas generation curves for the *conservative* and the *refined* approach are shown for the Åre Fm. sample G001965, the Spekk Fm. sample G001955, the Green River Shale sample G004750, and the synthetic mix Type I/III sample G0047501965. It is obvious that for all samples primary  $C_{6+}$  generation is still ongoing under open-system conditions while secondary cracking exceeds primary  $C_{6+}$  generation under closed-system conditions. There is a temperature gap of at least 50°C between open-system cumulative plateau yields and closed-system peak yields. Thus, the refined evaluation approach would be more appropriate for calculation of primary and secondary gas evolution curves as the prerequisite for the conservative evaluation method, that secondary cracking of oil starts when primary generation of oil ends does not hold to be true.

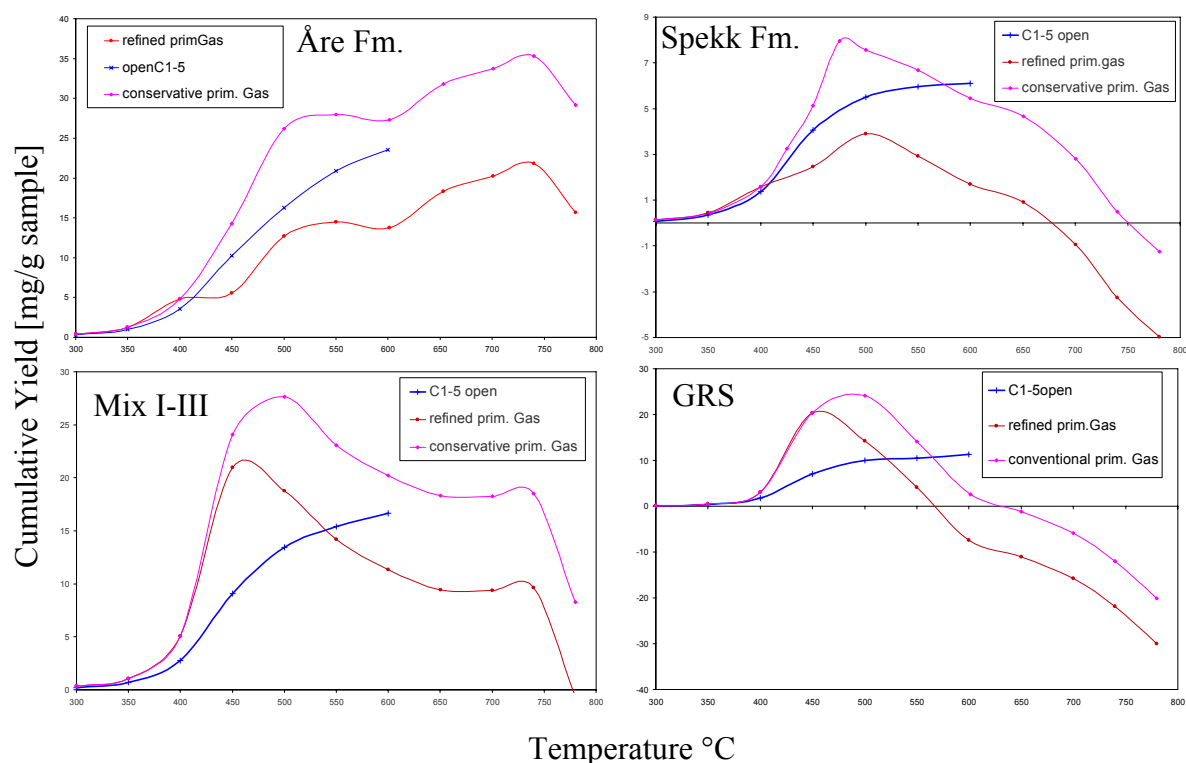


**Figure 4.5:** Comparison of measured primary gas yields (open pyrolysis) and calculated primary gas yields using “conservative” and “refined” approach models for the Åre Fm., Spekk Fm., Green River Shale (GRS), and synthetic mixture I/III

Calculated amounts of secondary gas are therefore higher for the refined approach whereas the additional amount of secondary gas is formed in the temperature range between open-system  $C_{6+}$  products plateau and closed-system  $C_{6+}$  peak yields. The shape of the secondary gas evolution curve is identical for the conservative as well as for the refined evaluation method for temperatures in excess of 550°C as measured primary oil generation

comes to an end at 550°C for all source rocks and calculation of secondary gas is left to only depend on the degradation of oil compounds within the MSSV vessel (equation (14)).

Nevertheless, independent of the evaluation method one feature is striking. The shape of the calculated primary gas evolution curve seems to be highly unrealistic for all source rocks and starts to decrease too early at temperature stages where primary gas generation has not come to an end under open-system conditions. In Fig. 4.5 measured open primary gas yields are directly compared to calculated primary gas yields. It is obvious that none of the calculated curves closely resembles the measured curve and thus, reality. For example, the *conservative* approach strongly underestimates secondary gas generation up to 500°C in all cases. The *refined* approach still underestimates secondary gas generation for the Green River Shale and the synthetic I/III mixture in this temperature range, but overestimates it for the Type III Åre Fm and the Type II Spekk Fm sample, indicating that some aromatisation or recombination of C<sub>6+</sub> compounds might occur reducing primary hydrocarbons content available for normal secondary cracking.

The decline in calculated primary gas amounts at temperatures higher than 600°C for all source rocks except the Åre Fm sample is mainly due to decreasing total MSSV Gas yields related to secondary cracking of C<sub>2-5</sub> wet gases to methane and coke, and only tributary to an overestimation of secondary gas generation. Thus only the Åre Fm. sample shows increasing, calculated primary gas yields after a plateau between 550 and 600°C at elevated temperature even though the slope of the primary gas evolution curve in the open system seems to level out at somewhat higher temperatures indicating the end of primary gas generation. Calculated primary gas formed between 600 and 740°C seems therefore to be the late gas under investigation formed from a thermally stabilised, not directly GC-detectable moiety during maturation and thus, is not of primary origin. In the context of this thesis this late gas is termed secondary gas (B) and its yield  $M_{\text{sec.B}}(T_x)$  can be calculated by subtracting plateau closed system primary gas yields  $M_{\text{prim.G}}(T_p)$  from post plateau primary gas yields  $M_{\text{prim.G}}(T_x)$  as shown in Fig. 4.6 using equation (15):

$$M_{\text{sec.B}}(T_x) = M_{\text{prim.G}}(T_x) - M_{\text{prim.G}}(T_p) \quad (15)$$

It can be seen in Fig. 4.6 that the secondary gas (B) yield at 740°C for both approaches adds up to 8.06 mg/g sample for the Åre Fm sample.



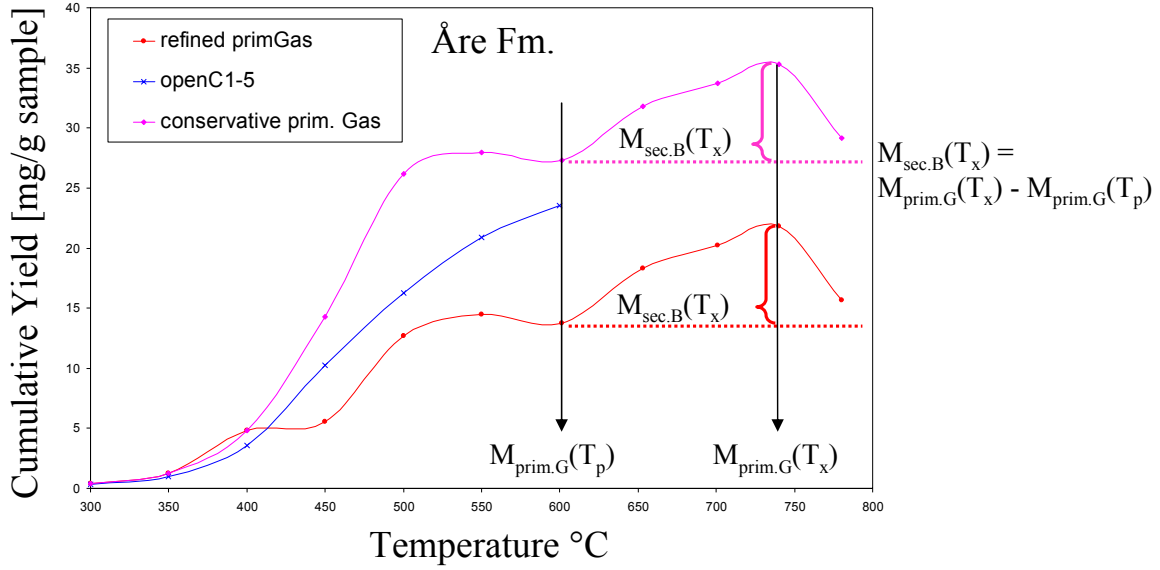


Figure 4.6: Calculation of late gas yields, i.e. secondary gas (B) yields based on calculated primary gas evolution curves

### Considering a “direct” open-versus-closed pyrolysis approach

The poor fit of measured and calculated primary gas evolution curves shown in Fig. 4.5 is still somewhat unsatisfactory. A more precise way would be to directly calculate secondary gas amounts by subtracting measured open pyrolysis primary gas  $M_{G.op}(T_x)$  from total MSSV gas yields  $M_{tot.G}(T_x)$  (equation (16)). In this context Berner et al. (1995) outlined that the primary cracking of the kerogen structure to form gas could be simulated by open system pyrolysis based on isotopic variations in hydrocarbon gases. For this reason, the open system pyrolysis-gas ( $C_{1-5}$ ) is considered to be a reasonable measure for the amounts of primary gas.

$$M_{sec.G}(T_x) = M_{tot.G}(T_x) - M_{G.op}(T_x) \quad (16)$$

A problem arising from this approach is that the open-system analytical device cannot be operated safely at temperatures in excess of 600°C degree due to the maximal application temperature of the used heating cartridges. Nevertheless primary gas evolution curves flatten out around 600°C for all four investigated source rocks and can be extrapolated to higher temperatures as shown in Fig. 4.7. One consequence of this approach is that none of the calculated yields are negative and a more realistic curve shape is obtained compared to the curve shapes observed for the *conservative* or *refined* approach.

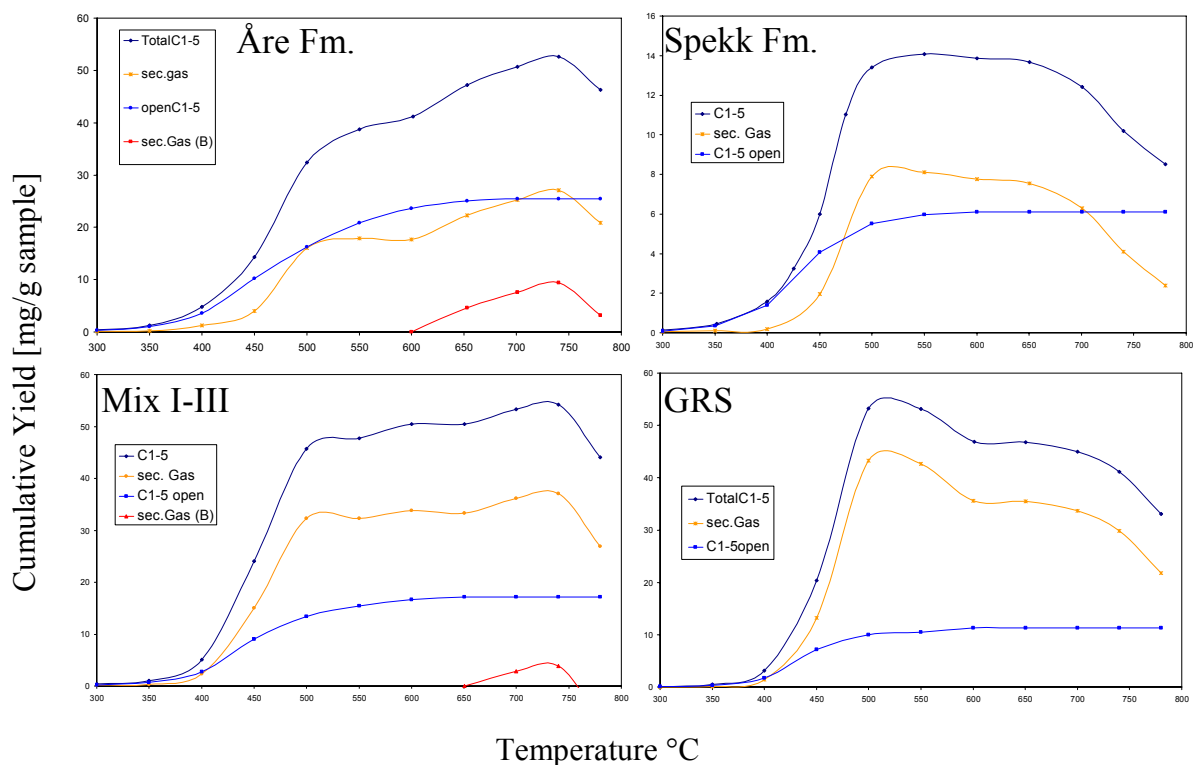


Figure 4.7: Evolution curves of calculated secondary gas (Equation 16), calculated secondary gas (B) (Equation 17), and directly measured open- and closed-system pyrolysis total gas yields for the Åre Fm., Spekk Fm., Green River Shale (GRS), and synthetic mixture I/III

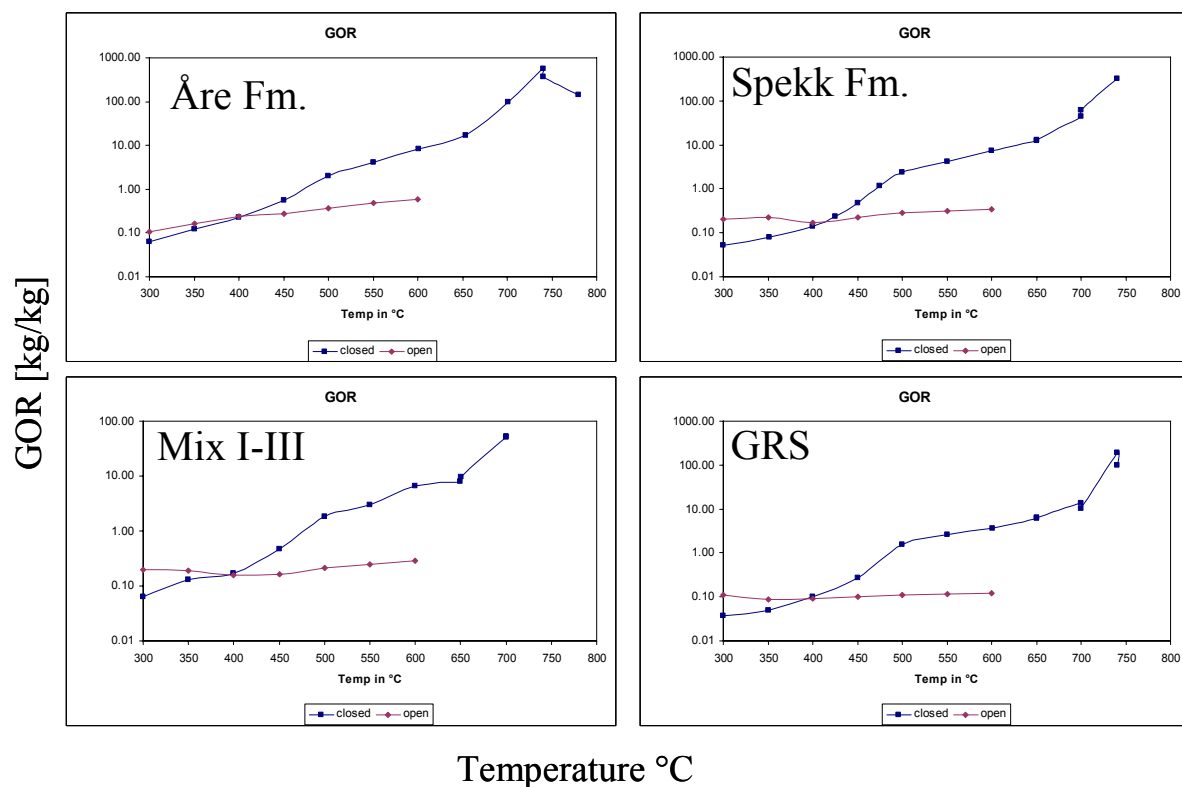


Figure 4.8: Evolution of GOR (C<sub>1-5</sub>/C<sub>6+</sub>) under open- and closed-system pyrolysis conditions for the Åre Fm., Spekk Fm., Green River Shale (GRS), and synthetic mixture I/III

Open-system gas yields fit very well closed-system gas yields up to temperatures around 350°C and then start to diverge possessing lower product amounts. Thus, secondary gas generation is starting at least as early as 400°C probably related to the cracking of  $C_{15+}$  compounds which is in accordance with MSSV  $C_{15+}$  yields being maximal around those temperatures (Fig. 4.2). Therefore not only smaller  $C_{6-14}$  products are being generated while  $C_{15+}$  cracking but also gas which is confirmed by intersecting open- and closed-system GOR ratio curves at 400°C (Fig. 4.8).

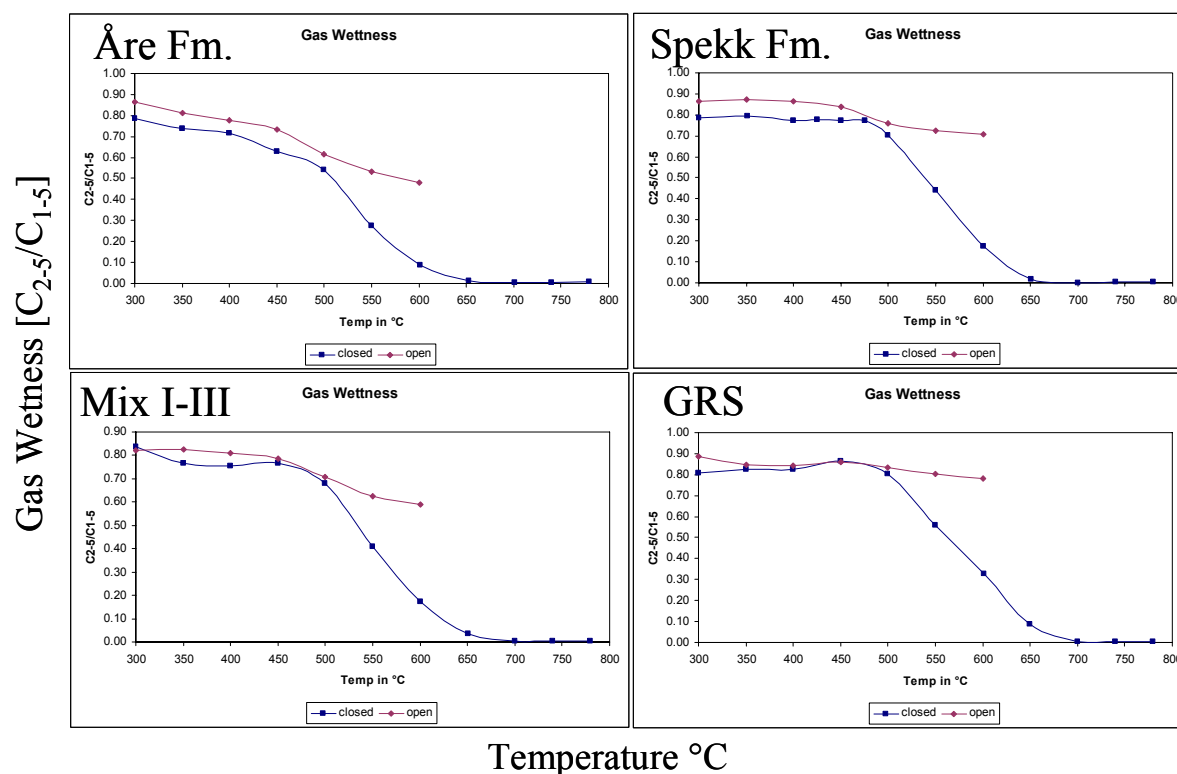


Figure 4.9: Evolution of gas wetness ( $C_{2-5}/C_{1-5}$ ) under open- and closed-system pyrolysis conditions for the Åre Fm., Spekk Fm., Green River Shale (GRS), and synthetic mixture I/III

Maximal calculated secondary gas yields or a plateau of cumulative formed secondary gas is reached between 500 and 550°C (Fig. 4.7) indicating that the main stage of secondary gas generation by  $C_{6+}$  cracking is completed and ongoing generation overcompensated by the beginning degradation of  $C_{2-5}$  wet gas components to methane and coke at 500°C (Fig. 4.2). The cracking of wet gas can also be demonstrated by a strong decrease in gas wetness starting at 500°C (Fig. 4.9). The shape of the secondary gas evolution curve at temperatures in excess of 550 to 600°C (Fig. 4.7) reflects closely the shape of the total measured closed system gas evolution curve, with decreasing product yields in the case of the Spekk Fm. and Green River Shale sample. This can be explained by the formation of coke by wet gas cracking but is somewhat unrealistic with respect to secondary gas which should keep on being formed

related to remaining C<sub>6+</sub> compounds within the closed system. It is obvious that primary gas is as prone to gas cracking as secondary gas, but due to the calculation method primary gas yields are fixed and thus, coke formation only affects calculated secondary gas amounts.

With respect to late gas generation this is very interesting as C<sub>6+</sub> compounds remain in all of the four samples closed-systems and wet gas is degraded in all cases, but only the Åre Fm. and the synthetic Type I/III mixture sample show late gas generation (methane) by increasing calculated secondary gas yields at high temperatures. This is late secondary gas (B) and its yield M<sub>sec.B</sub>(T<sub>x</sub>) can be calculated in close relation to equation (15) by subtracting plateau closed-system secondary gas yields M<sub>sec.G</sub>(T<sub>p</sub>) from post plateau secondary gas yields M<sub>sec.G</sub>(T<sub>x</sub>) as shown in Fig. 4.6 using equation (17):

$$M_{\text{sec.B}}(T_x) = M_{\text{sec.G}}(T_x) - M_{\text{sec.G}}(T_p) \quad (17).$$

Secondary gas (B) yields at 740°C amount up to 9.45 mg/g sample for the Åre Fm. and 3.82 mg/g sample for the synthetic Type I/III sample. For the latter a late gas generation could only be demonstrated by the last applied calculation approach. This and increased secondary gas (B) yields generated by the Åre Fm. sample compared to conservative and refined approach secondary gas (B) yields can be ascribed to the fact that C<sub>6+</sub> compound evolution is not taken into account neglecting possible input of regular secondary cracking gas into the late gas pool.

### ***Recalculation of the conversion factor $f_c$***

Here the question arises how much of the C<sub>6+</sub> products are converted into secondary gas between 600 and 740°C as the molecular composition of GC-amenable oil compounds and its H/C ratio is strongly changed in the course of maturation influencing the conversion factor  $f_c$  (equation (12)).

In Fig. 4.10 the H/C ratio and aromaticity of the MSSV C<sub>6+</sub> boiling range fraction is shown for all source rocks. The H/C ratio is calculated as the sum of all component H/C ratios weighted by their abundance, and the aromaticity is the ratio of the sum of all identified aromatic and phenolic compounds over the sum of all identified C<sub>6+</sub> compounds. It is self evident that at 600°C the average H/C-ratio of C<sub>6+</sub> compounds decreased to values as low as 1 for all investigated samples as the oil fraction is severely thermally degraded and almost completely made up of aromatic compounds such as benzene and minor amounts of methylated alkylbenzenes. Consequently, secondary gas generated at such temperatures from C<sub>6+</sub> cracking will be essentially methane with an H/C ratio of 4, which is confirmed by decreasing gas wetness and increasing methane yields.

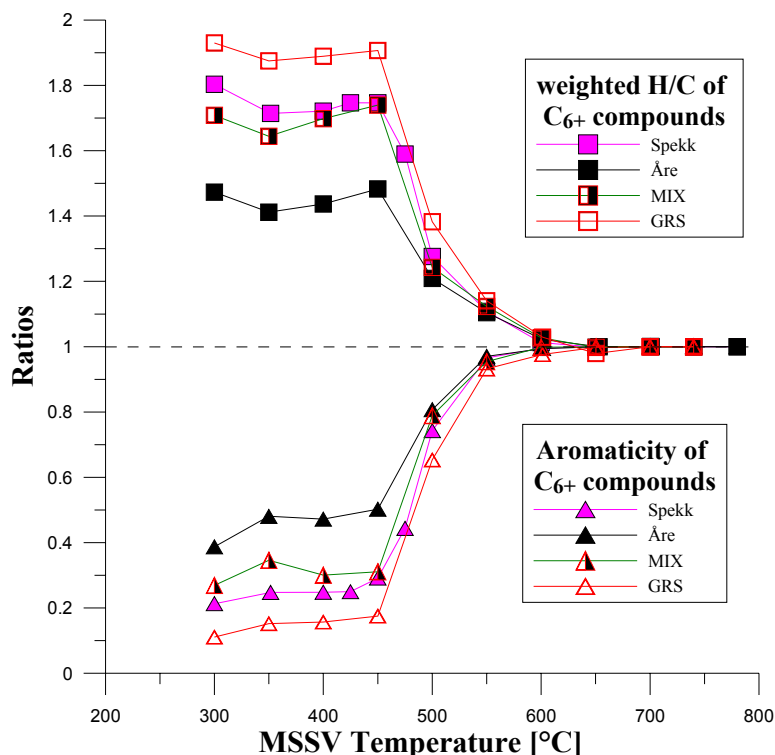
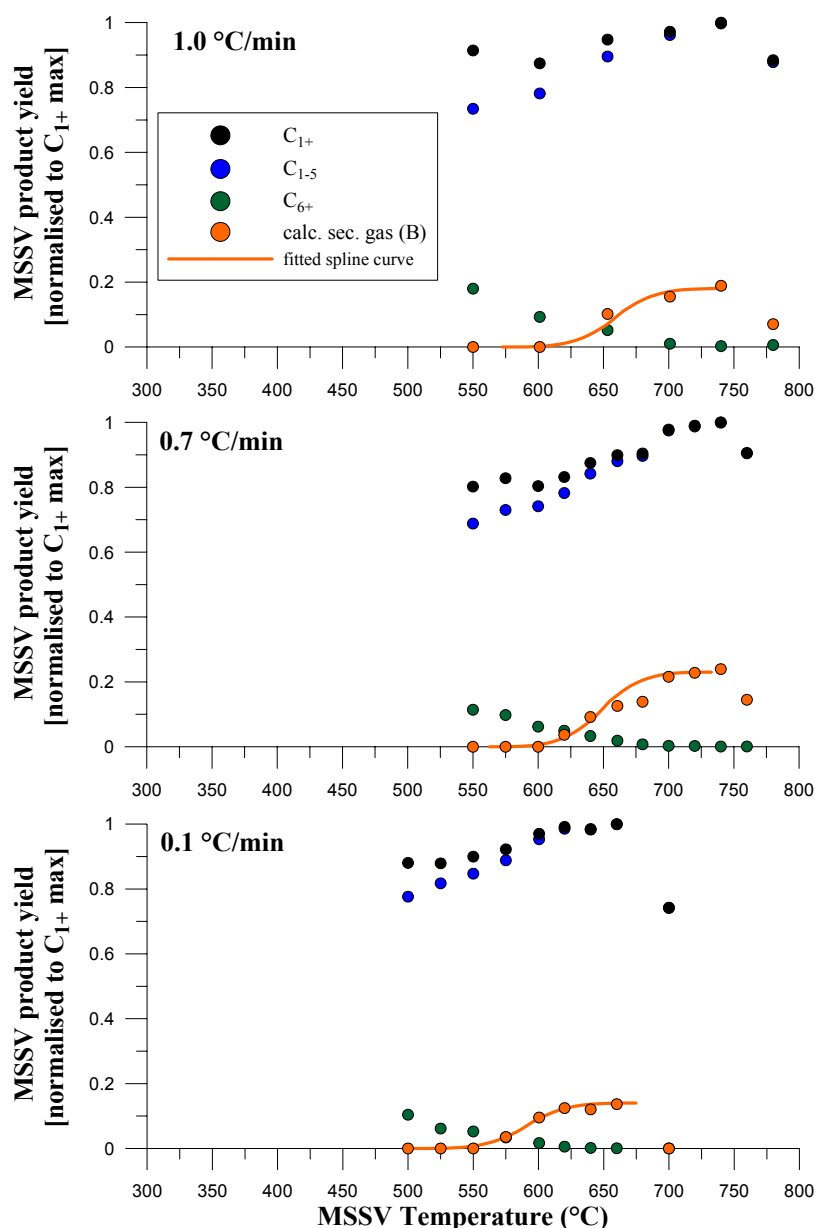


Figure 4.10: Evolution of H/C ratios and aromaticity of the MSSV C<sub>6+</sub> boiling range fraction for the Åre Fm., Spekk Fm., Green River Shale (GRS), and synthetic mixture I/III. The H/C ratio is defined as the sum of all components H/C ratios weighted by their abundance. The aromaticity is defined as the ratio of the sum of all identified aromatic and phenolic compounds over the sum of all identified C<sub>6+</sub> compounds.

Thus, the average conversion factor  $f_c$  of  $\sim 0.7$  is far too optimistic for these maturities and reassessed using equations (10) – (12). Assuming  $n = 1$  (average H/C-ratio of C<sub>6+</sub> compounds),  $m = 4$  (H/C-ratio of methane), and  $u = 0.2$  (average H/C ratio of pyrobitumen), the conversion factor is determined to be  $f_c = 0.3$ . This lower conversion factor is probably still too optimistic and should be viewed as a maximum possible conversion as aromatic ring structures will not be converted to methane as easily as during regular chain shortening of alkanes. Methyl groups of aromatic compounds can be cracked at the  $\alpha$ -position but non-substituted species such as benzene would have to be cracked via ring opening reactions. Nevertheless, secondary gas formation from oil cracking can be calculated using equation (9) with the maximal conversion factor 0.3 instead of 0.7. Secondary gas yields determined between 600 and 740°C amount to 1.43 mg/g sample for the Åre Fm. and 1.56 mg/g sample for the synthetic Type I/III sample and can be subtracted from secondary gas (B) yields. Calculated secondary gas (B) yields would then be 8.02 mg/g sample for the Åre Fm. sample, incidentally matching closely earlier calculations using the *conservative* and *refined* evaluation approach, and 2.26 mg/g sample for the synthetic Type I/III sample.

### 4.1.5 Kinetics of late Secondary Gas Formation

#### *Fitting of Spline Curves*



**Figure 4.11:** Normalised C<sub>1+</sub>, C<sub>1-5</sub>, and C<sub>6+</sub> boiling fractions as well as calculated cumulative secondary gas (B) yields and manually fitted spline curves for MSSV-pyrolysis at three heating rates 0.1, 0.7, and 1.0°C/min.

Calculation of reaction kinetic parameters using KINETICS05 for late secondary gas (B) generation is, as described in Sub-Chapter 2.2.2 under kinetic modelling, based on the determination of generation rate curves at three MSSV heating rates 0.1, 0.7, and 1.0°C/min for the Åre Fm sample G001965. Generation rate curves are obtained by differentiation of spline curves, which were manually fitted to the relatively few calculated cumulative secondary gas (B) yields shown in Fig. 4.11 together with C<sub>1+</sub>, C<sub>1-5</sub>, and C<sub>6+</sub> boiling fractions

at temperatures relevant for late gas generation. As only minimal primary gas generation can be expected for this high temperature pyrolysis interval, secondary gas (B) is simply calculated by subtracting calculated secondary gas (A) yields determined using equation (9) with the maximal conversion factor 0.3 instead of 0.7 from measured total C<sub>1-5</sub> yields. All yields are normalised to the maximal C<sub>1+</sub> value detected for the respective heating rate and displayed in Tab. 4-1.

**Table 4-1: Normalised C<sub>1+</sub>, C<sub>1-5</sub>, methane, C<sub>6+</sub> MSSV-pyrolysis yields as well as calculated cumulative secondary gas (B) and (A) yields for the three heating rates 0.1, 0.7, and 1.0°C/min. The red labelled late secondary gas (B) value indicates the factor the manually fitted spline curve was multiplied with.**

<b>1 K/min Yields normalised to C<sub>1+</sub> max: 1.00 = 52.76 mg/g sasample</b>						
Temperature °C	C <sub>1+</sub>	C <sub>1-5</sub>	Methane measured	C <sub>6+</sub>	late sec. Gas (B) calculated	sec. Gas (A)
550.0	0.91	0.73	0.53	0.18	0.00	0.00
601.1	0.87	0.78	0.71	0.09	0.00	0.03
653.1	0.95	0.90	0.88	0.05	0.10	0.04
700.9	0.97	0.96	0.96	0.01	0.16	0.05
740.1	1.00	1.00	0.99	0.00	0.19	0.05
780.0	0.88	0.88	0.87	0.01	0.07	0.05
<b>0.7K/min Yields normalised to C<sub>1+</sub> max: 1.00 = 59.39 mg/g sasample</b>						
Temperature °C	C <sub>1+</sub>	C <sub>1-5</sub>	Methane measured	C <sub>6+</sub>	late sec. Gas (B) calculated	sec. Gas (A)
550.0	0.80	0.69	0.53	0.11	0.00	0.00
575.0	0.83	0.73	0.63	0.10	0.00	0.00
600.0	0.80	0.74	0.69	0.06	0.00	0.02
620.0	0.83	0.78	0.76	0.05	0.04	0.02
640.0	0.88	0.84	0.82	0.03	0.09	0.02
660.7	0.90	0.88	0.86	0.02	0.13	0.03
680.0	0.90	0.90	0.88	0.01	0.14	0.03
700.0	0.98	0.97	0.96	0.00	0.22	0.03
720.0	0.99	0.99	0.99	0.00	0.23	0.03
740.0	1.00	1.00	1.00	0.00	0.24	0.03
760.0	0.91	0.90	0.90	0.00	0.14	0.03
<b>0.1K/min Yields normalised to C<sub>1+</sub> max: 1.00 = 49.66 mg/g sasample</b>						
Temperature °C	C <sub>1+</sub>	C <sub>1-5</sub>	Methane measured	C <sub>6+</sub>	late sec. Gas (B) calculated	sec. Gas (A)
500.0	0.88	0.78	0.53	0.10	0.00	0.00
525.0	0.88	0.82	0.69	0.06	0.00	0.01
550.0	0.90	0.85	0.77	0.05	0.00	0.02
575.0	0.92	0.89	0.87	0.03	0.04	0.02
600.5	0.97	0.95	0.93	0.02	0.10	0.03
620.0	0.99	0.99	0.97	0.01	0.12	0.03
640.0	0.98	0.98	0.97	0.00	0.12	0.03
660.0	1.00	1.00	0.99	0.00	0.14	0.03
700.0	0.74	0.74	0.73	0.00	0.00	0.00

The amount of generated late gas is not similar for the three used heating rates. Nevertheless, this is not necessarily a sign for a heating rate dependence of the reaction as observed for e.g. thiophenic compounds or single aromatic or aliphatic compounds (Dieckmann *et al.*, 2000a). Here, gas yields do not decrease systematically with decreasing heating rate. This rather implies problems with the reproducibility of measurements at such

extreme pyrolysis temperatures and is probably also related to the very low sample amounts used for one pyrolysis run to inhibit the explosion of MSSV-tubes caused by high gas pressures. Especially for the slow 0.1°C/min heating rate runs a maximum of 1 mg of material had to be used at high temperatures to prevent explosion of sample vials. Nevertheless, for all splines one curve multiplied by individual factors was used indicating a similar reaction mechanism under the three heating rate conditions.

The late gas (B) forming reaction proceeds over a relative small temperature interval of 100°C starting at approximately 550°C for the slowest heating rate 0.1°C/min and at 620°C for the fastest heating rate 1.0°C/min (Fig. 4.11 and 4.14). From this it is obvious that the application of an even faster heating rate to ensure accuracy for the determination of a start-frequency factor (van Heek and Jüntgen, 1968) is not really possible as late gas generation would be shifted to exceedingly high temperatures not manageable by the heating cartridge of the pyrolysis oven. The small reaction interval of 100°C for late gas generation is partly related to secondary degradation or loss of methane at high laboratory temperatures under all heating rate conditions (as discussed in Sub-Chapter 4.1.3 - experimental findings of Sackett (1995)). It is thinkable that late methane generation under milder, natural conditions proceeds over a wider range at the high temperature side and therefore, present results should be viewed as a minimum coverage of the reaction.

### ***Determination of Kinetic Parameters***

The first derivations of cumulative secondary gas (B) yield curves (generation rate curves) could be approximated using a best-fit model (KINETICS05) resulting in the kinetic parameter set displayed in Fig. 4.12. Parameters are given for calculations based on 2 or 3 heating rates. Not entirely surprisingly and related to the narrow temperature interval, the reaction itself can be mainly described by a single activation energy  $E_a$  ranging between 55 and 56 kcal/mol depending on whether 2 or 3 heating rates are used as input for the calculation. It also implies that a well-defined reaction mechanism is responsible for the occurrence of late methane.

Nevertheless, both the main activation energies and frequency factors of only 4.04E+09 or 6.91 E+09 (1/s) are surprisingly low for such a high temperature degradation process of a thermally stable moiety, which is explainable by the large  $T_{max}$  shift of almost 70°C between the 0.1 and 1.0°C heating rate. It should be noted that the frequency factor for late gas generation is lower by 5-6 orders of magnitude than values reported by e.g. Reynolds and Burnham (1993) for total hydrocarbon generation from coals from the San Juan Basin,



USA, or lower by 6 orders of magnitude than total hydrocarbon generation from the Åre Fm. sample G001965 itself in the current study.

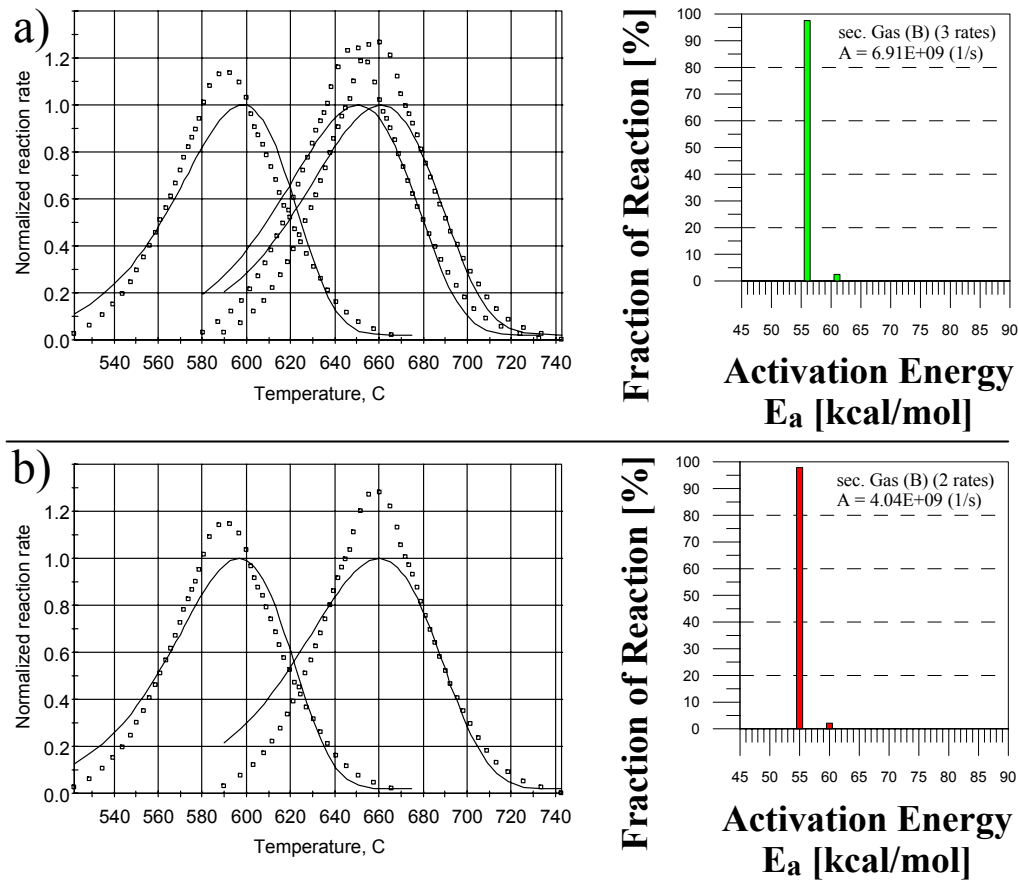


**Figure 4.12:** Differentiated spline curves (points) and calculated generation rate curves (lines) for secondary gas (B) generation at heating rates a) 0.1, 0.7, and 1.0°C/min and b) 0.1 and 1.0°C/min as well as respective kinetic parameters.

On the other hand, and as documented in Fig. 4.13 where the expression  $E/(\ln A - \ln r)$  as a measure of  $T_{\max}$  is displayed versus the logarithm of the heating rate ( $\ln r$ ), laboratory late gas generation remains a high temperature process and occurs subsequent to calculated bulk hydrocarbon formation even under geologic conditions. This can be deduced from the relative order of bulk and secondary gas (B) values in Fig. 4.13, which remains essentially the same for all laboratory and geological heating rates even though the curve for secondary gas (B) is somewhat steeper related to less stable kinetic parameters.

Furthermore, literature review reveals that low frequency factors are often encountered for high temperature gas generating processes. The pre-exponential factor for late methane generation from humic coal under non-isothermal (0.1, 0.5, 2.0°C/min), open-system experimental conditions was found to be  $3.18 \cdot 10^9$  (1/s) in experiments of Krooss *et al.* (1995), which is very close to the data presented here. However, the authors claimed, but

without closer specification and suspecting kinetic parameters to be too low, that more recent experiments yielded in some instances substantially higher frequency factors for methane ( $10^{16}$  1/s) with correspondingly higher activation energies. Nevertheless, low kinetic parameters are indicative of certain secondary gas generation mechanisms. Lorant and Behar (2002) as well as earlier studies (Behar *et al.*, 1999; Lorant *et al.*, 2000) showed that the generation of methane during the thermal cracking of methylated aromatic nuclei is characterized by a low frequency factor, typically in the range  $10^{10}$ - $10^{12}$  s<sup>-1</sup>, and by an activation energy close to 55 kcal/mol. Activation parameters derived for this demethylation reaction tend to confirm that methane generation via this reaction is relevant to the here investigated high temperature gas formation.

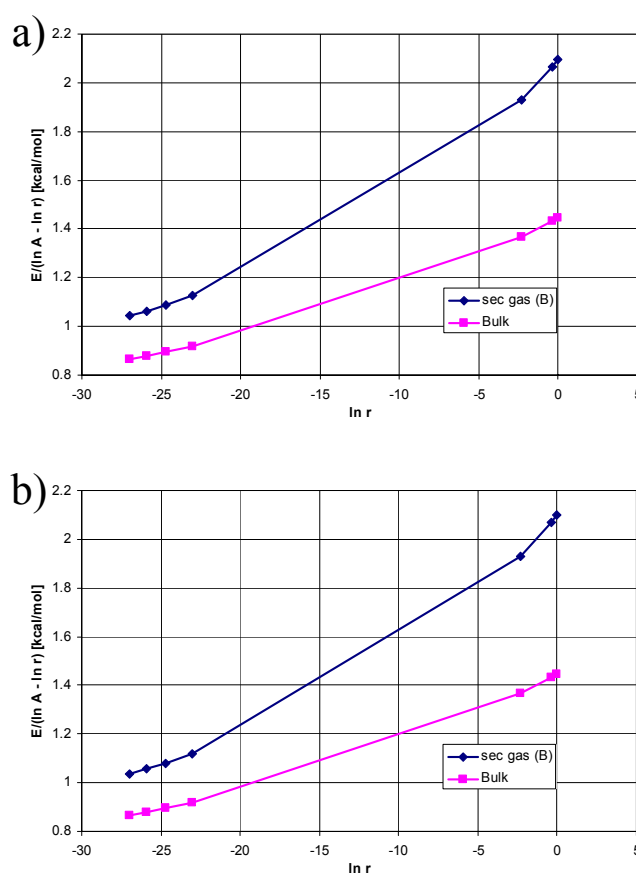


**Figure 4.13:  $T_{\max}$  as an expression of kinetic parameters and heating rate for secondary gas (B) and bulk hydrocarbon generation from Åre Fm. Sample G001965 at heating rates of a) 0.1, 0.7, and 1.0°C/min and b) 0.1 and 1.0°C/min.**

Furthermore, Horsfield *et al.* (1992b) suggested that aromatic compounds can undergo condensation reactions to form pyrobitumen and hydrogen whereas these second-order recombination reactions are likely to have lower pre-exponential factors and activation energies than those of the first-order  $\beta$ -scission reactions. The formed “free” hydrogen could enter into gas forming reactions leading to alpha-cleavage of methyl groups to form methane

(Horsfield and Schenk, 1995) which would explain low kinetic parameters observed for late gas generation.

As an aside, the present kinetic description of late gas generation helps to demonstrate that elevated methane yields detected for high MSSV-pyrolysis temperatures are geological relevant and not related to the postulated late hydrogenation reaction described in Lorant and Behar (2002) for mature Brent Coal and Toarcian Shale. The latter reaction seems to be characterized by even lower activation energies around 40-42 kcal/mol; values very close to those obtained for the hydrogenation during methylpyrene pyrolysis (Lorant *et al.*, 2000).

### ***Extrapolation to Geological Heating Rates***

Laboratory and predicted geological generation rate curves for secondary gas (B) derived from MSSV-pyrolysis are compared to bulk product formation rate curves derived from open-system (SRA)-pyrolysis in Fig. 4.14. Bulk curves describe a total potential of ~70 mg HC/g sample (S2 Rock Eval) and secondary gas (B) curves describe a calculated cumulative MSSV-yield of ~10 mg HC/g sample. Calculated temperatures and vitrinite reflectances for geologic  $T_{\max}$  and onset, middle, and end of product generation for a linear heating rate of 3°C/ma are given in Tab. 4-2.

**Table 4-2: Calculated, variable frequency factors, geologic  $T_{\max}$ , and transformation ratios 10%, 50%, and 90% in °C and % vitrinite reflectance for an applied geologic heating rate of 3°C/Ma for secondary gas (B) generation (MSSV-pyrolysis) and bulk hydrocarbon generation (SRA).**

Rates °C/min	Fraction	Frequency	geologic			
		factor A 1/s	10% TR °C	50% TR °C	90% TR °C	$T_{\max}$ °C
0.1; 1.0	Sec gas (B)	4.04E+09	217.1	233.5	245.0	236.2
0.1; 0.7; 1.0	Sec gas (B)	6.91E+09	221.3	237.7	249.3	240.4
0.7; 2; 5; 15	Bulk HC	4.42E+15	120.1	154.8	194.3	154.4
			% $R_0$	% $R_0$	% $R_0$	% $R_0$
0.1; 1.0	Sec gas (B)	4.04E+09	2.476	2.975	3.320	3.064
0.1; 0.7; 1.0	Sec gas (B)	6.91E+09	2.604	3.111	3.447	3.191
0.7; 2; 5; 15	Bulk HC	4.42E+15	0.696	1.073	1.857	1.066

It becomes clear that in accordance with previously published data (Erdmann and Horsfield, 2006) late methane generation takes place at much higher geologic temperatures than regular primary petroleum generation with onset temperatures exceeding 200°C (217°C or 221°C) equalling calculated vitrinite reflectances around 2.5%  $R_0$ . In contrast, bulk hydrocarbon generation is already completed (TR 90%) at 194.5°C or 1.9%  $R_0$ . The geologic  $T_{\max}$  of secondary gas (B) formation ranges between 236 and 240°C (3.1%  $R_0$ ) and comes to an end (TR 90%) before 250°C (3.5%  $R_0$ ) is reached. This is somewhat earlier than calculated by Erdmann and Horsfield (2006) who estimated the geologic  $T_{\max}$  to range around 250°C. It

should be kept in mind though that the authors could only estimate kinetic parameters of this gas forming mechanism as no cumulative plateau of late gas could be reached for the used analytical set-up. Nevertheless, slightly higher geologic  $T_{\max}$  and completion temperatures are plausible because in the present work methane is degraded at high laboratory thermal stress possibly overprinting ongoing methane formation and inhibiting broader generation rate curves at the high temperature end. Overall, determination of kinetic parameters and extrapolation of late gas generation to geologic conditions yields satisfying results, which are in accordance with observed high temperature methane generation behaviour of naturally matured samples (German Carboniferous coals) discussed in Chapter 5.1.

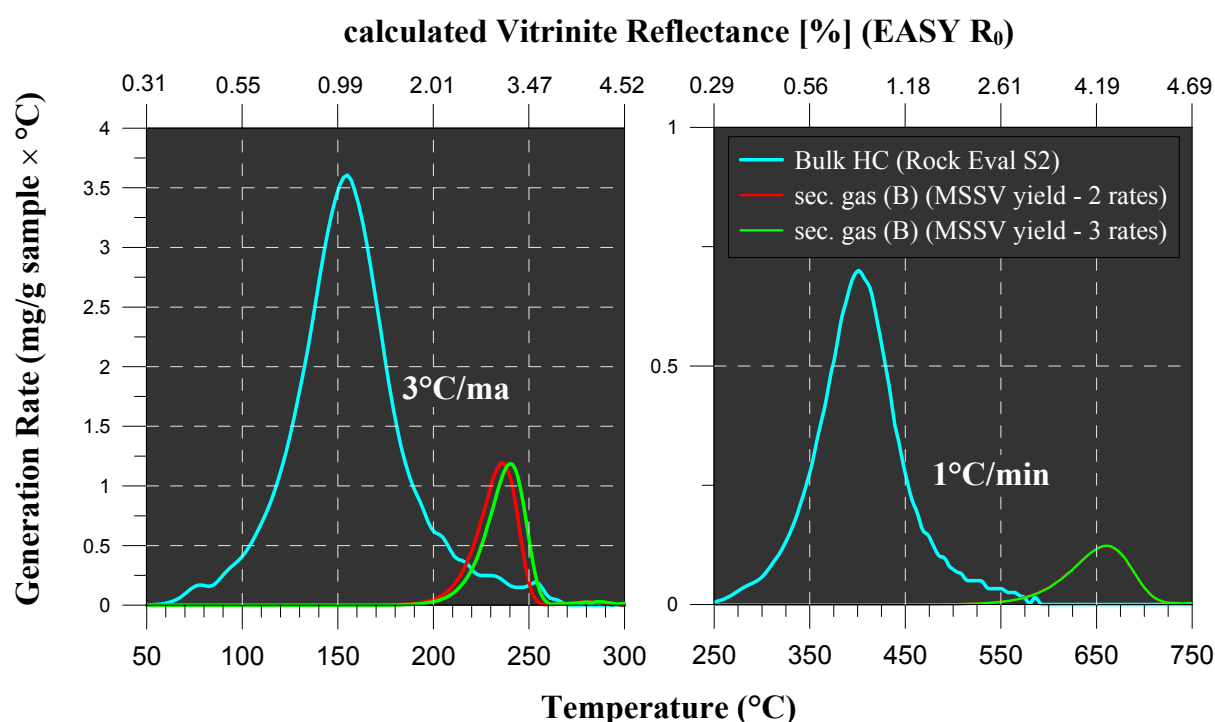


**Figure 4.14:** Laboratory (right) and predicted geological (left) generation rate curves of secondary gas (B) formation derived from MSSV-pyrolysis and bulk product formation rate curves derived from open-system (SRA)-pyrolysis

## 4.2 Late Gas Potential Evaluation for a large Sample Set

### 4.2.1 Screening Method

In order to evaluate the late gas potential of a large sample set of immature shales and coals from different depositional environments a method has to be applied which is not as time consuming as the previously described method of complete evolution curve determination using stepwise open- and closed-pyrolysis to various end temperatures between 300 and 780°C. Thus, non-isothermal closed-system micro-scale sealed vessels pyrolysis (MSSV-Pyrolysis (Horsfield et al., 1989)) was employed to characterise late gas generation behaviour of investigated samples as high temperature methane formation was only observed during the closed-system analytical set-up.

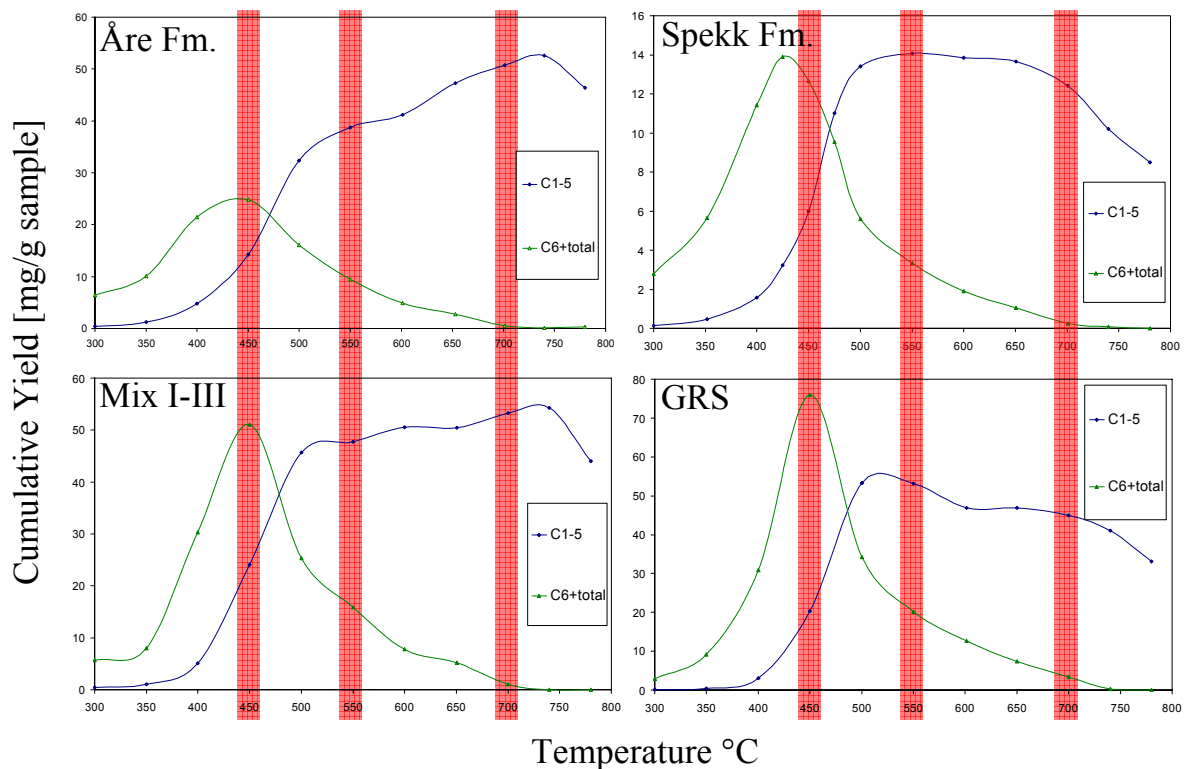


**Figure 4.15: MSSV-pyrolysis end temperatures (red shaded area) used for the late gas potential screening; complete cumulative yield curves for boiling fractions C<sub>1-5</sub> and C<sub>6+</sub> of Åre Fm., Spekk Fm., Green River Shale (GRS), and synthetic mixture I/III sample during MSSV-pyrolysis at 1°C/min.**

It can be seen in Fig. 4.15 that the use of only 3 MSSV end temperatures is sufficient to roughly evaluate the end of cumulative oil generation (450°C), the end of cumulative primary and secondary gas generation (550°C) and the main stage of late gas generation (700°C), if generation occurs, for any investigated source rock. It should be stated here, that at 700°C the maximal late gas yield is not necessarily reached but it can be discriminated in

general if late gas generation occurs or not. To accelerate the analytical procedure faster heating rates were applied, first 5°C/min and later 2°C/min for the greatest part of the sample set. End temperatures were adjusted according to kinetic considerations as product formation is shifted to higher temperatures with faster heating rates. Thus 460°C, 560°C and 700°C were used for the 2°C/min heating rate and 480°C, 580°C, and 700°C were used for the 5°C/min heating rate. In course of the late gas potential evaluation the screening was reduced to two end temperatures as the C<sub>6+</sub> compounds yield at 450°C (460°C, 480°C) is not a crucial parameter for high temperature methane formation between 600°C and 700°C. A start temperature of 200°C was applied to allow in-situ bitumen to be eventually cracked to secondary gas or to interact with the residual organic matter at low temperature stages either featuring (Dieckmann et al., 2006; Erdmann and Horsfield, 2006) or preventing (Vu et al., 2008) the formation of a recombination residue (via cross linking and/or aromatisation reactions) with a late gas potential.

#### 4.2.2 Late Gas Generation Behaviour (MSSV Py-GC)

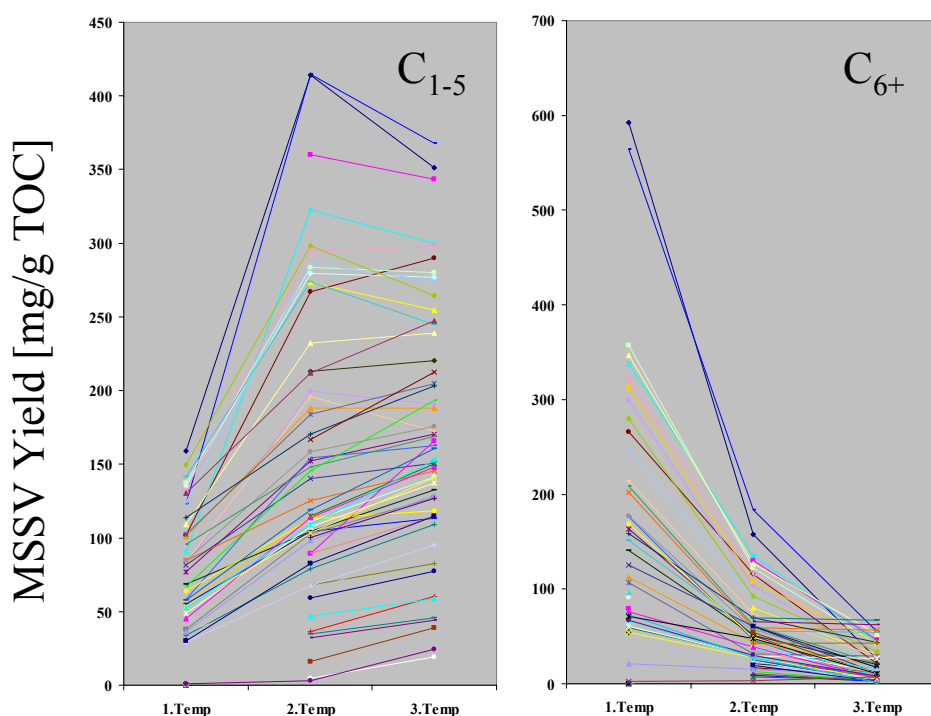


Figure 4.16: MSSV-pyrolysis yields at the three (two) screening end-temperatures

In Fig. 4.16 and Tab. 4-3 MSSV C<sub>1-5</sub> gas and C<sub>6+</sub> oil yields of investigated samples are shown for the 3 (or 2) end temperatures. Additional data and ratios based on those yields are provided in Tab. 4-4.

## 4 EVALUATING THE LATE GAS POTENTIAL OF IMMATURE SOURCE ROCKS

**Table 4-3: C<sub>1-5</sub> and C<sub>6+</sub> yields at three (two) screening end-temperatures during MSSV-pyrolysis. The exactly used end-temperatures as well as heating rates are given in Table A 7.**

GFZ Code	Formation/ Basin	Age	t depositional environment	C <sub>1-5</sub>			C <sub>6+</sub>			
				1.Temp	2.Temp	3.Temp	1.Temp	2.Temp	3.Temp	
				mg/g TOC						
G004750	Green River	Tertiary	lacustrine	158.90	414.29	351.07	592.75	157.66	25.81	
G006536	Wealden Shales	Cretaceous		0.00	360.35	343.40	0.00	130.23	45.83	
G006547	Wealden Shales	Cretaceous		0.00	273.58	254.42	0.00	79.66	30.79	
G000697	Boghead Coal	Pennsylvanian		90.65	322.44	299.71	337.66	135.37	43.61	
	Mix type I/III		Mixed	76.98	152.40	170.27	163.14	50.83	3.23	
G000859	Messel Oil Shale	Eocene	lacustrine	102.10	267.27	289.90	265.58	115.35	21.17	
G000698	Cannel Coal	Cretaceous	- terrestrial	33.76	79.18	109.17	58.90	29.83	5.26	
G000693	Alaskan	Jurassic	Marine Mesozoic- Cenozoic	123.17	414.52	367.92	564.10	183.24	54.85	
G000731	Brown Limestone	Late		647.32	1336.99	1411.80	1687.49	737.08	133.73	
G006208	Toarcian Shale	Jurassic		134.94	279.31	276.94	357.21	122.44	42.06	
G006209	Toarcian Shale	Jurassic		137.37	283.80	280.04	347.07	127.17	52.21	
G004072	Schöneck Fm.	Eocene-		109.07	232.30	238.80	245.66	89.47	19.57	
G004070	Schöneck Fm.	Eocene-		124.12	286.39	274.38	321.56	116.25	33.07	
G004071	Schöneck Fm.	Eocene-		132.36	294.67	298.00	298.80	103.82	26.33	
G000883	Autun Oil Shale	Jurassic		81.02	199.52	190.90	214.34	73.87	28.11	
G001955	Spekk Fm.	Upper		83.40	195.74	172.56	176.19	46.44	2.85	
G000689	Botneheia Shale	Triassic		58.28	154.14	162.73	150.80	55.71	53.83	
G005812	Irati Fm.	Perm	Marine Paleozoic	141.13	273.72	244.74	280.05	91.82	34.18	
G004563	Domanik Fm.	Devonian		149.84	298.18	264.75	312.70	107.51	42.55	
G000690	Woodford Shale	Devonian		55.99	114.51	117.88	112.59	43.88	18.52	
G006153	Woodford Shale	Devonian		100.65	188.12	188.36	202.48	58.84	56.45	
G006154	Woodford Shale	Devonian		84.82	125.07	145.24	107.05	31.72	28.81	
G006156	New Albany	Devonian		102.51	183.92	204.81	176.97	57.03	18.07	
G006155	Caney Shale	Carboniferous		84.67	158.51	175.50	158.39	69.44	43.94	
G005298	Bakken Shale	Mississippian		113.86	170.64	203.09	208.71	61.66	21.04	
G000692	Chattanooga	Devonian		95.54	148.14	169.06	140.35	51.25	20.60	
G004564	Murzuq Basin	Silurian		68.51	104.23	132.68	54.30	21.14	12.29	
G007160	Murzuq Basin	Silurian	org. lean marine	0.00	212.90	220.27	0.00	53.94	9.45	
G006949	Middle East	Silurian		0.00	15.88	38.85	0.00	10.42	3.45	
G000753	Alum Shale	Cambrian		130.25	212.05	247.32	125.59	60.62	11.34	
G000758	Alum Shale	Cambrian		81.69	140.44	150.76	91.52	38.01	11.08	
G005936	Middle East	Silurian		14.54	0.20	5.20	13.78	18.88	25.25	
G006948	Middle East	Silurian		0.00	4.92	19.34	0.00	13.21	3.17	
G007161	Ghadames Basin	Silurian		0.00	36.41	60.52	0.00	8.52	2.16	
G005935	Akata Shale	Paleogene		Mixed	67.11	145.51	193.56	168.64	48.63	10.83
G005762	Hekkingen Fm.	Jurassic		marine-	55.07	104.22	113.23	79.08	24.35	9.39
G005763	Hekkingen Fm.	Jurassic		terrestrial	64.15	112.51	118.73	96.09	36.10	15.27
G006204	Douala Basin	Cretaceous	org. lean mixed marine terrestrial	0.00	89.55	165.85	0.00	16.72	7.87	
G006205	Douala Basin	Cretaceous		0.00	46.72	58.75	0.00	7.54	3.93	
G006206	Mahakam Delta			0.00	167.04	212.41	0.00	60.79	16.77	
G007162	Farsund Fm.	upper Jurassic		0.00	115.06	150.40	0.00	42.68	42.68	
G007163	Farsund Fm.	upper Jurassic		0.00	59.12	77.57	0.00	65.20	62.02	
G007164	Farsund Fm.	upper Jurassic		0.00	68.01	82.57	0.00	69.48	67.27	
G007165	Farsund Fm.	upper Jurassic		0.00	32.29	43.95	0.00	26.05	14.47	
G007166	Farsund Fm.	upper Jurassic		0.00	35.03	45.60	0.00	15.04	10.87	
G000206	Kugmallit Fm.	Oligocene		fluvio- deltaic – terrestrial	36.12	64.37	92.82	21.06	15.58	8.26
G000721	Westphalian	Carboniferous			37.91	102.83	127.56	60.64	29.07	26.28
G001965	Åre Fm.	Lower	36.23		98.43	128.91	63.09	24.09	1.34	
G000696	Jet Rock	Lower	265.73		688.71	779.26	1122.15	607.28	146.62	
G006207	Mahakam Delta		48.87		107.48	137.07	94.73	34.60	10.26	
G006533	Wealden Coals	Cretaceous	0.00		111.06	141.45	0.00	25.45	2.51	
G006538	Wealden Coals	Cretaceous	0.00		100.37	126.61	0.00	20.45	5.71	
G006548	Wealden Coals	Cretaceous	0.00		89.61	114.17	0.00	19.79	2.31	
G000899	Talang Akar Coal	Eocene-	57.60		119.22	160.57	76.11	38.50	5.68	
G000726	Talang Akar Coal	Eocene-	29.13		67.48	95.19	54.11	27.37	5.05	
G000670	Talang Akar Coal	Eocene-	30.36	82.74	114.58	66.48	28.25	9.63		
G000950	Arang Coal	Miocene	44.99	113.63	148.21	66.80	29.94	8.03		
SN6750	Taglu Fm.	Eocene	migrated oil	53.35	103.58	140.82	72.76	27.12	1.26	
G001983	New Zealand	Eocene-		52.42	109.14	152.98	71.35	47.51	10.15	
G005937	Middle East	Silurian		0.99	3.36	24.45	2.23	3.29	7.09	

A rise in  $C_{1-5}$  gas yields can be observed for all analysed immature source rocks between the first (460°C; 450°C; 480°C) and the second (560°C; 550°C; 580°C) end temperature, which is relatable to the cracking of  $C_{6+}$  oil compounds within the closed system. In contrast, diverse late gas generation behaviour is recognisable between the second (560°C; 550°C; 580°C) and the third temperature (700°C). Source rocks generating late gas yield higher amounts of gas at 700°C than at 560°C, source rocks generating no late gas yield lower amounts of gas. For a quantitative comparison of the late gas potentials a late gas ratio LGR (1) was established, as the absolute gas yield at 700°C is not necessarily related to the gas formed at very high temperatures, but also depends on the earlier  $C_{6+}$  oil input and its gaseous cracking products (Fig. 4.16; Fig. 4.17b). For the late gas ratio (1) (LGR (1)) calculation using equation (18) gas yields at the highest temperature (3<sup>rd</sup> Temperature 700°C) are divided by the sum of gas yields at the 2<sup>nd</sup> temperature (560°C; 550°C; 580°C) and 3<sup>rd</sup> temperature.

$$\text{LGR (1)} = (\text{C}_{1-5} \text{ Yield}_3) / (\text{C}_{1-5} \text{ Yield}_2 + \text{C}_{1-5} \text{ Yield}_3) \quad (18)$$

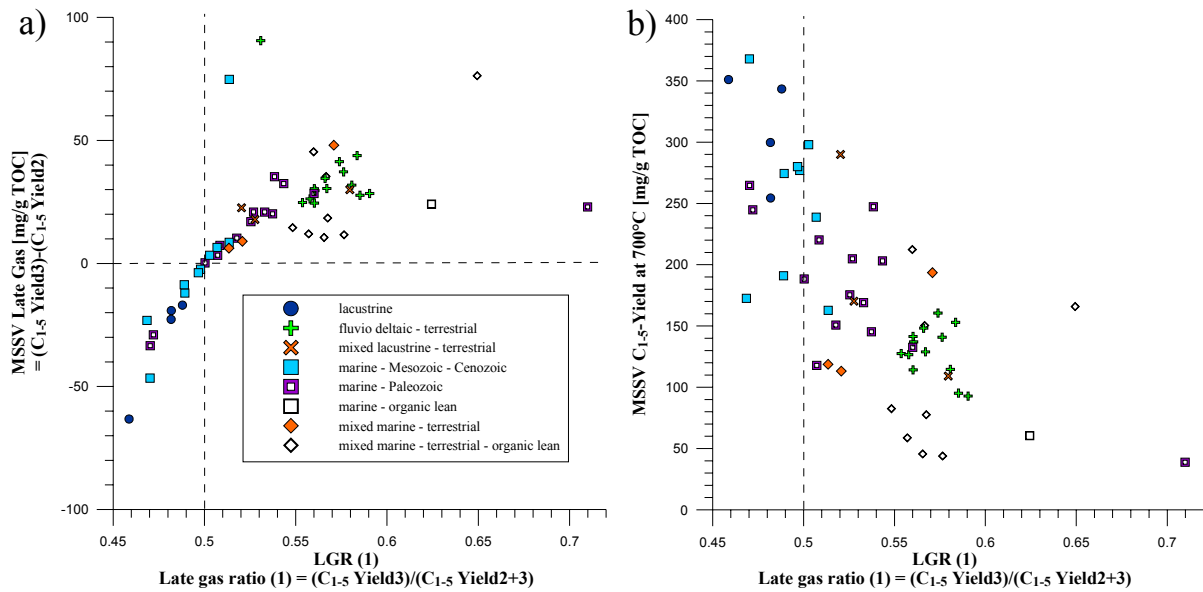


**Figure 4.17: Comparison of late gas ratio 1 (LGR1) to a) the late gas amount generated between the second (for most samples 560°C) and third temperature (for most samples 700°C) and to b) the absolute gas amount at the third temperature (for most samples 700°C). Data is provided in Tab. 4-4.**

Thus, ratios  $> 0.5$  are seen for source rocks yielding greater amounts of total  $C_{1-5}$  at the higher temperature state (late gas potential), ratios  $< 0.5$  for source rocks yielding lower amounts of gas (no late gas potential) (Fig. 4.17). To demonstrate the relation between the applied late gas ratio (1) and the late gas generation in the high temperature interval between ~560°C and 700°C, LGR (1) is plotted against late gas yields between the 2<sup>nd</sup> and 3<sup>rd</sup> temperature stage (Fig. 4.17a).



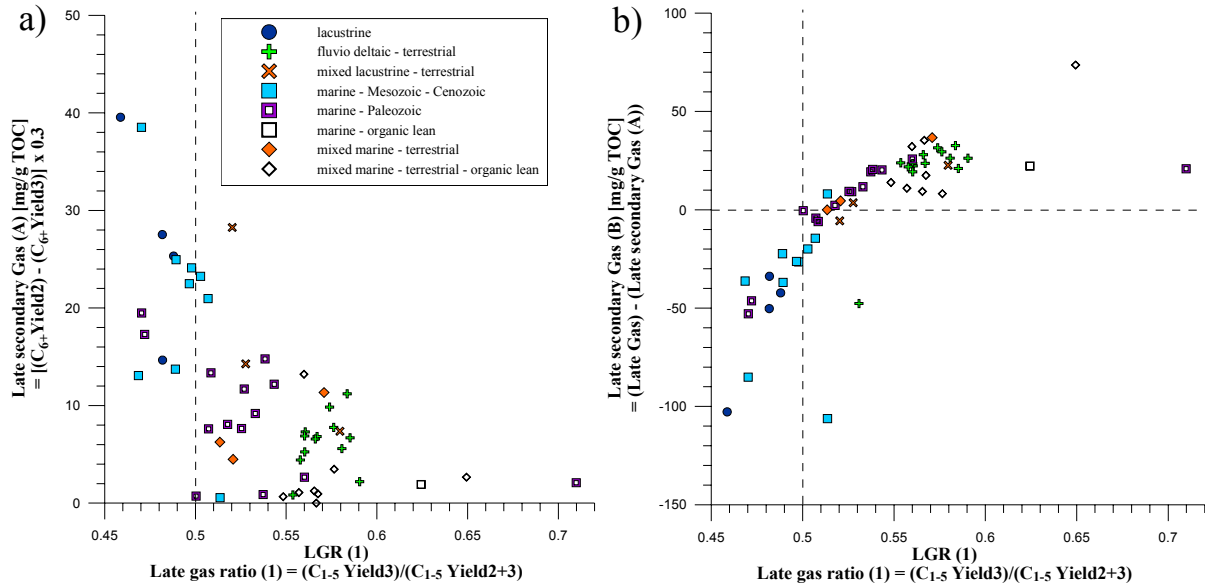


**Figure 4.18: Comparison of late gas ratio 1 (LGR1) to a) the late secondary gas (A) amount generated between the second (for most samples 560°C) and third temperature (for most samples 700°C) by cracking of  $C_{6+}$  compounds and to b) the secondary gas (B) amount generated between the second (for most samples 560°C) and third temperature (for most samples 700°C). Data is provided in Tab. 4-4.**

Furthermore, rising  $C_{1-5}$  yields between the 2<sup>nd</sup> and the 3<sup>rd</sup> temperatures can be partly attributed to the cracking of  $C_{6+}$  oil compounds remaining within the closed system generating what is here termed late secondary gas (A). In Fig. 4.18a the late gas ratio (1) is plotted against this late secondary gas (A) yield which is calculated using equation (9) by subtraction of gross  $C_{6+}$  yields at the 2<sup>nd</sup> temperature from gross  $C_{6+}$  yields at the 3<sup>rd</sup> temperature multiplied by the previously discussed conversion factor  $f_c \sim 0.3$ , assuming that for reasons of hydrogen balance only 30% of  $C_{6+}$  compounds are converted into gas and 70% into pyrobitumen (Coke). It is revealed that late secondary gas (A) makes up a relatively high proportion of the total late gas yield generated between 560°C and 700°C and can be made responsible even for the total late gas yields of some samples. This is demonstrated in Fig. 4.18b in which late secondary gas (B) yields, produced from a thermally stabilised recombination structure and simply calculated by subtracting late secondary gas (A) from total amounts of late gas, are plotted against the late gas ratio (1). It is apparent that late gas potentials of some source rocks can be solely attributed to late secondary  $C_{6+}$  cracking and need not to be explained by the decomposition of a recombination structure. For immature source rocks possessing  $\text{LGR}(1) > 0.55$ , secondary gas (B) makes up at least half of the total late gas yield (Fig. 4.17a, Fig. 4.18b).

By implementation of a second late gas ratio ( $\text{LGR}(2)$ ), calculated using equation (19) by division of gas yields at the highest temperature (3<sup>rd</sup> temperature 700°C) through the sum

of gas yields at the 2<sup>nd</sup> temperature (560°C; 550°C; 580°C) and late secondary gas (A), the late gas potential in relation to secondary gas (A) or (B) generation can be evaluated.

$$\text{LGR (2)} = (\text{C}_{1-5} \text{ Yield3}) / (\text{C}_{1-5} \text{ Yield 2} + \text{secondary gas (A)}) \quad (19)$$

LGR (2) ratios of less than unity are seen for source rocks whose late gas potential is mainly due to C<sub>6+</sub> cracking, LGR (2) ratios > 1 are seen for source rocks whose late gas potential can only be explained by a thermally stabilised moiety which yields additional amounts of secondary late gas (B) at high temperature stages. Plotted together with LGR (1) (Fig. 4.19), LGR (2) provides a tool for distinguishing between source rocks with high, intermediate or low late gas potentials. Immature source rocks with high late gas potentials (LGR (1) > 0.55) yield higher amounts of gas at 700°C than at 560°C whereas the extra amount of gas cannot be attributed to secondary cracking of C<sub>6+</sub> compounds alone (LGR (2) > 1), which, on the contrary, is the case for many of the samples with intermediate late gas potentials (LGR (1) 0.51 – 0.55 and LGR (2) < 1). Source rocks without or with only a very low late gas potential exhibit LGR (1)'s < 0.51.

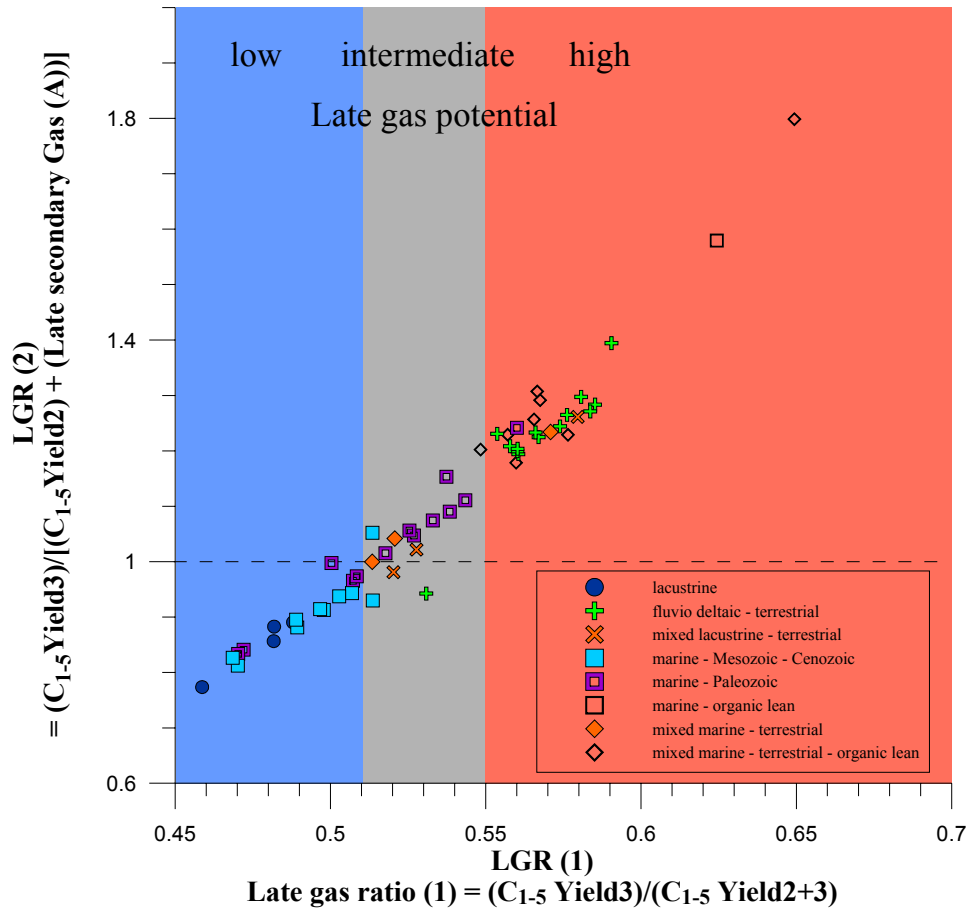


Figure 4.19: Discrimination of source rocks exhibiting low, high, and intermediate late gas potentials using the two Late Gas Ratios LGR1 and LGR2.

A good first impression of which source rocks possess a late gas potential, and which not, can be gained from Fig. 4.19 and Tab. 4-4 (see also Fig. 4.21). Mainly fluviodeltaic – terrestrial source rocks and organic lean source rocks possess a high late gas potential, whereas LGR1 ratios of some organic lean (marine) source rocks are extraordinarily high and plot outside of the chosen x-axis segment (0.45 – 0.7). Most organic-rich immature samples can be found within the 0.45 – 0.6 (LGR1) range. Therefore, it can't be ruled out that high late gas potentials or high temperature gas generation of organic lean source rocks are caused or influenced by mineral matrix effects. None of the source rocks deposited in a lacustrine environment exhibit late secondary gas (B) generation, and possess low late gas potentials. Marine source rocks display very diverse behaviour manifested by the presence of low, intermediate, and in some cases high late gas potentials (Silurian shales from the Murzuq Basin G004564 and Middle East G006949), whereas Mesozoic – Cenozoic shales exhibit rather low potentials and Paleozoic shales exhibit rather intermediate potentials. Terrestrially influenced mixed samples possess intermediate to high late gas potentials with higher LGR1 ratios observed for source rocks in which a higher fraction of terrestrial plant input is observed.

### **4.2.3 Secondary Gas Yields**

As previously discussed, it is revealed that late secondary gas (A) contributes a relative high proportion to the gas generated between 560°C and 700°C and is, in some cases, responsible for the total observed late gas (Tab. 4-4). Late secondary gas (B), produced from a thermally stabilised or neoformed refractory moiety, therefore accounts for the remaining late gas, as significant input of primary products can be ruled out at such elevated temperature levels. Its amount can be calculated by simply subtracting late secondary gas (A) from total late gas yields.

In Fig. 4.20b (also Fig. 4.18b) and Tab. 4-4 late secondary gas (B) yields are listed and correlated to LGR1. Late gas (B) amounts range between 0 and 40 mg C<sub>1-5</sub>/g TOC with averagely higher yields for higher LGR1's. Only the organic-lean shale G006204 from the Douala Basin (not shown in Fig. 4.20b) generates amounts as high as ~73 mg/g TOC. For immature source rocks possessing LGR1's > 0.55, secondary gas (B) contributes at least half of the total late gas yield and ranges between 10 and 40 mg C<sub>1-5</sub>/g TOC. Those samples possess a high late gas potential with respect to late secondary gas (B) generation and especially with respect to their total hydrocarbon generative potential defined by open-system C<sub>1+</sub> pyrolysis yields (Rock-Eval HI). Here, late secondary gas (B) contributes an additional 7

to 38% of the total primary petroleum potential, in the case of Douala Basin sample G006204 51% (Tab. 4-4). Intermediate late gas potentials are assigned to source rocks with LGR1's between 0.51 and 0.55 as the average late secondary gas (B) input is much lower, with amounts ranging between 0 and 20 mg C<sub>1-5</sub>/g TOC and proportions of late gas to total petroleum potential not exceeding 6% (Tab. 4-4). This is also owed to higher HI's of the respective samples compared to HI's of samples exhibiting high late gas potentials. In Fig. 4.20b this correlation is demonstrated by the bubble size of data points expressing the additional late secondary gas (B) input as percent of the total initial primary petroleum potential defined by Rock-Eval HI. One can easily recognise the importance of secondary gas (B) input for the evaluation of the total petroleum potential of a source rock. A high importance is evident for source rocks exhibiting high late gas potentials, whereas the importance of secondary gas (B) for a source rocks showing intermediate late gas potential is much lower compared to its primary petroleum potential.

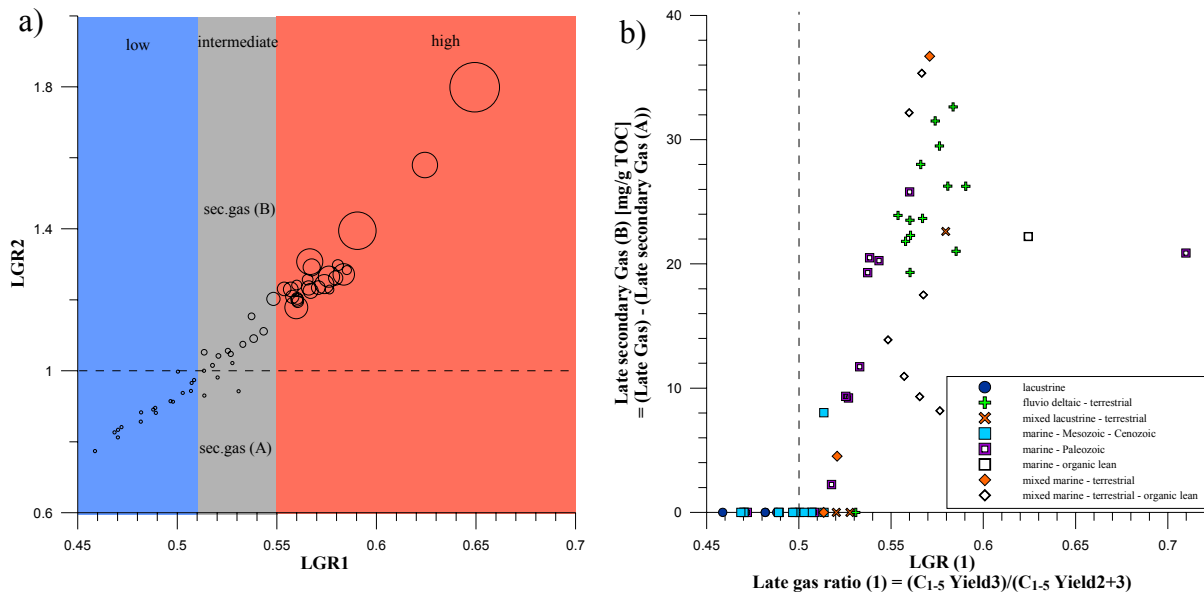


**Figure 4.20: Late secondary gas (B) amounts: a) Late Gas Potential classification based on LGR1 and LGR2 as well as on bubble sizes expressing additional late secondary gas (B) input as percent of the total initial primary petroleum potential (Rock-Eval HI), whereas smallest bubble = 0% and biggest bubble = 51%; b) Calculated late secondary gas (B) yield correlated to LGR1**

## 4 EVALUATING THE LATE GAS POTENTIAL OF IMMATURE SOURCE ROCKS

**Table 4-4: Calculated total late gas, late secondary gas (A), and late secondary gas (B) yields as well as late gas ratios LGR1 and LGR2 for all samples based on products generated between MSSV end temperatures 560°C and 700°C.**

GFZ Code	Formation/ Basin	depositional environmen	late gas	LGR1	sec. gas (A)	LGR2	late gas - sec. gas (A)	sec. gas (B)	Additional Gas Input sec. Gas (B)
			mg/g TOC	kg/kg	mg/g TOC	kg/kg	mg/g TOC	mg/g TOC	%
G004750	Green River Shale	lacustrine	-63.22	0.46	39.56	0.77	-102.78	0.00	0.00
G006536	Wealden Shales		-16.94	0.49	25.32	0.89	-42.27	0.00	0.00
G006540	Wealden Shales		-19.16	0.48	14.66	0.88	-33.82	0.00	0.00
G000697	Boghead Coal		-22.73	0.48	27.53	0.86	-50.25	0.00	0.00
	Mix type I/III	Mixed	17.87	0.53	14.28	1.02	3.59	0.00	0.00
G000859	Messel Oil Shale	lacustrine - terrestrial	22.63	0.52	28.26	0.98	-5.63	0.00	0.00
G000698	Cannel Coal		29.98	0.58	7.37	1.26	22.61	22.61	12.09
G000693	Alaskan	Marine Mesozoic- Cenozoic	-46.60	0.47	38.52	0.81	-85.12	0.00	0.00
G000731	Brown Limestone		74.81	0.51	181.01	0.93	-106.20	0.00	0.00
G006208	Toarcian Shale		-2.37	0.50	24.11	0.91	-26.49	0.00	0.00
G006209	Toarcian Shale		-3.76	0.50	22.49	0.91	-26.25	0.00	0.00
G004072	Schöneck Fm.		6.50	0.51	20.97	0.94	-14.47	0.00	0.00
G004070	Schöneck Fm.		-12.01	0.49	24.95	0.88	-36.97	0.00	0.00
G004071	Schöneck Fm.		3.33	0.50	23.25	0.94	-19.92	0.00	0.00
G000883	Autun Oil Shale		-8.62	0.49	13.73	0.90	-22.35	0.00	0.00
G001955	Spekk Fm.		-23.18	0.47	13.08	0.83	-36.26	0.00	0.00
G000689	Botneheia Shale		8.59	0.51	0.56	1.05	8.02	8.02	2.74
G005812	Irati Fm.	Marine Paleozoic	-28.98	0.47	17.29	0.84	-46.27	0.00	0.00
G004563	Domanik Fm.		-33.43	0.47	19.49	0.83	-52.92	0.00	0.00
G000690	Woodford Shale		3.37	0.51	7.61	0.97	-4.24	0.00	0.00
G006153	Woodford Shale		0.24	0.50	0.72	1.00	-0.48	0.00	0.00
G006154	Woodford Shale		20.17	0.54	0.87	1.15	19.30	19.30	3.93
G006156	New Albany		20.89	0.53	11.69	1.05	9.20	9.20	2.16
G006155	Caney Shale		16.99	0.53	7.65	1.06	9.34	9.34	2.07
G005298	Bakken Shale		32.45	0.54	12.19	1.11	20.26	20.26	4.87
G000692	Chattanooga		20.91	0.53	9.19	1.07	11.72	11.72	3.15
G004564	Murzuq Basin		28.45	0.56	2.66	1.24	25.79	25.79	7.50
G007160	Murzuq Basin		7.38	0.51	13.35	0.97	-5.97	0.00	0.00
G006949	Middle East		22.96	0.71	2.09	2.16	20.87	20.87	12.73
G000753	Alum Shale		35.28	0.54	14.79	1.09	20.49	20.49	5.10
G000758	Alum Shale		10.32	0.52	8.08	1.02	2.24	2.24	0.83
G005936	Middle East	org. lean marine	4.99	0.96	-1.91	-3.04	6.90	6.90	13.28
G006948	Middle East		14.42	0.80	3.01	2.44	11.41	11.41	22.81
G007161	Ghadames Basin		24.11	0.62	1.91	1.58	22.20	22.20	24.67
G005935	Akata Shale	Mixed marine- terrestrial	48.05	0.57	11.34	1.23	36.71	36.71	11.73
G005762	Hekkingen Fm.		9.01	0.52	4.49	1.04	4.52	4.52	1.65
G005763	Hekkingen Fm.		6.22	0.51	6.25	1.00	-0.02	0.00	0.00
G006204	Douala Basin	org. lean mixed marine terrestrial	76.30	0.65	2.66	1.80	73.64	73.64	51.50
G006205	Douala Basin		12.04	0.56	1.08	1.23	10.95	10.95	12.74
G006206	Mahakam Delta		45.37	0.56	13.20	1.18	32.17	32.17	21.88
G007162	Farsund Fm.		35.35	0.57	0.00	1.31	35.35	35.35	25.25
G007163	Farsund Fm.		18.45	0.57	0.95	1.29	17.50	17.50	15.35
G007164	Farsund Fm.		14.55	0.55	0.66	1.20	13.89	13.89	11.11
G007165	Farsund Fm.		11.66	0.58	3.48	1.23	8.18	8.18	6.15
G007166	Farsund Fm.		10.57	0.57	1.25	1.26	9.31	9.31	8.32
G000206	Kugmallit Fm.	fluvio- deltaic – terrestrial	28.44	0.59	2.20	1.39	26.25	26.25	38.04
G000721	Westphalian		24.74	0.55	0.84	1.23	23.90	23.90	11.49
G001965	Åre Fm.		30.48	0.57	6.82	1.22	23.66	23.66	13.14
G000696	Jet Rock		90.55	0.53	138.20	0.94	-47.65	0.00	0.00
G006207	Mahakam Delta		29.60	0.56	7.30	1.19	22.29	22.29	9.25
G006533	Wealden Coals		30.39	0.56	6.88	1.20	23.51	23.51	10.14
G006538	Wealden Coals		26.24	0.56	4.42	1.21	21.82	21.82	11.19
G006548	Wealden Coals		24.55	0.56	5.24	1.20	19.31	19.31	9.56
G000899	Talang Akar Coal		41.35	0.57	9.85	1.24	31.51	31.51	17.60
G000726	Talang Akar Coal		27.71	0.59	6.70	1.28	21.02	21.02	6.47
G000670	Talang Akar Coal		31.85	0.58	5.59	1.30	26.26	26.26	8.78
G000950	Arang Coal		34.58	0.57	6.57	1.23	28.01	28.01	12.39
SN6750	Taglu Fm.		37.25	0.58	7.76	1.26	29.49	29.49	19.92
G001983	New Zealand		43.84	0.58	11.21	1.27	32.63	32.63	20.30
G005937	Middle East	migrated oil	21.09	0.88	-1.14	11.03	22.23	22.23	185.26

#### 4.2.4 Impact of Kerogen Type and Structure

The late gas generation behaviour of immature shales and coals can be linked to the organic matter structure and depositional environment by using MSSV-based late gas potential assignments (Fig. 4.19) together with previously described open-system pyrolysis data. In the three ternary diagrams of Horsfield (1989), Eglinton *et al.* (1990) and Larter (1984) (Fig. 4. 22a, Fig. 25a, and Fig. 24.a) source rocks exhibiting low late gas potentials ( $LGR1 > 0.51$ ) are coloured light blue, source rocks exhibiting intermediate late gas potentials ( $LGR1\ 0.51 - 0.55$ ) are coloured black, and source rocks exhibiting high late gas potentials ( $LGR1 > 0.55$ ) are coloured red.

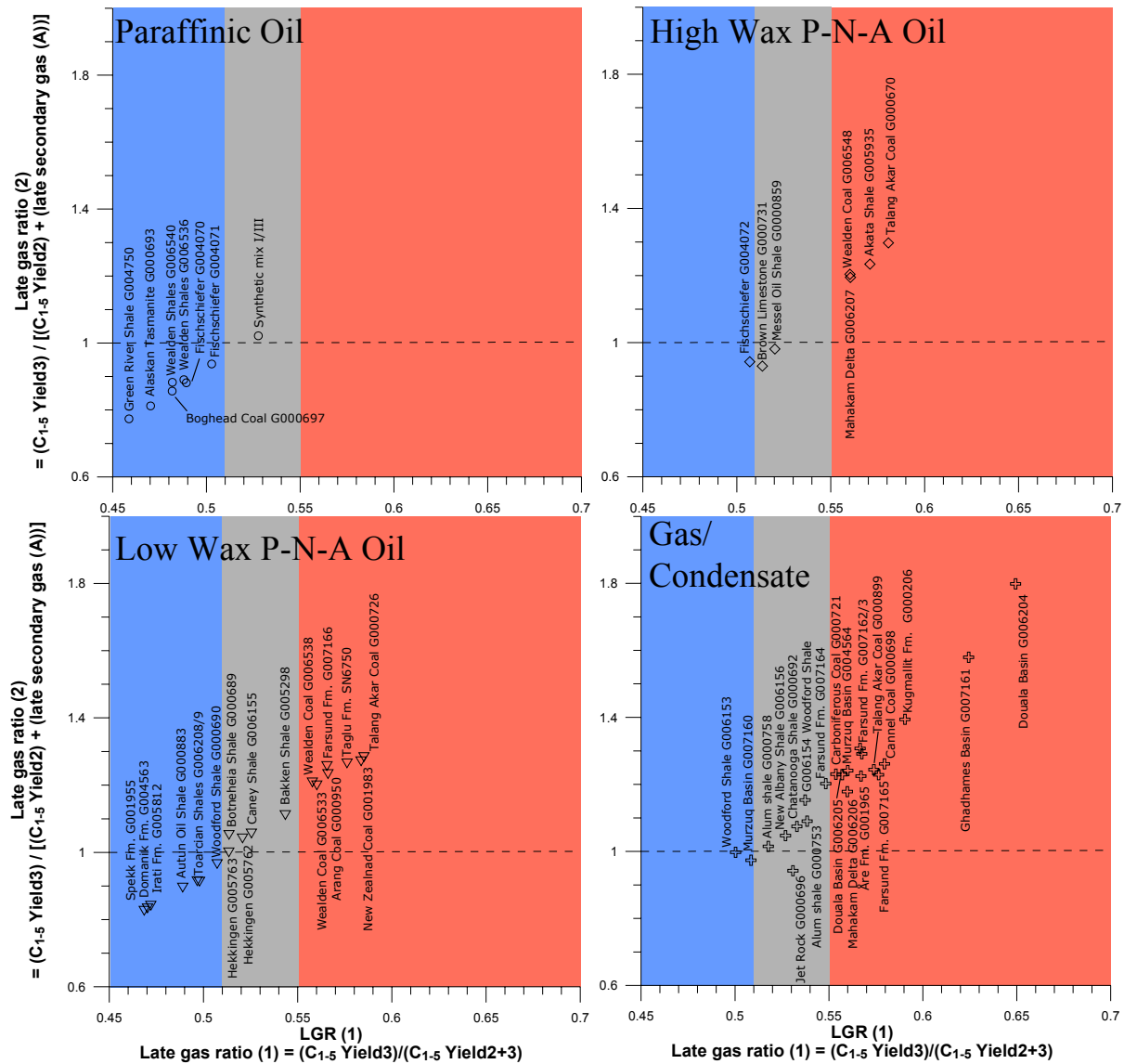


Figure 4.21: Comparison of open-system pyrolysis based alkyl chain length distribution classification and closed-system (MSSV)-pyrolysis based Late Gas Potential classification

### Chain Length Distribution - Petroleum Type Organofacies

The late gas potential of investigated immature source rocks is again depicted in Fig. 4.21 in relation to petroleum type organofacies based on the alkyl chain length distribution (ternary diagram in Fig. 4.22a (Horsfield, 1989)) in respective open-system pyrolysates. It stands out that for every petroleum type organofacies there are source rocks with low, intermediate, and high late gas potentials. Thus, late gas generation behaviour is not linkable to the alkyl chain length distribution within the kerogen structure alone, but has to be influenced by other structural moieties within the macromolecular organic matter whose chemistry is strongly related to the depositional environment.

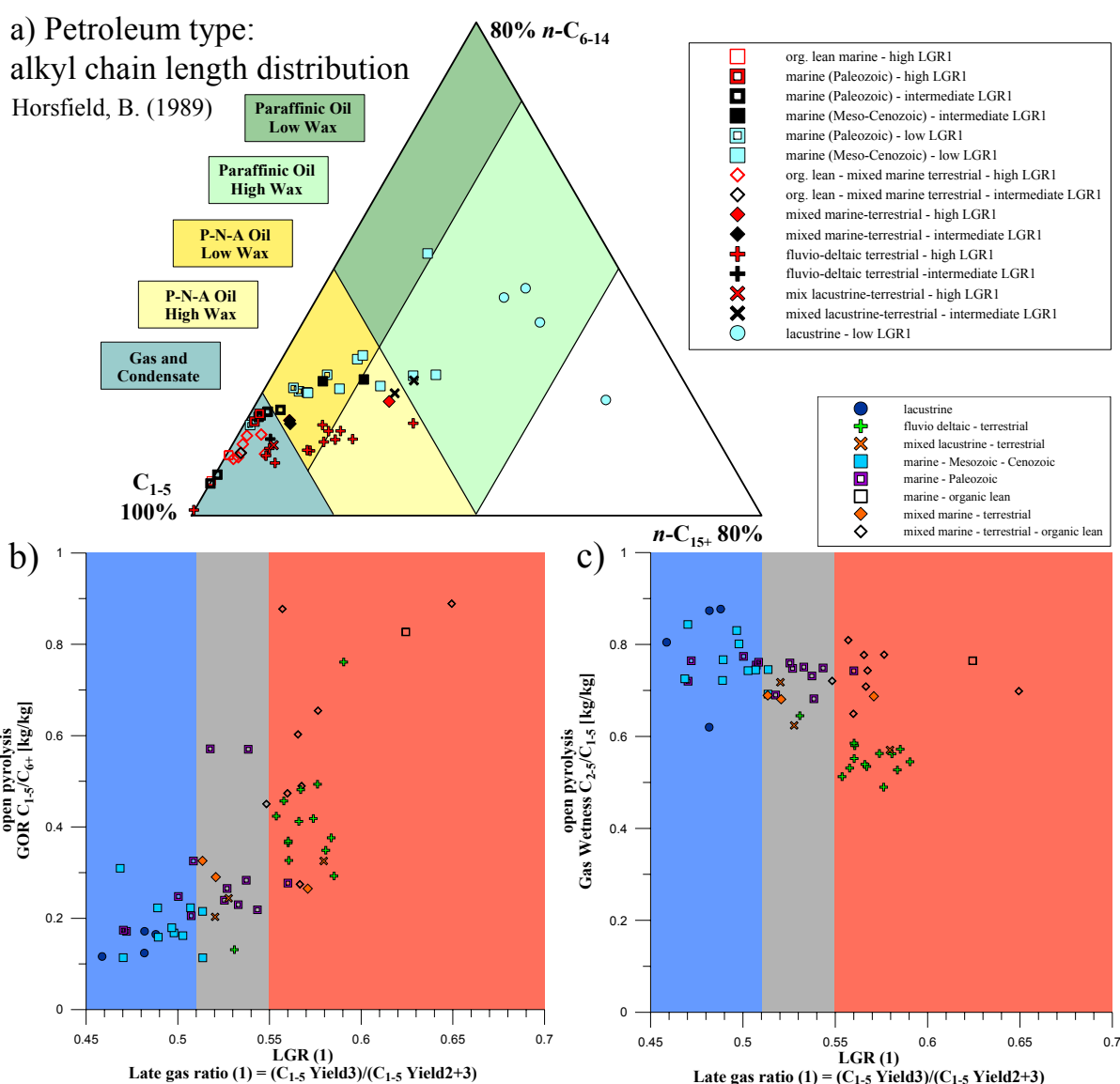


Figure 4.22: Merged Closed-System MSSV-Pyrolysis and Open-System Pyrolysis data – Alkyl chain length distribution: a) Late Gas Potential assignments in relation to organic matter structure and depositional environment in the ternary diagram of Horsfield (1989); b) Comparison of LGR1 and open-system pyrolysis GOR; c) Comparison of LGR1 and open-system pyrolysis gas wetness

### *High Late Gas Potentials*

High late gas potentials ( $LGR1 > 0.55$ ,  $LGR2 > 1$ ) are mainly seen for heterogeneous Type III to Type II/III terrigenous derived or influenced (deltaic) vitrinite rich coals (south-east Asian Talang Akar and Arang coals, New Zealand Coals, Canadian Kugmallit and Taglu Fm. Coals, German Coal, Norwegian Åre Fm. Coal) and mixed marine-terrestrial shales (Mahakam Delta Shale, Akata shale) or mixed lacustrine-terrestrial source rocks such as the spore-rich Cannel Coal (Fig. 4.21; Fig. 4.19, Fig. 4.26). Although not necessarily plotting in the gas and condensate field (Fig. 4.22a) terrestrial organic matter is characterised by higher open-system pyrolysis GOR's (Fig. 4.22b) and lower gas wetness values (Fig. 4.22c) compared to source rocks deposited in other environments.

Organic lean source rocks, with the exception of one Farsund Fm. sample, exhibit high late gas potentials (Fig. 4.26b) and are, due to high temperature mineral matrix effects, characterised by very high GOR's (Fig. 4.22b) and consequently by open-system pyrolysates inferring a gas and condensate petroleum type (Fig. 4.22a). The gas wetness, comprising values typical for marine source rocks, seems not to be influenced by those effects.

### *Low Late Gas Potentials*

The strongest contrast with lowest GOR's and highest gas wetness can be observed for algal derived, structurally homogenous lacustrine (Green River Shale, Wealden Shales, Boghead Coal) and marine shales of Mesozoic – Cenozoic age (Alaskan Tasmanite, Toarcian Shale, Spekk Fm. Shale, Fischschiefer), in some cases of Paleozoic age (Domanik Fm. Shale, Irati Fm. Shale), which contain Type I to Type II kerogen yielding pyrolysates plotting in the paraffinic and low or high wax, paraffinic-naphthenic-aromatic crude oil generating facies (Fig. 4.21, 4.22, 4.26). Those source rocks exclusively exhibit low late gas potentials ( $LGR1 < 0.51$ ,  $LGR2 < 1$ ).

### *Intermediate Late Gas Potentials*

Intermediate late gas potentials ( $LGR1 0.51 - 0.55$ ,  $LGR2 < \text{or} > 1$ ) are mainly seen for Type II to Type II/III (Fig. 4.26) mixed marine-terrestrial (Hekkingen Fm.) or lacustrine-terrestrial source rocks (synthetic Mix I/III; Messel Oil shale) as well as heterogeneous marine shales of Paleozoic age. Exceptions are represented by the younger marine Brown Limestone and Botneheia Shale as well as the Jet Rock sample which also exhibit intermediate late gas potentials. For the Type I Brown Limestone from Jordan as well as for the Type II Messel Oil Shale and Jet Rock late gas is not related to secondary gas (B) generation but to the cracking



of  $C_{6+}$  compounds. The mixed and marine Paleozoic source rocks are characterised by averagely higher GOR's and lower gas wetness than other marine or lacustrine source rocks, but lower GOR's and higher gas wetness than fluviodeltaic-terrestrial source rocks. Nevertheless, two Alum Shale samples exhibit GOR's ( $\sim 0.57$  kg/kg) exceeding those of most terrestrial coals (Fig. 4.22b) which demonstrates that high initial gas potentials are not necessarily indicative of a high late gas potential.

### *Influence of Oxygen-bearing Compounds on the Late Gas Potential*

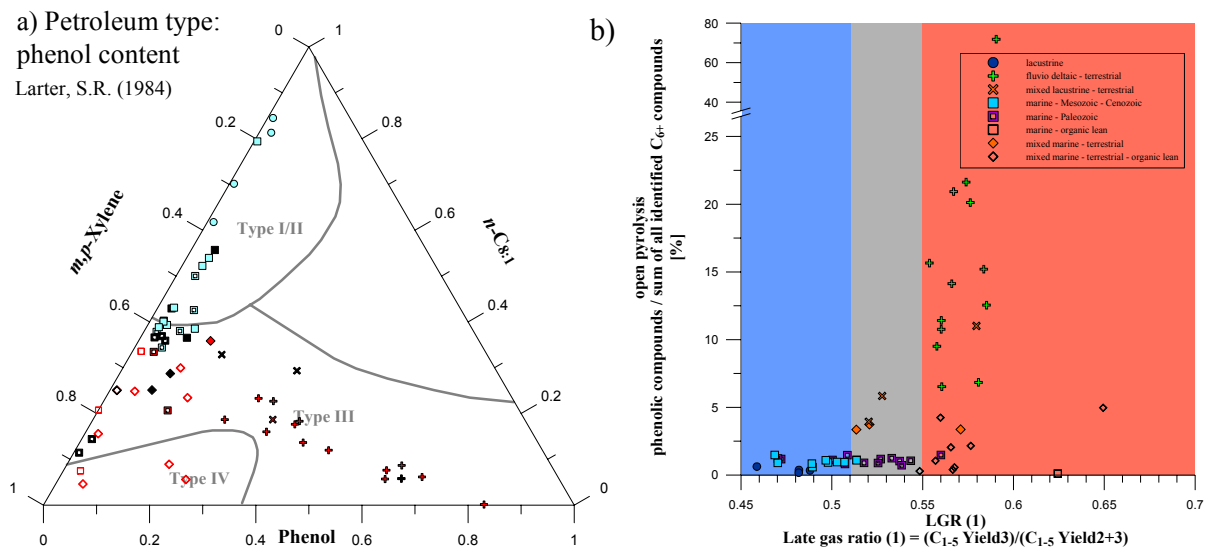


**Figure 4.23: Merged Closed-System MSSV-Pyrolysis and Open-System Pyrolysis data – Phenol content:** a) Late Gas Potential assignments in relation to organic matter structure and depositional environment in the ternary diagram of Larter (1984); b) Comparison of LGR1 and the percentage of phenolic compounds on all identified  $C_{6+}$  compounds (open-system pyrolysis)

In the ternary diagram of Larter (1984)(Fig. 4.23a), originally implemented to distinguish between phenol-rich and phenol-poor Type III source rocks, open-pyrolysis yields of phenol, representing land plant derived moieties of the organic matter, is plotted against *n*-octene and *m,p*-xylene. Corroborating previous statements, low late gas potentials are mainly seen for homogeneous lacustrine and marine Type I to Type II source rocks whose organic matter are dominated by short and long chain aliphatic structures and, thus yield higher amounts of *n*-octene over phenol and *m,p*-xylenes upon open-system pyrolysis. The pyrolysate of more heterogeneous source rocks is enriched in *m,p*-xylenes, representing aromatic moieties, or phenol or both. These samples exhibit intermediate to high late gas potentials, the latter strongly associated with terrigenously influenced depositional settings (high phenol contents). These observations are in accordance with the work of Erdmann and Horsfield (2006) and Dieckmann *et al.* (2006), who stated that terrestrial influenced organic

matter is more aromatic and phenolic in character, which results in recombination-aromatisation reactions of first formed petroleum and residual organic matter during maturation creating a thermally stabilised refractory moiety that generates methane at elevated levels of thermal stress by the  $\alpha$ -cleavage of alkylaromatic compounds.

Nevertheless, there is no clear interdependence between phenolic compounds content, expressed as the percentage of phenolic compounds on all identified  $C_{6+}$  compounds, and  $LGR1 > 0.55$  (Fig. 4.23b). For instance, the mixed marine-terrestrial or lacustrine-terrestrial source rocks clearly show higher phenol contents than the purely marine or lacustrine source rocks, but only the Akata Shale as well as the Cannel Coal possess high late gas potentials.

### *Influence of Kerogen-aromaticity on the Late Gas Potential*

Higher late gas potentials are rather linked to the heterogeneity (or aromaticity) of the organic matter in general which is demonstrated in Fig. 4.24 by a positive correlation of the aromaticity of oil compounds and  $LGR1$  (Fig. 4.24a), and consequently by a negative correlation of the average H/C ratio as an expression of aliphaticity of oil compounds and  $LGR1$  (Fig. 4.24b). Here, the aromaticity is defined as the sum of identified aromatic and phenolic compounds divided by the sum of all identified  $C_{6+}$  compounds whereas the average H/C ratio is defined as the sum of all  $C_{6+}$  component H/C ratios weighted by their abundance. Especially those source rocks showing low late gas potentials are characterised by a much lower aromaticity than most intermediate or high late gas potential source rocks, even though a real “cut-off”-value cannot really be discriminated.

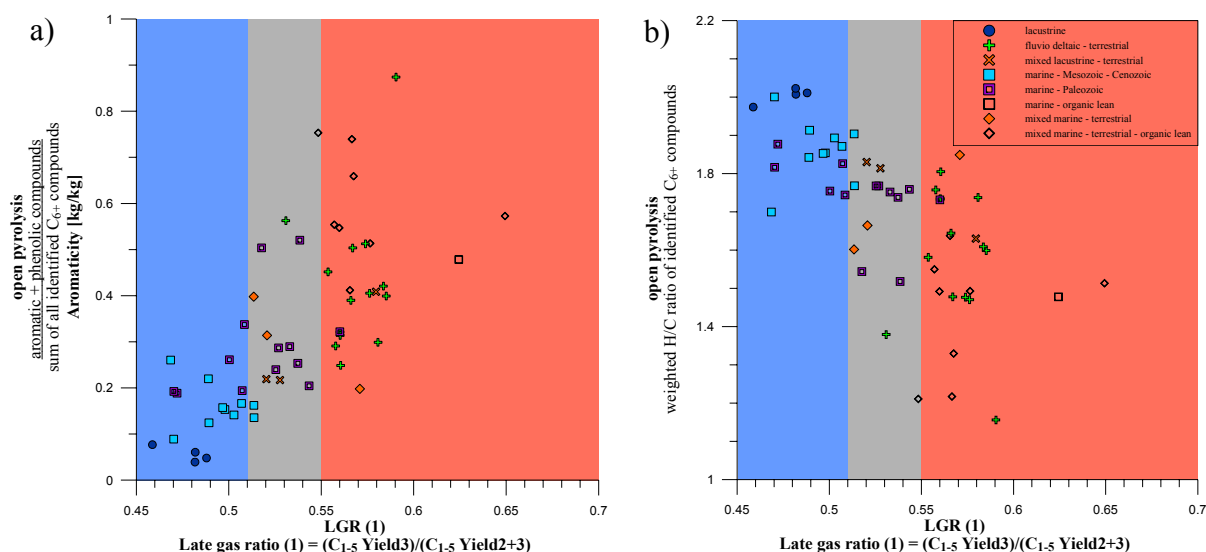


**Figure 4.24:** Comparison of  $LGR1$  to a) aromaticity of open-system pyrolysis  $C_{6+}$  compounds as expressed by the sum of identified aromatic and phenolic compounds divided by the sum of all identified  $C_{6+}$  compounds and to b) aliphaticity of open-system pyrolysis  $C_{6+}$  compounds as expressed by the weighted H/C ratio of all identified  $C_{6+}$  compounds

As discussed earlier, many of the Type II to Type III Paleozoic black shales, especially those of Cambrian, Silurian, and Devonian age, for which higher land plant input can be more or less ruled out (low phenol content Fig. 4.23) are nevertheless characterised by an overall higher aromaticity than their Mesozoic to Cenozoic counterparts and tend to possess intermediate late gas potentials showing secondary gas (B) generation. Thus, the intrinsic more aromatic nature of early Paleozoic source rocks or the presence of a short chain linked carotenoid structures might lead to enhanced aromatisation or polycondensation reactions upon closed-system pyrolysis, resulting in the formation of refractory, and methylated aromatic moieties, which decompose at high levels of thermal stress, again by  $\alpha$ -cleavage, to yield late secondary gas (B). In close relation and based on mass balance calculations of natural maturity series of the marine Alum and Bakken shales, Horsfield *et al.* (1992a) and Muscio and Horsfield (1996) proposed that some dead carbon (inert kerogen) in the “Cooles model” (Cooles *et al.*, 1986) is formed from labile kerogen in the course of maturation, presumably by the incorporation of cross-linked structures. As an alternative, this “dead” carbon might still comprise refractory precursor structures which yield late secondary gas (B) only at the very high temperature stages applied in the current study.

As an aside, the organic lean source rocks also exhibit a very high aromaticity or low aliphaticity besides high late gas potentials.

### ***Influence of Sulphur-bearing Compounds on the Late Gas Potential***

Open-pyrolysis yields of 2,3-dimethylthiophene, representing sulphur containing moieties in the kerogen structure, is plotted against *n*-nonene and *o*-xylene in the ternary diagram of Eglinton *et al.* (1990)(Fig. 4.25a) to distinguish between sulphur-rich and sulphur-poor petroleum generating source rocks. Low-sulphur depositional environments can be mainly found in lacustrine – terrestrial settings, whereas lacustrine source rocks are characterised by low late gas potentials and terrestrial source rocks are characterised by high late gas potentials. As previously observed (Fig. 4.22, 4.23, as well as Fig. 4.26), for sulphur enriched marine source rocks low late gas potentials are mainly seen for homogeneous Type I to Type II shales yielding higher amounts of *n*-nonene over 2,3-dimethylthiophene and *o*-xylene upon pyrolysis, intermediate to high late gas potentials are seen for heterogeneous Type II to Type III organic matter yielding higher amounts of *o*-xylene over 2,3-dimethylthiophene and *n*-nonene. This relation of late gas potential to aromaticity of generated products during open-system pyrolysis confirms the previously described positive correlation of LGR1 to aromaticity of the C<sub>6+</sub> pyrolysate (Fig. 4.24). Therefore, sulphur-richness of the organic matter structure itself seems not to be a major influence on the late gas

generation behaviour as additional comparison of LGR1 and thiophenic content of the pyrolysate, expressed as the ratio of identified thiophenes over all identified  $C_{6+}$  components, only shows data scattering (Fig. 4.25b). The slightly negative trend of LGR1 compared to the ratio of thiophenic compounds over mono-aromatic compounds (Fig. 4.25c) is rather explainable by a higher aliphaticity of the kerogen structure of source rocks with low late gas potentials than by sulphur richness.

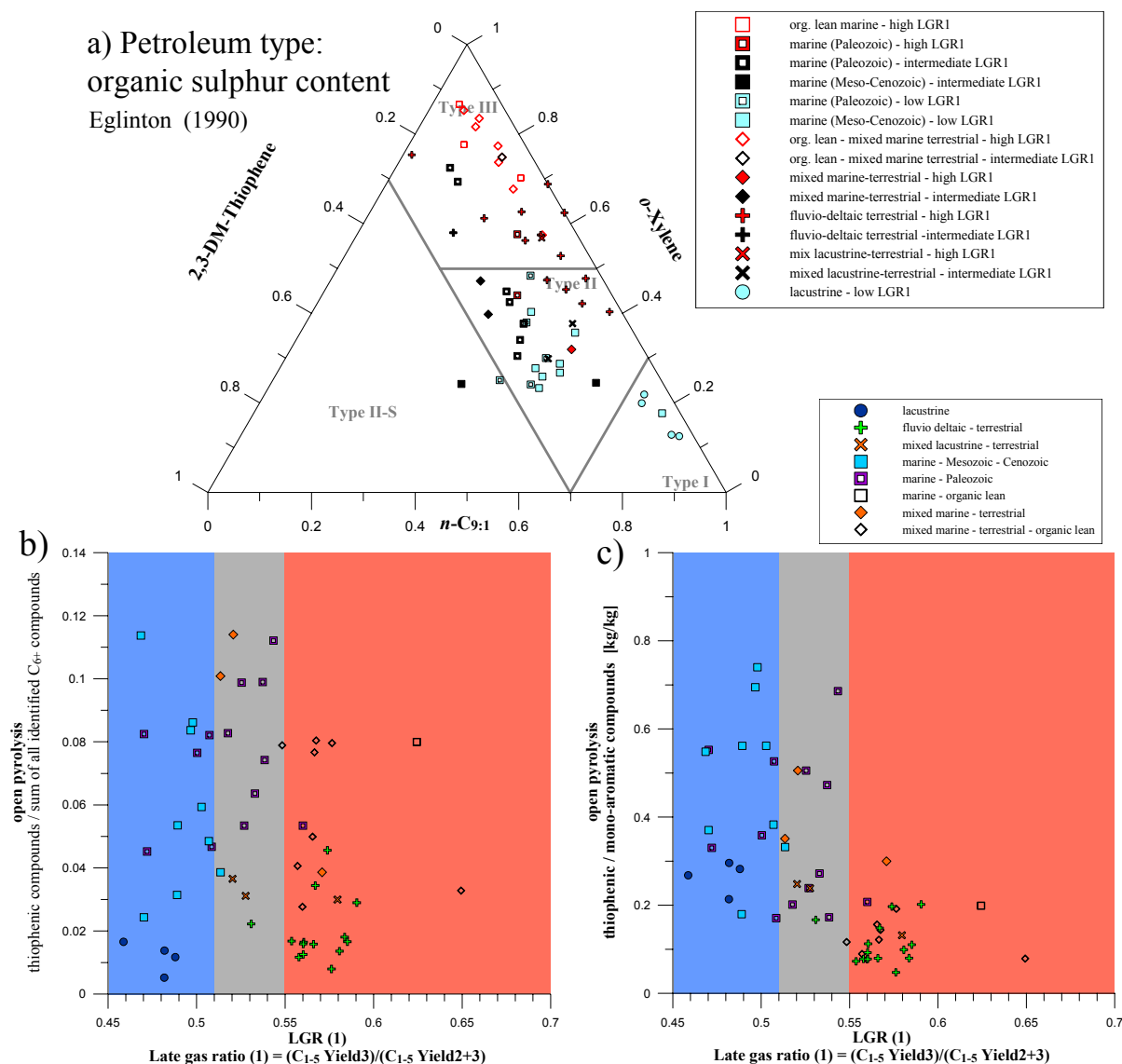
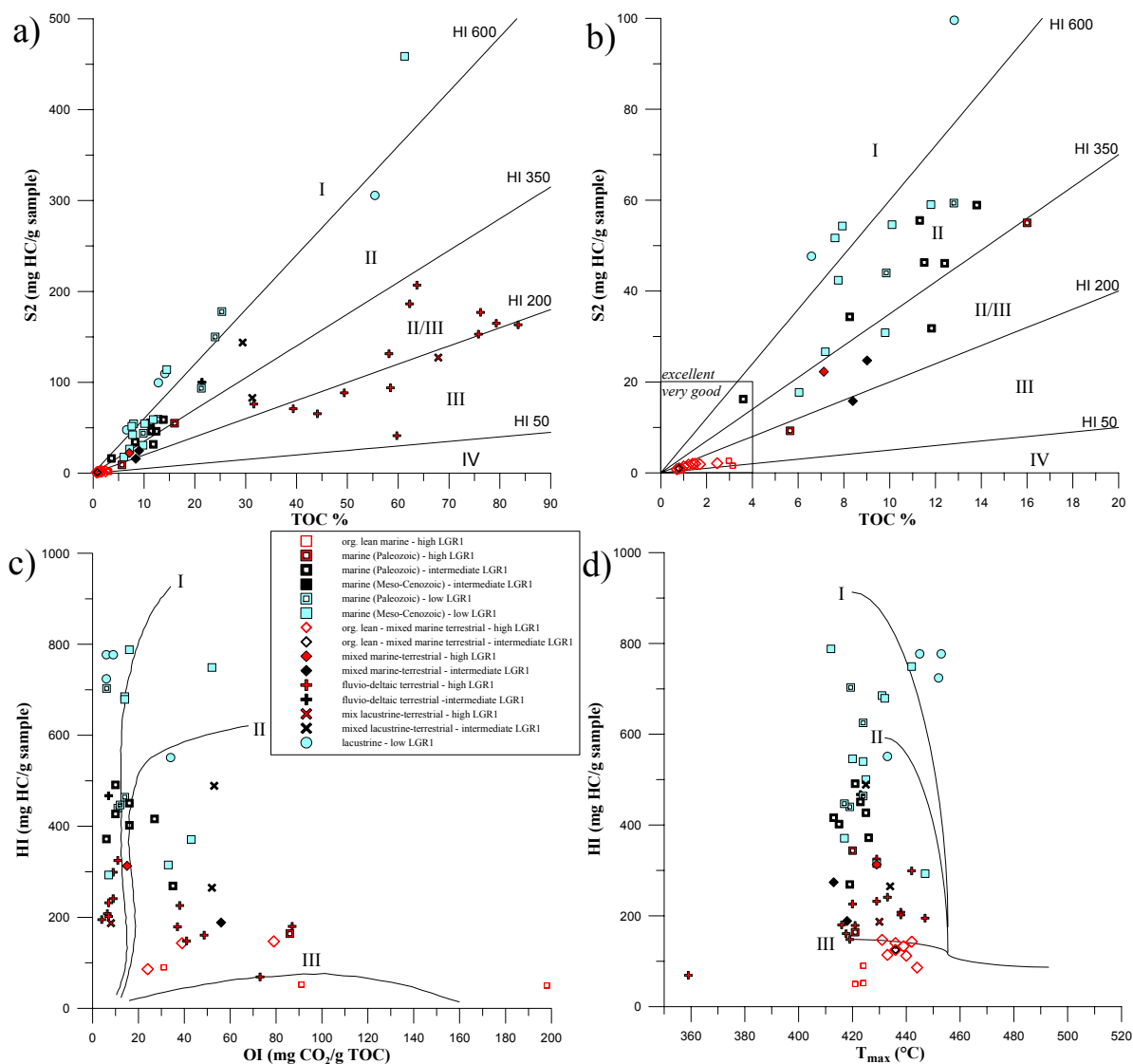


Figure 4.25: Merged Closed-System MSSV-Pyrolysis and Open-System Pyrolysis data – Organic sulphur content: a) Late Gas Potential assignments in relation to organic matter structure and depositional environment in the ternary diagram of Eglinton *et al.* (1990); b) Comparison of LGR1 and the ratio of thiophenic compounds over all identified  $C_{6+}$  compounds (open-system pyrolysis); c) Comparison of LGR1 and the ratio of thiophenic compounds over mono-aromatic compounds (open-system pyrolysis)

### *Influence of Kerogen-Type as defined by Rock-Eval Pyrolysis*

In Fig. 4.26 late gas potentials of immature source rocks are depicted in standard Rock-Eval diagrams. As previously stated it can be seen that mostly gas prone Type III to oil and gas prone Type II/III source rocks possess high or intermediate late gas potentials. Low late gas potentials are mainly related to oil prone Type I to Type II source rocks. Nevertheless, some uncertainty especially for coals and shales with a Hydrogen Index between 300 and 500 mg HC/g TOC is apparent, making bulk open-pyrolysis alone not an useful tool to discriminate between source rocks which might generate late gas from a thermally stabilised moiety during maturation and source rocks which are not late secondary gas (B) prone.



**Figure 4.26: Merged Closed-System MSSV-Pyrolysis and Open-System Pyrolysis data – Rock-Eval Bulk Parameter: Late Gas Potential assignments in relation to a) TOC versus S2, to b) the same as in a) in a smaller resolution, to c) OI versus HI, and d) T<sub>max</sub> versus HI**

### 4.3 Conclusion

In this chapter it was shown how late gas generation can be evidenced under laboratory conditions in general and to what extent the initial organic matter structure, depositional environment or precursor biota is responsible for the occurrence of late gas generation.

A fluvio deltaic-terrestrial Type III coal from the Åre Fm (G001965), a marine Type II shale from the Spekk Fm. (G001955), as well as a lacustrine Type I Green River Shale (G004750) and a synthetic Type I/III source rock (G0047501965) were used to study primary and secondary gas generation mechanisms in detail by non-isothermal ( $1^{\circ}\text{C}/\text{min}$ ), stepwise open-system pyrolysis (profiles only up to  $600^{\circ}\text{C}$ ) and closed-system MSSV-pyrolysis (up to  $780^{\circ}\text{C}$ ). The kinetic parameters of high temperature gas generation were determined for the type III Åre Fm. sample, which showed a distinct late gas potential, using 3 MSSV heating rates ( $0.1$ ,  $0.7$ ,  $1.0^{\circ}\text{C}$ ) and elevated pyrolysis temperatures. The late methane forming reaction itself can be described by a single activation energy  $E_a$  ( $\sim 55$  kcal/mol) and a surprisingly low frequency factor (only  $\sim 5.00\text{E}+09$  1/s), which nevertheless seems to be characteristically for the thermal cracking of methylated aromatic nuclei by  $\alpha$ -cleavage mechanisms. Furthermore, extrapolation to a linear geologic heating rate of  $3^{\circ}\text{C}/\text{ma}$  revealed, in accordance with previously published data of Erdmann and Horsfield (2006), onset temperatures exceeding  $200^{\circ}\text{C}$  ( $\sim 220^{\circ}\text{C}$ ; calculated  $R_o \sim 2.5\%$ ). A geologic  $T_{\text{max}}$  of  $\sim 240^{\circ}\text{C}$  ( $3.1\%$   $R_o$ ) and the calculated end of the reaction at temperatures of  $\sim 250^{\circ}\text{C}$  ( $3.5\%$   $R_o$ ) seemed rather low but are most likely related to the degradation of methane at high pyrolysis temperatures and consequently to the possible overprinting of ongoing methane formation by cracking of methane.

The ability of source rocks to generate significant additional amounts of gas at high maturities ( $R_o > 2.0\%$ ;  $T > 200^{\circ}\text{C}$ ) was studied and linked to the initial organic matter structure, depositional environment and precursor biota. A large selection of immature source rocks and putative gas shales covering all main kerogen types (I, II, II/III and III, from gas prone to oil prone) and depositional environments ( $\sim 60$  samples) were investigated using both open- and closed-system pyrolysis methods for the characterisation of kerogen type, molecular structure, and late gas generative behaviour. Using a rapid, two- (or three)-step MSSV-pyrolysis screening method, spanning the main stage of late gas generation subsequent to primary gas generation and secondary gas generation by cracking of aliphatic  $\text{C}_{6+}$  compounds, discrimination of source rocks with low, high, or intermediate late gas potential is possible. Two Late Gas Ratios based on MSSV  $\text{C}_{1-5}$  and  $\text{C}_{6+}$  yields for end temperatures of

the two high temperature stages were implemented, as gas generation between the first and the second stage was dominated by  $C_{6+}$  cracking alone for all samples in the closed-system. Immature source rocks with low, intermediate and high late gas potentials can be distinguished, whereas low late gas potentials ( $LGR1 < 0.51$ ) are defined by lower or constant gas yields at the highest temperature compared to the 2<sup>nd</sup> end temperature. Intermediate ( $LGR1\ 0.51 - 0.55$ ) and high late gas potentials ( $LGR1 > 0.55$ ) are defined by higher yields which can whether be due to cracking of  $C_{6+}$  compounds still present in the confined system ( $LGR2 < 1$ ) or which must be explained by an extra amount of gas generated from a neoformed or thermally stabilised structure ( $LGR2 > 1$ ). High late gas potentials are mainly associated with heterogeneous aromatic and/or phenolic Type III and Type II/III shales and coals stemming from fluvio deltaic – terrestrial or mixed marine – terrestrial environments confirming earlier findings of Erdmann and Horsfield (2006) and Dieckman *et al.* (2006). In some cases purely marine source rocks of high intrinsic aromatic nature show high late gas potentials. Here, late secondary gas (B) contributes an additional 10 to 40 mg  $C_{1-5}$ /g TOC or 6 to 52% to the total primary petroleum potential determined by routinely used open-system pyrolysis methods. Low late gas potentials, defined by lack of late secondary gas (B) generation, are associated with homogeneous, paraffinic organic matter of aquatic lacustrine and marine origin. Source rocks exhibiting intermediate late gas potentials, generate late gas, which is related to regular late  $C_{6+}$  cracking gas or to lower average late secondary gas (B) input in the range 0-20 mg  $C_{1-5}$ /g TOC. Here, proportions of late secondary gas (B) on the total petroleum potential do not exceed 6% and are mainly associated with heterogeneous marine source rocks containing algal or bacterial derived precursor structures of high aromaticity, or with source rocks deposited in aquatic environments containing minor amounts of aromatic/phenolic higher land plant material. Sulphur components within the kerogen structure do not seem to influence the late gas generation behaviour.





## 5 EVOLUTION OF LATE GAS POTENTIAL WITH MATURITY

The purpose of this chapter is to investigate whether late gas generative properties are influenced by structural and chemical changes within the organic matter during natural maturation or artificial maturation under open- and closed-system pyrolysis conditions.

In Chapter 5.1 five maturity series (39 samples) comprising two Type II marine shale series (Exshaw Fm. And Barnett Shale) and three Type III humic coal series (New Zealand Coals and German Carboniferous as well as Wealden Coals) are investigated by the MSSV-pyrolysis two-step (end-temperature) screening method described in Sub-Chapter 4.2.1. As indeed marked differences of late gas potential with maturity can be observed for all kerogen types, the evolution of secondary gas (B) generation is directly compared to organic matter structural changes as defined by open-system pyrolysis methods, IR and literature review.

In Chapter 5.2 results of the application of the same methods to five different artificially matured immature source rocks are discussed.

### 5.1 *Natural Maturity series*

#### 5.1.1 Late Gas Generation Behaviour (MSSV Py-GC)

MSSV C<sub>1-5</sub> gas and C<sub>6+</sub> compound yields at the 2 MSSV-screening temperatures as well as additional data and ratios based on those yields are provided in Tab. 5-1 for the five investigated natural maturation series. The position of the samples within the late gas potential ratios plot is displayed in Fig. 5.1. An extended scale up to a maximal possible LGR1 of 1 is implemented, as the more mature samples within one maturity sequence exhibit late gas potentials with increasingly higher values (> 0.6). Theoretically, maximal LGR2 could be infinitely high and is artificially fixed at 8. Rising LGR1 and LGR2 values with maturity signify that more and more of the late gas, generated between 560°C and 700°C, can be assigned to late secondary gas (B) production (see also Fig. 5.4). Interestingly, the location of all naturally matured samples within the LGR1 – LGR2 plot can be described by one exponential function for all investigated series (Fig. 5.2), even though initial late gas potentials are different. Thus, an increase of late gas potential can be ascribed to maturity induced structural evolution of the residual organic matter, which seems to be mechanistically similar for the different organic matter types.

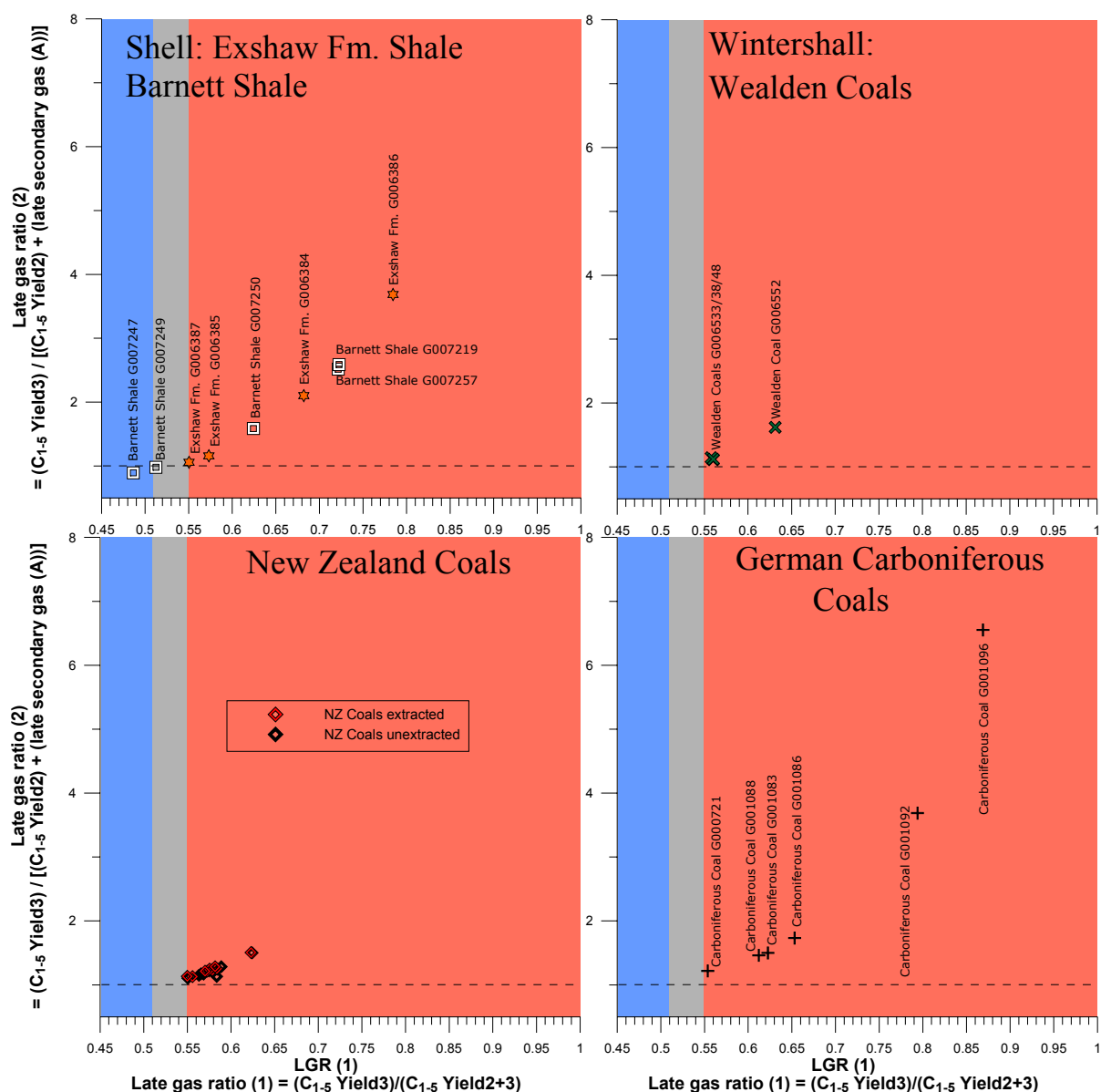


Figure 5.1: Late Gas Potentials Classification using MSSV-pyrolysis based LGR1 and LGR2 for investigated natural maturity series samples.

### 5.1.2 Product Amounts

#### *Yields versus Late Gas Ratio 1 (LGR1)*

The MSSV late gas yield data between 560°C and 700°C of investigated natural maturation series samples is provided in Fig. 5.3 and Tab. 5-1. Total gas yields are composed of secondary gas (A), which is due to the cracking of  $C_{6+}$  compounds within the closed-system MSSV-tubes, and secondary gas (B), generated from a thermally stabilised moiety. The percentage of late secondary gas (B) on the total late gas potential is shown in Fig. 5.4.

For the Exshaw Fm. maturity series, provided by Shell, total late gas yields range between 20 and 55 mg  $C_{1-5}$ /g TOC, whereas for the two more immature samples G006387

(LGR1 = 0.55) and G006385 (LGR1 = 0.57) about 20-30% of this amount can be ascribed to  $C_{6+}$  cracking. In contrast, late gas generated from the two more mature samples G006384 (LGR1 = 0.68) and G006386 (LGR1 = 0.78) is almost exclusively contributed by late secondary gas (B).

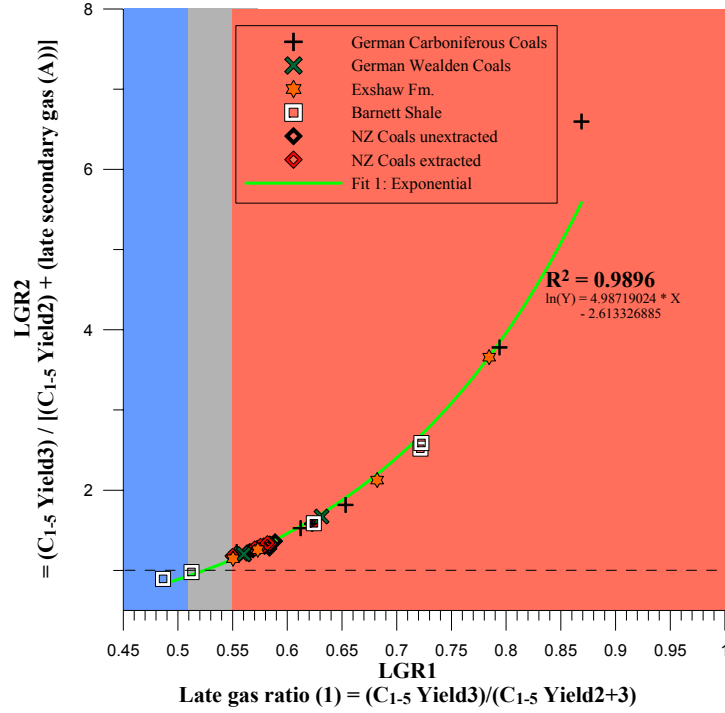


Figure 5.2: Exponential function describing the position of all investigated maturity series samples in the LGR1 – LGR2 plot.

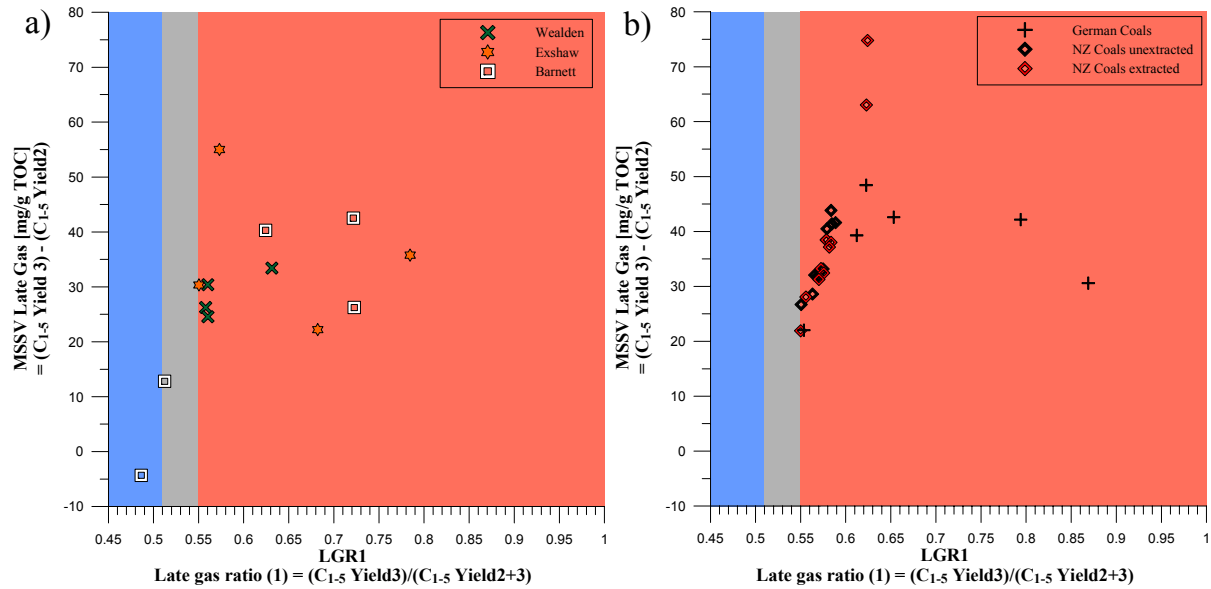
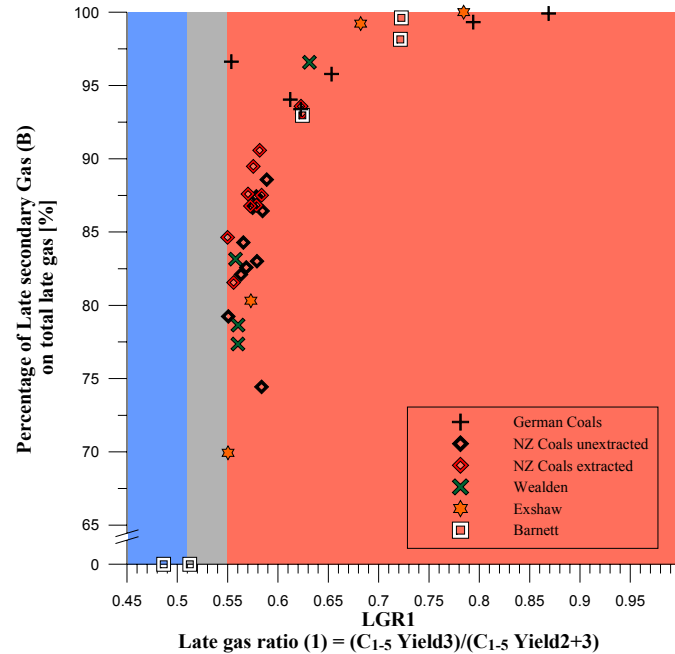


Figure 5.3: Comparison of LGR1 and total late gas generated between MSSV end temperatures 560° and 700°C for a) Barnett Shales and shales of the Exshaw Fm. as well as coals of the German Wealden and b) for German Carboniferous and unextracted and extracted New Zealand Coals.

The same is true for investigated Wealden Coals, provided by Wintershall. The percentage of late secondary gas (B) on total late gas yields of the three immature samples G006533, G006538, and G006548 (all LGR1 = 0.56) ranges around 80%, for the more mature sample G006552 ( $T_{\max}$  474°C; LGR1 = 0.63) proportions increase up to about 97%.



**Figure 5.4: Relation of LGR1 to the percentage of late secondary gas (B) on the total late gas generated between 560° and 700°C.**

The Barnett Shale sample set shows a somewhat diverse behaviour as for the two immature samples which exhibit only intermediate (G007249) and low (G007247) late gas potentials, none of the observed total late gas, if seen, can be ascribed to secondary gas (B) generation. This changes with maturity as LGR1 ratios increase and late gas, ranging between 0 – 41 mg/g TOC, is made up of increasingly higher proportions of secondary gas (B). Nevertheless, sample G007219, with the highest LGR1, exhibits the lowest late gas yields of the more mature samples (Fig. 5.3a.).

For the German Coals maturation series, for which total late gas exhibits values between 20 and 47 mg/g TOC, a similar trend can be observed in Fig. 5.3b with decreasing total late gas amounts for the sample with the highest LGR1. The percentage of late secondary gas (B) on the total late gas yield ranges, related to the overall relative high maturity of the German Coal sample set, between 93 and 100%. Interestingly, total late gas yields (20 – 75 mg/g TOC) and proportions of late secondary gas (B) on the total late gas yield (75 -90%) of the immature New Zealand Coals series show a positive correlation with LGR (1), but a negative correlation with maturity (see also Fig. 5.5 or Tab. 5-1).

**Table 5-1: Calculated late gas, secondary gas (A) and (B) yields as well as LGR1 and LGR2 for natural maturity series samples based on products generated between MSSV end temperatures 560°C and 700°C.**

Company	GFZ Code	R0 %	Formation	MSSV C <sub>1-5</sub>			LGR1	MSSV C <sub>6+</sub>		C <sub>1-5</sub> sec. Gas (A)	LGR2	C <sub>1-5</sub> sec. Gas (B)	sec. Gas (A) /Late Gas %	sec. Gas (B) /Late Gas %
				2.Temp	3.Temp	Late Gas	kg/kg	2.Temp	3.Temp	mg/g TOC	kg/kg	mg/g TOC	%	%
Shell	G006385	0.76	Exshaw Fm.	160.75	215.76	55.02	0.57	40.35	4.24	10.83	1.26	44.18	19.69	80.31
	G006387	0.89		135.58	165.93	30.35	0.55	42.30	11.89	9.12	1.15	21.22	30.06	69.94
	G006384	1.25		19.39	41.61	22.22	0.68	10.21	9.63	0.17	2.13	22.04	0.78	99.22
	G006386	3.33		13.55	49.32	35.78	0.78	6.48	6.71	-0.07	3.66	35.85	-0.20	100.20
Wintershall	G006533	0.56	Wealden	111.06	141.45	30.39	0.56	25.45	2.51	6.88	1.20	23.51	22.64	77.36
	G006548	0.72		89.61	114.17	24.55	0.56	19.79	2.31	5.24	1.20	19.31	21.35	78.65
	G006538	0.89		100.37	126.61	26.24	0.56	20.45	5.71	4.42	1.21	21.82	16.85	83.15
	G006552	1.37		46.96	80.39	33.42	0.63	6.56	2.75	1.14	1.67	32.28	3.42	96.58
GFZ natural maturity series	G007249	0.40	Barnett Shale	252.03	264.83	12.79	0.51	74.31	13.80	18.15	0.98	-5.36	100.00	0.00
	G007247	0.94		81.72	77.39	-4.33	0.49	19.99	3.78	4.86	0.89	-9.19	0.00	0.00
	G007250	1.35		60.93	101.22	40.30	0.62	10.59	1.13	2.84	1.58	37.46	7.04	92.96
	G007257	1.93		26.71	69.22	42.51	0.72	3.15	0.52	0.79	2.52	41.73	1.85	98.15
	G007219	3.21	Carboniferous Coals	16.35	42.58	26.23	0.72	1.63	1.29	0.10	2.59	26.13	0.39	99.61
	G000721	0.99		91.55	113.57	22.02	0.55	25.88	23.40	0.74	1.23	21.28	3.38	96.62
	G001088	1.26		67.95	107.23	39.29	0.61	10.74	2.94	2.34	1.53	36.95	5.96	94.04
	G001083	1.37		74.56	123.00	48.43	0.62	12.93	2.25	3.21	1.58	45.23	6.62	93.38
	G001086	1.58	New Zealand Coals	48.21	90.79	42.58	0.65	7.52	1.53	1.80	1.82	40.79	4.22	95.78
	G001092	2.09		14.78	56.95	42.17	0.79	1.47	0.52	0.29	3.78	41.88	0.68	99.32
	G001096	2.81		5.43	36.03	30.59	0.87	0.67	0.58	0.03	6.60	30.57	0.09	99.91
	G001983	0.41		109.14	152.98	43.84	0.58	47.51	10.15	11.21	1.27	32.63	25.57	74.43
	G001982	0.40	New Zealand Coals	107.68	148.15	40.47	0.58	26.50	3.58	6.88	1.29	33.60	16.99	83.01
	G001984	0.45		99.90	131.64	31.74	0.57	21.23	2.80	5.53	1.25	26.21	17.42	82.58
	G001981	0.45		103.41	141.88	38.47	0.58	18.81	2.69	4.83	1.31	33.63	12.57	87.43
	G001980	0.44		101.61	143.00	41.39	0.58	21.55	2.82	5.62	1.33	35.78	13.57	86.43
	G001997	0.52	New Zealand Coals extracted	96.37	137.99	41.62	0.59	17.77	1.93	4.75	1.36	36.87	11.42	88.58
	G001996	0.52		94.24	127.40	33.16	0.57	16.69	1.94	4.42	1.29	28.74	13.34	86.66
	G001990	0.71		118.70	145.39	26.69	0.55	20.54	2.07	5.54	1.17	21.15	20.76	79.24
	G001994	0.61		98.73	127.33	28.60	0.56	18.79	1.72	5.12	1.23	23.48	17.90	82.10
	G001991	0.80		106.19	138.25	32.07	0.57	18.32	1.52	5.04	1.24	27.03	15.72	84.28
	G001983K	0.41	New Zealand Coals extracted	113.12	187.90	74.78	0.62	20.85	3.67	5.16	1.59	69.63	6.89	93.11
	G001982K	0.40		103.05	141.50	38.45	0.58	19.58	2.69	5.07	1.31	33.38	13.18	86.82
	G001984K	0.45		94.54	132.55	38.01	0.58	18.08	2.26	4.75	1.33	33.26	12.49	87.51
	G001981K	0.45		97.85	131.08	33.23	0.57	17.20	2.55	4.39	1.28	28.84	13.22	86.78
	G001980K	0.44	New Zealand Coals extracted	96.78	159.82	63.04	0.62	16.98	3.50	4.05	1.59	58.99	6.42	93.58
	G001997K	0.52		91.27	123.71	32.44	0.58	13.78	2.40	3.41	1.31	29.03	10.52	89.48
	G001996K	0.52		94.99	132.16	37.16	0.58	13.41	1.74	3.50	1.34	33.66	9.42	90.58
	G001990K	0.71		111.57	139.62	28.05	0.56	20.00	2.75	5.17	1.20	22.88	18.45	81.55
	G001994K	0.61		95.53	126.79	31.26	0.57	14.95	2.02	3.88	1.28	27.38	12.41	87.59
	G001991K	0.80		98.72	120.63	21.91	0.55	12.52	1.30	3.37	1.18	18.55	15.36	84.64

### Yields, LGR1 versus Maturity (Vitrinite Reflectance)

For a better overview, LGR1 and late secondary gas (B) yields of all natural maturity series samples are plotted against maturity respective vitrinite reflectance (Fig. 5.5). Vitrinite reflectance of New Zealand coal samples ( $R_o = 0.4 - 0.8\%$ ) and higher rank German Coal samples ( $R_o = 0.99 - 2.81\%$ ) was directly measured by R. Sykes (GNS-New Zealand) whereas values for Exshaw Fm, Barnett Shale and Wealden Coal samples were calculated from Rock-Eval  $T_{max}$  data using the empirical formula of Jarvie *et al.* (2001) ( $R_o = T_{max} * 0.0180 - 7.16$ ).

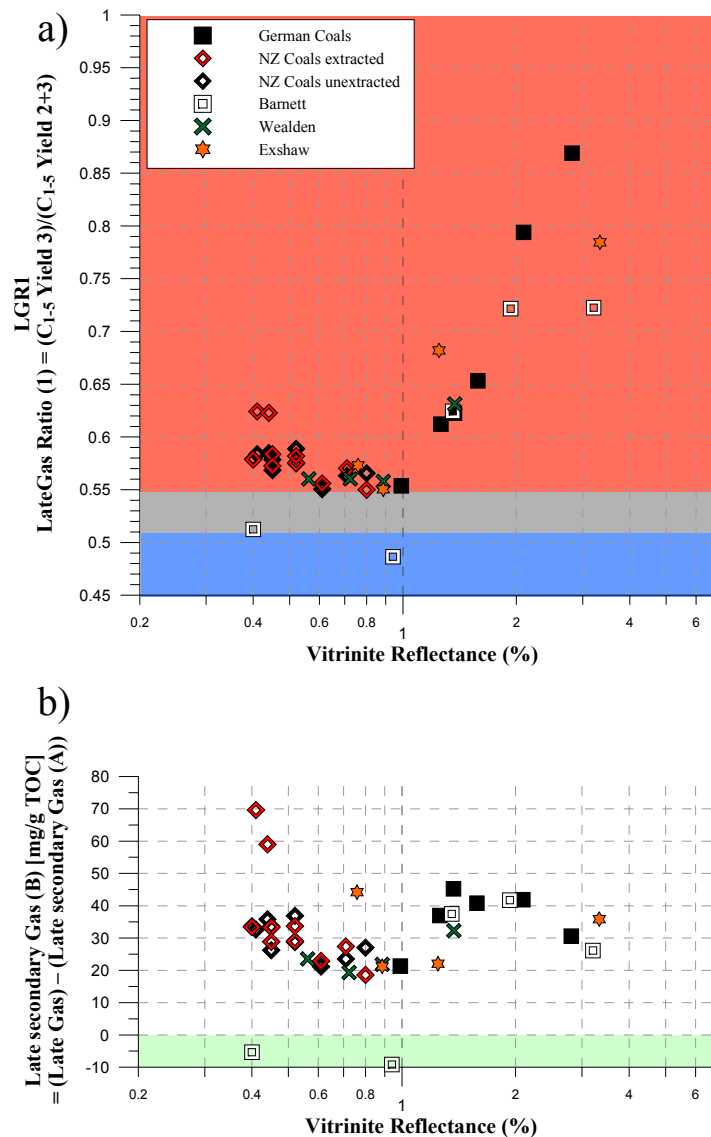


**Figure 5.5: Relation of measured (German Carboniferous Coals, New Zealand Coals) or calculated Vitrinite Reflectance (%  $R_o$ ) to a) LGR1 and b) secondary gas (B) yield**

One first important observation is that neither the late gas potential, expressed as LGR1 (Fig. 5.5a), nor the absolute amount of generated late secondary gas (B) (Fig. 5.5b) stays the same for maturities ranging from diagenesis ( $R_o < 0.5\%$ ) over catagenesis ( $R_o \sim 0.5$

– 2.0%) to metagenesis ( $R_o > 2.0\%$ ). This finding underlines the importance of using natural maturity sequences in addition to only immature source rocks as a calibration tool for the evaluation of late gas generation under geologic conditions at high levels of thermal stress.

For unextracted and extracted New Zealand Coals, there is a notable loss of late gas potential from sub-bituminous coal ranks ( $R_o$  range 0.4-0.5%) to high volatile bituminous coal ranks ( $R_o$  range 0.6-0.8%), where values stay about the same (Fig. 5.5). The three immature Wealden Coal samples exhibit more or less identical late gas potentials than the bituminous New Zealand coals in the respective maturity range. Interestingly, Barnett Shale samples experience the same downwards trend going from  $R_o \sim 0.4\%$  (intermediate late gas potential) to 0.93% (low late gas potential) which also holds true for the Exshaw Fm source rocks ( $R_o \sim 0.77\%$  and  $\sim 0.89\%$ ).

After this initial decrease, a late gas potential “jump”, i.e. strong increase, is evident for all investigated sequences in the catagenesis zone or at the end of the “oil window”. Late secondary gas (B) yields double from about  $\sim 20$  mg/g TOC to  $\sim 40$  mg/g TOC for the German Coal series going from high volatile bituminous coal ranks ( $R_o = 0.99\%$ ) to medium and low volatile bituminous coal ranks ( $R_o = 1.26 - 2.09\%$ ). Late secondary gas (B) yields of the more mature Wealden coal sample ( $R_o = 1.36\%$ ) are also significantly increased compared to lower maturity samples. The most striking “jump” can be observed for mature Barnett Shale samples for which late secondary gas (B) yields rise from 0 to  $\sim 40$  mg/g TOC between  $R_o = 1.35$  and 1.93% (Fig. 5.5b). This trend is not as marked for the Exshaw Fm. shales, which could be due to a somewhat lower maturity of the respective sample G006384.

It is noteworthy that maximal secondary gas (B) yields of all investigated maturity sequences range around 40 mg/g TOC at the end of catagenesis independent of kerogen type. Nevertheless, it should be kept in mind that true amounts might be higher as gas generation is most likely to proceed at laboratory temperatures in excess of  $700^\circ\text{C}$ , the final screening temperature. For example, Behar *et al.* (1992; Behar *et al.*, 1997) found, based on closed-system and open-system pyrolysis experiments and mass balance calculations, that mature kerogens of Type I, II, and III generate similar amounts of high temperature methane, approximately 50 mg/g TOC, at geologic temperatures between 200 and  $230^\circ\text{C}$ .

After maximal secondary gas (B) yields are reached in the catagenesis zone ( $\sim 40$  mg/g TOC), amounts decrease again during metagenesis. The anthracite sample ( $R_o = 2.81\%$ ) of the German coal series shows a lower yield of 30.53 mg  $\text{C}_{1-5}$ /g TOC whereas the most mature Barnett Shale sample ( $R_o = 3.21\%$ ) exhibits values around 26.13 mg/g TOC. It can be deduced that this latter fall in gas yield is due to the decomposition of late gas precursors from

the macromolecular organic matter under natural maturation conditions indicating  $R_o \sim 2\%$  to be the onset point of late gas generation. This conclusion is confirmed by previous MSSV-based kinetic calculations of late gas generation by Erdmann and Horsfield (2006), Dieckmann *et al.* (2006), and present kinetic calculations on an immature Åre Fm. sample G001965 (Chapter 4.1.5).

### **5.1.3 Relation of Late Gas Generation Behaviour to the Evolution of Kerogen/Coal Structure**

Open-system pyrolysis is a tool to crack the macromolecular organic matter into smaller GC-amenable products indirectly yielding information about predominant chemical moieties within the kerogen structure, which changes in the course of maturation. To compare the evolution of late gas generation behaviour to the evolution of kerogen structure during maturation, closed-system pyrolysis data of all investigated natural maturity series samples, i.e. late secondary gas (B) yields, is compared to open-system data, such as HI and OI (Rock Eval) as well as GOR, gas wetness, aromaticity, and phenol content (GC-FID) in relation to measured or calculated vitrinite reflectance in Fig. 5.6.

To further elucidate the correlation of changing late gas potentials and kerogen structure evolution during natural maturation, secondary gas (B) yields of unextracted New Zealand Coals and German Coals are compared to infrared spectroscopic analytical results and open-system pyrolytical yields in Fig. 5.7. Infrared and open pyrolysis data for New Zealand Coals were taken from Vu (2008); data for German Coals were taken from Horsfield and Schenk (1995) and Schenk and Richter (1995). Infrared data is listed in Tab. 5-2. The astonishingly smooth fit of ratios and yields in the maturity interval from 0.7 to 0.99%  $R_o$  justifies the usage of the two maturation series despite the different geographic origin of these coals, which was already previously noted by Vu (2008).

As described above, three maturity ranges with inherent structural changes of the organic matter are of special interest as far as late gas potential evolution is concerned. Those are firstly, vitrinite reflectances between 0.4 and 0.9% with an associated loss of late gas potential, secondly, vitrinite reflectances between 1 and 2% with an associated “jump” in late gas potentials, and thirdly, vitrinite reflectances above 2% with decreasing late gas potentials due to natural late gas generation. Based on open-system pyrolysis and infrared spectroscopy the structural evolution of the different types of organic matter within these three maturity ranges is described in detail in the following three sub-chapters.



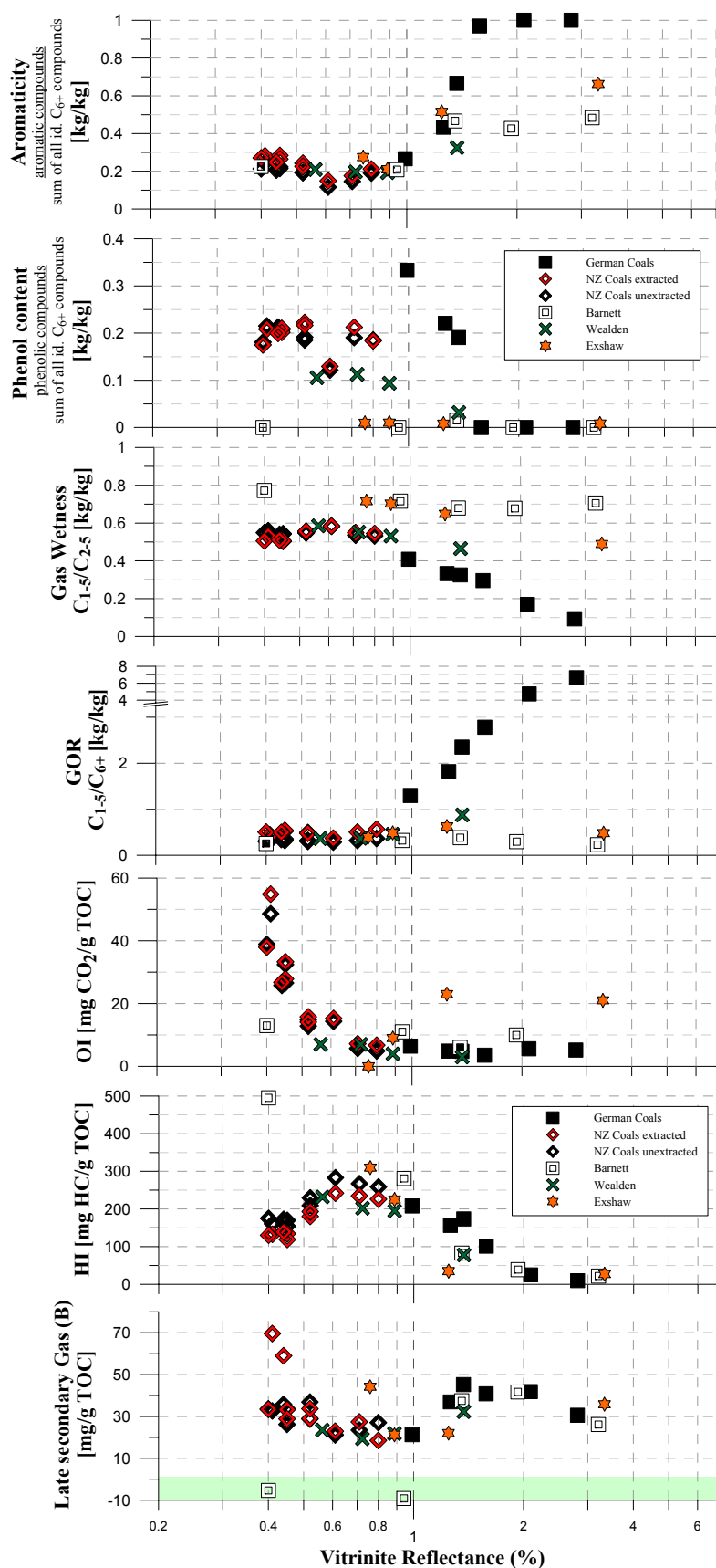
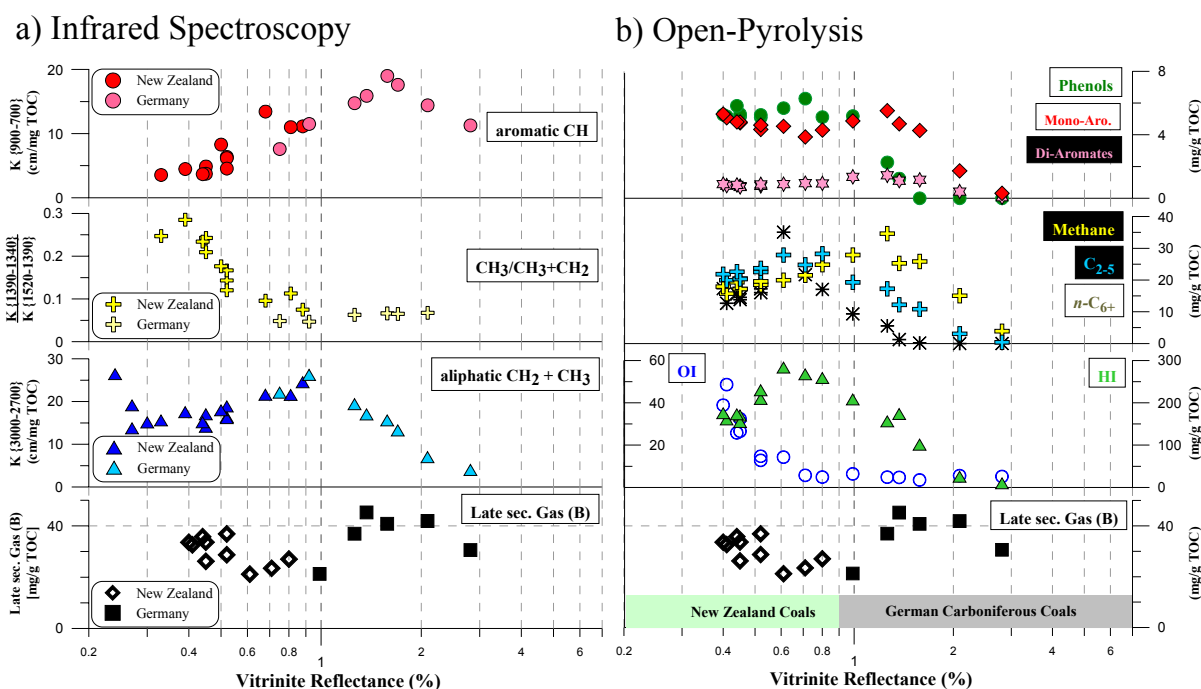


Figure 5.6: Evolution of late secondary gas (B) yields (MSSV-pyrolysis) and organic matter structure, as revealed by open-system pyrolysis HI, OI (Rock Eval) as well as GOR, gas wetness, aromaticity, and phenol content (GC-FID), in the course of maturation (vitrinite reflectance) for all maturity series.

### *Late Gas Potential loss during early maturation stages*

#### *General evolution of parameters (open-system pyrolysis and IR)*

In the first maturity range between 0.4 and 0.9% vitrinite reflectance late gas potential loss is accompanied by strongly decreasing Oxygen Indices and a slightly decreasing aromaticity of samples of all maturity series (Fig. 5.6). An opposite behaviour can be observed for the evolution of the Hydrogen Index which strongly increases for the New Zealand Coal samples, at least between 0.5 and 0.6%, but decreases for the Barnett Shale and Exshaw Fm. samples. Changes in GOR, gas wetness and phenol content are not significant in this maturity range. The decrease in late secondary gas (B) yield and oxygen index OI (mg CO<sub>2</sub>/g TOC) from sub-bituminous coal ranks (R<sub>o</sub> range 0.4-0.5%) to high volatile bituminous coal ranks (R<sub>o</sub> range 0.6-0.7%) for the New Zealand Coals is accompanied by a strong decrease of methyl groups over total aliphatic groups (CH<sub>3</sub>/(CH<sub>3</sub>+CH<sub>2</sub>)) (Fig. 5.7), whereas rising HI values are accompanied by rising total aliphatic groups (CH<sub>2</sub> + CH<sub>3</sub>) and an increase in C<sub>1+</sub> alkyl chain yields upon open-system pyrolysis. An increase of protonated aromatic carbon (CH) due to aromatisation of alicyclic ring components (Schenk and Richter, 1995; Vu, 2008) can also be observed.



**Figure 5.7: Evolution of late secondary gas (B) yields (MSSV-pyrolysis) and organic matter structure, as revealed by a) infrared spectroscopic analytical results and b) open-system pyrolytical yields, in the course of maturation (vitrinite reflectance) for New Zealand and German Carboniferous Coals.**

**Table 5-2: Integrated infrared absorption (cm/mg TOC) in selected spectral ranges of New Zealand Coals (extracted coals) and non-extracted German coals (table taken from Vu, 2008 (Table 6-1); data of Schenk & Richter, 1995 and Vu, 2008)**

Sample-nr.	R <sub>0</sub>	K 3000-2700	K 1520-1390	K 1390-1340	K 900-700	K1390-1340/ K1520-1390	C <sub>aliphatic</sub>
	(%)	cm <sup>-1</sup>					mg/gTOC
New Zealand Coals							
G001988	0.27	13.75	n.d	n.d	n.d	n.d	71.5
G001986	0.27	19.1	n.d	n.d	n.d	n.d	99.3
G001977	0.39	17.53	7.4	2.11	4.47	0.29	91.2
G001984	0.45	17.03	6.06	1.47	4.87	0.24	88.6
G001981	0.45	14.1	5.59	1.17	3.73	0.21	73.3
G001980	0.44	15.17	5.51	1.29	3.67	0.23	78.9
G001995	0.52	16.41	9.35	1.34	6.36	0.14	85.3
G001997	0.52	16.13	7.79	1.3	6.18	0.17	83.9
G001996	0.52	18.87	10.32	1.24	4.54	0.12	98.1
G001991	0.88	24.53	12.55	0.94	11.13	0.07	127.6
G002610	0.24	26.4	n.d	n.d	n.d	nd	137.3
G002600	0.3	15.13	n.d	n.d	n.d	n.d	78.7
G002570	0.33	15.6	5.83	1.44	3.54	0.25	81.1
G002590	0.5	17.95	8.39	1.48	8.28	0.18	93.3
G002587	0.68	21.6	11.8	1.13	13.43	0.10	112.3
G002585	0.81	21.54	11.25	1.27	11	0.11	112.0
German Coals							
E22794-PA1	0.75	22.08	10.62	0.51	7.59	0.05	114.8
E36213	0.92	26.25	12.00	0.56	11.50	0.05	136.5
G001088	1.26	19.39	8.18	0.51	14.74	0.06	100.8
G001083	1.37	17.01	-	-	15.88		88.5
G001086	1.58	15.60	6.34	0.42	18.99	0.07	81.1
E36216	1.70	13.25	5.07	0.33	17.60	0.07	68.9
G001092	2.09	6.99	2.70	0.18	14.41	0.07	36.3
G001096	2.81	4.00	-	-	11.27		20.8

*The phenomenon of HI increase during maturation of Type III organic matter*

Concerning increasing bulk petroleum potential (HI) and decreasing Oxygen Indices (OI) with maturity (Fig. 5.6, 5.7), Vandenbroucke and Largeau (2007) claimed that during diagenesis, the loss of O-containing molecules (decreasing OI and O/C) results in a concentration of potential hydrocarbon generating structures, and hence an increase in HI (Fig. 5.6 and Fig. 5.7b) and consequently also total aliphatic groups (CH<sub>2</sub> + CH<sub>3</sub>) (Fig. 5.7a). Vu (2008) could show, by using an empirical equation for the calculation of pyrolysis yields based on elemental composition (H/C and O/C) implemented by Orr (1983), that simple oxygen loss can largely explain the increase in Hydrogen Index occurring within the New Zealand Coal Band up to vitrinite reflectances ~ 0.7% and thus, the latter has not to be tracked back to a rearrangement of the coal structure (see Schenk and Horsfield, 1998) which had been suggested by Sykes and Snowdon (2002) and Killops *et al.* (1998). In addition, the

observed constant GOR and gas wetness values for all maturity series samples in the first maturity range support the concentration concept, as rearrangement of the organic matter structure with a postulated re-incorporation of hydrogen-rich volatile components into the coal matrix leading to a higher oil-proneness of mature coals compared to immature coals (Boreham *et al.*, 1999; Sykes and Snowdon, 2002) would have to have a noticeably lowering effect on the GOR. Almost unchanged phenol contents of New Zealand coals and Wealden coals (Fig. 5.6) can be explained by the preferential loss of oxygen fixed within labile functional groups in carboxylic acid or ester, whereas more stable phenolic -OH groups are preserved throughout the according maturity range (Levine *et al.*, 1982; Levine, 1993). The relative increase in Hydrogen Index depends on oxygen abundance in the kerogen and therefore is high for Type III kerogen as seen for New Zealand Coals, in which at sub-bituminous coal ranks around ¼ of organic mass occurs as C, O, and H in oxygen functional groups (Levine *et al.*, 1982), and hardly visible for Types I and II like the Exshaw and Barnett shale samples, for which the beginning of petroleum generation already led to decreasing Hydrogen Index values Fig. 5.6.

#### *The connection between Oxygen-loss and decreasing Late Gas Potentials*

With respect to high temperature methane generation, it is quite interesting to observe that the most pronounced oxygen loss, presumably in the form of H<sub>2</sub>O and CO<sub>2</sub> by dehydrogenation- and decarboxylation-reactions (Boudou *et al.*, 1984; Tissot and Welte, 1984; Boudou *et al.*, 1994), leads to an increase in normal hydrocarbon potential (HI) by concentration of petroleum forming precursor structures but also to a significant early loss of late gas potential (Fig. 5.6). This observation firstly points to the different nature of precursor structures of conventional petroleum and late secondary gas (B) and secondly is in contrast to previous assumptions that loss of heterocompounds during early maturation results in a stabilisation of organic matter via cross-linking or recombination reactions of first formed bitumen and residual kerogen leading to an enhancement of the late gas potential (Dieckmann *et al.*, 2006; Erdmann and Horsfield, 2006).

More likely, late gas precursor structures, presumably methyl groups yielding methane upon high temperature closed-system pyrolysis, are lost together with the most unstable O-bearing functional groups, which is directly confirmed by a strong decrease of methyl groups over total aliphatic groups ( $\text{CH}_3/(\text{CH}_3+\text{CH}_2)$ ) (Fig. 5.7a) in the respective maturity range up to  $R_o \sim 0.6\%$ . This illustrates the disadvantage of using immature samples when evaluating the late gas generating potential of source rocks. In this context, e.g. Glombitza *et al.* (2009)

report for immature New Zealand coals by applying alkaline ester cleavage experiments that concentrations of liberated low molecular weight compounds such as acetate, which possesses a methyl group within its chemical structure, considerably decrease during early catagenesis up to maturity levels of about 0.6%  $R_o$ , thus indicating a continuous loss of kerogen-linked small organic acids during maturation of organic matter, whether by release from or incorporation into the residual kerogen.

*The effect of bitumen on the Late Gas Potential*

Differences between extracted and unextracted New Zealand Coal samples are basically restricted to lower HI's and higher GOR's of extracted compared to non-extracted samples and additionally to a somewhat higher aromaticity (Fig. 5.6). New Zealand coals show high extraction yields of bitumen enriched in heavy ends, asphaltenes and resins (NSO's)(Vu, 2008), components which contribute considerably to the S2 yield related to their relative non-volatility for pyrolysis temperatures below 350°C (Orr, 1983; Wilhelms *et al.*, 1991). The loss of these  $C_{6+}$ -compounds during extraction explains lower Hydrogen Index values and higher GORs observed for extracted coals. Higher aromaticity of extracted samples can simply be related to the absence of the bitumen fraction as Vu (2008) showed that extracted coals exhibit clearly shorter chain length distributions of *n*-alkyl moieties ( $C_{1-5}$  total, *n*- $C_{6-14}$ , *n*- $C_{15+}$ ) in a ternary plot of Horsfield (1989), but more or less similar proportions of paraffins (*n*-octene), aromatics (*m,p*-xylenes), and phenolic compounds (phenol) in a ternary plot of Larter (1984) compared to original, non-extracted coals. The bitumen fraction in contrast is enriched in long chain *n*-alkane/alkene homologues causing, if absent, petroleum types to be shifted from a P-N-A-high wax (non-extracted coals) to a more gas and condensate dominated organofacies (extracted coals). These observations are in accordance with results published by Michels *et al.* (2000) and Behar *et al.* (2008) focussing on the role of NSO compounds (or polars) during maturation and cracking, confirming the model previously proposed by Tissot (1969) in which the main source of hydrocarbons is not the insoluble organic matter, but the NSO fraction. Michels *et al.* (2000) proposes that during the main stage of bitumen generation, a great part of the initial oil potential is transferred to the polars and Behar *et al.* (2008) postulate that kerogen and lignite first decompose into dichloromethane soluble NSO's with minor generation of hydrocarbons. Then, the main source of petroleum potential originates from secondary cracking of both DCM and *n*-pentane soluble NSO's through successive decomposition reactions.

Interestingly, secondary gas (B) yields (Fig. 5.6) are, with the exception of two immature samples, almost identical for extracted and unextracted New Zealand coals indicating that late gas precursor structures should be found within the insoluble kerogen and that they not have to be necessarily formed by secondary recombination reaction of bitumen and residual organic matter.

### ***Late Gas Potential increase during Catagenesis***

#### *General evolution of parameters (open-system pyrolysis and IR)*

In the second maturity range between 1 and 2%  $R_o$  a strong late gas potential increase can be observed for all investigated maturity series with the highest “jump” between 1 and 1.4%  $R_o$  (Fig. 5.6). The most striking increase from 0 to ~40 mg/g TOC can be reported for the Barnett Shale. Late gas potential increase is accompanied by strongly decreasing HI's and a strongly increasing aromaticity of all maturity series samples pyrolysates whereas phenol contents for Type III kerogens strongly decrease. Oxygen Index uniformly stays below 10 mg  $CO_2$ /g TOC for most maturity series with the exception of Exshaw Fm. samples. Here, high OI (> 20 mg  $CO_2$ /g TOC) can be explained by low TOC (< 2.5%) and raised carbonate contents (Peters, 1986; Cornford *et al.*, 1998) as more immature samples posses lower values and “organic  $CO_2$ ” precursor structures should be rather depleted by the reached maturity stages. For all maturity series a steady increase in GOR and decrease in gas wetness with maturity can be reported whereas the trend is much more pronounced for the German Coals. This contrasting pyrolytic behaviour of coals and Type II kerogens can be related to their respective basic structural units (Horsfield and Dueppenbecker, 1991) as coal is somewhat more heterogeneous than the marine shales and the respective chain length distribution stays relatively less fixed over the according maturity interval.

For the natural coal series the strong increase in late secondary (B) yields, paralleled by a decrease in HI values, and proceeding from high volatile bituminous coal ranks ( $R_o$  0.7 – 0.81%) to medium bituminous coal ranks ( $R_o$  = 1.26-1.37%) is accompanied by a simultaneous decrease in aliphatic carbon ( $CH_2 + CH_3$ )(Fig. 5.7). These changes can be explained by the generation of oil and gas or partly by the incorporation of aliphatic structures via aromatisation into the refractory residual organic matter under natural conditions. This chain shortening by  $\beta$ -cleavage (Horsfield and Schenk, 1995) results in lower  $C_{6+}$  alkyl chain and wet gas production from the residual coal structure and to an enrichment of methyl groups mirrored by increasing methane yields (increasing GOR's and decreasing gas wetness; see also Fig. 5.6). The gain of protonated aromatic carbon by continuing aromatisation of alicyclics and concentration of aromatic clusters due to the release of paraffinic oil gives rise

to labile aromatic moieties paralleled by increasing mono- and di-aromatic compound yields during open-system pyrolysis, whereas phenolic compounds decrease. Aromatisation of the macromolecular coal structure and concomitant methyl group enrichment seems to be an explanation for increasing late secondary gas (B) yields generated at high temperatures under artificial closed-system conditions. For medium to low volatile bituminous coal ranks ( $R_o = 1.26 - 2.09\%$ ) late secondary (B) yields stay about the same which is mirrored by a constant methyl group enrichment. The residual coal consists at this stage of a network of methylated and short chain alkylated polyaromatic nuclei linked together by alkyl bridges (Horsfield and Schenk, 1995). Extensive condensation of these aromatic rings causes a decrease in protonated aromatic carbon, mirrored in decreasing mono- and di-aromatic compounds yields, leading to  $\beta$ -cleavage (methyl group formation) and some  $\alpha$ -cleavage of aromatic ring-substituents. Thus, wet gases and methane are generated under natural conditions explaining still diminishing HI values and aliphatic carbon contents.

*Importance of methyl-group enrichment for the Late Gas Potential Increase*

The decrease in gas wetness (Fig. 5.6) points to the growing importance of methane over wet gas precursors with maturity for all investigated maturity series samples and different kerogen types in general. As indicated above, chain shortening reactions via  $\beta$ -cleavage, whatever the size of the alkyl chain, lead to the concomitant enrichment and formation of methyl-groups during petroleum generation (Freund and Olmstead, 1989; Smith and Savage, 1992; Savage, 2000) which is evidenced by progressively lower petroleum potentials (HI values) (Fig. 5.6). NMR experiments performed by Kelemen *et al.* (2002; 2007) illustrated that the average aliphatic carbon chain length decreases with increasing maturity approaching values of 1.0 (methyl-groups) for kerogens and coals with the highest levels of aromatic carbon. This indicates firstly, that almost all aliphatic carbon exists as methyl groups (acting as late gas precursor structures) for kerogens that have passed through the oil window and secondly, that aromatic carbon is concentrated if not neoformed in residual organic matter. The latter is indirectly confirmed by the present data, i.e. strongly increasing aromaticity of open-system pyrolysates with maturity (Fig. 5.6) can be observed for all maturity series samples. Again Kelemen *et al.* (2002, 2007) showed that, independent of organic matter type and initial aromatic carbon content, aromatic carbon increases linearly with decreasing hydrogen content during thermal maturation leading to a similar aromatic carbon content of ~80% for all types of naturally matured organic matter prior to metagenesis stage. This evolution is paralleled by an average ring size increase of aromatic core structures from 2 (10 aromatic carbon per

cluster) to 5 (20 aromatic carbon per cluster) with maturity for all kerogen types. These structural changes can occur through the selective loss of smaller aromatic ring sizes or by aromatization of adjacent aliphatic carbon structures during kerogen maturation (Kelemen *et al.*, 2007). As phenolic compounds are to a large extent not released into migrating petroleum during natural maturation but retained within the kerogen structure or undergo condensation reactions (Horsfield, 1997), it can be deduced that they also add to the discussed aromatic carbon pool. Depletion of phenols within pyrolysates of Wealden and Carboniferous coals up to maturity levels of  $\sim 1.5\%$   $R_o$  (Fig. 5.6) hint to the importance of this process for terrigenous derived organic matter. Nevertheless, for the late gas potential “jump” itself, the retention of phenolic precursor structures seems not to be an overall prerequisite as Exshaw Formation and Barnett Shale samples, being deposited in anoxic marine environments, are depleted in phenolic moieties. The observed late gas potential increase with maturity for the investigated and perhaps any kerogen types up to  $\sim 40$  mg/g TOC is thus more likely related to the concentration and formation via  $\beta$ -cleavage of thermally stable precursor structures, i.e. refractory kerogen in the form of methyl-aromatics, within the residual organic matter in the course of petroleum generation within the catagenesis zone. Behar and Vandenbroucke (1987) state that at the end of catagenesis kerogen has lost a large part of its hydrogen related to petroleum formation, averagely two H atoms are lost for one C atom, and has undergone aromatization and some structural rearrangement. Therefore, H/C atomic ratios of residual organic matter decrease to values about  $\sim 0.5$ , reflecting increasing aromatization. Concomitant loss of CO, CO<sub>2</sub> and H<sub>2</sub>O as well as NSO compounds within the oil fraction during petroleum formation leads to similar elemental compositions and hence a similar location in the van Krevelen diagram for all residual kerogens at the end of the catagenesis zone. This indicates a similar ratio of aliphatic to aromatic C for every naturally matured kerogen prior to metagenesis and helps to explain the observed similarity in  $\sim 40$  mg/g TOC secondary gas (B) potential for high temperature closed-system pyrolysis conditions, more or less confirming previously findings of Behar *et al.* (1997) who calculated similar potentials of around 50 mg/g TOC.

#### *Carbon loss during Catagenesis and its impact on the Late Gas Potential*

The amount of late gas generated from mature source rocks is strongly coupled to its TOC content which in return is related to initial TOC content and carbon loss during catagenesis. The latter is mainly influenced by the chemical structure of the organic matter type (Behar and Vandenbroucke, 1987). Like coal, low maturity kerogen can be considered as a plastic



substance, with aromatic stacks suspended in a metaplast made of mobile aliphatic units. The latter are progressively removed by thermal cracking upon catagenesis, up to the transition to metagenesis where a brittle solid is obtained (Oberlin *et al.*, 1980). Thermal maturation of homogeneous Type I kerogens leads to the genesis of a great amount of paraffinic oil and gas by the breaking of carbon-carbon bonds during catagenesis, resulting in the loss of about 79% carbon by weight. In contrast, for Type III kerogens, although the production of minor amounts of paraffinic oil can lead to the loss of 15 – 35% carbon, the main fraction of the carbon remains in the residual kerogen as polyaromatic domains. This is attributed to the high condensation of aromatic nuclei which inhibits their solution in the oil phase leading to retention within the residue. For Type II kerogens lower condensation of aromatic nuclei allows naphthenoaromatic compounds to be soluble in the oil phase causing a relatively high oil potential with up to 60% carbon loss after expulsion. Thus it can be said in general, that all kerogen types are chemically very similar after the catagenesis stage as reflected by their position in the Van Krevelen diagram and by their similar late gas potential.

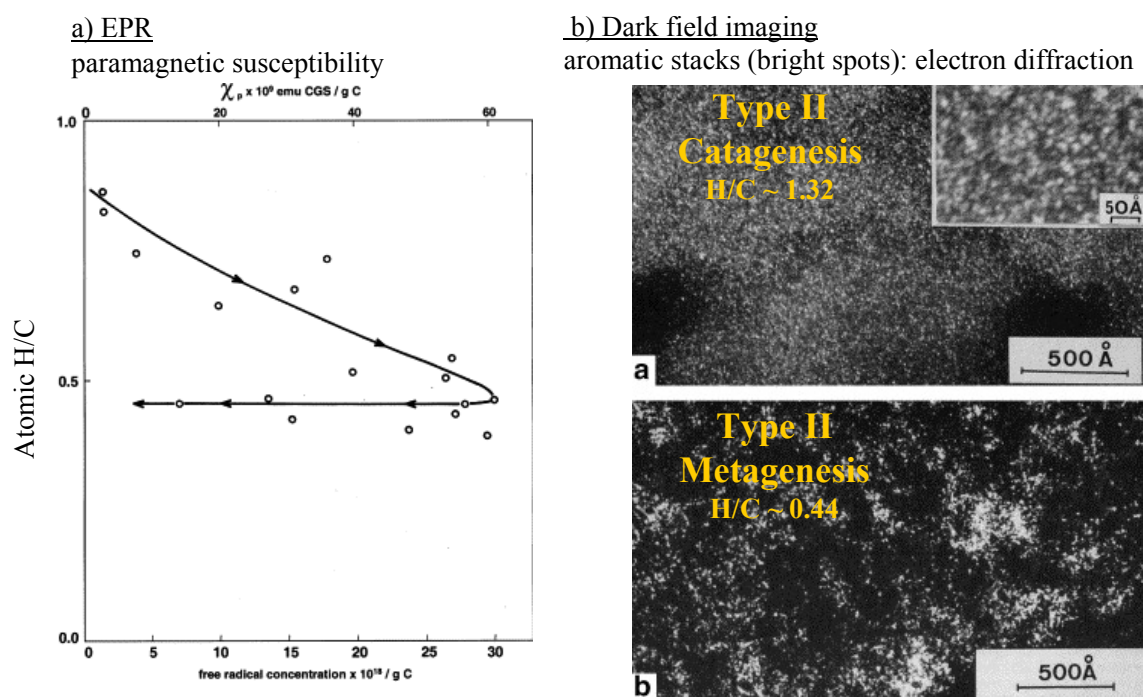
Nevertheless, the difference in carbon loss during catagenesis also induces a difference in the residual organic matter structure marked by a difference in size of aromatic clusters in the solid residue: ~50 Å for Type III, 100–200 Å for Type II and up to 1000 Å for Type I (Oberlin *et al.*, 1980). The extent of parallel formation or reorientation of aromatic stacks depends on the elimination efficiency of low molecular weight moieties during catagenesis allowing individual aromatic stacks a more or less free rotation. For Type I kerogens, expulsion of the greatest part of the labile organic matter allows the small number of polyaromatic nuclei, which is left, to undergo reorientation to a large extent resulting in a graphite-like structure formed of quasi parallel layers of aromatic condensed rings (Behar and Vandenbroucke, 1987). Residual polyaromatic structures within Type II kerogen also undergo reorganisation, but to a lesser extent than in Type I kerogen. For Type III, reorientation is very limited, as only few carbon structures are eliminated. This leads to the formation of a microporous solid in which the hydrocarbons formed during catagenesis are partly trapped and cannot be expelled until they are further cracked into gas (Oberlin *et al.*, 1980; Behar and Vandenbroucke, 1987).

### ***Late Gas Potential loss during Metagenesis***

#### *General evolution of parameters (open-system pyrolysis and IR)*

At vitrinite reflectances above 2%, late gas potential loss, presumably related to natural late gas generation, is accompanied by rather small changes in open-system pyrolysis parameters as the labile kerogen fraction is more or less already eliminated. Metagenesis is rather the

stage of reorganization of the aromatic network of the residual kerogen associated with an aromaticity increase, mainly by elimination of aromatic  $\text{CH}_3$  groups as  $\text{CH}_4$ , but also by release of hetero elements as  $\text{CO}_2$ ,  $\text{N}_2$  and  $\text{H}_2\text{S}$  (Vandenbroucke and Largeau, 2007). Thus, in Fig. 5.6, HI, OI and gas wetness further decreases to even smaller values whereas aromaticity and GOR slightly increase for samples of all maturity series. Phenol contents stay generally low for all source rocks as phenolic moieties are already depleted at such high thermally induced natural stress.



Marchand and Conard; 1980

**Figure 5.8: Aromatic ring condensation during metagenesis stage as evidenced by a) EPR and b) dark field imaging. Pictures are taken from Marchand and Conard (1980) and Oberlin *et al.* (1980).**

#### *Condensation reactions as driving force for late gas generation*

Falling protonated aromatic carbon contents for German Coals (Fig. 5.7a) can be explained by an extensive condensation of aromatic rings leading to decreasing labile mono- and di-aromatic moieties. Oberlin *et al.* (1980), using dark field imaging, directly observed an increase of ring condensation in the residual kerogen by an increasing diameter of aromatic stacks (Fig. 5.8b). This is also confirmed by electron paramagnetic resonance spectroscopy (Fig. 5.8a) with which the concentration of free radicals can be measured. The number of free radicals in kerogen increases during catagenesis due to radical formation related to bond breaking in the course of petroleum generation and then begins to decrease during metagenesis due to radical re-condensation triggered by condensation of aromatic ring

systems (Durand *et al.*, 1977a; Marchand and Conard, 1980; Horsfield, 1984). According to Horsfield and Schenk (1995), these condensation reactions “free” hydrogen which then could enter into gas forming reactions leading to  $\alpha$ -cleavage of methyl groups to form methane. The responsible demethylation pathway, in essence, involves a substitution reaction in which the methyl group of the alkyl-aromatic moiety is replaced by a hydrogen atom from a donor species (Smith and Savage, 1991), whether by hydrogen atom *ipso*-substitution (Vernon, 1980), molecular disproportionation (Billmers *et al.*, 1986), or radical hydrogen transfer (McMillen *et al.*, 1987; Malhotra and McMillen, 1990). Methane generation by  $\alpha$ -cleavage would be additionally facilitated by the gain in mesomeric energy as the aromatic system grew larger, as confirmed by pyrolysis experiments on authentic standards (Smith and Savage, 1991). Demethylation of methyl aromatics together with cleavage of aromatic ether bridges, yielding gases such as CH<sub>4</sub>, CO and CO<sub>2</sub>, and also some N<sub>2</sub> is also the advocated methane formation pathway at the metagenesis stage described in publications of Lorant and Behar (2002) and Behar *et al.* (2000).

*Accordance of late gas generation kinetics and late gas potential loss*

Thus, the decrease in late gas potential at maturity stages  $R_o > 2\%$  observed for the Barnett Shale and German Coals can be ascribed to the final demethylation of residual organic matter by  $\alpha$ -cleavage related to condensation reactions leading to dry gas production under natural conditions. The onset of natural late secondary gas (B) generation consequently seems to kick in for maturity levels in excess of  $R_o \sim 2\%$  confirming the kinetic predictions of Erdmann and Horsfield (2006), and the kinetic predictions based on an immature Åre Fm. sample presented earlier in this thesis (Chapter 4.1.5). For the latter case, the onset of high temperature methane generation can be expected for a calculated  $R_o$  of  $\sim 2.5\%$  with a geologic  $T_{max}$  at about  $3.1\%$ , which is more or less the trend observed for the most mature German Coal ( $R_o \sim 2.81\%$ ) and Barnett Shale ( $R_o \sim 3.21\%$ ) samples (Tab. 5-1, Fig. 5.6). Both samples produce lower secondary gas (B) amounts than at  $\sim 2\%$   $R_o$  but still possess a potential of more than 20 mg/g TOC.

## 5.2 Artificial Maturation: Simulating organic matter evolution

Table 5-3: Evolution of organic matter artificially matured under open- or closed-system conditions – Open pyrolysis of residues: Normalised single compound yields as input parameters for ternary diagrams of Horsfield (1989) and Larter (1984) as well as routinely used ratios such as GOR, Gas Wetness and Aromaticity.

Method	GFZ Code	Residue Temp.	GOR	Gas Wetness	Horsfield (1989)			Larter (1984)			Aromaticity
					Chain length distr.			Terrestrial Input			
		Total C <sub>1-C5</sub>	<i>n</i> -C <sub>6-14</sub>	<i>n</i> -C <sub>15+</sub>	<i>n</i> -C <sub>8:1</sub>	<i>m,p</i> -Xylene	Phenol	kg/kg			
		°C	kg/kg	kg/kg	Normalised Yields			Normalised Yields			
closed system (MSSV)	Åre Fm. G001965	original	0.44	0.58	85.03	9.41	5.56	6.85	28.54	64.61	0.51
		300	0.40	0.57	83.74	10.23	6.03	6.16	27.45	66.39	0.52
		350	0.45	0.55	84.18	10.02	5.80	6.46	26.85	66.69	0.51
		400	0.67	0.50	87.41	8.42	4.17	9.96	36.06	53.98	0.49
		450	0.93	0.33	94.64	2.75	2.61	2.43	36.85	60.72	0.65
		500	0.56	0.26	92.81	4.48	2.71	0.68	36.24	63.08	0.80
		550	0.20	0.46	97.46	2.54	0.00	0.27	53.30	46.43	0.97
	Mix I/III	original	0.28	0.69	61.20	22.60	16.20	30.91	36.52	32.57	0.24
		350	0.25	0.67	60.04	21.74	18.23	31.67	32.55	35.79	0.21
		400	0.36	0.63	65.92	20.53	13.55	43.88	34.55	21.57	0.20
		450	0.66	0.40	89.32	4.89	5.79	14.75	57.01	28.24	0.42
		500	0.59	0.25	95.26	2.54	2.20	1.25	54.53	44.23	0.75
	GRS G004750	original	0.15	0.86	41.58	32.00	26.42	63.67	35.42	0.91	0.09
		350	0.15	0.86	42.16	32.10	25.75	68.61	30.43	0.95	0.08
		400	0.18	0.84	43.75	31.78	24.47	77.72	21.68	0.60	0.07
		450	0.28	0.57	72.49	15.68	11.83	62.41	37.36	0.23	0.16
		500	0.47	0.40	97.90	2.10	0.00	13.72	86.28	0.00	0.84
	Spekk Fm. G001955	original	0.24	0.76	73.41	19.57	7.03	37.56	59.55	2.89	0.26
		350	0.28	0.75	73.47	19.54	6.99	44.63	53.14	2.23	0.23
		400	0.41	0.70	74.52	19.13	6.35	54.30	42.69	3.00	0.21
		450	1.21	0.42	93.22	3.17	3.61	18.89	80.93	0.18	0.43
		500	0.92	0.30	98.26	1.74	0.00	3.22	96.78	0.00	0.81
	Westph. Coal G000271	original	0.47	0.53	83.05	11.64	5.31	10.85	39.03	50.12	0.45
		400	0.47	0.50	84.76	10.45	4.79	11.43	39.75	48.81	0.46
		450	0.62	0.34	94.56	3.78	1.66	3.29	43.48	53.23	0.63
		500	0.78	0.17	98.96	0.80	0.24	0.11	40.72	59.16	0.88
open system (SRA)	Åre Fm. G001965	original	0.44	0.58	85.03	9.41	5.56	6.85	28.54	64.61	0.51
		400	1.36	0.47	92.03	7.29	0.68	7.20	34.00	58.80	0.65
		450	3.36	0.31	99.29	0.71	0.00	2.03	50.14	47.83	0.90
		500	3.33	0.13	100.00	0.00	0.00	0.00	100.00	0.00	1.00
	Westph. Coal G000271	original	0.47	0.53	83.05	11.64	5.31	10.85	39.03	50.12	0.45
		400	0.58	0.50	85.75	10.44	3.82	11.54	42.39	46.07	0.48
		450	1.38	0.38	94.80	4.47	0.73	4.69	46.57	48.74	0.66
		500	5.18	0.17	99.54	0.28	0.18	0.24	47.86	51.90	0.89

Pyrolysis residues were prepared by applying non-isothermal open- and closed-system pyrolysis in order to simulate natural maturation and to investigate if secondary reactions between first formed primary products and residual kerogen play a key role for the development of a late gas potential of source rocks during artificial maturation. Interestingly,

the latter seems not to be the case, as late gas generative properties of residues prepared under open-system conditions from Type III Westphalian Coal sample G000721 and Åre Fm. sample G001965 exhibit the same evolution as late gas generative properties of the respective residues prepared under closed-system conditions even though primary products are transported out of the hot reaction zone and cannot act as an additional source of late methane formation. Furthermore, increasing late gas potentials with increasing artificial maturity can be observed for residues of the Type II Spekk Fm. sample G001955, the Type I Green River Shale sample G004750 and the synthetic Mix type I/III sample G0047501965 prepared under closed-system conditions. This indicates that not only terrigenous derived organic matter but also other kinds of organic matter form at least small amounts of methane at high maturities, which confirms observations on the Barnett Shale natural maturity series discussed in Chapter 5.1. Preparative details are given in the methodology Sub-Chapter 2.2.3.

Most open- and closed-system residues were further analysed by open-system pyrolysis to gain information on structural changes within the residual macromolecular organic matter, and by the closed-system MSSV-pyrolysis based late gas potential screening method approach (two end temperatures) to investigate the impact of those structural changes on the high temperature methane generation. The results are discussed in the following.

### **5.2.1 Detailed Kerogen Composition of the Residues (Open Py)**

As stated before, pyrolysis-GC provides detailed insights into kerogen structure and has been employed to study the composition of the remaining organic matter after artificial maturation under open and closed-system pyrolysis conditions. Results such as the chain length distribution and phenol content are displayed in the ternary diagrams of Horsfield (1989) and Larter (1984) (Fig. 5.9 and Fig. 5.11), normalised yields of single compounds of the latter as well as GOR, gas wetness, and aromaticity are given in Tab. 5-3 and Fig. 5.10 and 5.12.

#### ***Closed-System Maturation***

Closed-system residues were prepared for the Åre Fm. sample G001965, the Spekk Fm. sample G001955, the Green River Shale sample G004750, and the synthetic Mix Type I/III sample G0047501965. The most immature ( $R_o = 0.99\%$ ) Westphalian Coal sample G000721 was also chosen for preparative pyrolysis to compare results of artificial maturation experiments directly to the evolution of a natural maturity sequence. The pyrolysate composition of all original, not artificially matured samples was already discussed in previous chapters, but is again indicated in Fig. 5.9 and Tab. 5-3. For the Åre Fm. sample G001965

residues were prepared exhibiting maturation stages of 300, 350, 400, 450, 500, and 550°C, for the Spekk Fm. sample G001955, the Green River Shale sample G004750, and the synthetic Mix Type I/III sample G0047501965 residues were prepared exhibiting maturation stages of 350, 400, 450, and 500°C. Three residues are available for the Westphalian Coal sample G000721, which experienced temperatures up to 400, 450, and 500°C.

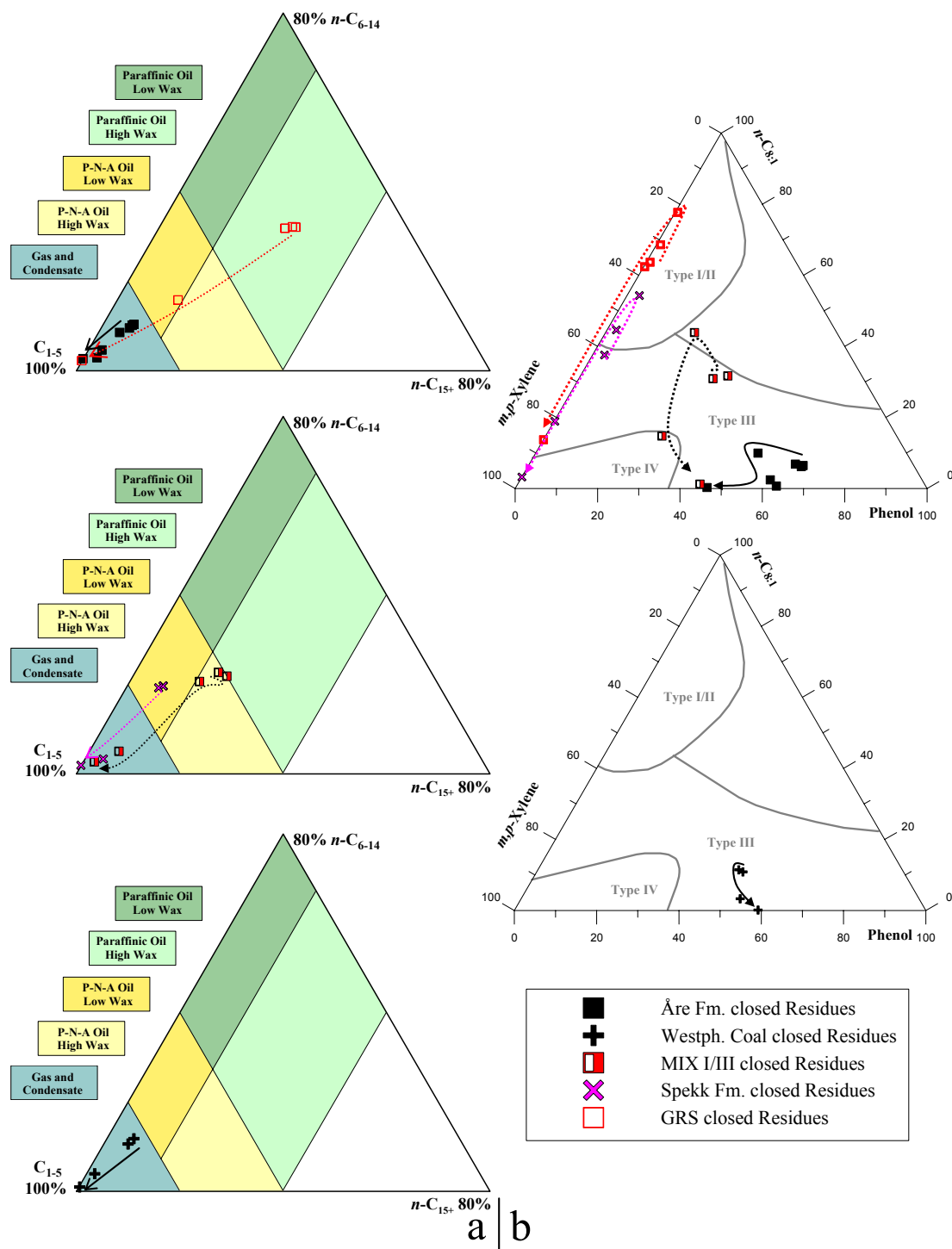
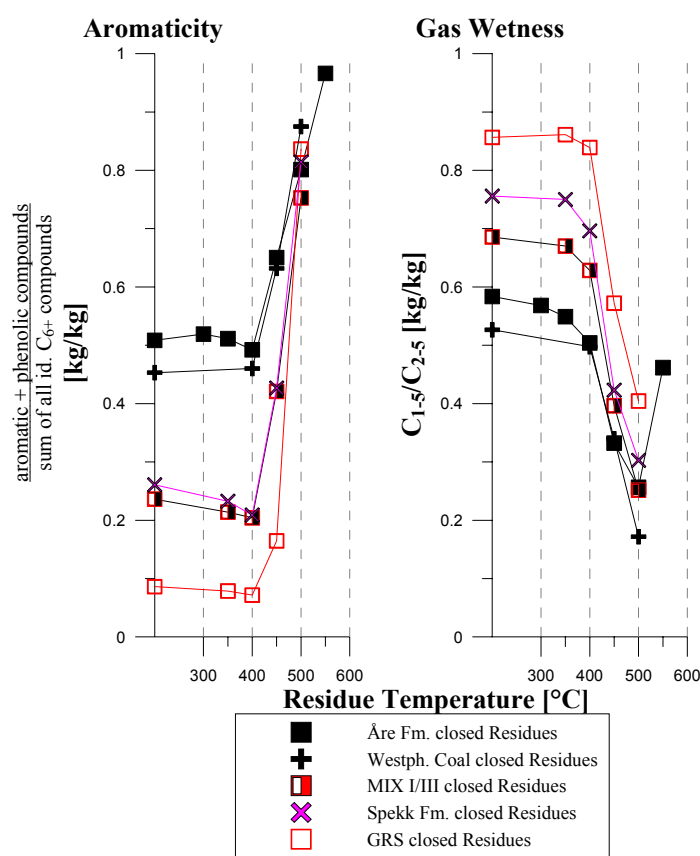


Figure 5.9: Evolution of the residue composition during closed-system artificial maturation displayed in ternary diagrams of a) Horsfield (1989) and b) Larter (1984). Arrows indicate the evolution pathway.

In the ternary diagrams of Horsfield (1989) and Larter (1984)(Fig. 5.9) it can be seen that artificial maturation of all immature source rocks under closed-system conditions causes changes within the remaining organic matter which generally resemble the natural maturation trends. By the removal of both long and short alkyl-chains during the breakdown of labile parts of the kerogen, pyrolysate compositions are progressively shifted to the lower left gas and higher aromaticity corner where source rocks mainly yield low molecular weight components and mono aromatic compounds. This is also reflected by a strong increase in aromaticity and decrease in gas wetness of the residues with increasing maturity as displayed in Fig. 5.10. Nevertheless, compositional changes in the residue structure are relatively subtle for artificial maturation stages below 450°C (Fig. 5.9 and Fig. 5.10) and only become obvious at higher temperature stages indicating the depletion of aliphatic C<sub>6+</sub> precursor material and a relative increase of methylated and alkylated aromatic ring systems.



**Figure 5.10: Evolution of the residue composition during closed-system artificial maturation as defined by Aromaticity and Gas Wetness (Open-Pyrolysis)**

Interestingly, it can be seen in Fig. 5.9b that in residues of the Type III Westphalian Coal sample G000721 and Åre Fm. sample G001965, which exhibit the highest artificial maturation levels, precursor structures yielding phenolic compounds upon open pyrolysis are

still present. This is in contrast to the natural maturation trends observed for the German Coal series (German Coals:  $R_o$  0.99% to 2.81%) for which phenol compounds progressively decrease and vanish at 1.58%  $R_o$  (Fig. 3.7a; Tab. 3-2). Nevertheless, similar positions of pyrolysates in the ternary diagram of Horsfield (1989)(Fig. 5.9a) of natural matured coal sample G001086 ( $R_o$  = 1.58%) and the Westphalian Coal residue artificially matured to 500°C suggest similar maturation levels or organic matter structure. One conclusion could be that during artificial maturation not all chemical reactions occurring under natural conditions can be simulated, an observation previously made by Schenk and Horsfield (1998) who reported that generation rate curves of more mature coals step out of the generation rate curve envelope defined by less mature coals. This natural stabilisation of the organic matter structure, attributed to solid state aromatisation reactions which compete with product generation during natural coalification, could not be simulated using both, open- or closed-system maturation methods (pyrolysis) on the lowest rank sample, a possible reason being the presence of structural moieties that yield phenolic compounds upon pyrolysis.

### ***Open-System Maturation***

Open-system residues were prepared for the Åre Fm. sample G001965 and the Westphalian Coal sample G000721 for the maturation stages 400, 450, and 500°C with a heating rate of 1°C/min and a start temperature 250°C using the Source Rock Analyser SRA (Humble).

Open pyrolysis results of open-system residues are shown together with those of closed-system residues in the ternary diagrams of Horsfield (1989) and Larter (1984) in Fig. 5.11. The general trend of product composition is similar for both artificial maturation methods whereas differences can be easily recognised. The extent of difference also differs for the two coal series because the shapes of arrows which indicate the molecular evolution pathway of the residues are more comparable for the open and closed Westphalian Coal series than for the open and closed Åre Fm. series. This can be best seen in Fig. 5.12b where values of aromaticity as well as gas wetness are almost identical for residues of the Westphalian Coal sample G000721 at similar maturation stages, with open-system residues showing only a slightly elevated aromaticity. The chemical structure of the remaining organic matter is therefore closely related with only phenolic moieties being relatively depleted in open-system residues compared to closed-system residues (Fig. 5.11a). This relative depletion is much more pronounced in residues of the Åre Fm. coal sample G001965, for which the open-system residue artificially matured to 500°C plots in the lowermost left corner of the ternary diagram of Larter (1984) (Fig. 5.11b) and the open-system residue artificially matured to



450°C is compositionally rather comparable to the closed-system residue artificially matured to 500°C. This “quicker” increase in maturation can also be noticed in the ternary diagram of Horsfield (1989) (Fig. 5.11a) and in Fig. 5.12a, where the aromaticity of open-system residues increases much faster than the aromaticity of closed-system residues and the gas wetness of open-system residues decreases much faster than the gas wetness of closed-system residues.

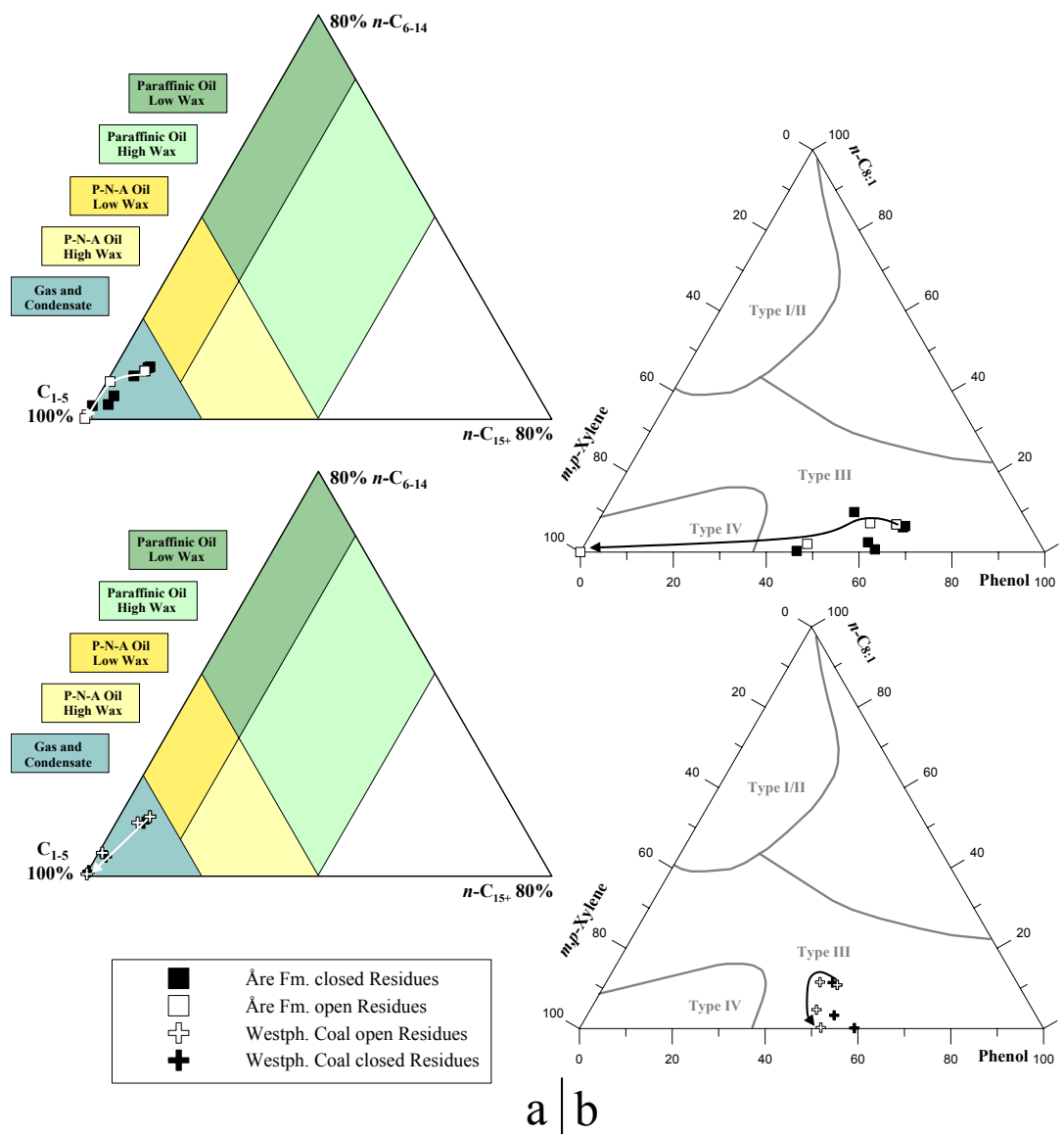


**Figure 5.11: Evolution of the residue composition during open- vs. closed-system artificial maturation displayed in ternary diagrams of a) Horsfield (1989) and b) Larter (1984). Arrows indicate the evolution pathway.**

The discrepancy between relative amounts of products generated from artificially prepared closed- or open-system residues of the Åre Fm. Coal sample G001965 versus the Westphalian Coal sample G000721 might be caused by the difference in maturity of the parent organic matter and therefore by the difference in organic matter structure. The original

Åre Fm. sample G001965 can be classified, according to its  $T_{\max}$  of  $415^{\circ}\text{C}$ , as a lignite to sub-bituminous coal (Sykes and Snowdon, 2002) and still possesses much more labile compounds in the form of e.g. oxygen containing functional groups ( $\text{OI} = 87 \text{ mg CO}_2/\text{g TOC}$ ) than the Westphalian Coal sample G000721 ( $\text{OI} = 6 \text{ mg CO}_2/\text{g TOC}$ ), which can be classified as an high volatile bituminous coal ( $R_o = 0.99\%$ ) that has lost its most labile parts and might exhibit a more stabilised and rearranged (by aromatisation and cross-linking) kerogen structure (Killops *et al.*, 1998; Schenk and Horsfield, 1998; Sykes and Snowdon, 2002). Upon open-system maturation using an SRA, aliphatic  $\text{C}_{6+}$  compounds loosely linked by functional groups to the macromolecular part of the coal (Given, 1984; Levine, 1993) might be swept away by the carrier gas in contrast to closed-system maturation using MSSV-tubes. The chemical composition of the less mature Åre Fm. residues is more strongly influenced by this process than the chemical composition of the more mature Westphalian coal sample residues, which is also indirectly confirmed by a much lower hydrocarbon rest potentials ( $\text{C}_{1+}$  yields) of open-system residues vs. closed-system residues of residues prepared from the Åre Fm. sample compared to residues prepared from the Westphalian Coal (Fig. 5.12).

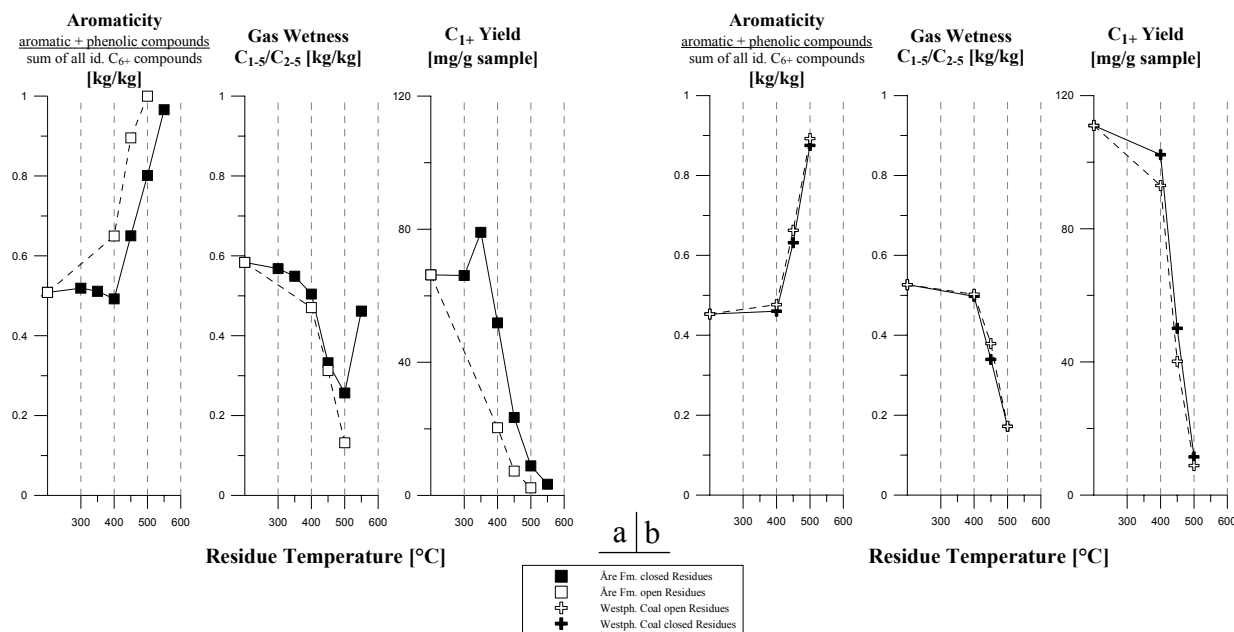


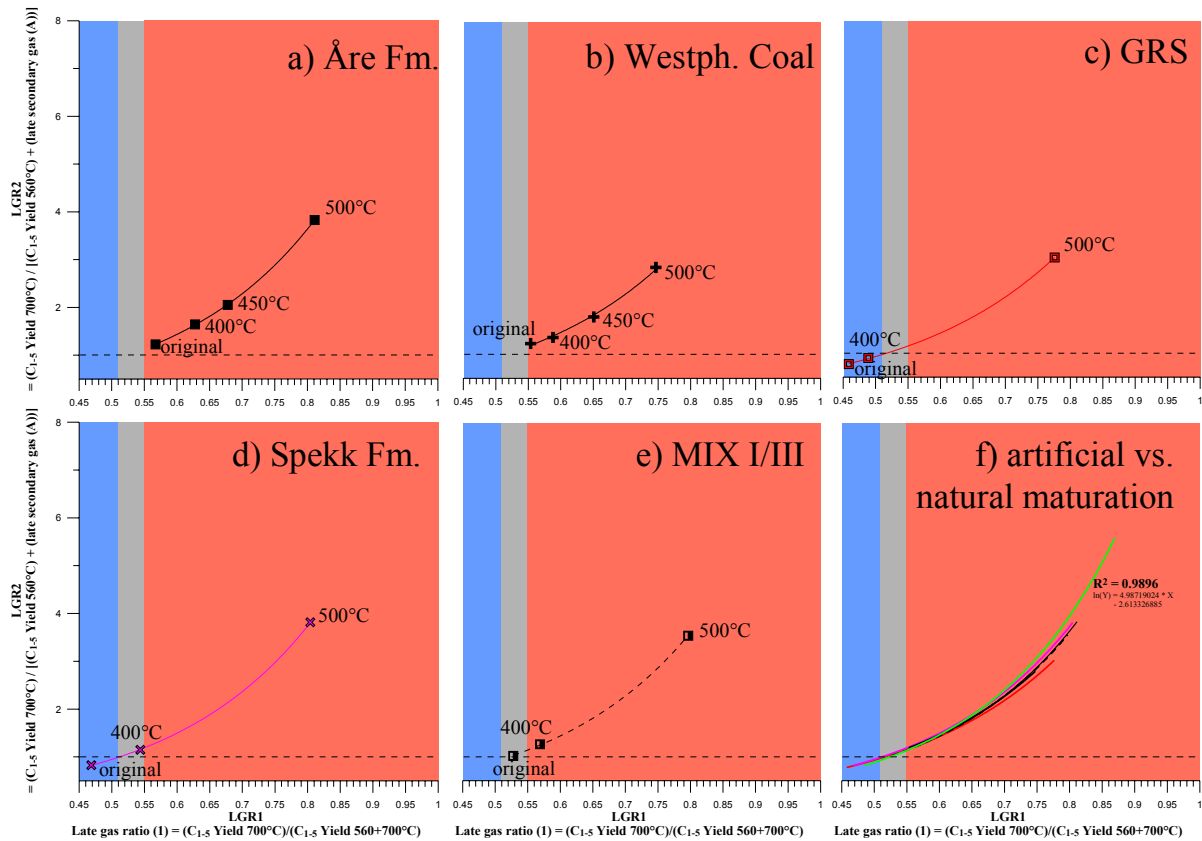
**Figure 5.12:** Evolution of open pyrolysis yields and composition of the residues during open- vs. closed-system artificial maturation as defined by Aromaticity and Gas Wetness (Open-Pyrolysis) for a) Åre Fm. sample G001965 and b) Westphalian Coal sample G000721.

### 5.2.2 Late Gas Generation Behaviour of the Residues (MSSV Py-GC)

MSSV C<sub>1-5</sub> gas and C<sub>6+</sub> compound yields at the 2 MSSV-screening temperatures as well as the two late gas ratios and calculated yields of late gas, secondary gas (A) and secondary gas (B) are provided in Tab. 5-4 for residues matured under closed- and open-system pyrolysis conditions.

**Table 5-4: Calculated late gas, secondary gas (A), and secondary gas (B) yields as well as LGR1 and LGR2 ratios for residues artificially prepared under open- or closed-system conditions based on products generated between MSSV end temperatures 560°C and 700°C.**

Method	GFZ Code	Residue Temp. °C	MSSV C <sub>1-5</sub> 560°C mg/g sample	MSSV C <sub>1-5</sub> 700°C mg/g sample	Late Gas	LGR1 kg/kg	MSSV C <sub>6+</sub> 560°C mg/g sample	MSSV C <sub>6+</sub> 700°C mg/g sample	MSSV C <sub>1-5</sub> sec. Gas (A) kg/kg	LGR2 kg/kg	MSSV C <sub>1-5</sub> sec. Gas (B) mg/g sample
closed system (MSSV)	Åre Fm. G001965	original	38.74	50.74	12.00	0.57	9.48	0.53	2.69	1.22	9.31
		400	29.57	49.84	20.27	0.63	3.73	1.29	0.73	1.64	19.54
		450	18.20	38.27	20.08	0.68	2.91	1.43	0.45	2.05	19.63
		500	8.23	35.29	27.07	0.81	3.61	0.31	0.99	3.83	26.08
		550	0.20	24.70	24.50	0.99	4.82	0.24	1.37	15.75	23.13
	Mix I/III	original	47.70	53.29	5.59	0.53	15.91	1.01	4.47	1.02	1.12
		400	32.59	43.01	10.42	0.57	6.77	2.06	1.41	1.26	9.00
	GRS G004750	500	4.49	17.56	13.08	0.80	1.79	0.23	0.47	3.54	12.61
		original	53.11	45.01	-8.10	0.46	20.21	3.31	5.07	0.77	-13.18
		400	46.28	44.26	-2.03	0.49	14.14	4.65	2.85	0.90	-4.88
	Spekk Fm. G001955	500	1.00	3.46	2.46	0.78	0.55	0.06	0.15	3.02	2.31
		original	14.07	12.41	-1.67	0.47	3.34	0.21	0.94	0.83	-2.61
		400	8.24	9.82	1.58	0.54	1.51	0.47	0.31	1.15	1.27
open system (SRA)	Westph. Coal G000271	500	0.89	3.66	2.77	0.80	0.31	0.09	0.07	3.82	2.70
		original	72.60	90.06	17.46	0.55	20.52	18.56	0.59	1.23	16.87
		400	58.06	82.88	24.82	0.59	11.90	2.06	2.95	1.36	21.87
		450	34.75	64.77	30.02	0.65	5.94	1.17	1.43	1.79	28.59
		500	16.24	47.81	31.57	0.75	2.80	0.65	0.64	2.83	30.92
	Åre Fm. G001965	original	38.74	50.74	12.00	0.57	9.48	0.53	2.69	1.22	9.31
		400	30.58	51.96	21.38	0.63	3.36	2.73	0.19	1.69	21.19
		450	18.96	45.56	26.60	0.71	2.27	1.34	0.28	2.37	26.32
	Westph. Coal G000271	500	11.35	36.65	25.30	0.76	1.68	1.68	0.00	3.23	25.30
		original	72.60	90.06	17.46	0.55	20.52	18.56	0.59	1.23	16.87
		400	53.88	82.88	29.00	0.61	10.24	2.62	2.29	1.48	26.72
		450	34.93	61.99	27.06	0.64	3.37	0.36	0.90	1.73	26.16
		500	17.13	47.83	30.71	0.74	0.99	0.32	0.20	2.76	30.51

*Closed-System Maturation*

**Figure 5.13: Late Gas Potentials Classification using MSSV-pyrolysis based LGR1 and LGR2 for closed-system artificially prepared residues of a) Åre Fm sample G001965, b) Westphalian Coal sample G000721, c) Green River Shale sample G004750, d) Spekk Fm sample G001955, and e) the synthetic Type I/III source rock mixture; in f) exponential functions describing the positions of residues in the LGR1 – LGR2 plot are compared to the exponential function describing the position of all investigated natural maturity series samples.**

The position of the samples matured under closed-system conditions within the late gas potential ratios plot is displayed in Fig. 5.13. Increasing LGR1 values signify that more and more late gas is generated with artificial maturity for all kerogen types. Additionally, LGR2-ratios exceed the value 1 for all samples at highest maturity levels, which means that the late gas generated between 560°C and 700°C has to be assigned to late secondary gas (B) production even in the case of the initially very homogeneous Type I Green River Shale (Fig. 5.13c). This result had not been expected, as homogeneous Type I source rocks were earlier classified as possessing only low late gas potentials and not thought to produce a bitumen intermediate capable of forming a thermally stabilised neobitumen. The location of all original samples and their respective residues within the LGR1 – LGR2 plot can be again described by exponential functions (Fig. 5.13a-e), which are compared in Fig. 5.13f to the unique exponential function applied to describe positions of naturally matured samples (see also Fig. 5.2). Interestingly, the natural trend is very well simulated by the artificial

maturation of immature organic matter under closed-system conditions. Artificial trends only show some divergence at the “high temperature end“, which implies that not all reactions occurring under natural conditions, for instance aromatisation reactions, can be reproduced in the lab. Nevertheless, the increase of late gas potentials with maturity induced structural evolution of residual organic matter seems to be mechanistically similar for all kerogen types as well as for kerogen matured whether in natural or artificial systems.

### Open-System Maturation

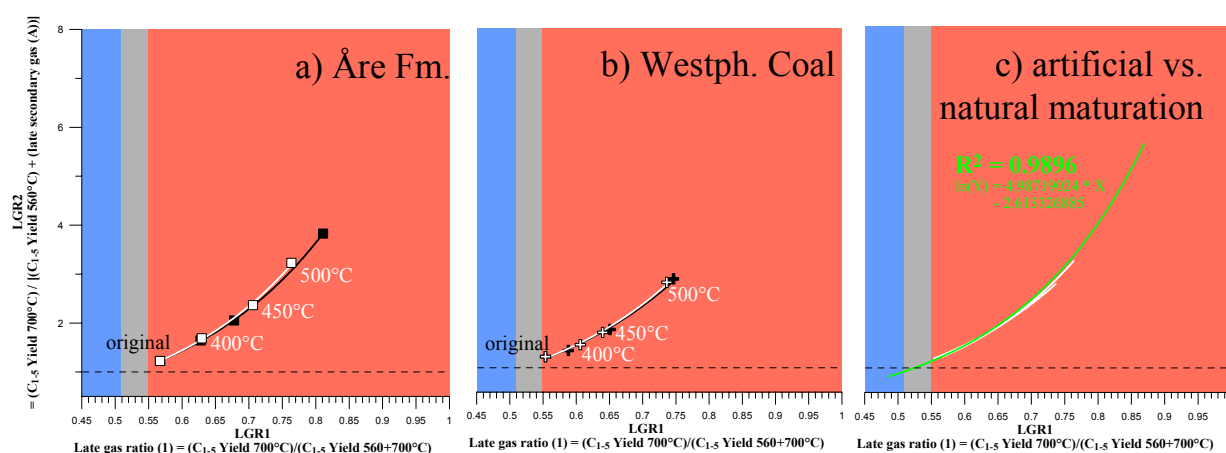


**Figure 5.14: Late Gas Potentials Classification using MSSV-pyrolysis based LGR1 and LGR2 for open-versus-closed-system artificially prepared residues of a) Åre Fm sample G001965 and b) Westphalian Coal sample G000721; in c) exponential functions describing the positions of open-system residues in the LGR1 – LGR2 plot are compared to the exponential function describing the position of all investigated natural maturity series samples.**

The position of the Åre Fm. sample G001965 and the Westphalian Coal sample G000721 matured under open-system conditions within the late gas potential ratios plot is displayed in Fig. 5.14a and 5.14b together with positions of previously discussed closed-system residues. It is easy to recognise that late gas potentials of open-system residues follow exactly the same trend as late gas potentials of closed-system residues and can be described by an almost identical exponential function. Consequentially and as shown in Fig. 5.14c, the evolution of the late gas potential with maturity can be as well simulated under open-system pyrolysis conditions. As results of open pyrolysis already suggested, open-system residues of Westphalian Coal resemble closed-system counterparts more closely than open-system residues of Åre Fm. sample G001965 resemble their closed-system counterparts.

Generally spoken, this is a very surprising result as one of the theoretical prerequisites for the formation of a thermally stabilised moiety yielding late gas at unusually high levels of thermal stress was thought to be the interaction of first formed bitumen with residual organic matter at lower maturity levels, a process only simulatable under closed-system conditions

like MSSV pyrolysis (Erdmann and Horsfield, 2006). Under open-system pyrolysis conditions products are transported out of the reaction zone and should not be able to assist in the genesis of a late gas potential. One simple conclusion would be that retrograde reactions between bitumen and residue are not a crucial factor in the development of a late gas potential and that precursor structures of late methane are to find in the initial refractory organic material. The question remains why late gas is only observable under closed- but not under open-system pyrolysis conditions.

### 5.2.3 Product Amounts

#### *Closed-System Maturation*

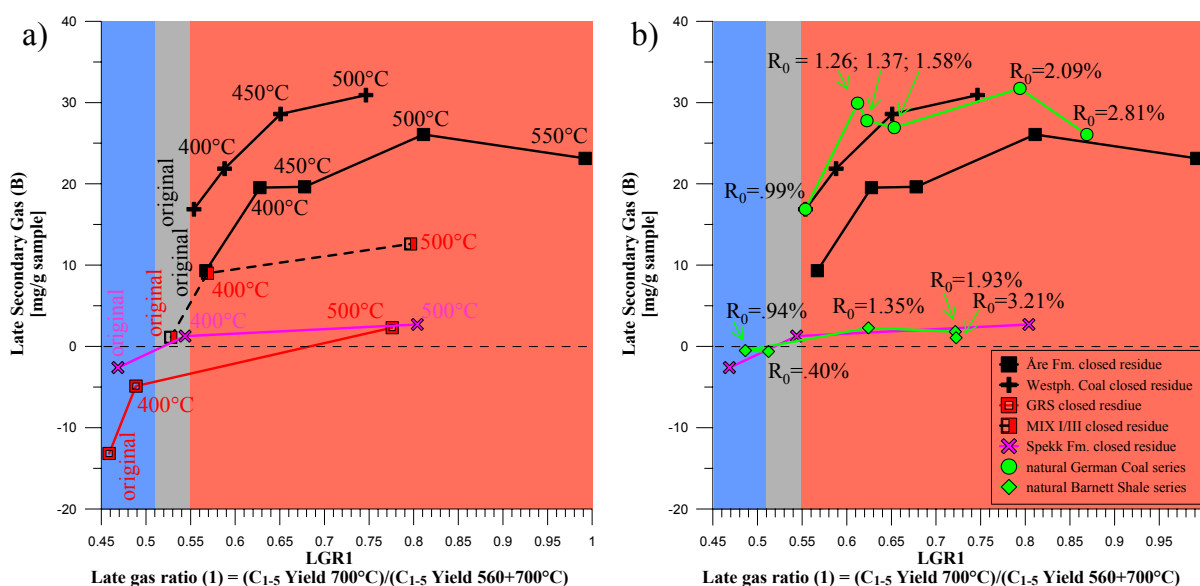


**Figure 5.15: Late secondary gas (B) yields: a) LGR1 and late secondary gas (B) yields of all original samples and their related residues matured under closed-system conditions; b) Comparison of naturally matured and artificially matured Type II (Barnett vs. Spekk) and Type III (natural Westph. Coal series versus Westph. Coal and Åre Fm.) source rocks.**

MSSV late secondary gas (B) yields, generated between 560 and 700°C, of original and under closed-systems conditions artificially matured samples are displayed in Fig. 5.15a together with LGR1. Yields are given in mg/g sample because the TOC content of residues was not identified. As increasing late gas potentials had already suggested (Fig. 5.13), secondary gas (B) input increases for all kerogen types and samples with artificial maturity irrespective of initial late gas generation behaviour of the original immature source rock. I.e. in the case of Green River Shale sample G004750, for which no late gas generation can be detected at immature levels, artificial maturation to 500°C brings about a secondary gas (B) potential of ca. 2.31 mg/g sample. This is in the same order of magnitude as secondary gas (B) potential of the Spekk Fm residue that exhibits a similar level of artificial maturation. Late

secondary gas (B) yields of Coal samples from the Åre Fm. and Germany are generally higher at all maturity stages with maximal amounts of 26 mg/g sample and 31mg/g sample respectively for the 500°C residue. This can be easily explained by a higher TOC content of Coals compared to shales. The synthetic Type I/III kerogen mixture exhibits intermediate yields ranging between its parent source materials provided by the Green River Shale and Åre Fm. sample.

Natural trends are very well simulated by artificial closed-system maturation as can be seen in Fig. 5.15b. The evolution pathway of secondary gas (B) yields from residues of the Type II Spekk Fm. sample G001955 traces very well the evolution pathway of secondary gas (B) yields from samples of the Type II Barnett Shale natural maturity series. This holds also true for residues of Westphalian coal sample G000721 ( $R_o = 0.99\%$ ), which is as well part of the German Coals natural maturity sequence. The Åre Fm. Sample G001965 based artificial maturity series follows the same trend with only lower absolute yields probably related to a lower initial TOC content of 40% compared to 80%. Interestingly, with further artificial maturation to 550°C of the Åre Fm. Sample G001965 the decrease in late secondary gas (B) yield observed for German Coals in the maturity interval between  $R_o = 2.09$  and  $2.81\%$  is also simulated.

### ***Open-System Maturation***

Late secondary gas (B) yields of Åre Fm. sample G001965 and Westphalian Coal sample G000721 matured under open-system conditions are displayed in Fig. 5.16a together with late secondary gas (B) yields of the respective closed-system residues. Again, it is very surprising that for the open-system maturation method the same trend of increasing yields can be observed even though bitumen material is swept away and cannot act as a source of late methane. Thus, this phenomenon is only explainable by the concentration of material with a late gas potential in both systems, in contrast to the neoformation theory of a thermally stabilised moiety by interaction between first-formed bitumen and residual organic matter. Nevertheless, the latter process plays an important role during the retention of organic matter and leads to increased TOC contents and therefore higher late gas potentials for the same quantity of source rock.

Nevertheless, slight differences for late secondary gas (B) generation can be observed for residues matured under closed- versus open-system conditions, with stronger impacts being obvious for the Åre Fm. sample G001965 most likely related to differences already noticed during open-system pyrolysis (Fig. 5.11 and 5.12a). Here artificial maturation led to a higher aromaticity of residues matured under open-system conditions compared to residues

matured under closed-system conditions at similar levels of thermal stress, which could be also described as a higher artificial maturity as the organic remainder is depleted in aliphatic compounds typical for coals of higher rank. Therefore, and also according to late secondary gas (B) yields of Åre Fm. residues (Fig. 5.16a), samples artificially heated to ca. 450°C under open-system conditions exhibit similar maturity levels than samples artificially heated to ca. 500°C under closed-system conditions. For the artificial Westphalian Coal series the impact is not as significant as for the Åre Fm. series most likely due to the maturity induced difference in the initial organic matter structure.

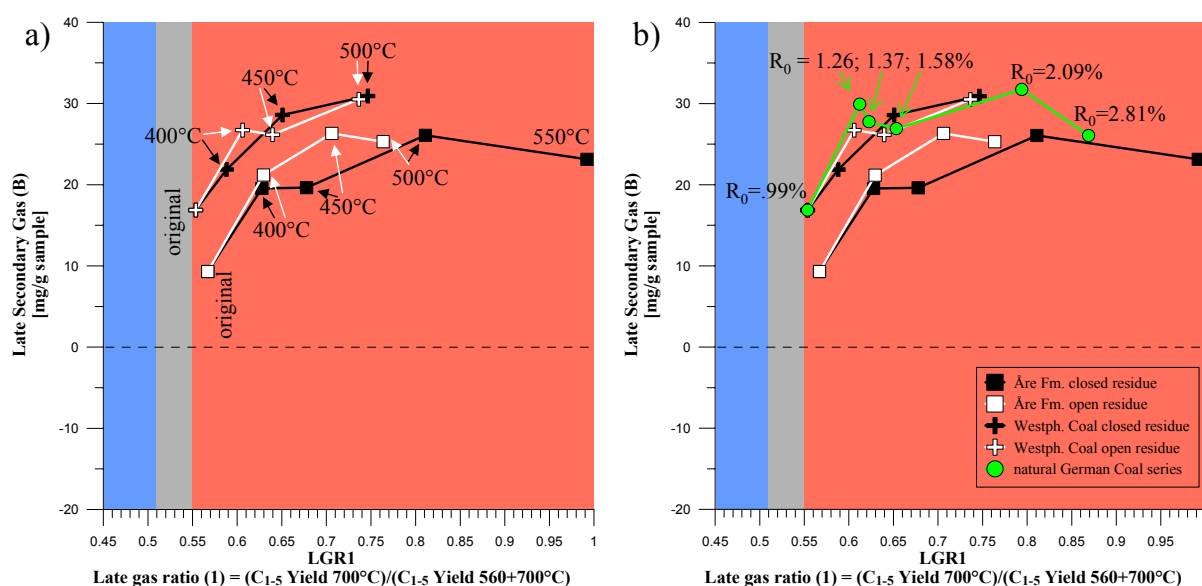


**Figure 5.16: Late secondary gas (B) yields: a) LGR1 and late secondary gas (B) yields of Åre Fm sample G001965 and Westphalian Coal sample G000721 and their related residues matured under open- vs. closed-system conditions; b) Comparison of naturally matured Westphalian Coal series and under open- vs. closed-system artificially matured Åre Fm sample G001965 and Westphalian Coal sample G000721.**

In Fig. 5.16b evolution pathways of secondary gas (B) yields from open- and closed-system residues of the Westphalian Coals sample G000721 trace very well the evolution pathway of secondary gas (B) yields from samples of the natural German Coals maturity sequence. It can be therefore concluded that both, open- and closed-system artificial maturation methods, are valid tools to simulate natural organic matter evolution. Thus, it is possible to relate LGR1 ratios of the different residues of the Westphalian Coal sample G000721 to the maturity parameter vitrinite reflectance of the natural German Coals maturity series. In Fig. 5.17a a linear function is used to fit LGR1 and vitrinite reflectance of the natural maturity series. Applying this function to the LGR1 ratio of the residues, a vitrinite reflectance value can be ascribed, which allows correlating late secondary gas (B) yields and maturity (Fig. 5.17b). It can be seen that secondary gas (B) yields of residues follow the



natural trend between 0.99 and 2.09%  $R_0$  perfectly tracing the jump in late gas potential previously described for this maturity interval (Sub-Chapter 5.1.2).

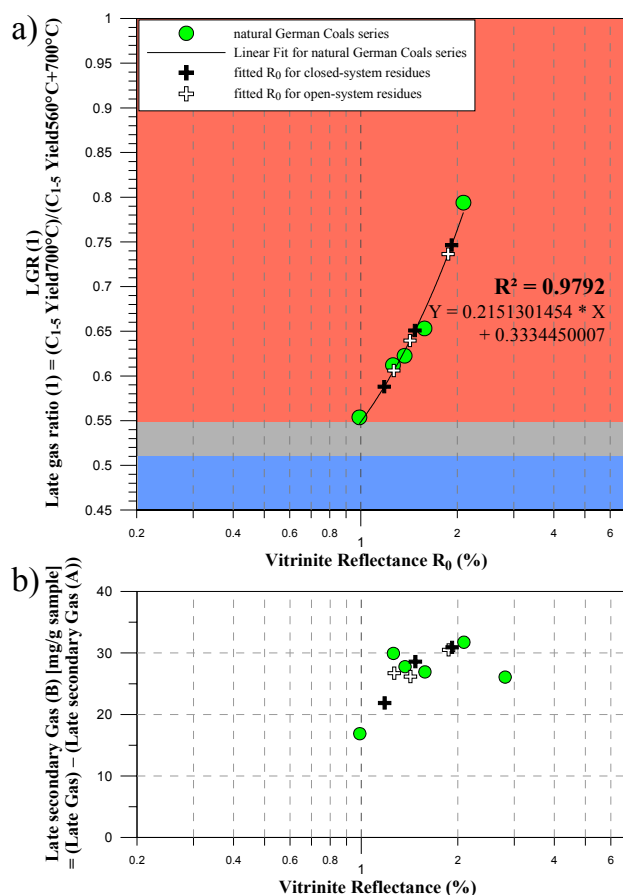


Figure 5.17: Calculated Vitritine Reflectance values for open- and closed-system residues of Westphalian Coals sample G000721 based on a) LGR1 ratios and a linear fit through data points of the natural maturity coal series from Germany between 0.99 and 2.09%  $R_0$ ; b) evolution of secondary gas (B) yields with artificial and natural maturation ( $R_0$ ).

### *Weight loss correction for late secondary gas (B) yields*

An interesting question to be answered is whether observed increasing secondary gas (B) yields are solely due to the concentration of refractory late gas precursor structures during artificial maturation and product generation or if other processes might play a role. This can be best done by taking into account the weight loss occurring during the preparation procedure (pyrolysis) of residues and using it as an input parameter for calculating yields normalised to the initial potential of the original sample. Yields can also be compared to theoretical yields, which are based only on the initial secondary gas (B) potential of the original sample and the weight loss. Measured, renormalized, and theoretical yields are displayed in Tab. 5-5 and Fig. 5.18 for open-system artificial maturation residues of Åre Fm. sample G001965 and Westphalian Coals sample G000721. Open-system residues were

chosen because firstly the natural trend is simulated as good as during closed-system maturation and secondly the weight before and after heating the sample to the desired residue end-temperature can be much easier determined using the SRA than MSSV tubes. The latter have to be manually crushed to collect the residue material which leads to the loss of small amounts of sample material. It should be kept in mind that this weight loss correction is not necessary to testify if natural trends are simulated correctly, as secondary gas (B) yields of natural maturity series samples are not weight loss corrected either, but to get information about processes leading to an increased late gas potential.

**Table 5-5: The effect of weight loss occurring during open-system artificial maturation using a SRA on Late secondary gas (B) yields of open-system residues of Åre Fm sample G001965 and Westphalian Coal sample G000721. Measured, theoretical (based on secondary gas (B) yield of the original sample and weight loss), and normalised (measured secondary gas (B) yields are normalised to original sample weight) yields are given.**

Maturation Method	Sample	Residue Temp.	Secondary Gas (B) Yield			Weight Loss during maturation	Residue Weight
			measured	theoretical concentration	measured and normalised		
		°C	mg/g sample				
Open-system (SRA)	Åre Fm. G001965	original	9.31	9.31	9.31	0.00	1000.00
		400	21.19	11.27	17.52	173.42	826.58
		450	26.32	12.17	20.14	234.77	765.23
		500	25.30	12.96	18.18	281.30	718.70
	Westph. Coal G000271	original	16.87	16.87	16.87	0.00	1000.00
		400	26.72	18.12	24.89	68.55	931.45
		450	26.16	20.01	22.05	156.88	843.12
		500	30.51	21.55	23.89	216.79	783.21

From Tab. 5-5 and Fig. 5.18 it can be deduced that an additional process besides concentration of late gas precursor structures has to be responsible for the evolution of the high temperature methane potential. The directly measured secondary gas (B) yields are much higher than calculated theoretical secondary gas (B) yields with 10-14 mg/g sample difference in the case of Åre Fm. residues and 6-9 mg/g sample difference in the case of Westphalian Coal residues. If measured secondary gas (B) yields are renormalized to the original sample weight intermediate yields are obtained which still exceed by far the initial late methane potential of the original sample. It is therefore clear that besides concentration of refractory precursor structures new ones must have been formed during artificial maturation. As neoformation of a thermally stabilised moiety by second-order reactions between first formed bitumen and residual organic matter can be excluded due to the removal of primary products in the open-system, a sensible alternative explanation is the enrichment and formation of methyl-groups concomitant to chain shortening reactions via  $\beta$ -cleavage during petroleum generation (Freund and Olmstead, 1989; Smith and Savage, 1992; Savage, 2000). The

relevance of such reactions in the catagenesis zone was already discussed in Sub-Chapter 5.1.3 under “Late Gas Potential increase during Catagenesis” for various natural maturity sequences.

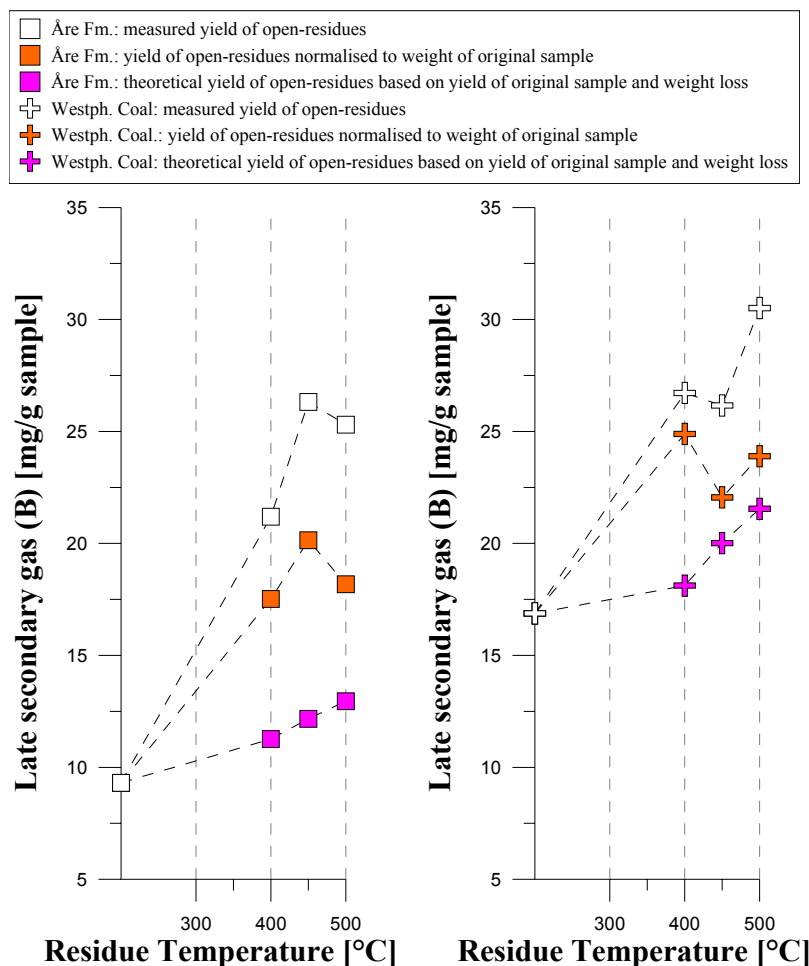


Figure 5.18: Measured, theoretical, and normalised late secondary gas yields of Åre Fm sample G001965, and Westphalian Coal sample G000721, as well as their respective open-system residues.

It should be stated here that even though the timing might be different, closed-system maturation brings about changes of the same intensity as open-system maturation regarding late secondary gas (B) potential. Thus, processes leading to the formation of high temperature methane precursor structures seem to be mechanistically similar under both artificial heating conditions. Second-order reactions between bitumen and residual organic matter leading to the neoformation of a thermally stable moiety are therefore not crucial for the development of a late gas potential.

### 5.3 Conclusion

The purpose of this chapter was to investigate if late gas generative properties are influenced by structural and chemical changes within the organic matter during natural maturation or artificial maturation under open- and closed-system pyrolysis conditions. It can be shown that this is the case and absolute late gas amounts cannot be safely predicted using immature samples alone because late gas precursor structures are formed during both, natural and artificial maturation, regardless of the initial organic matter structure.

Using the two-step MSSV-pyrolysis screening method described in Sub-Chapter 4.2.1, late gas potentials of samples (39) from five natural maturity series, comprising material of two Type II marine shale series (Exshaw Fm. and Barnett Shale) and three Type III humic coal series (New Zealand Coals and German Carboniferous as well as Wealden Coals), are shown to increase up to ~40 mg/g TOC at maturity levels ~2.0%  $R_o$  for all kerogen types. The advocated cause is an enrichment of methyl-aromatics, acting as precursor structures of late methane, within the residual organic matter related to chain shortening reactions by  $\beta$ -scission during hydrocarbon generation within the oil window and simple concentration of refractory organic matter due to product release. The observation that natural behaviour, i.e. late gas potential increase, can be simulated for immature organic matter using both, open-system (Type II Spekk Fm. sample G001955, Type I Green River Shale sample G004750, synthetic Mix Type I/III sample G0047501965, Type III Westphalian Coal sample G000721, and Åre Fm. sample G001965) and closed-system (Type III Westphalian Coal sample G000721 and Åre Fm. sample G001965) preparative pyrolysis confirms the relevance of the suggested mechanism and shows that interactions between first-formed bitumen and residual organic matter seem not to be a crucial factor for the development of a late gas potential as previously thought. Nevertheless, second-order recombination reactions, observed especially for heterogeneous kerogens or coals under natural conditions, promote the retention of  $C_{6+}$  compounds within the residual organic matter leading to retention of TOC. If the late gas potential is indeed 40 mg/g TOC after the catagenesis stage for any given kerogen type, the amount of high temperature methane generated from mature source rocks would be strongly coupled to initial TOC contents and carbon loss during catagenesis. The previously established late gas potential classification tool based on the two late gas ratios LGR1 and LGR2 is therefore still relevant. E.g. homogeneous, paraffinic organic matter of aquatic lacustrine and marine origin generally exhibits low late gas potentials at low maturity levels and loses much of its carbon during catagenesis. The remaining TOC content is

consequently much lower than observed for more heterogeneous marine source rocks containing algal or bacterial derived precursor structures of high aromaticity or terrestrial derived source rocks exhibiting intermediate to high late gas potentials.

The decrease of late gas potential evidenced for the highly mature Westphalian Coal sample ( $R_o = 2.81\%$ ) and Barnett Shale sample ( $R_o = 3.21\%$ ) indicates that high temperature methane is being generated under geologic conditions in the metagenesis zone for vitrinite reflectances exceeding  $\sim 2\% R_o$ . This not only confirms the validity of previous (Dieckmann *et al.*, 2006; Erdmann and Horsfield, 2006) and present closed-system kinetic predictions (Sub-Chapter 4.1.5) for late secondary gas (B) generation based on the evaluation of immature source rocks, but also that high temperature methane generation is most likely a process occurring under natural conditions and does not only represent a laboratory artefact. The advocated mechanism for late dry gas production is the final demethylation of residual organic matter by  $\alpha$ -cleavage concomitant to condensation reactions of the aromatic cluster.

An interesting observation was that late gas potentials decrease in the maturity interval  $0.4 - 0.8\% R_o$  for unextracted and extracted coals from New Zealand. Most likely, late gas precursor structures, presumably methyl groups yielding methane upon high temperature closed-system pyrolysis, are lost together with the most unstable O-bearing functional groups and low molecular weight compounds such as acetate. As this process also leads to an increase in normal hydrocarbon potential (HI) by concentration of petroleum forming precursor structures, the different nature of precursor structures for conventional petroleum and late secondary gas (B) generation is revealed. As a practical consequence one should avoid to use very low maturity samples for the determination of absolute late gas yields.



## 6 FURTHER COMPOSITIONAL CONSIDERATIONS

### 6.1 *Stable carbon isotopes of Gas (MSSV-Pyrolysis)*

The  $\delta^{13}\text{C}$  compositions of methane, ethylene, ethane, propene, propane, and butane were determined for 11 MSSV pyrolysis temperatures in triplicate for the Åre Fm. sample G001965, the Spekk Fm. sample G001955, the Green River Shale sample G004750, and the synthetic Mix Type I/III sample G0047501965 at a heating rate of 1 °C/min. The chosen start temperature was 250°C and end temperatures were spaced by 50°C between 300 and 800°C covering the whole temperature interval used during MSSV pyrolysis. Under closed-system conditions, primary and secondary processes and its accompanying fractionation effects influence the isotopic composition of the generated cumulative gas and thus, are observable. Isotopic values of cumulative gas are not directly comparable to isotopic values of primary open-system-formed gas, as carbon isotopes from gases formed at lower temperatures remain in the tube and therefore, have an influence on values measured on products at higher temperatures. To overcome this problem, instantaneous gas values can be calculated if the amount of gas generated between two temperatures is known. Nevertheless, a direct comparison with open-system data is still somewhat erroneous especially for temperatures exceeding 450°C, when secondary cracking processes become very pronounced.

#### 6.1.1 Evolution of $\delta^{13}\text{C}$ Compositions of Individual Gas Compounds

The methane, ethylene, ethane, propene, propane, and butane were measured (Table A 13). Fig. 6.1 shows stable carbon isotope ratios for methane and the  $\text{C}_2$  to  $\text{C}_4$  alkanes at various MSSV end temperatures together with cumulative MSSV pyrolysis yields. The observed trends are essentially the same for all four source rocks and molecular species in that isotopic values decrease with increasing temperature up to 400 or 450°C and then start to increase again for higher temperatures showing a divergence. The shift to extremely heavy isotopic compositions for propane and ethane beginning at 500°C and 550°C respectively can be ascribed clearly to the secondary cracking of these compounds as the respective cumulative pyrolysis yields decrease at higher temperatures (Fig. 6.1)(Lorant *et al.*, 1998; Erdmann, 1999). At the initial stages of this process preferential cracking of the  $^{12}\text{C}$ - $^{12}\text{C}$  bond (Silverman, 1967; Sackett *et al.*, 1970) within ethane or propane will result in a concentration of the heavier, primary molecule and in the generation of light methane as a secondary product. Thus, methane should become isotopically lighter at temperatures exceeding 550°C, which is actually not the case probably related to a counterbalancing by primary high

## 6 FURTHER COMPOSITIONAL CONSIDERATIONS

temperature  $^{13}\text{C}$  methane production. Increasing propane and ethane isotopic ratios at MSSV temperatures below  $500^\circ\text{C}$  might be caused by the conventionally postulated kinetic isotope effect fractionation during primary generation and/or the input of heavy secondary product species by the cracking of higher alkane homologues.

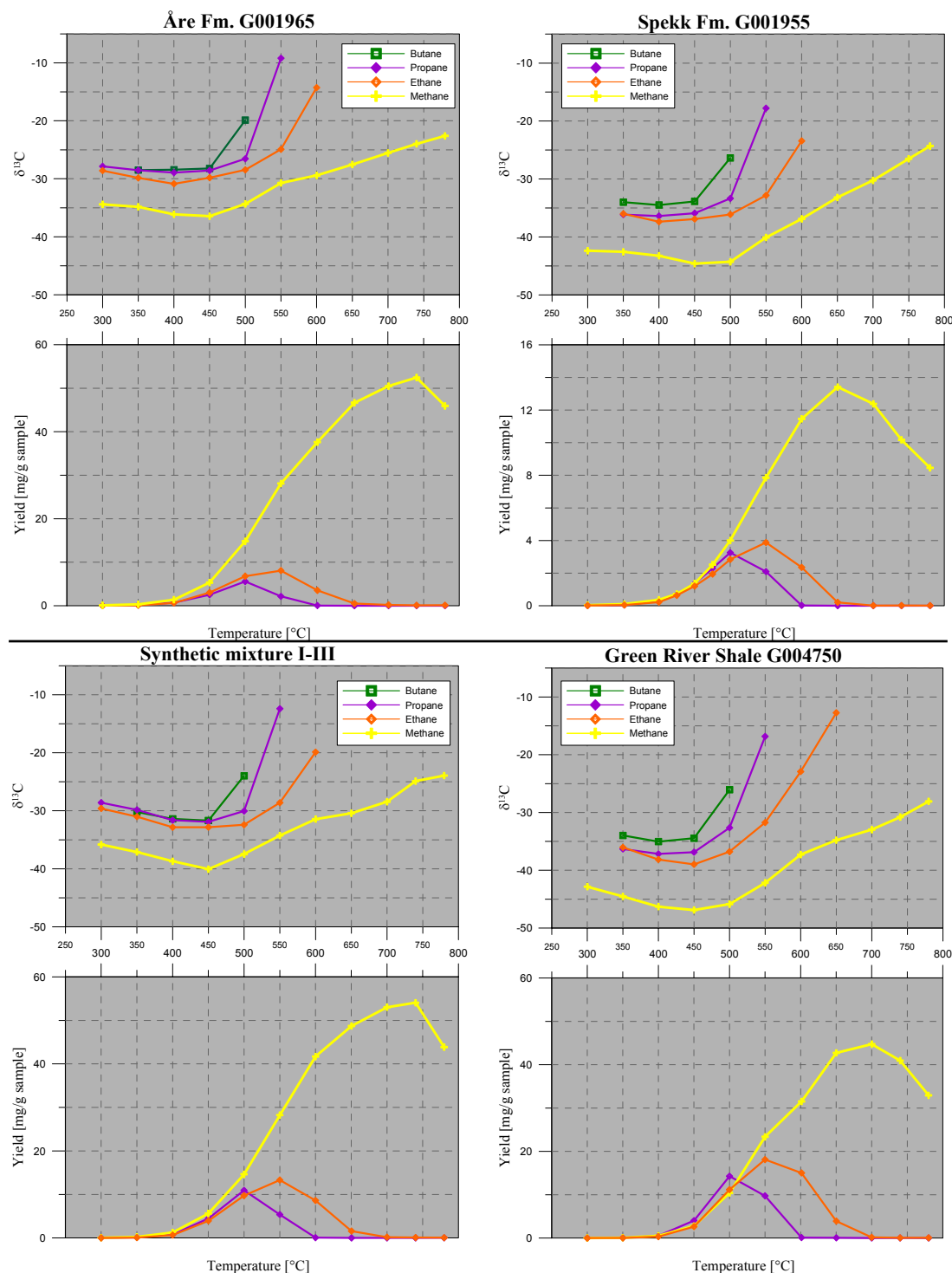


**Figure 6.1: Stepwise MSSV-pyrolysis at  $1^\circ\text{C}/\text{min}$ : Cumulative stable carbon isotope ratio curves of  $\text{C}_{1-4}$  alkanes as well as cumulative MSSV-pyrolysis yield curves of  $\text{C}_{1-3}$  alkanes for the Åre Fm. sample G001965, the Spekk Fm. sample G001955, the Green River Shale sample G004750, and the synthetic Mix type I/III sample G0047501965.**



### 6.1.2 Evolution of $\delta^{13}\text{C}$ Compositions of Methane

Generally it can be said that the observed stable carbon isotope ratio trend for methane of all source rocks, with or without late gas potential, resembles the v-shape already described in various publications where closed-system pyrolysis was used for investigation (Sackett, 1978; Chung and Sackett, 1980; Arneth and Matzigkeit, 1986; Lorant *et al.*, 1998; Erdmann, 1999; Tang *et al.*, 2000) and does not monotonically increase with extent of kerogen cracking as inferred from many field studies. It should be stated here that all of the laboratory research of these authors was undertaken using temperatures below 600°C. The “w”-shape observed by Dieckmann *et al.* (2006), which was attributed to the recombination of  $\text{C}_{6+}$  gas precursor structures and neoformation of a thermally stable gas precursor yielding additional methane at extreme maturities, could not be replicated in the present work. However, end temperature intervals of 50°C could be too large to recognise such an isotopic trend.

#### *Temperature Interval 300 – 450°C*

All source rocks show the formation of initially “heavy” methane followed quickly by the usual lighter methane with a minimum at 450°C. The Åre Fm. sample G001965 shows the heaviest overall isotopic composition with a starting ratio of -34.4‰ which is in accordance with the theory of terrestrial or lipid-poor organic matter being  $^{13}\text{C}$  enriched (Silverman, 1967; Degens, 1989). Consequently, the lipid-rich Type I Green River Shale sample G004750 possesses the lightest starting ratio of -42.8‰ followed by the Type II Spekk Fm. sample G001955 with -42.4‰ and the synthetic Mix Type I/III sample G0047501965 with -35.8‰. The shift to the lighter carbon isotope ratios at the “minimum” temperature covers a range of 2‰ for the Åre Fm. sample, 2.2‰ for the Spekk Fm sample, 4.2‰ for the synthetic mixture, and 4‰ for the Green River Shale sample.

Most authors explain this early heavy-light trend by hypothesising two different precursor structures. Here, the earliest methane is generated from a pool of isotopically heavy methyl groups bound with relatively labile heteroatomic bonds (for example C-O or C-S linkages)(Chung and Sackett, 1980; Smith *et al.*, 1985; Arneth and Matzigkeit, 1986; Sackett and Conkright, 1997; Lorant *et al.*, 1998; Cramer, 2004). Decreasing  $\delta^{13}\text{C}$  values could then be explained by mixing with methane generated by the cracking of different, isotopically light precursor structures, presumably C-C bonds. At those temperatures cracking would occur preferentially at  $^{12}\text{C}$ - $^{12}\text{C}$  bonds. In contrast, Sackett and Conkright (1997) and Arneth and Matzigkeit (1986) suggest that catalysis due to the presence of inorganic minerals with carbonium ion inducing catalytic properties may play a role. Based on cracking experiments

with model compounds (*n*-octadecane) and sodium montmorillonite (Sackett, 1978), the described carbon isotope ratio trend was replicated and explained by an early, catalytically (carbonium ion mechanism) produced methane, with little carbon isotope fractionation, and a subsequently, thermally produced methane (free radical mechanism), with a relatively large carbon isotope fractionation. A third, alternative possibility is assumed by Tang *et al.* (2000), who observed the same kind of decreasing isotope ratio trend during pyrolysis experiments on pure n-alkane compounds, meaning that the decomposition of a precursor structure with one unique initial  $\delta^{13}\text{C}$  value can also yield such a complex isotopic product composition. The authors could kinetically model this complex trend by a hypothetical parallel reaction scheme for the generation of methane and assigning one of two different isotopic fractionation factors  $\Delta E_a$  to reactions with activation energies  $> 50$  kcal/mol or activation energies  $< 50$  kcal/mol.

### ***Temperature Interval 450 - 780°C***

From 450°C on, carbon isotopic ratios of methane increase for all investigated source rocks with increasing temperatures up to 780°C. The shift to heavier carbon isotope ratios covers a range of 13.9‰ for the Åre Fm. sample, 20.3‰ for the Spekk Fm sample, 16.1‰ for the synthetic mixture, and 18.8‰ for the Green River Shale sample. The increase in  $^{13}\text{C}_1$  between 450°C and 600°C can be explained by the kinetic isotope effect (Sackett *et al.*, 1970; Schoell, 1980), as  $^{12}\text{C}$  forms slightly weaker chemical bonds than does  $^{13}\text{C}$  (Silverman, 1967; Sackett *et al.*, 1970) leading to an isotopically light gas at low temperatures and a progressively “heavier” gas subsequently formed at higher temperatures (Clayton, 1991; Whiticar, 1999). The isotopic trend within this temperature region is, as stated above, regularly observed for closed-system experiments (Sackett, 1978; Chung and Sackett, 1980; Arneth and Matzigkeit, 1986; Lorant *et al.*, 1998; Erdmann, 1999; Tang *et al.*, 2000) as well as for open-system experiments (Friedrich and Jüntgen, 1973; Berner *et al.*, 1995; Cramer *et al.*, 2001; Gaschnitz *et al.*, 2001; Cramer, 2004) making primary thermal cracking of increasingly heavy gas precursor structures (C-C bonds) with maturity the most pronounced mechanism. Nevertheless, methane isotopic ratios are most likely also influenced by secondarily generated methane in the closed system.

For temperatures in excess of 600°C carbon isotopic ratios of methane rather unexpectedly still increase for all investigated source rocks. The data cannot be compared to other closed-system data as this temperature interval is not covered in literature. Nevertheless, open-system experiments were conducted, mainly for coals. The shape of the methane isotopic trend at comparable heating rates shows a characteristic inflexion around 600°C and decreasing  $\delta^{13}\text{C}$  values with a shift of about 10‰ towards isotopically lighter methane at

temperatures around  $\sim 750^{\circ}\text{C}$  (Friedrich and Jüntgen, 1973; Cramer *et al.*, 2001; Gaschnitz *et al.*, 2001; Cramer, 2004). This inflexion coincides with the onset of a more or less distinct shoulder observed in the relevant generation rate curves (bulk) and can be explained by a different precursor pool, which produces lighter methane at high temperatures (Gaschnitz *et al.*, 2001). Reactions between aromatic substances might be responsible for the release of this late methane (Friedrich and Jüntgen, 1973; Payne and Ortoleva, 2001; Lorant and Behar, 2002; Cramer, 2004; Xiong *et al.*, 2004; Dieckmann *et al.*, 2006). Decreasing  $\delta^{13}\text{C}$  values are not observable in the present closed-system experiments but one could argue that the slope of the methane isotopic trend flattens out between  $600^{\circ}\text{C}$  and  $700^{\circ}\text{C}$  at least for the Åre Fm. sample G001965, the Green River Shale sample G004750, and the synthetic Mix type I/III sample.

At least two mechanisms could explain the still increasingly heavy isotope signature of methane for increasing pyrolysis temperatures. Firstly, the input of secondary methane from cracking of increasingly heavy ethane and secondly, the decomposition of methane as  $^{12}\text{C}$ - $^{12}\text{C}$  bonds are more labile than  $^{13}\text{C}$ - $^{12}\text{C}$  bonds. Pure methane begins to decompose at temperatures of  $700^{\circ}\text{C}$  with a half time of about 44 days into amorphous carbon and hydrogen gas (Sackett, 1995). The author used pure methane sealed in precombusted Vycor (quartz) glass tubing at one atmosphere pressure for isothermal pyrolysis. Time series of temperatures at 600, 700, 800, 900, and  $1000^{\circ}\text{C}$  allowed decomposition rates to be determined. Half times were calculated to be 108 hours for  $800^{\circ}\text{C}$ , 34 hours for  $900^{\circ}\text{C}$  and 4 hours for  $1000^{\circ}\text{C}$ . A large kinetic isotope fractionation was observed in the decomposition of methane to amorphous carbon with methane being enriched in  $\delta^{13}\text{C}$ . Decomposition of methane might even start at lower temperatures if pyrolysed in an “impure” system together with its carbon-rich source rock as is the case for the present analytical set-up. For example, Greensfelder *et al.* (1949) demonstrated a high dehydrogenation activity of activated carbon by decalin transformation to naphthalene and showed that cracking of *n*-hexadecane was greatly accelerated or catalysed by the high surface area of the activated carbon. That cracking of methane at least influences the isotopic signature can be best seen for the Spekk Fm. sample. Here cumulative methane yields start to decrease at temperatures exceeding  $650^{\circ}\text{C}$  leading to a steep slope in the  $\delta^{13}\text{C}$  trend.

An additional topic to discuss would be the ability of carbonaceous species to undergo isotopic re-equilibration after they have been generated and remain in a closed system. Very little information, experimental or theoretical, exists in literature. For example, carbon isotope exchange between methane and carbon dioxide seems not to be the reason for the change in

$\delta^{13}\text{C}$  values of cumulative methane in the pyrolysis temperature region between 450°C and 800°C. Sackett and Chung (1979) reported no exchange at 500°C for periods up to 136 hours and Sackett (1995) showed no exchange for 524 hours at 600°C. When the experimental temperature was raised to 800°C, methane decayed with a half life of 108 hours, whereas  $\text{CO}_2$  exhibited little if any change in amount and  $\delta^{13}\text{C}$  for experimental times up to 44.5 hours.

### 6.1.3 Isotopic Reversals (Rollover) in Shale Gases

Cumulative  $\delta^{13}\text{C}$  ratios of methane and the  $\text{C}_2$  to  $\text{C}_4$  alkanes of all 4 immature samples are characterised by  $\delta^{13}\text{C}_{\text{methane}} < \delta^{13}\text{C}_{\text{ethane}} < \delta^{13}\text{C}_{\text{propane}}$  and  $< \delta^{13}\text{C}_{\text{butane}}$  at all MSSV pyrolysis end temperatures with an increasingly heavy isotope signature at higher temperatures. This is consistent with theoretical models of kinetic isotope effect (KIE) and carbon isotopic compositions observed in most conventional, natural gas accumulations (Burruss and Laughrey, 2010). An interesting isotopic reversal of  $\delta^{13}\text{C}_2$ , i.e. “rollover” of the ethane carbon isotope composition to lighter values at high maturities leading to e.g.  $\delta^{13}\text{C}_{\text{methane}} > \delta^{13}\text{C}_{\text{ethane}}$ , is observed for many highly productive shale gas wells in the U.S. (e.g. Barnett, Haynesville, and Woodford Shales)(Zumberge *et al.*, 2012) but could not be reproduced under the confined laboratory conditions in the current thesis. This indicates that in-situ gas cracking of ethane and propane during MSSV-pyrolysis is not a reasonable explanation for the observed natural trend. The responsible mechanism is still far from determined, but momentarily Tang and Xia (2011) suggested a generally accepted reaction pathway involving “water-reforming” of highly mature organic matter to  $\text{CO}_2$  and  $\text{H}_2$  in a rate limiting step and a subsequent Fischer-Tropsch like process in which  $\text{CO}_2$  and hydrogen react to methane and minor amounts of ethane and propane (Ji *et al.*, 2008). Iron (II) oxide may act as a possible catalyst under the reducing subsurface hydrocarbon reservoir conditions (Tang and Xia, 2011). The proposed reaction pathway is characterised by a light  $\delta^{13}\text{C}$  signature in  $\text{CO}_2$  as well as in a reversed series of  $\delta^{13}\text{C}_{\text{methane}} > \delta^{13}\text{C}_{\text{ethane}}$  and  $> \delta^{13}\text{C}_{\text{propane}}$  encountered in unconventional hydrocarbon reservoirs exhibiting the reversal phenomenon (Burruss and Laughrey, 2010; Tang and Xia, 2011; Zumberge *et al.*, 2012). This also indicates a similar, originally organic carbon source of the respective gases.

Nevertheless, input of „light” ethane generated directly from highly mature organic matter or neoformed residue (char/coke) cannot be ruled out as a formation mechanism based on the results shown within the current thesis. All used samples are immature and a possible late “light” gas signature is therefore overprinted by the secondary cracking of previously formed primary and secondary ethane during closed-system MSSV pyrolysis. To test if

primary cracking or cracking of thermally stabilised organic matter leads to lighter carbon isotopic ratios naturally matured samples could be analysed in future works using the MSSV-pyrolysis approach for high temperatures (Chapter 4.2.1).

## **6.2 *Second order reactions and their effect on Late Gas Generation - Synthetic Source Rock Mixture (Type I/III)***

The role of second order reactions between pyrolysis products from different kerogen types in natural mixed kerogen assemblages was simulated (open- and closed-system pyrolysis) using admixtures. Mahlstedt *et al.* (2008) have already demonstrated, as well using synthetic mixtures of immature source rock samples stemming from different sedimentary environments during closed-system artificial maturation experiments, that second-order reactions are revealed by a strongly increased recovery of phenolic compounds in the pyrolysate of blended material exceeding that of the parent coal sample. Phenolic/aromatic moieties were therefore suggested to be of high importance during organic matter maturation and the development of a thermally stabilised moiety because the presence of aliphatic material in the admixture possibly served to suppress “char” formation by cross-linking reactions between first formed products and residual organic matter (Dieckmann *et al.*, 2006; Erdmann and Horsfield, 2006).

### **6.2.1 Open-System Pyrolysis**

#### ***TOC/Rock-Eval***

In Fig. 6.2 TOC/Rock-Eval data is displayed for a synthetic Type I/III source rock mixture and its parent material Green River Shale G004750 and Åre Fm G001965. Data for the Åre Fm sample is plotted on left y-axis; data for the Green River Shale sample is plotted on the right y-axis. Consequently, data for the synthetic mixture can be found in the middle of the diagram in the 50% coal and 50% Type I position. Values not plotting on a linear line connecting values of the parent source rocks might indicate the occurrence of second-order reactions during pyrolysis, which is not necessarily the case, as will be explained in due course. In Fig. 6.2a directly measured Rock-Eval parameters such as S1, S2, S3, and TOC are depicted, in Fig. 6.2b parameters such as  $T_{\max}$ , HI and OI, which are based on the previous parameters.

It can be seen in Fig. 6.2a that S1, S2, and S3 of the synthetic mixture reveal only very subtle deviation from linear behaviour with S2-yields being only slightly lower than expected. Thus, the blending of the parent materials seems to have created a real 50:50 mixture. Interestingly, the TOC is much too high for a 50:50 blend, which nevertheless is more likely related to an invalid TOC measurement performed by the sub-contractor APT (detected S1, S2, S3 amounts are ok).

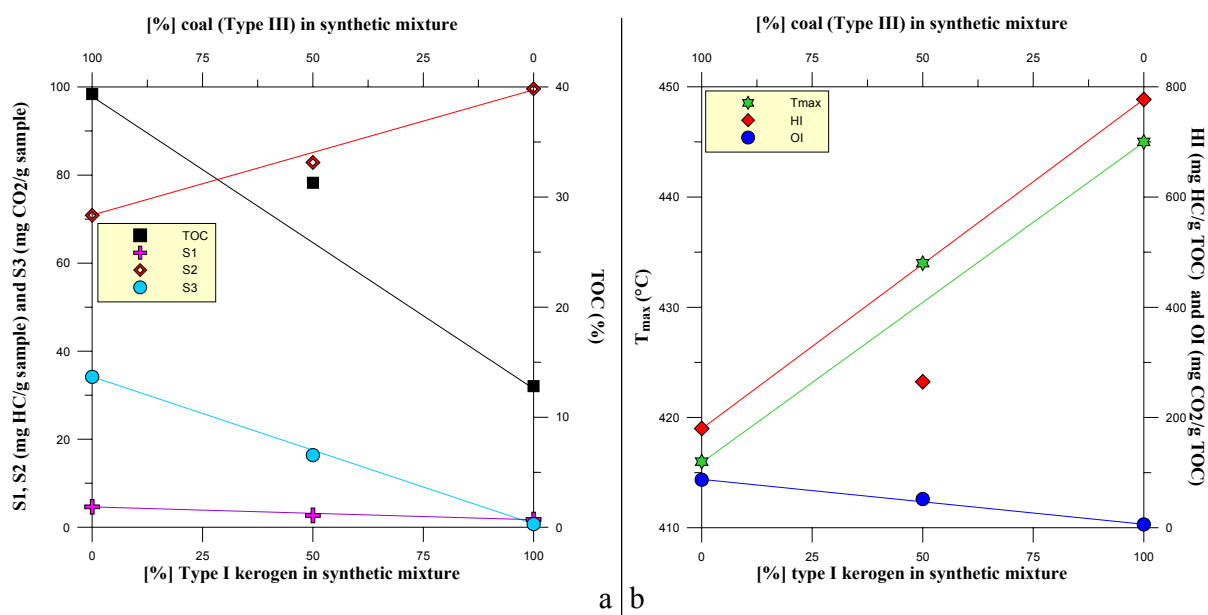


**Figure 6.2: TOC/Rock-Eval screening data for the synthetic Type I/III source rock mixture and its parent material; a) TOC, S1, S2, S3; b)  $T_{max}$ , HI, OI**

The much too high TOC as an input parameter of course causes the HI (mg HC/g TOC) of the synthetic Type I/III mixture to be unrealistically low (Fig. 6.2b). Thus, in the following diagrams the yield unit mg/g sample will be used for comparison to avoid problems based on an uncertain TOC content. The  $T_{max}$  is higher than a linear relationship would suggest due to an overprinting effect of the higher S2 yield of the more stable Type I Green River shale sample compared to the lower S2 yields of the Åre Fm. Coal sample. Thus, deviation from linear behaviour is not evidence for second-order reaction in the case of HI, OI, or  $T_{max}$ .

Bimolecular (second-order) recombination reactions cannot really be evidenced for open-system Rock-Eval (Rock-Eval 6) pyrolysis as S1-, S2- and S3-yields of the synthetic mixture largely depend linearly on yields of its original source rock samples.

### ***Open-system Pyrolysis GC-FID***

In Fig. 6.3 open-system pyrolysis (300-600°C at 60°C/min) yields of Åre Fm sample G001965, Green River Shale sample G004750 and the physical 50:50 source rock mixture of the latter two samples (synthetic Type I/III MIX) are displayed. In order to be able to recognise differences more easily theoretical yields for a 50:50 source rock mixture of the parent material were calculated on the basis of measured product amounts and compared to the physical source rock mixture. One can easily notice that gas yields, i.e. methane and C<sub>2-5</sub>, of the physical mixture meet expectations, i.e. are identical to yields of a theoretical mixture,

on the premise no second-order reactions are taking place during open-system pyrolysis. On the other hand,  $C_{6+}$  yields are slightly lower than expected, which influences of course also the total yield.

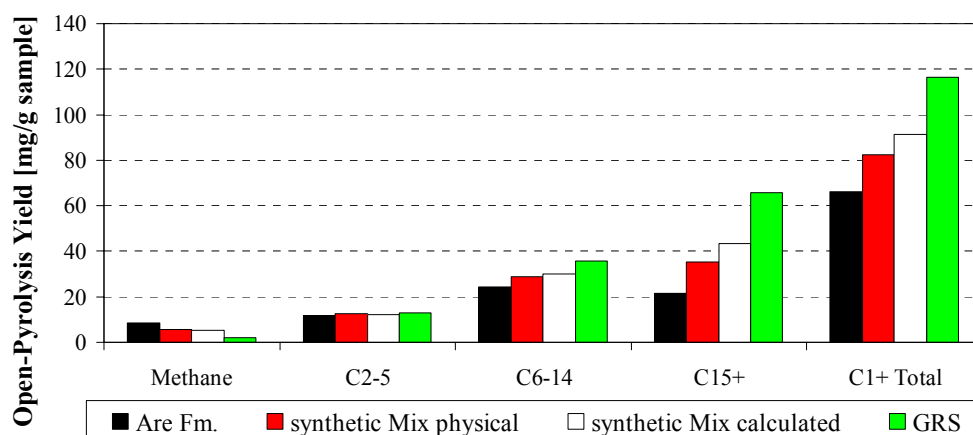


Figure 6.3: Open-Pyrolysis (300-600°C) yields of Åre Fm sample G001965, Green River Shale sample G004750, a physical 50:50 source rock mixture of the latter two samples (synthetic Type I/III MIX) and a theoretical 50:50 source rock mixture of those samples

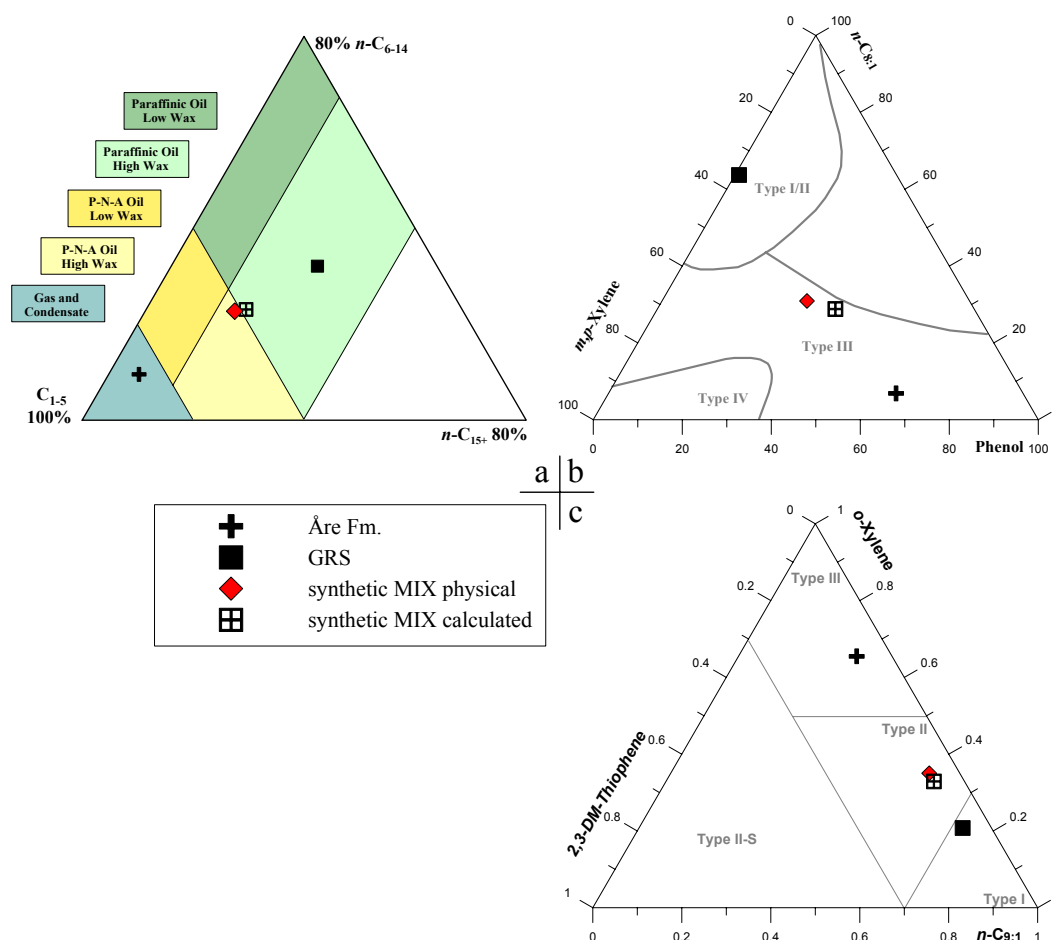


Figure 6.4: Composition of open-system pyrolysates of Åre Fm sample G001965, Green River Shale sample G004750, the physical 50:50 source rock mixture of the latter two samples (synthetic Type I/III MIX) and a theoretical 50:50 source rock mixture of those samples displayed in ternary diagrams of a) Horsfield (1989), b) Larter (1984), and c) Eglinton *et al.* (1990).



The composition of pyrolysates for the same samples is displayed in Fig. 6.4 in ternary diagrams of Horsfield (1989), Larter (1984), and Eglinton *et al.* (1990). No significant differences between measured and theoretical composition of synthetic mixtures can be observed with the exception of a relative, slight depletion in phenolic compounds represented by phenol (Fig. 6.4b). Interestingly, even under open-system conditions, phenolic compounds are again involved in the only real discrepancy between expected and measured values, perhaps hinting on bimolecular reactions. To elucidate this more closely stepwise open-system pyrolysis was performed, which is described in the following subchapter.

### ***Stepwise Open-System Pyrolysis (GC-FID)***

Cumulative yield curves of boiling fractions  $C_{1+}$ , methane,  $C_{2-5}$ ,  $C_{6-14}$ , and  $C_{15+}$  are shown in Fig. 6.5 for Åre Fm sample G001965, Green River Shale sample G004750 and the physical and theoretical 50:50 Type I/III source rock mixture. Stepwise open-system pyrolysis curves are based on heating samples from 250°C to end temperatures regularly spaced by 50°C using a 1°C/min heating rate. As already observed for open-system pyrolysis using a faster heating rate of 60°C/min to heat samples from 300 to 600°C in a single run, gas yields, i.e. methane and  $C_{2-5}$ , almost perfectly meet expectations assuming no bimolecular are taking place, but  $C_{6+}$  yields are again lower in the higher temperature regime, i.e. above 450°C. This subtly hints to the occurrence of second-order reactions in spite of a relatively short residence time of first formed products in the pyrolyser.

Another interesting observation is that  $C_{6-14}$  and  $C_{15+}$  fraction yields of physical source rock mixtures exhibit maxima at 500°C and then slightly decrease for 550°C and 600°C end temperatures. This feature, also observable for Åre Fm sample G001965, should actually not occur during open-system pyrolysis because cumulative yields should always increase or stay the same once the maximum yield is reached and no more products are formed. Consequently, the detected decrease of  $C_{6+}$ -compounds for temperatures above 450°C can only be related to reactions taking place in the liquid nitrogen cooled trap, which could be due to increasingly long holdback times of formed substances within the latter before the ballistic heating and release of products onto the GC-column for higher end temperatures (for details see Chapter 2.2.2). The discrepancy between measured and theoretical yields of the synthetic Type I/III sample is therefore not a direct sign of second-order reactions being of importance during open-system pyrolysis product generation but rather a sign of second-order reactions occurring in the trap between primary products partly forming a “coke“ which is retained.

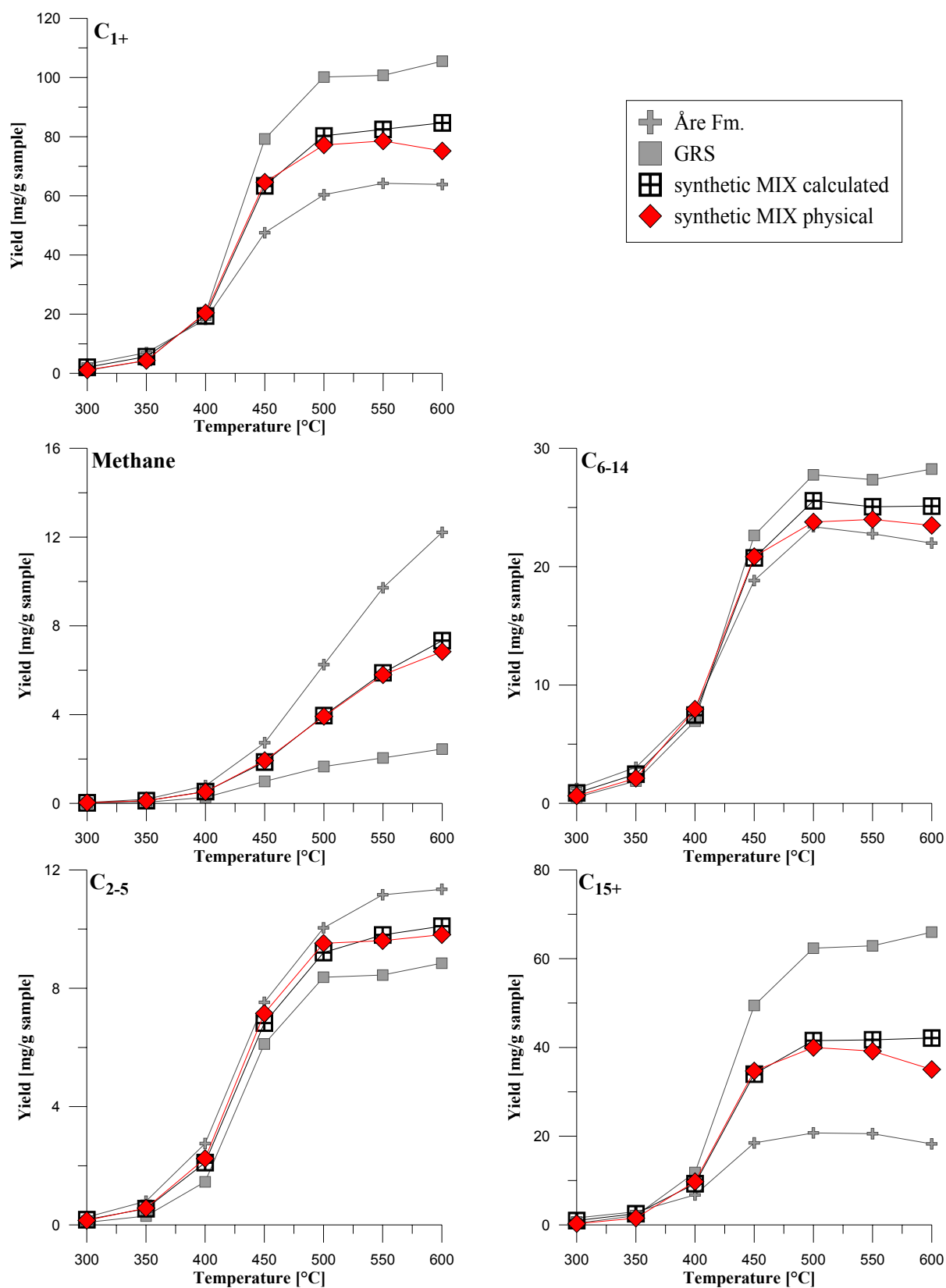


Figure 6.5: Stepwise open-pyrolysis at 1°C/min: cumulative yield curves of boiling fractions methane, C<sub>2-5</sub>, C<sub>6-14</sub>, C<sub>15+</sub> and totals for the Åre Fm., Green River Shale (GRS), as well as measured and calculated synthetic mixture I/III

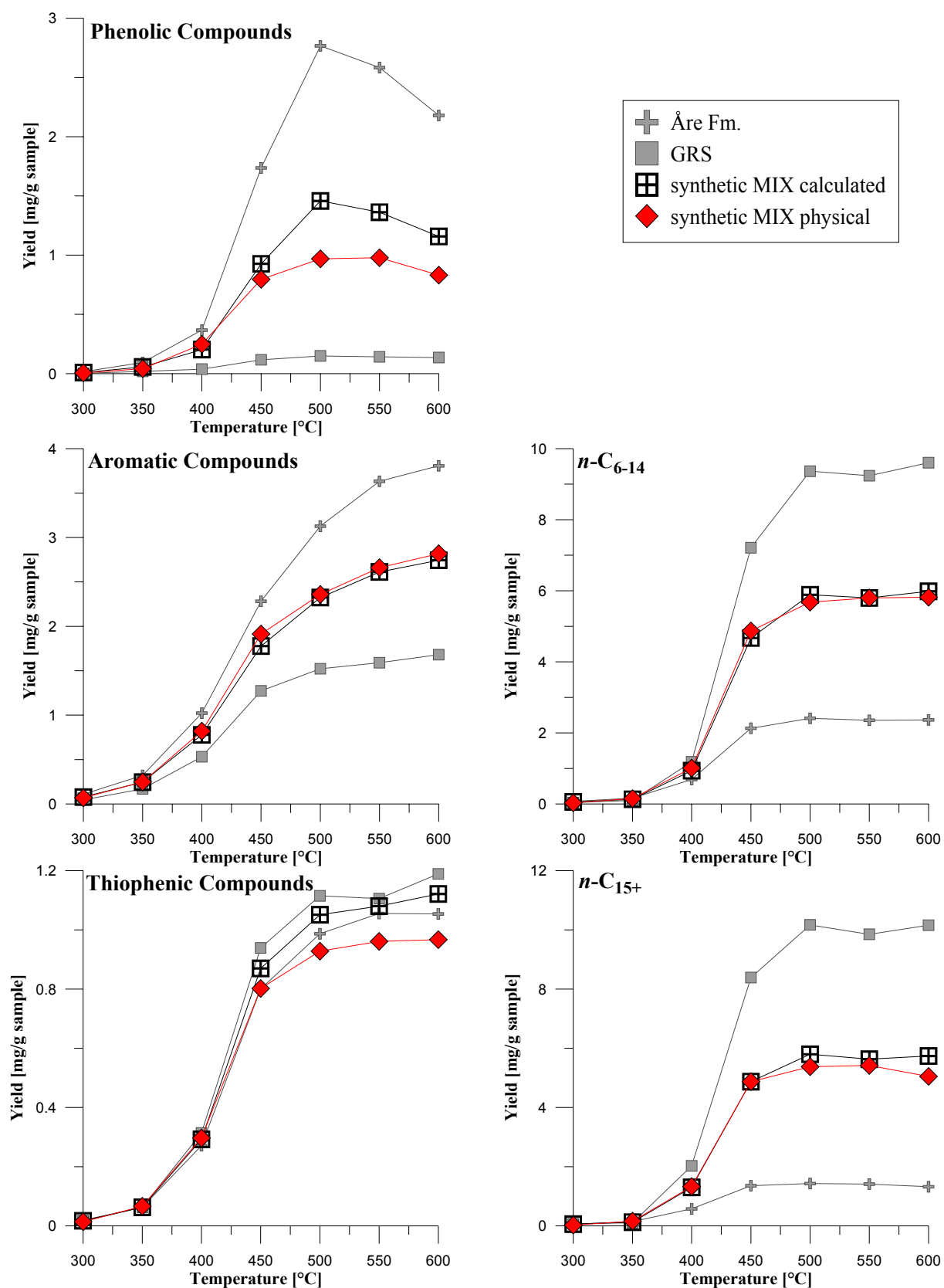


Figure 6.6: Stepwise open-pyrolysis at 1°C/min: cumulative yield curves of single compound fractions phenolic compounds, aromatic compounds, thiophenic compounds and aliphatic compounds  $n\text{-C}_{6-14}$  and  $n\text{-C}_{15+}$  for the Åre Fm., Green River Shale, as well as measured and calculated synthetic mixture I/III

To elucidate more closely which  $C_{6+}$  product classes might be involved in second-order reactions occurring within the pyrolyser or trap, cumulative yield curves of resolved compound fractions phenolic compounds, aromatic compounds, thiophenic compounds and aliphatic compounds  $n-C_{6-14}$  and  $n-C_{15+}$  are displayed in Fig. 6.6 for the same samples. Dry gas and wet gas production is not influenced during all open-system pyrolysis steps (Fig. 6.5) and are therefore not depicted in Fig. 6.6. Resolved aromatic compounds, comprising the most prominent mono- and diaromatic compounds such as alkyl-benzenes and alkyl naphthalenes, as well as aliphatic straight chains of the  $n-C_{6-14}$  and  $n-C_{15+}$  fraction seem not to be heavily influenced by second-order reactions, whereas aromatic compounds yield is slightly increased and  $n-C_{15+}$  yield is slightly decreased. Nevertheless, deviation from expected yield is relatively subtle for the latter compound fractions. In contrast, resolved phenolic and thiophenic compound yields of the physical Type I/III source rock mixture are much lower for temperatures exceeding 450°C than theoretical yields would suggest. Thiophenic compounds yields are even lower than yields of both parent source rocks indicating that compounds which contain heteroelements are involved to a significant extent in second-order reactions once they are generated within the. Bimolecular reactions taking place in the cryogenic trap presumably linked to condensation and cross-linking reactions in the course of rapid cooling are evident for phenolic compounds by decreasing product yields for pyrolysis temperatures in excess of 500°C.

### 6.2.2 Closed-System Pyrolysis

#### *(Stepwise) MSSV-Yields*

Cumulative yield curves of boiling fractions  $C_{1+}$ , methane,  $C_{2-5}$ ,  $C_{6-14}$ , and  $C_{15+}$  are shown in Fig. 6.7 for Åre Fm sample G001965, Green River Shale sample G004750 and the physical and theoretical 50:50 Type I/III source rock mixtures. Stepwise closed-system MSSV-pyrolysis curves are based on heating samples from 250°C to end temperatures up to 780°C regularly spaced by ca. 50°C using a 1°C/min heating rate. Deviations from linearity, which is represented by values defining the theoretical yield curves, can be observed for all boiling fractions but not for all temperature stages. The most pronounced discrepancy between measured and theoretical yields is the enhanced total  $C_{1+}$  compounds generation (or preservation) for temperatures from 400°C up to the latest temperature stage 780°C. This discrepancy can or has to be explained solely by methane being present in higher amounts than expected for temperatures exceeding 450°C. In this temperature region (500 to 780°C) all other boiling fractions of the physical source rock mixture, i.e.  $C_{2-5}$ ,  $C_{6-14}$ , and  $C_{15+}$ , exhibit

values closely resembling those of the theoretical mixture. In contrast, at 450°C  $C_{15+}$  yields are about 5 mg/g sample lower than expected and  $C_{2-5}$  and  $C_{6-14}$  yields are each about 5 to 6 mg/g sample higher than expected which leads together with minor additional methane input to increased  $C_{1+}$  values. It should be kept in mind though that the extra amount of  $C_{1-14}$  compounds can therefore not be solely tracked back to secondary cracking of  $C_{15+}$  compounds. This is even more obvious at end temperature 400°C where all boiling fractions of the physical source rock mixture positively deviate from linearity. One possible explanation for this observation is that the presence of aliphatic material in the admixture provided by the Type I Green River Shale sample G004750 may serve to enhance the solvating properties of the reaction medium and suppress “char” formation at early artificial maturation stages typical for Type III organic matter such as the Åre Fm sample G001965. Nevertheless, in what way this early crosslinking-suppression could lead to unexpected high methane yields at higher temperature stages is not clear yet.

To elucidate more closely which  $C_{6+}$  product classes might be involved in the suppression of “char”-forming reactions cumulative yield curves of resolved compound fractions phenolic compounds, aromatic compounds, thiophenic compounds and aliphatic compounds  $n-C_{6-14}$  and  $n-C_{15+}$  are displayed in Fig. 6.8 for the same samples discussed in Fig. 6.7. Interestingly, aliphatic compounds  $n-C_{6-14}$  and  $n-C_{15+}$  behave like the  $C_{6-14}$  and  $C_{15+}$  boiling fractions previously described. They follow the expected theoretical trend with the exception being found at 400°C and 450°C. At 400°C both fractions show somewhat enhanced product amounts; at 450°C  $n-C_{6-14}$  aliphatic chain yields exceed theoretical yields by 2 mg/g sample but  $n-C_{15+}$  yields are lower by 1 mg/g sample. As discussed in Mahlstedt *et al.* (2008) higher amounts of  $n-C_{6-14}$  and  $n-C_{15+}$  aliphatic chains in the closed-system between 400°C and 450°C might enhance the solvating properties of the reaction medium thereby promoting the mobility of organic species such as polar compounds which provide the agents of hydrogen transfer necessary for the stabilisation of initially formed free radicals (Mitchell *et al.*, 1992; Mansuy *et al.*, 1995; Michels *et al.*, 2000). This improvement of hydrogen transfer efficiency would retard recombination reactions in which phenolic compounds might be involved, e.g. via formation of ether bridges, and inhibit cross-linking between radical sites and adjacent carbons as proposed by Lewan (1997). This is more or less confirmed by phenolic compound yields (Fig. 6.8), which are much higher between 450 and 550°C than theoretical yields would suggest, at 550°C yields even exceed those of the Åre Fm coal sample G001965. A similar trend can be observed for aromatic compounds between 400°C and 550°C hinting to their involvement in recombination reactions.

## 6 FURTHER COMPOSITIONAL CONSIDERATIONS

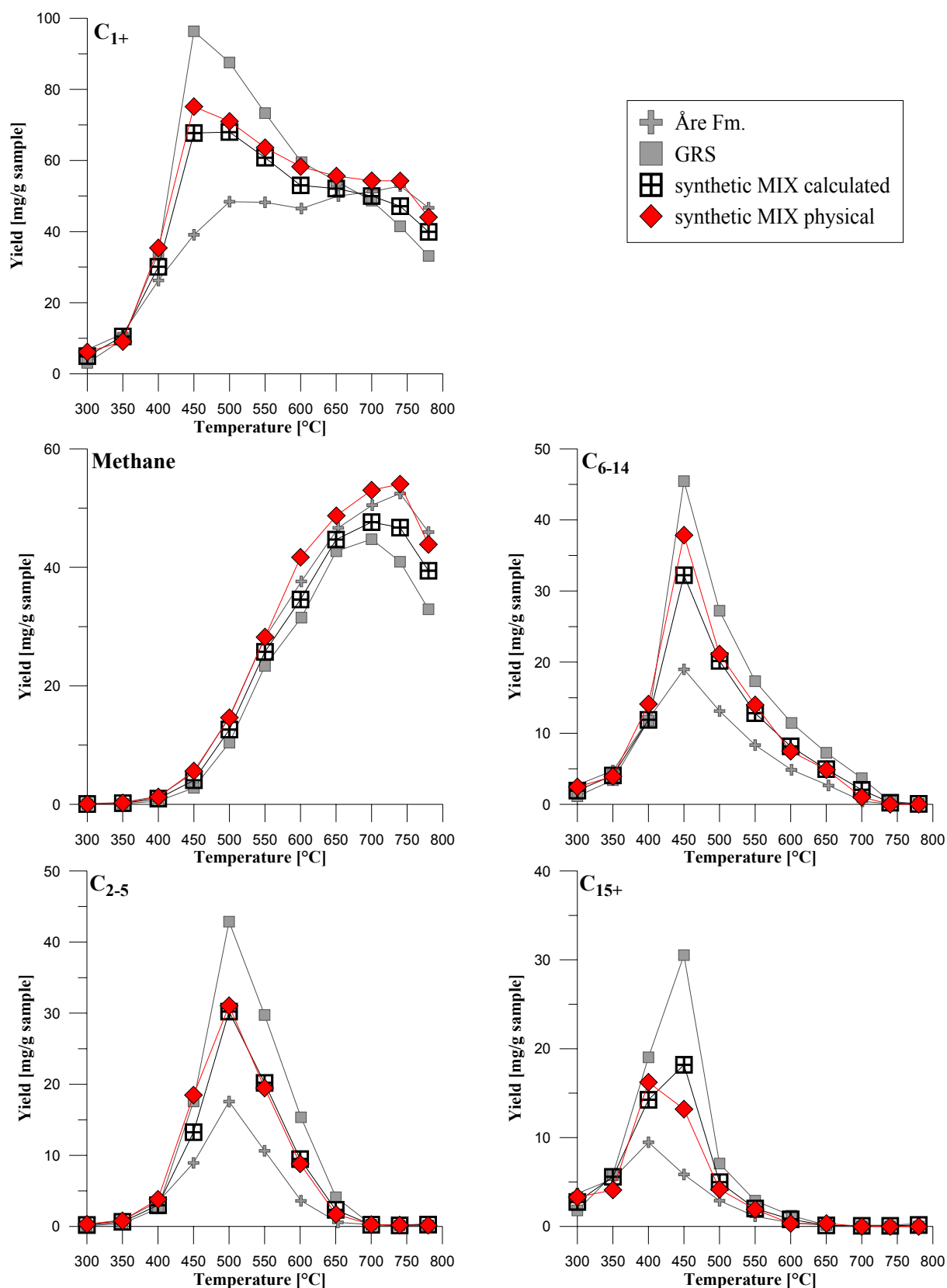


Figure 6.7: Stepwise MSSV-pyrolysis at 1°C/min: cumulative yield curves of boiling fractions methane,  $C_{2-5}$ ,  $C_{6-14}$ ,  $C_{15+}$  and totals for the Åre Fm., Green River Shale, as well as measured and calculated synthetic mixture I/III

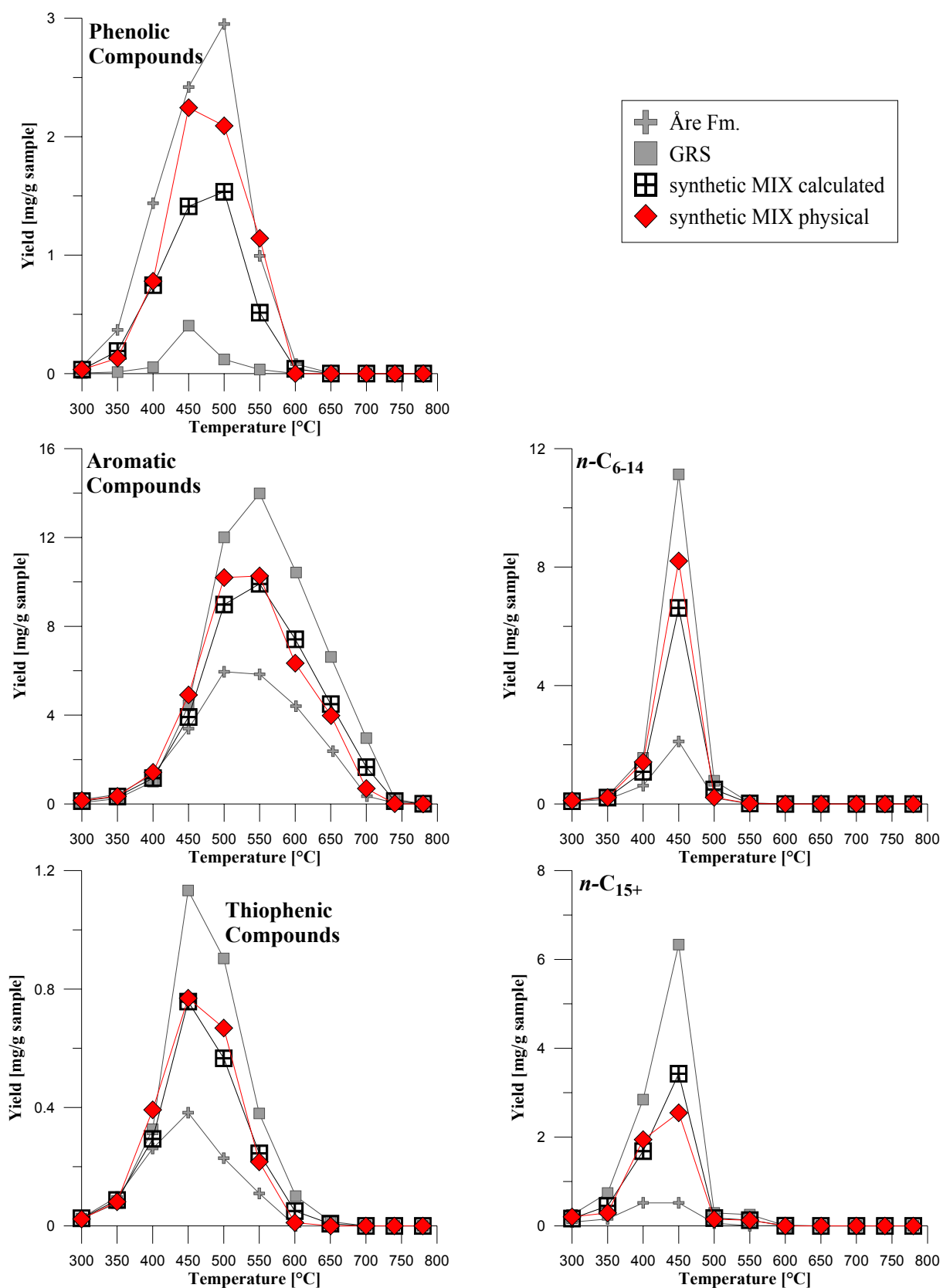


Figure 6.8: Stepwise MSSV-pyrolysis at 1°C/min: cumulative yield curves of single compound fractions phenolic compounds, aromatic compounds, thiophenic compounds and aliphatic compounds  $n\text{-C}_{6-14}$  and  $n\text{-C}_{15+}$  for the Åre Fm., Green River Shale, as well as measured and calculated synthetic mixture I/III

The proposed suppression of recombination reactions seems to be most pronounced between 400°C and 450°C as effects are observable for the aliphatic chains and discrepancies between measured and theoretical yields are highest for phenolic and aromatic compounds. Still enhanced amounts of phenolic and aromatic compounds in the pyrolysate up to 550°C, a temperature region in which partial secondary cracking of those compounds proceeds, are most likely simply an expression of an enhanced presence of the latter at earlier temperature stages. Thiophenic compounds show diverse behaviour probably related to relative low overall yields of single specimen and uncertainties during quantification. Nevertheless, deviation from linearity is subtle.

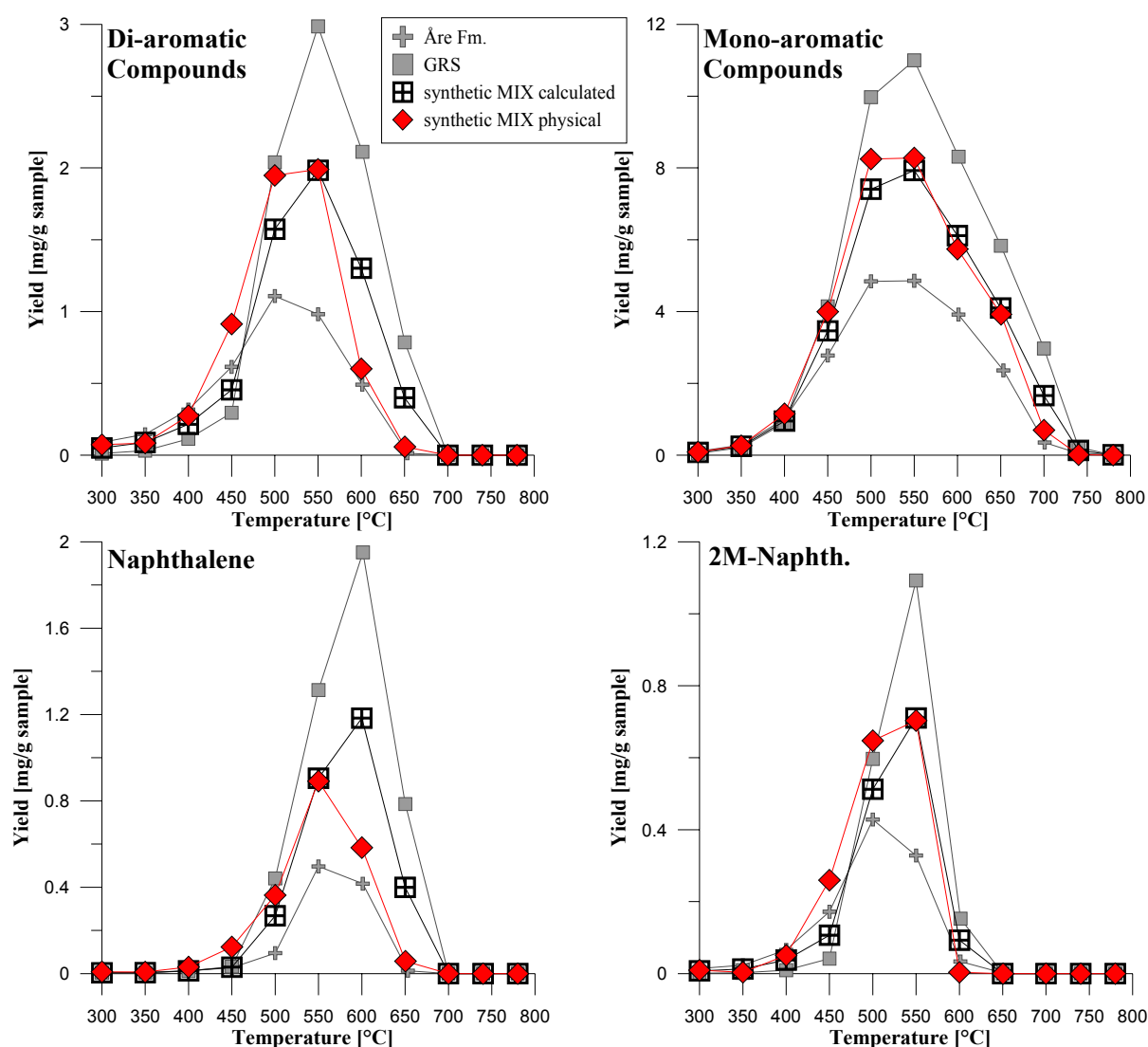


Figure 6.9: Stepwise MSSV-pyrolysis at 1°C/min: cumulative yield curves of di- and mono-aromatic compound fractions as well as Naphthalene and 1M-Naphthalene for the Åre Fm., Green River Shale, as well as measured and calculated synthetic mixture I/III



At 600°C an very interesting feature occurs which is the complete degradation of phenolic compounds in accordance with theoretical trends (as well observed for  $n$ -C<sub>6-14</sub> and  $n$ -C<sub>15+</sub>-fraction) and a fall of measured aromatic compound yields below expected yields, a trend continuing up to 740°C where aromatic compounds vanish. This observation is not easy to explain but falls together with methane yields of the physical source rock mixture markedly jumping above theoretical as well as Åre Fm coal yields at 600°C (Fig. 6.7). It could be presumed here that phenolic compounds undergo second-order reactions during secondary cracking with aromatic compounds or structural moieties within residual organic matter producing coke and extra amounts of methane by the loss of their methyl/alkyl-substituents. It can be best seen in Fig. 6.9 that mono-aromatic compounds are not as strongly influenced by this process than di-aromatic compounds such as naphthalene and 1-methylnaphthalene. The precise mechanism is of course not known and the relevance of second-order reactions for the extra methane input highly speculative. Nevertheless, the concomitant occurrence suggests a connection of both features. The subsequent, constantly higher methane yields of the source rock mixture following theoretical trends up to 740°C simply imply that similar gas generating mechanisms prevail in this temperature region with the “extra”-methane, generated between 550°C and 650°C, being preserved in the closed system. As a consequence it can be stated that secondary late gas (B) generation, taking place in excess of 600°C for similar heating rates under laboratory conditions, is not directly influenced by the previously described bimolecular reactions.

### ***Stable Carbon Isotopes***

In Fig. 6.10 closed-system MSSV pyrolysis based cumulative stable carbon isotopic ratio curves of methane, ethane, and propane are displayed for Åre Fm sample G001965, Green River Shale sample G004750 and the physical and theoretical 50:50 Type I/III source rock mixtures. Theoretical ratio curves (blue) are calculated using isotopic ratios of the parent material weighted by product yield at the relevant pyrolysis temperature. It can be seen at first sight, that measured and theoretical  $\delta^{13}\text{C}$  values fit very well with differences being lower than 2‰ for all temperature stages. Nevertheless, deviations higher than 1‰ can be observed for methane at MSSV temperatures exceeding 450°C and for ethane and propane at temperatures exceeding 400°C. At lower temperature stages, where only primary product generation can be assumed to occur for the respective gases, expected  $\delta^{13}\text{C}$  values are detected rendering the influence of bimolecular reactions to be very unlikely. At higher temperature stages  $\delta^{13}\text{C}$  gas values are uniformly slightly heavier than expected, i.e.  $\delta^{13}\text{C}$  gas

## 6 FURTHER COMPOSITIONAL CONSIDERATIONS

values resemble more closely  $\delta^{13}\text{C}$  gas values of the original Åre Fm coal sample G001965, hinting to the presence of an associated mechanism of relevance.

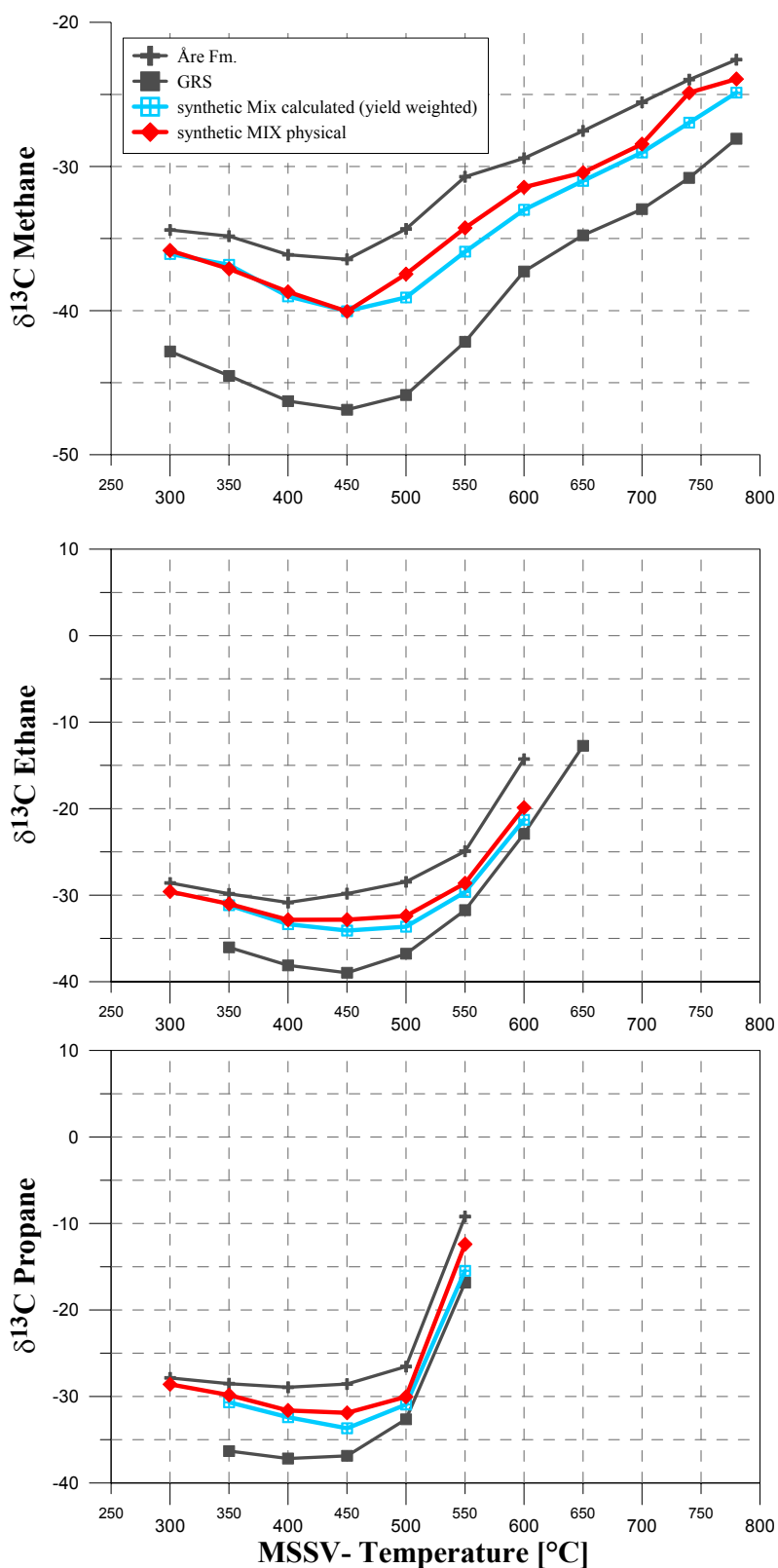


Figure 6.10: Stepwise MSSV-pyrolysis at 1°C/min: methane, ethane, and propane isotopic carbon composition for the Åre Fm., Green River Shale, as well as measured and calculated synthetic mixture I/III

A corresponding mechanism might be found in enhanced  $C_{1+}$  yields observed for temperatures exceeding 350°C with maxima around 450°C for the  $C_{1-14}$  boiling fraction related to a postulated suppression or retardation of “char”-forming reactions relevant for the Åre Fm coal sample G001965. Terrestrial gas precursor structures possess an initially heavier  $\delta^{13}C$  signature than lipid-rich Type I source rocks such as the Green River Shale sample (Silverman, 1967; Degens, 1989). If “char”-forming reactions are indeed suppressed and excess amounts of the original, heavier terrestrial material can be “freed”, isotopic signatures of products of the synthetic source rock mixture should more closely resemble isotopic signature of product of the terrestrial parent organic matter. This should also be valid for secondary cracking products.

### **6.2.3 Closed-System Artificial Maturation: Residues**

Residues of the synthetic Type I/III source rock mixture were prepared under closed-system artificial conditions using a 1°C/min heating rate from 250°C to maturation stages of 350, 400, 450, and 500°C. Those residues were further analysed by open-system pyrolysis to gain information on structural changes within the residual macromolecular organic matter, and by the closed-system MSSV-pyrolysis based late gas potential screening method approach (two end temperatures) to investigate the impact of those structural changes on the high temperature methane generation; results are compared to theoretical results of a hypothetical Type I/III source rock mixture based on open- and closed-system yields of residues of the parent material .

#### ***Residual Organic Matter Composition (Open-Py)***

Pyrolysis-GC has been employed to study the composition of the remaining organic matter after artificial maturation under closed-system pyrolysis conditions. Measured and calculated results such as the chain length distribution and phenol content are displayed in the ternary diagrams of Horsfield (1989) and Larter (1984)(Fig. 6.11a and b) for the synthetic Type I/III source rocks mixture. Further parameters such as Aromaticity, GOR and gas wetness are given in Fig. 6.11c. Generally it can be seen that measured compositional trends resemble expected, theoretical trends but show some major discrepancies revealing bimolecular reactions to take place during artificial maturation. For instance, the relative amount of phenol in the residual organic matter is much lower for the physical than for the hypothetical source rock mixture even though the overall evolutionary trend indicated by the arrow is similar (Fig. 6.11b). This holds not only true for relative but also for absolute phenolic compound yields (Fig. 6.12).

## 6 FURTHER COMPOSITIONAL CONSIDERATIONS

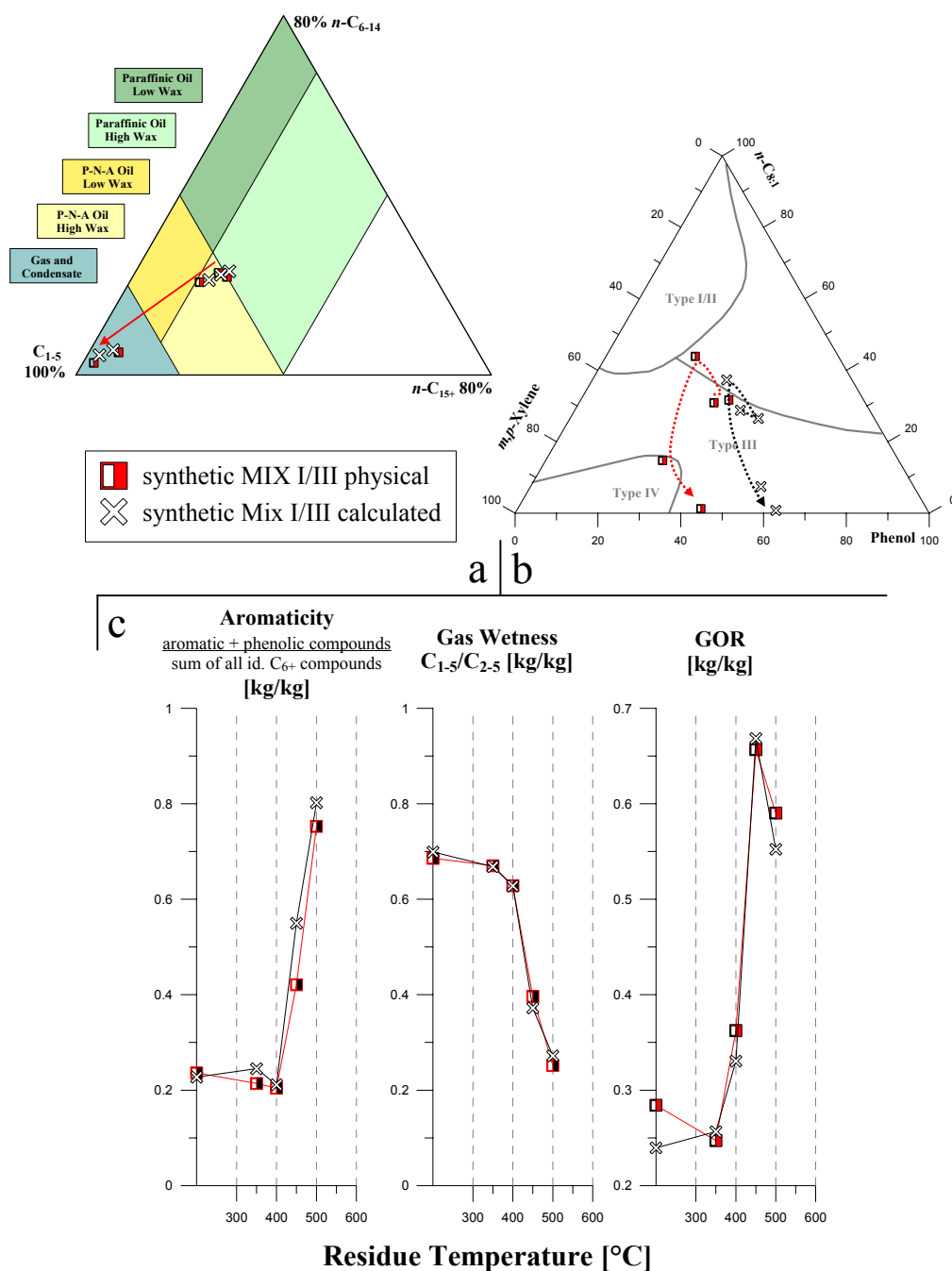


**Figure 6.11: Open-Pyrolysis GC-FID: Evolution of the measured and calculated residue composition of synthetic Type I/III source rock mixture during closed-system artificial maturation displayed in ternary diagrams of a) Horsfield (1989) and b) Larter (1984) as well as expressed in c) gas wetness, GOR, and aromaticity. Arrows indicate the evolution pathway.**

In contrast, the evolution of the chain length distribution within the residue structure seems to behave in the expected way (Fig. 6.11a) leading to almost identical gas wetness and more or less similar GOR's at all heating stages (Fig. 6.11c). The aromaticity, defined as the sum of phenolic and aromatic compounds over all identified  $\text{C}_{6+}$  compounds, follows theoretical trends but is markedly lower for the 450 $^{\circ}\text{C}$  and 500 $^{\circ}\text{C}$  residues related to not only lower absolute phenolic compound yields but also lower absolute aromatic compound yields.

In Fig. 6.12 it can be seen that at the latter temperature stages both compound fractions are the only ones showing major deviation from linearity, thereby explaining deviations from linearity within the  $C_{6-14}$  boiling fraction, whereas methane-, wet gases-,  $C_{15+}$  hydrocarbons-,  $n-C_{6-14}$  and  $n-C_{15+}$  aliphatic chains-, and thiophenic compounds-rest potentials are almost identical. It can be therefore concluded that primarily phenolic and also aromatic compounds are influenced by second-order reactions during artificial maturation in the closed-system. Interestingly, especially with respect to late secondary gas (B) generation, this does not seem to have an overly strong effect on methane and wet gas precursor structures.

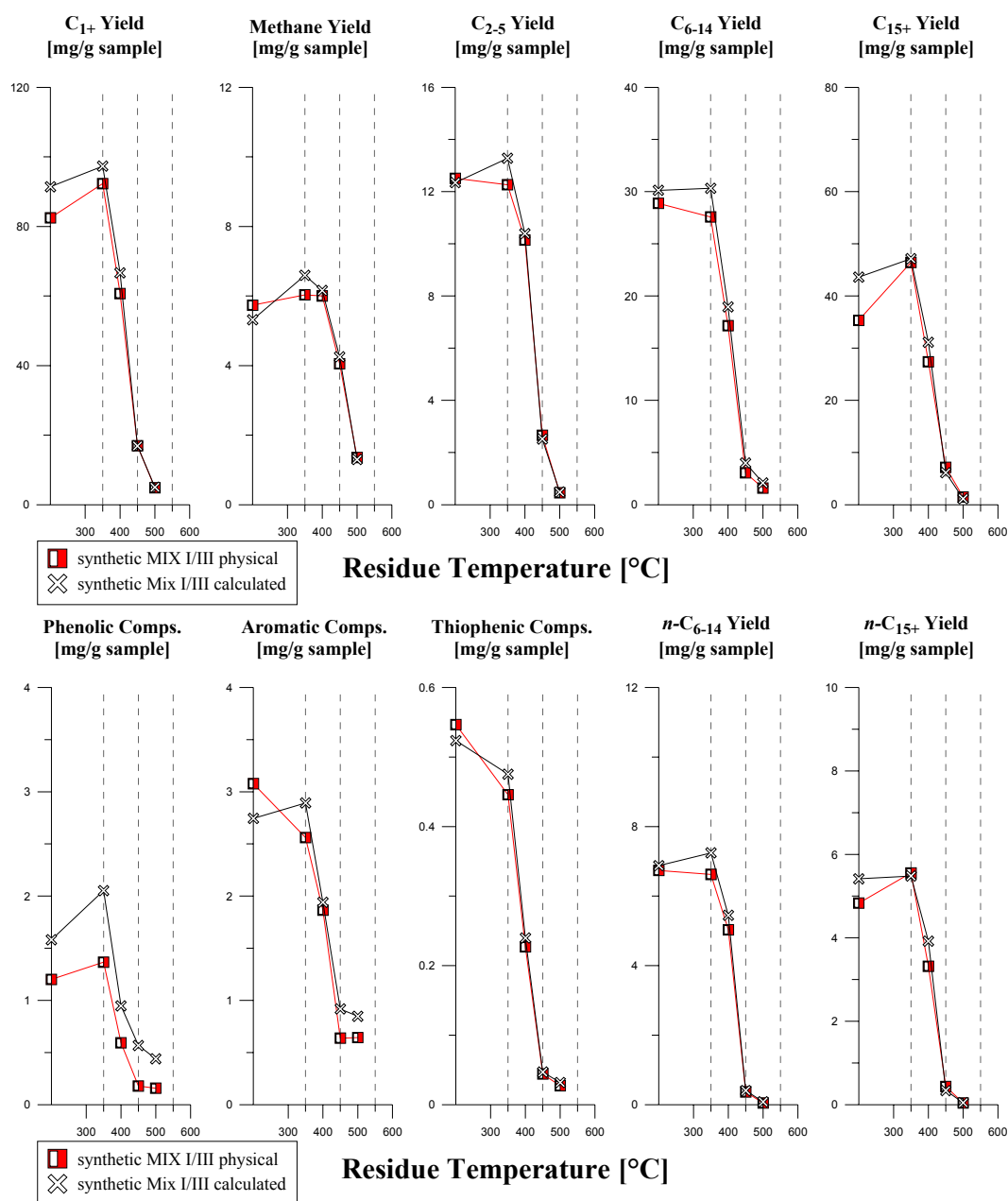


**Figure 6.12: Open-Pyrolysis GC-FID: Evolution of the measured and calculated residue yields of the synthetic Type I/III source rock mixture for boiling fractions methane,  $C_{2-5}$ ,  $C_{6-14}$ , and  $C_{15+}$  as well as for single compound fractions phenolic compounds, aromatic compounds, thiophenic compounds and aliphatic compounds  $n-C_{6-14}$  and  $n-C_{15+}$ .**

For residues exhibiting artificial maturity stages of 350°C and 400°C all measured boiling and compound fraction rest potentials fall under theoretical target values. This is most likely related to the previously discussed suppression of bimolecular, “char”-forming or at least retention reactions leading to an enhanced product release during stepwise MSSV-pyrolysis up to temperatures around 450°C (Fig. 6.7), which leaves the residue depleted in those precursor structures. Identical rest potentials at higher artificial maturity stages point to a reproaching of hydrocarbon generation characteristics due to the concentration of more stable material of similar structure.

### *Late Gas Generation Behaviour and Amount (MSSV-Py GC)*

In Fig. 6.13 measured and theoretical late gas potential screening method results for the 400°C and 500°C residue of the synthetic Type I/III source rock mixture are compared.

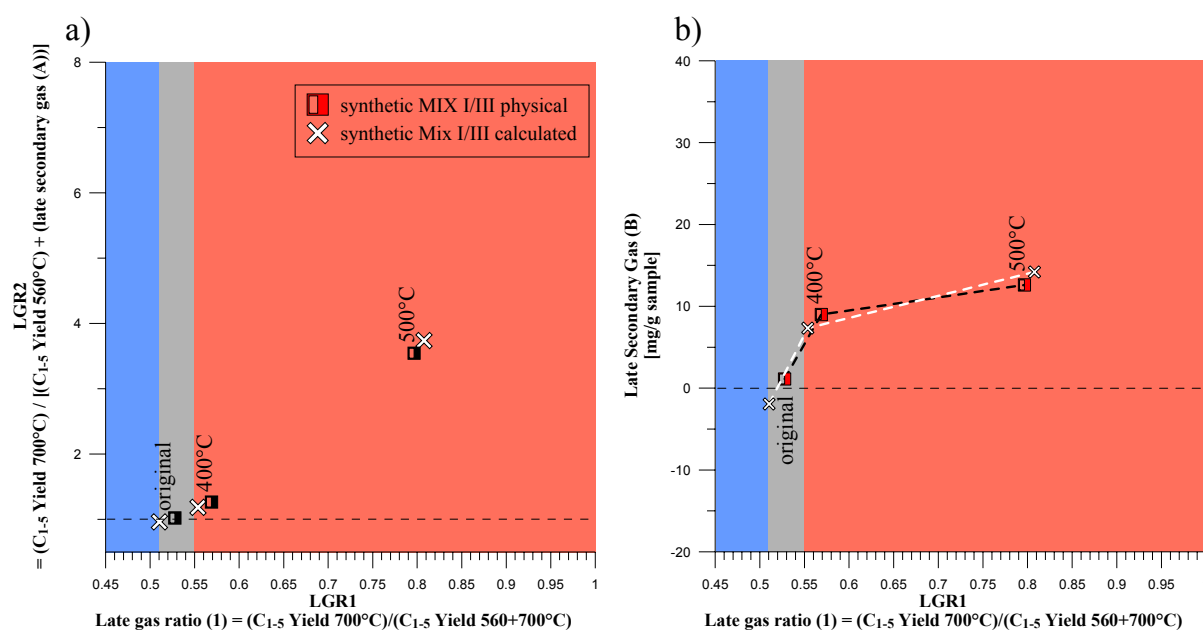


**Figure 6.13: closed-system MSSV-Pyrolysis: Comparison of a) Late Gas Potential (LGR1-LGR2 plot) and b) late secondary gas (B) yield for measured and calculated closed-system artificially prepared residues of the synthetic Type I/III source rock mixture.**

It can be generally said that measured late gas ratios (Fig. 6.13a) of the physical 50:50 mixture residues do not deviate substantially from a linear dependency as calculated late gas ratios are almost similar. It should be kept in mind the great amount of preparative steps when comparing measured to calculated ratios or yields; calculated ratios or yields are based on directly measured ratios or yields of residue of the parent material Åre Fm coal G001965 and Green River Shale G004750. It is in fact striking that especially measured and theoretical absolute secondary gas (B) yields of the synthetic Type I/III residues are very much alike

(Fig. 6.13b). One very important conclusion can be drawn from this observation, which is that even though bimolecular (second-order) reactions influence the evolution of the residual organic matter structure as well as the generated compounds composition and yield for temperatures up to 500°C, late gas generative properties are not seriously effected, at least not during artificial closed-system maturation.. This could again hint to an initially refractory organic matter moiety with a high late gas potential (methylated aromatics) which is simply concentrated during maturation due to chain shortening reactions by  $\beta$ -scission during hydrocarbon generation and product release.

### 6.3 ESR-Measurements (Residues Are Fm. Coal)

ESR signals were detected for Åre Fm Coal sample G001965 as well as for seven corresponding residues prepared under closed-system pyrolysis conditions using a start temperature of 250°C, a heating rate of 1 °C/min and end temperatures 300°C, 350°C, 400°C, 450°C, 500°C, 550°C, and 600°C (Fig. 6.14).

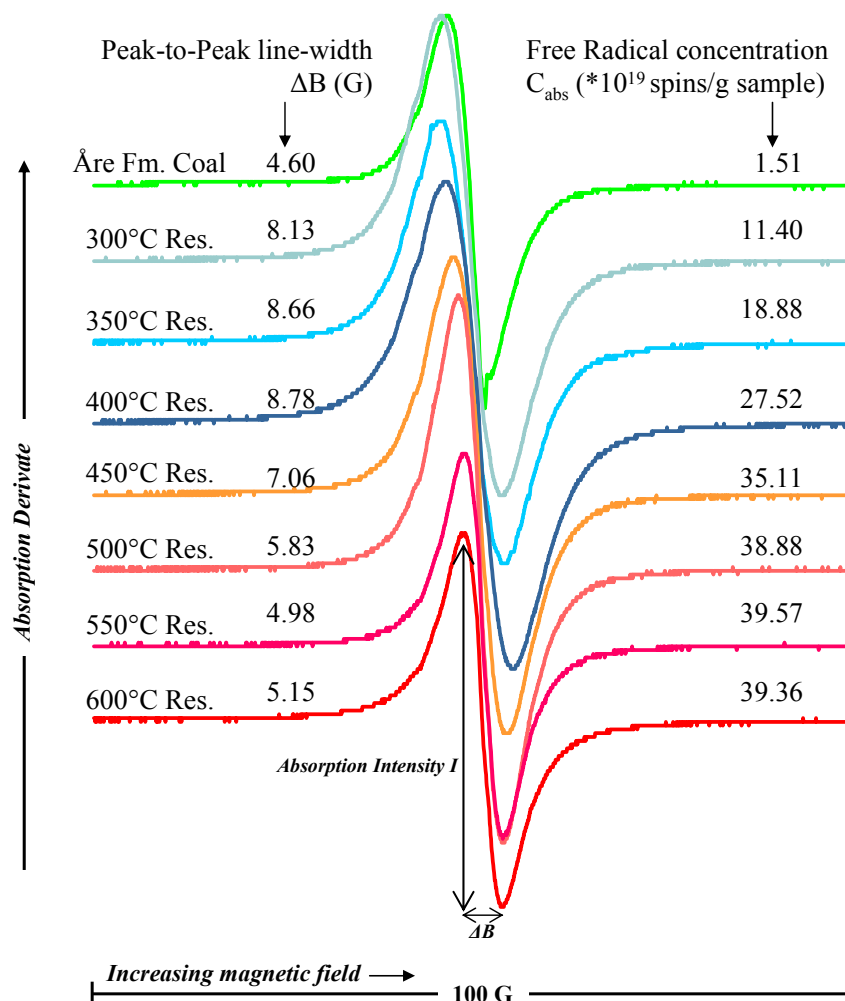


Figure 6.14: ESR Spectra of Åre Fm. Coal sample G001965 and seven corresponding residues artificially matured under close-system pyrolysis conditions to end temperatures between 300 and 600°C.

#### 6.3.1 Evolution of the Free Radical Concentration

According to Marchand and Conard (1980), artificial degradation of immature coals by pyrolysis methods proceeds via the free-radical mechanism (Greensfelder *et al.*, 1949) and will result in larger free radical concentrations and increasing aromatic character of these radicals. During thermal cracking volatile products of small molecular mass are torn off the carbon skeleton of the parent macromolecule leaving “scars” on the latter: one unpaired



electron for each broken chemical bond. Those unpaired electrons, free radicals, can of course recombine via new electron pairings, bond rearrangements or hydrogen saturation, but some free radicals are stabilised by delocalisation throughout an aromatic polynuclear structure and can be measured by ESR-methods as they remain for a quasi-infinite time. Various ESR parameters indicate that unpaired electrons in coals and kerogens as well as signals in Fig. 6.14 are associated with similar aromatic clusters in which they are stabilised as  $\pi$ -electrons (Premovic, 1992, and personal communication with Pöppl). Increasing radical concentrations with artificial or natural maturity throughout the catagenesis zone are therefore an expression of an increasing amount of polyaromatic paramagnetic structures within the residual organic matter related to the loss of labile kerogen. This trend can be as well observed in Fig. 6.15 for the present artificial maturity sequence of Åre Fm Coal sample G001965. Free radical concentrations increase from an initial concentration of  $1.51\text{E}+19$  spins/g sample for the original coal sample to a maximal concentration of  $3.96\text{E}+20$  spins/g sample for the  $550^\circ\text{C}$  residue.

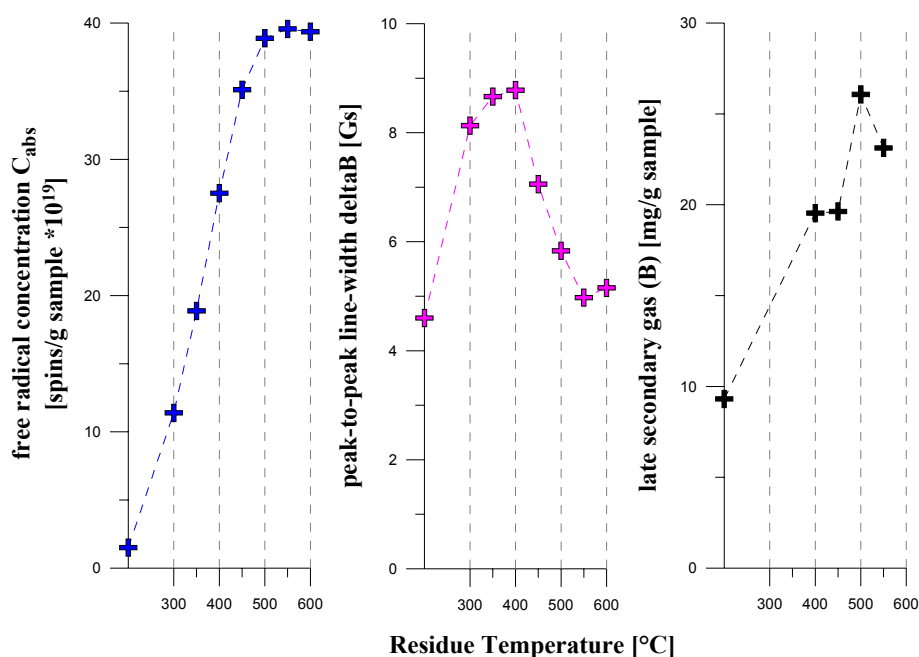


**Figure 6.15:** Closed-system maturation end temperature versus ESR-parameter absolute free radical concentration  $C_{abs}$ , peak-to-peak line-width  $\Delta B$ , as well as late secondary gas (B) yields for investigated Åre Fm. sample and corresponding residues.

Interestingly, the slope of the free radical concentration curve begins to already flatten out at artificial maturity stages around  $500^\circ\text{C}$  ( $C_{abs.} = 3.89\text{E}+20$  spins/g sample) and even decreases for temperatures exceeding  $550^\circ\text{C}$ . Marchand and Conard (1980) state that at such high concentrations the mean distance between radicals is in the order of 30-40 Å and small enough to allow direct combinations. When the rate of recombination, ostensibly proceeding

via condensation reactions of aromatic nuclei (Oberlin *et al.*, 1980), grows larger than the rate of creation of free radicals, their concentration starts decreasing. As condensation reactions were suggested to be partly responsible for triggering high temperature methane generation, late secondary gas (B) yields of residues are also depicted in Fig. 6.15. It is noteworthy that late gas generative properties increase together with the free radical concentrations up to 500°C (residue temperature) and then decline for higher temperature stages. A contribution of condensation reactions on the degradation of late gas precursor structures can therefore not easily be neglected. Furthermore, the closed-system residue of Westphalian Coal sample G000721 matured to 500°C was extrapolated to possess maturity levels around ~2.0%  $R_o$  (Fig. 5.17). Artificial maturation to 550°C of the Åre Fm Coal sample G001965 should therefore have brought about maturity levels exceeding ~2.0%  $R_o$  adding evidence to the conclusion that onset of late gas generation can be found at such elevated temperature levels.

### 6.3.2 Evolution of the Peak-to-Peak Line-Width

The peak-to-peak line-width  $\Delta B$  is measured on the first derivative (pictured in Fig. 6.14) of the absorption spectrum and is probably an expression of the proximity of the unpaired electron to nuclei with magnetic moments (Marchand and Conard, 1980; Premovic, 1992). In Fig. 6.15 it can be seen that the line-width increases from 4.60 Gs at immature stages to 8.78 Gs for the 400°C residue concomitant to the cracking and release of the most labile heteroelement-containing compounds leading to a decrease in overall aromaticity and increase in  $C_{1+}$  yield (compare Fig. 5.12). The subsequent hydrocarbon generation and release via chain shortening reactions leads to an increasing aromaticity and concentration of polyaromatic structures within the residual organic matter possibly explaining the trend of decreasing line-width up to 4.98 Gs for the 550°C residue. According to Bakr *et al.* (1990) aromatic molecules may have a tendency to stack thereby causing the radical electron to hop from one aromatic electron host to an adjacent one. This leads to an overlapping of the electronic wave functions of adjacent radicals which promotes a phenomenon called radical exchange perhaps responsible for the narrowing of the resonance line. Interestingly, the line-width flattens out for higher temperature stages (Fig. 6.15) in correspondence with the free radical concentration trend indicating that aromatic nuclei are too closely stacked and start to condense.

It can be concluded that results of ESR measurement on artificially matured residues of immature coal fit very well in the general scheme constructed to explain late gas, i.e. high temperature methane generation.

## 6.4 Conclusion

The purpose of this chapter was to discuss additional experiments shedding some more light on compositional changes of organic matter during pyrolysis. Here especially the role of second order reactions, i.e. interaction between bitumen and residual kerogen, during maturation and their effect on late gas generation are considered by gas isotopic composition at high-temperature closed-system pyrolysis conditions for four different immature source rocks stemming from various depositional environments and by applying open- and closed-system pyrolysis methods to a synthetic source rock mixture (Type I/III). Furthermore ESR measurements on coal residues yielded information on changes within the residual organic matter during artificial maturation.

Observed stable carbon isotope ratio trends of methane for the immature samples Type III Åre Fm. Coal G001965, Type I Green River Shale G004750, synthetic Type I/III source rock mixture, and Type II Spekk Fm. shale G001955 resemble the v-shape already described in various publications where closed-system pyrolysis was used for investigation with minima around 450°C MSSV-temperature. The consecutive double v-shape observed by Dieckmann *et al.* (2006) indicating the recombination of C<sub>6+</sub> gas precursor structures and neoformation of a thermally stable gas precursor possibly yielding additional methane at extreme maturities could not be replicated in the present work. In addition, an isotopic reversal of methane or ethane at high artificial maturity stages (up to 780°C) could not be simulated, which would have yielded further evidence for the existence and degradation of a high temperature gas precursor structure. Nevertheless, based on the relative heavier carbon isotopic signature of gases from a physical synthetic Type I/III source rock mixture in comparison to a theoretical synthetic Type I/III source rock mixture one can assume that aliphatic material provided by the Type I parent material led to a suppression of second-order recombination reactions occurring in the terrestrial Type III parent material “freeing” higher amounts of terrestrial products with an terrestrial isotopic signature.

From comparing open- and closed-system pyrolysis data of the synthetic Type I/III source rock mixture and its corresponding closed-system residues to data of its parent material Åre Fm. Coal G001965 and Green River Shale G004750 it can be learnt that second-order reactions can be evidenced under closed-system conditions as well as under open-system conditions, whereas under open-system conditions bimolecular reactions do not occur between first formed bitumen and residual organic matter but between primary products in the liquid nitrogen cooled trap. In both systems presence of phenolic compounds, initially found

in the terrestrial organic matter, plays the most important role. It can be generally concluded that second-order reactions are only indirectly evidenced to occur during the maturation of terrestrial organic matter as recombination reactions are suppressed or retarded by the presence of Type I organic matter or its pyrolysis products. One major conclusion can be drawn from using the established late gas screening method on artificially matured residues. Even though bimolecular (second-order) reactions influence the evolution of the residual organic matter structure as well as composition and yield of generated compounds for temperatures up to 500°C, late gas generative properties are not seriously effected hinting to the presence of an initially refractory organic matter moiety with a high late gas potential (methylated aromatics), which is simply concentrated during maturation due to chain shortening reactions by  $\beta$ -scission during hydrocarbon generation and product release.

ESR measurement on artificially matured residues of the immature Åre Fm. Coal G001965 fit very well in the general scheme constructed to explain late gas generation. During hydrocarbon generation via  $\beta$ -scission and product release not only an enrichment of methyl aromatics occurs, but also an increase in the free radical concentration within the residual organic matter explainable by an increasingly aromatic character. The advocated mechanism of high temperature methane production is the final demethylation of residual aromatic nuclei within spent organic matter by  $\alpha$ -cleavage mechanisms involving condensation reactions of aromatic clusters. Decreasing radical concentrations between 550°C and 600°C in residues of the Åre Fm. Coal G001965 represent additional support for the relevance of this process.

## 7 CONCLUSION AND PERSPECTIVES

### 7.1 *Major Conclusions*

It can be concluded that the major goal, to assess amount and timing of late dry gas generation from source rocks at high thermal maturity levels, was reached.

- The existence of a late gas potential of ~40 mg/g TOC for every type of source rock at maturities around 2.0%  $R_o$  was demonstrated. The absolute amount of high temperature methane generated from a mature source rock in a given kitchen area of defined dimensions would therefore be strongly coupled to the TOC content of the source rock.
- The late methane forming reaction itself can be described by a single activation energy  $E_a$  of ~55 kcal/mol and a surprisingly low frequency factor of only ~5.00E+09 1/s. Extrapolation to a linear geologic heating rate of 3°C/ma revealed in accordance with previously published data of Erdmann and Horsfield (2006) onset temperatures of ~220°C for a calculated  $R_o$  of ~2.5% and a geologic  $T_{max}$  of ~240°C at 3.1%  $R_o$ . The calculated end of the reaction at temperatures of ~250°C (3.5%  $R_o$ ) seems to be rather low but is most likely related to the degradation of methane at high pyrolysis temperatures and consequently to the overprinting of ongoing methane formation by cracking of methane under laboratory conditions.
- A decrease of the late gas potential for naturally matured source rocks exhibiting vitrinite reflectances exceeding 2.0%  $R_o$  confirms that previous and present timing predictions based on the evaluation of immature organic matter are valid and that high temperature methane generation under geologic conditions is a reality and not a laboratory artefact.

Three key questions related to high temperature methane generation were answered in the course of the project.

1.) “Which types of source rocks possess a late gas potential in general?”

- The usage of natural and artificial maturity series as a calibration tool led to one major outcome of the thesis which is that any kerogen type possesses a late gas potential of ~40 mg/g TOC at maturities around 2.0%  $R_o$ . Nevertheless, the amount of high temperature methane generated is strongly influenced by initial TOC contents and carbon loss during catagenesis. Homogeneous, paraffinic Type I and Type II organic matter of aquatic lacustrine and marine origin e.g. could be assigned a low late gas potential as they are good expeller during natural maturation and “loose” great amounts of their initial carbon content. In contrast, more heterogeneous marine or mixed marine-terrestrial to terrestrial

source rocks could be assigned intermediate to high late gas potentials as retention of C<sub>6+</sub> compounds within the residual organic matter potentially leads to preservation of TOC.

- Using a novel, rapid MSSV-pyrolysis screening method spanning the main stage of late gas generation subsequent to primary gas generation and secondary gas generation by cracking of oil compounds, source rocks can be assigned low, high, or intermediate late gas potentials on the basis of a newly implemented index that comprises two late gas ratios (LGR1; LGR2). With those discrimination between late gas derived from cracking of remaining C<sub>6+</sub> compounds, called late secondary gas (A), and late gas derived from degradation of a residual, thermally stable moiety, called late secondary gas (B), is possible. High late gas potentials (LGR1 >0.55; LGR2 >1) are mainly associated with heterogeneous aromatic and/or phenolic Type III and Type II/III shales and coals stemming from fluvio deltaic – terrestrial or mixed marine – terrestrial environments. Low late gas potentials (LGR1 <0.51; LGR2 <1) can be recognised for Type I or Type II homogeneous, paraffinic organic matter of aquatic lacustrine and marine origin. Source rocks exhibiting intermediate late gas potentials (LGR1 0.51-0.55; LGR2 <1 or >1) are mainly associated with heterogeneous marine source rocks containing algal or bacterial derived precursor structures of high aromaticity, or with source rocks deposited in aquatic environments containing minor amounts of aromatic/phenolic higher land plant material.
- The employment of a large series of immature source rocks (65 samples), shales and coals covering all main kerogen types and depositional environments, puts the relationship of initial organic matter structure and late gas potential on a statistically more powerful basis than any other previously published study.

2.) “Which molecular compositional changes of initial kerogen structure and early formed bitumen might be involved?”

- Using natural maturity sequences and under both, open- and closed –system conditions artificially matured samples from different depositional environments as well as synthetic source rock mixtures, it could be shown that second-order reactions between first formed bitumen and residual organic matter, a process Erdmann and Horsfield (2006) and Dieckmann *et al.* (2006) assumed to be a prerequisite for high temperature methane generation, do not play a crucial role for the development of a late gas potential during natural and artificial maturation (only for TOC preservation).
- The most likely mechanism responsible for the increase of the late gas potential to ~40 mg/g TOC at 2.0% R<sub>o</sub> is an enrichment of late methane precursor structures (methyl-

aromatics), which proceeds via chain shortening reactions by  $\beta$ -scission during hydrocarbon generation within the oil window and via simple concentration of refractory organic matter due to the release of labile compounds.

- Natural maturation in the diagenesis to early catagenesis zone seems to cause a slight late gas potential loss as evidenced for unextracted and extracted coals from New Zealand (0.4 – 0.8%  $R_o$ ) which possibly is related to the loss of late gas precursor structures together with the most unstable O-bearing functional groups and low molecular weight compounds such as acetate.

3.) “How are these changes manifested in kinetic parameters and stable isotopic compositions?”

- As natural trends confirm calculations conducted using an immature coal sample, kinetic parameters of late gas generation seem not be influenced by compositional changes of the initial kerogen structure during maturation. The kinetic parameters are characteristic for the advocated mechanism of high temperature methane production which is the final demethylation of residual aromatic nuclei within spent organic matter by  $\alpha$ -cleavage mechanisms involving condensation reactions of aromatic clusters. Late dry gas formation takes place after possible second-order stabilisation reactions observed e.g. for naturally matured Carboniferous coals at lower maturity stages (Schenk and Horsfield, 1998) and is therefore kinetically unaffected of those. The latter reactions have only an effect on the absolute late gas potential (TOC influence) as they were shown to lead to the retention of organic matter marking predictions of primary hydrocarbon generation or composition as invalid.
- Confirming the conclusion that second-order processes do not play a crucial role for the development of a late dry gas potential, the observed stable carbon isotope ratio trend for methane is similar in terms of shape (v-shape) for all investigated immature source rocks from various depositional settings initially exhibiting low to high late gas potentials. A w-shape hinting to the recombination of  $C_{6+}$  gas precursor structures and neoformation of a thermally stable gas precursor yielding additional methane at extreme maturities as reported by Dieckmann *et al.* (2006) could not be replicated for any sample in the present work. Nevertheless, measurements on naturally matured samples were not conducted which prohibits excluding a possible effect of second-order reactions on isotopic signatures to occur.

## 7.2 *Perspectives*

The amount and timing of late dry gas generation from source rocks at high thermal maturity levels was assessed and calculated. This has important implications for the exploration of deeply situated conventional hydrocarbon systems as well as for unconventional, overmature shale gas plays. In the future, the existence of a late gas potential of ~40 mg/g TOC at maturities around 2.0%  $R_o$  should be taken into account for the calculation of total gas in place (GIP) because precursor structures are sure to remain in the source rock during maturation, in contrast to retained oil which in many cases may have already left the source rock soon after its generation. In addition, high levels of organic matter conversion potentially provide, besides input of additional amounts of late gas, high-flow-rate gas systems (Jarvie *et al.*, 2001; Jarvie *et al.*, 2007).

### *The impact of additional late gas generation on the total petroleum potential*

One logical consequence of the existence of a late gas potential (40 mg/g TOC) which is not detectable by routinely used open-system pyrolysis evaluation methods is that its impact on the total hydrocarbon potential as defined by Rock-Eval pyrolysis is much higher for source rocks with an initially low Hydrogen Index. For instance, typical Type III kerogens or humic coals exhibit Hydrogen Indices greater than 150 mg HC/g TOC and late gas (40 mg/g TOC) would add an extra charge amounting up to ~27% of the initial potential. This extra charge would be much smaller for a lacustrine Type I source rock exhibiting an HI of 900 mg/g TOC (up to ~4.5%). For marine shales, especially for those Paleozoic in age, Hydrogen Indices are lower and late gas input can be as high as up to ~10% of the initial petroleum potential (for an HI of 400 mg/g TOC). Nevertheless and because the absolute late gas yield strongly depends on the TOC content prior to metagenesis, source rocks comprising Type I or Type II kerogen should not be neglected when evaluating e.g. thermogenic shale gas plays because especially marine source rock successions can be very thick and often persist over very large geographical areas equalling high total late gas volumes.

To exemplify the importance of such an additional late gas input during metagenesis of any source rock type, i.e. in addition to secondary gas formed by the cracking of retained oil compounds, the value 40 mg methane/g TOC was used to calculate gas amounts in Tcf gas/km<sup>3</sup> rock or m<sup>3</sup> gas/m<sup>3</sup> rock as a function of rock density and TOC (Fig. 7.1 left side). One can see at first sight that yields are significant, especially for coals or coaly shales for which more than 1 Tcf gas/km<sup>3</sup> can be expected when TOC contents exceed 25%. For organic-rich shales exhibiting TOC contents between 5 and 10% yields are much lower, but 0.25 – 0.5 Tcf



gas/km<sup>3</sup> rock or 7 – 14 m<sup>3</sup> gas/m<sup>3</sup> rock might be formed. Generation of this gas would still add e.g. ~10% to the estimated total generation potential of the Barnett Shale (84.0 m<sup>3</sup>/m<sup>3</sup>) as evaluated by Jarvie *et al.* (2007).

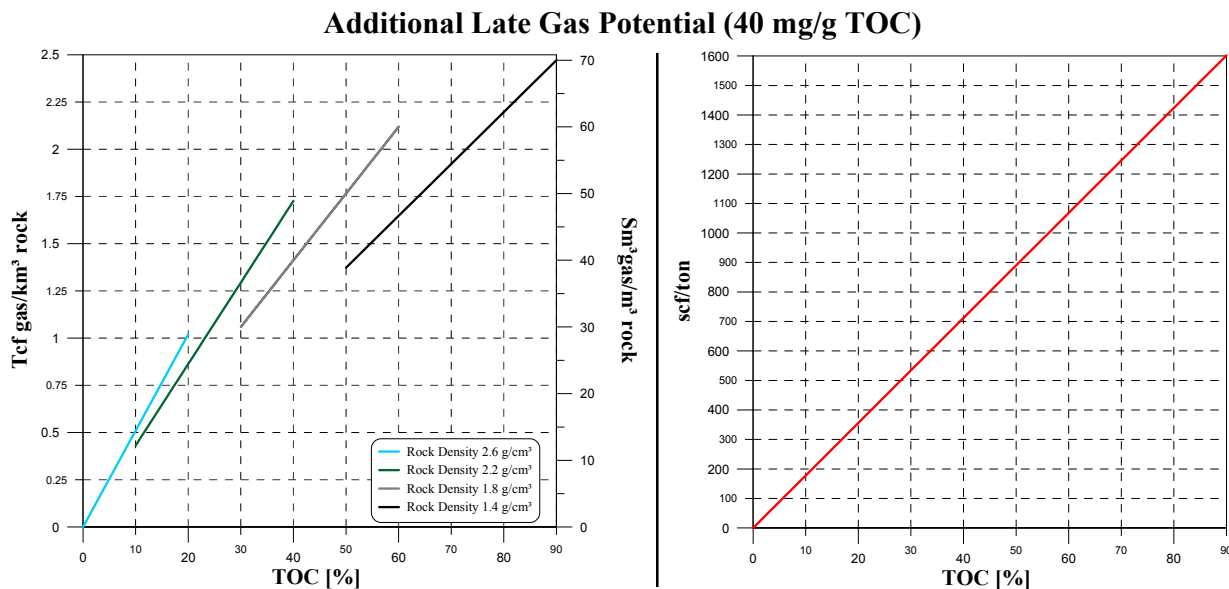


**Figure 7.1: Additional Late Gas Input in Tcf/km<sup>3</sup>, Sm<sup>3</sup>/m<sup>3</sup>, and scf/ton as a function of TOC**

#### *Importance of TOC content and consequences for “late gas exploration”*

As TOC content has such a strong impact on the total amount of generated late gas, source rocks which tend to retain organic matter by second-order recombination reactions between first formed C<sub>6+</sub> compounds and residual organic matter appear to be “late gas prone” and attractive late gas exploration targets. Besides humic coals, this applies to heterogeneous source rocks which comprise fractions of higher land plant derived organic matter or source rocks whose organic matter is of an intrinsic aromatic character. The latter was demonstrated for especially Paleozoic source rocks, previously e.g. for the Cambrian Alum Shale in Sweden (Horsfield *et al.*, 1992a) or the Pennsylvanian-Mississippian Bakken Shale in North America (Muscio and Horsfield, 1996), or in the current work and using open-system pyrolysis GC-FID for detailed kerogen characterisation for various Silurian source rocks from North-Africa and The Middle-East, but also for many paleozoic black shales from North America (Woodford Shale, Barnett Shale, Caney Shale, Exshaw Fm., etc.). Silurian Hot Shales exhibited, besides the Cambrian Alum Shale, highest aromaticity and sometimes already high late gas potentials (LGR1 > 0.55) at immature stages prior to the documented late gas potential increase during catagenesis.

Therefore and mirrored by the interest and activity of many petroleum companies, Silurian Shale appears to be a very attractive candidate for shale gas exploration. It is thick, organic-rich, and laterally extensive throughout North-Africa and The Middle-East, e.g. Illizi Basin (Algeria), Ghadames Basin (Tunisia, Algeria, Western Libya, Jordan (West Risha), but also e.g. in Poland (and Ukraine) with sufficient maturity levels for late gas generation e.g. in the Baltic Depression of North Poland (Lane Energy, BNK, ExxonMobil, ConocoPhillips). Cambrian Alum Shale of Sweden is also of interest (Shell) for late and shale gas and comprises beneficial maturity levels, TOC content and lateral extension. Cambrian to Silurian strata of a not necessarily marine origin is also appraised for shale gas outside Europe, e.g. in the Sichuan Province, China (Shell, Petrochina) or in various basins throughout Australia (e.g. Cooper Basin, Perth Basin, Georgina Basin). It should be stated here that of course not all potential (and thermogenic) shale gas prospects in Europe are early Paleozoic in age. The most important and promising ones are the Toarcian Posidonia Shale (Germany, France), the Cretaceous Wealden (Lower Saxony Basin), and the Namurian Bowland Shales (U.K.).

#### *Gas storage capacity*

One important consideration is whether the gas storage capacity of shales or coals suffices to store the additional late gas or not. To solve that question is not really easy as storage capacity changes with maturity of the organic matter, kerogen type, TOC content, mineralogy, reservoir pressure, and reservoir temperature. Generally it can be said that at maturities  $>2\%$   $R_o$  (anthracite) adsorption capacity of organic matter is much higher than at immature stages (Jenkins and Boyer, 2008) caused by an increased microporosity (Ross and Bustin, 2009) due to the separation of stacked layers of polyaromatic rings by about 0.34 - 0.80 nm (Oberlin *et al.*, 1980; Jarvie *et al.*, 2007). Furthermore, reservoir pressure increases with increasing burial depth allowing more gas to be sorbed. In addition, secondary porosity is created by organic matter decomposition for maturity levels  $>1.4\%$   $R_o$  potentially providing the space for generated late methane. Jarvie *et al.* (2007) calculated for a source rock (Barnett Shale) with an average TOC of 6.41 wt.-%, equalling 12.7 vol.-% using an assumed organic matter density of 1.18 g/cm<sup>3</sup>, that 4.3 vol.-% secondary porosity would be generated in the dry gas window.

In Fig. 7.1 (right side) the additional late methane input, if completely realised (40 mg/g TOC), is given in scf/ton as a function of TOC. Organic-rich shale exhibiting a TOC content of 5% would generate ~100 scf/ton late methane. Jarvie *et al.* (2007) calculated for a Barnett shale comprising 6% porosity that it provides a maximal storage capacity of 159

scf/ton at typical reservoir conditions (70°C, 26.2 MPa) and a maximal storage capacity of 250 scf/ton at maximum burial depth (180°C, 55.2 MPa). Therefore and by numbers, late gas could be easily collected within the shale reservoir at maximum burial depth (of the Barnett Shale), of course also depending on how much primary and secondary gas already occupies sorption sites or free pore space. By any means, subsequent uplift would result in a decrease of pressure leading to desorption of gas and filling of pore spaces which might impact on an easier release of gas during initial production.

For coals, absolute additional late methane amounts are much higher. For a TOC of 85% (previous to metagenesis) 1500 scf/ton could be expected (Fig. 7.1 right side) which is about as high as the absolute methane sorption capacity of many anthracites (Langmuir Volume), of course depending on TOC content, reservoir temperature and pressure. As nearly all coalbed gas is considered to be sorbed gas (Jenkins and Boyer, 2008) sorption capacity defines maximal gas storage capacity. Thus, it will not be possible to accumulate all additional generated late gas within the coal matrix because during coalification coals already generate more gas than their capacity to retain gas increases (Meissner, 1984; Clayton, 1998; Bustin and Bustin, 2008). Nevertheless, excess methane may migrate into adjacent strata resulting in saturation of otherwise undersaturated coals or it may help to fill the cleat system to account for dry coals. For gas production from coalbed reservoirs, gas saturation and dryness (no water) are beneficial during initial completion as dewatering could require years (Jenkins and Boyer, 2008).



## REFERENCES

- Abella, C., Moutesinos, E., Guerrero, R.M., 1980. Field studies on the competition between the purple and green sulfur bacteria for available light. *Dev. Hydrobiol* 3, 173-181.
- Abrajano, T.A., Sturchio, N.C., Bohlke, J.K., Lyon, G.L., Poreda, R.J., Stevens, C.M., 1988. Methane-hydrogen gas seeps, Zambales Ophiolite, Philippines: Deep or shallow origin? *Chemical Geology - Origins of Methane in the Earth* 71, 211-222.
- Al Darouich, T., Behar, F., Largeau, C., 2006. Thermal cracking of the light aromatic fraction of Safaniya crude oil - experimental study and compositional modelling of molecular classes. *Organic Geochemistry* 37, 1130-1154.
- Arneth, J.-D., Matzigkeit, U., 1986. Variations in the carbon isotope composition and production yield of various pyrolysis products under open and closed system conditions. *Organic Geochemistry* 10, 1067-1071.
- Atkins, P., de Paula, J., 2002. *Atkins' Physical Chemistry*. Oxford University Press, Oxford.
- Bakr, M., Akiyama, M., Sanada, Y., 1991. In situ high temperature ESR measurements for kerogen maturation. *Organic Geochemistry* 17, 321-328.
- Bakr, M., Akiyama, M., Sanada, Y., Yokono, T., 1988. Radical concentration of kerogen as a maturation parameter. *Organic Geochemistry* 12, 29-32.
- Bakr, M.Y., Akiyama, M., Sanada, Y., 1990. ESR assessment of kerogen maturation and its relation with petroleum genesis. *Organic Geochemistry* 15, 595-599.
- Baskin, D.K., 1997. Atomic H/C ratio of kerogen as an estimate of thermal maturity and organic matter conversion. *AAPG Bulletin* 81, 1437-1450.
- Baskin, D.K., Peters, K.E., 1992. Early generation characteristics of a sulfur-rich Monterey kerogen. *AAPG Bulletin* 76, 1-13.
- Behar, F., Beaumont, V., De, B.P.H.L., 2001. Rock-Eval 6 technology: Performances and developments. *Oil and Gas Science and Technology* 56, 111-134.
- Behar, F., Budzinski, H., Vandenbroucke, M., Tang, Y., 1999. Methane Generation from Oil Cracking: Kinetics of 9-Methylphenanthrene Cracking and Comparison with Other Pure Compounds and Oil Fractions. *Energy & Fuels* 13, 471-481.
- Behar, F., Gillaizeau, B., Derenne, S., Largeau, C., 2000. Nitrogen Distribution in the Pyrolysis Products of a Type II Kerogen (Cenomanian, Italy). Timing of Molecular Nitrogen Production versus Other Gases. *Energy & Fuels* 14, 431-440.
- Behar, F., Kressmann, S., Rudkiewicz, J.L., Vandenbroucke, M., 1991a. Experimental simulation in a confined system and kinetic modelling of kerogen and oil cracking. *Organic Geochemistry* 19, 173-189.
- Behar, F., Kressmann, S., Rudkiewicz, J.L., Vandenbroucke, M., 1992. Experimental simulation in a confined system and kinetic modelling of kerogen and oil cracking *Advances in Organic Geochemistry 1991, Advances and Applications in Energy and the Natural Environment*. Vol. 19, Pergamon, Oxford, p. 173-189.
- Behar, F., Lorant, F., Lewan, M., 2008. Role of NSO compounds during primary cracking of a Type II kerogen and a Type III lignite. *Organic Geochemistry* 39, 1-22.

- Behar, F., Pelet, R., 1985. Pyrolysis-gas chromatography applied to organic geochemistry: Structural similarities between kerogens and asphaltenes from related rock extracts and oils. *Journal of Analytical and Applied Pyrolysis* 8, 173-187.
- Behar, F., Pelet, R., 1988. Hydrogen-transfer reactions in the thermal cracking of asphaltenes. *Energy & Fuels* 2, 259-264.
- Behar, F., Ungerer, P., Kressmann, S., Rudkiewicz, J., L., 1991b. Evolution thermique des huiles dans les bassins sédimentaires : simulation expérimentale par pyrolyse en milieu confiné et modélisation cinétique. *Oil & Gas Science and Technology - Rev. IFP* 46, 151-181.
- Behar, F., Vandenbroucke, M., 1987. Chemical modelling of kerogens. *Organic Geochemistry* 11, 15-24.
- Behar, F., Vandenbroucke, M., Tang, Y., Marquis, F., Espitalie, J., 1997. Thermal cracking of kerogen in open and closed systems: determination of kinetic parameters and stoichiometric coefficients for oil and gas generation. *Organic Geochemistry* 26, 321-339.
- Behar, F., Vandenbroucke, M., Teermann, S.C., Hatcher, P.G., Leblond, C., Lerat, O., 1995. Experimental simulation of gas generation from coals and a marine kerogen. *Chemical Geology - Processes of Natural Gas Formation* 126, 247-260.
- Berkaloff, C., Casadevall, E., Largeau, C., Peracca, M.S., Virlet, J., 1983. The resistant polymer of the walls of the hydrocarbon-rich alga *Botryococcus braunii*. *Phytochemistry* 22, 389-397.
- Berner, U., Faber, E., 1988. Maturity related mixing model for methane, ethane and propane, based on carbon isotopes. *Organic Geochemistry - Proceedings of the 13th International Meeting on Organic Geochemistry* 13, 67-72.
- Berner, U., Faber, E., Scheeder, G., Panten, D., 1995. Primary cracking of algal and landplant kerogens: Kinetic models of isotope variations in methane, ethane and propane. *Chemical Geology - Processes of Natural Gas Formation* 126, 233-245.
- Billmers, R., Griffith, L.L., Stein, S.E., 1986. Hydrogen transfer between anthracene structures. *The Journal of Physical Chemistry* 90, 517-523.
- Boreham, C.J., Horsfield, B., Schenk, H.J., 1999. Predicting the quantities of oil and gas generated from Australian Permian coals, Bowen Basin using pyrolytic methods. *Marine and Petroleum Geology* 16, 165-188.
- Bostick, N.H., Daws, T.A., 1994. Relationships between data from Rock-Eval pyrolysis and proximate, ultimate, petrographic, and physical analyses of 142 diverse U.S. coal samples. *Organic Geochemistry* 21, 35-49.
- Boudou, J.-P., Durand, B., Oudin, J.-L., 1984. Diagenetic trends of a tertiary low-rank coal series. *Geochimica et Cosmochimica Acta* 48, 2005-2010.
- Boudou, J.P., Espitalie, J., Bimer, J., Salbut, P.D., 1994. Oxygen Groups and Oil Suppression During Coal Pyrolysis. *Energy & Fuels* 8, 972-977.
- Bowker, K.A., 2007. Barnett Shale gas production, Fort Worth Basin: Issues and discussion. *AAPG Bulletin* 91, 523-533.
- Brassell, S.C., Lewis, C.A., de Leeuw, J.W., de Lange, F., Damste, J.S.S., 1986. Isoprenoid thiophenes: novel products of sediment diagenesis? 320, 160-162.
- Braun, R.L., Burnham, A.K., 1987. Analysis of chemical reaction kinetics using a distribution of activation energies and simpler models. *Energy & Fuels* 1, 153-161.

- Braun, R.L., Burnham, A.K., 1992. PMOD: a flexible model of oil and gas generation, cracking, and expulsion. *Organic Geochemistry* 19, 161-172.
- Braun, R.L., Burnham, A.K., Reynolds, J.G., Clarkson, J.E., 1991. Pyrolysis kinetics for lacustrine and marine source rocks by programmed micropyrolysis. *Energy & Fuels* 5, 192-204.
- Braun, R.L., Rothman, A.J., 1975. Oil-shale pyrolysis: Kinetics and mechanism of oil production. *Fuel* 54, 129-131.
- Burlingame, A.L., Haug, P.A., Schnoes, H.K., Simoneit, B.R.T., 1969. Fatty acids derived from the Green River Formation oil shale by extraction and oxidation—a review. In: Schenck, P.A., Havenaar, I. (Eds.), *Advances in Organic Geochemistry* 1968. Pergamon Press, Oxford, p. 68–71.
- Burnham, A.K., Braun, R.L., 1990. Development of a detailed model of petroleum formation, destruction, and expulsion from lacustrine and marine source rocks. *Organic Geochemistry* 16, 27-39.
- Burnham, A.K., Braun, R.L., Gregg, H.R., Samoun, A.M., 1987. Comparison of methods for measuring kerogen pyrolysis rates and fitting kinetic parameters. *Energy & Fuels* 1, 452-458.
- Burnham, A.K., Braun, R.L., Samoun, A.M., 1988. Further comparison of methods for measuring kerogen pyrolysis rates and fitting kinetic parameters. *Organic Geochemistry* 13, 839-845.
- Burnham, A.K., Happe, J.A., 1984. On the mechanism of kerogen pyrolysis. *Fuel* 63, 1353-1356.
- Burnham, A.K., Oh, M.S., Crawford, R.W., Samoun, A.M., 1989. Pyrolysis of Argonne premium coals: activation energy distributions and related chemistry. *Energy & Fuels* 3, 42-55.
- Burruss, R.C., Laughrey, C.D., 2010. Carbon and hydrogen isotopic reversals in deep basin gas: Evidence for limits to the stability of hydrocarbons. *Organic Geochemistry* 41, 1285-1296.
- Bustin, A.M.M., Bustin, M.R., 2008. Coal Reservoir Saturation: Impact of Temperature and Pressure. *Aapg Bulletin* 92, 77-86.
- Campbell, J.H., Gallegos, G., Gregg, M., 1980. Gas evolution during oil shale pyrolysis. 2. Kinetic and stoichiometric analysis. *Fuel* 59, 727-732.
- Cane, R.F., Albion, P.R., 1973. The organic geochemistry of torbanite precursors *Geochimica et Cosmochimica Acta* 37, 1543-1549.
- Carr, A.D., Snape, C.E., Meredith, W., Uguna, C., Scotchman, I.C., Davis, R.C., 2009. The effect of water pressure on hydrocarbon generation reactions: some inferences from laboratory experiments. *Petroleum Geoscience* 15, 17-26.
- Carruthers, R.G., Caldwell, W., Steuart, D.R., 1912. *The Oil Shales of the Lothians*. HMSO, Edinburgh.
- Castelli, A., Chiamonte, M.A., Beltrame, P.L., Carniti, P., Del Bianco, A., Stroppa, F., 1990. Thermal degradation of kerogen by hydrous pyrolysis. A kinetic study. *Organic Geochemistry - Proceedings of the 14th International Meeting on Organic Geochemistry* 16, 75-82.

- Chung, H.M., Sackett, W.M., 1980. Carbon isotope effects during the pyrolytic formation of early methane from carbonaceous materials *Advances in Organic Geochemistry* 1979. Pergamon Press, p. 705–710.
- Clayton, C., 1991. Carbon isotope fractionation during natural gas generation from kerogen. *Marine and Petroleum Geology* 8, 232-240.
- Clayton, J.L., 1998. Geochemistry of coalbed gas - A review. *International Journal of Coal Geology* 35, 159-173.
- Clegg, H., Horsfield, B., Stasiuk, L., Fowler, M., Vliex, M., 1997. Geochemical characterisation of organic matter in Keg River Formation (Elk point group, Middle Devonian), La Crete Basin, Western Canada. *Organic Geochemistry* 26, 627-643.
- Clementz, D.M., 1979. Effects of oil and bitumen saturation on source rock pyrolysis. *AAPG Bulletin* 63, 2227–2232.
- Cooles, G.P., Mackenzie, A.S., Quigley, T.M., 1986. Calculation of petroleum masses generated and expelled from source rocks. *Organic Geochemistry* 10, 235-245.
- Cornford, C., Gardner, P., Burgess, C., 1998. Geochemical truths in large data sets. I: Geochemical screening data. *Organic Geochemistry - Advances in Organic Geochemistry 1997 Proceedings of the 18th International Meeting on Organic Geochemistry Part I. Petroleum Geochemistry* 29, 519-530.
- Costa Neto, C., 1991. The effect of pressure on geochemical maturation: theoretical considerations. *Organic Geochemistry* 17, 579-584.
- Craig, H., 1957. Isotopic standards for carbon and oxygen and correction factors for mass-spectrometric analysis of carbon dioxide. *Geochimica et Cosmochimica Acta* 12, 133-149.
- Craig, H., 1961. Standard for Reporting Concentrations of Deuterium and Oxygen-18 in Natural Waters. *Science* 133, 1833-1834.
- Cramer, B., 2004. Methane generation from coal during open system pyrolysis investigated by isotope specific, Gaussian distributed reaction kinetics. *Organic Geochemistry - Conference on Emerging Concepts in Organic Petrology and Geochemistry* 35, 379-392.
- Cramer, B., Faber, E., Gerling, P., Krooss, B.M., 2001. Reaction Kinetics of Stable Carbon Isotopes in Natural Gas Insights from Dry, Open System Pyrolysis Experiments. *Energy & Fuels* 15, 517-532.
- Cummins, J.J., Robinson, W.E., 1972. Thermal degradation of Green River Kerogen at 150–350 °C – rate of product formation. *US Bureau of Mines Report of Investigation* 7620, 15.
- Dahl, B., Bojesen-Koefoed, J., Holm, A., Justwan, H., Rasmussen, E., Thomsen, E., 2004. A new approach to interpreting Rock-Eval S2 and TOC data for kerogen quality assessment. *Organic Geochemistry - Advances in Organic Geochemistry 2003. Proceedings of the 21st International Meeting on Organic Geochemistry* 35, 1461-1477.
- Dahl, J., Hallberg, R., Kaplan, I.R., 1988. The effects of radioactive decay of uranium on elemental and isotopic ratios of Alum shale kerogen. *Applied Geochemistry* 3, 583-589.
- Damtoft, K., Nielsen, L.H., Johannessen, P.N., Thomsen, E., Andersen, P.R., 1992. Hydrocarbon plays of the Danish Central Trough. In: Spencer, A.M. (Ed.) *Generation, accumulation and production of Europe's hydrocarbons II. Special publication of the European Association of Petroleum Geoscientists, Vol. 2*, Springer Verlag, Berlin, Heidelberg.



- Degens, E.T., 1989. Perspectives on Biogeochemistry. Springer, Berlin.
- Dembicki, H., Jr., 2009. Three common source rock evaluation errors made by geologists during prospect or play appraisals. AAPG Bulletin 93, 341-356.
- di Primio, R., Dieckmann, V., Mills, N., 1998. PVT and phase behaviour analysis in petroleum exploration. Organic Geochemistry - Advances in Organic Geochemistry 1997 Proceedings of the 18th International Meeting on Organic Geochemistry Part I. Petroleum Geochemistry 29, 207-222.
- di Primio, R., Horsfield, B., 1996. Predicting the generation of heavy oils in carbonate/evaporitic environments using pyrolysis methods. Organic Geochemistry - Proceedings of the 17th International Meeting on Organic Geochemistry 24, 999-1016.
- di Primio, R., Horsfield, B., 2006. From petroleum-type organofacies to hydrocarbon phase prediction. AAPG Bulletin 90, 1031-1058.
- di Primio, R., Skeie, J.E., 2004. Development of a compositional kinetic model for hydrocarbon generation and phase equilibria modelling: a case study from Snorre Field, Norwegian North Sea. In: Cubitt, J.M., England, W.A., Larter, S.R. (Eds.), Understanding Petroleum Reservoirs: Towards an Integrated Reservoir Engineering and Geochemical Approach, Vol. 237, Geological Society Special Publication, London, pp. 157-174.
- Dieckmann, V. (1999) Zur Vorhersage der Erdöl- und Erdgaszusammensetzung durch die Integration von Labor- und Fallstudien. In *Berichte des Forschungszentrums Jülich*, p. 285. RWTH Aachen.
- Dieckmann, V., 2005. Modelling petroleum formation from heterogeneous source rocks: the influence of frequency factors on activation energy distribution and geological prediction. Marine and Petroleum Geology 22, 375-390.
- Dieckmann, V., Horsfield, B., Schenk, H.J., 2000a. Heating rate dependency of petroleum-forming reactions: implications for compositional kinetic predictions. Organic Geochemistry 31, 1333-1348.
- Dieckmann, V., Ondrak, R., Cramer, B., Horsfield, B., 2006. Deep basin gas: New insights from kinetic modelling and isotopic fractionation in deep-formed gas precursors. Marine and Petroleum Geology 23, 183-199.
- Dieckmann, V., Schenk, H.J., Horsfield, B., 2000b. Assessing the overlap of primary and secondary reactions by closed- versus open-system pyrolysis of marine kerogens. Journal of Analytical and Applied Pyrolysis 56, 33-46.
- Dieckmann, V., Schenk, H.J., Horsfield, B., Welte, D.H., 1998. Kinetics of petroleum generation and cracking by programmed-temperature closed-system pyrolysis of Toarcian Shales. Fuel 77, 23-31.
- Domine, F., 1991. High pressure pyrolysis of n-hexane, 2,4-dimethylpentane and 1-phenylbutane. Is pressure an important geochemical parameter? Organic Geochemistry 17, 619-634.
- Dubin, M.M., 1975. Physical adsorption of gases and vapours in micropores. In: Cadenhead, D.A., Danielli, J.F., Rosenberg, M.D. (Eds.), Progress in Surface and Membrane Science. Vol. 9, Academic Press, New York, p. 1-70.
- Dueppenbecker, S., Horsfield, B., 1990. Compositional information for kinetic modelling and petroleum type prediction. Organic Geochemistry 16, 259-266.
- Durand, B., 1980. Kerogen: insoluble organic matter from sedimentary rocks. Editions Technip, Paris.

- Durand, B., Marchand, A., Amiell, J., Combaz, A., 1977a. Etude de kérogènes par résonance paramagnétique électronique. In: Campos, R., Goñi, J. (Eds.), *Advances in Organic Geochemistry 1975*. ENADISMA, Madrid, p. 753–779.
- Durand, B., Monin, J.C., 1980. Elemental analysis of kerogens (C, H, O, N, S, Fe). In: Durand, B. (Ed.) *Kerogen: Insoluble organic matter from sedimentary rocks*. Editions Technip, Paris, pp. 113-142.
- Durand, B., Nicaise, G., Roucaché, J., Vandenbroucke, M., Hagemann, H.W., 1977b. Etude géochimique d'une série de charbons. In: Campo, R., Goñi, J. (Eds.), *Advances in Organic Geochemistry 1975*. ENADISMA, Madrid, p. 601–631.
- Durand, B., Paratte, M., 1983. *Oil Potential of Coals: A Geochemical Approach*. Geological Society, London, Special Publications 12, 255-265.
- Eglinton, T.I., Sinninghe Damsté, J.S., Kohnen, M.E.L., de Leeuw, J.W., 1990. Rapid estimation of the organic sulphur content of kerogens, coals and asphaltenes by pyrolysis-gas chromatography. *Fuel* 69, 1394-1404.
- EIA. (2009) *International Energy Outlook 2009*, p. 274. Energy Information Administration.
- Eisma, E., Jurg, J.W., 1969. Fundamental aspects of the generation of petroleum. In: Eglinton, G., Murphy, M.T.J. (Eds.), *Organic Geochemistry*. Springer-Verlag, p. 676–698.
- England, W., Mackenzie, A., 1989. Some aspects of the organic geochemistry of petroleum fluids. *Geologische Rundschau* 78, 291-303.
- Erdmann, M. (1999) *Gas Generation from Overmature Upper Jurassic Source Rocks, Northern Viking Graben*, p. 128. RWTH Aachen.
- Erdmann, M., Horsfield, B., 2006. Enhanced late gas generation potential of petroleum source rocks via recombination reactions: Evidence from the Norwegian North Sea. *Geochimica et Cosmochimica Acta* 70, 3943-3956.
- Ericsson, I., Lattimer, R., 1989. Pyrolysis nomenclature. *Journal of Analytical and Applied Pyrolysis* 14, 219-221.
- Espitalié, J., Bordenave, M.L., 1993. Rock-Eval Pyrolysis. In: Bordenave, M.L. (Ed.) *Applied petroleum geochemistry*. Editions Technip, Paris, pp. 237-261.
- Espitalié, J., Deroo, G., Marquis, F., 1985. Rock-Eval pyrolysis and its applications. *Revue de l'Institut Français du Pétrole* 40, 563-579.
- Espitalié, J., Laporte, J., L., Madec, M., Marquis, F., Leplat, P., Paulet, J., Boutefeu, A., 1977. Méthode rapide de caractérisation des roches mères, de leur potentiel pétrolier et de leur degré d'évolution. *Oil & Gas Science and Technology - Rev. IFP* 32, 23-42.
- Espitalié, J., Madec, M., Tissot, B., 1980. Role of mineral matrix in kerogen pyrolysis; influence on petroleum generation and migration. *AAPG Bulletin* 64, 59-66.
- Espitalié, J., Ungerer, P., Irwin, I., Marquis, F., 1988. Primary cracking of kerogens. Experimenting and modelling C1, C2-C5, C6-C15 and C15+ classes of hydrocarbons formed. *Organic Geochemistry - Proceedings of the 13th International Meeting on Organic Geochemistry* 13, 893-899.
- Evans, C.R., Rogers, M.A., Bailey, N.J.L., 1971. Evolution and alteration of petroleum in western Canada. *Chemical Geology - Contributions to Petroleum Geochemistry* 8, 147-170.

- Evans, R.J., Felbeck Jr., G.T., 1983. High temperature simulation of petroleum formation--II. Effect of inorganic sedimentary constituents on hydrocarbon formation. *Organic Geochemistry* 4, 145-152.
- Faber, E., Stahl, W.J., Whiticar, M.J., 1992. Distinction of bacterial and thermogenic hydrocarbons. In: Vially, R. (Ed.) *Bacterial Gas*. Editions Technip, Paris.
- Fausett, D.W., Miknis, F.P., 1981. Simplified kinetics of oil shale pyrolysis. In: Gary, J. (Ed.) *Proc. of 14th Oil Shale Symposium*, Colo. Sch. of Mines. Golden, Co, p. 154–160.
- Fitzgerald, D., Van Krevelen, D.W., 1959. Chemical structure and properties of coal: the kinetics of coal carbonization. *Fuel* 38, 17-37.
- Forbes, P.I., Ungerer, P.M., Kuhfuss, A.B., Riis, F., Eggen, S., 1991. Compositional modeling of petroleum generation and expulsion: trial application to a local mass balance in the Smørbukk Sør field, Haltenbanken Area, Norway. *Am. Assoc. Petr. Geol. Bull.* 75, 873–893.
- Forsman, J.P., Hunt, J.M., 1958. Insoluble organic matter (kerogen) in sedimentary rocks. *Geochimica et Cosmochimica Acta* 15, 170-182.
- Franks, A.J., Goodier, B.D., 1922. Preliminary study of the organic matter of Colorado Oil shales. *Quarterly of the Colorado School of Mines* 17, 3–16.
- Freund, H., Olmstead, W.N., 1989. Detailed chemical kinetic modeling of butylbenzene pyrolysis. *International Journal of Chemical Kinetics* 21, 561-574.
- Freund, H., Walters, C.C., Kelemen, S.R., Siskin, M., Gorbaty, M.L., Curry, D.J., Bence, A.E., 2007. Predicting oil and gas compositional yields via chemical structure-chemical yield modeling (CS-CYM): Part 1 - Concepts and implementation. *Organic Geochemistry* 38, 288-305.
- Friedrich, H.-U., Jüntgen, H., 1973. Aussagen zum  $^{13}\text{C}/^{12}\text{C}$ -Verhältnis des bei der Inkohlung gebildeten Methans aufgrund von Pyrolyseversuchen. *Erdöl und Kohle–Erdgas–Petrochemie vereinigt mit Brennstoff-Chemie* 26, 636–639.
- Galimov, E.M., 1980.  $^{13}\text{C}/^{12}\text{C}$  in kerogen. In: Durand, B. (Ed.) *Kerogen – Insoluble Organic Matter from Sedimentary Rocks*. Editions Technip, Paris, p. 271–299.
- Gaschnitz, R., Krooss, B.M., Gerling, P., Faber, E., Littke, R., 2001. On-line pyrolysis-GC-IRMS: isotope fractionation of thermally generated gases from coals. *Fuel* 80, 2139-2153.
- Given, P.H., 1960. The distribution of hydrogen in coals and its relation to coal structure. *Fuel* 39, 147-153.
- Given, P.H., 1984. An essay on the organic geochemistry of coal. In: Gorbaty, M.L. (Ed.) *Coal Science*. Vol. 3, Academic Press, New York, pp. 63-252, 339-341.
- Glombitza, C., Mangelsdorf, K., Horsfield, B., 2009. A novel procedure to detect low molecular weight compounds released by alkaline ester cleavage from low maturity coals to assess its feedstock potential for deep microbial life. *Organic Geochemistry* 40, 175-183.
- Goth, K., de Leeuw, J.W., Puttmann, W., Tegelaar, E.W., 1988. Origin of Messel Oil Shale kerogen. 336, 759-761.
- Greensfelder, B.S., Voge, H.H., Good, G.M., 1949. Catalytic and Thermal Cracking of Pure Hydrocarbons: Mechanisms of Reaction. *Industrial & Engineering Chemistry* 41, 2573-2584.
- Haenel, M.W., 1992. Recent progress in coal structure research. *Fuel* 71, 1211-1223.

- Hartgers, W.A., Damsté, J.S.S., de Leeuw, J.W., 1994a. Geochemical significance of alkylbenzene distributions in flash pyrolysates of kerogens, coals, and asphaltenes. *Geochimica et Cosmochimica Acta* 58, 1759-1775.
- Hartgers, W.A., Sinninghe Damsté, J.S., Requejo, A.G., Allan, J., Hayes, J.M., Ling, Y., Xie, T.-M., Primack, J., de Leeuw, J.W., 1994b. A molecular and carbon isotopic study towards the origin and diagenetic fate of diaromatic carotenoids. *Organic Geochemistry* 22, 703-725.
- Hatcher, P.G., Faulon, J.L., Wenzel, K.A., Cody, G.D., 1992. A structural model for lignin-derived vitrinite from high-volatile bituminous coal (coalified wood). *Energy & Fuels* 6, 813-820.
- Henderson, W., Eglinton, G., Simmons, P., Lovelock, J.E., 1968. Thermal Alteration as a Contributory Process to the Genesis of Petroleum. 219, 1012-1016.
- Hershkowitz, F., Olmstead, W.N., Rhodes, R.P., Rose, K.D., 1983. Molecular Mechanism of Oil Shale Pyrolysis in Nitrogen and Hydrogen Atmospheres *Geochemistry and Chemistry of Oil Shales. ACS Symposium Series, AMERICAN CHEMICAL SOCIETY*, pp. 301-316 SE - 15.
- Hill, R.J., Tang, Y., Kaplan, I.R., Jenden, P.D., 1996. The Influence of Pressure on the Thermal Cracking of Oil. *Energy & Fuels* 10, 873-882.
- Hill, R.J., Zhang, E., Katz, B.J., Tang, Y., 2007. Modeling of gas generation from the Barnett Shale, Fort Worth Basin, Texas. *AAPG Bulletin* 91, 501-521.
- Hoering, T.C., 1984. Thermal reactions of kerogen with added water, heavy water and pure organic substances. *Organic Geochemistry* 5, 267-278.
- Horsfield, B., 1984. Pyrolysis Studies and Petroleum Exploration. In: Brooks, J., Welte, D.H. (Eds.), *Advances in Petroleum Geochemistry. Vol. 1*, Academic Press, London, pp. 47-298.
- Horsfield, B., 1989. Practical criteria for classifying kerogens: Some observations from pyrolysis-gas chromatography. *Geochimica et Cosmochimica Acta* 53, 891-901.
- Horsfield, B., 1997. The bulk composition of first-formed petroleum in source rocks. In: Welte, D.H., Horsfield, B., Backer, D.R. (Eds.), *Petroleum and Basin Evolution. Insights from Petroleum geochemistry, Geology and Basin modelling*, Springer, Berlin, pp. 335-402.
- Horsfield, B., Bharati, S., Larter, S.R., Leistner, F., Littke, R., Schenk, H.J., Dypvik, H., 1992a. On the atypical petroleum-generation characteristics of alginite in the Cambrian Alum Shale. In: Schidlowski, M. (Ed.) *Early organic evolution: Implications for mineral and energy resources*. Springer-Verlag, pp. 257-266.
- Horsfield, B., Dembicki, H., Jr., Ho, T.T.Y., 1983. Some potential applications of pyrolysis to basin studies. *Journal of the Geological Society* 140, 431-443.
- Horsfield, B., Disko, U., Leistner, F., 1989. The micro-scale simulation of maturation: outline of a new technique and its potential applications. *Geologische Rundschau* 78, 361-374.
- Horsfield, B., Douglas, A.G., 1980. The influence of minerals on the pyrolysis of kerogens. *Geochimica et Cosmochimica Acta* 44, 1119-1131.
- Horsfield, B., Dueppenbecker, S.J., 1991. The decomposition of posidonia shale and green river shale kerogens using microscale sealed vessel (MSSV) pyrolysis. *Journal of Analytical and Applied Pyrolysis* 20, 107-123.

- Horsfield, B., Schenk, H.J. (1995) The composition and yield of gases associated with coals of high volatile bituminous through anthracite rank from northern Germany: macromolecular structure and gas generating potential. KFA internal report.
- Horsfield, B., Schenk, H.J., Mills, N., Welte, D.H., 1992b. An investigation of the in-reservoir conversion of oil to gas: compositional and kinetic findings from closed-system programmed-temperature pyrolysis. *Organic Geochemistry* 19, 191-204.
- Horsfield, B., Schenk, H.J., Zink, K., Ondrak, R., Dieckmann, V., Kallmeyer, J., Mangelsdorf, K., di Primio, R., Wilkes, H., Parkes, R.J., Fry, J., Cragg, B., 2006. Living microbial ecosystems within the active zone of catagenesis: Implications for feeding the deep biosphere. *Earth and Planetary Science Letters* 246, 55-69.
- Horsfield, B., Yordy, K.L., Crelling, J.C., 1988. Determining the petroleum-generating potential of coal using organic geochemistry and organic petrology. *Organic Geochemistry* 13, 121-129.
- Hubbard, A.B., Robinson, W.E., Savage, J.W. (1948) A Thermal Decomposition Study of Colorado Oil Shale, p. 24. Petroleum and Oil-Shale Experiment Station - US Bureau of Mines.
- Huc, A.Y., 1980. Origin and formation of organic matter in recent sediments and its relation to kerogen. In: Durand, B. (Ed.) *Kerogen, Insoluble Organic Matter from Sedimentary Rocks*. Edition Technip, Paris, p. 445-474.
- Huc, A.Y., B., D., J., R., M., V., J.L., P., 1986. Comparison of three series of organic matter of continental origin. In: Leythaeuser, D., Rullkötter, J. (Eds.), *Advances in Organic Geochemistry 1985*. Vol. *Organic Geochemistry*, p. 65-72.
- Huc, A.Y., Durand, B., 1974. Etude des acides humiques et de l'humine de sédiments récents considérés comme précurseurs des kérogènes. In: Tissot, B., Bienner, F. (Eds.), *Advances in Organic Geochemistry 1973*. Editions Technip, Paris, p. 53-72.
- Huizinga, B.J., Tannenbaum, E., Kaplan, I.R., 1987. The role of minerals in the thermal alteration of organic matter--III. Generation of bitumen in laboratory experiments. *Organic Geochemistry* 11, 591-604.
- Hunt, J.M., 1979. *Petroleum Geochemistry and Geology*. W.H. Freeman, San Francisco.
- Hunt, J.M., 1995. *Petroleum Geochemistry and Geology*. W.H. Freeman and Company, New York.
- Huss, E.B., Burnham, A.K., 1982. Gas evolution during pyrolysis of various Colorado oil shales. *Fuel* 61, 1188-1196.
- Ineson, J.R., Bojesen-Koefoed, J.A., Dybkjær, K., Nielsen, L.H., 2003. Volgian-Ryazanian 'hot shales' of the Bo Member (Farsund Formation) in the Danish Central Graben, North Sea: stratigraphy, facies and geochemistry. *Geological Survey Of Denmark And Greenland Bulletin* 1, 403-436.
- Isaksen, G.H., Curry, D.J., Yeakel, J.D., Jenssen, A.I., 1998. Controls on the oil and gas potential of humic coals. *Organic Geochemistry - Advances in Organic Geochemistry 1997 Proceedings of the 18th International Meeting on Organic Geochemistry Part I*. *Petroleum Geochemistry* 29, 23-44.
- Ishiwatari, R., Ishiwatari, M., Kaplan, I.R., Rohrback, B.G., 1976. Thermal alteration of young kerogen in relation to petroleum genesis. 264, 347-349.

- Ishiwatari, R., Ishiwatari, M., Rohrbach, B.G., Kaplan, I.R., 1977. Thermal alteration experiments on organic matter from recent marine sediments in relation to petroleum genesis. *Geochimica et Cosmochimica Acta* 41, 815-828.
- Jarvie, D.M., Claxton, B., Henk, B., Breyer, J. 2001. Oil and Shale Gas from Barnett Shale, Ft. Worth Basin, Texas. AAPG National Convention.
- Jarvie, D.M., Hill, R.J., Pollastro, R.M., 2004. Assessment of the gas potential and yields from shales: The Barnett Shale model. In: Cardott, B.J. (Ed.) *Unconventional Energy Resources in the Southern Mid-continent*, 2004 Conference: Oklahoma Geological Survey Circular 110. p. 34.
- Jarvie, D.M., Hill, R.J., Ruble, T.E., Pollastro, R.M., 2007. Unconventional shale-gas systems: The Mississippian Barnett Shale of north-central Texas as one model for thermogenic shale-gas assessment. *AAPG Bulletin* 91, 475-499.
- Jarvie, D.M., Lundell, L.L., 2001. Amount, type, and kinetics of thermal transformation of organic matter in the Miocene Monterey Formation. In: Isaacs, C.M., Rullkötter, J. (Eds.), *The Monterey Formation: From Rocks to Molecules*. Columbia University Press, New York, pp. 268-295.
- Javai, A.A. (2000) PVT modelling of reservoir fluids from the Norwegian North Sea. Oslo University.
- Jenkins, C.D., Boyer, C.M., 2008. Coalbed-and shale-gas reservoirs. *Journal of Petroleum Technology SPE* 103514, 92-99.
- Ji, F., Zhou, H., Yang, Q. (2008) The Abiotic Formation of Hydrocarbons from Dissolved CO<sub>2</sub> Under Hydrothermal Conditions with Cobalt-Bearing Magnetite. In *Origins of Life and Evolution of Biospheres*, Vol. 38, pp. 117-125. Springer Netherlands.
- Jones, R.W., 1987. Organic facies. In: Brooks, J., Welte, D.H. (Eds.), *Advances in Petroleum Geochemistry* 2. Academic Press, London, p. 1–90.
- Jüntgen, H., 1964. Reaktionskinetische Überlegungen zur Deutung von Pyrolyse-Reaktionen. *Erdöl und Kohle-Erdgas-Petrochemie* 17, 180-186.
- Jüntgen, H., 1984. Review of the kinetics of pyrolysis and hydrolypyrolysis in relation to the chemical constitution of coal. *Fuel* 63, 731-737.
- Jüntgen, H., Klein, J., 1975. Entstehung von Erdgas aus Kohligen Sedimenten. *Erdöl und Kohle-Erdgas-Petrochemie vereinigt mit Brennstoff-Chemie* 28, 65–73.
- Jüntgen, H., Van Heek, K.H., 1968. Gas release from coal as a function of the rate of heating. *Fuel* 48, 103–117.
- Jurg, J.W., Eisma, E., 1964. Petroleum Hydrocarbons: Generation from Fatty Acid. *Science* 144, 1451-1452.
- Katz, B.J., 1981. Limitations of Rock-Eval pyrolysis for typing organic matter. *American Association of Petroleum Geologists Bulletin* 65, 994.
- Katz, B.J., 1983. Limitations of 'Rock-Eval' pyrolysis for typing organic matter. *Organic Geochemistry* 4, 195-199.
- Kelemen, S.R., Afeworki, M., Gorbaty, M.L., Cohen, A.D., 2002. Characterization of Organically Bound Oxygen Forms in Lignites, Peats, and Pyrolyzed Peats by X-ray Photoelectron Spectroscopy (XPS) and Solid-State <sup>13</sup>C NMR Methods. *Energy Fuels* 16, 1450-1462.

- Kelemen, S.R., Afeworki, M., Gorbaty, M.L., Sansone, M., Kwiatek, P.J., Walters, C.C., Freund, H., Siskin, M., Bence, A.E., Curry, D.J., Solum, M., Pugmire, R.J., Vandenbroucke, M., Leblond, M., Behar, F., 2007. Direct Characterization of Kerogen by X-ray and Solid-State <sup>13</sup>C Nuclear Magnetic Resonance Methods. *Energy Fuels* 21, 1548-1561.
- Killops, S.D., Funnell, R.H., Suggate, R.P., Sykes, R., Peters, K.E., Walters, C., Woolhouse, A.D., Weston, R.J., Boudou, J.-P., 1998. Predicting generation and expulsion of paraffinic oil from vitrinite-rich coals. *Organic Geochemistry - Advances in Organic Geochemistry 1997 Proceedings of the 18th International Meeting on Organic Geochemistry Part I. Petroleum Geochemistry* 29, 1-21.
- Kissin, Y.V., 1987. Catagenesis and composition of petroleum: Origin of n-alkanes and isoalkanes in petroleum crudes. *Geochimica et Cosmochimica Acta* 51, 2445-2457.
- Klomp, U.C., Wright, P.A., 1990. A new method for the measurement of kinetic parameters of hydrocarbon generation from source rocks. *Organic Geochemistry - Proceedings of the 14th International Meeting on Organic Geochemistry* 16, 49-60.
- Knauss, K.G., Copenhaver, S.A., Braun, R.L., Burnham, A.K., 1997. Hydrous pyrolysis of New Albany and Phosphoria Shales: production kinetics of carboxylic acids and light hydrocarbons and interactions between the inorganic and organic chemical systems. *Organic Geochemistry* 27, 477-496.
- Kossiakoff, A., Rice, F.O., 1943. Thermal Decomposition of Hydrocarbons, Resonance Stabilization and Isomerization of Free Radicals<sup>1</sup>. *Journal of the American Chemical Society* 65, 590-595.
- Krooss, B.M., Littke, R., Muller, B., Frielingsdorf, J., Schwochau, K., Idiz, E.F., 1995. Generation of nitrogen and methane from sedimentary organic matter: Implications on the dynamics of natural gas accumulations. *Chemical Geology - Processes of Natural Gas Formation* 126, 291-318.
- Landais, P., Gerard, L., 1996. Coalification stages from confined pyrolysis of an immature humic coal. *International Journal of Coal Geology - Coalification and Coal Petrology* 30, 285-301.
- Largeau, C., Casadevall, E., Kadouri, A., Metzger, P., 1984. Formation of Botryococcus-derived kerogens--Comparative study of immature torbanites and of the extant alga *Botryococcus braunii*. *Organic Geochemistry* 6, 327-332.
- Largeau, C., Derenne, S., 1993. Relative efficiency of the Selective Preservation and Degradation Recondensation pathways in kerogen formation. Source and environment influence on their contributions to type I and II kerogens. *Organic Geochemistry* 20, 611-615.
- Largeau, C., Derenne, S., Casadevall, E., Kadouri, A., Sellier, N., 1986. Pyrolysis of immature Torbanite and of the resistant biopolymer (PRB A) isolated from extant alga *Botryococcus braunii*. Mechanism of formation and structure of torbanite. *Organic Geochemistry* 10, 1023-1032.
- Larter, S.R., 1984. Application of Analytical Pyrolysis Techniques to Kerogen Characterisation and Fossil Fuel Exploration/Exploitation. In: Voorhees, K. (Ed.) *Analytical pyrolysis, methods and applications*. Butterworth, London, pp. 212-275.
- Larter, S.R., Horsfield, B., 1993. Determination of structural components of kerogens by the use of analytical pyrolysis methods. In: Engel, M.H., Macko, S.A. (Eds.), *Organic Geochemistry – Principles and Applications*. Plenum Press, New York, p. 271–287.

- Larter, S.R., Senftle, J.T., 1985. Improved kerogen typing for petroleum source rock analysis. 318, 277-280.
- Lehne, E., Dieckmann, V., 2007. The significance of kinetic parameters and structural markers in source rock asphaltenes, reservoir asphaltenes and related source rock kerogens, the Duvernay Formation (WCSB). *Fuel* 86, 887-901.
- Levine, D.G., Schlosberg, R.H., Silbernagel, B.G., 1982. Understanding the chemistry and physics of coal structure (A Review). *Proceedings of the National Academy of Sciences of the United States of America* 79, 3365-3370.
- Levine, J.R., 1993. Coalification: The evolution of coal as source rock and reservoir rock for oil and gas. In: Law, B.E., Dudley, D.R. (Eds.), *Hydrocarbons from coal. AAPG Studies in Geology*, Vol. 38, pp. 39-77.
- Lewan, M.D., 1985. Evaluation of petroleum generation by hydrous pyrolysis experimentation. *Philosophical Transactions of the Royal Society, London, Series A* 315, 123-134.
- Lewan, M.D., 1992a. Primary oil migration and expulsion as determined by hydrous pyrolysis. *Proceedings of the Thirteenth World Petroleum Congress: Chichester*, John Wiley & Sons, 215-223.
- Lewan, M.D., 1992b. Water as a source of hydrogen and oxygen in petroleum formation by hydrous pyrolysis. *American Chemical Society, Reprints, Division of Fuel Chemistry* 37, 1643-1649.
- Lewan, M.D., 1993. Laboratory simulation of petroleum formation: hydrous pyrolysis. In: Engel, M.H., Macko, S. (Eds.), *Organic Geochemistry Principles and Applications*. Plenum Press, New York, p. 419-442.
- Lewan, M.D., 1994. Laboratory simulation of petroleum formation: hydrous pyrolysis. In: Engel, M.H., Macko, S.A. (Eds.), *Organic Geochemistry*. Plenum, New York.
- Lewan, M.D., 1997. Experiments on the role of water in petroleum formation. *Geochimica et Cosmochimica Acta* 61, 3691-3723.
- Lewan, M.D., Buchardt, B., 1989. Irradiation of organic matter by uranium decay in the Alum Shale, Sweden. *Geochimica et Cosmochimica Acta* 53, 1307-1322.
- Lewan, M.D., Ruble, T.E., 2002. Comparison of petroleum generation kinetics by isothermal hydrous and nonisothermal open-system pyrolysis. *Organic Geochemistry* 33, 1457-1475.
- Lewan, M.D., Winters, J.C., McDonald, J.H., 1979. Generation of oil-like pyrolyzates from organic rich shales. *Science* 203, 897-899.
- Lin, R., Davis, A., Bensley, D.F., Derbyshire, F.J., 1986. Vitrinite secondary fluorescence: Its chemistry and relation to the development of a mobile phase and thermoplasticity in coal. *International Journal of Coal Geology* 6, 215-228.
- Lorant, F., Behar, F., 2002. Late Generation of Methane from Mature Kerogens. *Energy Fuels* 16, 412-427.
- Lorant, F., Behar, F., Vandenbroucke, M., McKinney, D.E., Tang, Y., 2000. Methane Generation from Methylated Aromatics: Kinetic Study and Carbon Isotope Modeling. *Energy Fuels* 14, 1143-1155.
- Lorant, F., Prinzhofer, A., Behar, F., Huc, A.-Y., 1998. Carbon isotopic and molecular constraints on the formation and the expulsion of thermogenic hydrocarbon gases. *Chemical Geology* 147, 249-264.



- Mackenzie, A., Quigley, T.M., 1988. Principles of geochemical prospect appraisal. American Association of Petroleum Geologists Bulletin 72, 399-415.
- Mahlstedt, N., Horsfield, B., Dieckmann, V., 2008. Second order reactions as a prelude to gas generation at high maturity. Organic Geochemistry - Advances in Organic Geochemistry 2007 - Proceedings of the 23rd International Meeting on Organic Geochemistry 39, 1125-1129.
- Maier, C.G., Zimmerly, S.R., 1924. The chemical dynamics of the transformation of the organic matter to bitumen in oil shale. University of Utah Bulletin 14, 62-81.
- Malhotra, R., McMillen, D.F., 1990. A mechanistic numerical model for coal liquefaction involving hydrogenolysis of strong bonds. Rationalization of interactive effects of solvent aromaticity and hydrogen pressure. Energy & Fuels 4, 184-193.
- Mallinson, R.G., Braun, R.L., Westbrook, C.K., Burnham, A.K., 1992. Detailed chemical kinetics study of the role of pressure in butane pyrolysis. Industrial & Engineering Chemistry Research 31, 37-45.
- Mango, F.D., 1992a. Transition metal catalysis in the generation of petroleum and natural gas. Geochimica et Cosmochimica Acta 56, 553-555.
- Mango, F.D., 1992b. Transition metal catalysis in the generation of petroleum: A genetic anomaly in Ordovician oils. Geochimica et Cosmochimica Acta 56, 3851-3854.
- Mango, F.D., 1997. The light hydrocarbons in petroleum: a critical review. Organic Geochemistry 26, 417-440.
- Mango, F.D., 2000. The origin of light hydrocarbons. Geochimica et Cosmochimica Acta 64, 1265-1277.
- Mango, F.D., Elrod, L.W., 1999. The carbon isotopic composition of catalytic gas: a comparative analysis with natural gas. Geochimica et Cosmochimica Acta 63, 1097-1106.
- Mango, F.D., Hightower, J., 1997. The catalytic decomposition of petroleum into natural gas. Geochimica et Cosmochimica Acta 61, 5347-5350.
- Mango, F.D., Hightower, J.W., James, A.T., 1994. Role of transition-metal catalysis in the formation of natural gas. Nature 368, 536-538.
- Mansuy, L., Landais, P., 1995. Importance of the reacting medium in artificial maturation of a coal by confined pyrolysis. 2. Water and polar compounds. Energy Fuels 9, 809-821.
- Mansuy, L., Landais, P., Ruau, O., 1995. Importance of the Reacting Medium in Artificial Maturation of a Coal by Confined Pyrolysis. 1. Hydrocarbons and Polar Compounds. Energy Fuels 9, 691-703.
- Marchand, A., Conard, J., 1980. Electron paramagnetic resonances in kerogen studies. In: Durand, B. (Ed.) Kerogen: insoluble organic matter from sedimentary rocks. Editions Technip, Paris, pp. 243-270.
- McKee, R.H., Lyder, E.E., 1921. The Thermal Decomposition of Shales: I - Heat Effects. Journal of Industrial & Engineering Chemistry 13, 613-618.
- McMillen, D.F., Malhotra, R., 2006. Hydrogen Transfer in the Formation and Destruction of Retrograde Products in Coal Conversion. The Journal of Physical Chemistry A 110, 6757-6770.
- McMillen, D.F., Malhotra, R., Chang, S.-J., Ogier, W.C., Nigenda, S.E., Fleming, R.H., 1987. Mechanisms of hydrogen transfer and bond scission of strongly bonded coal structures in donor-solvent systems. Fuel 66, 1611-1620.

- Meissner, F.F., 1984. Cretaceous and lower Tertiary coals as sources for gas accumulations in the Rocky Mountain area. In: Woodward, J., Meissner, F.F., Clayton, J.L. (Eds.), *Hydrocarbon Source Rocks of the Greater Rocky Mountain Region*. Rocky Mountain Association of Geologists, Denver, p. 401–431.
- Michels, R., Burkle, V., Mansuy, L., Langlois, E., Ruau, O., Landais, P., 2000. Role of Polar Compounds as Source of Hydrocarbons and Reactive Medium during the Artificial Maturation of Mahakam Coal. *Energy Fuels* 14, 1059-1071.
- Michels, R., Landais, P., Philp, R.P., Torkelson, B.E., 1994. Effects of Pressure on Organic Matter Maturation during Confined Pyrolysis of Woodford Kerogen. *Energy & Fuels* 8, 741-754.
- Michels, R., Landis, P., Philp, R.P., Torkelson, B.E., 1995. Influence of Pressure and the Presence of Water on the Evolution of the Residual Kerogen during Confined, Hydrous, and High-Pressure Hydrous Pyrolysis of Woodford Shale. *Energy & Fuels* 9, 204-215.
- Michels, R., Langlois, E., Ruau, O., Mansuy, L., Elie, M., Landais, P., 1996. Evolution of Asphaltenes during Artificial Maturation: A Record of the Chemical Processes. *Energy Fuels* 10, 39-48.
- Mitchell, S., McArthur, C., Snape, C.E., Taulbee, D., Hower, J.C., 1992. Evidence for maceral synergism in catalytic hydrolysis and hydrogenation of a sub-bituminous coal. *Preprints of Papers-American Chemical Society, Division of Fuel Chemistry* 37, 1583-1587.
- Monin, J.C., Connan, J., Oudin, J.L., Durand, B., 1990. Quantitative and qualitative experimental approach of oil and gas generation: Application to the North Sea source rocks. *Organic Geochemistry* 16, 133-142.
- Monin, J.C., Durand, B., Vandenbroucke, M., Huc, A.Y., 1980. Experimental simulation of the natural transformation of kerogen. *Physics and Chemistry of The Earth - Proceedings of the 9th International Meeting on Organic Geochemistry* 12, 517-530.
- Monnier, F., Powell, T.G., Snowdon, L.R., 1983. Qualitative and quantitative aspects of gas generation maturation of sedimentary organic matter. Examples from Canadian frontier basins. In: Bjorey (Ed.) *Advances in Organic Geochemistry 1981*. Wiley, Chichester, p. 487–495.
- Monthioux, M., Landais, P., Durand, B., 1986. Comparison between extracts from natural and artificial maturation series of Mahakam delta coals. *Organic Geochemistry* 10, 299-311.
- Monthioux, M., Landais, P., Monin, J.-C., 1985. Comparison between natural and artificial maturation series of humic coals from the Mahakam delta, Indonesia. *Organic Geochemistry* 8, 275-292.
- Muscio, G.P.A., Horsfield, B., 1996. Neoformation of Inert Carbon during the Natural Maturation of a Marine Source Rock: Bakken Shale, Williston Basin. *Energy Fuels* 10, 10-18.
- Muscio, G.P.A., Horsfield, B., Welte, D.H., 1994. Occurrence of thermogenic gas in the immature zone--implications from the Bakken in-source reservoir system. *Organic Geochemistry* 22, 461-476.
- Nissenbaum, A., Kaplan, I.R., 1972. Chemical and isotopic evidence for the in situ origin of marine humic substances. *Limnology and Oceanography* 17, 570–582.
- Oberlin, A., Boulmier, J.L., Villey, M., 1980. Electron microscopic study of kerogen microtexture. Selected criteria for determining the evolution path and evolution stage of

- kerogen. In: Durand, B. (Ed.) *Kerogen. Insoluble Organic Matter from Sedimentary Rocks*. Editions Technip, Paris, p. 191–241.
- Orr, W.L., 1983. Comments on pyrolytic hydrocarbon yields in source-rock evaluation. In: Bjoroy, M. (Ed.) *Advances in Organic Geochemistry 1981*. Wiley, Chichester, p. 775–787.
- Orr, W.L., 1986. Kerogen/asphaltene/sulfur relationships in sulfur-rich Monterey oils. *Organic Geochemistry* 10, 499-516.
- Payne, D.F., Ortoleva, P.J., 2001. A model for lignin alteration--part I: a kinetic reaction-network model. *Organic Geochemistry* 32, 1073-1085.
- Pelet, R., Behar, F., Monin, J.C., 1986. Resins and asphaltenes in the generation and migration of petroleum. *Organic Geochemistry* 10, 481-498.
- Pepper, A.S., Corvi, P.J., 1995a. Simple kinetic models of petroleum formation. Part I: oil and gas generation from kerogen. *Marine and Petroleum Geology* 12, 291-319.
- Pepper, A.S., Corvi, P.J., 1995b. Simple kinetic models of petroleum formation. Part III: Modelling an open system. *Marine and Petroleum Geology* 12, 417-452.
- Pepper, A.S., Dodd, T.A., 1995. Simple kinetic models of petroleum formation. Part II: oil-gas cracking. *Marine and Petroleum Geology* 12, 321-340.
- Peters, K.E., 1986. Guidelines for evaluating petroleum source rock using programmed pyrolysis. *AAPG Bulletin* 70, 318-329.
- Philippi, G.T., 1965. On the depth, time and mechanism of petroleum generation. *Geochimica et Cosmochimica Acta* 29, 1021-1049.
- Philp, R.P., Calvin, M., 1976. Possible origin for insoluble organic (kerogen) debris in sediments from insoluble cell-wall materials of algae and bacteria. *Nature* 262, 134-136.
- Pitt, G.J. 1961. The kinetics of the evolution of volatile products from coal. 4th Int. Conf. on Coal Science.
- Polanyi, M., Wigner, E., 1928. Über die Interferenz von Eigenschwingungen als Ursache von Energieschwankungen und chemischer Umsetzungen. *Zeitschrift für Physikalische Chemie* A139, 439-452.
- Poutsma, M.L., 1990. Free-radical thermolysis and hydrogenolysis of model hydrocarbons relevant to processing of coal. *Energy Fuels* 4, 113-131.
- Powell, T.G., Boreham, C.J., Smyth, M., Russell, N., Cook, A.C., 1991. Petroleum source rock assessment in non-marine sequences: pyrolysis and petrographic analysis of Australian coals and carbonaceous shales. *Organic Geochemistry* 17, 375-394.
- Premovic, P.I., 1992. Organic Free Radicals in Precambrian and Paleozoic Rocks: Origin and Significance. In: Schidlowski, M. (Ed.) *Early organic evolution: Implication for mineral and energy resources*. Springer-Verlag, pp. 241-256.
- Price, L.C., 1981. Organic geochemistry of 300°C, 7 km core samples, south Texas. *Chemical Geology* 37, 205–214.
- Price, L.C., 1989. Primary petroleum migration from shales with oxygen-rich organic matter. *Journal of Petroleum Geology* 12, 289-324.
- Price, L.C., 2001. A Possible Deep-Basin High-Rank Gas Machine Via Water Organic-Matter Redox Reactions. In: Dyman, T.S., Kuuskraa, V.A. (Eds.), *Geologic Studies of Deep*

- Natural Gas Resources. U. S. Geological Survey Digital Data Series, U. S. Geological Survey, Denver.
- Price, L.C., Wenger, L.M., 1992. The influence of pressure on petroleum generation and maturation as suggested by aqueous pyrolysis. *Organic Geochemistry - Proceedings of the 15th International Meeting on Organic Geochemistry* 19, 141-159.
- Quigley, T.M., Mackenzie, A.S., 1988. The temperatures of oil and gas formation in the sub-surface. *Nature* 333, 549-552.
- Quigley, T.M., Mackenzie, A.S., Gray, J.R., 1987. Kinetic theory of petroleum generation. In: Doligez, B. (Ed.) *Migration of hydrocarbons in sedimentary basins*. Editions Technip, p. 649-666.
- Rayleigh, J.W.S., 1896. Theoretical considerations respecting the separation of gases by diffusion and similar processes. 493-499.
- Reed, J.D., Illich, H.A., Horsfield, B., 1986. Biochemical evolutionary significance of Ordovician oils and their sources. In: Leythaeuser, D., Rullkötter, J. (Eds.), *Advances in Organic Geochemistry*. Pergamon Press, Oxford, pp. 347-358.
- Requejo, A.G., Allan, J., Creaney, S., Gray, N.R., Cole, K.S., 1992. Aryl isoprenoids and diaromatic carotenoids in Paleozoic source rocks and oils from the Western Canada and Williston Basins. *Organic Geochemistry - Proceedings of the 15th International Meeting on Organic Geochemistry* 19, 245-264.
- Reynolds, J.G., Burnham, A.K., 1993. Pyrolysis kinetics and maturation of coals from the San Juan basin. *Energy & Fuels* 7, 610-619.
- Reynolds, J.G., Burnham, A.K., 1995. Comparison of kinetic analysis of source rocks and kerogen concentrates. *Organic Geochemistry* 23, 11-19.
- Rice, D.D., Claypool, G.E., 1981. Generation, accumulation, and resource potential of biogenic gas. *AAPG Bulletin* 65, 5-25.
- Rice, F.O., 1933. The Thermal Decomposition of Organic Compounds from the Standpoint of Free Radicals. III. The Calculation of the Products Formed from Paraffin Hydrocarbons. *Journal of the American Chemical Society* 55, 3035-3040.
- Robinson, W.E., Heady, H.H., Hubbard, A.B., 1953. Alkaline Permanganate Oxidation of Oil-Shale Kerogen. *Industrial & Engineering Chemistry* 45, 788-791.
- Ross, D.J.K., Bustin, M.R., 2009. The importance of shale composition and pore structure upon gas storage potential of shale gas reservoirs. *Marine and Petroleum Geology* 26, 916-927.
- Rullkötter, J., Michaelis, W., 1990. The structure of kerogen and related materials. A review of recent progress and future trends. *Organic Geochemistry - Proceedings of the 14th International Meeting on Organic Geochemistry* 16, 829-852.
- Sachsenhofer, R.F., 1994. Petroleum generation and migration in the Styrian Basin (Pannonian Basin system, Austria): an integrated geochemical and numerical modelling study. *Marine and Petroleum Geology* 11, 684-701.
- Sackett, W.M., 1978. Carbon and hydrogen isotope effects during the thermocatalytic production of hydrocarbons in laboratory simulation experiments. *Geochimica et Cosmochimica Acta* 42, 571-580.
- Sackett, W.M., 1995. The thermal stability of methane from 600 to 1000°C. *Organic Geochemistry* 23, 403-406.

- Sackett, W.M., Chung, H.M., 1979. Experimental confirmation of the lack of carbon isotope exchange between methane and carbon oxides at high temperatures. *Geochimica et Cosmochimica Acta* 43, 273-276.
- Sackett, W.M., Conkright, M.E., 1997. Summary and re-evaluation of the high-temperature isotope geochemistry of methane. *Geochimica et Cosmochimica Acta* 61, 1941-1952.
- Sackett, W.M., Nakaparskin, S., Dalrymple, 1970. Carbon isotope effects in methane production by thermal cracking. In: Hobson, G.D., Speers, G.C. (Eds.), *Advances in Organic Geochemistry*. Pergamon Press, p. 37-53.
- Sandvik, E.I., Young, W.A., Curry, D.J., 1992. Expulsion from hydrocarbon sources: the role of organic absorption. *Organic Geochemistry - Proceedings of the 15th International Meeting on Organic Geochemistry* 19, 77-87.
- Santamaria-Orozco, D., Horsfield, B., 2004. Gas generation potential of Upper Jurassic (Tithonian) source rocks in the Sonda de Campeche, Mexico. In: Bartolini, C., Buffler, R.T., Blickwede, R.F. (Eds.), *The Circum-Gulf of Mexico and the Caribbean: Hydrocarbon Habitats, Basin Formation and Plate Tectonics*; AAPG Memoir. Vol. 79, American Association of Petroleum Geologists, Tulsa.
- Savage, P.E., 2000. Mechanisms and kinetics models for hydrocarbon pyrolysis. *Journal of Analytical and Applied Pyrolysis* 54, 109-126.
- Schaefer, R.G., Schenk, H.J., Hardelauf, H., Harms, R., 1990. Determination of gross kinetic parameters for petroleum formation from Jurassic source rocks of different maturity levels by means of laboratory experiments. *Organic Geochemistry* 16, 115-120.
- Schenk, H.J., Di Primio, R., Horsfield, B., 1997a. The conversion of oil into gas in petroleum reservoirs. Part 1: Comparative kinetic investigation of gas generation from crude oils of lacustrine, marine and fluviodeltaic origin by programmed-temperature closed-system pyrolysis. *Organic Geochemistry* 26, 467-481.
- Schenk, H.J., Dieckmann, V., 2004. Prediction of petroleum formation: the influence of laboratory heating rates on kinetic parameters and geological extrapolations. *Marine and Petroleum Geology* 21, 79-95.
- Schenk, H.J., Horsfield, B., 1993. Kinetics of petroleum generation by programmed-temperature closed-versus open-system pyrolysis. *Geochimica et Cosmochimica Acta* 57, 623-630.
- Schenk, H.J., Horsfield, B., 1998. Using natural maturation series to evaluate the utility of parallel reaction kinetics models: an investigation of Toarcian shales and Carboniferous coals, Germany. *Organic Geochemistry* 29, 137-154.
- Schenk, H.J., Horsfield, B., Krooss, B., Schaefer, R.G., Schwochau, K., 1997b. Kinetics of petroleum formation and cracking. In: Welte, D.H., Horsfield, B., Backer, D.R. (Eds.), *Petroleum and Basin Evolution. Insights from Petroleum geochemistry, Geology and Basin modelling*, Springer, Berlin, pp. 231-270.
- Schenk, H.-J., Richter, A. (1995) Investigation of Carboniferous coals by Infrared Spectroscopy and Kinetic Measurements: Data Report. KFA Internal Report.
- Schenk, H.J., Witte, E.G., Muller, P.J., Schwochau, K., 1986. Infrared estimates of aliphatic kerogen carbon in sedimentary rocks. *Organic Geochemistry* 10, 1099-1104.
- Schoell, M., 1980. The hydrogen and carbon isotopic composition of methane from natural gases of various origins. *Geochimica et Cosmochimica Acta* 44, 649-661.
- Schoell, M., 1983. Genetic characterization of natural gases. *AAPG Bulletin* 67, 2225-2238.

- Schoell, M., 1988. Multiple origins of methane in the Earth. *Chemical Geology - Origins of Methane in the Earth* 71, 1-10.
- Schulz, H.-M., Sachsenhofer, R.F., Bechtel, A., Polesny, H., Wagner, L., 2002. The origin of hydrocarbon source rocks in the Austrian Molasse Basin (Eocene-Oligocene transition). *Marine and Petroleum Geology* 19, 683-709.
- Scott, A.C., 1989. Observations on the nature and origin of fusain. *International Journal of Coal Geology* 12, 443-475.
- Seewald, J.S., 1994. Evidence for metastable equilibrium between hydrocarbons under hydrothermal conditions. 370, 285-287.
- Senftle, J.T., Larter, S.R., Bromley, B.W., Brown, J.H., 1986. Quantitative chemical characterization of vitrinite concentrates using pyrolysis-gas chromatography. Rank variation of pyrolysis products. *Organic Geochemistry* 9, 345-350.
- Short, K.C., Stäuble, A.J., 1965. Outline of geology of Niger Delta. *AAPG Bulletin* 51, 761-779.
- Silverman, S., 1967. Carbon isotopic evidence for the role of lipids in petroleum formation. *Journal of the American Oil Chemists' Society* 44, 691-695.
- Sinninghe Damste, J.S., De Leeuw, J.W., 1990. Analysis, structure and geochemical significance of organically-bound sulphur in the geosphere: State of the art and future research. *Organic Geochemistry - Proceedings of the 14th International Meeting on Organic Geochemistry* 16, 1077-1101.
- Sinninghe Damsté, J.S., Eglinton, T.I., Rijpstra, W.I.C., de Leeuw, J.W., 1990. Characterisation of organically-bound sulfur in high-molecular-weight sedimentary organic matter using flash pyrolysis and Raney Ni desulfurisation. In: Orr, W.L., White, C.M. (Eds.), *Geochemistry of Sulfur in Fossil Fuels*. 429. ACS Symposium Series, Washington DC, pp. 486-528.
- Sinninghe Damsté, J.S., Kohnen, M.E.L., Horsfield, B., 1998. Origin of low-molecular-weight alkylthiophenes in pyrolysates of sulphur-rich kerogens as revealed by micro-scale sealed vessel pyrolysis. *Organic Geochemistry* 29, 1891-1903.
- Smith, C.M., Savage, P.E., 1991. Reactions of polycyclic alkylaromatics: Structure and reactivity. *AIChE Journal* 37, 1613-1624.
- Smith, C.M., Savage, P.E., 1992. Reactions of polycyclic alkylaromatics. 4. Hydrogenolysis mechanisms in 1-alkylpyrene pyrolysis. *Energy & Fuels* 6, 195-202.
- Smith, G.C., Cook, A.C., 1984. Petroleum occurrence in the Gippsland Basin and its relationship to rank and organic matter type. *Australian Petroleum Exploration Association Journal* 24, 196-216.
- Smith, J.W., Rigby, D., Gould, K.W., Hart, G., Hargraves, A.J., 1985. An isotopic study of hydrocarbon generation processes. *Organic Geochemistry*
- Organic Geochemistry 2 A Selection of Papers from the 2nd Australian Organic Geochemistry Conference* 8, 341-347.
- Snowdon, L.R., 1971. Source rock analysis in Alberta and the N.W. Territories, utilising borehole cuttings. *Geological Survey of Canada Paper* 71-1 (part-b) 105.
- Snowdon, L.R., 2001. Natural gas composition in a geological environment and the implications for the processes of generation and preservation. *Organic Geochemistry* 32, 913-931.

- Solomon, P.R., Hamblen, D.G., Carangelo, R.M., Serio, M.A., Deshpande, G.V., 1988. General model of coal devolatilization. *Energy & Fuels* 2, 405-422.
- Stach, E., Mackowsky, M.-T., Teichmüller, M., Taylor, G.H., Chandra, D., Teichmüller, R., 1982. *Stach's Textbook of Coal Petrology*. Gebrüder Borntraeger, Stuttgart.
- Stacher, P., 1995. Present understanding of the Niger Delta hydrocarbon habitat. In: Oti, M.N., Postma, G. (Eds.), *Geology of Deltas*. A.A. Balkema, Rotterdam, pp. 257-267.
- Stahl, W.J., Carey Jr., B.D., 1975. Source-rock identification by isotope analyses of natural gases from fields in the Val Verde and Delaware basins, west Texas. *Chemical Geology* 16, 257-267.
- Stevenson, F.J., 1974. Non biological transformations of amino acids in soils and sediments. In: Tissot, B., Bienner, F. (Eds.), *Advances in Organic Geochemistry 1973*. Editions Technip, Paris, pp. 701-714.
- Stout, S.A., Boon, J.J., 1994. Structural characterization of the organic polymers comprising a lignite's matrix and megafossils. *Organic Geochemistry* 21, 953-970.
- Stout, S.A., Emsbo-Mattingly, S.D., 2008. Concentration and character of PAHs and other hydrocarbons in coals of varying rank - Implications for environmental studies of soils and sediments containing particulate coal. *Organic Geochemistry* 39, 801-819.
- Stuermer, D.H., Peters, K.E., Kaplan, I.R., 1978. Source indicators of humic substances and proto-kerogen. Stable isotope ratios, elemental compositions and electron spin resonance spectra. *Geochimica et Cosmochimica Acta* 42, 989-997.
- Suggate, R.P., Boudou, J.P., 1993. Coal Rank and Type Variation in Rock-Eval Assessment of New Zealand Coals. *Journal of Petroleum Geology* 16, 73-88.
- Summons, R.E., 1993. Biogeochemical cycles: A review of fundamental aspects of organic matter formation, preservation, and composition. In: Engel, M.H., Macko, S.A. (Eds.), *Organic geochemistry—Principles and applications*. Plenum Press, New York, pp. 3-21.
- Sweeney, J.J., Burnham, A.K., Braun, R.L., 1987. A model of hydrocarbon generation from type I kerogen; application to Uinta Basin, Utah. *AAPG Bulletin* 71, 967-985.
- Sykes, R., Snowdon, L.R., 2002. Guidelines for assessing the petroleum potential of coaly source rocks using Rock-Eval pyrolysis. *Organic Geochemistry* 33, 1441-1455.
- Tang, Y., Perry, J.K., Jenden, P.D., Schoell, M., 2000. Mathematical modeling of stable carbon isotope ratios in natural gases. *Geochimica et Cosmochimica Acta* 64, 2673-2687.
- Tang, Y., Xia, X. (2011) Kinetics and Mechanism of Shale Gas Formation: A Quantitative Interpretation of Gas Isotope "Rollover" for Shale Gas Formation. In *AAPG Search and Discovery Article #90122©2011 AAPG Hedberg Conference, December 5-10, 2010, Austin, Texas*.
- Tannenbaum, E., Kaplan, I.R., 1985. Role of minerals in the thermal alteration of organic matter--I: Generation of gases and condensates under dry condition. *Geochimica et Cosmochimica Acta* 49, 2589-2604.
- Tarafa, M.E., Hunt, J.M., Ericsson, I., 1983. Effect of hydrocarbon volatility and adsorption on source-rock pyrolysis. *Journal of Geochemical Exploration* 18, 75-85.
- Tarafa, M.E., Whelan, J.K., Farrington, J.W., 1988. Investigation on the effects of organic solvent extraction on whole-rock pyrolysis: Multiple-lobed and symmetrical P2 peaks. *Organic Geochemistry* 12, 137-149.

- Tegelaar, E.W., de Leeuw, J.W., Derenne, S., Largeau, C., 1989a. A reappraisal of kerogen formation. *Geochimica et Cosmochimica Acta* 53, 3103-3106.
- Tegelaar, E.W., Matthezing, R.M., Jansen, J.B.H., Horsfield, B., Leeuw, J.W.d., 1989b. Possible origin of n-alkanes in high-wax crude oils. *Nature* 342, 529 - 531.
- Tegelaar, E.W., Noble, R.A., 1994. Kinetics of hydrocarbon generation as a function of the molecular structure of kerogen as revealed by pyrolysis-gas chromatography. *Organic Geochemistry* 22, 543-574.
- Teichmüller, M., 1989. The genesis of coal from the viewpoint of coal petrology. *International Journal of Coal Geology* 12, 1-87.
- Teichmüller, M., Durand, B., 1983. Fluorescence microscopical rank studies on liptinites and vitrinites in peat and coals, and comparison with results of the rock-eval pyrolysis. *International Journal of Coal Geology* 2, 197-230.
- Thompson, K.F.M., 2002. Compositional regularities common to petroleum reservoir fluids and pyrolysates of asphaltenes and kerogens. *Organic Geochemistry* 33, 829-841.
- Thompson, S., Cooper, B.S., Morley, R.J., Barnard, P.C., 1985. Oil-generating coals. In: Thomas, B.M. (Ed.) *Petroleum Geochemistry in Exploration of the Norwegian Shelf*. Graham and Trotman, London, p. 59-73.
- Tissot, B., Califet-Debyser, Y., Deroo, G., Oudin, J.L., 1971. Origin and evolution of hydrocarbons in Early Toarcian shales, Paris Basin, France. *American Association of Petroleum Geologists Bulletin* 55, 177-2193.
- Tissot, B., Deroo, G., Hood, A., 1978. Geochemical study of the Uinta Basin: formation of petroleum from the Green River formation. *Geochimica et Cosmochimica Acta* 42, 1469-1485.
- Tissot, B.P., 1969. Premières données sur les mécanismes et la cinétique de la formation du pétrole dans les sédiments - Simulation d'un schéma réactionnel sur ordinateur. *Oil & Gas Science and Technology - Rev. IFP* 24, 470-501.
- Tissot, B.P., Durand, B., Espitalié, J., Combaz, A., 1974. Influence of nature and diagenesis of organic matter in formation of petroleum. *AAPG Bulletin* 58, 499-506.
- Tissot, B.P., Espitalié, J., 1975. L'évolution de la matière organique des sédiments: application d'une simulation mathématique. *Rev. IFP* 30, 743-777.
- Tissot, B.P., Pelet, R., Ungerer, P., 1987. Thermal history of sedimentary basins, maturation indices, and kinetics of oil and gas generation. *AAPG Bulletin* 71, 1445-1466.
- Tissot, B.P., Welte, D.H., 1984. *Petroleum Formation and Occurrence*. Springer-Verlag, Berlin.
- Ungerer, P., 1990. State of the art of research in kinetic modelling of oil formation and expulsion. *Organic Geochemistry - Proceedings of the 14th International Meeting on Organic Geochemistry* 16, 1-25.
- Ungerer, P., Behar, F., Villalba, M., Heum, O.R., Audibert, A., 1988. Kinetic modelling of oil cracking. *Organic Geochemistry - Proceedings of the 13th International Meeting on Organic Geochemistry* 13, 857-868.
- Ungerer, P., Pelet, R., 1987. Extrapolation of the kinetics of oil and gas formation from laboratory experiments to sedimentary basins. *Nature* 327, 52-54.
- Urov, K.E., 1980. Thermal decomposition of kerogens : Mechanism and analytical application. *Journal of Analytical and Applied Pyrolysis* 1, 323-338.



- USDOE. (2009) Modern Shale Gas Development in the United States: A Primer, p. 116. U.S. Department of Energy, Office of Fossil Energy, National Energy Technology Laboratory.
- Van Aarssen, B.G.K., Cox, H.C., Hoogendoorn, P., De Leeuw, J.W., 1990. A cadinene biopolymer in fossil and extant dammar resins as a source for cadinanes and bicadinanes in crude oils from South East Asia. *Geochimica et Cosmochimica Acta* 54, 3021-3031.
- van Aarssen, B.G.K., de Leeuw, J.W., Horsfield, B., 1991. A comparative study of three different pyrolysis methods used to characterise a biopolymer isolated from fossil and extant dammar resins. *Journal of Analytical and Applied Pyrolysis* 20, 125-139.
- van Aarssen, B.G.K., Hessels, J.K.C., Abbink, O.A., de Leeuw, J.W., 1992. The occurrence of polycyclic sesqui-, tri-, and oligoterpenoids derived from a resinous polymeric cadinene in crude oils from southeast Asia. *Geochimica et Cosmochimica Acta* 56, 1231-1246.
- van de Meent, D., Brown, S.C., Philp, R.P., Simoneit, B.R.T., 1980. Pyrolysis-high resolution gas chromatography and pyrolysis gas chromatography-mass spectrometry of kerogens and kerogen precursors. *Geochimica et Cosmochimica Acta* 44, 999-1013.
- van Heek, K.H., Jüntgen, H., 1968. Bestimmung der reaktionskinetischen Parameter aus nicht-isothermen Messungen. *Ber Bunsenges Physical Chemistry* 72, 1223-1231.
- Van Krevelen, D.W., 1961. *Coal: Typology – Chemistry – Physics – Constitution*. Elsevier, The Netherlands.
- Van Krevelen, D.W., 1993. *Coal: Typology, Physics, Chemistry, and Constitution*. Elsevier, New York.
- van Krevelen, D.W., van Heerden, C., Huntjens, F.J., 1951. Physicochemical aspects of the pyrolysis of coal and related organic compounds. *Fuel* 30, 253-259.
- Vandenbroucke, M., Largeau, C., 2007. Kerogen origin, evolution and structure. *Organic Geochemistry* 38, 719-833.
- Vernon, L.W., 1980. Free radical chemistry of coal liquefaction: role of molecular hydrogen. *Fuel* 59, 102-106.
- Voge, H.H., Good, G.M., 1949. Thermal Cracking of Higher Paraffins. *Journal of the American Chemical Society* 71, 593-597.
- Vu, T.A.T. (2008) Origin and maturation of organic matter in New Zealand coals. University of Greifswald.
- Vu, T.A.T., Horsfield, B., Sykes, R., 2008. Influence of in-situ bitumen on the generation of gas and oil in New Zealand coals. *Organic Geochemistry* 39, 1606-1619.
- Vu, T.T.A., Zink, K.-G., Mangelsdorf, K., Sykes, R., Wilkes, H., Horsfield, B., 2009. Changes in bulk properties and molecular compositions within New Zealand Coal Band solvent extracts from early diagenetic to catagenetic maturity levels. *Organic Geochemistry* 40, 963-977.
- Walters, C.C., Freund, H., Kelemen, S.R., Peczak, P., Curry, D.J., 2007. Predicting oil and gas compositional yields via chemical structure-chemical yield modeling (CS-CYM): Part 2 - Application under laboratory and geologic conditions. *Organic Geochemistry* 38, 306-322.
- Wang, C., Du, J., Wang, W., Xie, H., Chen, G., Duan, Y., Zhou, X., 2006. Experimental study to confirm the existence of hydrocarbon under high pressure and temperature of deep lithosphere. *Chinese Science Bulletin* 51, 1633-1638.

- Waples, D.W., 2000. The kinetics of in-reservoir oil destruction and gas formation: Constraints from experimental and empirical data and from thermodynamics. *Organic Geochemistry* 31, 553–575.
- Weiss, H.M., Wilhelms, A., Mills, N., Scotchmer, J., Hall, P.B., Lind, K., Brekke, T., 2000. NIGOGA—The Norwegian Industry Guide to Organic Geochemical Analysis. Edition 4.0. Norsk Hydro, Statoil, Geolab Nor, SINTEF Petroleum Research and the Norwegian Petroleum Directorate. [www.npd.no](http://www.npd.no).
- Welhan, J.A., 1988. Origins of methane in hydrothermal systems. *Chemical Geology - Origins of Methane in the Earth* 71, 183-198.
- Welte, D.H., 1974. Recent advances in organic geochemistry of humic substances and kerogen. A review. In: Tissot, B., Bienner, F. (Eds.), *Advances in Organic Geochemistry 1973*. Editions Technip, Paris, p. 3–13.
- Weres, O., Newton, A.S., Tsao, L., 1988. Hydrous pyrolysis of alkanes, alkenes, alcohols and ethers. *Organic Geochemistry* 12, 433-444.
- Whiticar, M.J., 1994. Correlation of natural gases with their source. In: Magoon, L., Dow, W. (Eds.), *The Petroleum System: from Source to Trap*. Vol. 60, AAPG Memoir, pp. 261-283.
- Whiticar, M.J., 1999. Carbon and hydrogen isotope systematics of bacterial formation and oxidation of methane. *Chemical Geology* 161, 291-314.
- Whiticar, M.J., Faber, E., Schoell, M., 1986. Biogenic methane formation in marine and freshwater environments: CO<sub>2</sub> reduction vs. acetate fermentation--Isotope evidence. *Geochimica et Cosmochimica Acta* 50, 693-709.
- Wilhelms, A., Larter, S.R., Leythaeuser, D., 1991. Influence of bitumen-2 on Rock-Eval pyrolysis. *Organic Geochemistry* 17, 351-354.
- Wilkins, R.W.T., George, S.C., 2002. Coal as a source rock for oil: a review. *International Journal of Coal Geology* 50, 317-361.
- Wiser, W.H., 1968. Kinetic Study of the Thermal Dissolution of High-Volatile Bituminous Coal. *Fuel* 47, 475.
- Xiong, Y., Zhang, H., Geng, X., Geng, A. (2004) Thermal cracking of *n*-octodecane and its geochemical significance. In *Chinese Science Bulletin*, Vol. 49, pp. 79-83. Science China Press, co-published with Springer.
- Yarzab, R.F., Abdel-Baset, Z., Given, P.H., 1979. Hydroxyl contents of coals: new data and statistical analyses. *Geochimica et Cosmochimica Acta* 43, 281-287.
- Yen, T.F., 1974. A new structural model of oil shale kerogen. *Prepr. Div. Fuel. Chem. Am. Chem. Soc* 19, 109–114.
- Zumberge, J., Ferworn, K., Brown, S., 2012. Isotopic reversal ('rollover') in shale gases produced from the Mississippian Barnett and Fayetteville formations. *Marine and Petroleum Geology - Insights into Shale Gas Exploration and Exploitation* 31, 43-52.

## INDEX OF APPENDIX

Table A 1: Sample Provenance and TOC/Rock-Eval .....	249
Table A 2: Open-System Pyrolysis GC-FID.....	252
Table A 3: Bulk Kinetics .....	290
Table A 4: IR-ATR Mineralogy Screen.....	294
Table A 5: stepwise open-system pyrolysis GC-FID.....	295
Table A 6: stepwise closed-system (MSSV)-pyrolysis.....	303
Table A 7: Late Gas Potential Screening (immature samples).....	309
Table A 8: Late Gas Potential Screening (maturity series).....	323
Table A 9: Open-system pyrolysis GC-FID of residues prepared by MSSV-pyrolysis.....	330
Table A 10: Late Gas Potential Screening of residues prepared by MSSV-pyrolysis .....	336
Table A 11: Open-system Pyrolysis GC-FID of residues prepared by open-system pyrolysis (SRA) .....	339
Table A 12: Late Gas Potential Screening of residues prepared by open-system pyrolysis (SRA) .....	341
Table A 13: $\delta^{13}\text{C}$ composition of $\text{C}_{1-4}$ gases at different MSSV-pyrolysis end temperatures .....	342

## APPENDIX

Table A 1: Sample Provenance and TOC/Rock-Eval

Table A 1: Sample Provenance and TOC/Rock-Eval

Company	Company Code/Wells	GFZ Code	APT Code	Formation/Basin	Age	TOC (%)	S1 (mg HC/g rock)	S2 (mg HC/g rock)	S3 (mg CO2/g rock)	HI (mg HC/g TOC)	OI (mg CO2/g TOC)	T <sub>max</sub> (°C)	PI S1/(S1+S2)	R <sub>o</sub> % calculated
Shell	Plogbene-2	G005935	53354	Akata Shale	Paleogene	7.12	1.54	22.25	1.08	313	15	429	0.06	0.56
	Nr.4	G005936	53385			9.93	0.03	0.48	0.85	52	91	424	0.06	0.47
		G005937	53386	Middle East	Silurian	4.29	0.30	0.50	0.70	12	16	285	0.38	
	A-ST 003 GSC 14348	G006948	64456			3.14	0.14	1.57	6.22	50	198	421	0.08	0.42
	B-STQ 003 GSC 14380	G006949	64457			5.65	0.93	9.26	4.84	164	86	421	0.09	0.42
Total		G006204		Douala Basin	Cretaceous	1.39	0.21	1.98	0.54	143	39	442	0.10	0.80
		G006205				2.46	0.24	2.11	0.59	86	24	444	0.10	0.83
	165345-1	G006206		Mahakam Delta		1.21	0.12	1.78	0.96	147	79	431	0.06	0.60
	165344-1	G006207	57629			31.60	3.00	76.01	2.93	241	9	433	0.04	0.63
		G006208		Toarcian Shale	Jurassic	7.93	1.23	54.30	1.11	685	14	431	0.02	0.60
ENI		G006209				7.61	1.28	51.69	1.07	679	14	432	0.02	0.62
	A-TD	G004563		Domanik Fm.	Devonian	24.00	10.50	150.00		625		424	0.07	0.47
	B-NSH	G004564		Murzuq Basin	Silurian	16.00	5.21	55.00		344		420	0.09	0.40
	sample C	G007160	64458			12.80	10.58	59.37	1.75	464	14	424	0.15	0.47
	sample D	G007161	64459	Ghadames Basin	Silurian	2.97	0.44	2.67	0.92	90	31	424	0.14	0.47
Petrobras	sample A	G005762		Hekkingen Fm.	Jurassic	9.01	0.60	24.71		274		413	0.02	0.27
	sample B	G005763	57628			8.39	1.19	15.82	4.71	189	56	418	0.07	0.36
	80590752	G005812		Irati Fm.	Perm	25.30	9.68	177.87	1.55	703	6	419	0.05	0.39
		G006153	53392	Woodford Shale	Devonian	9.85	1.22	43.99	1.22	447	12	417	0.03	0.35
	06-4015-159521	G006154		Caney Shale	Carboniferous	11.31	0.89	55.53	1.15	491	10	421	0.02	0.42
Devon	06-4015-159520	G006155		New Albany Shale	Devonian	3.60	0.23	16.23	0.59	451	16	423	0.01	0.45
		G006156	53391			13.80	2.57	58.91	1.37	427	10	425	0.04	0.49
	Rheden-18-SP-845	G006533	57612			76.20	24.22	176.97	5.65	232	7	429	0.12	0.56
	Rheden-19-SP-845	G006535	57613			14.10	0.81	108.88	1.12	772	8	453	0.01	0.99
	Rheden-19-SP-870	G006536	57614			14.10	0.86	109.60	1.23	777	9	453	0.01	0.99
Wintershall	Rheden-19-SP-890	G006538	57615			83.60	20.04	163.27	3.75	195	4	447	0.11	0.89
	Rheden-19-SP-955	G006540	57616			6.19	0.93	38.18	0.37	617	6	452	0.02	0.98
	Rheden-23-SP-605	G006542	57617			78.60	30.84	207.43	3.25	264	4	439	0.13	0.74
	Rheden-24-SP-870	G006544	57618			85.10	21.69	175.13	3.05	206	4	440	0.11	0.76
	Rheden-26-SP-800	G006547	57619			6.58	1.15	47.66	0.40	724	6	452	0.02	0.98
	Rheden-29-SP-865	G006548	57620			75.80	15.47	152.92	4.94	202	7	438	0.09	0.72
	Rheden-29-SP-870	G006550	57621			80.20	18.09	174.63	4.12	218	5	440	0.09	0.76
	Bahrenborstel-Z-8-SP-365	G006553	57623			9.12	2.10	58.36	0.51	640	6	453	0.03	0.99
	Bahrenborstel-Z-8SP-355	G006554	57624			8.28	1.90	53.32	0.58	644	7	451	0.03	0.96
	Annalie-1 4215 m	G007162				1		1.40		140		436		0.69
Maersk	Annalie-1 4400 m	G007163		Farsund Fm.	upper Jurassic	0.7		0.80		114		433		0.63
	Annalie-1 4635 m	G007164		Danish Central Graben		0.8		1.00		125		436		0.69
	Annalie-1 4720 m	G007165				1.5		2.00		133		439		0.74
	Annalie-1 4805 m	G007166				1.7		1.90		112		440		0.76

Calculated R<sub>o</sub> = 0.0180 \* T<sub>max</sub> - 7.16 (Jarvie *et al.* 2001)

Table A 1: Sample Provenance and TOC/Rock-Eval

Table A 1 continued (immature GFZ samples)

Company	Company Code/Wells	GFZ Code	APT Code	Formation/Basin	Age	TOC	S1 (mg HC/g rock)	S2 (mg HC/g rock)	S3 (mg CO2/g rock)	HI (mg HC/g TOC)	OI (mg CO2/g TOC)	T <sub>max</sub> (°C)	PI (°C)(S1/(S1+S2))	R <sub>o</sub> % calculated
GFZ immature		G000206		Kugmallit Fm.	Oligocene	59.74	3.30	41.28	43.57	69	73	359	0.07	
		G000670		Talang Akar Coal	Eocene-Oligocene	62.25	21.03	186.33	5.82	299	9	442	0.10	0.80
		G000689	57630	Botheheia Shale	Triassic	6.04	1.00	17.71	0.41	293	7	447	0.05	0.89
		G000690		Woodford Shale	Devonian	21.27	4.53	93.53	2.44	440	11	419	0.05	0.38
		G000692	53387	Chatanooga Shale	Devonian	12.40	2.06	46.12	0.80	372	6	426	0.04	0.51
		G000693		Alaskan Tasmanite	Jurassic	61.26	11.09	458.72	31.91	749	52	442	0.02	0.80
		G000696		Jet Rock	Lower Jurassic	21.40	10.05	100.00	1.55	467	7	423	0.09	0.45
		G000697		Boghead Coal	Pennsylvanian	55.42	4.98	305.63	18.60	551	34	433	0.02	0.63
		G000698	53388	Cannel Coal	Cretaceous	67.90	1.65	127.27	5.14	187	8	430	0.01	0.58
		G000726		Talang Akar Coal	Eocene-Oligocene	63.70	12.39	206.98	6.94	325	11	429	0.06	0.56
		G000731		Brown Limestone	Late Cretaceous	14.47	3.71	114.09	2.35	788	16	412	0.03	0.26
		G000753		Alum Shale	Cambrian	11.51	1.20	46.30	1.90	402	16	415	0.03	0.31
		G000758		Alum Shale	Cambrian	11.83	1.60	31.80	4.20	269	35	419	0.05	0.38
		G000859	53390	Messel Oil Shale	Eocene	29.40	3.55	143.74	15.56	489	53	425	0.02	0.49
		G000883	53389	Autun Oil Shale	Jurassic	9.80	0.91	30.85	3.19	315	33	429	0.03	0.56
		G000899		Talang Akar Coal	Eocene-Oligocene	49.40	4.20	88.49	18.18	179	37	421	0.05	0.42
		G000950		Arang Coal	Miocene	58.19	4.51	131.44	22.39	226	38	420	0.03	0.40
		G001955		Spekk Fm.	Upper Jurassic	7.19	2.03	26.65	3.11	371	43	417	0.07	0.35
		G001965		Are Fm.	Lower Jurassic	39.36	4.65	70.87	34.17	180	87	416	0.06	0.33
	Fischschiefer/Osch-1	G004070		Schöneck Fm.	Eocene-Oligocene	10.10	2.34	54.62		540		424	0.04	0.47
	Fischschiefer/Osch-1	G004071		Schöneck Fm.	Eocene-Oligocene	11.80	2.96	59.04		500		425	0.05	0.49
	Fischschiefer/Osch-1	G004072		Schöneck Fm.	Eocene-Oligocene	7.75	1.08	42.36		546		420	0.02	0.40
		G004750		Green River Shale	Tertiary	12.82	1.79	99.58	0.73	777	6	445	0.02	0.85
		G0047501965	53383	Mix type I/III		31.30	2.70	82.87	16.39	265	52	434	0.03	0.65
		G005298		Bakken Shale	Mississippian	8.25	0.79	34.34	2.20	416	27	413	0.02	0.27
		SN6750	53382	Taglu Fm.	Eocene	44.10	1.44	65.44	17.92	148	41	419	0.02	0.38

Table A 1: Sample Provenance and TOC/Rock-Eval

Table A 1 continued (maturity series)

Company	Company Code/Wells	GFZ Code	APT Code	Formation/Basin	Age	TOC (%)	S1 (mg HC/g rock)	S2 (mg HC/g rock)	S3 (mg CO2/g rock)	HI (mg HC/g TOC)	OI (mg CO2/g TOC)	T <sub>max</sub> (°C)	PI β1/(S1+S2))	% R <sub>o</sub> calculated measured	
Shell	FPC-271538	G006385		Exshaw Fm.	Devonian	8.83		27.36		310		440		0.76	
	FPC-826949	G006387	57627			2.65	1.13	5.95	0.23	225	9	447	0.16	0.89	
	FPC-271536	G006384	57625			1.20	0.15	0.42	0.28	35	23	467	0.26	1.25	
	FPC-378121	G006386	57626			2.25	0.10	0.61	0.47	27	21	583	0.14	3.33	
Wintershall	Rheden-18-SP-845	G006533	57612	Wealden	Cretaceous	76.20	24.22	176.97	5.65	232	7	429	0.12	0.56	
	Rheden-29-SP-865	G006548	57620			75.80	15.47	152.92	4.94	202	7	438	0.09	0.72	
	Rheden-19-SP-890	G006538	57615			83.60	20.04	163.27	3.75	195	4	447	0.11	0.89	
	Bahrenborstel-Z-2-SP-285	G006552	57622			47.20	2.18	36.76	1.49	78	3	474	0.06	1.37	
GFZ natural maturity series	Quarry South of San Saba, TX	G007249	63181	Barnett Shale	Carboniferous late Mississippian	11.70	1.09	57.90	1.47	495	13	420	0.02	0.40	
	Ron Cheek #1	G007247	63179			5.59	11.00	15.73	0.64	281	11	450	0.18	0.94	
	W.C. Young-2	G007250	63182			6.11	6.00	5.08	0.38	83	6	473	0.33	1.35	
	Mitchell T P Sims-2	G007257	63189			4.37	10.00	1.71	0.42	39	10	505	0.30	1.93	
	Oliver-1	G007219	63151	Westphalian Coals	Carboniferous	4.08	0.54	0.90	2.81	22	69	576	0.38	3.21	
	Sandbochum1	G007221	70096			79.30	3.25	164.90	5.08	208	6	438	0.02	0.99	
	Wlastedde	G001088	70099			81.00	4.90	126.61	3.94	156	5	468	0.04	1.26	
	Dickebank-2	G001083	70097			61.40	4.52	106.56	2.92	174	5	482	0.04	1.37	
	Verden-1	G001086	70098			66.00	2.25	66.76	2.33	101	4	492	0.03	1.58	
	Siedenburg Z-1	G001092	70100			75.80	0.55	19.22	4.23	25	6	550	0.03	2.09	
	Granterath-1	G001096	70101			85.30	1.19	8.39	4.42	10	5	596	0.12	2.81	
	GFZ natural maturity series		G001983		NZ-Coal	Cenozoic	58.47	7.27	93.98	28.42	161	49	418	0.07	0.41
			G001982				60.01	3.96	105.19	23.33	175	39	419	0.04	0.40
			G001984				63.90	3.75	108.54	16.97	170	27	423	0.03	0.45
			G001981				61.20	3.04	94.51	19.85	154	32	422	0.03	0.45
			G001980				60.20	3.00	104.04	15.52	173	26	420	0.03	0.44
		G001997		67.40			2.87	141.05	9.94	209	15	424	0.02	0.52	
		G001996		65.50			4.03	150.45	8.39	230	13	423	0.03	0.52	
		G001994		63.52			6.23	179.93	9.10	283	14	430	0.03	0.61	
		G001990		74.18			7.65	198.29	4.25	267	6	431	0.04	0.71	
		G001991		75.00			13.67	194.01	3.68	259	5	436	0.07	0.80	
		G001983K		56.64			7.84	75.39	31.05	133	55	420	0.09	0.41	
		G001982K		59.91			7.57	78.17	22.74	130	38	424	0.09	0.40	
		G001984K		61.80			9.08	83.06	17.21	134	28	422	0.10	0.45	
		G001981K		59.60			11.13	70.92	19.84	119	33	425	0.14	0.45	
		G001980K		58.30			10.50	81.18	15.58	139	27	423	0.11	0.44	
		G001997K		65.90			9.81	118.74	10.37	180	16	426	0.08	0.52	
	G001996K		62.00	9.85	119.68	8.74	193	14	426	0.08	0.52				
	G001994K		61.47	7.47	148.73	9.39	242	15	431	0.05	0.61				
	G001990K		69.31	9.70	162.51	4.99	235	7	432	0.06	0.71				
	G001991K		69.80	8.54	157.97	4.71	226	7	436	0.05	0.80				

Table A 2: Open-System Pyrolysis GC-FID

Table A 2: Open-System Pyrolysis GC-FID

Company	Shell				
Formation/Basin	Akata Shale	Middle East - Silurian Hot Shale			
GFZ Code	G005935	G005936	G005937	G006948	G006949
File	G005935AD	G005936AD	G005937AD	G006948AA	G006949AA
Temperature [°C]	200-560	200-560	200-560	300-600	300-600
Rate	2K/min	2K/min	2K/min	60K/min	60K/min
Totals	mg/g TOC	mg/g TOC	mg/g TOC	mg/g TOC	mg/g TOC
C <sub>1+</sub> (-blank)	307.62	143.31	49.35	23.39	89.37
C <sub>1-5</sub>	64.43	22.01	3.25	13.43	30.25
C <sub>2-5</sub>	44.28	18.13	2.02	11.78	25.58
C <sub>6-14</sub> (-blank)	94.31	10.88	6.10	9.96	43.97
C <sub>6-14</sub> Hump	61.20	8.99	4.14	7.81	29.43
C <sub>6-14</sub> Resolved	33.11	1.88	1.96	2.15	14.54
C <sub>15+</sub> (-blank)	148.88	110.43	40.00	0.00	15.15
C <sub>15+</sub> Hump	31.35	0.14	1.17	0.00	2.19
C <sub>15+</sub> Resolved	117.53	110.29	38.82	0.00	12.96
GOR	0.26	0.18	0.07	1.35	0.51
Gas Wetness (C2-5/C1-5)	0.69	0.82	0.62	0.88	0.85
Compounds Summation	mg/g TOC	mg/g TOC	mg/g TOC	mg/g TOC	mg/g TOC
n-C <sub>6-14</sub>	18.78	2.37	1.29	0.78	6.03
n-C <sub>15+</sub>	18.99	0.10	0.51	0.01	0.51
Mono-aromatic Compounds	7.19	2.24	0.51	3.36	5.89
Di-aromatic Compounds	2.41	0.01	0.11	0.14	1.05
Phenolic Compounds	1.88	0.00	0.03	0.01	0.38
Thiophenic Compounds	2.16	0.47	0.06	0.44	1.56
Single Compounds	mg/g TOC	mg/g TOC	mg/g TOC	mg/g TOC	mg/g TOC
Methane	20.15	3.88	1.23	1.65	4.67
Ethene	2.82	4.27	0.26	0.21	0.29
Ethane	9.73	1.10	0.11	2.21	4.26
Propane	10.85	4.47	0.30	1.93	4.76
i-Butane	0.38	0.19	0.09	0.11	0.42
1-Butene	3.87	1.06	0.20	0.45	2.02
n-Butane	2.62	1.22	0.07	0.60	1.49
i-Pentane	1.00	0.19	0.07	0.39	0.63
Pentene	1.55	0.45	0.04	0.37	0.92
n-Pentane	1.55	0.89	0.03	0.32	1.12
Cyclopentane	0.17	0.06	0.01	0.03	0.09
2-Methylpentane	0.41	0.17	0.06	0.10	0.27
3-Methylpentane	0.12	0.05	0.04	0.05	0.13
1-Hexene	1.60	0.14	0.02	0.13	0.85
n-Hexane	1.16	0.44	0.10	0.17	0.67
Methylcyclopentane	0.21	0.01	0.01	0.04	0.16
Benzene	0.73	0.86	0.16	1.01	1.22
Thiophene	0.12	0.16	0.02	0.25	0.22
Cyclohexane	0.13	0.00	0.01	0.06	0.13
2-Methylhexane	0.11	0.05	0.04	0.03	0.11
2,3-Dimethylpentane	0.13	0.03	0.01	0.03	0.06
1,1-Dimethylpentane	0.00	0.00	0.00	0.00	0.00
3-Methylhexane	0.11	0.05	0.04	0.03	0.13
1-Heptene	1.31	0.10	0.02	0.04	0.51
n-Heptane	1.32	0.50	0.03	0.13	0.67
Methyl-Cyclohexane	0.23	0.07	0.02	0.03	0.16
Ethylcyclopentane	0.10	0.04	0.00	0.02	0.07
2,5-Dimethylhexane	0.30	0.02	0.01	0.02	0.11
2,4-Dimethylhexane	0.08	0.00	0.00	0.00	0.00
3,3-Dimethylhexane	0.25	0.00	0.00	0.00	0.02
2,3,4-Trimethylpentane	0.39	0.01	0.01	0.01	0.11
Toluene	1.51	0.61	0.14	0.55	1.22
2-Methylthiophene	0.41	0.18	0.01	0.10	0.24
3-Methylthiophene	0.22	0.05	0.00	0.02	0.13
1-Octene	1.21	0.06	0.01	0.03	0.35
n-Octane	1.19	0.37	0.04	0.09	0.48
Ethylbenzene	0.50	0.08	0.02	0.07	0.44
Ethylthiophene	0.26	0.01	0.01	0.03	0.03
2,5-Dimethylthiophene	0.25	0.01	0.00	0.00	0.04
m/p-Xylene	1.71	0.23	0.07	0.38	1.12
2,4-Dimethylthiophene	0.16	0.02	0.00	0.02	0.06
2,3-Dimethylthiophene	0.25	0.03	0.02	0.02	0.10
Styrene	0.18	0.00	0.00	0.01	0.10
o-Xylene	0.59	0.20	0.03	0.21	0.50
1-Nonene	0.99	0.03	0.00	0.01	0.27
n-Nonane	0.99	0.22	0.04	0.05	0.37
2-Propylthiophene	0.13	0.00	0.00	0.00	0.11
Propylbenzene	0.13	0.00	0.00	0.03	0.11
2-Ethyl-5-Methylthiophene	0.17	0.00	0.00	0.00	0.64
(?)-Benzene	0.48	0.04	0.01	0.72	0.13
1,3,5-Trimethylbenzene	0.17	0.00	0.01	0.06	0.10
Phenol	0.46	0.00	0.03	0.01	0.22
1-Ethyl-2-Methylbenzene	0.57	0.03	0.01	0.06	0.02
2,3,5-Trimethylthiophene	0.18	0.00	0.00	0.00	0.00



Table A 2: Open-System Pyrolysis GC-FID

Company	Shell				
Formation/Basin	Akata Shale	Middle East - Silurian Hot Shale			
GFZ Code	G005935	G005936	G005937	G006948	G006949
1,2,4-Trimethylbenzene	0.50	0.09	0.04	0.11	0.52
1-Decene	0.92	0.02	0.01	0.01	0.22
n-Decane	0.85	0.15	0.07	0.03	0.28
1,2,3-Trimethylbenzene	0.32	0.10	0.02	0.16	0.49
o-Cresol	0.56	0.00	0.00	0.00	0.04
m/p-Cresol	0.69	0.00	0.00	0.00	0.09
Dimethylphenol	0.18	0.00	0.00	0.00	0.02
1-Undecene	0.90	0.02	0.01	0.01	0.19
n-Undecane	0.84	0.11	0.09	0.02	0.23
1,2,3,4-Tetramethylbenzene	0.34	0.04	0.00	0.04	0.52
Naphthalene	0.38	0.01	0.02	0.10	0.24
1-Dodecene	0.86	0.01	0.02	0.01	0.19
n-Dodecane	0.98	0.09	0.17	0.02	0.20
2-Methylnaphthalene	0.44	0.00	0.00	0.01	0.22
1-Tridecene	0.81	0.00	0.01	0.01	0.14
1-Methylnaphthalene	0.61	0.00	0.01	0.01	0.18
n-Tridecane	1.02	0.08	0.31	0.01	0.17
1-Tetradecene	0.80	0.01	0.02	0.00	0.11
n-Tetradecane	1.03	0.03	0.30	0.01	0.13
Dimethylnaphthalene	0.55	0.00	0.05	0.01	0.26
1-Pentadecene	0.70	0.00	0.01	0.00	0.08
n-Pentadecane	1.13	0.02	0.23	0.00	0.12
Trimethylnaphthalene	0.09	0.00	0.00	0.00	0.06
Trimethylnaphthalene	0.24	0.00	0.02	0.00	0.07
Trimethylnaphthalene	0.10	0.00	0.00	0.00	0.02
1-Hexadecene	0.62	0.00	0.00	0.00	0.03
n-Hexadecane	1.02	0.02	0.15	0.00	0.05
Isopropylidimethylnaphthalene	0.07	0.00	0.00	0.00	0.00
1-Heptadecene	0.59	0.00	0.00	0.00	0.02
n-Heptadecane	1.05	0.02	0.07	0.00	0.05
Pristane	0.55	0.00	0.03	0.00	0.00
Prist.-1-ene	0.27	0.00	0.00	0.00	0.00
1-Octadecene	0.52	0.00	0.00	0.00	0.01
n-Octadecane	0.86	0.03	0.02	0.00	0.03
Phytane	0.24	0.00	0.01	0.00	0.00
1-Nonadecene	0.52	0.00	0.00	0.00	0.02
n-Nonadecane	0.86	0.00	0.01	0.00	0.03
1-Icosene	0.45	0.00	0.00	0.00	0.00
n-Icosane	0.75	0.01	0.00	0.00	0.02
1-Henicosene	0.45	0.00	0.00	0.00	0.01
n-Henicosane	0.71	0.00	0.00	0.00	0.01
1-Docosene	0.38	0.00	0.00	0.00	0.00
n-Docosane	0.69	0.00	0.00	0.00	0.01
1-Tricosene	0.36	0.00	0.00	0.00	0.00
n-Tricosane	0.68	0.00	0.00	0.00	0.01
1-Tetracosene	0.29	0.00	0.00	0.00	0.00
n-Tetracosane	0.66	0.00	0.00	0.00	0.01
1-Pentacosene	0.29	0.00	0.00	0.00	0.00
n-Pentacosane	0.61	0.00	0.00	0.00	0.00
1-Hexacosene	0.25	0.00	0.00	0.00	0.00
n-Hexacosane	0.58	0.00	0.00	0.00	0.00
1-Heptacosene	0.22	0.00	0.00	0.00	0.00
n-Heptacosane	0.57	0.00	0.00	0.00	0.00
1-Octacosene	0.18	0.00	0.00	0.00	0.00
n-Octacosane	0.48	0.00	0.00	0.00	0.00
1-Nonacosene	0.16	0.00	0.00	0.00	0.00
n-Nonacosane	0.43	0.00	0.00	0.00	0.00
1-Triacontene	0.12	0.00	0.00	0.00	0.00
n-Triacontane	0.40	0.00	0.00	0.00	0.00
n-C31:1	0.11	0.00	0.00	0.00	0.00
n-C31	0.34	0.00	0.00	0.00	0.00
n-C32:1	0.21	0.00	0.00	0.00	0.00
n-C32	0.21	0.00	0.00	0.00	0.00
n-C33:1	0.03	0.00	0.00	0.00	0.00
n-C33	0.20	0.00	0.00	0.00	0.00
n-C34:1	0.05	0.00	0.00	0.00	0.00
n-C34	0.08	0.00	0.00	0.00	0.00
n-C35:1	0.03	0.00	0.00	0.00	0.00
n-C35	0.06	0.00	0.00	0.00	0.00
n-C36:1	0.01	0.00	0.00	0.00	0.00
n-C36	0.03	0.00	0.00	0.00	0.00
n-C37:1	0.00	0.00	0.00	0.00	0.00
n-C37	0.03	0.00	0.00	0.00	0.00
n-C38:1	0.00	0.00	0.00	0.00	0.00
n-C38	0.02	0.00	0.00	0.00	0.00
n-C39:1	0.00	0.00	0.00	0.00	0.00
n-C39	0.01	0.00	0.00	0.00	0.00

Table A 2 continued: samples provided by Shell

Table A 2: Open-System Pyrolysis GC-FID

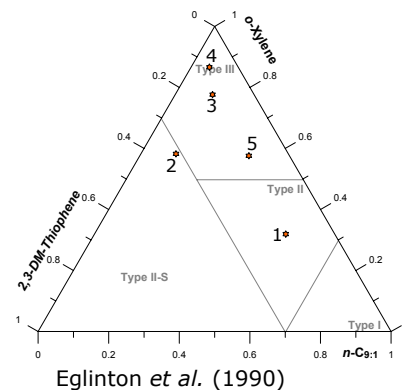
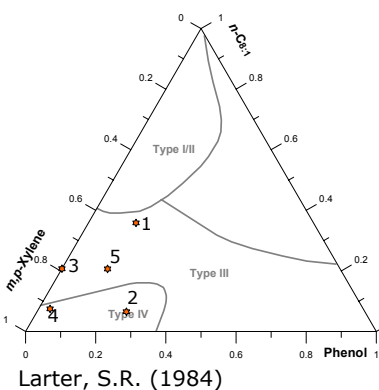
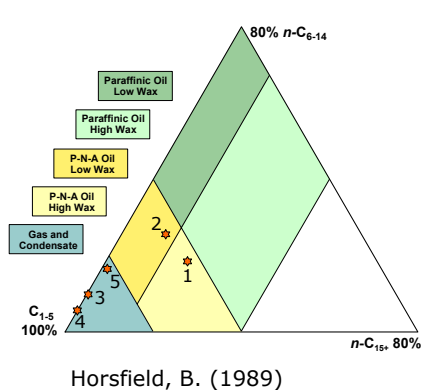
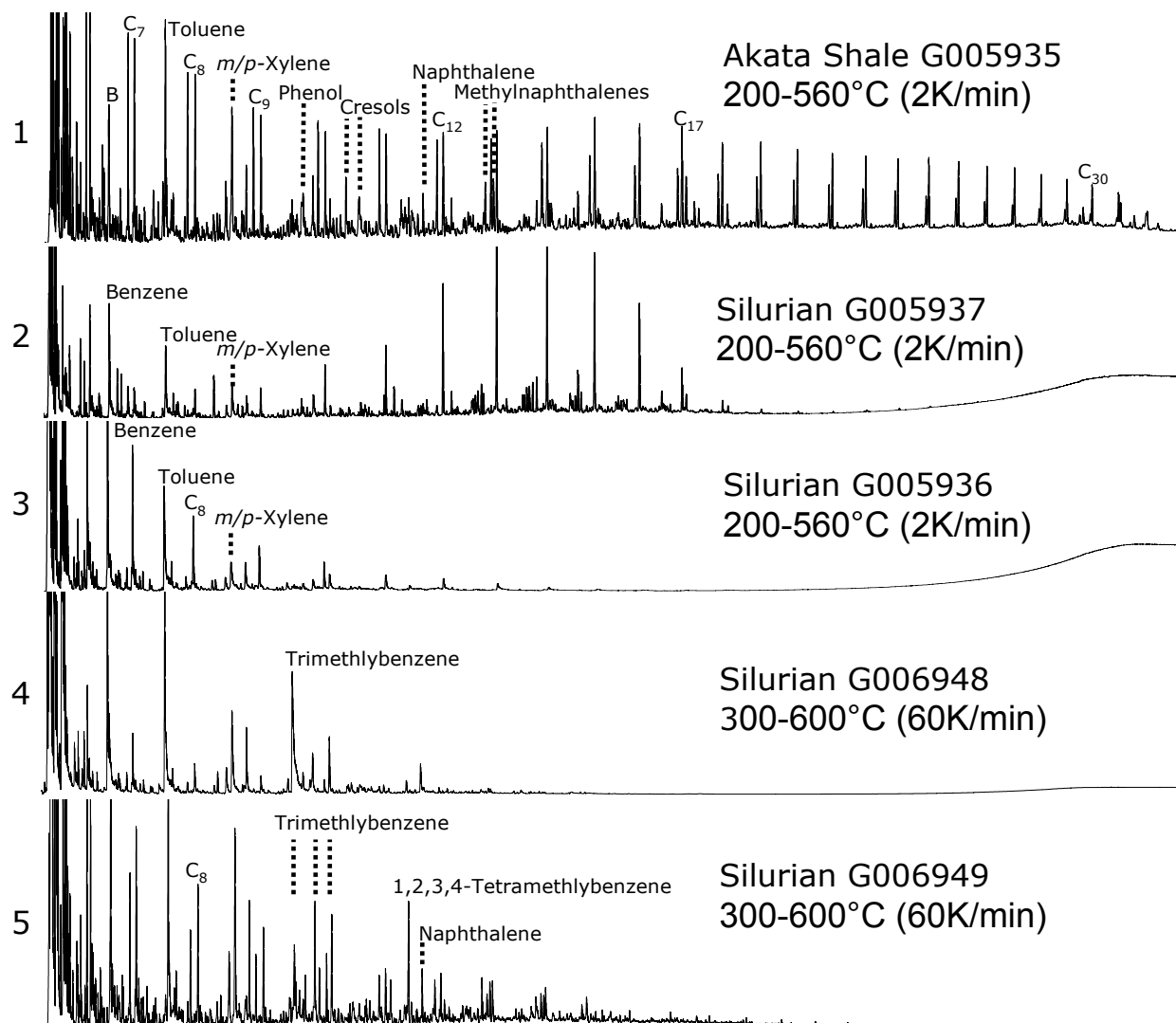


Table A 2 continued: samples provided by Shell

Table A 2: Open-System Pyrolysis GC-FID

Company	Total					
Formation/Basin	Douala Basin		Mahakam Delta		Toarcian Shale	
GFZ Code	G006204	G006205	G006206	G006207	G006208	G006209
File	G006204AE	G006205AE	G006206AE	G006207AD	G006208AD	G006209AD
Temperature [°C]	300-600	300-600	300-600	200-560	200-560	200-560
Rate	60K/min	60K/min	60K/min	2K/min	2K/min	2K/min
Totals	mg/g TOC	mg/g TOC	mg/g TOC	mg/g TOC	mg/g TOC	mg/g TOC
C <sub>1+</sub> (-blank)	116.09	66.85	222.55	215.33	588.73	536.76
C <sub>1-5</sub>	54.63	31.24	71.54	53.02	84.68	81.64
C <sub>2-5</sub>	38.16	25.29	46.46	30.75	67.84	67.78
C <sub>6-14</sub> (-blank)	43.53	24.42	82.03	62.68	175.52	174.70
C <sub>6-14</sub> Hump	36.76	21.23	65.07	41.96	97.23	97.83
C <sub>6-14</sub> Resolved	6.77	3.19	16.96	20.72	78.30	76.87
C <sub>15+</sub> (-blank)	17.93	11.19	68.97	99.63	328.52	280.42
C <sub>15+</sub> Hump	3.92	1.37	17.14	27.92	25.52	26.28
C <sub>15+</sub> Resolved	14.00	9.83	51.83	71.71	303.00	254.13
GOR	0.89	0.88	0.47	0.33	0.17	0.18
Gas Wetness (C2-5/C1-5)	0.70	0.81	0.65	0.58	0.80	0.83
Compounds Summation	mg/g TOC	mg/g TOC	mg/g TOC	mg/g TOC	mg/g TOC	mg/g TOC
n- C <sub>6-14</sub>	5.74	3.15	8.30	12.79	33.37	33.50
n- C <sub>15+</sub>	1.19	0.49	4.58	20.49	14.12	14.43
Mono-aromatic Compounds	9.41	5.31	14.84	7.42	8.38	8.69
Di-aromatic Compounds	2.72	1.13	7.19	2.33	2.36	2.13
Phenolic Compounds	1.12	0.12	1.75	3.31	0.67	0.78
Thiophenic Compounds	0.74	0.48	1.14	0.84	6.20	6.04
Single Compounds	mg/g TOC	mg/g TOC	mg/g TOC	mg/g TOC	mg/g TOC	mg/g TOC
Methane	16.47	5.95	25.09	22.27	16.84	13.86
Ethene	1.33	0.57	2.61	2.57	2.80	6.03
Ethane	6.90	2.81	9.02	7.15	13.37	9.85
Propane	7.60	4.11	9.23	7.57	16.61	13.98
i-Butane	0.32	0.23	0.54	0.43	0.64	0.65
1-Butene	2.53	2.20	2.83	2.56	6.51	6.80
n-Butane	1.59	0.95	2.10	1.70	5.13	5.08
i-Pentane	2.06	2.15	3.37	0.67	0.70	0.65
Pentene	0.62	0.46	1.25	0.99	2.93	2.96
n-Pentane	0.95	0.58	1.10	1.04	3.17	3.10
Cyclopentane	0.08	0.04	0.15	0.10	0.39	0.36
2-Methylpentane	0.30	0.25	0.53	0.31	0.73	0.54
3-Methylpentane	0.08	0.07	0.18	0.09	0.30	0.36
1-Hexene	0.37	0.39	0.98	0.94	3.52	3.39
n-Hexane	0.72	0.38	0.67	0.85	2.40	2.24
Methylcyclopentane	0.11	0.06	0.21	0.17	0.48	0.45
Benzene	1.26	0.59	2.54	0.92	1.05	1.32
Thiophene	0.12	0.08	0.09	0.05	0.23	0.24
Cyclohexane	0.10	0.05	0.14	0.13	0.28	0.31
2-Methylhexane	0.13	0.12	0.22	0.08	0.21	0.24
2,3-Dimethylpentane	0.05	0.02	0.11	0.10	0.08	0.11
1,1-Dimethylpentane	0.00	0.00	0.00	0.00	0.00	0.00
3-Methylhexane	0.06	0.06	0.12	0.06	0.26	0.24
1-Heptene	0.23	0.14	0.55	0.82	2.47	2.41
n-Heptane	0.66	0.32	0.86	0.98	2.55	2.40
Methyl-Cyclohexane	0.12	0.04	0.17	0.21	0.67	0.61
Ethylcyclopentane	0.04	0.02	0.07	0.07	0.23	0.28
2,5-Dimethylhexane	0.05	0.05	0.21	0.13	0.34	0.37
2,4-Dimethylhexane	0.01	0.01	0.03	0.02	0.05	0.07
3,3-Dimethylhexane	0.06	0.05	0.12	0.10	0.39	0.34
2,3,4-Trimethylpentane	0.10	0.07	0.42	0.26	0.76	0.68
Toluene	2.66	1.24	3.72	2.31	1.34	1.37
2-Methylthiophene	0.09	0.06	0.15	0.14	1.52	1.30
3-Methylthiophene	0.10	0.06	0.28	0.13	0.68	0.66
1-Octene	0.13	0.05	0.33	0.69	2.25	2.21
n-Octane	0.62	0.32	0.69	0.81	2.25	2.14
Ethylbenzene	0.49	0.32	0.80	0.46	0.79	0.70
Ethylthiophene	0.05	0.04	0.07	0.03	0.38	0.34
2,5-Dimethylthiophene	0.02	0.01	0.02	0.03	0.69	0.71
m/p-Xylene	1.67	1.00	2.66	1.42	1.89	1.71
2,4-Dimethylthiophene	0.06	0.03	0.16	0.07	0.60	0.63
2,3-Dimethylthiophene	0.07	0.05	0.10	0.10	0.83	0.80
Styrene	0.10	0.04	0.21	0.09	0.23	0.33
o-Xylene	0.73	0.49	1.05	0.54	0.79	0.92
1-Nonene	0.10	0.04	0.27	0.55	1.78	1.83
n-Nonane	0.45	0.21	0.46	0.69	1.81	1.83
2-Propylthiophene	0.16	0.11	0.16	0.12	0.19	0.34
Propylbenzene	0.06	0.03	0.12	0.11	0.21	0.24
2-Ethyl-5-Methylthiophene	0.06	0.03	0.08	0.05	0.60	0.55
(?)-Benzene	0.82	0.49	1.09	0.33	0.57	0.56
1,3,5-Trimethylbenzene	0.28	0.14	0.35	0.16	0.22	0.25
Phenol	0.57	0.06	0.71	0.86	0.17	0.17
1-Ethyl-2-Methylbenzene	0.30	0.18	0.40	0.54	0.40	0.46
2,3,5-Trimethylthiophene	0.01	0.01	0.03	0.12	0.47	0.46

Table A 2 continued: samples provided by Total

Table A 2: Open-System Pyrolysis GC-FID

Company	Total					
Formation/Basin	Douala Basin		Mahakam Delta		Toarcian Shale	
GFZ Code	G006204	G006205	G006206	G006207	G006208	G006209
1,2,4-Trimethylbenzene	0.68	0.59	1.47	0.41	0.73	0.76
1-Decene	0.06	0.02	0.23	0.58	1.65	1.80
n-Decane	0.43	0.20	0.44	0.72	1.59	1.69
1,2,3-Trimethylbenzene	0.46	0.26	0.63	0.23	0.39	0.41
o-Cresol	0.26	0.02	0.40	1.01	0.06	0.07
m/p-Cresol	0.24	0.04	0.55	1.30	0.30	0.31
Dimethylphenol	0.05	0.01	0.09	0.15	0.14	0.23
1-Undecene	0.09	0.03	0.28	0.60	1.60	1.75
n-Undecane	0.38	0.16	0.42	0.74	1.45	1.51
1,2,3,4-Tetramethylbenzene	0.20	0.10	0.43	0.16	0.62	0.62
Naphthalene	0.60	0.28	1.07	0.37	0.23	0.21
1-Dodecene	0.11	0.03	0.32	0.52	1.37	1.46
n-Dodecane	0.45	0.20	0.45	0.88	1.47	1.45
2-Methylnaphthalene	0.68	0.33	1.60	0.54	0.45	0.44
1-Tridecene	0.04	0.02	0.20	0.47	1.31	1.30
1-Methylnaphthalene	0.49	0.21	1.07	0.45	0.54	0.49
n-Tridecane	0.45	0.31	0.45	0.78	1.51	1.54
1-Tetradecene	0.06	0.03	0.23	0.49	1.14	1.26
n-Tetradecane	0.39	0.30	0.46	0.67	1.25	1.30
Dimethylnaphthalene	0.67	0.25	2.29	0.52	0.76	0.75
1-Pentadecene	0.04	0.01	0.19	0.45	0.82	0.90
n-Pentadecane	0.34	0.18	0.54	0.74	1.11	1.19
Trimethylnaphthalene	0.09	0.03	0.35	0.05	0.12	0.09
Trimethylnaphthalene	0.11	0.03	0.56	0.26	0.24	0.14
Trimethylnaphthalene	0.10	0.01	0.26	0.13	0.02	0.01
1-Hexadecene	0.03	0.01	0.25	0.48	0.78	0.92
n-Hexadecane	0.19	0.09	0.34	0.74	0.98	1.04
Isopropylidimethylnaphthalene	0.00	0.00	0.00	0.27	0.02	0.01
1-Heptadecene	0.02	0.01	0.11	0.44	0.73	0.76
n-Heptadecane	0.16	0.06	0.39	0.77	1.04	0.99
Pristane	0.01	0.00	0.06	0.23	0.26	0.13
Prist.-1-ene	0.01	0.00	0.03	0.32	0.41	0.39
1-Octadecene	0.01	0.00	0.06	0.41	0.54	0.55
n-Octadecane	0.11	0.04	0.28	0.74	0.75	0.74
Phytane	0.01	0.00	0.07	0.07	0.19	0.14
1-Nonadecene	0.04	0.02	0.16	0.41	0.48	0.49
n-Nonadecane	0.08	0.03	0.25	0.79	0.66	0.67
1-Icosene	0.00	0.00	0.05	0.41	0.42	0.45
n-Icosane	0.06	0.02	0.28	0.80	0.61	0.59
1-Henicosene	0.01	0.00	0.07	0.44	0.43	0.41
n-Henicosane	0.04	0.01	0.23	0.84	0.50	0.48
1-Docosene	0.00	0.00	0.04	0.47	0.34	0.32
n-Docosane	0.02	0.01	0.22	0.89	0.44	0.40
1-Tricosene	0.00	0.00	0.02	0.50	0.25	0.23
n-Tricosane	0.01	0.00	0.19	0.91	0.39	0.35
1-Tetracosene	0.00	0.00	0.03	0.00	0.21	0.20
n-Tetracosane	0.01	0.00	0.19	1.49	0.31	0.32
1-Pentacosene	0.00	0.00	0.03	0.43	0.17	0.17
n-Pentacosane	0.00	0.00	0.15	0.97	0.28	0.26
1-Hexacosene	0.00	0.00	0.03	0.38	0.10	0.12
n-Hexacosane	0.00	0.00	0.13	0.84	0.20	0.21
1-Heptacosene	0.00	0.00	0.01	0.33	0.08	0.10
n-Heptacosane	0.00	0.00	0.10	0.86	0.19	0.19
1-Octacosene	0.00	0.00	0.02	0.28	0.09	0.10
n-Octacosane	0.00	0.00	0.08	0.69	0.17	0.17
1-Nonacosene	0.00	0.00	0.01	0.25	0.08	0.09
n-Nonacosane	0.00	0.00	0.06	0.59	0.14	0.13
1-Triacontene	0.00	0.00	0.00	0.14	0.07	0.07
n-Triacontane	0.00	0.00	0.04	0.51	0.14	0.13
n-C31:1	0.00	0.00	0.00	0.12	0.04	0.06
n-C31	0.00	0.00	0.02	0.40	0.18	0.15
n-C32:1	0.00	0.00	0.00	0.08	0.04	0.03
n-C32	0.00	0.00	0.02	0.33	0.11	0.10
n-C33:1	0.00	0.00	0.00	0.05	0.02	0.03
n-C33	0.00	0.00	0.00	0.19	0.07	0.07
n-C34:1	0.00	0.00	0.00	0.04	0.01	0.02
n-C34	0.00	0.00	0.00	0.09	0.04	0.04
n-C35:1	0.00	0.00	0.00	0.02	0.02	0.01
n-C35	0.00	0.00	0.00	0.07	0.04	0.04
n-C36:1	0.00	0.00	0.00	0.01	0.02	0.02
n-C36	0.00	0.00	0.00	0.03	0.01	0.03
n-C37:1	0.00	0.00	0.00	0.01	0.01	0.02
n-C37	0.00	0.00	0.00	0.02	0.02	0.01
n-C38:1	0.00	0.00	0.00	0.01	0.00	0.01
n-C38	0.00	0.00	0.00	0.01	0.00	0.01
n-C39:1	0.00	0.00	0.00	0.01	0.00	0.01
n-C39	0.00	0.00	0.00	0.00	0.00	0.01

Table A 2 continued: samples provided by Total

Table A 2: Open-System Pyrolysis GC-FID

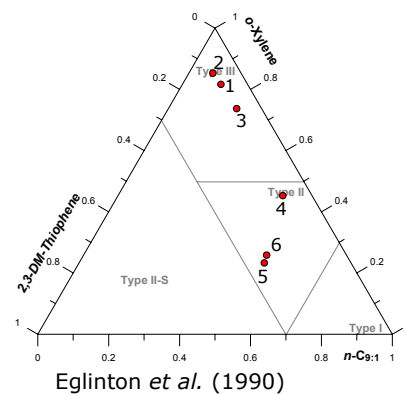
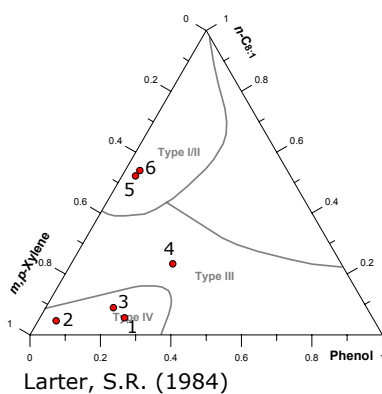
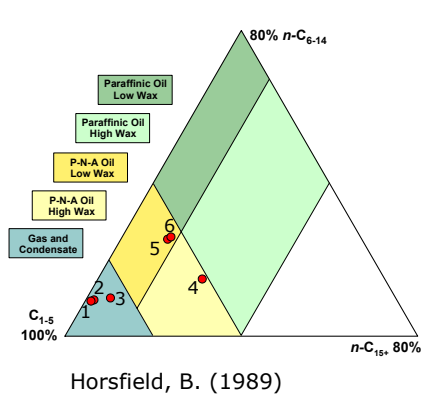
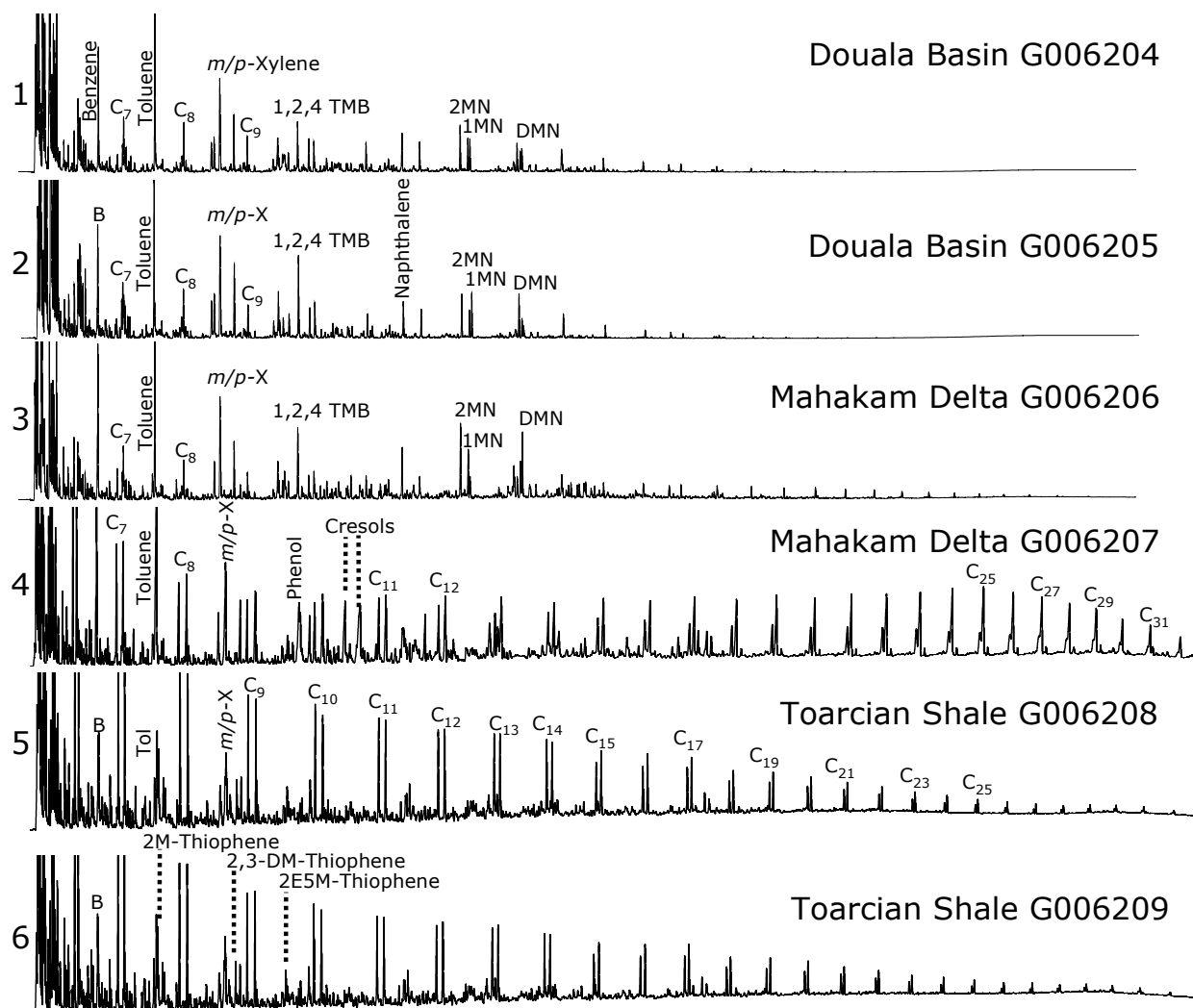


Table A 2 continued: samples provided by Total

Table A 2: Open-System Pyrolysis GC-FID

Company	ENI					
	Domanik Fm.	Murzuq Basin		Ghadames Basin	Hekkingen Fm.	
Formation/Basin						
GFZ Code	G004563	G004564	G007160	G007161	G005762	G005763
File	G004563BD	G004564BD	G007160AA	G007161AA	G005762AD	G005763AD
Temperature [°C]	200-580	200-580	300-600	300-600	200-580	200-580
Rate	5K/min	5K/min	60K/min	60K/min	5K/min	5K/min
Totals	mg/g TOC	mg/g TOC	mg/g TOC	mg/g TOC	mg/g TOC	mg/g TOC
<b>C<sub>1+</sub></b> (-blank)	566.87	352.53	340.41	53.21	208.28	183.56
<b>C<sub>1-5</sub></b>	84.01	76.52	83.60	24.09	46.87	45.12
<b>C<sub>2-5</sub></b>	60.51	56.82	63.65	18.42	31.91	31.10
<b>C<sub>6-14</sub></b> (-blank)	138.62	107.35	107.18	22.80	69.44	73.44
<b>C<sub>6-14</sub> Hump</b>	76.08	56.67	63.55	15.49	38.56	44.28
<b>C<sub>6-14</sub> Resolved</b>	62.54	50.68	43.63	7.31	30.88	29.16
<b>C<sub>15+</sub></b> (-blank)	344.23	168.66	149.63	6.32	91.97	65.00
<b>C<sub>15+</sub> Hump</b>	17.23	6.81	3.86	1.37	8.84	8.54
<b>C<sub>15+</sub> Resolved</b>	327.00	161.85	145.77	4.95	83.13	56.46
<b>GOR</b>	0.17	0.28	0.33	0.83	0.29	0.33
<b>Gas Wetness (C2-5/C1-5)</b>	0.72	0.74	0.76	0.76	0.68	0.69
Compounds Summation	mg/g TOC	mg/g TOC	mg/g TOC	mg/g TOC	mg/g TOC	mg/g TOC
<i>n</i> -C <sub>6-14</sub>	22.47	13.83	14.41	2.57	8.78	8.78
<i>n</i> -C <sub>15+</sub>	5.73	1.21	0.98	0.13	3.89	3.54
Mono-aromatic Compounds	7.20	8.20	9.32	3.54	6.14	8.90
Di-aromatic Compounds	1.95	2.00	2.06	0.69	1.64	2.61
Phenolic Compounds	0.59	0.47	0.50	0.01	1.02	1.04
Thiophenic Compounds	3.98	1.70	1.59	0.70	3.10	3.13
Single Compounds	mg/g TOC	mg/g TOC	mg/g TOC	mg/g TOC	mg/g TOC	mg/g TOC
Methane	23.51	19.69	19.95	5.67	14.96	14.02
Ethene	2.67	3.28	2.64	0.53	2.23	1.94
Ethane	14.31	10.87	13.46	1.94	8.24	6.71
Propane	14.41	14.32	15.81	3.67	8.07	7.16
i-Butane	0.71	0.57	0.69	0.18	0.24	0.30
1-Butene	4.27	5.01	5.45	0.99	2.35	2.44
<i>n</i> -Butane	4.72	4.47	4.84	0.70	1.80	2.03
i-Pentane	0.97	0.76	1.18	0.12	0.29	0.85
Pentene	2.11	2.26	2.18	0.59	0.99	1.07
<i>n</i> -Pentane	3.08	2.65	3.00	0.43	0.96	1.05
Cyclopentane	0.33	0.18	0.23	0.05	0.08	0.08
2-Methylpentane	0.92	0.70	0.83	0.10	0.24	0.25
3-Methylpentane	0.33	0.32	0.33	0.05	0.12	0.15
1-Hexene	2.34	2.18	2.15	0.55	1.01	1.07
<i>n</i> -Hexane	2.10	1.72	2.01	0.23	0.68	0.72
Methylcyclopentane	0.52	0.33	0.41	0.04	0.13	0.14
Benzene	0.27	0.65	0.87	0.71	0.63	1.54
Thiophene	0.10	0.09	0.09	0.21	0.17	0.30
Cyclohexane	0.18	0.17	0.21	0.06	0.09	0.13
2-Methylhexane	0.22	0.25	0.33	0.03	0.03	0.05
2,3-Dimethylpentane	0.09	0.07	0.10	0.01	0.01	0.08
1,1-Dimethylpentane	0.00	0.00	0.00	0.00	0.00	0.00
3-Methylhexane	0.00	0.34	0.38	0.03	0.06	0.08
1-Heptene	1.60	1.34	1.39	0.29	0.69	0.68
<i>n</i> -Heptane	2.22	1.50	1.92	0.18	0.67	0.70
Methyl-Cyclohexane	0.41	0.34	0.48	0.06	0.20	0.26
Ethylcyclopentane	0.22	0.15	0.22	0.01	0.06	0.07
2,5-Dimethylhexane	0.26	0.36	0.83	0.02	0.17	0.16
2,4-Dimethylhexane	0.03	0.05	0.11	0.01	0.04	0.03
3,3-Dimethylhexane	0.24	0.23	0.29	0.02	0.16	0.15
2,3,4-Trimethylpentane	0.52	0.38	0.52	0.05	0.25	0.24
Toluene	0.99	1.43	1.85	0.97	1.60	2.53
2-Methylthiophene	0.74	0.34	0.26	0.11	0.74	0.71
3-Methylthiophene	0.20	0.23	0.35	0.10	0.21	0.18
1-Octene	1.48	0.94	1.06	0.21	0.58	0.61
<i>n</i> -Octane	1.83	1.17	1.28	0.16	0.57	0.60
Ethylbenzene	1.08	0.76	0.75	0.36	0.39	0.50
Ethylthiophene	0.13	0.10	0.10	0.05	0.23	0.25
2,5-Dimethylthiophene	0.49	0.17	0.13	0.02	0.33	0.33
<i>m/p</i> -Xylene	1.74	1.76	1.87	0.40	1.26	1.63
2,4-Dimethylthiophene	0.30	0.15	0.14	0.05	0.27	0.17
2,3-Dimethylthiophene	0.73	0.30	0.20	0.02	0.34	0.35
Styrene	0.13	0.17	0.17	0.58	0.17	0.21
<i>o</i> -Xylene	0.59	0.72	0.72	0.36	0.52	0.69
1-Nonene	1.03	0.62	0.57	0.13	0.45	0.42
<i>n</i> -Nonane	1.41	0.73	0.74	0.09	0.47	0.49
2-Propylthiophene	0.18	0.16	0.14	0.08	0.16	0.18
Propylbenzene	0.29	0.09	0.14	0.05	0.08	0.07
2-Ethyl-5-Methylthiophene	0.49	0.05	0.06	0.02	0.31	0.28
(?)-Benzene	0.51	0.73	0.84	0.19	0.41	0.45
1,3,5-Trimethylbenzene	0.27	0.29	0.30	0.06	0.12	0.14
Phenol	0.24	0.11	0.16	0.01	0.19	0.19
1-Ethyl-2-Methylbenzene	0.30	0.39	0.40	0.21	0.50	0.67
2,3,5-Trimethylthiophene	0.60	0.10	0.11	0.03	0.34	0.38

Table A 2 continued: samples provided by ENI

Table A 2: Open-System Pyrolysis GC-FID

Company	ENI					
Formation/Basin	Domanik Fm.	Murzuq Basin		Ghadames Basin	Hekkingen Fm.	
GFZ Code	G004563	G004564	G007160	G007161	G005762	G005763
1,2,4-Trimethylbenzene	0.64	0.88	1.00	0.15	0.38	0.43
1-Decene	1.07	0.48	0.43	0.11	0.44	0.40
<i>n</i> -Decane	1.17	0.56	0.58	0.08	0.40	0.38
1,2,3-Trimethylbenzene	0.53	0.51	0.58	0.08	0.24	0.25
<i>o</i> -Cresol	0.06	0.04	0.09	0.00	0.20	0.25
<i>m/p</i> -Cresol	0.17	0.22	0.15	0.00	0.57	0.54
Dimethylphenol	0.11	0.09	0.10	0.00	0.05	0.05
1-Undecene	0.93	0.41	0.35	0.10	0.32	0.32
<i>n</i> -Undecane	0.97	0.41	0.43	0.07	0.36	0.34
1,2,3,4-Tetramethylbenzene	1.19	0.76	0.69	0.07	0.22	0.27
Naphthalene	0.25	0.26	0.25	0.24	0.31	0.53
1-Dodecene	0.79	0.34	0.32	0.09	0.31	0.29
<i>n</i> -Dodecane	0.94	0.38	0.30	0.06	0.43	0.39
2-Methylnaphthalene	0.35	0.41	0.47	0.11	0.36	0.71
1-Tridecene	0.60	0.20	0.21	0.05	0.36	0.34
1-Methylnaphthalene	0.41	0.32	0.35	0.20	0.31	0.51
<i>n</i> -Tridecane	0.75	0.29	0.32	0.08	0.40	0.34
1-Tetradecene	0.62	0.33	0.16	0.04	0.32	0.29
<i>n</i> -Tetradecane	0.62	0.23	0.20	0.04	0.32	0.39
Dimethylnaphthalene	0.48	0.60	0.60	0.11	0.41	0.63
1-Pentadecene	0.44	0.12	0.07	0.03	0.20	0.21
<i>n</i> -Pentadecane	0.57	0.26	0.26	0.03	0.36	0.42
Trimethylnaphthalene	0.13	0.18	0.00	0.00	0.07	0.06
Trimethylnaphthalene	0.28	0.17	0.21	0.01	0.13	0.09
Trimethylnaphthalene	0.06	0.06	0.18	0.02	0.05	0.07
1-Hexadecene	0.31	0.06	0.12	0.02	0.20	0.16
<i>n</i> -Hexadecane	0.43	0.16	0.12	0.03	0.24	0.28
Isopropylidimethylnaphthalene	0.02	0.02	0.00	0.00	0.10	0.07
1-Heptadecene	0.26	0.05	0.04	0.01	0.17	0.14
<i>n</i> -Heptadecane	0.44	0.16	0.09	0.01	0.24	0.26
Pristane	0.18	0.05	0.00	0.00	0.07	0.16
Prist.-1-ene	0.30	0.04	0.00	0.00	0.19	0.32
1-Octadecene	0.21	0.03	0.03	0.00	0.14	0.12
<i>n</i> -Octadecane	0.31	0.05	0.06	0.00	0.17	0.20
Phytane	0.16	0.02	0.00	0.00	0.06	0.11
1-Nonadecene	0.25	0.09	0.06	0.00	0.14	0.12
<i>n</i> -Nonadecane	0.36	0.05	0.05	0.00	0.20	0.18
1-Icosene	0.17	0.04	0.01	0.00	0.10	0.08
<i>n</i> -Icosane	0.28	0.05	0.04	0.00	0.14	0.13
1-Henicosene	0.09	0.05	0.01	0.00	0.12	0.11
<i>n</i> -Henicosane	0.19	0.03	0.02	0.00	0.13	0.13
1-Docosene	0.10	0.00	0.00	0.00	0.08	0.06
<i>n</i> -Docosane	0.18	0.00	0.00	0.00	0.12	0.10
1-Tricosene	0.06	0.00	0.00	0.00	0.07	0.06
<i>n</i> -Tricosane	0.14	0.00	0.00	0.00	0.12	0.10
1-Tetracosene	0.06	0.00	0.00	0.00	0.04	0.04
<i>n</i> -Tetracosane	0.11	0.00	0.00	0.00	0.12	0.10
1-Pentacosene	0.05	0.00	0.00	0.00	0.05	0.03
<i>n</i> -Pentacosane	0.10	0.00	0.00	0.00	0.10	0.08
1-Hexacosene	0.03	0.00	0.00	0.00	0.05	0.03
<i>n</i> -Hexacosane	0.09	0.00	0.00	0.00	0.08	0.07
1-Heptacosene	0.05	0.00	0.00	0.00	0.04	0.02
<i>n</i> -Heptacosane	0.06	0.00	0.00	0.00	0.08	0.06
1-Octacosene	0.03	0.00	0.00	0.00	0.02	0.02
<i>n</i> -Octacosane	0.04	0.00	0.00	0.00	0.05	0.04
1-Nonacosene	0.03	0.00	0.00	0.00	0.01	0.01
<i>n</i> -Nonacosane	0.07	0.00	0.00	0.00	0.08	0.06
1-Triacontene	0.06	0.00	0.00	0.00	0.02	0.01
<i>n</i> -Triacontane	0.14	0.00	0.00	0.00	0.05	0.04
<i>n</i> -C31:1	0.00	0.00	0.00	0.00	0.01	0.01
<i>n</i> -C31	0.00	0.00	0.00	0.00	0.05	0.03
<i>n</i> -C32:1	0.00	0.00	0.00	0.00	0.01	0.00
<i>n</i> -C32	0.00	0.00	0.00	0.00	0.03	0.01
<i>n</i> -C33:1	0.00	0.00	0.00	0.00	0.02	0.02
<i>n</i> -C33	0.00	0.00	0.00	0.00	0.02	0.01
<i>n</i> -C34:1	0.00	0.00	0.00	0.00	0.01	0.01
<i>n</i> -C34	0.00	0.00	0.00	0.00	0.01	0.00
<i>n</i> -C35:1	0.00	0.00	0.00	0.00	0.01	0.00
<i>n</i> -C35	0.00	0.00	0.00	0.00	0.01	0.00
<i>n</i> -C36:1	0.00	0.00	0.00	0.00	0.00	0.00
<i>n</i> -C36	0.00	0.00	0.00	0.00	0.00	0.00
<i>n</i> -C37:1	0.00	0.00	0.00	0.00	0.00	0.00
<i>n</i> -C37	0.00	0.00	0.00	0.00	0.00	0.00
<i>n</i> -C38:1	0.00	0.00	0.00	0.00	0.00	0.00
<i>n</i> -C38	0.00	0.00	0.00	0.00	0.00	0.00
<i>n</i> -C39:1	0.00	0.00	0.00	0.00	0.00	0.00
<i>n</i> -C39	0.00	0.00	0.00	0.00	0.00	0.00

Table A 2 continued: samples provided by ENI

Table A 2: Open-System Pyrolysis GC-FID

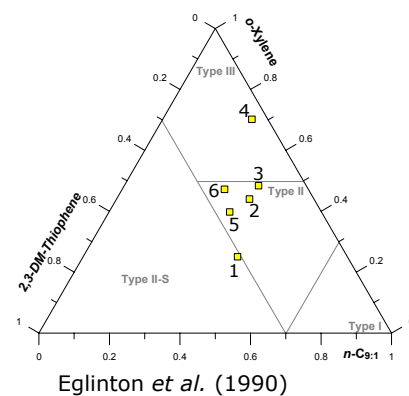
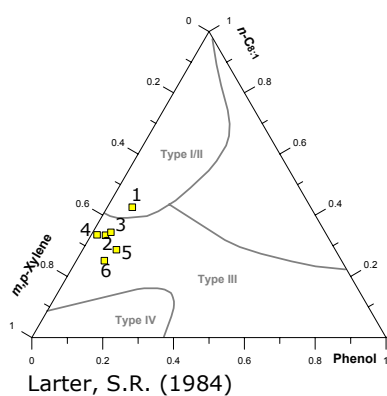
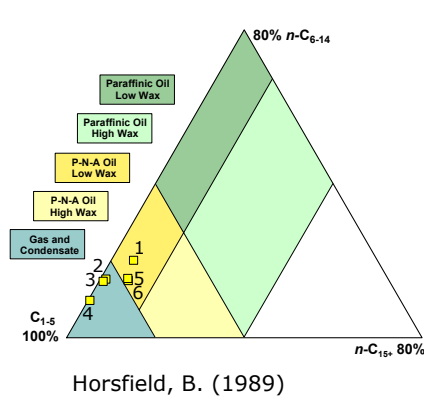
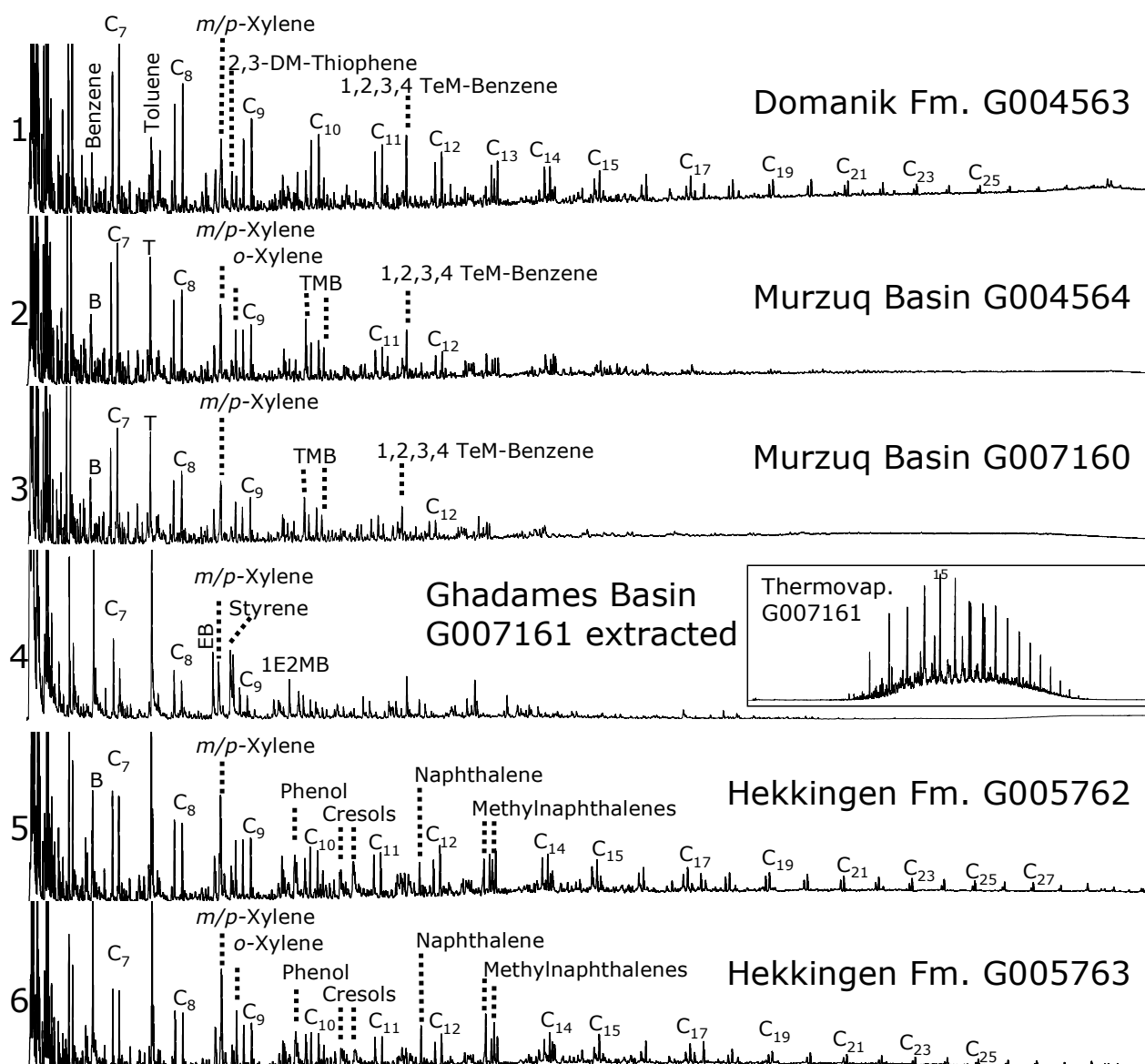


Table A 2 continued: samples provided by ENI



Table A 2: Open-System Pyrolysis GC-FID

Company	Petrobras	Devon			
Formation/Basin	Irati Fm.	Woodford Shale	Caney Shale	New Albany Shale	
GFZ Code	G005812	G006153	G006154	G006155	G006156
File	G005812AD	G006153AD	G006154AD	G006155AD	G006156AD
Temperature [°C]	200-580	200-560	200-560	200-560	200-560
Rate	5K/min	2K/min	2K/min	2K/min	2K/min
Totals	mg/g TOC	mg/g TOC	mg/g TOC	mg/g TOC	mg/g TOC
C <sub>1+</sub> (-blank)	524.32	417.26	356.04	370.64	405.40
C <sub>1-5</sub>	76.72	82.86	78.62	71.63	84.97
C <sub>2-5</sub>	58.66	64.13	57.53	54.42	63.57
C <sub>6-14</sub> (-blank)	137.56	119.63	105.91	114.07	120.61
C <sub>6-14</sub> Hump	78.41	64.37	58.12	59.44	64.88
C <sub>6-14</sub> Resolved	59.14	55.26	47.79	54.63	55.73
C <sub>15+</sub> (-blank)	310.05	214.77	171.51	184.93	199.81
C <sub>15+</sub> Hump	24.40	7.45	7.36	8.70	7.14
C <sub>15+</sub> Resolved	285.66	207.32	164.15	176.23	192.67
GOR	0.17	0.25	0.28	0.24	0.27
Gas Wetness (C2-5/C1-5)	0.76	0.77	0.73	0.76	0.75
Compounds Summation	mg/g TOC	mg/g TOC	mg/g TOC	mg/g TOC	mg/g TOC
n- C <sub>6-14</sub>	25.04	17.13	16.17	15.42	16.32
n- C <sub>15+</sub>	8.50	2.44	2.27	3.63	1.56
Mono-aromatic Compounds	7.23	8.08	7.51	6.85	8.18
Di-aromatic Compounds	2.59	1.78	1.54	1.49	2.29
Phenolic Compounds	0.62	0.42	0.37	0.31	0.43
Thiophenic Compounds	2.39	2.90	3.55	3.46	1.96
Single Compounds	mg/g TOC	mg/g TOC	mg/g TOC	mg/g TOC	mg/g TOC
Methane	18.06	18.73	21.09	17.21	21.41
Ethene	1.83	2.50	3.50	2.50	2.90
Ethane	11.78	13.66	11.78	12.24	13.48
Propane	14.41	15.50	14.56	13.50	15.74
i-Butane	1.07	0.64	0.45	0.50	0.98
1-Butene	5.36	4.26	4.55	4.41	0.60
n-Butane	4.35	4.62	4.11	3.44	4.70
i-Pentane	1.24	0.65	0.69	0.54	4.72
Pentene	1.99	2.30	2.29	1.95	0.81
n-Pentane	2.91	2.52	2.42	1.93	2.29
Cyclopentane	0.15	0.21	0.19	0.21	0.29
2-Methylpentane	1.28	0.57	0.43	0.32	0.70
3-Methylpentane	0.36	0.27	0.19	0.21	0.39
1-Hexene	2.42	2.36	2.22	2.11	2.11
n-Hexane	1.95	1.82	1.68	1.33	2.10
Methylcyclopentane	0.30	0.29	0.24	0.23	0.46
Benzene	0.15	0.46	0.70	0.41	0.32
Thiophene	0.04	0.16	0.21	0.14	0.06
Cyclohexane	0.10	0.20	0.18	0.18	0.22
2-Methylhexane	0.31	0.14	0.10	0.11	0.26
2,3-Dimethylpentane	0.12	0.04	0.07	0.03	0.17
1,1-Dimethylpentane	0.00	0.00	0.00	0.00	0.00
3-Methylhexane	0.39	0.22	0.15	0.13	0.40
1-Heptene	1.66	1.55	1.51	1.45	1.45
n-Heptane	2.37	1.72	1.59	1.32	2.04
Methyl-Cyclohexane	0.37	0.32	0.25	0.27	0.40
Ethylcyclopentane	0.10	0.16	0.14	0.10	0.19
2,5-Dimethylhexane	0.27	0.45	0.33	0.30	0.37
2,4-Dimethylhexane	0.04	0.06	0.05	0.06	0.06
3,3-Dimethylhexane	0.24	0.36	0.28	0.33	0.31
2,3,4-Trimethylpentane	0.53	0.52	0.48	0.56	0.62
Toluene	0.71	1.32	1.58	1.24	1.39
2-Methylthiophene	0.59	0.71	0.87	0.82	0.39
3-Methylthiophene	0.24	0.42	0.40	0.43	0.23
1-Octene	1.53	1.27	1.20	1.12	1.13
n-Octane	2.08	1.34	1.23	1.12	1.57
Ethylbenzene	1.22	0.78	0.52	0.57	0.77
Ethylthiophene	0.08	0.13	0.24	0.22	0.14
2,5-Dimethylthiophene	0.16	0.11	0.38	0.34	0.14
m/p-Xylene	2.23	2.01	1.53	1.59	1.81
2,4-Dimethylthiophene	0.20	0.16	0.21	0.20	0.16
2,3-Dimethylthiophene	0.53	0.41	0.39	0.43	0.35
Styrene	0.05	0.20	0.19	0.15	0.17
o-Xylene	0.49	0.79	0.73	0.65	0.79
1-Nonene	1.03	0.88	0.81	0.82	0.62
n-Nonane	1.49	0.96	0.86	0.79	1.00
2-Propylthiophene	0.13	0.21	0.21	0.21	0.21
Propylbenzene	0.25	0.18	0.20	0.23	0.15
2-Ethyl-5-Methylthiophene	0.18	0.26	0.34	0.40	0.10
(?)-Benzene	0.17	0.60	0.53	0.54	0.79
1,3,5-Trimethylbenzene	0.19	0.24	0.20	0.23	0.29
Phenol	0.27	0.08	0.08	0.07	0.12
1-Ethyl-2-Methylbenzene	0.28	0.35	0.32	0.33	0.40
2,3,5-Trimethylthiophene	0.25	0.32	0.30	0.26	0.17

Table A 2 continued: samples provided by Petrobras and Devon

Table A 2: Open-System Pyrolysis GC-FID

Company	Petrobras	Devon			
Formation/Basin	Irati Fm.	Woodford Shale		Caney Shale	New Albany Shale
GFZ Code	G005812	G006153	G006154	G006155	G006156
1,2,4-Trimethylbenzene	0.65	0.78	0.70	0.66	0.94
1-Decene	1.09	0.81	0.75	0.77	0.55
<i>n</i> -Decane	1.28	0.76	0.70	0.68	0.73
1,2,3-Trimethylbenzene	0.87	0.58	0.51	0.40	0.53
<i>o</i> -Cresol	0.03	0.05	0.04	0.04	0.06
<i>m/p</i> -Cresol	0.21	0.22	0.21	0.14	0.16
Dimethylphenol	0.11	0.08	0.04	0.06	0.10
1-Undecene	0.96	0.61	0.60	0.62	0.41
<i>n</i> -Undecane	1.25	0.57	0.54	0.53	0.57
1,2,3,4-Tetramethylbenzene	0.39	1.02	0.98	0.42	0.65
Naphthalene	0.24	0.22	0.19	0.17	0.32
1-Dodecene	0.87	0.52	0.43	0.50	0.35
<i>n</i> -Dodecane	1.09	0.50	0.50	0.51	0.51
2-Methylnaphthalene	0.22	0.32	0.30	0.29	0.54
1-Tridecene	0.61	0.38	0.40	0.45	0.25
1-Methylnaphthalene	0.92	0.28	0.28	0.28	0.39
<i>n</i> -Tridecane	1.22	0.37	0.41	0.47	0.39
1-Tetradecene	1.15	0.39	0.38	0.38	0.23
<i>n</i> -Tetradecane	1.00	0.34	0.34	0.45	0.30
Dimethylnaphthalene	0.72	0.57	0.44	0.50	0.62
1-Pentadecene	0.51	0.20	0.22	0.24	0.11
<i>n</i> -Pentadecane	1.17	0.32	0.33	0.39	0.27
Trimethylnaphthalene	0.15	0.13	0.11	0.06	0.14
Trimethylnaphthalene	0.25	0.22	0.18	0.17	0.22
Trimethylnaphthalene	0.09	0.04	0.04	0.03	0.05
1-Hexadecene	0.53	0.19	0.16	0.22	0.09
<i>n</i> -Hexadecane	0.58	0.24	0.18	0.27	0.22
Isopropylidimethylnaphthalene	0.06	0.03	0.01	0.00	0.02
1-Heptadecene	0.24	0.13	0.12	0.18	0.07
<i>n</i> -Heptadecane	0.76	0.25	0.19	0.30	0.20
Pristane	0.47	0.05	0.05	0.04	0.04
Prist.-1-ene	1.75	0.06	0.07	0.13	0.04
1-Octadecene	0.28	0.09	0.09	0.14	0.04
<i>n</i> -Octadecane	0.34	0.14	0.14	0.18	0.11
Phytane	0.35	0.03	0.03	0.03	0.02
1-Nonadecene	0.25	0.10	0.08	0.14	0.05
<i>n</i> -Nonadecane	0.32	0.11	0.09	0.14	0.07
1-Icosene	0.23	0.05	0.06	0.11	0.02
<i>n</i> -Icosane	0.25	0.09	0.09	0.14	0.06
1-Henicosene	0.31	0.09	0.09	0.14	0.03
<i>n</i> -Henicosane	0.24	0.08	0.07	0.13	0.04
1-Docosene	0.10	0.03	0.04	0.07	0.01
<i>n</i> -Docosane	0.21	0.05	0.05	0.11	0.03
1-Tricosene	0.13	0.03	0.03	0.06	0.00
<i>n</i> -Tricosane	0.22	0.05	0.05	0.10	0.03
1-Tetracosene	0.07	0.03	0.03	0.04	0.02
<i>n</i> -Tetracosane	0.19	0.04	0.04	0.08	0.03
1-Pentacosene	0.08	0.03	0.03	0.03	0.01
<i>n</i> -Pentacosane	0.17	0.03	0.03	0.06	0.02
1-Hexacosene	0.05	0.02	0.01	0.03	0.02
<i>n</i> -Hexacosane	0.12	0.02	0.02	0.06	0.02
1-Heptacosene	0.05	0.01	0.00	0.02	0.00
<i>n</i> -Heptacosane	0.12	0.02	0.02	0.05	0.00
1-Octacosene	0.04	0.00	0.00	0.01	0.00
<i>n</i> -Octacosane	0.08	0.00	0.00	0.03	0.00
1-Nonacosene	0.11	0.00	0.00	0.02	0.00
<i>n</i> -Nonacosane	0.07	0.00	0.00	0.02	0.00
1-Triacontene	0.04	0.00	0.00	0.01	0.00
<i>n</i> -Triacontane	0.12	0.00	0.00	0.02	0.00
<i>n</i> -C31:1	0.10	0.00	0.00	0.04	0.00
<i>n</i> -C31	0.19	0.00	0.00	0.01	0.00
<i>n</i> -C32:1	0.04	0.00	0.00	0.01	0.00
<i>n</i> -C32	0.10	0.00	0.00	0.00	0.00
<i>n</i> -C33:1	0.01	0.00	0.00	0.01	0.00
<i>n</i> -C33	0.08	0.00	0.00	0.01	0.00
<i>n</i> -C34:1	0.00	0.00	0.00	0.00	0.00
<i>n</i> -C34	0.00	0.00	0.00	0.00	0.00
<i>n</i> -C35:1	0.00	0.00	0.00	0.00	0.00
<i>n</i> -C35	0.00	0.00	0.00	0.00	0.00
<i>n</i> -C36:1	0.00	0.00	0.00	0.00	0.00
<i>n</i> -C36	0.00	0.00	0.00	0.00	0.00
<i>n</i> -C37:1	0.00	0.00	0.00	0.00	0.00
<i>n</i> -C37	0.00	0.00	0.00	0.00	0.00
<i>n</i> -C38:1	0.00	0.00	0.00	0.00	0.00
<i>n</i> -C38	0.00	0.00	0.00	0.00	0.00
<i>n</i> -C39:1	0.00	0.00	0.00	0.00	0.00
<i>n</i> -C39	0.00	0.00	0.00	0.00	0.00

Table A 2 continued: samples provided by Petrobras and Devon

Table A 2: Open-System Pyrolysis GC-FID

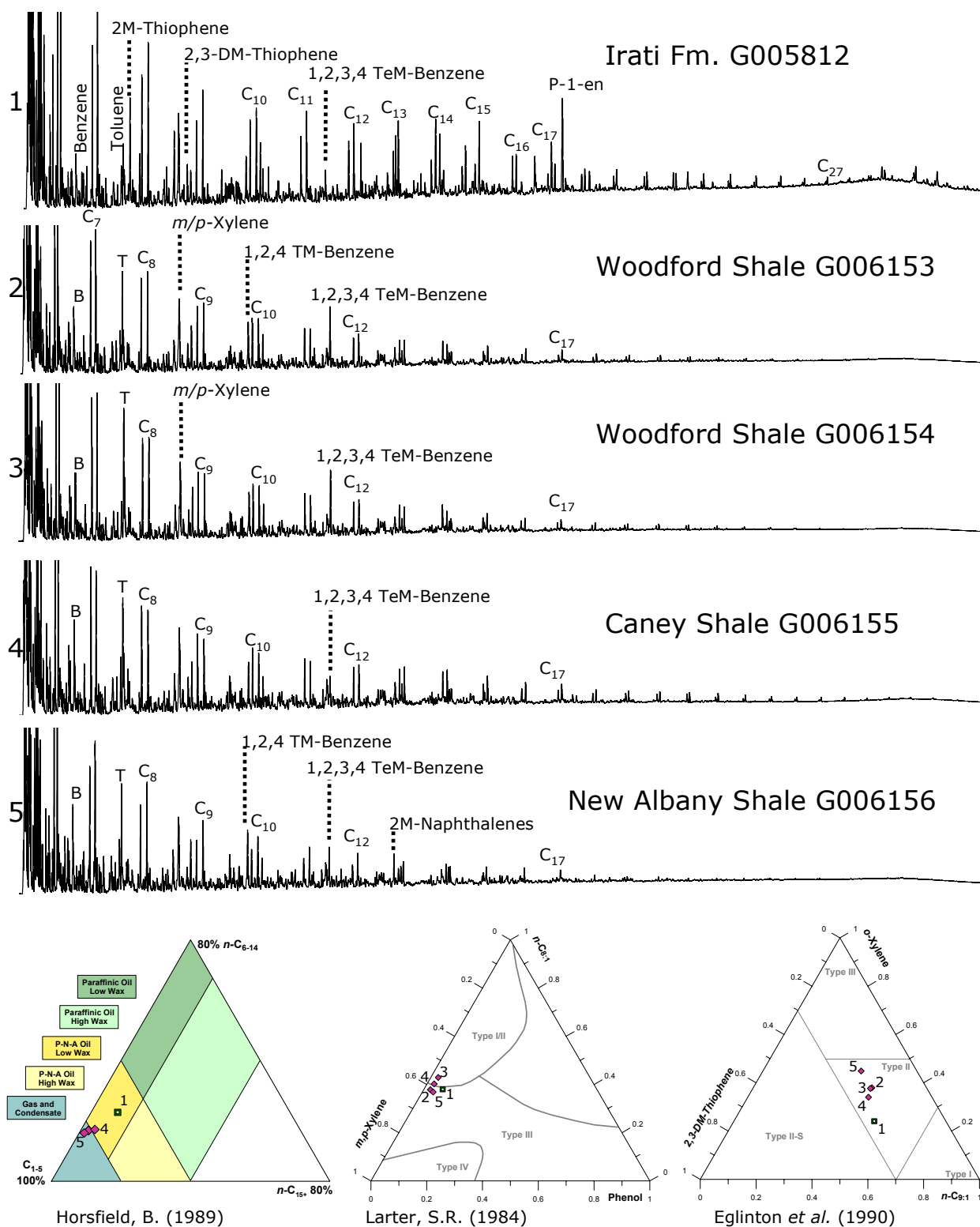


Table A 2 continued: samples provided by Petrobras and Devon

Table A 2: Open-System Pyrolysis GC-FID

Company	Wintershall					
Formation/Basin	German Wealden Coals					
GFZ Code	G006533	G006538	G006542	G006544	G006548	G006550
File	G006533AA	G006538AA	G006542AA	G006544AA	G006548AA	G006550AA
Temperature [°C]	300-600	300-600	300-600	300-600	300-600	300-600
Rate	60K/min	60K/min	60K/min	60K/min	60K/min	60K/min
Totals	mg/g TOC	mg/g TOC	mg/g TOC	mg/g TOC	mg/g TOC	mg/g TOC
C <sub>1+</sub> (-blank)	171.94	149.68	178.23	147.06	150.29	153.76
C <sub>1-5</sub>	45.99	46.95	48.57	41.13	40.53	44.68
C <sub>2-5</sub>	26.92	24.94	30.31	22.29	22.37	24.86
C <sub>6-14</sub> (-blank)	45.54	36.10	49.55	35.45	36.90	38.49
C <sub>6-14</sub> Hump	30.82	28.86	37.20	27.14	27.28	29.47
C <sub>6-14</sub> Resolved	14.72	7.24	12.35	8.31	9.63	9.02
C <sub>15+</sub> (-blank)	80.41	66.63	80.11	70.48	72.86	70.59
C <sub>15+</sub> Hump	11.41	13.35	15.57	12.78	13.59	14.18
C <sub>15+</sub> Resolved	69.00	53.28	64.54	57.70	59.27	56.41
GOR	0.37	0.46	0.37	0.39	0.37	0.41
Gas Wetness (C2-5/C1-5)	0.59	0.53	0.62	0.54	0.55	0.56
Compounds Summation	mg/g TOC	mg/g TOC	mg/g TOC	mg/g TOC	mg/g TOC	mg/g TOC
n-C <sub>6-14</sub>	8.43	9.19	13.84	7.73	7.60	8.34
n-C <sub>15+</sub>	7.76	7.04	10.03	8.25	7.95	8.39
Mono-aromatic Compounds	4.96	4.08	4.82	4.24	4.32	4.62
Di-aromatic Compounds	1.42	1.51	1.43	1.39	1.36	1.52
Phenolic Compounds	3.10	2.59	2.34	2.98	3.07	3.05
Thiophenic Compounds	0.46	0.32	0.51	0.31	0.34	0.36
Single Compounds	mg/g TOC	mg/g TOC	mg/g TOC	mg/g TOC	mg/g TOC	mg/g TOC
Methane	19.07	22.01	18.26	18.84	18.16	19.82
Ethene	1.78	1.56	2.06	1.69	1.83	1.97
Ethane	7.29	7.89	8.06	6.71	6.31	7.15
Propane	8.04	6.59	7.73	5.62	5.58	6.24
i-Butane	0.24	0.26	0.29	0.22	0.21	0.24
1-Butene	1.64	1.49	2.28	1.51	1.57	1.75
n-Butane	1.41	1.48	1.97	1.23	1.23	1.38
i-Pentane	0.58	0.37	0.49	0.35	0.40	0.44
Pentene	0.68	0.68	1.06	0.61	0.66	0.70
n-Pentane	0.83	0.93	1.31	0.74	0.72	0.80
Cyclopentane	0.11	0.12	0.16	0.09	0.08	0.09
2-Methylpentane	0.20	0.16	0.24	0.16	0.17	0.19
3-Methylpentane	0.06	0.05	0.08	0.05	0.05	0.05
1-Hexene	0.71	0.68	1.20	0.63	0.68	0.79
n-Hexane	0.66	0.75	1.07	0.57	0.59	0.66
Methylcyclopentane	0.13	0.15	0.20	0.12	0.11	0.13
Benzene	0.38	0.37	0.40	0.41	0.38	0.42
Thiophene	0.02	0.01	0.01	0.01	0.01	0.01
Cyclohexane	0.11	0.11	0.15	0.08	0.08	0.09
2-Methylhexane	0.07	0.07	0.11	0.08	0.08	0.08
2,3-Dimethylpentane	0.03	0.03	0.04	0.03	0.02	0.03
1,1-Dimethylpentane	0.00	0.00	0.00	0.00	0.00	0.00
3-Methylhexane	0.05	0.06	0.07	0.04	0.04	0.05
1-Heptene	0.55	0.56	0.93	0.51	0.54	0.58
n-Heptane	0.68	0.75	1.10	0.61	0.58	0.63
Methyl-Cyclohexane	0.15	0.13	0.20	0.11	0.11	0.10
Ethylcyclopentane	0.06	0.06	0.09	0.05	0.04	0.05
2,5-Dimethylhexane	0.24	0.10	0.17	0.13	0.15	0.14
2,4-Dimethylhexane	0.03	0.03	0.05	0.03	0.02	0.03
3,3-Dimethylhexane	0.07	0.03	0.05	0.04	0.04	0.04
2,3,4-Trimethylpentane	0.18	0.11	0.14	0.11	0.11	0.11
Toluene	1.46	1.10	1.38	1.26	1.27	1.34
2-Methylthiophene	0.05	0.02	0.04	0.02	0.02	0.02
3-Methylthiophene	0.15	0.11	0.14	0.09	0.08	0.08
1-Octene	0.47	0.49	0.82	0.42	0.44	0.49
n-Octane	0.58	0.66	0.97	0.50	0.49	0.54
Ethylbenzene	0.36	0.28	0.39	0.29	0.30	0.33
Ethylthiophene	0.02	0.01	0.01	0.01	0.01	0.01
2,5-Dimethylthiophene	0.02	0.03	0.06	0.03	0.03	0.05
m/p-Xylene	1.16	0.99	1.02	0.97	1.03	1.11
2,4-Dimethylthiophene	0.06	0.05	0.07	0.04	0.04	0.05
2,3-Dimethylthiophene	0.02	0.02	0.06	0.04	0.05	0.05
Styrene	0.10	0.07	0.05	0.04	0.04	0.05
o-Xylene	0.36	0.28	0.36	0.27	0.29	0.31
1-Nonene	0.37	0.40	0.65	0.34	0.35	0.39
n-Nonane	0.46	0.55	0.79	0.42	0.41	0.44
2-Propylthiophene	0.06	0.05	0.08	0.05	0.05	0.05
Propylbenzene	0.08	0.05	0.08	0.05	0.05	0.05
2-Ethyl-5-Methylthiophene	0.05	0.03	0.04	0.03	0.04	0.04
(?)-Benzene	0.35	0.34	0.37	0.31	0.31	0.34
1,3,5-Trimethylbenzene	0.14	0.17	0.13	0.15	0.14	0.16
Phenol	1.02	0.70	0.68	0.89	0.95	0.94
1-Ethyl-2-Methylbenzene	0.15	0.12	0.19	0.12	0.13	0.13
2,3,5-Trimethylthiophene	0.01	0.00	0.01	0.00	0.01	0.01

Table A 2 continued: samples provided by Wintershall (Coals)

Table A 2: Open-System Pyrolysis GC-FID

Company	Wintershall					
Formation/Basin	German Wealden Coals					
GFZ Code	G006533	G006538	G006542	G006544	G006548	G006550
1,2,4-Trimethylbenzene	0.35	0.30	0.34	0.29	0.29	0.31
1-Decene	0.35	0.36	0.61	0.33	0.34	0.36
<i>n</i> -Decane	0.44	0.52	0.78	0.42	0.40	0.42
1,2,3-Trimethylbenzene	0.15	0.08	0.14	0.13	0.14	0.12
<i>o</i> -Cresol	0.71	0.67	0.53	0.79	0.80	0.79
<i>m/p</i> -Cresol	1.25	1.07	1.02	1.15	1.16	1.16
Dimethylphenol	0.12	0.15	0.11	0.16	0.16	0.16
1-Undecene	0.36	0.36	0.59	0.33	0.34	0.36
<i>n</i> -Undecane	0.43	0.55	0.79	0.41	0.39	0.42
1,2,3,4-Tetramethylbenzene	0.18	0.15	0.14	0.11	0.16	0.16
Naphthalene	0.20	0.20	0.25	0.18	0.16	0.18
1-Dodecene	0.36	0.35	0.56	0.34	0.34	0.36
<i>n</i> -Dodecane	0.56	0.59	0.81	0.52	0.43	0.44
2-Methylnaphthalene	0.29	0.36	0.29	0.28	0.29	0.33
1-Tridecene	0.31	0.36	0.49	0.29	0.31	0.38
1-Methylnaphthalene	0.27	0.24	0.22	0.16	0.15	0.19
<i>n</i> -Tridecane	0.47	0.48	0.66	0.41	0.39	0.42
1-Tetradecene	0.28	0.32	0.45	0.29	0.27	0.29
<i>n</i> -Tetradecane	0.38	0.45	0.58	0.39	0.32	0.36
Dimethylnaphthalene	0.44	0.47	0.42	0.47	0.44	0.48
1-Pentadecene	0.33	0.26	0.42	0.27	0.27	0.31
<i>n</i> -Pentadecane	0.42	0.42	0.61	0.39	0.37	0.40
Trimethylnaphthalene	0.07	0.10	0.11	0.10	0.11	0.14
Trimethylnaphthalene	0.12	0.12	0.10	0.13	0.11	0.11
Trimethylnaphthalene	0.02	0.02	0.05	0.07	0.09	0.11
1-Hexadecene	0.26	0.34	0.46	0.34	0.35	0.34
<i>n</i> -Hexadecane	0.36	0.39	0.55	0.37	0.34	0.37
Isopropylidimethylnaphthalene	0.00	0.00	0.00	0.00	0.00	0.00
1-Heptadecene	0.21	0.26	0.34	0.23	0.25	0.28
<i>n</i> -Heptadecane	0.36	0.39	0.50	0.33	0.30	0.33
Pristane	0.03	0.04	0.04	0.02	0.02	0.03
Prist.-1-ene	0.21	0.01	0.09	0.13	0.09	0.10
1-Octadecene	0.20	0.20	0.31	0.21	0.22	0.24
<i>n</i> -Octadecane	0.34	0.35	0.49	0.34	0.33	0.35
Phytane	0.04	0.07	0.06	0.06	0.07	0.06
1-Nonadecene	0.21	0.28	0.32	0.22	0.25	0.26
<i>n</i> -Nonadecane	0.34	0.37	0.46	0.34	0.34	0.36
1-Icosene	0.16	0.18	0.26	0.19	0.21	0.21
<i>n</i> -Icosane	0.34	0.34	0.44	0.34	0.35	0.36
1-Henicosene	0.16	0.16	0.23	0.16	0.20	0.20
<i>n</i> -Henicosane	0.32	0.28	0.40	0.32	0.31	0.33
1-Docosene	0.14	0.14	0.22	0.15	0.17	0.19
<i>n</i> -Docosane	0.31	0.26	0.38	0.33	0.31	0.34
1-Tricosene	0.14	0.12	0.16	0.12	0.16	0.16
<i>n</i> -Tricosane	0.32	0.24	0.35	0.36	0.31	0.34
1-Tetracosene	0.13	0.11	0.14	0.14	0.15	0.17
<i>n</i> -Tetracosane	0.34	0.23	0.34	0.38	0.32	0.35
1-Pentacosene	0.13	0.10	0.13	0.14	0.13	0.15
<i>n</i> -Pentacosane	0.32	0.22	0.31	0.36	0.31	0.34
1-Hexacosene	0.14	0.13	0.13	0.10	0.11	0.12
<i>n</i> -Hexacosane	0.29	0.21	0.30	0.34	0.28	0.30
1-Heptacosene	0.07	0.05	0.07	0.07	0.07	0.07
<i>n</i> -Heptacosane	0.24	0.16	0.26	0.30	0.25	0.26
1-Octacosene	0.07	0.07	0.08	0.06	0.06	0.07
<i>n</i> -Octacosane	0.20	0.14	0.24	0.26	0.22	0.23
1-Nonacosene	0.03	0.02	0.04	0.03	0.03	0.03
<i>n</i> -Nonacosane	0.17	0.10	0.20	0.21	0.18	0.18
1-Triacontene	0.03	0.04	0.03	0.03	0.03	0.04
<i>n</i> -Triacontane	0.15	0.11	0.17	0.17	0.15	0.15
<i>n</i> -C31:1	0.02	0.02	0.02	0.02	0.02	0.02
<i>n</i> -C31	0.12	0.08	0.15	0.15	0.13	0.13
<i>n</i> -C32:1	0.01	0.01	0.01	0.01	0.02	0.02
<i>n</i> -C32	0.10	0.05	0.12	0.12	0.11	0.10
<i>n</i> -C33:1	0.01	0.01	0.01	0.01	0.01	0.01
<i>n</i> -C33	0.07	0.03	0.08	0.09	0.06	0.07
<i>n</i> -C34:1	0.01	0.01	0.01	0.01	0.00	0.01
<i>n</i> -C34	0.05	0.03	0.07	0.07	0.06	0.06
<i>n</i> -C35:1	0.01	0.00	0.01	0.01	0.01	0.01
<i>n</i> -C35	0.05	0.02	0.05	0.05	0.04	0.04
<i>n</i> -C36:1	0.01	0.01	0.01	0.00	0.01	0.01
<i>n</i> -C36	0.03	0.03	0.04	0.04	0.03	0.03
<i>n</i> -C37:1	0.00	0.01	0.01	0.01	0.00	0.00
<i>n</i> -C37	0.03	0.03	0.03	0.03	0.02	0.03
<i>n</i> -C38:1	0.00	0.02	0.01	0.01	0.01	0.01
<i>n</i> -C38	0.02	0.02	0.03	0.03	0.03	0.02
<i>n</i> -C39:1	0.00	0.01	0.01	0.00	0.00	0.00
<i>n</i> -C39	0.02	0.02	0.02	0.03	0.02	0.02

Table A 2 continued: samples provided by Wintershall (Coals)

Table A 2: Open-System Pyrolysis GC-FID

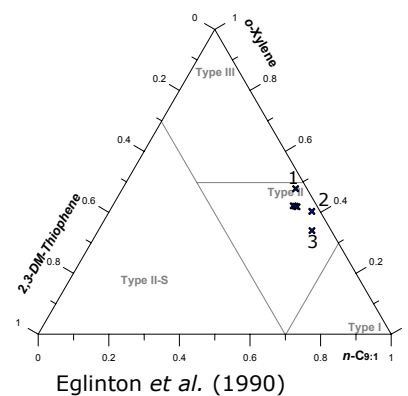
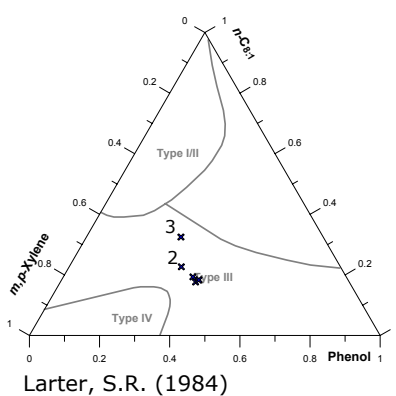
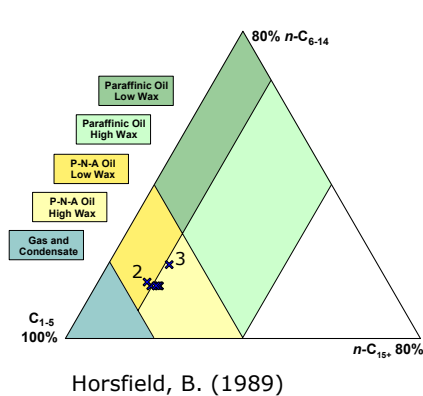
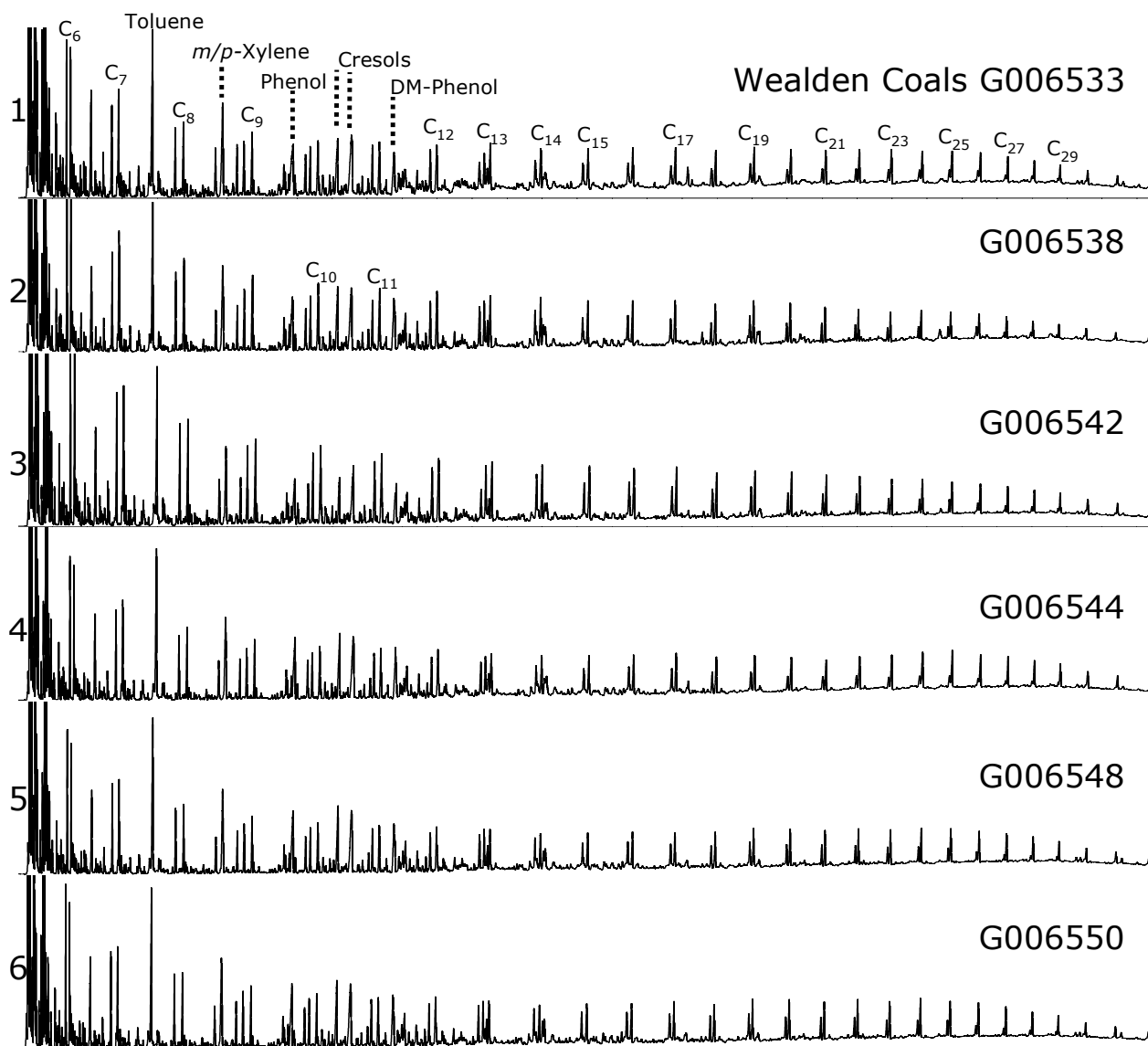


Table A 2 continued: samples provided by Wintershall (Coals)

Table A 2: Open-System Pyrolysis GC-FID

Company	Wintershall					
Formation/Basin	German Wealden Shales					
GFZ Code	G006535	G006536	G006540	G006547	G006553	G006554
File	G006535AA	G006536AA	G006540AA	G006547AA	G006553AA	G006554AA
Temperature [°C]	300-600	300-600	300-600	300-600	300-600	300-600
Rate	60K/min	60K/min	60K/min	60K/min	60K/min	60K/min
Totals	mg/g TOC	mg/g TOC	mg/g TOC	mg/g TOC	mg/g TOC	mg/g TOC
C <sub>1+</sub> (-blank)	607.32	615.46	520.19	572.45	526.34	552.95
C <sub>1-5</sub>	95.86	87.12	76.14	88.38	77.41	73.83
C <sub>2-5</sub>	83.96	76.41	66.52	78.16	66.94	64.92
C <sub>6-14</sub> (-blank)	203.64	193.25	167.72	180.77	159.30	167.45
C <sub>6-14</sub> Hump	158.63	152.93	132.29	140.24	120.75	124.14
C <sub>6-14</sub> Resolved	45.01	40.32	35.43	40.54	38.54	43.30
C <sub>15+</sub> (-blank)	307.82	335.09	276.32	303.30	289.64	311.68
C <sub>15+</sub> Hump	92.60	91.60	73.24	81.77	70.91	72.28
C <sub>15+</sub> Resolved	215.22	243.49	203.09	221.53	218.72	239.39
GOR	0.19	0.16	0.17	0.18	0.17	0.15
Gas Wetness (C2-5/C1-5)	0.88	0.88	0.87	0.88	0.86	0.88
Compounds Summation	mg/g TOC	mg/g TOC	mg/g TOC	mg/g TOC	mg/g TOC	mg/g TOC
n- C <sub>6-14</sub>	95.14	92.31	72.37	81.00	73.97	74.37
n- C <sub>15+</sub>	69.85	71.58	50.95	60.26	56.04	57.12
Mono-aromatic Compounds	8.01	7.53	6.49	7.44	5.90	6.21
Di-aromatic Compounds	1.93	1.41	2.21	2.13	1.80	1.79
Phenolic Compounds	0.47	0.62	0.52	0.80	0.72	0.80
Thiophenic Compounds	2.50	2.12	1.92	2.35	1.83	1.86
Single Compounds	mg/g TOC	mg/g TOC	mg/g TOC	mg/g TOC	mg/g TOC	mg/g TOC
Methane	11.90	10.71	9.62	10.22	10.46	8.91
Ethene	5.98	6.22	4.01	6.91	5.50	4.63
Ethane	14.22	11.91	11.27	12.51	11.04	10.12
Propane	19.90	18.07	16.18	18.71	16.05	15.47
i-Butane	0.47	0.35	0.38	0.32	0.34	0.34
1-Butene	7.32	7.20	6.09	7.46	6.14	6.18
n-Butane	6.98	6.31	5.83	6.29	5.72	5.73
i-Pentane	0.32	0.34	0.36	0.32	0.28	0.33
Pentene	6.03	5.88	4.76	5.85	4.88	4.81
n-Pentane	4.68	4.27	3.95	4.03	3.74	3.75
Cyclopentane	0.42	0.37	0.30	0.33	0.33	0.33
2-Methylpentane	0.35	0.30	0.28	0.32	0.25	0.32
3-Methylpentane	0.13	0.11	0.12	0.11	0.11	0.12
1-Hexene	9.74	9.41	7.48	9.29	7.67	7.71
n-Hexane	4.55	4.15	3.80	3.73	3.51	3.71
Methylcyclopentane	0.65	0.60	0.43	0.49	0.50	0.54
Benzene	1.65	1.37	0.92	1.36	0.98	1.10
Thiophene	0.08	0.06	0.05	0.07	0.07	0.10
Cyclohexane	0.46	0.40	0.31	0.36	0.34	0.37
2-Methylhexane	0.21	0.18	0.19	0.19	0.14	0.17
2,3-Dimethylpentane	0.04	0.04	0.03	0.03	0.04	0.04
1,1-Dimethylpentane	0.00	0.00	0.00	0.00	0.00	0.00
3-Methylhexane	0.20	0.15	0.17	0.17	0.14	0.19
1-Heptene	7.01	6.83	5.44	6.40	5.51	5.78
n-Heptane	4.72	4.38	4.12	4.06	3.72	3.75
Methyl-Cyclohexane	0.90	0.67	0.50	0.56	0.52	0.58
Ethylcyclopentane	0.41	0.38	0.27	0.29	0.29	0.31
2,5-Dimethylhexane	0.68	0.54	0.38	0.49	0.43	0.43
2,4-Dimethylhexane	0.26	0.27	0.08	0.13	0.18	0.19
3,3-Dimethylhexane	0.23	0.21	0.22	0.21	0.20	0.20
2,3,4-Trimethylpentane	0.47	0.41	0.46	0.52	0.40	0.40
Toluene	1.78	1.78	1.28	1.63	1.31	1.33
2-Methylthiophene	0.37	0.33	0.20	0.33	0.29	0.28
3-Methylthiophene	0.76	0.70	0.65	0.81	0.59	0.57
1-Octene	5.94	5.76	4.30	5.19	4.60	4.36
n-Octane	4.54	4.26	3.83	3.86	3.54	3.39
Ethylbenzene	0.51	0.61	0.50	0.58	0.47	0.54
Ethylthiophene	0.12	0.05	0.05	0.05	0.03	0.04
2,5-Dimethylthiophene	0.18	0.09	0.15	0.27	0.15	0.17
m/p-Xylene	1.06	0.99	0.95	1.05	0.86	0.91
2,4-Dimethylthiophene	0.29	0.29	0.26	0.29	0.22	0.24
2,3-Dimethylthiophene	0.25	0.17	0.16	0.23	0.20	0.20
Styrene	0.49	0.56	0.19	0.30	0.30	0.27
o-Xylene	0.80	0.78	0.64	0.72	0.61	0.61
1-Nonene	5.37	5.27	3.87	4.62	4.16	4.06
n-Nonane	4.19	4.00	3.42	3.46	3.30	3.21
2-Propylthiophene	0.23	0.19	0.19	0.16	0.13	0.15
Propylbenzene	0.33	0.32	0.33	0.32	0.22	0.24
2-Ethyl-5-Methylthiophene	0.14	0.17	0.18	0.09	0.09	0.07
(?)-Benzene	0.60	0.55	0.63	0.58	0.43	0.44
1,3,5-Trimethylbenzene	0.14	0.13	0.13	0.13	0.11	0.11
Phenol	0.06	0.07	0.12	0.14	0.10	0.13
1-Ethyl-2-Methylbenzene	0.46	0.41	0.45	0.41	0.37	0.40
2,3,5-Trimethylthiophene	0.07	0.08	0.03	0.05	0.05	0.03

Table A 2 continued: samples provided by Wintershall (Shales)

Table A 2: Open-System Pyrolysis GC-FID

Company	Wintershall					
Formation/Basin	German Wealden Shales					
GFZ Code	G006535	G006536	G006540	G006547	G006553	G006554
1,2,4-Trimethylbenzene	0.48	0.43	0.47	0.46	0.38	0.38
1-Decene	5.80	5.82	4.10	4.87	4.51	4.45
<i>n</i> -Decane	4.27	3.99	3.41	3.40	3.35	3.17
1,2,3-Trimethylbenzene	0.20	0.17	0.19	0.20	0.16	0.16
<i>o</i> -Cresol	0.11	0.21	0.05	0.20	0.22	0.22
<i>m/p</i> -Cresol	0.24	0.24	0.22	0.22	0.18	0.23
Dimethylphenol	0.07	0.10	0.13	0.24	0.23	0.22
1-Undecene	5.70	5.70	3.79	4.86	4.46	4.43
<i>n</i> -Undecane	4.71	4.50	3.88	3.88	3.67	3.57
1,2,3,4-Tetramethylbenzene	0.24	0.22	0.23	0.30	0.25	0.28
Naphthalene	0.02	0.02	0.02	0.32	0.30	0.31
1-Dodecene	5.49	5.45	3.70	4.36	4.09	4.18
<i>n</i> -Dodecane	4.77	4.59	3.82	3.93	3.70	3.73
2-Methylnaphthalene	0.24	0.22	0.56	0.47	0.33	0.27
1-Tridecene	4.84	4.94	3.24	3.97	3.79	3.99
1-Methylnaphthalene	0.39	0.32	0.34	0.34	0.28	0.28
<i>n</i> -Tridecane	4.49	4.42	3.73	3.89	3.63	3.77
1-Tetradecene	4.70	4.68	3.02	3.69	3.46	3.74
<i>n</i> -Tetradecane	4.34	4.14	3.42	3.56	3.30	3.36
Dimethylnaphthalene	0.39	0.00	0.52	0.45	0.32	0.35
1-Pentadecene	4.47	4.51	2.60	3.29	3.25	3.36
<i>n</i> -Pentadecane	4.35	4.32	3.32	3.57	3.33	3.29
Trimethylnaphthalene	0.21	0.18	0.21	0.17	0.15	0.13
Trimethylnaphthalene	0.39	0.34	0.42	0.28	0.30	0.28
Trimethylnaphthalene	0.29	0.31	0.15	0.11	0.11	0.17
1-Hexadecene	4.00	4.56	2.57	3.17	2.98	3.12
<i>n</i> -Hexadecane	3.92	4.28	2.99	3.32	3.00	3.03
Isopropylidimethylnaphthalene	0.00	0.00	0.00	0.00	0.00	0.00
1-Heptadecene	3.59	3.88	2.10	2.76	2.63	2.75
<i>n</i> -Heptadecane	3.74	3.88	2.81	3.17	2.83	2.87
Pristane	0.22	0.20	0.27	0.23	0.13	0.11
Prist.-1-ene	0.08	0.07	0.01	0.01	0.04	0.04
1-Octadecene	2.98	3.11	1.89	2.53	2.35	2.38
<i>n</i> -Octadecane	3.37	3.35	2.69	3.08	2.63	2.59
Phytane	0.20	0.18	0.29	0.29	0.18	0.18
1-Nonadecene	2.67	2.79	1.68	2.24	2.16	2.18
<i>n</i> -Nonadecane	3.11	3.04	2.50	2.81	2.39	2.36
1-Icosene	2.38	2.34	1.39	1.91	1.84	1.87
<i>n</i> -Icosane	2.73	2.57	2.21	2.50	2.13	2.08
1-Henicosene	2.16	2.10	1.24	1.67	1.57	1.69
<i>n</i> -Henicosane	2.49	2.31	2.02	2.23	1.89	1.86
1-Docosene	2.05	2.00	1.13	1.48	1.49	1.44
<i>n</i> -Docosane	2.32	2.18	1.88	2.00	1.72	1.69
1-Tricosene	1.70	1.69	0.89	1.18	1.27	1.30
<i>n</i> -Tricosane	2.14	2.04	1.82	1.88	1.63	1.61
1-Tetracosene	1.49	1.54	0.83	1.10	1.16	1.15
<i>n</i> -Tetracosane	1.92	1.81	1.68	1.77	1.50	1.46
1-Pentacosene	1.17	1.19	0.62	0.96	0.96	1.00
<i>n</i> -Pentacosane	1.60	1.52	1.43	1.61	1.37	1.31
1-Hexacosene	0.90	0.98	0.49	0.69	0.77	0.84
<i>n</i> -Hexacosane	1.35	1.41	1.31	1.39	1.27	1.29
1-Heptacosene	0.65	0.74	0.32	0.41	0.52	0.59
<i>n</i> -Heptacosane	1.05	1.12	1.07	1.11	1.06	1.10
1-Octacosene	0.56	0.58	0.35	0.50	0.48	0.58
<i>n</i> -Octacosane	0.74	0.80	0.82	0.87	0.85	0.89
1-Nonacosene	0.40	0.41	0.25	0.33	0.40	0.43
<i>n</i> -Nonacosane	0.55	0.60	0.65	0.64	0.66	0.68
1-Triacontene	0.27	0.35	0.18	0.26	0.28	0.30
<i>n</i> -Triacontane	0.43	0.49	0.55	0.55	0.54	0.57
<i>n</i> -C31:1	0.21	0.26	0.13	0.19	0.20	0.25
<i>n</i> -C31	0.36	0.41	0.48	0.48	0.47	0.50
<i>n</i> -C32:1	0.13	0.19	0.07	0.12	0.14	0.17
<i>n</i> -C32	0.33	0.38	0.41	0.42	0.39	0.40
<i>n</i> -C33:1	0.12	0.14	0.06	0.10	0.13	0.12
<i>n</i> -C33	0.25	0.29	0.30	0.31	0.29	0.35
<i>n</i> -C34:1	0.08	0.10	0.04	0.10	0.10	0.14
<i>n</i> -C34	0.21	0.21	0.24	0.26	0.25	0.26
<i>n</i> -C35:1	0.07	0.09	0.04	0.07	0.07	0.10
<i>n</i> -C35	0.18	0.21	0.22	0.23	0.22	0.22
<i>n</i> -C36:1	0.06	0.07	0.04	0.07	0.09	0.10
<i>n</i> -C36	0.14	0.20	0.16	0.21	0.19	0.21
<i>n</i> -C37:1	0.04	0.08	0.06	0.05	0.05	0.06
<i>n</i> -C37	0.14	0.13	0.16	0.16	0.13	0.16
<i>n</i> -C38:1	0.05	0.06	0.04	0.14	0.12	0.11
<i>n</i> -C38	0.11	0.13	0.12	0.17	0.14	0.14
<i>n</i> -C39:1	0.05	0.03	0.01	0.05	0.04	0.04
<i>n</i> -C39	0.09	0.11	0.10	0.13	0.11	0.14

Table A 2 continued: samples provided by Wintershall (Shales)



Table A 2: Open-System Pyrolysis GC-FID

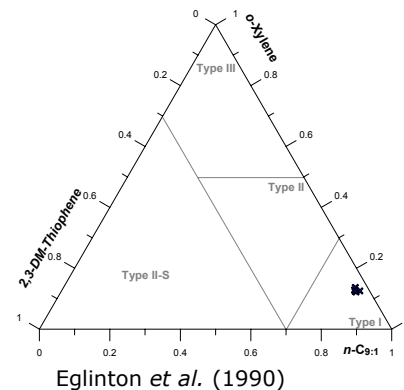
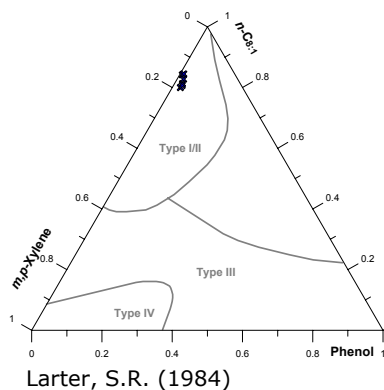
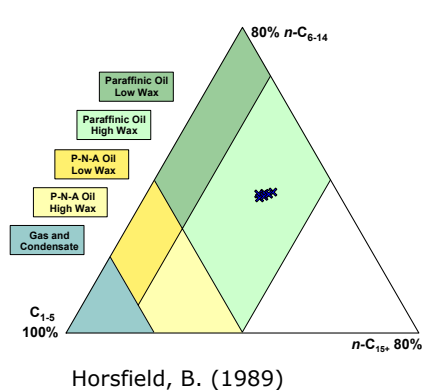
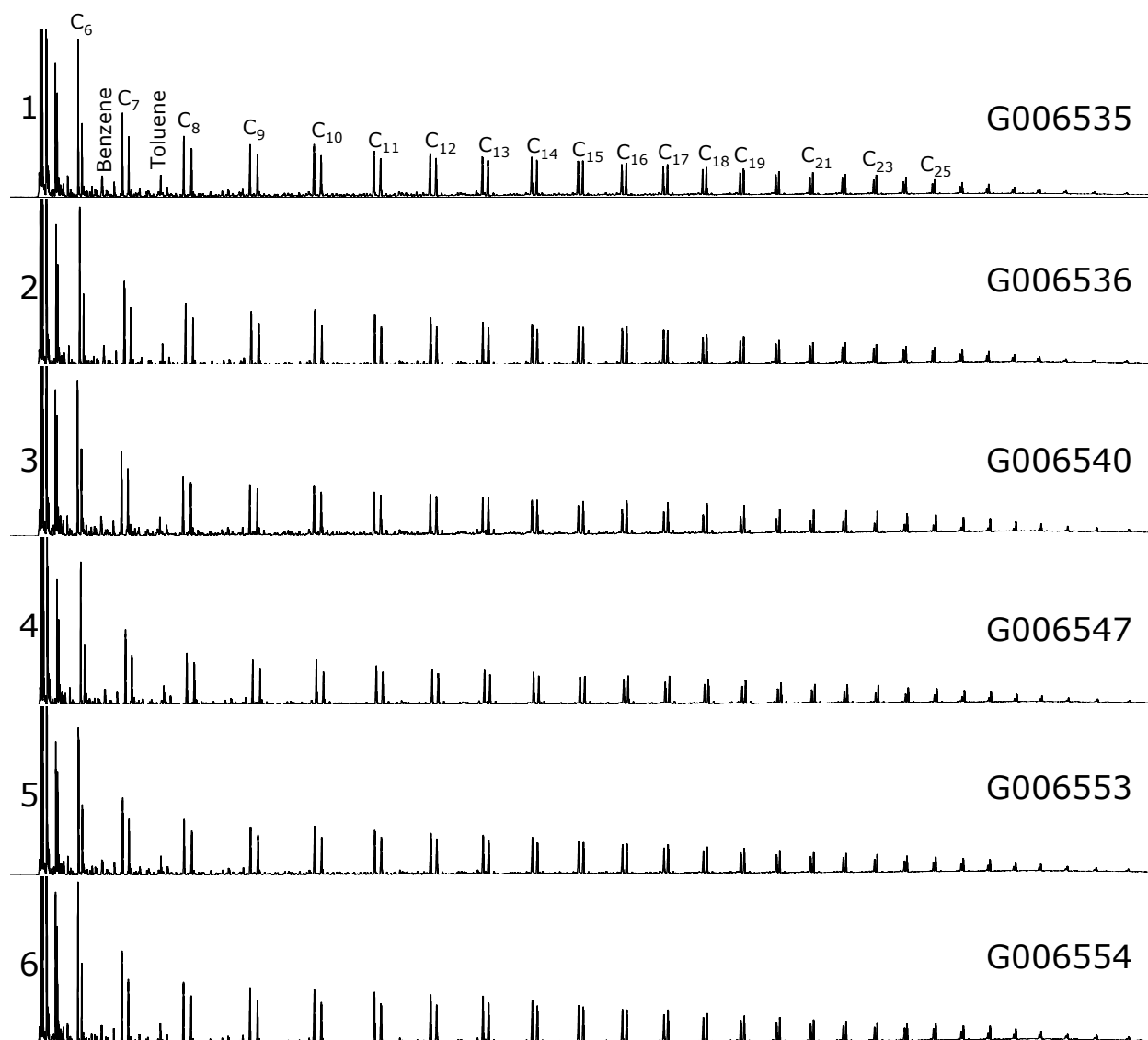


Table A 2 continued: samples provided by Wintershall (Shales)

Table A 2: Open-System Pyrolysis GC-FID

Company	Maersk				
Formation/Basin	Farsund Fm.				
GFZ Code	G007162	G007163	G007164	G007165	G007166
File	G007162AA	G007163AA	G007164AA	G007165AA	G007166AA
Temperature [°C]	300-600	300-600	300-600	300-600	300-600
Rate	60K/min	60K/min	60K/min	60K/min	60K/min
Totals	mg/g TOC	mg/g TOC	mg/g TOC	mg/g TOC	mg/g TOC
C <sub>1+</sub> (-blank)	85.86	81.44	52.83	54.82	76.88
C <sub>1-5</sub>	18.50	26.77	16.40	21.69	28.91
C <sub>2-5</sub>	13.11	19.90	11.82	16.87	22.48
C <sub>6-14</sub> (-blank)	31.19	34.20	27.56	24.29	34.52
C <sub>6-14</sub> Hump	27.63	28.79	23.50	19.76	27.63
C <sub>6-14</sub> Resolved	3.56	5.42	4.06	4.53	6.90
C <sub>15+</sub> (-blank)	36.18	20.46	8.87	8.84	13.45
C <sub>15+</sub> Hump	2.19	2.06	2.03	3.19	6.13
C <sub>15+</sub> Resolved	33.99	18.40	6.83	5.65	7.32
GOR	0.27	0.49	0.45	0.65	0.60
Gas Wetness (C2-5/C1-5)	0.71	0.74	0.72	0.78	0.78
Compounds Summation	mg/g TOC	mg/g TOC	mg/g TOC	mg/g TOC	mg/g TOC
n-C <sub>6-14</sub>	2.76	3.52	1.86	3.37	5.63
n-C <sub>15+</sub>	0.31	0.47	0.36	0.86	2.25
Mono-aromatic Compounds	13.87	11.17	12.34	5.52	5.68
Di-aromatic Compounds	2.34	1.87	1.33	1.02	1.27
Phenolic Compounds	0.09	0.11	0.05	0.29	0.36
Thiophenic Compounds	1.69	1.60	1.44	1.06	0.89
Single Compounds	mg/g TOC	mg/g TOC	mg/g TOC	mg/g TOC	mg/g TOC
Methane	5.39	6.87	4.58	4.82	6.44
Ethene	1.39	1.19	0.83	0.62	0.71
Ethane	1.82	2.24	1.30	2.11	3.31
Propane	2.62	3.79	2.12	2.71	3.93
i-Butane	0.13	0.26	0.17	0.21	0.19
1-Butene	0.73	1.32	0.65	0.94	1.31
n-Butane	0.81	1.45	0.90	1.19	1.16
i-Pentane	0.18	0.17	0.10	0.93	2.20
Pentene	0.42	0.57	0.32	0.62	1.06
n-Pentane	0.55	0.64	0.38	0.55	0.77
Cyclopentane	0.06	0.08	0.05	0.06	0.09
2-Methylpentane	0.14	0.18	0.10	0.12	0.18
3-Methylpentane	0.06	0.06	0.04	0.06	0.08
1-Hexene	0.34	0.45	0.22	0.43	0.78
n-Hexane	0.40	0.46	0.24	0.36	0.51
Methylcyclopentane	0.09	0.10	0.06	0.08	0.10
Benzene	10.06	6.10	9.08	1.81	1.22
Thiophene	1.32	1.08	1.00	0.33	0.12
Cyclohexane	0.15	0.24	0.19	0.13	0.14
2-Methylhexane	0.07	0.09	0.06	0.06	0.08
2,3-Dimethylpentane	0.05	0.05	0.03	0.02	0.04
1,1-Dimethylpentane	0.00	0.00	0.00	0.00	0.00
3-Methylhexane	0.06	0.06	0.04	0.05	0.07
1-Heptene	0.20	0.24	0.18	0.29	0.50
n-Heptane	0.35	0.41	0.20	0.34	0.53
Methyl-Cyclohexane	0.11	0.11	0.07	0.10	0.15
Ethylcyclopentane	0.04	0.04	0.02	0.04	0.05
2,5-Dimethylhexane	0.03	0.03	0.02	0.03	0.11
2,4-Dimethylhexane	0.00	0.00	0.00	0.00	0.01
3,3-Dimethylhexane	0.00	0.00	0.00	0.00	0.01
2,3,4-Trimethylpentane	0.02	0.02	0.01	0.03	0.12
Toluene	2.20	2.22	1.45	1.46	1.56
2-Methylthiophene	0.08	0.13	0.12	0.24	0.15
3-Methylthiophene	0.11	0.09	0.08	0.09	0.17
1-Octene	0.14	0.13	0.12	0.21	0.38
n-Octane	0.30	0.35	0.18	0.32	0.50
Ethylbenzene	0.30	0.44	0.22	0.41	0.53
Ethylthiophene	0.04	0.09	0.05	0.07	0.07
2,5-Dimethylthiophene	0.00	0.00	0.00	0.03	0.05
m/p-Xylene	0.39	0.69	0.36	0.54	0.74
2,4-Dimethylthiophene	0.02	0.02	0.03	0.06	0.09
2,3-Dimethylthiophene	0.02	0.04	0.02	0.04	0.05
Styrene	0.25	0.31	0.23	0.29	0.27
o-Xylene	0.36	0.61	0.28	0.38	0.40
1-Nonene	0.08	0.08	0.07	0.14	0.25
n-Nonane	0.20	0.22	0.11	0.22	0.31
2-Propylthiophene	0.08	0.12	0.07	0.17	0.16
Propylbenzene	0.06	0.05	0.03	0.04	0.04
2-Ethyl-5-Methylthiophene	0.01	0.01	0.00	0.01	0.02
(?)-Benzene	0.15	0.29	0.21	0.30	0.43
1,3,5-Trimethylbenzene	0.04	0.08	0.04	0.06	0.08
Phenol	0.03	0.02	0.01	0.14	0.14
1-Ethyl-2-Methylbenzene	0.16	0.29	0.53	0.24	0.28
2,3,5-Trimethylthiophene	0.01	0.03	0.07	0.02	0.01

Table A 2 continued: samples provided by Maersk

Table A 2: Open-System Pyrolysis GC-FID

Company	Maersk				
Formation/Basin	Farsund Fm.				
GFZ Code	G007162	G007163	G007164	G007165	G007166
1,2,4-Trimethylbenzene	0.10	0.25	0.09	0.18	0.28
1-Decene	0.06	0.05	0.06	0.10	0.18
<i>n</i> -Decane	0.16	0.18	0.09	0.18	0.27
1,2,3-Trimethylbenzene	0.06	0.13	0.06	0.10	0.12
<i>o</i> -Cresol	0.01	0.01	0.00	0.06	0.10
<i>m/p</i> -Cresol	0.05	0.08	0.04	0.09	0.13
Dimethylphenol	0.00	0.00	0.00	0.00	0.00
1-Undecene	0.04	0.05	0.05	0.08	0.18
<i>n</i> -Undecane	0.12	0.15	0.07	0.14	0.23
1,2,3,4-Tetramethylbenzene	0.02	0.06	0.02	0.06	0.09
Naphthalene	2.12	1.14	1.09	0.44	0.40
1-Dodecene	0.05	0.05	0.04	0.07	0.17
<i>n</i> -Dodecane	0.10	0.14	0.05	0.13	0.21
2-Methylnaphthalene	0.09	0.26	0.09	0.18	0.30
1-Tridecene	0.03	0.07	0.05	0.07	0.13
1-Methylnaphthalene	0.09	0.26	0.10	0.19	0.28
<i>n</i> -Tridecane	0.09	0.21	0.05	0.13	0.23
1-Tetradecene	0.04	0.04	0.03	0.05	0.09
<i>n</i> -Tetradecane	0.08	0.25	0.05	0.10	0.19
Dimethylnaphthalene	0.04	0.20	0.05	0.21	0.30
1-Pentadecene	0.02	0.02	0.02	0.02	0.06
<i>n</i> -Pentadecane	0.06	0.18	0.04	0.06	0.22
Trimethylnaphthalene	0.00	0.00	0.00	0.00	0.00
Trimethylnaphthalene	0.00	0.00	0.00	0.00	0.00
Trimethylnaphthalene	0.00	0.00	0.00	0.00	0.00
1-Hexadecene	0.01	0.01	0.01	0.02	0.07
<i>n</i> -Hexadecane	0.06	0.10	0.06	0.11	0.20
Isopropylidimethylnaphthalene	0.00	0.00	0.00	0.00	0.00
1-Heptadecene	0.02	0.01	0.01	0.01	0.03
<i>n</i> -Heptadecane	0.04	0.07	0.06	0.12	0.24
Pristane	0.01	0.00	0.03	0.04	0.08
Prist.-1-ene	0.00	0.00	0.00	0.00	0.00
1-Octadecene	0.01	0.00	0.00	0.01	0.02
<i>n</i> -Octadecane	0.03	0.04	0.05	0.12	0.24
Phytane	0.01	0.00	0.01	0.03	0.06
1-Nonadecene	0.01	0.01	0.01	0.04	0.06
<i>n</i> -Nonadecane	0.02	0.02	0.04	0.11	0.24
1-Icosene	0.00	0.00	0.00	0.00	0.02
<i>n</i> -Icosane	0.01	0.01	0.02	0.08	0.22
1-Henicosene	0.00	0.00	0.00	0.01	0.02
<i>n</i> -Henicosane	0.01	0.01	0.02	0.06	0.19
1-Docosene	0.00	0.00	0.00	0.00	0.01
<i>n</i> -Docosane	0.00	0.00	0.01	0.03	0.14
1-Tricosene	0.00	0.00	0.00	0.00	0.00
<i>n</i> -Tricosane	0.00	0.00	0.01	0.02	0.10
1-Tetracosene	0.00	0.00	0.00	0.00	0.01
<i>n</i> -Tetracosane	0.00	0.00	0.00	0.01	0.06
1-Pentacosene	0.00	0.00	0.00	0.00	0.00
<i>n</i> -Pentacosane	0.00	0.00	0.00	0.01	0.04
1-Hexacosene	0.00	0.00	0.00	0.00	0.00
<i>n</i> -Hexacosane	0.00	0.00	0.00	0.00	0.02
1-Heptacosene	0.00	0.00	0.00	0.00	0.00
<i>n</i> -Heptacosane	0.00	0.00	0.00	0.00	0.01
1-Octacosene	0.00	0.00	0.00	0.00	0.00
<i>n</i> -Octacosane	0.00	0.00	0.00	0.00	0.00
1-Nonacosene	0.00	0.00	0.00	0.00	0.00
<i>n</i> -Nonacosane	0.00	0.00	0.00	0.00	0.00
1-Triacontene	0.00	0.00	0.00	0.00	0.00
<i>n</i> -Triacontane	0.00	0.00	0.00	0.00	0.00
<i>n</i> -C31:1	0.00	0.00	0.00	0.00	0.00
<i>n</i> -C31	0.00	0.00	0.00	0.00	0.00
<i>n</i> -C32:1	0.00	0.00	0.00	0.00	0.00
<i>n</i> -C32	0.00	0.00	0.00	0.00	0.00
<i>n</i> -C33:1	0.00	0.00	0.00	0.00	0.00
<i>n</i> -C33	0.00	0.00	0.00	0.00	0.00
<i>n</i> -C34:1	0.00	0.00	0.00	0.00	0.00
<i>n</i> -C34	0.00	0.00	0.00	0.00	0.00
<i>n</i> -C35:1	0.00	0.00	0.00	0.00	0.00
<i>n</i> -C35	0.00	0.00	0.00	0.00	0.00
<i>n</i> -C36:1	0.00	0.00	0.00	0.00	0.00
<i>n</i> -C36	0.00	0.00	0.00	0.00	0.00
<i>n</i> -C37:1	0.00	0.00	0.00	0.00	0.00
<i>n</i> -C37	0.00	0.00	0.00	0.00	0.00
<i>n</i> -C38:1	0.00	0.00	0.00	0.00	0.00
<i>n</i> -C38	0.00	0.00	0.00	0.00	0.00
<i>n</i> -C39:1	0.00	0.00	0.00	0.00	0.00
<i>n</i> -C39	0.00	0.00	0.00	0.00	0.00

Table A 2 continued: samples provided by Maersk

Table A 2: Open-System Pyrolysis GC-FID

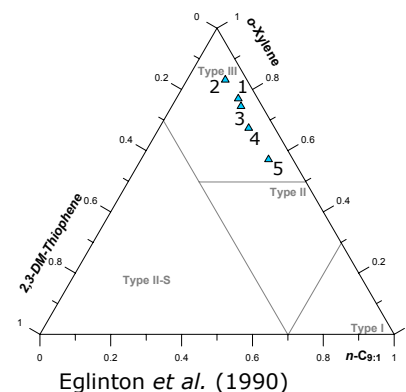
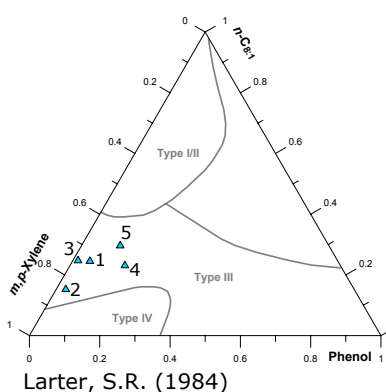
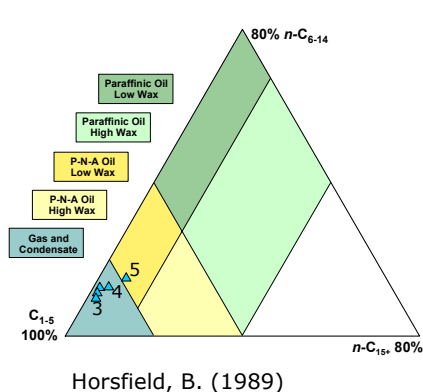
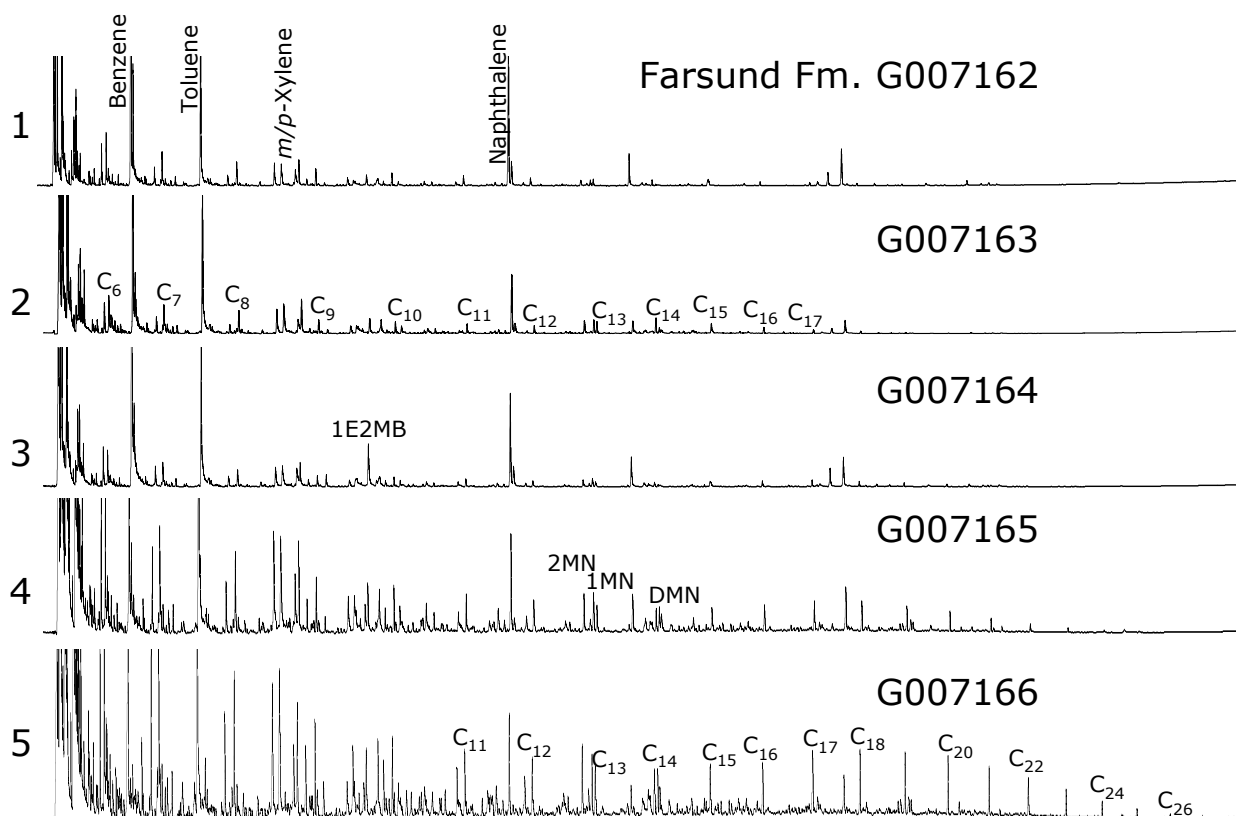


Table A 2 continued: samples provided by Maersk

Table A 2: Open-System Pyrolysis GC-FID

GFZ immature: Organofacies	GAS + Condensate: Coals						Gas + Condensate: Shales		
Formation/Basin	Kugmallit Fm.	Jet Rock	Cannel Coal	Sandbochum1 Westf. Coal	Talang Akar Coal	Are Fm.	Chattanooga Shale	Alum Shale	Alum Shale
GFZ Code	G000206	G000696	G000698	G000721	G000899	G001965	G000692	G000753	G000758
File	EE	AD	AD	A	AD	BO	AD	AD	AD
Temperature [°C]	200-580	200-560	200-560	300-600	200-560	200-550	200-560	200-560	200-560
Rate	5K/min	2K/min	2K/min	60K/min	2K/min	1k/min	2K/min	2K/min	2K/min
Totals	mg/g TOC	mg/g TOC	mg/g TOC	mg/g TOC	mg/g TOC	mg/g TOC	mg/g TOC	mg/g TOC	mg/g TOC
C <sub>1+</sub> (-blank)	84.03	1875.44	188.67	207.89	177.23	163.15	458.42	461.06	276.74
C <sub>1-5</sub>	36.32	217.65	46.33	61.86	52.28	53.04	85.65	167.39	100.59
C <sub>2-5</sub>	19.79	140.42	26.43	31.70	29.43	28.35	64.33	114.14	69.42
C <sub>6-14</sub> (-blank)	34.76	584.32	45.73	52.31	60.33	57.87	121.06	135.59	89.31
C <sub>6-14</sub> Hump	24.80	420.09	29.89	36.99	39.02	43.87	70.69	89.40	55.31
C <sub>6-14</sub> Resolved	9.96	164.23	15.84	15.32	21.31	14.00	50.37	46.19	34.00
C <sub>15+</sub> (-blank)	12.96	1073.47	96.61	93.72	64.62	52.25	251.71	158.08	86.84
C <sub>15+</sub> Hump	1.96	89.81	8.74	9.40	10.61	12.99	7.43	13.98	8.08
C <sub>15+</sub> Resolved	11.00	983.66	87.87	84.32	54.01	39.26	244.28	144.09	78.76
GOR	0.76	0.13	0.33	0.42	0.42	0.48	0.23	0.57	0.57
Gas Wetness (C2-5/C1-5)	0.54	0.65	0.57	0.51	0.56	0.53	0.75	0.68	0.69
Compounds Summation	mg/g TOC	mg/g TOC	mg/g TOC	mg/g TOC	mg/g TOC	mg/g TOC	mg/g TOC	mg/g TOC	mg/g TOC
n-C <sub>6-14</sub>	0.26	32.21	6.30	7.93	5.21	5.98	16.78	8.89	6.99
n-C <sub>15+</sub>	0.00	13.08	3.32	4.14	4.70	3.59	1.76	0.32	0.47
Mono-aromatic Compounds	2.10	37.86	4.86	7.09	7.61	7.28	9.40	17.47	10.95
Di-aromatic Compounds	0.18	12.99	1.83	2.36	2.55	2.30	2.03	4.01	2.61
Phenolic Compounds	10.54	109.94	2.36	4.82	7.11	6.57	0.50	0.30	0.24
Thiophenic Compounds	0.42	6.32	0.64	0.52	1.50	1.08	2.56	3.01	2.21
Single Compounds	mg/g TOC	mg/g TOC	mg/g TOC	mg/g TOC	mg/g TOC	mg/g TOC	mg/g TOC	mg/g TOC	mg/g TOC
Methane	16.53	77.23	19.90	30.16	22.85	24.69	21.33	53.25	31.17
Ethene	0.86	7.13	1.94	2.67	2.80	3.38	3.67	8.73	6.18
Ethane	1.52	37.83	7.58	9.30	6.56	6.54	13.01	27.06	14.92
Propane	0.86	36.75	6.75	8.27	6.33	6.95	14.96	27.60	17.27
i-Butane	4.28	2.36	0.22	0.32	0.28	0.25	0.86	1.08	0.57
1-Butene	2.56	9.03	1.75	2.14	3.90	2.01	4.96	9.24	5.61
n-Butane	4.33	9.25	1.53	1.66	0.72	1.21	5.08	6.75	4.20
i-Pentane	0.75	2.81	0.16	0.42	0.74	1.15	1.13	2.74	1.72
Pentene	0.08	2.87	0.78	0.99	0.59	0.70	2.29	2.86	2.06
n-Pentane	0.06	5.15	0.86	1.03	0.57	0.63	3.26	3.11	2.04
Cyclopentane	0.01	1.40	0.16	0.19	0.06	0.05	0.37	0.23	0.13
2-Methylpentane	0.02	2.06	0.17	0.22	0.30	0.18	0.98	0.74	0.61
3-Methylpentane	0.04	0.94	0.07	0.07	0.05	0.04	0.49	0.56	0.33
1-Hexene	0.02	2.59	0.70	0.84	0.48	0.62	2.15	2.00	1.45
n-Hexane	0.02	3.04	0.61	0.77	0.36	0.49	2.26	1.81	1.18
Methylcyclopentane	0.00	2.66	0.14	0.21	0.07	0.07	0.72	0.35	0.20
Benzene	0.46	2.64	0.47	0.61	0.86	1.02	0.47	1.05	0.85
Thiophene	0.12	0.26	0.03	0.02	0.23	0.15	0.33	0.45	0.26
Cyclohexane	0.01	1.88	0.10	0.14	0.04	0.06	0.41	0.25	0.14
2-Methylhexane	0.00	0.83	0.05	0.07	0.04	0.11	0.35	0.42	0.26
2,3-Dimethylpentane	0.01	0.39	0.05	0.07	0.12	0.06	0.14	0.14	0.07
1,1-Dimethylpentane	0.00	0.00	0.00	0.00	0.00	0.00	0.00	0.00	0.00
3-Methylhexane	0.02	0.88	0.04	0.06	0.06	0.05	0.51	0.50	0.25
1-Heptene	0.01	1.41	0.50	0.66	0.31	0.45	1.37	0.90	0.70
n-Heptane	0.02	3.11	0.56	0.74	0.43	0.50	2.01	1.28	0.84
Methyl-Cyclohexane	0.02	3.55	0.14	0.28	0.07	0.07	0.68	0.52	0.20
Ethylcyclopentane	0.00	0.79	0.07	0.07	0.03	0.05	0.26	0.16	0.08
2,5-Dimethylhexane	0.01	1.11	0.09	0.12	0.19	0.16	0.39	0.57	0.32
2,4-Dimethylhexane	0.01	0.15	0.03	0.02	0.07	0.05	0.07	0.15	0.06
3,3-Dimethylhexane	0.01	0.69	0.08	0.06	0.14	0.11	0.27	0.40	0.19
2,3,4-Trimethylpentane	0.02	1.99	0.16	0.13	0.23	0.19	0.49	0.71	0.33
Toluene	0.79	9.70	1.55	2.20	2.34	2.26	1.79	4.03	2.51
2-Methylthiophene	0.13	1.03	0.08	0.04	0.32	0.27	0.36	0.60	0.45
3-Methylthiophene	0.07	1.03	0.10	0.13	0.14	0.12	0.29	0.26	0.21
1-Octene	0.00	2.18	0.42	0.52	0.29	0.37	1.22	0.54	0.44
n-Octane	0.01	2.54	0.49	0.56	0.39	0.43	1.47	0.94	0.54
Ethylbenzene	0.05	2.60	0.35	0.44	0.50	0.39	0.88	1.08	0.67
Ethylthiophene	0.02	0.46	0.04	0.03	0.09	0.11	0.22	0.14	0.15
2,5-Dimethylthiophene	0.01	0.26	0.05	0.01	0.08	0.07	0.17	0.24	0.20
m/p-Xylene	0.45	11.14	1.07	1.62	1.66	1.54	2.01	4.15	2.57
2,4-Dimethylthiophene	0.03	1.04	0.08	0.06	0.12	0.08	0.16	0.26	0.18
2,3-Dimethylthiophene	0.03	0.79	0.06	0.05	0.13	0.07	0.42	0.35	0.25
Styrene	0.02	0.40	0.09	0.06	0.12	0.33	0.25	0.49	0.29
o-Xylene	0.10	1.93	0.45	0.48	0.50	0.57	0.87	1.50	1.01
1-Nonene	0.00	0.61	0.29	0.38	0.19	0.27	0.76	0.22	0.20
n-Nonane	0.01	1.73	0.36	0.42	0.29	0.33	1.01	0.35	0.31
2-Propylthiophene	0.01	1.09	0.08	0.09	0.14	0.14	0.27	0.39	0.24
Propylbenzene	0.01	0.47	0.09	0.10	0.05	0.09	0.19	0.10	0.06
2-Ethyl-5-Methylthiophene	0.01	0.37	0.03	0.02	0.09	0.06	0.14	0.13	0.08
(?) -Benzene	0.08	3.47	0.32	0.48	0.46	0.47	0.82	1.84	1.06
1,3,5-Trimethylbenzene	0.00	2.47	0.14	0.26	0.11	0.13	0.39	0.63	0.39
Phenol	2.19	24.22	0.77	1.10	3.11	2.97	0.17	0.05	0.06
1-Ethyl-2-Methylbenzene	0.00	0.00	0.00	0.36	0.39	0.05	0.46	0.63	0.42
2,3,5-Trimethylthiophene	0.00	0.00	0.09	0.07	0.15	0.00	0.19	0.20	0.19

Table A 2 continued: samples provided by GFZ

Table A 2: Open-System Pyrolysis GC-FID

GFZ immature: Organofacies	GAS + Condensate: Coals						Gas + Condensate: Shales		
Formation/Basin	Kugmallit Fm.	Jet Rock	Cannel Coal	Sandbochum1 Westf. Coal	Talang Akar Coal	Are Fm.	Chattanooga Shale	Alum Shale	Alum Shale
GFZ Code	G000206	G000696	G000698	G000721	G000899	G001965	G000692	G000753	G000758
1,2,4-Trimethylbenzene	0.06	2.46	0.31	0.41	0.46	0.42	0.96	1.85	1.05
1-Decene	0.00	0.71	0.24	0.31	0.19	0.24	0.61	0.15	0.14
n-Decane	0.17	1.31	0.33	0.39	0.23	0.27	0.79	0.20	0.22
1,2,3-Trimethylbenzene	0.10	0.98	0.11	0.14	0.27	0.35	0.56	0.62	0.36
o-Cresol	0.82	18.03	0.62	1.55	1.21	0.94	0.06	0.03	0.03
m/p-Cresol	7.53	67.68	0.80	1.85	2.58	2.56	0.18	0.22	0.15
Dimethylphenol	0.00	0.00	0.17	0.32	0.21	0.10	0.10	0.00	0.00
1-Undecene	0.00	1.45	0.21	0.29	0.21	0.33	0.49	0.08	0.14
n-Undecane	0.00	1.30	0.28	0.33	0.26	0.24	0.54	0.13	0.19
1,2,3,4-Tetramethylbenzene	0.06	5.23	0.12	0.13	0.32	0.25	0.75	0.00	0.36
Naphthalene	0.18	1.73	0.24	0.33	0.31	0.41	0.26	0.54	0.39
1-Dodecene	0.00	0.91	0.17	0.30	0.17	0.25	0.42	0.06	0.11
n-Dodecane	0.00	2.64	0.34	0.42	0.49	0.24	0.43	0.14	0.18
2-Methylnaphthalene	0.00	2.43	0.40	0.53	0.49	0.58	0.47	0.89	0.66
1-Tridecene	0.00	3.44	0.16	0.17	0.17	0.21	0.31	0.00	0.10
1-Methylnaphthalene	0.00	1.74	0.39	0.43	0.50	0.33	0.40	0.64	0.43
n-Tridecane	0.00	1.54	0.28	0.35	0.30	0.24	0.36	0.03	0.09
1-Tetradecene	0.00	0.55	0.14	0.21	0.22	0.30	0.33	0.00	0.09
n-Tetradecane	0.00	1.16	0.21	0.28	0.22	0.22	0.24	0.06	0.07
Dimethylnaphthalene	0.00	6.36	0.49	0.70	0.83	0.63	0.62	1.27	0.76
1-Pentadecene	0.00	0.53	0.11	0.13	0.11	0.25	0.17	0.00	0.22
n-Pentadecane	0.00	1.69	0.25	0.33	0.32	0.20	0.29	0.12	0.10
Trimethylnaphthalene	0.00	0.05	0.07	0.11	0.17	0.11	0.02	0.31	0.16
Trimethylnaphthalene	0.00	0.30	0.14	0.16	0.10	0.04	0.19	0.25	0.15
Trimethylnaphthalene	0.00	0.38	0.10	0.09	0.15	0.19	0.08	0.10	0.06
1-Hexadecene	0.00	0.71	0.14	0.14	0.12	0.18	0.13	0.00	0.00
n-Hexadecane	0.00	1.98	0.21	0.22	0.22	0.17	0.17	0.04	0.00
Isopropyldimethylnaphthalene	0.00	0.00	0.02	0.02	0.49	0.03	0.00	0.14	0.07
1-Heptadecene	0.00	0.38	0.09	0.16	0.11	0.13	0.10	0.00	0.00
n-Heptadecane	0.00	1.88	0.23	0.27	0.22	0.17	0.16	0.08	0.07
Pristane	0.00	0.76	0.09	0.11	0.03	0.06	0.04	0.03	0.03
Prist.-1-ene	0.00	0.64	0.05	0.15	0.31	0.23	0.04	0.02	0.00
1-Octadecene	0.00	0.27	0.09	0.13	0.10	0.10	0.07	0.00	0.00
n-Octadecane	0.00	1.01	0.18	0.23	0.17	0.22	0.08	0.01	0.01
Phytane	0.00	0.98	0.04	0.03	0.03	0.06	0.02	0.05	0.03
1-Nonadecene	0.00	0.04	0.15	0.12	0.10	0.11	0.09	0.00	0.00
n-Nonadecane	0.00	0.84	0.24	0.22	0.19	0.23	0.06	0.03	0.05
1-Icosene	0.00	0.00	0.08	0.08	0.08	0.11	0.05	0.00	0.00
n-Icosane	0.00	0.63	0.16	0.21	0.17	0.16	0.06	0.04	0.03
1-Henicosene	0.00	0.00	0.08	0.08	0.07	0.09	0.07	0.00	0.00
n-Henicosane	0.00	0.37	0.15	0.19	0.16	0.15	0.06	0.00	0.00
1-Docosene	0.00	0.00	0.06	0.09	0.07	0.09	0.02	0.00	0.00
n-Docosane	0.00	0.40	0.12	0.18	0.15	0.14	0.03	0.00	0.00
1-Tricosene	0.00	0.00	0.06	0.05	0.08	0.08	0.02	0.00	0.00
n-Tricosane	0.00	0.39	0.11	0.16	0.17	0.14	0.04	0.00	0.00
1-Tetracosene	0.00	0.00	0.05	0.04	0.07	0.08	0.01	0.00	0.00
n-Tetracosane	0.00	0.29	0.10	0.16	0.20	0.14	0.02	0.00	0.00
1-Pentacosene	0.00	0.00	0.04	0.04	0.07	0.07	0.02	0.00	0.00
n-Pentacosane	0.00	0.34	0.08	0.13	0.19	0.13	0.02	0.00	0.00
1-Hexacosene	0.00	0.00	0.04	0.06	0.06	0.06	0.01	0.00	0.00
n-Hexacosane	0.00	0.37	0.08	0.14	0.17	0.10	0.02	0.00	0.00
1-Heptacosene	0.00	0.00	0.03	0.03	0.06	0.04	0.00	0.00	0.00
n-Heptacosane	0.00	0.14	0.06	0.10	0.17	0.07	0.00	0.00	0.00
1-Octacosene	0.00	0.00	0.03	0.02	0.07	0.04	0.00	0.00	0.00
n-Octacosane	0.00	0.13	0.05	0.08	0.16	0.06	0.00	0.00	0.00
1-Nonacosene	0.00	0.00	0.01	0.03	0.05	0.03	0.00	0.00	0.00
n-Nonacosane	0.00	0.10	0.03	0.06	0.13	0.05	0.00	0.00	0.00
1-Triacontene	0.00	0.00	0.03	0.01	0.05	0.00	0.00	0.00	0.00
n-Triacontane	0.00	0.17	0.03	0.03	0.16	0.00	0.00	0.00	0.00
n-C31:1	0.00	0.00	0.02	0.03	0.04	0.00	0.00	0.00	0.00
n-C31	0.00	0.11	0.04	0.05	0.16	0.00	0.00	0.00	0.00
n-C32:1	0.00	0.00	0.02	0.01	0.01	0.00	0.00	0.00	0.00
n-C32	0.00	0.13	0.04	0.06	0.09	0.00	0.00	0.00	0.00
n-C33:1	0.00	0.00	0.04	0.03	0.02	0.00	0.00	0.00	0.00
n-C33	0.00	0.11	0.02	0.02	0.06	0.00	0.00	0.00	0.00
n-C34:1	0.00	0.00	0.00	0.00	0.01	0.00	0.00	0.00	0.00
n-C34	0.00	0.04	0.00	0.00	0.03	0.00	0.00	0.00	0.00
n-C35:1	0.00	0.00	0.00	0.00	0.02	0.00	0.00	0.00	0.00
n-C35	0.00	0.04	0.00	0.00	0.02	0.00	0.00	0.00	0.00
n-C36:1	0.00	0.00	0.00	0.00	0.00	0.00	0.00	0.00	0.00
n-C36	0.00	0.00	0.00	0.00	0.01	0.00	0.00	0.00	0.00
n-C37:1	0.00	0.00	0.00	0.00	0.01	0.00	0.00	0.00	0.00
n-C37	0.00	0.00	0.00	0.00	0.01	0.00	0.00	0.00	0.00
n-C38:1	0.00	0.00	0.00	0.00	0.00	0.00	0.00	0.00	0.00
n-C38	0.00	0.00	0.00	0.00	0.01	0.00	0.00	0.00	0.00
n-C39:1	0.00	0.00	0.00	0.00	0.00	0.00	0.00	0.00	0.00
n-C39	0.00	0.00	0.00	0.00	0.00	0.00	0.00	0.00	0.00

Table A 2 continued: samples provided by GFZ

Table A 2: Open-System Pyrolysis GC-FID

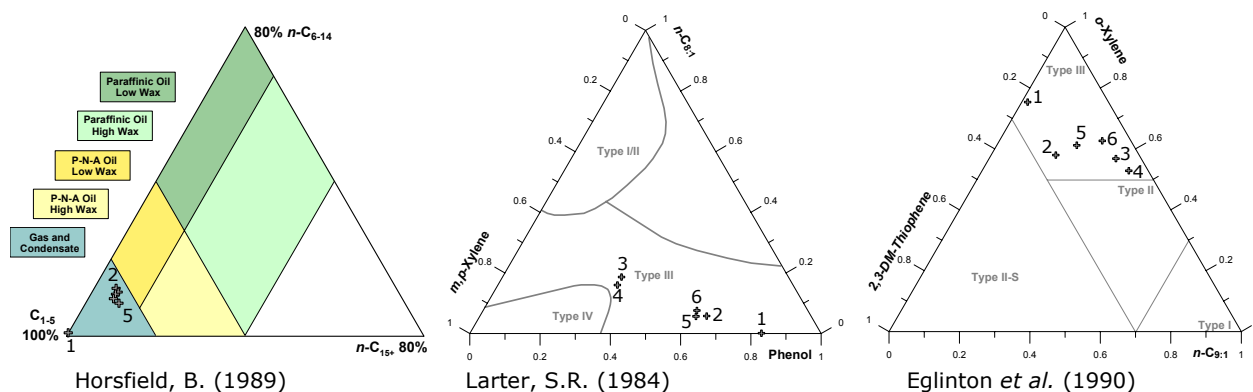
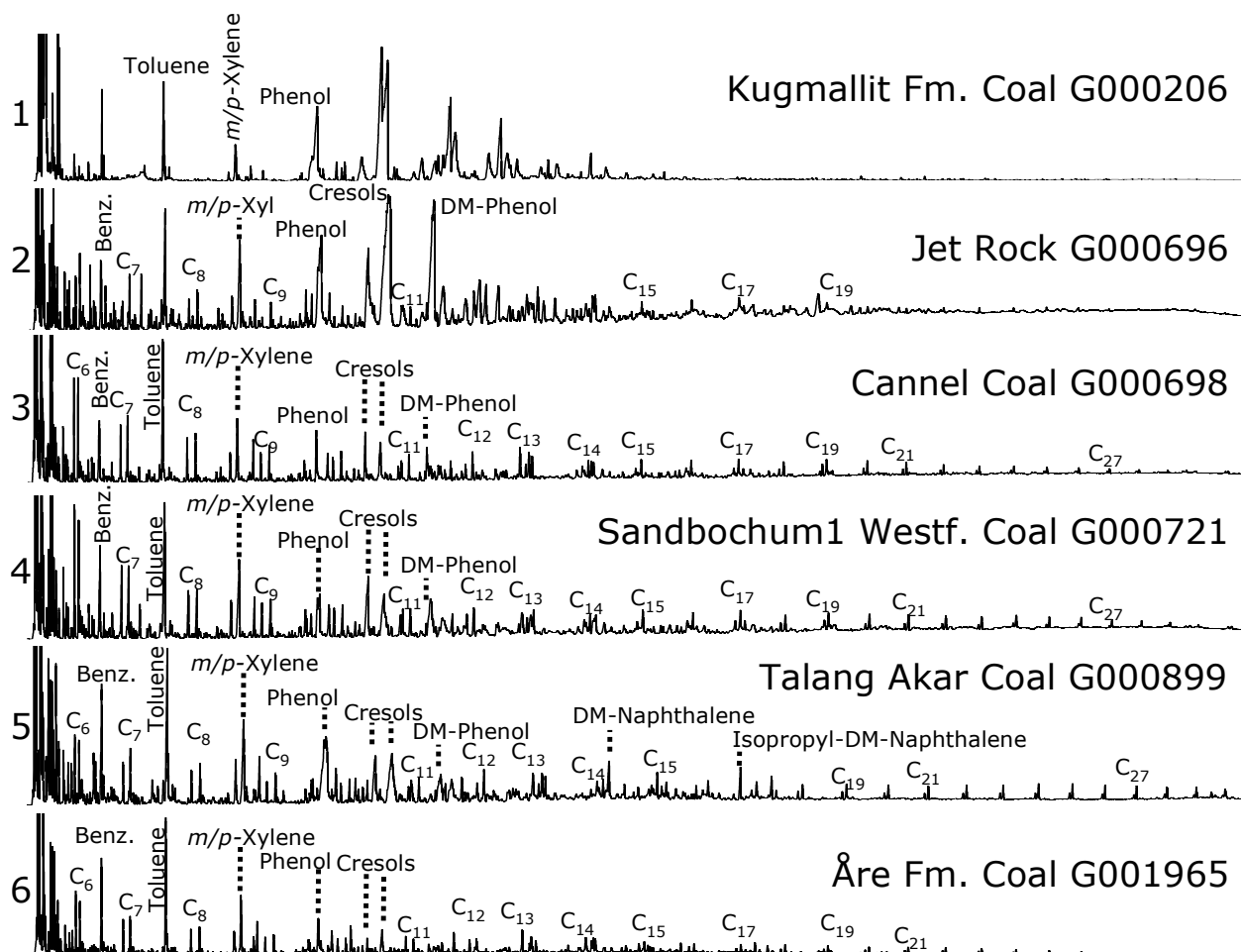


Table A 2 continued: samples provided by GFZ

Table A 2: Open-System Pyrolysis GC-FID

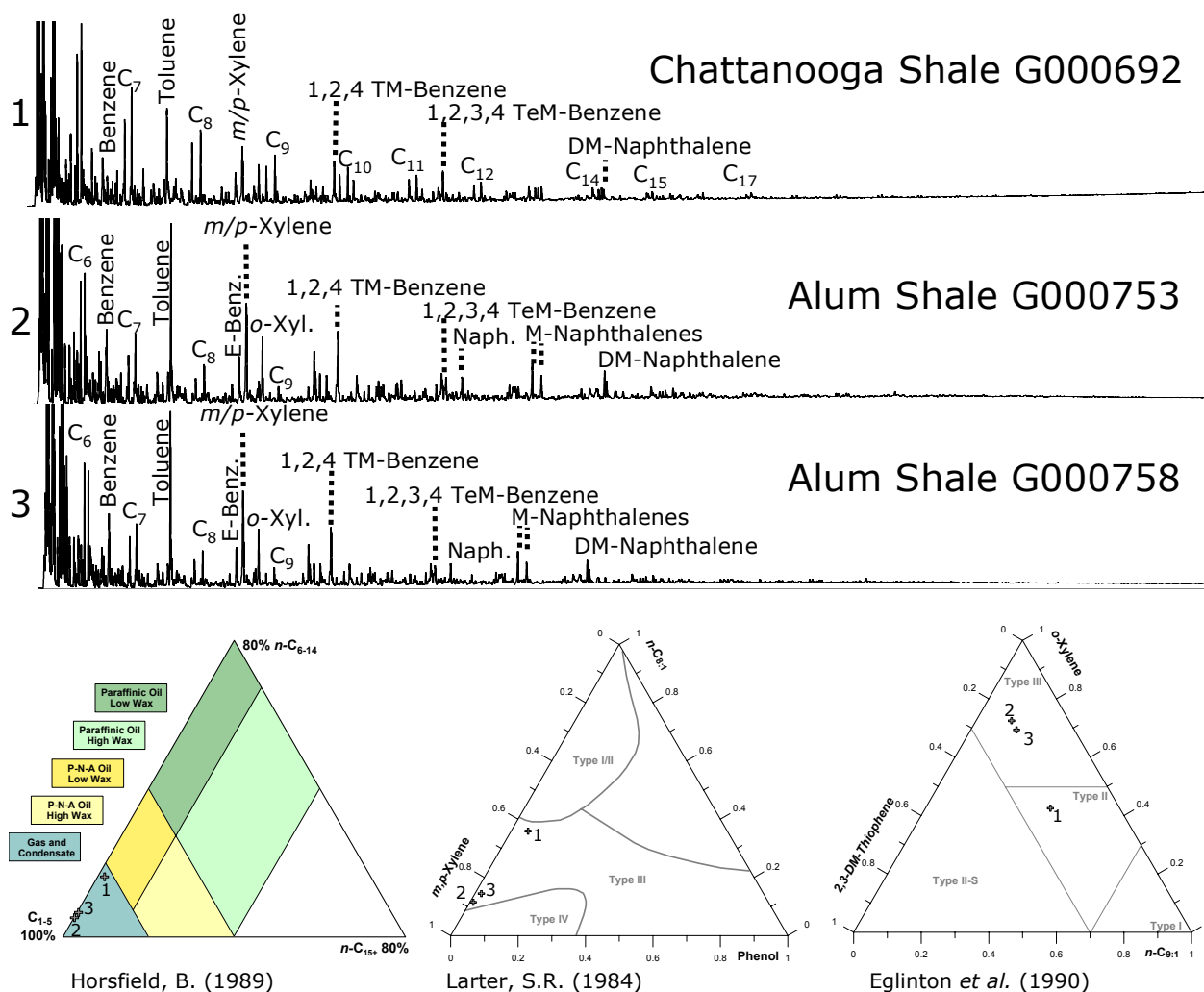


Table A 2 continued: samples provided by GFZ



Table A 2: Open-System Pyrolysis GC-FID

GFZ immature: Organofacies	PNA low wax Oil: Coals			PNA low wax Oil: shales				
Formation/Basin	Talang Akar Coal	Arang Coal	Taglu Fm.	Botneheia Shale	Woodford Shale	Autun Oil Shale	Spekk Fm.	Bakken Shale
GFZ Code	G000726	G000950	SN6750	G000689	G000690	G000883	G001955	G005298
File	G000726AD	G000950AD	SN6750HD	G000689AD	G000690AD	G000883AD	G001955FF	G005298CD
Temperature [°C]	200-560	200-560	200-560	200-560	200-560	200-560	200-550	200-560
Rate	2K/min	2K/min	1K/min	2K/min	2K/min	2K/min	1K/min	2K/min
Totals	mg/g TOC	mg/g TOC	mg/g TOC	mg/g TOC	mg/g TOC	mg/g TOC	mg/g TOC	mg/g TOC
C <sub>1+</sub> (-blank)	162.35	193.81	124.62	453.61	287.50	437.88	350.87	431.19
C <sub>1-5</sub>	36.75	56.58	41.18	80.31	49.01	79.78	82.94	77.39
C <sub>2-5</sub>	21.03	30.51	20.16	55.57	37.02	57.58	60.16	57.95
C <sub>6-14</sub> (-blank)	43.03	58.15	43.88	99.52	72.04	124.87	138.59	142.70
C <sub>6-14</sub> Hump	27.68	39.88	35.02	65.25	42.86	72.04	95.18	78.22
C <sub>6-14</sub> Resolved	15.36	18.27	8.86	34.27	29.18	52.83	43.41	64.48
C <sub>15+</sub> (-blank)	82.56	79.07	39.56	273.78	166.44	233.23	129.35	211.10
C <sub>15+</sub> Hump	11.27	16.45	17.53	14.88	6.83	19.52	19.29	15.25
C <sub>15+</sub> Resolved	71.29	62.62	22.03	258.90	159.61	213.71	110.06	195.85
GOR	0.29	0.41	0.49	0.22	0.21	0.22	0.31	0.22
Gas Wetness (C2-5/C1-5)	0.57	0.54	0.49	0.69	0.76	0.72	0.73	0.75
Compounds Summation	mg/g TOC	mg/g TOC	mg/g TOC	mg/g TOC	mg/g TOC	mg/g TOC	mg/g TOC	mg/g TOC
n-C <sub>6-14</sub>	4.87	8.84	5.48	24.59	13.39	23.63	22.23	20.81
n-C <sub>15+</sub>	5.40	9.52	5.79	8.69	2.64	12.25	7.31	6.63
Mono-aromatic Compounds	3.69	7.52	5.61	5.46	4.07	9.47	12.39	8.27
Di-aromatic Compounds	3.45	2.45	2.04	1.93	0.98	2.64	2.60	2.04
Phenolic Compounds	3.08	5.36	6.78	0.51	0.21	0.46	0.88	0.53
Thiophenic Compounds	0.41	0.60	0.27	1.81	2.14	1.70	6.79	5.67
Single Compounds	mg/g TOC	mg/g TOC	mg/g TOC	mg/g TOC	mg/g TOC	mg/g TOC	mg/g TOC	mg/g TOC
Methane	15.72	26.07	21.02	24.74	11.99	22.19	22.78	19.44
Ethane	1.90	2.99	2.46	2.74	2.40	2.68	4.59	2.88
Propane	5.02	6.70	5.33	13.10	7.63	11.24	12.04	13.42
i-Butane	5.76	7.46	5.31	13.11	9.07	13.61	13.41	12.55
1-Butene	0.36	0.37	0.22	0.79	0.32	0.66	0.53	0.57
n-Butane	1.50	2.69	1.59	3.76	2.99	5.16	5.63	5.14
i-Pentane	1.01	1.36	0.86	4.22	2.94	3.59	3.49	3.70
Pentene	0.50	0.66	0.62	0.66	0.39	0.96	0.99	0.57
n-Pentane	0.45	0.74	0.44	2.23	1.58	2.22	2.44	2.17
Cyclopentane	0.51	0.82	0.49	2.37	1.84	2.41	2.18	2.15
2-Methylpentane	0.10	0.07	0.04	0.27	0.16	0.16	0.18	0.15
3-Methylpentane	0.33	0.35	0.20	0.61	0.34	0.73	0.57	0.77
1-Hexene	0.09	0.08	0.03	0.22	0.15	0.30	0.13	0.15
n-Hexane	0.43	0.72	0.42	2.52	1.61	2.46	2.56	2.34
Methylcyclopentane	0.34	0.67	0.38	1.85	1.35	1.76	1.64	1.58
Benzene	0.21	0.09	0.08	0.47	0.21	0.21	0.19	0.19
Thiophene	0.30	0.76	0.84	0.64	0.22	1.13	1.53	0.46
Cyclohexane	0.03	0.07	0.02	0.10	0.13	0.08	0.44	0.17
2-Methylhexane	0.09	0.06	0.05	0.28	0.13	0.12	0.14	0.12
2,3-Dimethylpentane	0.06	0.06	0.07	0.21	0.11	0.15	0.32	0.12
1,1-Dimethylpentane	0.06	0.08	0.04	0.08	0.03	0.04	0.10	0.23
3-Methylhexane	0.00	0.00	0.00	0.00	0.00	0.00	0.00	0.00
1-Heptene	0.06	0.05	0.03	0.25	0.14	0.22	0.16	0.14
n-Heptane	0.31	0.53	0.30	1.85	1.18	1.73	1.97	1.64
Methyl-Cyclohexane	0.39	0.69	0.39	1.91	1.24	1.80	1.71	1.61
Ethylcyclopentane	0.21	0.08	0.10	0.61	0.26	0.22	0.27	0.25
2,5-Dimethylhexane	0.04	0.04	0.03	0.21	0.12	0.11	0.12	0.10
2,4-Dimethylhexane	0.12	0.15	0.19	0.20	0.19	0.29	0.53	0.29
3,3-Dimethylhexane	0.02	0.05	0.03	0.03	0.04	0.04	0.11	0.07
2,3,4-Trimethylpentane	0.08	0.09	0.07	0.13	0.14	0.23	0.36	0.30
Toluene	0.16	0.18	0.15	0.32	0.24	0.55	0.55	0.53
2-Methylthiophene	0.94	2.25	1.53	0.69	0.80	1.55	3.13	1.41
3-Methylthiophene	0.07	0.10	0.05	0.49	0.45	0.29	1.95	1.25
1-Octene	0.06	0.09	0.07	0.35	0.22	0.33	0.35	0.25
n-Octane	0.29	0.46	0.27	1.69	0.96	1.43	1.69	1.31
Ethylbenzene	0.33	0.64	0.37	1.77	0.98	1.66	1.42	1.33
Ethylthiophene	0.28	0.51	0.30	0.50	0.28	0.69	0.81	0.33
2,5-Dimethylthiophene	0.03	0.02	0.00	0.09	0.15	0.08	0.74	0.73
m/p-Xylene	0.02	0.02	0.00	0.12	0.21	0.10	0.96	0.63
2,4-Dimethylthiophene	0.95	1.56	1.13	1.21	0.89	2.05	2.56	2.18
2,3-Dimethylthiophene	0.02	0.04	0.00	0.17	0.16	0.28	0.56	0.44
Styrene	0.06	0.07	0.00	0.27	0.27	0.25	0.51	0.63
o-Xylene	0.05	0.12	0.19	0.06	0.13	0.15	0.68	0.21
1-Nonene	0.31	0.57	0.41	0.51	0.42	0.80	1.18	0.76
n-Nonane	0.18	0.35	0.19	1.31	0.70	1.19	1.24	1.11
2-Propylthiophene	0.24	0.51	0.29	1.37	0.74	1.28	1.11	1.10
Propylbenzene	0.05	0.14	0.09	0.17	0.14	0.18	0.34	0.20
2-Ethyl-5-Methylthiophene	0.05	0.06	0.09	0.10	0.12	0.13	0.17	0.26
(?)-Benzene	0.02	0.04	0.00	0.02	0.18	0.03	0.93	0.67
1,3,5-Trimethylbenzene	0.28	0.45	0.33	0.43	0.36	0.79	0.84	0.51
Phenol	0.13	0.14	0.09	0.19	0.14	0.24	0.25	0.22
1-Ethyl-2-Methylbenzene	0.90	1.85	3.02	0.13	0.07	0.09	0.10	0.09
2,3,5-Trimethylthiophene	0.00	0.53	0.18	0.34	0.21	0.42	0.50	0.31
	0.05	0.02	0.04	0.03	0.22	0.07	0.00	0.70

Table A 2 continued: samples provided by GFZ

Table A 2: Open-System Pyrolysis GC-FID

GFZ immature: Organofacies	PNA low wax Oil: Coals			PNA low wax Oil: shales				
Formation/Basin	Talang Akar Coal	Arang Coal	Taglu Fm.	Botneheia Shale	Woodford Shale	Autun Oil Shale	Spekk Fm. Bakken Shale	
GFZ Code	G000726	G000950	SN6750	G000689	G000690	G000883	G001955	G005298
1,2,4-Trimethylbenzene	0.32	0.41	0.31	0.58	0.40	0.91	0.86	0.86
1-Decene	0.19	0.35	0.20	1.19	0.63	1.19	1.05	1.12
n-Decane	0.23	0.49	0.30	1.27	0.64	1.19	0.88	0.99
1,2,3-Trimethylbenzene	0.13	0.28	0.40	0.26	0.22	0.77	0.58	0.98
o-Cresol	0.82	1.22	1.11	0.07	0.03	0.06	0.20	0.07
m/p-Cresol	1.16	2.08	2.54	0.20	0.09	0.26	0.45	0.25
Dimethylphenol	0.20	0.21	0.11	0.10	0.02	0.05	0.13	0.11
1-Undecene	0.20	0.39	0.27	1.12	0.53	1.03	1.14	0.93
n-Undecane	0.24	0.49	0.32	1.12	0.50	1.05	0.90	0.78
1,2,3,4-Tetramethylbenzene	0.10	0.14	0.50	0.16	0.35	0.55	0.25	2.83
Naphthalene	0.36	0.25	0.25	0.18	0.14	0.34	0.53	0.22
1-Dodecene	0.20	0.40	0.24	0.97	0.46	0.96	0.96	0.77
n-Dodecane	0.32	0.63	0.35	1.05	0.46	1.07	0.80	1.18
2-Methylnaphthalene	0.51	0.37	0.26	0.38	0.22	0.43	0.67	0.33
1-Tridecene	0.18	0.28	0.26	0.80	0.41	0.81	0.74	0.67
1-Methylnaphthalene	0.59	0.43	0.28	0.44	0.17	0.39	0.49	0.45
n-Tridecane	0.31	0.53	0.37	1.09	0.37	1.11	0.84	0.87
1-Tetradecene	0.26	0.29	0.23	0.76	0.35	0.86	0.83	0.78
n-Tetradecane	0.24	0.42	0.32	0.94	0.29	1.02	0.74	0.68
Dimethylnaphthalene	1.58	0.87	0.47	0.65	0.25	0.82	0.60	0.55
1-Pentadecene	0.11	0.24	0.15	0.56	0.22	0.61	0.96	0.48
n-Pentadecane	0.29	0.48	0.30	0.86	0.30	1.07	0.71	0.70
Trimethylnaphthalene	0.13	0.17	0.14	0.12	0.07	0.16	0.16	0.16
Trimethylnaphthalene	0.14	0.16	0.25	0.15	0.11	0.35	0.09	0.29
Trimethylnaphthalene	0.14	0.20	0.39	0.02	0.02	0.15	0.07	0.05
1-Hexadecene	0.13	0.20	0.17	0.54	0.20	0.47	0.49	0.29
n-Hexadecane	0.22	0.41	0.25	0.68	0.20	0.97	0.60	0.46
Isopropyldimethylnaphthalene	0.69	0.73	0.12	0.04	0.00	0.03	0.01	0.01
1-Heptadecene	0.13	0.22	0.19	0.42	0.13	0.50	0.36	0.26
n-Heptadecane	0.26	0.41	0.29	0.62	0.21	0.99	0.59	0.45
Pristane	0.14	0.04	0.03	0.04	0.02	0.11	0.09	0.12
Prist.-1-ene	0.19	0.27	0.18	0.09	0.03	0.12	0.26	0.33
1-Octadecene	0.13	0.20	0.14	0.36	0.10	0.45	0.26	0.23
n-Octadecane	0.22	0.36	0.27	0.48	0.13	0.82	0.42	0.30
Phytane	0.04	0.03	0.04	0.08	0.03	0.11	0.12	0.12
1-Nonadecene	0.12	0.18	0.15	0.34	0.11	0.46	0.19	0.23
n-Nonadecane	0.23	0.37	0.27	0.44	0.12	0.75	0.38	0.30
1-Icosene	0.11	0.17	0.16	0.25	0.08	0.35	0.20	0.18
n-Icosane	0.20	0.36	0.28	0.39	0.10	0.66	0.27	0.28
1-Henicosene	0.11	0.17	0.14	0.27	0.10	0.36	0.13	0.28
n-Henicosane	0.19	0.36	0.35	0.32	0.09	0.55	0.21	0.24
1-Docosene	0.10	0.20	0.16	0.18	0.05	0.28	0.13	0.12
n-Docosane	0.19	0.36	0.33	0.26	0.07	0.44	0.19	0.19
1-Tricosene	0.11	0.19	0.16	0.14	0.05	0.19	0.11	0.11
n-Tricosane	0.19	0.38	0.30	0.21	0.07	0.37	0.18	0.18
1-Tetracosene	0.09	0.16	0.12	0.10	0.02	0.14	0.07	0.06
n-Tetracosane	0.20	0.41	0.27	0.17	0.04	0.30	0.15	0.13
1-Pentacosene	0.10	0.17	0.12	0.09	0.03	0.14	0.04	0.08
n-Pentacosane	0.18	0.39	0.25	0.13	0.04	0.24	0.11	0.13
1-Hexacosene	0.08	0.15	0.08	0.06	0.01	0.09	0.03	0.05
n-Hexacosane	0.17	0.36	0.17	0.11	0.03	0.20	0.08	0.11
1-Heptacosene	0.08	0.14	0.06	0.05	0.01	0.06	0.02	0.04
n-Heptacosane	0.17	0.34	0.15	0.09	0.02	0.16	0.07	0.11
1-Octacosene	0.09	0.14	0.04	0.04	0.01	0.06	0.02	0.03
n-Octacosane	0.17	0.33	0.10	0.09	0.02	0.12	0.06	0.09
1-Nonacosene	0.06	0.12	0.04	0.04	0.01	0.04	0.02	0.04
n-Nonacosane	0.14	0.27	0.11	0.06	0.01	0.08	0.05	0.23
1-Triacontene	0.07	0.11	0.02	0.03	0.01	0.02	0.02	0.01
n-Triacontane	0.14	0.27	0.06	0.05	0.01	0.07	0.03	0.06
n-C31:1	0.06	0.08	0.01	0.02	0.01	0.05	0.02	0.05
n-C31	0.13	0.26	0.06	0.05	0.01	0.07	0.05	0.06
n-C32:1	0.03	0.05	0.00	0.02	0.00	0.02	0.01	0.02
n-C32	0.14	0.17	0.04	0.03	0.00	0.02	0.02	0.04
n-C33:1	0.03	0.04	0.02	0.01	0.00	0.02	0.02	0.02
n-C33	0.09	0.12	0.02	0.03	0.00	0.01	0.00	0.01
n-C34:1	0.02	0.02	0.00	0.01	0.00	0.01	0.00	0.00
n-C34	0.03	0.05	0.00	0.03	0.00	0.01	0.01	0.02
n-C35:1	0.02	0.02	0.00	0.01	0.00	0.00	0.00	0.00
n-C35	0.03	0.03	0.00	0.01	0.00	0.00	0.00	0.00
n-C36:1	0.01	0.01	0.00	0.01	0.00	0.00	0.00	0.00
n-C36	0.02	0.01	0.00	0.01	0.00	0.00	0.00	0.00
n-C37:1	0.01	0.01	0.00	0.00	0.00	0.00	0.00	0.00
n-C37	0.01	0.01	0.00	0.00	0.00	0.00	0.00	0.00
n-C38:1	0.01	0.01	0.00	0.00	0.00	0.00	0.00	0.00
n-C38	0.00	0.01	0.00	0.00	0.00	0.00	0.00	0.00
n-C39:1	0.00	0.00	0.00	0.00	0.00	0.00	0.00	0.00
n-C39	0.00	0.00	0.00	0.00	0.00	0.00	0.00	0.00

Table A 2 continued: samples provided by GFZ

Table A 2: Open-System Pyrolysis GC-FID

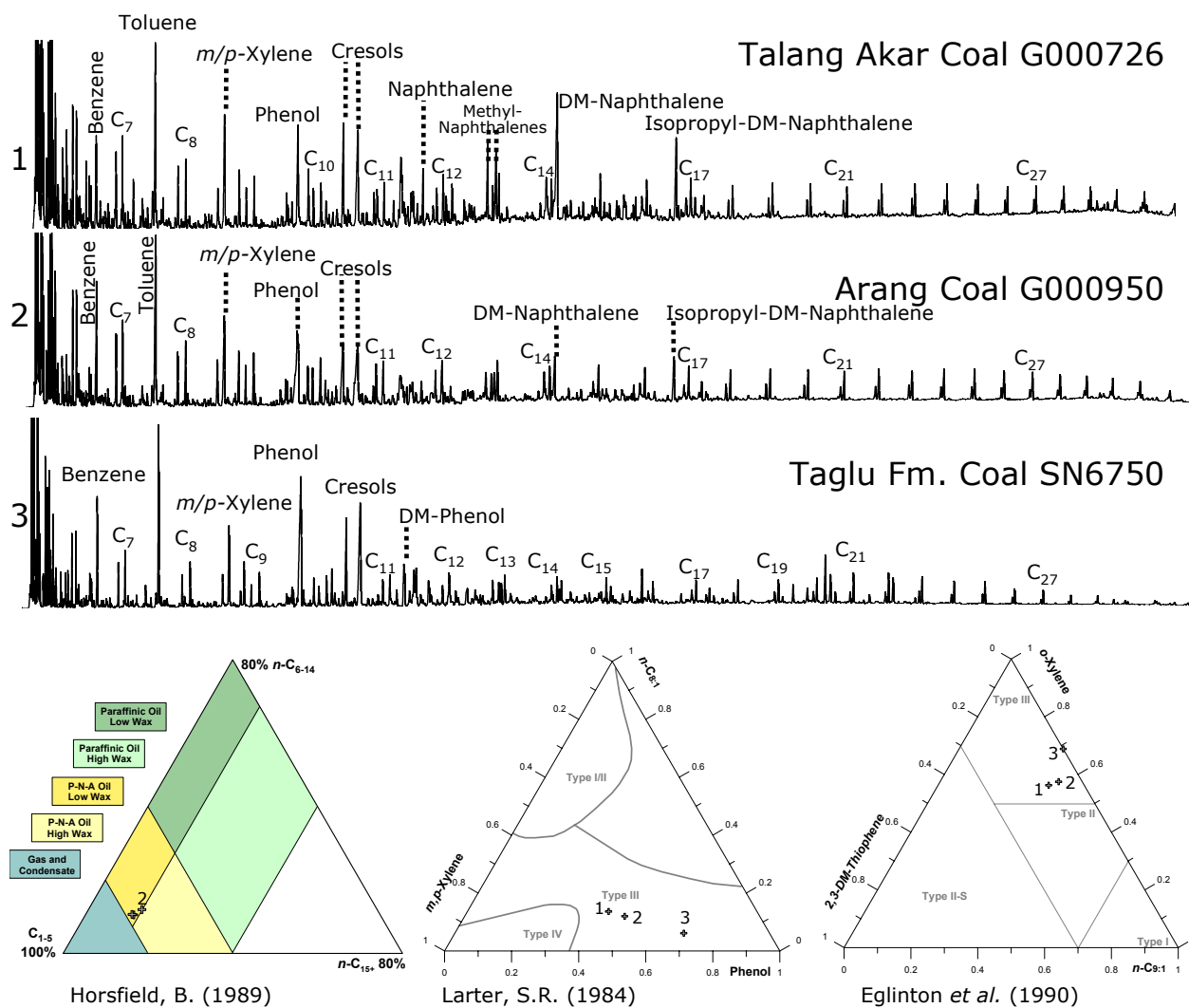


Table A 2 continued: samples provided by GFZ

Table A 2: Open-System Pyrolysis GC-FID

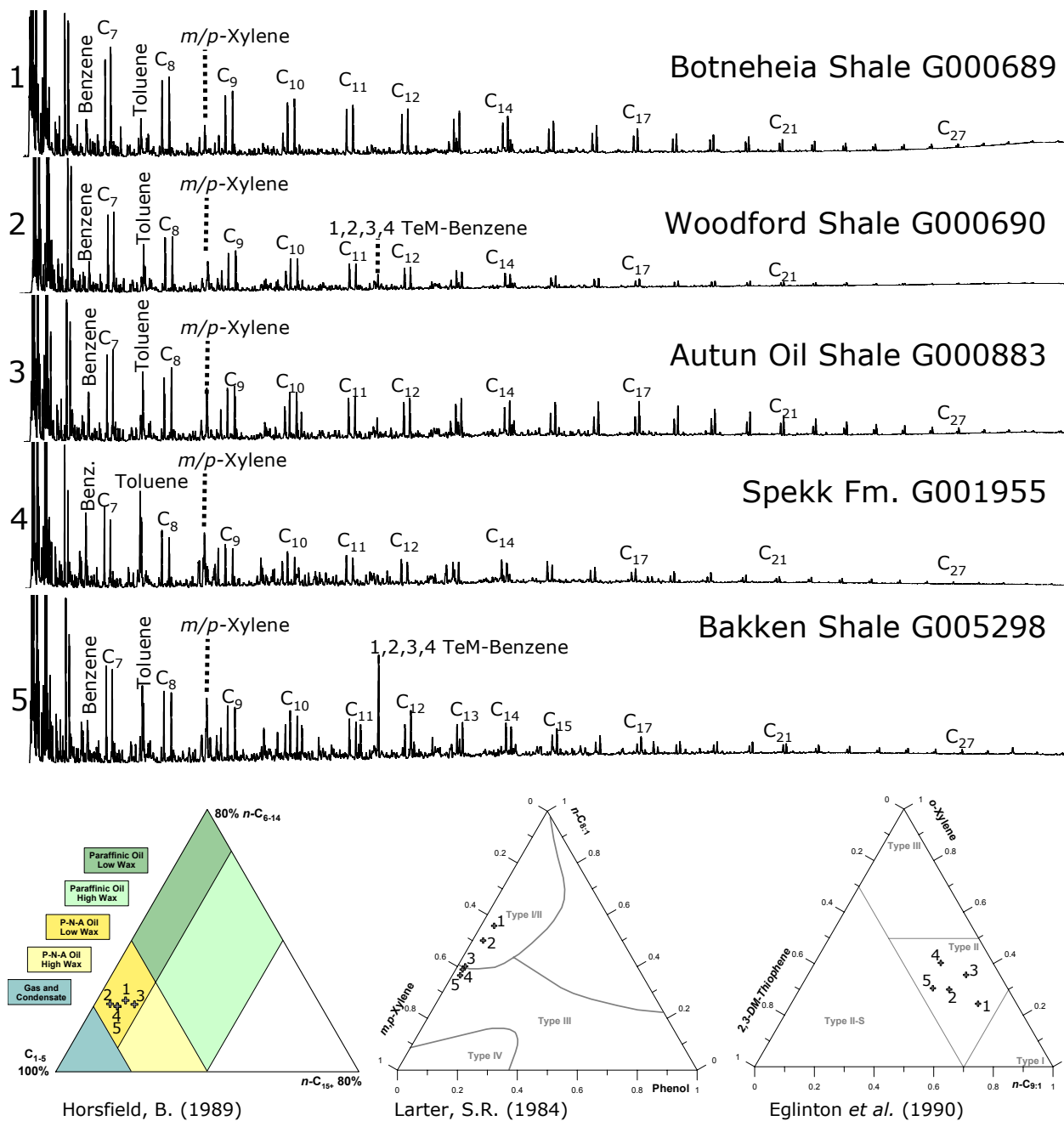


Table A 2 continued: samples provided by GFZ

Table A 2: Open-System Pyrolysis GC-FID

GFZ immature: Organofacies	PNA high wax Oil			
Formation/Basin	Talang Akar	Brown Coal	Messel Oil Shale	Fischschiefer
GFZ Code	G000670	G000731	G000859	G004072
File	G000670AD	G000731AE	G000859AD	G004072AD
Temperature [°C]	200-560	200-560	200-560	200-560
Rate	2K/min	2K/min	2K/min	2K/min
Totals	mg/g TOC	mg/g TOC	mg/g TOC	mg/g TOC
C <sub>1+</sub> (-blank)	170.86	2769.00	474.82	419.39
C <sub>1-5</sub>	44.20	282.35	80.17	76.52
C <sub>2-5</sub>	24.85	210.45	57.54	57.00
C <sub>6-14</sub> (-blank)	43.31	659.81	142.82	133.02
C <sub>6-14</sub> Hump	32.12	389.99	85.71	76.85
C <sub>6-14</sub> Resolved	11.19	269.82	57.11	56.16
C <sub>15+</sub> (-blank)	83.36	1826.84	251.83	209.85
C <sub>15+</sub> Hump	19.27	134.51	38.46	35.25
C <sub>15+</sub> Resolved	64.09	1692.34	213.37	174.60
GOR	0.35	0.11	0.20	0.22
Gas Wetness (C2-5/C1-5)	0.56	0.75	0.72	0.74
Compounds Summation	mg/g TOC	mg/g TOC	mg/g TOC	mg/g TOC
n-C <sub>6-14</sub>	7.60	95.66	25.64	25.34
n-C <sub>15+</sub>	10.26	57.70	24.35	19.55
Mono-aromatic Compounds	4.38	34.58	11.24	8.30
Di-aromatic Compounds	3.56	7.56	2.92	2.49
Phenolic Compounds	2.18	3.04	3.01	0.62
Thiophenic Compounds	0.43	48.17	2.79	3.18
Single Compounds	mg/g TOC	mg/g TOC	mg/g TOC	mg/g TOC
Methane	19.35	71.90	22.63	19.52
Ethene	1.84	8.54	3.74	2.84
Ethane	6.43	42.82	9.99	13.71
Propane	6.60	50.13	12.78	13.78
i-Butane	0.56	2.57	0.82	0.68
1-Butene	1.68	16.26	5.51	4.71
n-Butane	1.29	17.15	3.52	3.55
i-Pentane	0.67	3.17	2.26	0.72
Pentene	0.58	7.52	2.46	2.12
n-Pentane	0.69	11.46	2.09	2.17
Cyclopentane	0.10	1.00	0.15	0.23
2-Methylpentane	0.44	3.86	0.71	0.53
3-Methylpentane	0.14	0.89	0.20	0.24
1-Hexene	0.52	8.58	2.40	2.33
n-Hexane	0.51	7.87	1.72	1.67
Methylcyclopentane	0.21	1.12	0.20	0.28
Benzene	0.35	2.45	1.21	0.60
Thiophene	0.02	1.54	0.21	0.11
Cyclohexane	0.14	0.58	0.11	0.22
2-Methylhexane	0.12	0.63	0.30	0.14
2,3-Dimethylpentane	0.06	0.75	0.34	0.18
1,1-Dimethylpentane	0.00	0.00	0.00	0.00
3-Methylhexane	0.10	0.97	0.17	0.18
1-Heptene	0.43	5.63	1.80	1.77
n-Heptane	0.57	8.32	1.79	1.78
Methyl-Cyclohexane	0.30	1.10	0.33	0.34
Ethylcyclopentane	0.05	0.59	0.10	0.15
2,5-Dimethylhexane	0.10	1.12	0.39	0.34
2,4-Dimethylhexane	0.02	0.14	0.28	0.05
3,3-Dimethylhexane	0.05	0.73	0.20	0.28
2,3,4-Trimethylpentane	0.13	1.68	0.67	0.62
Toluene	1.00	5.19	2.55	1.38
2-Methylthiophene	0.07	9.58	0.45	0.70
3-Methylthiophene	0.01	0.93	0.35	0.46
1-Octene	0.40	5.14	1.55	1.51
n-Octane	0.52	7.20	1.65	1.69
Ethylbenzene	0.18	1.54	0.68	0.56
Ethylthiophene	0.09	4.98	0.16	0.43
2,5-Dimethylthiophene	0.02	3.81	0.19	0.28
m/p-Xylene	1.22	14.93	2.36	2.04
2,4-Dimethylthiophene	0.02	4.01	0.17	0.35
2,3-Dimethylthiophene	0.08	4.20	0.25	0.43
Styrene	0.04	0.00	0.26	0.27
o-Xylene	0.34	2.61	0.89	0.69
1-Nonene	0.30	3.97	1.22	1.29
n-Nonane	0.43	5.63	1.38	1.37
2-Propylthiophene	0.06	1.81	0.21	0.14
Propylbenzene	0.08	0.58	0.18	0.32
2-Ethyl-5-Methylthiophene	0.02	8.75	0.18	0.24
(?)-Benzene	0.33	1.32	0.84	0.58
1,3,5-Trimethylbenzene	0.24	0.95	0.20	0.37
Phenol	0.53	1.23	0.81	0.36
1-Ethyl-2-Methylbenzene	0.09	1.25	0.75	0.34
2,3,5-Trimethylthiophene	0.04	8.56	0.61	0.03

Table A 2 continued: samples provided by GFZ

Table A 2: Open-System Pyrolysis GC-FID

GFZ immature: Organofacies	PNA high wax Oil			
Formation/Basin	Talang Akar Coal	Brown Limestone	Messel Oil Shale	Fischschiefer
GFZ Code	G000670	G000731	G000859	G004072
1,2,4-Trimethylbenzene	0.39	2.31	0.85	0.80
1-Decene	0.31	5.13	1.31	1.22
<i>n</i> -Decane	0.42	5.30	1.27	1.25
1,2,3-Trimethylbenzene	0.15	1.46	0.73	0.62
<i>o</i> -Cresol	0.66	0.22	0.71	0.03
<i>m/p</i> -Cresol	0.78	1.20	1.39	0.24
Dimethylphenol	0.21	0.38	0.10	0.00
1-Undecene	0.32	4.81	1.21	1.18
<i>n</i> -Undecane	0.44	4.87	1.44	1.20
1,2,3,4-Tetramethylbenzene	0.10	3.25	0.64	0.75
Naphthalene	0.34	0.90	0.52	0.34
1-Dodecene	0.32	3.84	1.17	1.15
<i>n</i> -Dodecane	0.49	4.73	1.28	1.23
2-Methylnaphthalene	0.58	1.48	0.61	0.32
1-Tridecene	0.26	3.58	0.95	1.03
1-Methylnaphthalene	0.56	1.80	0.56	0.74
<i>n</i> -Tridecane	0.53	4.28	1.42	1.39
1-Tetradecene	0.40	3.23	0.95	1.04
<i>n</i> -Tetradecane	0.44	3.55	1.15	1.22
Dimethylnaphthalene	1.48	1.99	0.79	0.59
1-Pentadecene	0.26	2.81	0.84	0.84
<i>n</i> -Pentadecane	0.52	3.51	1.19	1.19
Trimethylnaphthalene	0.20	0.20	0.12	0.12
Trimethylnaphthalene	0.22	1.02	0.26	0.27
Trimethylnaphthalene	0.16	0.18	0.07	0.11
1-Hexadecene	0.28	1.92	0.79	0.72
<i>n</i> -Hexadecane	0.49	3.46	1.04	0.99
Isopropylidimethylnaphthalene	0.19	0.31	0.05	0.00
1-Heptadecene	0.21	2.43	0.67	0.63
<i>n</i> -Heptadecane	0.57	3.29	1.05	0.99
Pristane	0.48	0.49	0.05	0.27
Prist.-1-ene	0.08	1.82	0.73	0.99
1-Octadecene	0.20	1.89	0.53	0.63
<i>n</i> -Octadecane	0.42	2.92	0.77	0.90
Phytane	0.09	0.55	0.11	0.15
1-Nonadecene	0.24	1.57	0.47	0.54
<i>n</i> -Nonadecane	0.50	2.61	0.74	0.87
1-Icosene	0.19	1.93	0.45	0.65
<i>n</i> -Icosane	0.43	2.55	0.75	0.84
1-Henicosene	0.23	2.53	0.75	0.62
<i>n</i> -Henicosane	0.43	2.31	0.75	0.83
1-Docosene	0.17	1.20	0.49	0.44
<i>n</i> -Docosane	0.45	2.09	0.76	0.70
1-Tricosene	0.18	1.08	0.41	0.34
<i>n</i> -Tricosane	0.44	1.80	0.78	0.66
1-Tetracosene	0.17	0.86	0.46	0.31
<i>n</i> -Tetracosane	0.46	1.67	0.89	0.57
1-Pentacosene	0.16	1.00	0.45	0.27
<i>n</i> -Pentacosane	0.43	1.36	0.90	0.53
1-Hexacosene	0.14	0.70	0.40	0.21
<i>n</i> -Hexacosane	0.40	0.99	0.84	0.43
1-Heptacosene	0.11	0.53	0.32	0.18
<i>n</i> -Heptacosane	0.39	1.50	1.00	0.43
1-Octacosene	0.09	0.27	0.41	0.13
<i>n</i> -Octacosane	0.33	1.09	0.89	0.33
1-Nonacosene	0.09	0.70	0.35	0.09
<i>n</i> -Nonacosane	0.30	0.94	0.70	0.27
1-Triacontene	0.07	0.29	0.29	0.10
<i>n</i> -Triacontane	0.21	0.77	0.87	0.44
<i>n</i> -C31:1	0.04	0.48	0.14	0.15
<i>n</i> -C31	0.21	0.76	0.94	0.63
<i>n</i> -C32:1	0.03	0.45	0.21	0.09
<i>n</i> -C32	0.14	0.93	0.52	0.35
<i>n</i> -C33:1	0.01	0.10	0.00	0.08
<i>n</i> -C33	0.11	0.44	0.15	0.17
<i>n</i> -C34:1	0.01	0.00	0.07	0.11
<i>n</i> -C34	0.04	0.00	0.20	0.03
<i>n</i> -C35:1	0.01	0.00	0.03	0.06
<i>n</i> -C35	0.03	0.00	0.06	0.04
<i>n</i> -C36:1	0.00	0.00	0.00	0.04
<i>n</i> -C36	0.02	0.00	0.00	0.02
<i>n</i> -C37:1	0.01	0.00	0.00	0.03
<i>n</i> -C37	0.02	0.00	0.00	0.04
<i>n</i> -C38:1	0.01	0.00	0.00	0.01
<i>n</i> -C38	0.01	0.00	0.00	0.01
<i>n</i> -C39:1	0.00	0.00	0.00	0.01
<i>n</i> -C39	0.00	0.00	0.00	0.01

Table A 2 continued: samples provided by GFZ

Table A 2: Open-System Pyrolysis GC-FID

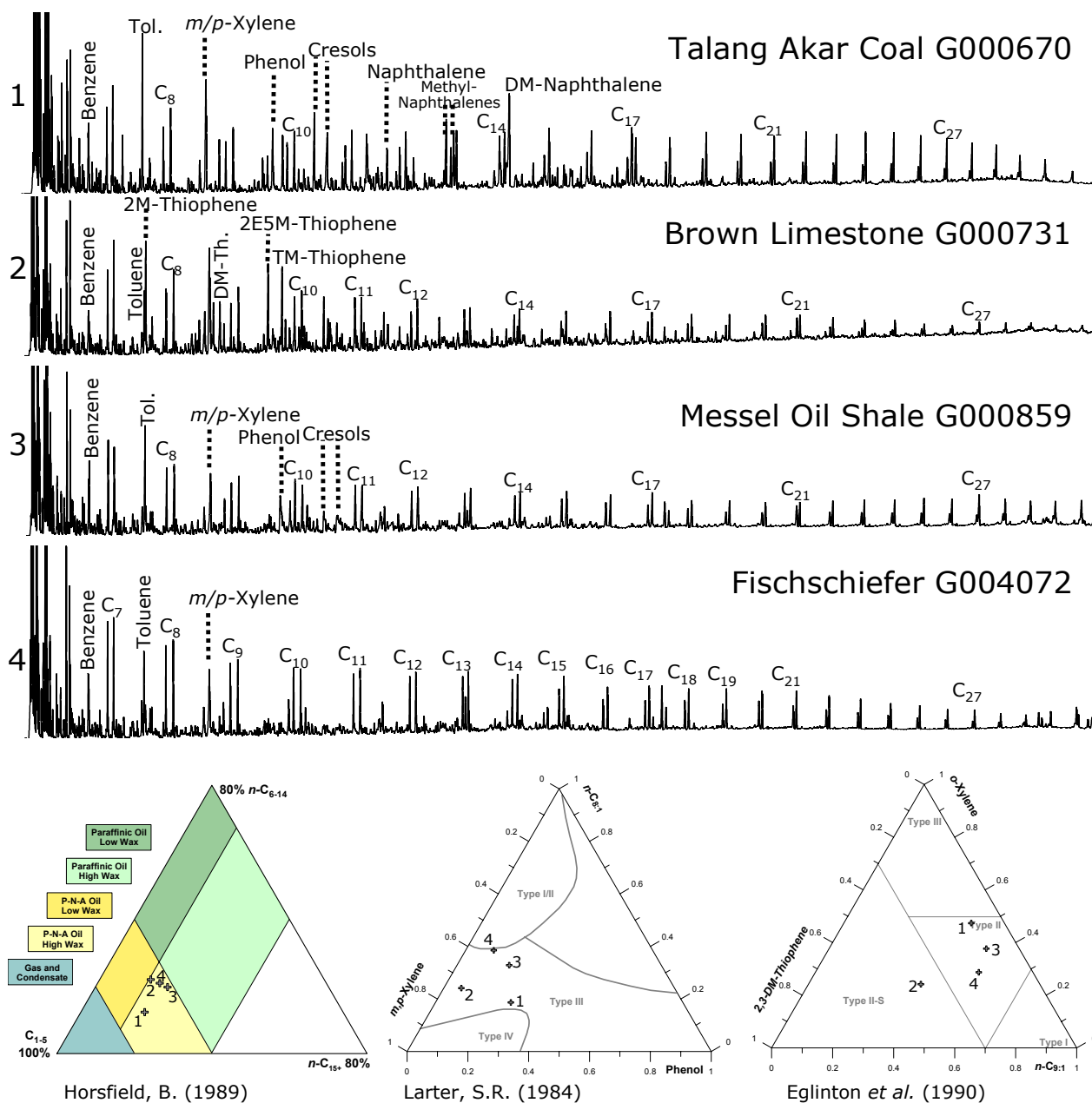


Table A 2 continued: samples provided by GFZ

Table A 2: Open-System Pyrolysis GC-FID

GFZ immature: Organofacies		Paraffinic Oil					
Formation/Basin		Alaskan Tasmanite	Boghead Coal	Fischschiefer	Fischschiefer	Green River Shale	Mix type I/III
GFZ Code		G000693	G000697	G004070	G004071	G004750	30047501965
File		G000693AD	G000697AD	G004070AD	G004071AD	G004750DF	G004750CF
Temperature [°C]		200-560	200-560	200-560	200-560	200-550	200-550
Rate		2K/min	2K/min	2K/min	2K/min	1k/min	1k/min
Totals		mg/g TOC	mg/g TOC	mg/g TOC	mg/g TOC	mg/g TOC	mg/g TOC
C <sub>1+</sub> (-blank)		666.83	452.67	527.97	523.98	785.79	251.01
C <sub>1-5</sub>		68.18	49.92	72.23	73.04	81.85	49.20
C <sub>2-5</sub>		57.52	30.95	55.41	54.28	65.87	30.70
C <sub>6-14</sub> (-blank)		174.06	80.82	142.43	142.58	213.37	76.67
C <sub>6-14</sub> Hump		121.28	51.97	87.17	85.38	153.29	55.86
C <sub>6-14</sub> Resolved		52.78	28.85	55.26	57.20	60.09	20.81
C <sub>15+</sub> (-blank)		424.60	321.92	313.31	308.37	490.57	125.14
C <sub>15+</sub> Hump		32.64	92.96	52.11	49.58	117.98	30.10
C <sub>15+</sub> Resolved		391.95	228.97	261.20	258.79	372.59	95.04
GOR		0.11	0.12	0.16	0.16	0.12	0.24
Gas Wetness (C2-5/C1-5)		0.84	0.62	0.77	0.74	0.80	0.62
Compounds Summation		mg/g TOC	mg/g TOC	mg/g TOC	mg/g TOC	mg/g TOC	mg/g TOC
n-C <sub>6-14</sub>		63.43	28.57	30.19	28.61	72.06	18.53
n-C <sub>15+</sub>		17.84	75.00	30.55	25.19	76.84	17.31
Mono-aromatic Compounds		6.38	2.70	7.83	8.01	10.83	6.99
Di-aromatic Compounds		1.65	1.81	2.38	2.47	1.93	1.84
Phenolic Compounds		0.87	0.19	0.48	0.73	1.10	3.13
Thiophenic Compounds		2.36	0.58	4.40	4.50	2.90	1.67
Single Compounds		mg/g TOC	mg/g TOC	mg/g TOC	mg/g TOC	mg/g TOC	mg/g TOC
Methane		10.65	18.96	16.83	18.76	15.97	18.50
Ethene		1.85	1.92	2.95	2.69	3.33	2.60
Ethane		10.79	7.81	11.25	10.91	9.77	5.98
Propane		13.25	7.53	12.62	13.23	15.84	7.76
i-Butane		0.24	0.16	0.64	0.55	0.67	0.26
1-Butene		4.21	2.26	4.62	4.63	6.82	2.67
n-Butane		6.35	2.21	3.96	3.63	5.56	1.91
i-Pentane		0.19	0.41	1.30	0.72	1.31	0.85
Pentene		3.78	1.46	2.44	2.16	4.08	1.30
n-Pentane		5.14	1.71	2.59	2.55	3.96	1.23
Cyclopentane		0.43	0.13	0.23	0.21	0.28	0.09
2-Methylpentane		0.15	0.19	0.77	0.65	0.70	0.30
3-Methylpentane		0.15	0.05	0.00	0.24	0.18	0.06
1-Hexene		4.93	1.67	2.47	2.41	5.84	1.51
n-Hexane		5.06	1.47	1.90	1.87	3.72	1.10
Methylcyclopentane		0.60	0.15	0.27	0.26	0.44	0.13
Benzene		0.54	0.41	0.61	0.54	1.38	1.05
Thiophene		0.06	0.02	0.18	0.15	0.16	0.12
Cyclohexane		0.40	0.09	0.21	0.19	0.34	0.09
2-Methylhexane		0.12	0.03	0.18	0.15	0.25	0.11
2,3-Dimethylpentane		0.14	0.08	0.33	0.35	0.14	0.06
1,1-Dimethylpentane		0.00	0.00	0.00	0.00	0.00	0.00
3-Methylhexane		0.12	0.04	0.21	0.22	0.23	0.07
1-Heptene		4.68	1.39	1.94	1.86	4.72	1.23
n-Heptane		5.45	1.48	2.03	2.05	4.12	1.17
Methyl-Cyclohexane		0.71	0.15	0.34	0.37	0.57	0.14
Ethylcyclopentane		0.42	0.09	0.13	0.15	0.31	0.08
2,5-Dimethylhexane		0.45	0.09	0.56	0.42	0.44	0.18
2,4-Dimethylhexane		0.06	0.02	0.06	0.06	0.06	0.04
3,3-Dimethylhexane		0.13	0.08	0.29	0.31	0.29	0.12
2,3,4-Trimethylpentane		0.39	0.16	0.59	0.62	0.62	0.24
Toluene		1.46	0.71	1.19	1.19	1.91	1.78
2-Methylthiophene		0.23	0.07	0.80	0.92	0.25	0.33
3-Methylthiophene		0.56	0.16	0.33	0.40	0.22	0.12
1-Octene		4.45	0.99	1.67	1.57	4.43	1.14
n-Octane		5.46	1.08	1.88	1.84	4.12	1.12
Ethylbenzene		0.39	0.22	0.43	0.42	0.67	0.39
Ethylthiophene		0.09	0.02	0.53	0.59	0.61	0.19
2,5-Dimethylthiophene		0.25	0.03	0.50	0.49	0.38	0.14
m/p-Xylene		1.12	0.41	2.09	2.28	2.66	1.45
2,4-Dimethylthiophene		0.54	0.04	0.36	0.30	0.30	0.12
2,3-Dimethylthiophene		0.17	0.06	0.50	0.60	0.34	0.37
Styrene		0.30	0.06	0.18	0.20	0.71	0.00
o-Xylene		0.83	0.26	0.71	0.73	1.08	0.58
1-Nonene		3.71	0.87	1.45	1.30	3.99	0.98
n-Nonane		4.66	1.02	1.62	1.52	3.82	1.01
2-Propylthiophene		0.23	0.06	0.22	0.18	0.28	0.12
Propylbenzene		0.21	0.08	0.34	0.35	0.40	0.12
2-Ethyl-5-Methylthiophene		0.07	0.03	0.45	0.41	0.36	0.15
(?)-Benzene		0.57	0.14	0.59	0.61	0.59	0.41
1,3,5-Trimethylbenzene		0.11	0.03	0.24	0.22	0.22	0.11
Phenol		0.03	0.01	0.12	0.14	0.08	1.28
1-Ethyl-2-Methylbenzene		0.36	0.19	0.42	0.41	0.40	0.23
2,3,5-Trimethylthiophene		0.17	0.10	0.53	0.46	0.00	0.00

Table A 2 continued: samples provided by GFZ



Table A 2: Open-System Pyrolysis GC-FID

Formation/Basin GFZ Code	Paraffinic Oil					
	Alaskan Tasmanite	Boghead Coal	Fischschiefer	Fischschiefer	Green River Shale	Mix type I/III
	G000693	G000697	G004070	G004071	G004750	G0047501965
1,2,4-Trimethylbenzene	0.59	0.18	0.68	0.69	0.76	0.40
1-Decene	3.14	0.93	1.58	1.46	4.18	0.99
<i>n</i> -Decane	4.09	1.11	1.57	1.49	3.72	0.93
1,2,3-Trimethylbenzene	0.19	0.08	0.54	0.58	0.78	0.47
<i>o</i> -Cresol	0.16	0.03	0.04	0.04	0.19	0.46
<i>m/p</i> -Cresol	0.42	0.12	0.26	0.46	0.58	1.29
Dimethylphenol	0.27	0.03	0.07	0.08	0.24	0.09
1-Undecene	2.63	1.10	1.48	1.37	3.90	0.99
<i>n</i> -Undecane	3.36	1.26	1.48	1.49	3.69	0.95
1,2,3,4-Tetramethylbenzene	0.14	0.13	0.55	0.62	0.05	0.16
Naphthalene	0.33	0.18	0.33	0.30	0.35	0.35
1-Dodecene	2.09	1.47	1.45	1.30	3.83	0.89
<i>n</i> -Dodecane	2.80	2.06	1.73	1.62	4.06	0.93
2-Methylnaphthalene	0.42	0.30	0.33	0.35	0.61	0.46
1-Tridecene	1.65	2.15	1.43	1.31	3.50	0.81
1-Methylnaphthalene	0.27	0.59	0.71	0.75	0.28	0.24
<i>n</i> -Tridecane	2.20	2.91	1.72	1.62	3.95	0.97
1-Tetradecene	1.30	2.43	1.26	1.13	2.94	0.90
<i>n</i> -Tetradecane	1.79	3.19	1.53	1.39	3.52	0.92
Dimethylnaphthalene	0.36	0.40	0.56	0.58	0.33	0.47
1-Pentadecene	1.12	2.40	1.11	0.93	2.97	0.71
<i>n</i> -Pentadecane	1.60	3.08	1.54	1.35	3.35	0.83
Trimethylnaphthalene	0.04	0.07	0.14	0.10	0.08	0.11
Trimethylnaphthalene	0.21	0.23	0.23	0.29	0.18	0.09
Trimethylnaphthalene	0.01	0.03	0.09	0.09	0.11	0.14
1-Hexadecene	1.07	2.26	0.97	0.76	2.89	0.67
<i>n</i> -Hexadecane	1.32	3.06	1.40	1.14	3.48	0.81
Isopropylidimethylnaphthalene	0.00	0.14	0.00	0.00	0.32	0.06
1-Heptadecene	0.89	2.13	0.96	0.76	2.65	0.58
<i>n</i> -Heptadecane	1.22	3.10	1.50	1.23	3.37	0.78
Pristane	0.01	0.06	0.29	0.30	0.12	0.06
Prist.-1-ene	0.04	0.62	1.03	1.05	0.99	0.32
1-Octadecene	0.66	1.69	0.94	0.76	2.25	0.47
<i>n</i> -Octadecane	1.03	2.52	1.38	1.12	2.74	0.67
Phytane	0.06	0.16	0.21	0.20	0.36	0.09
1-Nonadecene	0.67	1.52	0.84	0.73	1.93	0.43
<i>n</i> -Nonadecane	0.99	2.40	1.40	1.17	2.77	0.71
1-Icosene	0.54	1.47	1.02	0.93	2.08	0.45
<i>n</i> -Icosane	0.81	2.26	1.22	1.06	2.58	0.62
1-Henicosene	0.51	1.69	0.86	0.74	1.87	0.42
<i>n</i> -Henicosane	0.68	2.25	1.26	1.09	2.73	0.67
1-Docosene	0.44	1.52	0.60	0.53	2.11	0.45
<i>n</i> -Docosane	0.56	2.28	0.99	0.84	2.56	0.62
1-Tricosene	0.31	1.49	0.50	0.43	1.76	0.40
<i>n</i> -Tricosane	0.47	2.47	0.93	0.79	2.62	0.65
1-Tetracosene	0.26	1.57	0.46	0.37	1.63	0.36
<i>n</i> -Tetracosane	0.37	2.63	0.82	0.68	2.16	0.54
1-Pentacosene	0.19	1.63	0.41	0.33	1.57	0.32
<i>n</i> -Pentacosane	0.31	2.91	0.76	0.59	2.32	0.54
1-Hexacosene	0.11	1.72	0.35	0.26	1.67	0.33
<i>n</i> -Hexacosane	0.23	2.98	0.67	0.52	2.08	0.47
1-Heptacosene	0.09	1.52	0.29	0.22	1.32	0.27
<i>n</i> -Heptacosane	0.22	3.39	0.70	0.54	2.25	0.49
1-Octacosene	0.10	1.46	0.24	0.21	1.28	0.25
<i>n</i> -Octacosane	0.20	2.83	0.52	0.40	1.86	0.41
1-Nonacosene	0.09	1.30	0.09	0.17	0.99	0.18
<i>n</i> -Nonacosane	0.14	2.60	0.16	0.35	1.69	0.36
1-Triacontene	0.08	0.99	0.23	0.14	0.78	0.14
<i>n</i> -Triacontane	0.12	2.09	0.44	0.96	1.32	0.31
<i>n</i> -C31:1	0.06	0.62	0.17	0.34	0.91	0.18
<i>n</i> -C31	0.13	2.02	0.82	0.69	1.54	0.34
<i>n</i> -C32:1	0.03	0.27	0.00	0.27	0.57	0.12
<i>n</i> -C32	0.09	0.96	0.77	0.33	0.78	0.16
<i>n</i> -C33:1	0.01	0.14	0.19	0.06	0.24	0.04
<i>n</i> -C33	0.06	0.46	1.34	0.21	0.61	0.11
<i>n</i> -C34:1	0.03	0.11	0.21	0.32	0.25	0.04
<i>n</i> -C34	0.02	0.32	0.33	0.08	0.41	0.07
<i>n</i> -C35:1	0.01	0.13	0.26	0.19	0.23	0.02
<i>n</i> -C35	0.02	0.20	0.11	0.14	0.34	0.07
<i>n</i> -C36:1	0.01	0.01	0.19	0.10	0.14	0.02
<i>n</i> -C36	0.01	0.14	0.13	0.03	0.30	0.05
<i>n</i> -C37:1	0.01	0.03	0.10	0.06	0.14	0.01
<i>n</i> -C37	0.01	0.15	0.07	0.18	0.26	0.05
<i>n</i> -C38:1	0.00	0.01	0.04	0.02	0.08	0.01
<i>n</i> -C38	0.00	0.08	0.19	0.05	0.16	0.02
<i>n</i> -C39:1	0.00	0.02	0.00	0.01	0.06	0.01
<i>n</i> -C39	0.00	0.09	0.06	0.01	0.17	0.03

Table A 2 continued: samples provided by GFZ

Table A 2: Open-System Pyrolysis GC-FID

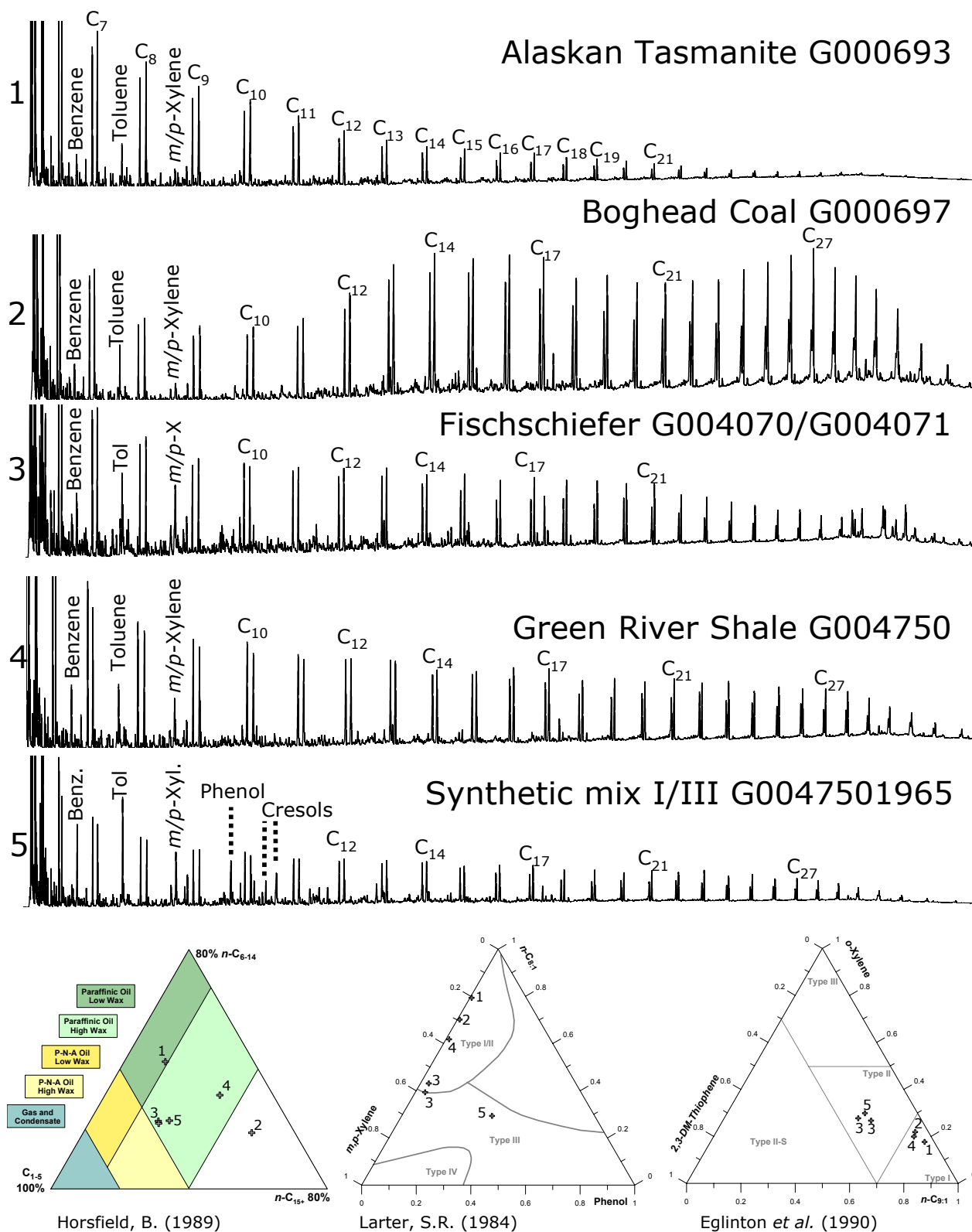


Table A 2 continued: samples provided by GFZ

Table A 2: Open-System Pyrolysis GC-FID

Company	Shell				Wintershall
Formation/Basin	Exshaw Fm.				Wealden Coal
GFZ Code	G006385	G006387	G006384	G006386	G006552
File	G006385AA	G006387AA	G006384AA	G006386AA	G006552AA
Temperature [°C]	300-600	300-600	300-600	300-600	300-600
Rate	60K/min	60K/min	60K/min	60K/min	60K/min
Totals	mg/g TOC	mg/g TOC	mg/g TOC	mg/g TOC	mg/g TOC
C <sub>1+</sub> (-blank)	238.31	164.08	34.22	28.49	58.98
C <sub>1-5</sub>	67.25	53.66	13.19	9.28	27.55
C <sub>2-5</sub>	48.14	37.74	8.56	4.54	12.81
C <sub>6-14</sub> (-blank)	75.96	58.01	7.28	4.30	12.57
C <sub>6-14</sub> Hump	50.92	41.33	5.62	3.20	9.54
C <sub>6-14</sub> Resolved	25.04	16.69	1.66	1.10	3.03
C <sub>15+</sub> (-blank)	95.10	52.40	13.75	14.91	18.85
C <sub>15+</sub> Hump	6.99	6.16	0.33	0.50	4.98
C <sub>15+</sub> Resolved	88.12	46.24	13.42	14.41	13.88
GOR	0.39	0.49	0.63	0.48	0.88
Gas Wetness (C2-5/C1-5)	0.72	0.70	0.65	0.49	0.46
Compounds Summation	mg/g TOC	mg/g TOC	mg/g TOC	mg/g TOC	mg/g TOC
n- C <sub>6-14</sub>	12.77	13.34	0.82	0.26	2.46
n- C <sub>15+</sub>	2.18	3.04	0.07	0.09	1.72
Mono-aromatic Compounds	6.85	4.83	1.58	1.34	2.06
Di-aromatic Compounds	1.69	0.97	0.24	0.13	0.62
Phenolic Compounds	0.30	0.28	0.03	0.02	0.26
Thiophenic Compounds	1.36	1.39	0.26	0.24	0.18
Single Compounds	mg/g TOC	mg/g TOC	mg/g TOC	mg/g TOC	mg/g TOC
Methane	19.11	15.92	4.63	4.74	14.74
Ethene	2.72	2.68	0.80	0.57	1.37
Ethane	10.11	7.17	1.55	0.71	4.00
Propane	11.75	8.94	1.21	0.80	3.12
i-Butane	0.65	0.48	0.14	0.06	0.12
1-Butene	4.21	3.64	0.51	0.28	0.83
n -Butane	3.76	2.68	0.43	0.20	0.61
i-Pentane	0.92	0.74	0.12	0.09	0.12
Pentene	1.61	1.63	0.20	0.13	0.30
n -Pentane	2.13	1.44	0.23	0.09	0.29
Cyclopentane	0.24	0.16	0.02	0.01	0.05
2-Methylpentane	0.58	0.41	0.07	0.02	0.06
3-Methylpentane	0.25	0.17	0.04	0.01	0.02
1-Hexene	1.64	1.81	0.13	0.04	0.27
n -Hexane	1.46	1.04	0.11	0.03	0.22
Methylcyclopentane	0.43	0.25	0.03	0.01	0.05
Benzene	0.59	0.70	0.29	0.61	0.29
Thiophene	0.04	0.05	0.12	0.10	0.00
Cyclohexane	0.22	0.17	0.06	0.02	0.06
2-Methylhexane	0.25	0.17	0.03	0.01	0.02
2,3-Dimethylpentane	0.05	0.04	0.01	0.00	0.00
1,1-Dimethylpentane	0.00	0.00	0.00	0.00	0.00
3-Methylhexane	0.28	0.19	0.03	0.01	0.02
1-Heptene	1.10	1.22	0.07	0.02	0.19
n -Heptane	1.44	1.02	0.08	0.02	0.21
Methyl-Cyclohexane	0.43	0.22	0.07	0.00	0.07
Ethylcyclopentane	0.18	0.13	0.01	0.00	0.02
2,5-Dimethylhexane	0.52	0.18	0.02	0.00	0.08
2,4-Dimethylhexane	0.06	0.02	0.00	0.00	0.01
3,3-Dimethylhexane	0.15	0.05	0.00	0.00	0.02
2,3,4-Trimethylpentane	0.36	0.15	0.04	0.00	0.05
Toluene	1.38	1.03	0.41	0.24	0.61
2-Methylthiophene	0.20	0.20	0.04	0.09	0.01
3-Methylthiophene	0.21	0.22	0.05	0.02	0.06
1-Octene	0.85	1.02	0.05	0.01	0.16
n -Octane	1.06	0.90	0.08	0.02	0.16
Ethylbenzene	0.66	0.37	0.06	0.03	0.14
Ethylthiophene	0.06	0.16	0.01	0.01	0.01
2,5-Dimethylthiophene	0.11	0.13	0.00	0.00	0.01
m/p -Xylene	1.41	0.95	0.30	0.11	0.47
2,4-Dimethylthiophene	0.15	0.13	0.01	0.00	0.03
2,3-Dimethylthiophene	0.34	0.18	0.02	0.00	0.01
Styrene	0.03	0.13	0.02	0.02	0.02
o -Xylene	0.55	0.35	0.12	0.06	0.12
1-Nonene	0.58	0.76	0.03	0.01	0.13
n -Nonane	0.71	0.65	0.05	0.01	0.13
2-Propylthiophene	0.10	0.11	0.00	0.00	0.03
Propylbenzene	0.13	0.12	0.03	0.01	0.02
2-Ethyl-5-Methylthiophene	0.09	0.18	0.00	0.00	0.01
(?)-Benzene	0.64	0.50	0.12	0.17	0.16
1,3,5-Trimethylbenzene	0.27	0.16	0.07	0.03	0.08
Phenol	0.13	0.09	0.01	0.00	0.07
1-Ethyl-2-Methylbenzene	0.34	0.21	0.04	0.02	0.04
2,3,5-Trimethylthiophene	0.06	0.04	0.00	0.00	0.00

Table A 2 continued: Maturity series provided by Shell and Wintershall

Table A 2: Open-System Pyrolysis GC-FID

Company	Shell				Wintershall
Formation/Basin	Exshaw Fm.				Wealden Coal
GFZ Code	G006385	G006387	G006384	G006386	G006552
1,2,4-Trimethylbenzene	0.58	0.29	0.11	0.04	0.11
1-Decene	0.46	0.69	0.02	0.01	0.11
<i>n</i> -Decane	0.60	0.56	0.04	0.01	0.12
1,2,3-Trimethylbenzene	0.32	0.16	0.04	0.02	0.02
<i>o</i> -Cresol	0.05	0.07	0.00	0.01	0.05
<i>m/p</i> -Cresol	0.11	0.09	0.01	0.01	0.11
Dimethylphenol	0.01	0.03	0.00	0.00	0.02
1-Undecene	0.40	0.58	0.02	0.01	0.09
<i>n</i> -Undecane	0.49	0.48	0.04	0.01	0.11
1,2,3,4-Tetramethylbenzene	0.25	0.08	0.00	0.00	0.03
Naphthalene	0.27	0.21	0.10	0.06	0.13
1-Dodecene	0.41	0.56	0.01	0.01	0.09
<i>n</i> -Dodecane	0.38	0.43	0.03	0.01	0.10
2-Methylnaphthalene	0.40	0.21	0.06	0.03	0.19
1-Tridecene	0.26	0.42	0.01	0.01	0.07
1-Methylnaphthalene	0.30	0.20	0.04	0.02	0.08
<i>n</i> -Tridecane	0.41	0.46	0.03	0.01	0.12
1-Tetradecene	0.22	0.36	0.01	0.00	0.07
<i>n</i> -Tetradecane	0.29	0.38	0.03	0.01	0.12
Dimethylnaphthalene	0.49	0.22	0.04	0.02	0.15
1-Pentadecene	0.15	0.26	0.00	0.01	0.05
<i>n</i> -Pentadecane	0.28	0.33	0.03	0.02	0.12
Trimethylnaphthalene	0.12	0.05	0.00	0.00	0.03
Trimethylnaphthalene	0.08	0.07	0.01	0.00	0.04
Trimethylnaphthalene	0.03	0.01	0.00	0.00	0.01
1-Hexadecene	0.18	0.21	0.00	0.00	0.07
<i>n</i> -Hexadecane	0.16	0.22	0.02	0.02	0.13
Isopropylidimethylnaphthalene	0.00	0.00	0.00	0.00	0.00
1-Heptadecene	0.08	0.15	0.00	0.00	0.04
<i>n</i> -Heptadecane	0.15	0.21	0.01	0.01	0.13
Pristane	0.02	0.04	0.00	0.00	0.00
Prist.-1-ene	0.02	0.01	0.00	0.00	0.00
1-Octadecene	0.07	0.13	0.00	0.00	0.03
<i>n</i> -Octadecane	0.12	0.19	0.01	0.01	0.14
Phytane	0.04	0.04	0.00	0.00	0.01
1-Nonadecene	0.10	0.13	0.00	0.00	0.09
<i>n</i> -Nonadecane	0.11	0.16	0.00	0.00	0.14
1-Icosene	0.05	0.09	0.00	0.00	0.02
<i>n</i> -Icosane	0.11	0.14	0.00	0.00	0.14
1-Henicosene	0.05	0.05	0.00	0.00	0.02
<i>n</i> -Henicosane	0.07	0.11	0.00	0.00	0.10
1-Docosene	0.03	0.05	0.00	0.00	0.02
<i>n</i> -Docosane	0.06	0.10	0.00	0.00	0.08
1-Tricosene	0.02	0.03	0.00	0.00	0.01
<i>n</i> -Tricosane	0.05	0.08	0.00	0.00	0.07
1-Tetracosene	0.03	0.02	0.00	0.00	0.01
<i>n</i> -Tetracosane	0.05	0.08	0.00	0.00	0.05
1-Pentacosene	0.02	0.02	0.00	0.00	0.03
<i>n</i> -Pentacosane	0.03	0.07	0.00	0.00	0.05
1-Hexacosene	0.02	0.01	0.00	0.00	0.03
<i>n</i> -Hexacosane	0.04	0.06	0.00	0.00	0.03
1-Heptacosene	0.00	0.01	0.00	0.00	0.00
<i>n</i> -Heptacosane	0.03	0.04	0.00	0.00	0.03
1-Octacosene	0.00	0.01	0.00	0.00	0.01
<i>n</i> -Octacosane	0.02	0.03	0.00	0.00	0.02
1-Nonacosene	0.01	0.00	0.00	0.00	0.01
<i>n</i> -Nonacosane	0.02	0.02	0.00	0.00	0.02
1-Triacontene	0.00	0.00	0.00	0.00	0.02
<i>n</i> -Triacontane	0.01	0.01	0.00	0.00	0.01
<i>n</i> -C31:1	0.00	0.00	0.00	0.00	0.01
<i>n</i> -C31	0.01	0.01	0.00	0.00	0.01
<i>n</i> -C32:1	0.00	0.00	0.00	0.00	0.00
<i>n</i> -C32	0.01	0.00	0.00	0.00	0.01
<i>n</i> -C33:1	0.00	0.00	0.00	0.00	0.00
<i>n</i> -C33	0.01	0.00	0.00	0.00	0.00
<i>n</i> -C34:1	0.00	0.00	0.00	0.00	0.00
<i>n</i> -C34	0.01	0.00	0.00	0.00	0.00
<i>n</i> -C35:1	0.00	0.00	0.00	0.00	0.00
<i>n</i> -C35	0.00	0.00	0.00	0.00	0.00
<i>n</i> -C36:1	0.00	0.00	0.00	0.00	0.00
<i>n</i> -C36	0.00	0.00	0.00	0.00	0.00
<i>n</i> -C37:1	0.00	0.00	0.00	0.00	0.00
<i>n</i> -C37	0.00	0.00	0.00	0.00	0.00
<i>n</i> -C38:1	0.00	0.00	0.00	0.00	0.00
<i>n</i> -C38	0.00	0.00	0.00	0.00	0.00
<i>n</i> -C39:1	0.00	0.00	0.00	0.00	0.00
<i>n</i> -C39	0.00	0.00	0.00	0.00	0.00

Table A 2 continued: Maturity series provided by Shell and Wintershall

Table A 2: Open-System Pyrolysis GC-FID

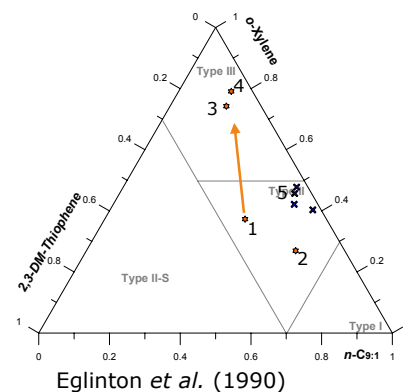
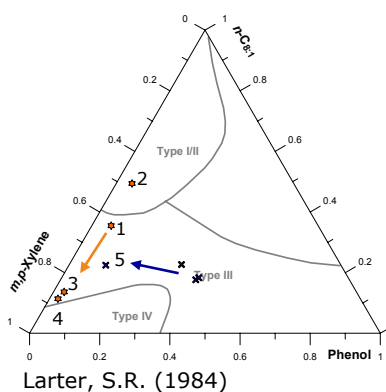
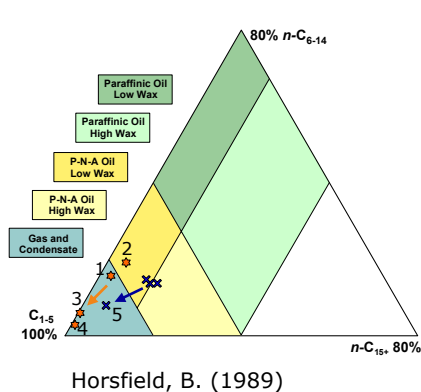
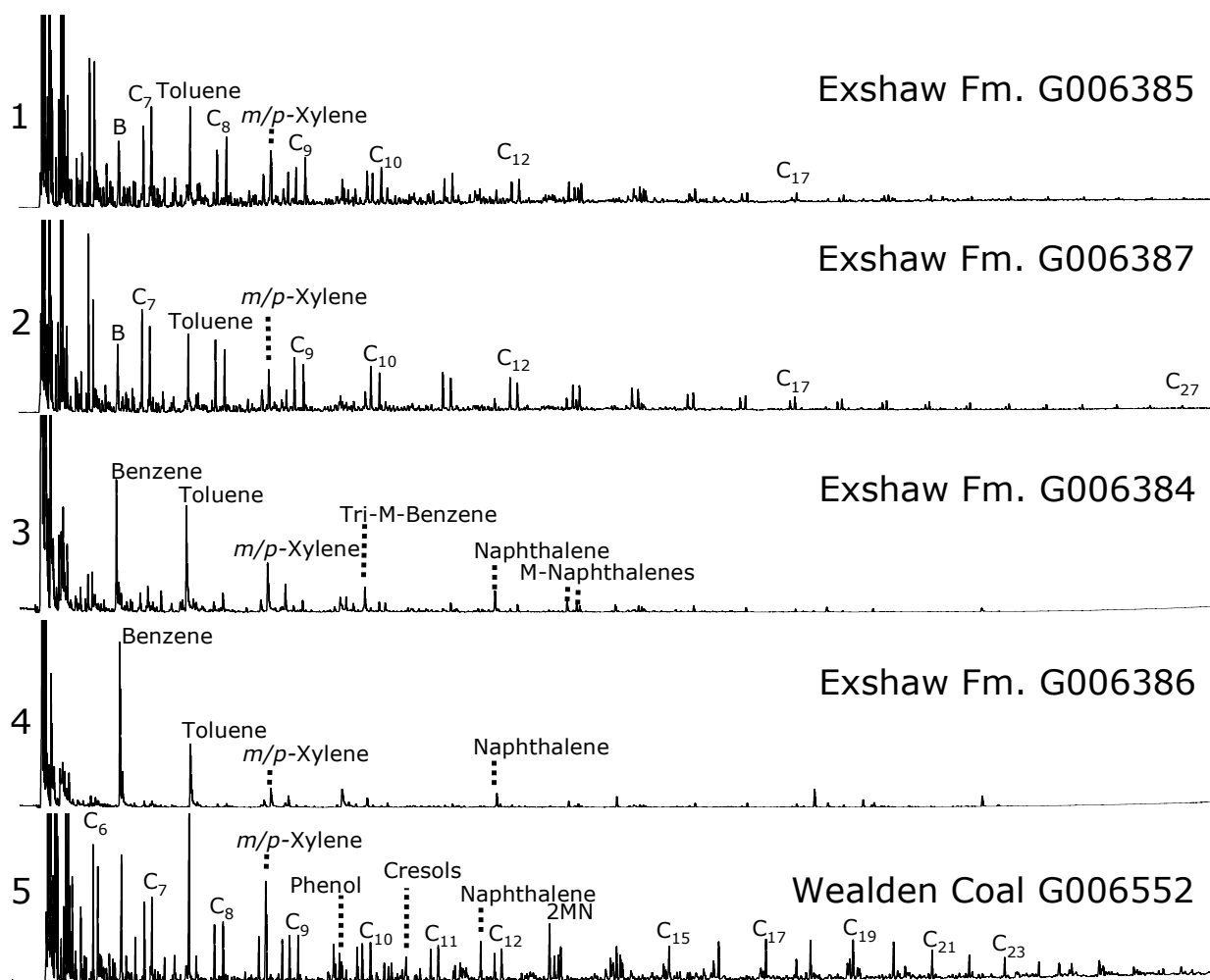


Table A 2 continued: Maturity series provided by Shell and Wintershall

Table A 3: Bulk Kinetics

Company/ Formation/Basin GFZ Code Fraction	ENI Domank Fm. G004563 Bulk 4.43E+13	Muziq Basin G004564 Bulk 3.69E+14	Hekkingen Fm. G005762 Bulk 4.29E+13	Hekkingen Fm. G005763 Bulk 6.28E+12	Petrobras Irat Fm. G005812 Bulk 1.36E+12	Devon Woodford Shale G006153 Bulk 2.17E+13	Woodford Shale G006154 Bulk 2.71E+13	Carrey Shale G006155 Bulk 2.06E+13	New Albany Shale G006156 Bulk 1.23E+13	Shell Akata Shale G005935 Bulk 1.89E+13	Total Douala Basin G006204 Bulk 2.96E+14	Douala Basin G006205 Bulk 8.86E+12	Mahakam Delta G006206 Bulk 9.05E+13	Mahakam Delta G006207 Bulk 3.07E+13	Toardian Shale G006208 Bulk 4.06E+12	Toardian Shale G006209 Bulk 3.64E+12
E (kJ/mol)	%	%	%	%	%	%	%	%	%	%	%	%	%	%	%	%
35																
36					0.02											
37					0.55											
38					0.19											
39				0.16	0.89											
40				0.16	0.34					0.21						
41	0.21		0.07	0.11	1.19	0.08	0.01	0.07	0.07	0.21					0.09	0.10
42	0.38		0.11	0.41	0.89	0.23	0.12	0.24	0.24	0.30					0.19	0.18
43	0.52	0.03	0.27	0.69	0.85	0.25	0.14	0.26	0.74	0.51				0.14	0.26	0.38
44	0.56	0.02	0.33	0.49		0.72	0.40	0.44	0.13	0.60				0.12	0.40	0.81
45	0.86	0.05	0.58	1.08	3.92	0.47	0.26	0.57	1.45	0.67		1.39	0.64	0.32	0.43	0.38
46	0.57	0.14	0.71	4.06	13.22	1.87	1.77	1.13	0.24	1.15		0.82	0.43	0.44	0.32	0.38
47	1.71	0.20	1.61	9.17	53.17	1.43	1.41	1.41	0.24	0.73		1.68	0.90	0.99	11.04	9.75
48	0.62		3.48	17.62	12.94	8.27	3.77	10.78	4.08	2.98		1.76	1.65	1.44	11.10	15.93
49	4.72	0.32	7.44	23.88	6.91	8.05	5.70	25.43	5.51	3.94			0.91	3.08	41.78	41.69
50	13.58	0.47	14.05	20.73	3.45	22.18	16.87	25.43	47.45	14.36		23.62	2.76	5.86	15.79	11.96
51	16.49		18.88	9.46	0.47	29.17	35.33	23.81	19.02	23.95	0.10	30.99	6.35	15.77	9.67	9.39
52	31.89	0.33	18.92	5.46	1.85	9.41	14.01	14.14	10.29	22.14	1.41	21.69	8.45	23.84	1.25	0.97
53	12.49	9.66	14.78	3.74		12.10	13.79	14.04	3.65	14.06	1.91	9.18	12.19	20.49	3.40	2.96
54	6.84	40.53	9.72	0.61	0.19		2.39		5.15	6.06	3.88	3.84	16.07	13.57		
55	3.66	20.94	2.01	0.92	0.06	4.86	3.50	6.78	5.15	1.49	17.53	2.84	17.75	2.37		
56	1.35	12.00	5.80			0.80	0.39	0.78	0.93	4.95	18.49		8.63	5.93	0.10	0.06
57	1.28	8.21	0.34	0.25			0.42		0.32		25.95		5.43	0.75		
58	0.68	2.96	0.52	0.18			0.34		0.26	0.26	8.02	0.12	3.85	1.08		
59	0.45	1.29				0.05		0.05	0.23	0.45	9.91		3.34	1.12		
60	0.37	1.14	0.21	0.52							1.61	1.95	1.77			
61	0.17	0.07	0.03								4.75		3.12	1.23		
62	0.33	0.43								0.30				0.10		
63		0.35									2.65		2.50			
64	0.28		0.14				0.77				0.11		0.74			
65											2.46		1.42	0.71		
66		0.86														
67																
68																
69											1.22					
70																
71																
72																
73																
74																
75																
76																
77																
78																
79																
80																

Table A 3: immature samples provided by ENI, Petrobras, Devon, Shell, and Total

Table A 3: Bulk Kinetics

Company	GFZ	Woodford Shale	Alaskan Tasmantite	Boghead Coal	Brown Limestone	Alang Coal	Spekk Fm.	Are Fm.	Green River Shale	Mix Type (III)	Schönbeck Fm.	Schönbeck Fm.	Schönbeck Fm.	Winterhall
Formation/Basin	Tagli Fm.	Woodford Shale	Alaskan Tasmantite	Boghead Coal	Brown Limestone	Alang Coal	Spekk Fm.	Are Fm.	Green River Shale	Mix Type (III)	Schönbeck Fm.	Schönbeck Fm.	Schönbeck Fm.	Winterhall
GFZ Code	SN6750	G000690	G000693	G000697	G000731	G000950	G001955	G001965	G004750	G0047501965	G004070	G004071	G004072	Walden Shale
Fraction	Bulk	Bulk	Bulk	Bulk	Bulk	Bulk	Bulk	Bulk	Bulk	Bulk	Bulk	Bulk	Bulk	Bulk
A (sec <sup>-1</sup> )	5.54E+14	2.57E+13	4.28E+13	3.54E+13	1.76E+12	3.10E+14	9.98E+14	4.42E+15	2.02E+14	2.36E+14	1.87E+14	1.56E+14	3.94E+14	9.27E+14
E (kcal/mol)	%	%	%	%	%	%	%	%	%	%	%	%	%	%
35														
36														
37														
38														
39														
40														
41														
42														
43														
44														
45														
46														
47														
48														
49														
50														
51														
52														
53														
54														
55														
56														
57														
58														
59														
60														
61														
62														
63														
64														
65														
66														
67														
68														
69														
70														
71														
72														
73														
74														
75														
76														
77														
78														
79														
80														

Table A 3 continued: immature samples provided by GFZ and Wintershall (Shales)

Table A 3: Bulk Kinetics

Company		GFZ																	
Formation/Basin GFZ Code Fraction	A (sec <sup>-1</sup> )	NZ-Coal G001983 Bulk	NZ-Coal G001982 Bulk	NZ-Coal G001981 Bulk	NZ-Coal G001980 Bulk	NZ-Coal G001997 Bulk	NZ-Coal G001994 Bulk	NZ-Coal G001990 Bulk	NZ-Coal G001991 Bulk	NZ-Coal extracted G001983K Bulk	NZ-Coal extracted G001981K Bulk	NZ-Coal extracted G001980K Bulk	NZ-Coal extracted G001997K Bulk	NZ-Coal extracted G001994K Bulk	NZ-Coal extracted G001990K Bulk	NZ-Coal extracted G001991K Bulk			
		6.07E+15	1.84E+15	1.51E+15	1.1549E+15	1.64E+15	2.72E+15	4.50E+15	1.15E+16	3.31E+15	1.50E+15	1.23E+15	1.07E+15	2.21E+15	1.74E+15	5.17E+15			
E (kcal/mol)		%	%	%	%	%	%	%	%	%	%	%	%	%	%	%			
45																			
46			0.85	0.88	0.70	0.42	0.48				0.24	0.12	0.16						
47	1.44					0.04	0.10	0.47		0.86	0.02	0.15	0.1	0.31	0.25				
48			1.09	1.03	0.98	0.71	0.65		0.77		0.50	0.38	0.33						
49	1.45	0.77	0.85	0.80	0.47	0.47	0.41	0.59		1.33	0.56	0.65	0.56	0.5	0.39	0.29			
50	1.00	1.93	1.59	1.60	1.24	1.24	0.79	0.32	0.81	0.91	1.12	1.11	0.83	0.32	0.28				
51	1.92	2.16	2.25	2.31	1.30	1.30	0.87	0.68	0.46	2.28	1.77	1.83	1.63	0.86	0.68	0.44			
52	2.34	3.89	3.24	3.57	2.57	2.57	1.14	0.75	0.95	2.6	2.83	2.95	2.2	0.89	0.8	0.35			
53	3.41	4.86	5.06	5.68	3.09	3.09	1.95	1.10	0.89	4.29	4.43	4.74	4.24	1.86	1.5	0.70			
54	4.74	7.39	6.92	7.45	5.76	5.76	2.36	1.63	1.33	5.62	6.21	6.63	5.23	2.7	2.33	1.02			
55	6.33	9.40	9.74	11.07	6.94	6.94	4.57	2.42	1.43	7.5	9.53	10.22	10.31	4.39	3.58	1.39			
56	8.19	12.69	13.35	14.37	13.68	13.68	6.51	3.85	2.33	9.96	13.69	14.67	15.7	7.8	7.93	2.46			
57	10.30	14.37	14.94	14.96	15.11	15.11	15.67	6.76	2.45	13.17	15.96	15.65	15.01	17.71	16.17	4.08			
58	12.70	13.46	13.47	12.40	13.52	13.52	18.47	15.27	5.11	13.56	13.70	13.26	12.48	17.31	15.04	8.61			
59	12.58	9.10	7.84	6.31	10.43	10.43	14.09	16.00	8.80	12.22	8.28	7.36	7.42	14.02	13.36	14.60			
60	11.38	4.55	4.53	4.21	5.58	5.58	11.52	13.49	15.70	7.94	4.98	4.60	5.3	9.85	8.6	14.56			
61	6.79	3.33	3.27	3.01	4.78	4.78	5.34	10.29	14.23	4.44	3.41	3.29	4.02	4.64	6.43	12.50			
62	4.21	2.12	2.45	2.15	3.02	3.02	4.15	6.38	12.36	3.32	2.82	2.52	2.95	4.24	5.01	8.78			
63	2.65	1.88	1.66	1.72	2.79	2.77	2.79	5.01	8.49	2.12	1.83	1.92	2.56	2.51	4.1	6.99			
64	2.26	1.09	1.63	1.29	1.54	1.54	2.00	4.13	5.84	1.95	2.01	1.63	1.37	2.42	2.83	5.45			
65	1.07	1.35	0.86	1.16	1.89	1.89	1.81	2.47	5.41	1.11	0.88	1.25	2.22	1.22	2.3	4.28			
66	1.79	0.51	1.29	0.94	0.37	0.37	0.39	2.87	2.92	1.38	1.75	1.22		1.77	1.93	3.00			
67		1.24	0.50	0.71	2.13	2.13	1.90	0.33	3.77	0.41	0.36	0.76	2.55	0.23	0.75	2.33			
68	1.78	0.23	1.06	1.01				2.65	0.31	1.36	1.40	1.18		2.01	2.47	2.01			
69		0.44							3.12							0.65			
70		1.29	1.58	1.58	2.63	2.63	2.03	2.54		0.62	1.73	1.91	2.82			2.46			
71	1.66								2.52	1.03				2.43	3.27				
72																			
73																3.04			
74																			
75																			
76																			
77																			
78																			
79																			
80																			
81																			
82																			
83																			
84																			
85																			
86																			
87																			
88																			
89																			
90																			

Table A 3 continued: extracted and unextracted New Zealand Coals provided by GFZ



Table A 3: Bulk Kinetics

Company/GFZ		German Coals				Company		Shell			Wintershall		
Formation/Basin GFZ Code	Sandbochum-1 G000721 Bulk	Wlastedde G001088 Bulk	Dickelbank-2 G001083 Bulk	Verden-1 G001086 Bulk	Siedenburg Z-1 G001092 Bulk	Granterath-1 G001096 Bulk	Formation/Basin GFZ Code Fraction	Exshaw Fm. G006384 Bulk	Exshaw Fm. G006385 Bulk	Exshaw Fm. G006387 Bulk	G006533 Bulk	Wealden Coals G006538 Bulk	G006552 Bulk
A (sec <sup>-1</sup> )	7.91E+14	6.32E+17	3.43E+17	1.67E+18	5.08E+14	1.28E+15	A (sec <sup>-1</sup> )	3.30E+13	1.77E+13	1.41E+13	1.99E+16	4.30E+15	6.97E+15
E (kcal/mol)	%	%	%	%	%	%	E (kcal/mol)	%	%	%	%	%	%
45	0.14						35						
46	0.10				0.35	0.56	36						
47	0.28						37						
48	0.26						38						
49	0.45						39						
50	0.47						40						
51	0.67						41		0.27				
52	0.82						42		0.71	0.55			
53	0.85						43		0.77	0.66			
54	0.94						44		1.01	0.90			
55					0.40		45		1.16	0.78			
56	22.10						46		1.00	1.41			
57	21.00				0.62		47		1.80	0.60		0.76	
58	12.45	0.78	0.73		0.57	0.56	48		1.09	2.79		0.33	0.53
59	11.11	0.98	0.84		0.68		49		3.12		0.88	1.11	0.41
60	6.13	1.14	0.92		1.82	0.63	50	0.08	0.61	6.34	0.47	0.77	0.76
61	5.75	1.24	1.38		2.84		51		22.76	13.34	1.42	1.25	0.71
62	4.39	1.89	1.53		5.29	0.56	52	0.05	22.19	28.72	0.62	1.11	0.91
63	2.42	1.73	1.98	0.91	8.30	1.05	53	10.97	22.80	17.28	1.74	1.39	1.04
64	3.51	2.03	1.63	1.10	9.26	1.36	54	9.29	6.11	15.13	0.62	1.55	1.33
65	0.02	3.03	3.86	1.12	10.74	2.16	55	25.21	9.15	7.62	3.11	1.90	1.61
66	2.95	4.25	2.70	1.55	9.43	6.15	56	8.23	3.20		0.62	2.82	2.35
67	0.37	8.15	10.49	1.89	9.03	2.31	57	19.09		0.94	3.81	3.65	3.25
68		12.99	10.34	2.04	8.35	14.38	58		1.05		4.30	7.32	6.41
69	2.83	13.14	15.33	3.76	7.05	2.63	59	11.94	0.39		7.93	12.97	13.75
70		11.53	11.13	5.27	6.19	14.14	60	0.22			14.05	15.43	16.33
71		9.28	10.72	9.91	5.05	6.39	61				14.41	13.52	13.69
72		6.42	5.15	12.14	3.64	11.58	62	14.92	0.80	2.95	10.30	9.21	10.56
73		4.74	6.25	12.32	3.01	5.36	63				13.37	5.85	6.12
74		4.29	2.16	9.77	1.65	8.15	64				6.49	5.85	5.32
75		2.35	3.38	7.99	2.33	3.36	65				4.26	2.81	4.12
76		2.49	1.97	5.75		5.59	66				3.67	4.20	2.50
77		1.76	2.22	4.47	1.65	1.36	67				1.90		3.21
78		1.53	1.47	3.68	0.79	3.91	68				2.48	3.51	3.52
79		1.38	0.96	3.11	0.72	0.72	69					0.25	3.01
80		1.14	1.02	2.22	0.28	2.80	70				2.15		0.04
81		0.87	1.13		0.68		71					2.46	3.15
82		0.89				2.16	72						2.04
83			0.71	0.96		0.72	73				1.42		
84				2.04			74						7.29
85				1.03		1.41	75						0.57
86				0.9			76						
87							77						7.39
88							78						
89							79						
90				1.4			80						

Table A 3 continued: maturity series provided by GFZ, Shell, and Wintershall

Table A 4: IR-ATR Mineralogy Screen

Table A 4: IR-ATR Mineralogy Screen

G/FZ Code	Formation/Basin	Quartz (%)	Feldspar (%)	Calcite (%)	Dolomite (%)	Kaolinite (%)	Chlorite (%)	Illite-Smectite (%)	Total (%)
G004750	Green River Shale	25	5	6	1	6	4	50	97
G006536	Walden Shales	10	4	6	1	10	4	60	95
G0047501965	Mix type I/III	19	5	10	1	12	5	46	98
G006208	Toarcian Shale	22	5	25	0	7	5	35	99
G001955	Spekk Fm.	20	4	6	0	14	4	51	98
G000689	Botneheia Shale	42	5	10	0	2	4	40	103
G005812	Irati Fm.	39	5	3	0	6	4	46	102
G006153	Woodford Shale	74	6	4	1	0	2	17	104
G006154	Woodford Shale	76	6	3	0	0	2	15	102
G006156	New Albany Shale	31	4	4	1	5	3	49	98
G006155	Caney Shale	56	6	5	0	0	3	29	99
G005298	Bakken Shale	39	5	3	1	5	3	48	103
G000692	Chattanooga Shale	32	4	3	1	6	3	48	97
G004564	Murzuq Basin	18	4	4	1	11	4	54	96
G007160	Murzuq Basin	10	4	5	0	13	4	63	99
G006949	Middle East	12	3	4	0	12	4	63	98
G000753	Alum Shale	49	5	2	0	4	3	37	101
G000758	Alum Shale	54	5	3	1	0	2	30	95
G006948	Middle East	18	4	4	0	13	4	56	99
G007161	Ghadames Basin	43	5	8	1	3	3	37	101
G005935	Akata Shale	20	6	8	3	12	4	45	99
G005763	Hekkingen Fm.	36	5	7	0	7	4	41	100
G006205	Douala Basin	2	2	6	0	13	3	72	98
G007165	Farsund Fm.	19	5	8	0	8	4	49	94
G007166	Farsund Fm.	22	4	11	0	6	4	50	98
G000721	Westphalian Coals	50	1	23	1	7	2	20	104
G001965	Are Fm.	19	5	15	2	17	5	42	104
G006207	Mahakam Delta	26	5	6	0	9	4	50	100
SN6750	Taglu Fm.	47	5	14	0	7	4	25	101
G006385	Exshaw Fm.	41	5	3	1	3	3	42	98
G006387	Exshaw Fm.	75	6	26	0	1	3	3	113
G006384	Exshaw Fm.	40	5	14	0	2	4	38	103

Table A 5: stepwise open-system pyrolysis GC-FID

Table A 5: stepwise open-system pyrolysis GC-FID

Formation/Basin	Are Fm. G001965						
GFZ Code	G001965BA	G001965BB	G001965BC	G001965BM	G001965BN	G001965BO	G001965BP
File	200-300	200-350	200-400	200-450	200-500	200-550	200-600
Temperature [°C]	1 K/min	1 K/min	1 K/min	1 K/min	1 K/min	1 K/min	1 K/min
Rate	1 K/min	1 K/min	1 K/min	1 K/min	1 K/min	1 K/min	1 K/min
Totals	mg/g sample	mg/g sample	mg/g sample	mg/g sample	mg/g sample	mg/g sample	mg/g sample
C1+ (-blank)	3.13	6.98	18.28	47.56	60.40	64.22	63.83
C1-5	0.31	0.98	3.55	10.26	16.29	20.88	23.56
C2-5	0.26	0.80	2.75	7.52	10.04	11.16	11.35
C6-14 (-blank)	1.24	3.04	7.97	18.83	23.38	22.78	22.00
C6-14Hump	0.51	1.10	2.55	5.34	6.50	5.51	5.63
C6-14 Resolved	0.74	1.94	5.42	13.49	16.88	17.27	16.36
C15+ (-blank)	1.58	2.96	6.77	18.48	20.73	20.56	18.27
C15+ Hump	1.26	2.12	4.70	14.00	15.80	15.45	13.59
C15+ Resolved	0.32	0.83	2.06	4.48	4.93	5.11	4.68
GOR	0.11	0.16	0.24	0.27	0.37	0.48	0.59
Gas Wetness (C <sub>2-5</sub> /C <sub>1-5</sub> )	0.87	0.81	0.78	0.73	0.62	0.53	0.48
Compounds Summation	mg/g sample	mg/g sample	mg/g sample	mg/g sample	mg/g sample	mg/g sample	mg/g sample
n- C <sub>6-14</sub>	0.08	0.16	0.69	2.13	2.41	2.36	2.36
n- C <sub>15+</sub>	0.05	0.15	0.58	1.36	1.43	1.41	1.32
Mono-aromatic Compounds	0.06	0.21	0.78	1.81	2.39	2.87	3.00
Di-aromatic Compounds	0.07	0.15	0.32	0.61	0.89	0.90	0.95
Phenolic Compounds	0.02	0.09	0.37	1.74	2.77	2.58	2.18
Thiophenic Compounds	0.02	0.06	0.23	0.37	0.42	0.43	0.44
Single Compounds	mg/g sample	mg/g sample	mg/g sample	mg/g sample	mg/g sample	mg/g sample	mg/g sample
Methane	0.04	0.18	0.80	2.73	6.25	9.72	12.22
Ethene	0.00	0.00	0.17	0.58	1.04	1.33	1.63
Ethane	0.03	0.11	0.35	1.31	2.08	2.57	2.61
Propane	0.03	0.17	0.67	2.08	2.47	2.73	2.64
i-Butane	0.00	0.01	0.03	0.08	0.11	0.10	0.09
1-Butene	0.03	0.07	0.21	0.64	0.79	0.79	0.82
n-Butane	0.01	0.04	0.16	0.39	0.46	0.48	0.48
i-Pentane	0.03	0.05	0.16	0.34	0.41	0.45	0.45
Pentene	0.00	0.02	0.06	0.23	0.27	0.28	0.25
n-Pentane	0.00	0.01	0.07	0.21	0.25	0.25	0.24
Cyclopentane	0.00	0.00	0.01	0.02	0.02	0.02	0.02
2-Methylpentane	0.00	0.01	0.03	0.07	0.08	0.07	0.07
3-Methylpentane	0.00	0.00	0.01	0.02	0.02	0.02	0.02
1-Hexene	0.00	0.01	0.04	0.20	0.24	0.24	0.25
n-Hexane	0.00	0.01	0.05	0.17	0.19	0.19	0.19
Methylcyclopentane	0.00	0.01	0.01	0.02	0.03	0.03	0.03
Benzene	0.01	0.04	0.09	0.16	0.24	0.40	0.55
Thiophene	0.00	0.01	0.02	0.04	0.05	0.06	0.05
Cyclohexane	0.00	0.00	0.01	0.02	0.02	0.02	0.02
2-Methylhexane	0.00	0.00	0.01	0.04	0.04	0.04	0.04
2,3-Dimethylpentane	0.00	0.00	0.01	0.02	0.02	0.02	0.03
1,1-Dimethylpentane	0.00	0.00	0.00	0.00	0.00	0.00	0.00
3-Methylhexane	0.00	0.00	0.01	0.02	0.02	0.02	0.02
1-Heptene	0.00	0.00	0.04	0.15	0.17	0.18	0.18
n-Heptane	0.00	0.01	0.06	0.17	0.19	0.20	0.20
Methyl-Cyclohexane	0.00	0.00	0.01	0.03	0.03	0.03	0.03
Ethylcyclopentane	0.00	0.00	0.01	0.02	0.02	0.02	0.01
2,5-Dimethylhexane	0.00	0.01	0.02	0.06	0.07	0.06	0.06
2,4-Dimethylhexane	0.00	0.00	0.00	0.02	0.02	0.02	0.02
3,3-Dimethylhexane	0.00	0.00	0.01	0.04	0.04	0.04	0.04
2,3,4-Trimethylpentane	0.00	0.01	0.03	0.06	0.06	0.08	0.06
Toluene	0.01	0.04	0.16	0.47	0.71	0.89	0.93
2-Methylthiophene	0.00	0.01	0.05	0.09	0.10	0.11	0.11
3-Methylthiophene	0.00	0.01	0.02	0.04	0.05	0.05	0.05
1-Octene	0.00	0.00	0.04	0.13	0.15	0.15	0.15
n-Octane	0.00	0.01	0.06	0.18	0.18	0.17	0.17
Ethylbenzene	0.00	0.01	0.04	0.11	0.15	0.15	0.15
Ethylthiophene	0.00	0.00	0.02	0.04	0.04	0.04	0.04
2,5-Dimethylthiophene	0.00	0.00	0.01	0.03	0.03	0.03	0.03
m/p-Xylene	0.01	0.04	0.15	0.38	0.53	0.61	0.59
2,4-Dimethylthiophene	0.00	0.01	0.02	0.03	0.03	0.03	0.03
2,3-Dimethylthiophene	0.00	0.01	0.05	0.03	0.03	0.03	0.03
Styrene	0.00	0.00	0.00	0.12	0.12	0.13	0.13
o-Xylene	0.00	0.01	0.07	0.18	0.22	0.22	0.22
1-Nonene	0.00	0.00	0.02	0.09	0.10	0.10	0.10
n-Nonane	0.00	0.01	0.04	0.12	0.13	0.13	0.13
2-Propylthiophene	0.00	0.01	0.02	0.04	0.05	0.05	0.05
Propylbenzene	0.00	0.00	0.02	0.03	0.03	0.04	0.03
2-Ethyl-5-Methylthiophene	0.00	0.00	0.02	0.03	0.03	0.02	0.05
(?)-Benzene	0.00	0.01	0.05	0.13	0.17	0.18	0.18
1,3,5-Trimethylbenzene	0.00	0.00	0.01	0.03	0.05	0.05	0.05
Phenol	0.01	0.05	0.17	0.74	1.22	1.17	1.01
1-Ethyl-2-Methylbenzene	0.00	0.01	0.03	0.07	0.00	0.02	0.02
2,3,5-Trimethylthiophene	0.00	0.00	0.00	0.00	0.00	0.00	0.00

Table A 5: Åre Fm. sample G001965

Table A 5: stepwise open-system pyrolysis GC-FID

Formation/Basin	Are Fm.						
GFZ Code	G001965						
Temperature [°C]	200-300	200-350	200-400	200-450	200-500	200-550	200-600
1,2,4-Trimethylbenzene	0.01	0.02	0.06	0.12	0.16	0.17	0.15
1-Decene	0.00	0.00	0.01	0.09	0.09	0.09	0.09
<i>n</i> -Decane	0.00	0.01	0.03	0.10	0.10	0.10	0.10
1,2,3-Trimethylbenzene	0.01	0.03	0.10	0.13	0.14	0.14	0.13
<i>o</i> -Cresol	0.00	0.01	0.04	0.24	0.36	0.37	0.31
<i>m/p</i> -Cresol	0.01	0.04	0.14	0.72	1.15	1.01	0.83
Dimethylphenol	0.00	0.00	0.02	0.03	0.03	0.04	0.03
1-Undecene	0.00	0.01	0.04	0.11	0.12	0.13	0.13
<i>n</i> -Undecane	0.00	0.01	0.04	0.09	0.09	0.09	0.09
1,2,3,4-Tetramethylbenzene	0.00	0.00	0.02	0.08	0.07	0.10	0.10
Naphthalene	0.00	0.01	0.03	0.06	0.10	0.16	0.20
1-Dodecene	0.00	0.01	0.04	0.09	0.10	0.10	0.09
<i>n</i> -Dodecane	0.01	0.01	0.04	0.09	0.10	0.10	0.10
2-Methylnaphthalene	0.01	0.02	0.06	0.13	0.22	0.23	0.22
1-Tridecene	0.00	0.01	0.02	0.08	0.09	0.08	0.08
1-Methylnaphthalene	0.01	0.01	0.04	0.08	0.14	0.13	0.13
<i>n</i> -Tridecane	0.00	0.01	0.04	0.09	0.11	0.09	0.10
1-Tetradecene	0.02	0.04	0.06	0.11	0.15	0.12	0.13
<i>n</i> -Tetradecane	0.00	0.01	0.04	0.09	0.10	0.09	0.08
Dimethylnaphthalene	0.03	0.07	0.12	0.20	0.29	0.25	0.26
1-Pentadecene	0.01	0.01	0.03	0.08	0.11	0.10	0.09
<i>n</i> -Pentadecane	0.01	0.01	0.03	0.07	0.09	0.08	0.08
Trimethylnaphthalene	0.01	0.01	0.02	0.04	0.05	0.04	0.05
Trimethylnaphthalene	0.00	0.00	0.01	0.02	0.02	0.02	0.02
Trimethylnaphthalene	0.01	0.02	0.04	0.08	0.08	0.08	0.08
1-Hexadecene	0.01	0.01	0.02	0.06	0.07	0.07	0.07
<i>n</i> -Hexadecane	0.00	0.01	0.03	0.07	0.07	0.07	0.07
Isopropyldimethylnaphthalene	0.00	0.01	0.01	0.01	0.01	0.01	0.01
1-Heptadecene	0.00	0.00	0.02	0.05	0.05	0.05	0.05
<i>n</i> -Heptadecane	0.00	0.01	0.03	0.07	0.07	0.07	0.07
Pristane	0.00	0.01	0.02	0.03	0.03	0.03	0.02
Prist.-1-ene	0.00	0.03	0.07	0.10	0.09	0.09	0.09
1-Octadecene	0.00	0.00	0.01	0.04	0.04	0.04	0.04
<i>n</i> -Octadecane	0.00	0.00	0.03	0.08	0.09	0.09	0.08
Phytane	0.00	0.00	0.01	0.01	0.02	0.02	0.01
1-Nonadecene	0.00	0.00	0.01	0.04	0.04	0.04	0.04
<i>n</i> -Nonadecane	0.00	0.01	0.03	0.09	0.09	0.09	0.08
1-Icosene	0.00	0.00	0.01	0.04	0.04	0.04	0.04
<i>n</i> -Icosane	0.00	0.00	0.02	0.06	0.06	0.06	0.06
1-Henicosene	0.00	0.00	0.01	0.03	0.03	0.03	0.03
<i>n</i> -Henicosane	0.00	0.01	0.03	0.06	0.06	0.06	0.05
1-Docosene	0.00	0.00	0.01	0.03	0.04	0.04	0.03
<i>n</i> -Docosane	0.00	0.01	0.03	0.06	0.05	0.06	0.05
1-Tricosene	0.00	0.00	0.01	0.03	0.03	0.03	0.03
<i>n</i> -Tricosane	0.00	0.01	0.03	0.05	0.05	0.05	0.05
1-Tetracosene	0.00	0.00	0.01	0.03	0.03	0.03	0.03
<i>n</i> -Tetracosane	0.00	0.01	0.02	0.05	0.05	0.05	0.05
1-Pentacosene	0.00	0.00	0.01	0.03	0.03	0.03	0.03
<i>n</i> -Pentacosane	0.00	0.00	0.02	0.05	0.05	0.05	0.05
1-Hexacosene	0.00	0.00	0.01	0.02	0.03	0.03	0.02
<i>n</i> -Hexacosane	0.00	0.00	0.02	0.04	0.04	0.04	0.04
1-Heptacosene	0.00	0.00	0.00	0.02	0.02	0.02	0.02
<i>n</i> -Heptacosane	0.00	0.00	0.01	0.03	0.03	0.03	0.03
1-Octacosene	0.00	0.00	0.00	0.01	0.01	0.01	0.01
<i>n</i> -Octacosane	0.00	0.00	0.01	0.02	0.02	0.02	0.02
1-Nonacosene	0.00	0.00	0.00	0.01	0.01	0.01	0.01
<i>n</i> -Nonacosane	0.00	0.00	0.01	0.02	0.02	0.02	0.02
1-Triacontene	0.00	0.00	0.00	0.00	0.00	0.00	0.00
<i>n</i> -Triacontane	0.00	0.00	0.02	0.00	0.00	0.00	0.00
<i>n</i> -C31:1	0.00	0.00	0.00	0.00	0.00	0.00	0.00
<i>n</i> -C31	0.00	0.00	0.01	0.00	0.00	0.00	0.00
<i>n</i> -C32:1	0.00	0.00	0.00	0.00	0.00	0.00	0.00
<i>n</i> -C32	0.00	0.00	0.01	0.00	0.00	0.00	0.00
<i>n</i> -C33:1	0.00	0.00	0.00	0.00	0.00	0.00	0.00
<i>n</i> -C33	0.00	0.00	0.00	0.00	0.00	0.00	0.00
<i>n</i> -C34:1	0.00	0.00	0.00	0.00	0.00	0.00	0.00
<i>n</i> -C34	0.00	0.00	0.00	0.00	0.00	0.00	0.00
<i>n</i> -C35:1	0.00	0.00	0.00	0.00	0.00	0.00	0.00
<i>n</i> -C35	0.00	0.00	0.00	0.00	0.00	0.00	0.00
<i>n</i> -C36:1	0.00	0.00	0.00	0.00	0.00	0.00	0.00
<i>n</i> -C36	0.00	0.00	0.00	0.00	0.00	0.00	0.00
<i>n</i> -C37:1	0.00	0.00	0.00	0.00	0.00	0.00	0.00
<i>n</i> -C37	0.00	0.00	0.00	0.00	0.00	0.00	0.00
<i>n</i> -C38:1	0.00	0.00	0.00	0.00	0.00	0.00	0.00
<i>n</i> -C38	0.00	0.00	0.00	0.00	0.00	0.00	0.00
<i>n</i> -C39:1	0.00	0.00	0.00	0.00	0.00	0.00	0.00
<i>n</i> -C39	0.00	0.00	0.00	0.00	0.00	0.00	0.00

Table A 5 continued: Are Fm. sample G001965

Table A 5: stepwise open-system pyrolysis GC-FID

Company							
Formation/Basin	I-III Mix						
GFZ Code	G0047501965						
File	G004750CA	G004750CB	G004750CC	G004750CD	G004750CE	G004750CF	G004750CG
Temperature [°C]	200-300	200-350	200-400	200-450	200-500	200-550	200-600
Rate	1 K/min	1 K/min	1 K/min	1 K/min	1 K/min	1 K/min	1 K/min
Totals	mg/g sample	mg/g sample	mg/g sample	mg/g sample	mg/g sample	mg/g sample	mg/g sample
C1+ (-blank)	1.13	4.35	20.47	64.62	77.19	78.56	75.18
C1-5	0.19	0.69	2.77	9.08	13.44	15.40	16.65
C2-5	0.15	0.57	2.24	7.15	9.52	9.61	9.81
C6-14 (-blank)	0.64	2.12	7.95	20.85	23.77	24.00	23.49
C6-14Hump	0.25	0.82	0.17	6.02	6.74	6.51	6.05
C6-14 Resolved	0.39	1.30	7.78	14.83	17.04	17.48	17.44
C15+ (-blank)	0.31	1.54	9.74	34.69	39.98	39.17	35.04
C15+ Hump	0.12	0.88	6.76	26.24	30.46	29.75	26.17
C15+ Resolved	0.18	0.66	2.98	8.46	9.52	9.42	8.87
GOR	0.20	0.19	0.16	0.16	0.21	0.24	0.28
Gas Wetness (C <sub>2-5</sub> /C <sub>1-5</sub> )	0.82	0.83	0.81	0.79	0.71	0.62	0.59
Compounds Summation	mg/g sample	mg/g sample	mg/g sample	mg/g sample	mg/g sample	mg/g sample	mg/g sample
n-C <sub>6-14</sub>	0.03	0.15	1.01	4.87	5.68	5.80	5.82
n-C <sub>15+</sub>	0.03	0.16	1.33	4.87	5.38	5.42	5.05
Mono-aromatic Compounds	0.04	0.19	0.66	1.59	1.95	2.19	2.34
Di-aromatic Compounds	0.04	0.09	0.22	0.42	0.50	0.58	0.57
Phenolic Compounds	0.01	0.04	0.25	0.80	0.97	0.98	0.83
Thiophenic Compounds	0.01	0.05	0.23	0.47	0.52	0.52	0.53
Single Compounds	mg/g sample	mg/g sample	mg/g sample	mg/g sample	mg/g sample	mg/g sample	mg/g sample
Methane	0.03	0.12	0.53	1.93	3.92	5.79	6.84
Ethene	0.00	0.00	0.00	0.37	0.74	0.82	0.88
Ethane	0.01	0.04	0.33	1.18	1.83	1.87	2.00
Propane	0.02	0.09	0.52	1.83	2.37	2.43	2.18
i-Butane	0.01	0.02	0.03	0.08	0.09	0.08	0.09
1-Butene	0.00	0.05	0.21	0.67	0.83	0.83	0.91
n-Butane	0.01	0.02	0.11	0.47	0.57	0.60	0.60
i-Pentane	0.01	0.02	0.09	0.22	0.27	0.27	0.27
Pentene	0.00	0.01	0.06	0.32	0.42	0.41	0.42
n-Pentane	0.00	0.01	0.07	0.33	0.40	0.39	0.38
Cyclopentane	0.00	0.00	0.01	0.02	0.03	0.03	0.03
2-Methylpentane	0.00	0.01	0.04	0.08	0.08	0.09	0.09
3-Methylpentane	0.00	0.00	0.01	0.02	0.02	0.02	0.02
1-Hexene	0.00	0.01	0.08	0.38	0.48	0.47	0.50
n-Hexane	0.00	0.01	0.06	0.30	0.34	0.34	0.35
Methylcyclopentane	0.00	0.00	0.01	0.04	0.05	0.04	0.04
Benzene	0.01	0.04	0.09	0.17	0.20	0.33	0.43
Thiophene	0.00	0.01	0.02	0.03	0.03	0.04	0.04
Cyclohexane	0.00	0.00	0.01	0.03	0.03	0.03	0.03
2-Methylhexane	0.00	0.00	0.01	0.03	0.04	0.03	0.03
2,3-Dimethylpentane	0.00	0.00	0.01	0.02	0.02	0.02	0.02
1,1-Dimethylpentane	0.00	0.00	0.00	0.00	0.00	0.00	0.00
3-Methylhexane	0.00	0.00	0.01	0.02	0.02	0.02	0.02
1-Heptene	0.00	0.01	0.05	0.31	0.39	0.38	0.40
n-Heptane	0.00	0.01	0.07	0.32	0.36	0.37	0.37
Methyl-Cyclohexane	0.00	0.00	0.01	0.04	0.05	0.04	0.05
Ethylcyclopentane	0.00	0.00	0.01	0.02	0.03	0.03	0.03
2,5-Dimethylhexane	0.00	0.00	0.03	0.07	0.06	0.06	0.05
2,4-Dimethylhexane	0.00	0.00	0.00	0.01	0.01	0.01	0.01
3,3-Dimethylhexane	0.00	0.00	0.02	0.04	0.04	0.04	0.03
2,3,4-Trimethylpentane	0.00	0.01	0.04	0.07	0.07	0.07	0.07
Toluene	0.00	0.03	0.12	0.34	0.48	0.56	0.59
2-Methylthiophene	0.00	0.01	0.05	0.10	0.11	0.10	0.10
3-Methylthiophene	0.00	0.00	0.02	0.03	0.04	0.04	0.04
1-Octene	0.00	0.01	0.05	0.29	0.36	0.36	0.36
n-Octane	0.00	0.01	0.07	0.31	0.35	0.35	0.35
Ethylbenzene	0.00	0.01	0.04	0.10	0.11	0.12	0.13
Ethylthiophene	0.00	0.01	0.03	0.06	0.07	0.06	0.06
2,5-Dimethylthiophene	0.00	0.00	0.01	0.04	0.04	0.04	0.04
m/p-Xylene	0.01	0.04	0.17	0.35	0.43	0.46	0.46
2,4-Dimethylthiophene	0.00	0.01	0.02	0.03	0.04	0.04	0.04
2,3-Dimethylthiophene	0.00	0.00	0.04	0.09	0.11	0.12	0.12
Styrene	0.00	0.00	0.00	0.00	0.00	0.00	0.00
o-Xylene	0.00	0.01	0.05	0.15	0.18	0.18	0.18
1-Nonene	0.00	0.00	0.04	0.25	0.31	0.31	0.31
n-Nonane	0.00	0.01	0.06	0.28	0.31	0.32	0.31
2-Propylthiophene	0.00	0.00	0.01	0.04	0.04	0.04	0.04
Propylbenzene	0.00	0.00	0.02	0.04	0.04	0.04	0.04
2-Ethyl-5-Methylthiophene	0.00	0.01	0.02	0.05	0.04	0.05	0.05
(?)-Benzene	0.00	0.01	0.04	0.10	0.12	0.13	0.13
1,3,5-Trimethylbenzene	0.00	0.00	0.01	0.03	0.03	0.04	0.04
Phenol	0.00	0.02	0.11	0.33	0.39	0.40	0.35
1-Ethyl-2-Methylbenzene	0.00	0.01	0.02	0.06	0.07	0.07	0.07
2,3,5-Trimethylthiophene	0.00	0.00	0.00	0.00	0.00	0.00	0.00

Table A 5 continued: synthetic mixture I-III

Table A 5: stepwise open-system pyrolysis GC-FID

Formation/Basin	I-III Mix						
GFZ Code	G0047501965						
Temperature [°C]	200-300	200-350	200-400	200-450	200-500	200-550	200-600
1,2,4-Trimethylbenzene	0.00	0.01	0.04	0.10	0.14	0.13	0.12
1-Decene	0.00	0.01	0.05	0.26	0.31	0.31	0.31
n-Decane	0.00	0.01	0.05	0.26	0.28	0.29	0.29
1,2,3-Trimethylbenzene	0.01	0.02	0.08	0.14	0.15	0.15	0.14
o-Cresol	0.00	0.00	0.03	0.11	0.14	0.14	0.13
m/p-Cresol	0.00	0.01	0.09	0.33	0.41	0.40	0.33
Dimethylphenol	0.00	0.00	0.01	0.03	0.03	0.03	0.03
1-Undecene	0.00	0.01	0.05	0.26	0.30	0.31	0.30
n-Undecane	0.00	0.01	0.05	0.26	0.28	0.30	0.28
1,2,3,4-Tetramethylbenzene	0.00	0.00	0.02	0.04	0.06	0.05	0.04
Naphthalene	0.00	0.01	0.02	0.05	0.07	0.11	0.12
1-Dodecene	0.00	0.01	0.05	0.24	0.28	0.28	0.28
n-Dodecane	0.00	0.01	0.06	0.26	0.27	0.29	0.28
2-Methylnaphthalene	0.00	0.01	0.04	0.09	0.13	0.14	0.14
1-Tridecene	0.00	0.01	0.04	0.20	0.24	0.25	0.25
1-Methylnaphthalene	0.00	0.01	0.02	0.05	0.07	0.07	0.08
n-Tridecane	0.00	0.01	0.07	0.26	0.29	0.30	0.30
1-Tetradecene	0.00	0.01	0.04	0.22	0.27	0.28	0.28
n-Tetradecane	0.00	0.01	0.07	0.22	0.27	0.29	0.31
Dimethylnaphthalene	0.02	0.03	0.07	0.13	0.14	0.15	0.14
1-Pentadecene	0.00	0.01	0.05	0.19	0.22	0.22	0.23
n-Pentadecane	0.00	0.01	0.07	0.23	0.25	0.26	0.26
Trimethylnaphthalene	0.00	0.01	0.02	0.03	0.03	0.03	0.03
Trimethylnaphthalene	0.01	0.01	0.02	0.02	0.02	0.03	0.02
Trimethylnaphthalene	0.00	0.01	0.03	0.04	0.04	0.04	0.04
1-Hexadecene	0.00	0.01	0.05	0.18	0.21	0.21	0.20
n-Hexadecane	0.00	0.01	0.07	0.23	0.25	0.25	0.25
Isopropylidimethylnaphthalene	0.00	0.00	0.01	0.01	0.02	0.02	0.02
1-Heptadecene	0.00	0.01	0.04	0.15	0.18	0.18	0.17
n-Heptadecane	0.00	0.01	0.08	0.22	0.23	0.24	0.24
Pristane	0.00	0.00	0.01	0.01	0.02	0.02	0.02
Prist.-1-ene	0.00	0.02	0.08	0.10	0.10	0.10	0.09
1-Octadecene	0.00	0.00	0.03	0.13	0.14	0.15	0.14
n-Octadecane	0.00	0.01	0.06	0.19	0.20	0.21	0.20
Phytane	0.00	0.00	0.01	0.03	0.03	0.03	0.03
1-Nonadecene	0.00	0.00	0.03	0.12	0.13	0.13	0.13
n-Nonadecane	0.00	0.01	0.06	0.20	0.21	0.22	0.21
1-Icosene	0.00	0.00	0.03	0.12	0.14	0.14	0.13
n-Icosane	0.00	0.01	0.05	0.17	0.19	0.20	0.18
1-Henicosene	0.00	0.00	0.03	0.11	0.13	0.13	0.12
n-Henicosane	0.00	0.01	0.06	0.19	0.20	0.21	0.20
1-Docosene	0.00	0.00	0.03	0.13	0.14	0.14	0.13
n-Docosane	0.00	0.01	0.06	0.18	0.19	0.19	0.18
1-Tricosene	0.00	0.00	0.02	0.11	0.12	0.13	0.12
n-Tricosane	0.00	0.01	0.06	0.18	0.19	0.20	0.19
1-Tetracosene	0.00	0.00	0.02	0.10	0.11	0.11	0.11
n-Tetracosane	0.00	0.01	0.05	0.16	0.17	0.17	0.17
1-Pentacosene	0.00	0.00	0.02	0.09	0.10	0.10	0.09
n-Pentacosane	0.00	0.01	0.05	0.16	0.17	0.17	0.16
1-Hexacosene	0.00	0.00	0.02	0.09	0.10	0.10	0.09
n-Hexacosane	0.00	0.00	0.04	0.14	0.15	0.15	0.13
1-Heptacosene	0.00	0.00	0.02	0.07	0.08	0.09	0.07
n-Heptacosane	0.00	0.00	0.05	0.15	0.16	0.15	0.14
1-Octacosene	0.00	0.00	0.01	0.07	0.08	0.08	0.07
n-Octacosane	0.00	0.00	0.04	0.12	0.13	0.13	0.11
1-Nonacosene	0.00	0.00	0.01	0.06	0.06	0.06	0.05
n-Nonacosane	0.00	0.00	0.03	0.11	0.12	0.11	0.10
1-Triacontene	0.00	0.00	0.02	0.06	0.06	0.04	0.05
n-Triacontane	0.00	0.00	0.02	0.09	0.10	0.10	0.08
n-C31:1	0.00	0.00	0.02	0.05	0.06	0.06	0.05
n-C31	0.00	0.00	0.03	0.09	0.10	0.11	0.08
n-C32:1	0.00	0.00	0.00	0.03	0.04	0.04	0.02
n-C32	0.00	0.00	0.01	0.05	0.06	0.05	0.05
n-C33:1	0.00	0.00	0.00	0.01	0.01	0.01	0.01
n-C33	0.00	0.00	0.01	0.03	0.04	0.04	0.04
n-C34:1	0.00	0.00	0.00	0.01	0.01	0.01	0.01
n-C34	0.00	0.00	0.00	0.02	0.02	0.02	0.02
n-C35:1	0.00	0.00	0.00	0.00	0.01	0.01	0.00
n-C35	0.00	0.00	0.00	0.02	0.02	0.02	0.02
n-C36:1	0.00	0.00	0.00	0.00	0.00	0.01	0.01
n-C36	0.00	0.00	0.00	0.02	0.02	0.02	0.01
n-C37:1	0.00	0.00	0.00	0.00	0.00	0.00	0.00
n-C37	0.00	0.00	0.00	0.01	0.02	0.01	0.01
n-C38:1	0.00	0.00	0.00	0.00	0.00	0.00	0.00
n-C38	0.00	0.00	0.00	0.01	0.01	0.01	0.01
n-C39:1	0.00	0.00	0.00	0.00	0.00	0.00	0.00
n-C39	0.00	0.00	0.00	0.01	0.01	0.01	0.01

Table A 5 continued: synthetic mixture I-III

Table A 5: stepwise open-system pyrolysis GC-FID

Formation/Basin	Green River Shale						
GFZ Code	G004750						
File	G004750DA	G004750DB	G004750DC	G004750DD	G004750DE	G004750DF	G004750DG
Temperature [°C]	200-300	200-350	200-400	200-450	200-500	200-550	200-600
Rate	1 K/min	1 K/min	1 K/min	1 K/min	1 K/min	1 K/min	1 K/min
Totals	mg/g sample	mg/g sample	mg/g sample	mg/g sample	mg/g sample	mg/g sample	mg/g sample
C1+ (-blank)	0.99	4.33	20.47	79.22	100.16	100.74	105.52
C1-5	0.10	0.35	1.73	7.11	10.03	10.49	11.29
C2-5	0.09	0.27	1.46	6.12	8.37	8.45	8.85
C6-14 (-blank)	0.52	1.89	6.95	22.64	27.76	27.35	28.25
C6-14Hump	0.20	1.02	2.54	6.62	7.83	7.70	7.68
C6-14 Resolved	0.31	0.87	4.40	16.02	19.93	19.65	20.57
C15+ (-blank)	0.38	2.09	11.80	49.46	62.36	62.89	65.98
C15+ Hump	0.15	1.65	8.19	36.73	46.80	47.77	50.41
C15+ Resolved	0.22	0.44	3.61	12.73	15.56	15.12	15.56
GOR	0.11	0.09	0.09	0.10	0.11	0.12	0.12
Gas Wetness (C <sub>2-5</sub> /C <sub>1-5</sub> )	0.89	0.77	0.84	0.86	0.83	0.80	0.78
Compounds Summation	mg/g sample	mg/g sample	mg/g sample	mg/g sample	mg/g sample	mg/g sample	mg/g sample
n-C <sub>6-14</sub>	0.04	0.10	1.19	7.21	9.36	9.24	9.60
n-C <sub>15+</sub>	0.07	0.11	2.03	8.39	10.17	9.85	10.15
Mono-aromatic Compounds	0.04	0.13	0.47	1.12	1.33	1.39	1.48
Di-aromatic Compounds	0.01	0.06	0.07	0.20	0.25	0.25	0.26
Phenolic Compounds	0.00	0.02	0.04	0.12	0.15	0.14	0.14
Thiophenic Compounds	0.01	0.04	0.17	0.35	0.38	0.37	0.40
Single Compounds	mg/g sample	mg/g sample	mg/g sample	mg/g sample	mg/g sample	mg/g sample	mg/g sample
Methane	0.01	0.08	0.27	0.99	1.66	2.05	2.45
Ethene	0.00	0.00	0.00	0.17	0.37	0.43	0.44
Ethane	0.01	0.03	0.18	0.87	1.30	1.25	1.40
Propane	0.00	0.06	0.30	1.37	1.84	2.03	2.04
i-Butane	0.00	0.01	0.03	0.07	0.09	0.09	0.10
1-Butene	0.01	0.04	0.17	0.61	0.89	0.87	0.90
n-Butane	0.00	0.01	0.09	0.53	0.70	0.71	0.77
i-Pentane	0.00	0.01	0.03	0.15	0.15	0.17	0.18
Pentene	0.00	0.01	0.06	0.37	0.53	0.52	0.53
n-Pentane	0.00	0.01	0.07	0.42	0.52	0.51	0.54
Cyclopentane	0.00	0.00	0.01	0.03	0.04	0.04	0.04
2-Methylpentane	0.00	0.00	0.03	0.08	0.09	0.09	0.09
3-Methylpentane	0.00	0.00	0.01	0.02	0.02	0.02	0.02
1-Hexene	0.00	0.00	0.09	0.54	0.75	0.75	0.77
n-Hexane	0.00	0.00	0.06	0.38	0.50	0.48	0.52
Methylcyclopentane	0.00	0.00	0.01	0.05	0.06	0.06	0.06
Benzene	0.01	0.03	0.05	0.14	0.15	0.18	0.19
Thiophene	0.00	0.00	0.01	0.02	0.02	0.02	0.02
Cyclohexane	0.00	0.00	0.01	0.04	0.05	0.04	0.05
2-Methylhexane	0.00	0.00	0.01	0.03	0.04	0.03	0.03
2,3-Dimethylpentane	0.00	0.00	0.01	0.02	0.02	0.02	0.02
1,1-Dimethylpentane	0.00	0.00	0.00	0.00	0.00	0.00	0.00
3-Methylhexane	0.00	0.00	0.01	0.03	0.03	0.03	0.03
1-Heptene	0.00	0.00	0.06	0.43	0.61	0.61	0.63
n-Heptane	0.00	0.01	0.07	0.44	0.54	0.53	0.57
Methyl-Cyclohexane	0.00	0.00	0.01	0.07	0.08	0.07	0.08
Ethylcyclopentane	0.00	0.00	0.01	0.03	0.04	0.04	0.04
2,5-Dimethylhexane	0.00	0.00	0.02	0.05	0.05	0.06	0.05
2,4-Dimethylhexane	0.00	0.00	0.00	0.01	0.01	0.01	0.01
3,3-Dimethylhexane	0.00	0.00	0.02	0.04	0.04	0.04	0.04
2,3,4-Trimethylpentane	0.01	0.01	0.04	0.08	0.09	0.08	0.09
Toluene	0.00	0.02	0.05	0.17	0.23	0.24	0.25
2-Methylthiophene	0.00	0.01	0.01	0.03	0.03	0.03	0.03
3-Methylthiophene	0.00	0.00	0.02	0.03	0.03	0.03	0.02
1-Octene	0.00	0.00	0.05	0.41	0.58	0.57	0.59
n-Octane	0.00	0.01	0.08	0.44	0.54	0.53	0.56
Ethylbenzene	0.00	0.00	0.02	0.06	0.08	0.09	0.09
Ethylthiophene	0.00	0.00	0.04	0.08	0.08	0.08	0.09
2,5-Dimethylthiophene	0.00	0.00	0.01	0.04	0.05	0.05	0.05
m/p-Xylene	0.01	0.03	0.16	0.30	0.34	0.34	0.37
2,4-Dimethylthiophene	0.00	0.00	0.02	0.04	0.04	0.04	0.04
2,3-Dimethylthiophene	0.00	0.00	0.03	0.04	0.05	0.04	0.05
Styrene	0.00	0.00	0.02	0.07	0.09	0.09	0.10
o-Xylene	0.00	0.01	0.03	0.10	0.14	0.14	0.14
1-Nonene	0.00	0.00	0.05	0.38	0.52	0.51	0.54
n-Nonane	0.00	0.00	0.07	0.41	0.50	0.49	0.53
2-Propylthiophene	0.00	0.00	0.01	0.03	0.03	0.04	0.04
Propylbenzene	0.00	0.00	0.02	0.04	0.05	0.05	0.05
2-Ethyl-5-Methylthiophene	0.00	0.01	0.02	0.04	0.04	0.05	0.05
(?)-Benzene	0.00	0.00	0.02	0.06	0.08	0.08	0.08
1,3,5-Trimethylbenzene	0.00	0.01	0.01	0.02	0.02	0.03	0.03
Phenol	0.00	0.00	0.01	0.01	0.01	0.01	0.01
1-Ethyl-2-Methylbenzene	0.00	0.00	0.02	0.04	0.05	0.05	0.06
2,3,5-Trimethylthiophene	0.00	0.00	0.00	0.00	0.00	0.00	0.00

Table A 5 continued: Green River Shale sample G004750

Table A 5: stepwise open-system pyrolysis GC-FID

Formation/Basin	Green River Shale						
GFZ Code	G004750						
Temperature [°C]	200-300	200-350	200-400	200-450	200-500	200-550	200-600
1,2,4-Trimethylbenzene	0.00	0.01	0.03	0.08	0.10	0.10	0.10
1-Decene	0.00	0.01	0.08	0.42	0.55	0.54	0.57
<i>n</i> -Decane	0.00	0.00	0.06	0.40	0.48	0.48	0.51
1,2,3-Trimethylbenzene	0.00	0.02	0.06	0.10	0.10	0.10	0.11
<i>o</i> -Cresol	0.00	0.00	0.01	0.02	0.03	0.02	0.02
<i>m/p</i> -Cresol	0.00	0.01	0.01	0.06	0.08	0.07	0.07
Dimethylphenol	0.00	0.00	0.01	0.03	0.03	0.03	0.03
1-Undecene	0.00	0.01	0.06	0.40	0.53	0.50	0.53
<i>n</i> -Undecane	0.00	0.00	0.06	0.40	0.49	0.47	0.50
1,2,3,4-Tetramethylbenzene	0.00	0.00	0.00	0.01	0.01	0.01	0.01
Naphthalene	0.00	0.01	0.01	0.03	0.04	0.04	0.05
1-Dodecene	0.00	0.01	0.06	0.37	0.50	0.49	0.49
<i>n</i> -Dodecane	0.00	0.01	0.07	0.41	0.52	0.52	0.52
2-Methylnaphthalene	0.00	0.01	0.02	0.06	0.07	0.08	0.08
1-Tridecene	0.00	0.00	0.05	0.31	0.42	0.45	0.43
1-Methylnaphthalene	0.00	0.01	0.01	0.02	0.03	0.04	0.03
<i>n</i> -Tridecane	0.00	0.01	0.08	0.39	0.48	0.51	0.50
1-Tetradecene	0.00	0.01	0.05	0.30	0.38	0.38	0.38
<i>n</i> -Tetradecane	0.00	0.01	0.08	0.38	0.46	0.45	0.47
Dimethylnaphthalene	0.00	0.02	0.02	0.04	0.05	0.04	0.04
1-Pentadecene	0.00	0.01	0.06	0.30	0.39	0.38	0.40
<i>n</i> -Pentadecane	0.01	0.01	0.09	0.37	0.44	0.43	0.45
Trimethylnaphthalene	0.00	0.00	0.00	0.01	0.02	0.01	0.01
Trimethylnaphthalene	0.00	0.01	0.01	0.02	0.03	0.02	0.03
Trimethylnaphthalene	0.00	0.01	0.00	0.01	0.02	0.01	0.02
1-Hexadecene	0.00	0.01	0.06	0.29	0.37	0.37	0.37
<i>n</i> -Hexadecane	0.01	0.01	0.10	0.38	0.46	0.45	0.46
Isopropylidimethylnaphthalene	0.00	0.00	0.00	0.03	0.03	0.04	0.03
1-Heptadecene	0.00	0.00	0.06	0.26	0.34	0.34	0.33
<i>n</i> -Heptadecane	0.01	0.01	0.10	0.35	0.44	0.43	0.44
Pristane	0.00	0.00	0.00	0.01	0.01	0.02	0.01
Prist.-1-ene	0.00	0.01	0.07	0.11	0.13	0.13	0.12
1-Octadecene	0.00	0.00	0.04	0.22	0.29	0.29	0.28
<i>n</i> -Octadecane	0.01	0.01	0.07	0.28	0.36	0.35	0.36
Phytane	0.01	0.00	0.02	0.04	0.04	0.05	0.05
1-Nonadecene	0.00	0.00	0.03	0.19	0.26	0.25	0.25
<i>n</i> -Nonadecane	0.01	0.01	0.07	0.29	0.37	0.36	0.36
1-Icosene	0.00	0.00	0.04	0.21	0.27	0.27	0.27
<i>n</i> -Icosane	0.01	0.01	0.07	0.27	0.34	0.33	0.34
1-Henicosene	0.00	0.00	0.04	0.20	0.24	0.24	0.24
<i>n</i> -Henicosane	0.00	0.01	0.08	0.29	0.36	0.35	0.36
1-Docosene	0.00	0.00	0.04	0.22	0.28	0.27	0.28
<i>n</i> -Docosane	0.00	0.01	0.08	0.28	0.33	0.33	0.34
1-Tricosene	0.00	0.00	0.04	0.19	0.23	0.23	0.24
<i>n</i> -Tricosane	0.00	0.01	0.09	0.30	0.35	0.34	0.36
1-Tetracosene	0.00	0.00	0.03	0.18	0.22	0.21	0.22
<i>n</i> -Tetracosane	0.00	0.00	0.07	0.26	0.29	0.28	0.29
1-Pentacosene	0.00	0.00	0.04	0.17	0.21	0.20	0.21
<i>n</i> -Pentacosane	0.00	0.00	0.07	0.27	0.31	0.30	0.31
1-Hexacosene	0.00	0.00	0.03	0.18	0.22	0.21	0.22
<i>n</i> -Hexacosane	0.00	0.00	0.06	0.25	0.28	0.27	0.29
1-Heptacosene	0.00	0.00	0.03	0.14	0.17	0.17	0.18
<i>n</i> -Heptacosane	0.00	0.00	0.08	0.27	0.30	0.29	0.32
1-Octacosene	0.00	0.00	0.02	0.14	0.17	0.16	0.16
<i>n</i> -Octacosane	0.00	0.00	0.06	0.22	0.26	0.24	0.26
1-Nonacosene	0.00	0.00	0.02	0.11	0.12	0.13	0.14
<i>n</i> -Nonacosane	0.00	0.00	0.06	0.21	0.24	0.22	0.25
1-Triacontene	0.00	0.00	0.02	0.10	0.11	0.10	0.12
<i>n</i> -Triacontane	0.00	0.00	0.05	0.16	0.19	0.17	0.18
<i>n</i> -C31:1	0.00	0.00	0.04	0.11	0.14	0.12	0.11
<i>n</i> -C31	0.00	0.00	0.06	0.18	0.20	0.20	0.20
<i>n</i> -C32:1	0.00	0.00	0.02	0.07	0.08	0.07	0.06
<i>n</i> -C32	0.00	0.00	0.03	0.10	0.12	0.10	0.11
<i>n</i> -C33:1	0.00	0.00	0.00	0.03	0.03	0.03	0.03
<i>n</i> -C33	0.00	0.00	0.02	0.07	0.08	0.08	0.09
<i>n</i> -C34:1	0.00	0.00	0.00	0.03	0.02	0.03	0.02
<i>n</i> -C34	0.00	0.00	0.01	0.05	0.05	0.05	0.05
<i>n</i> -C35:1	0.00	0.00	0.00	0.02	0.01	0.03	0.01
<i>n</i> -C35	0.00	0.00	0.01	0.04	0.05	0.04	0.04
<i>n</i> -C36:1	0.00	0.00	0.00	0.02	0.02	0.02	0.02
<i>n</i> -C36	0.00	0.00	0.01	0.03	0.04	0.04	0.04
<i>n</i> -C37:1	0.00	0.00	0.00	0.01	0.01	0.02	0.01
<i>n</i> -C37	0.00	0.00	0.01	0.03	0.03	0.03	0.03
<i>n</i> -C38:1	0.00	0.00	0.00	0.01	0.01	0.01	0.01
<i>n</i> -C38	0.00	0.00	0.00	0.02	0.03	0.02	0.02
<i>n</i> -C39:1	0.00	0.00	0.00	0.00	0.01	0.01	0.00
<i>n</i> -C39	0.00	0.00	0.00	0.02	0.02	0.02	0.01

Table A 5 continued: Green River Shale sample G004750



Table A 5: stepwise open-system pyrolysis GC-FID

Formation/Basin	Spekk Fm.						
GFZ Code	G001955						
File	G001955FA	G001955FB	G001955FC	G001955FD	G001055FE	G001955FF	G001955FG
Temperature [°C]	200-300	200-350	200-400	200-450	200-500	200-550	200-600
Rate	1 K/min	1 K/min	1 K/min	1 K/min	1 K/min	1 K/min	1 K/min
Totals	mg/g sample	mg/g sample	mg/g sample	mg/g sample	mg/g sample	mg/g sample	mg/g sample
C1+ (-blank)	0.51	1.94	9.58	21.76	24.65	25.23	23.95
C1-5	0.09	0.35	1.38	4.06	5.50	5.96	6.11
C2-5	0.07	0.31	1.19	3.41	4.17	4.33	4.32
C6-14 (-blank)	0.24	1.15	4.52	9.03	9.93	9.96	9.85
C6-14Hump	0.07	0.40	1.67	3.04	3.14	3.12	2.98
C6-14 Resolved	0.16	0.75	2.85	5.99	6.79	6.84	6.87
C15+ (-blank)	0.19	0.44	3.69	8.68	9.23	9.30	8.00
C15+ Hump	0.12	0.29	3.10	7.46	7.91	7.91	6.76
C15+ Resolved	0.07	0.15	0.58	1.21	1.31	1.39	1.24
GOR	0.20	0.22	0.17	0.23	0.29	0.31	0.34
Gas Wetness (C <sub>2-5</sub> /C <sub>1-5</sub> )	0.87	0.87	0.86	0.84	0.76	0.73	0.71
Compounds Summation	mg/g sample	mg/g sample	mg/g sample	mg/g sample	mg/g sample	mg/g sample	mg/g sample
<i>n</i> -C <sub>6-14</sub>	0.02	0.09	0.48	1.44	1.58	1.60	1.62
<i>n</i> -C <sub>15+</sub>	0.02	0.04	0.22	0.49	0.52	0.53	0.48
Mono-aromatic Compounds	0.02	0.10	0.32	0.67	0.84	0.89	0.91
Di-aromatic Compounds	0.01	0.03	0.08	0.14	0.18	0.19	0.19
Phenolic Compounds	0.00	0.00	0.03	0.06	0.07	0.06	0.07
Thiophenic Compounds	0.01	0.09	0.28	0.44	0.48	0.49	0.49
Single Compounds	mg/g sample	mg/g sample	mg/g sample	mg/g sample	mg/g sample	mg/g sample	mg/g sample
Methane	0.01	0.04	0.19	0.65	1.33	1.64	1.78
Ethene	0.00	0.01	0.05	0.14	0.27	0.33	0.37
Ethane	0.00	0.02	0.14	0.62	0.81	0.87	0.85
Propane	0.01	0.04	0.24	0.79	1.00	0.96	0.88
i-Butane	0.00	0.00	0.01	0.03	0.03	0.04	0.04
1-Butene	0.01	0.03	0.11	0.34	0.38	0.40	0.44
<i>n</i> -Butane	0.00	0.01	0.07	0.20	0.24	0.25	0.27
i-Pentane	0.00	0.00	0.05	0.11	0.13	0.07	0.08
Pentene	0.00	0.01	0.04	0.16	0.18	0.18	0.19
<i>n</i> -Pentane	0.00	0.01	0.05	0.14	0.15	0.16	0.16
Cyclopentane	0.00	0.00	0.00	0.01	0.01	0.01	0.01
2-Methylpentane	0.00	0.00	0.02	0.04	0.04	0.04	0.04
3-Methylpentane	0.00	0.00	0.01	0.01	0.01	0.01	0.01
1-Hexene	0.00	0.01	0.05	0.16	0.18	0.18	0.19
<i>n</i> -Hexane	0.00	0.01	0.03	0.11	0.11	0.12	0.12
Methylcyclopentane	0.00	0.00	0.00	0.01	0.01	0.01	0.01
Benzene	0.01	0.02	0.04	0.06	0.10	0.11	0.13
Thiophene	0.00	0.01	0.02	0.03	0.03	0.03	0.03
Cyclohexane	0.00	0.00	0.00	0.01	0.01	0.01	0.01
2-Methylhexane	0.00	0.00	0.01	0.02	0.02	0.02	0.02
2,3-Dimethylpentane	0.00	0.00	0.00	0.01	0.01	0.01	0.01
1,1-Dimethylpentane	0.00	0.00	0.00	0.00	0.00	0.00	0.00
3-Methylhexane	0.00	0.00	0.01	0.01	0.01	0.01	0.01
1-Heptene	0.00	0.00	0.03	0.12	0.14	0.14	0.15
<i>n</i> -Heptane	0.00	0.01	0.04	0.11	0.12	0.12	0.12
Methyl-Cyclohexane	0.00	0.00	0.01	0.01	0.02	0.02	0.02
Ethylcyclopentane	0.00	0.00	0.00	0.01	0.01	0.01	0.01
2,5-Dimethylhexane	0.00	0.00	0.02	0.03	0.04	0.04	0.04
2,4-Dimethylhexane	0.00	0.00	0.00	0.01	0.01	0.01	0.01
3,3-Dimethylhexane	0.00	0.00	0.01	0.03	0.03	0.03	0.02
2,3,4-Trimethylpentane	0.00	0.00	0.02	0.04	0.04	0.04	0.04
Toluene	0.00	0.02	0.07	0.16	0.21	0.22	0.23
2-Methylthiophene	0.01	0.03	0.08	0.13	0.13	0.14	0.14
3-Methylthiophene	0.00	0.00	0.01	0.02	0.02	0.03	0.03
1-Octene	0.00	0.00	0.03	0.11	0.12	0.12	0.13
<i>n</i> -Octane	0.00	0.01	0.03	0.10	0.10	0.10	0.11
Ethylbenzene	0.00	0.01	0.02	0.05	0.05	0.06	0.06
Ethylthiophene	0.00	0.01	0.03	0.05	0.06	0.05	0.05
2,5-Dimethylthiophene	0.00	0.01	0.03	0.06	0.07	0.07	0.07
<i>m/p</i> -Xylene	0.01	0.03	0.08	0.14	0.18	0.18	0.18
2,4-Dimethylthiophene	0.00	0.01	0.02	0.04	0.04	0.04	0.04
2,3-Dimethylthiophene	0.00	0.01	0.02	0.03	0.04	0.04	0.04
Styrene	0.00	0.00	0.02	0.04	0.05	0.05	0.05
<i>o</i> -Xylene	0.00	0.01	0.03	0.07	0.08	0.09	0.08
1-Nonene	0.00	0.00	0.02	0.08	0.09	0.09	0.09
<i>n</i> -Nonane	0.00	0.00	0.03	0.07	0.08	0.08	0.08
2-Propylthiophene	0.00	0.01	0.01	0.02	0.02	0.02	0.02
Propylbenzene	0.00	0.00	0.01	0.01	0.01	0.01	0.01
2-Ethyl-5-Methylthiophene	0.00	0.01	0.04	0.06	0.06	0.07	0.07
(?) -Benzene	0.00	0.01	0.02	0.05	0.06	0.06	0.06
1,3,5-Trimethylbenzene	0.00	0.00	0.01	0.01	0.02	0.02	0.02
Phenol	0.00	0.00	0.00	0.01	0.01	0.01	0.01
1-Ethyl-2-Methylbenzene	0.00	0.00	0.01	0.03	0.04	0.04	0.04
2,3,5-Trimethylthiophene	0.00	0.00	0.00	0.00	0.00	0.00	0.00

Table A 5 continued: Spekk Fm. ample G001955

Table A 5: stepwise open-system pyrolysis GC-FID

Formation/Basin	Spekk Fm.						
GFZ Code	G001955						
Temperature [°C]	200-300	200-350	200-400	200-450	200-500	200-550	200-600
1,2,4-Trimethylbenzene	0.00	0.01	0.02	0.05	0.06	0.06	0.06
1-Decene	0.00	0.00	0.02	0.07	0.08	0.08	0.08
<i>n</i> -Decane	0.00	0.00	0.02	0.06	0.06	0.06	0.06
1,2,3-Trimethylbenzene	0.00	0.01	0.03	0.04	0.04	0.04	0.04
<i>o</i> -Cresol	0.00	0.00	0.01	0.01	0.02	0.01	0.02
<i>m/p</i> -Cresol	0.00	0.00	0.02	0.03	0.04	0.03	0.04
Dimethylphenol	0.00	0.00	0.00	0.01	0.01	0.01	0.01
1-Undecene	0.00	0.00	0.03	0.07	0.08	0.08	0.08
<i>n</i> -Undecane	0.00	0.00	0.02	0.06	0.06	0.06	0.06
1,2,3,4-Tetramethylbenzene	0.00	0.00	0.00	0.01	0.01	0.02	0.02
Naphthalene	0.00	0.00	0.01	0.02	0.03	0.04	0.04
1-Dodecene	0.00	0.00	0.02	0.06	0.07	0.07	0.07
<i>n</i> -Dodecane	0.00	0.00	0.02	0.05	0.06	0.06	0.06
2-Methylnaphthalene	0.00	0.01	0.02	0.04	0.05	0.05	0.05
1-Tridecene	0.00	0.00	0.02	0.05	0.05	0.05	0.05
1-Methylnaphthalene	0.00	0.00	0.01	0.03	0.03	0.03	0.04
<i>n</i> -Tridecane	0.00	0.01	0.03	0.06	0.06	0.06	0.06
1-Tetradecene	0.00	0.01	0.02	0.05	0.06	0.06	0.06
<i>n</i> -Tetradecane	0.01	0.01	0.02	0.05	0.05	0.05	0.06
Dimethylnaphthalene	0.00	0.01	0.02	0.04	0.05	0.04	0.04
1-Pentadecene	0.00	0.00	0.02	0.06	0.07	0.07	0.07
<i>n</i> -Pentadecane	0.01	0.01	0.02	0.04	0.05	0.05	0.05
Trimethylnaphthalene	0.00	0.00	0.00	0.01	0.01	0.01	0.01
Trimethylnaphthalene	0.00	0.00	0.00	0.01	0.01	0.01	0.01
Trimethylnaphthalene	0.00	0.00	0.00	0.00	0.00	0.00	0.00
1-Hexadecene	0.00	0.00	0.01	0.03	0.04	0.04	0.03
<i>n</i> -Hexadecane	0.01	0.01	0.02	0.04	0.04	0.04	0.04
Isopropyldimethylnaphthalene	0.00	0.00	0.00	0.00	0.00	0.00	0.00
1-Heptadecene	0.00	0.00	0.01	0.03	0.03	0.03	0.02
<i>n</i> -Heptadecane	0.00	0.01	0.02	0.04	0.04	0.04	0.04
Pristane	0.00	0.00	0.00	0.01	0.01	0.01	0.01
Prist.-1-ene	0.00	0.00	0.01	0.02	0.02	0.02	0.02
1-Octadecene	0.00	0.00	0.01	0.02	0.02	0.02	0.02
<i>n</i> -Octadecane	0.00	0.00	0.01	0.03	0.03	0.03	0.03
Phytane	0.00	0.00	0.00	0.01	0.01	0.01	0.01
1-Nonadecene	0.00	0.00	0.01	0.01	0.01	0.01	0.01
<i>n</i> -Nonadecane	0.00	0.00	0.01	0.03	0.03	0.03	0.02
1-Icosene	0.00	0.00	0.00	0.01	0.01	0.01	0.01
<i>n</i> -Icosane	0.00	0.00	0.01	0.02	0.02	0.02	0.02
1-Henicosene	0.00	0.00	0.00	0.01	0.01	0.01	0.01
<i>n</i> -Henicosane	0.00	0.00	0.01	0.02	0.02	0.02	0.01
1-Docosene	0.00	0.00	0.00	0.01	0.01	0.01	0.01
<i>n</i> -Docosane	0.00	0.00	0.01	0.01	0.01	0.01	0.01
1-Tricosene	0.00	0.00	0.00	0.01	0.01	0.01	0.01
<i>n</i> -Tricosane	0.00	0.00	0.01	0.01	0.01	0.01	0.01
1-Tetracosene	0.00	0.00	0.00	0.00	0.01	0.01	0.00
<i>n</i> -Tetracosane	0.00	0.00	0.00	0.01	0.01	0.01	0.01
1-Pentacosene	0.00	0.00	0.00	0.00	0.00	0.00	0.00
<i>n</i> -Pentacosane	0.00	0.00	0.00	0.01	0.01	0.01	0.01
1-Hexacosene	0.00	0.00	0.00	0.00	0.00	0.00	0.00
<i>n</i> -Hexacosane	0.00	0.00	0.00	0.01	0.01	0.01	0.00
1-Heptacosene	0.00	0.00	0.00	0.00	0.00	0.00	0.00
<i>n</i> -Heptacosane	0.00	0.00	0.00	0.00	0.01	0.01	0.00
1-Octacosene	0.00	0.00	0.00	0.00	0.00	0.00	0.00
<i>n</i> -Octacosane	0.00	0.00	0.00	0.00	0.00	0.00	0.00
1-Nonacosene	0.00	0.00	0.00	0.00	0.00	0.00	0.00
<i>n</i> -Nonacosane	0.00	0.00	0.00	0.00	0.00	0.00	0.00
1-Triacontene	0.00	0.00	0.00	0.00	0.00	0.00	0.00
<i>n</i> -Triacontane	0.00	0.00	0.00	0.00	0.00	0.00	0.00
<i>n</i> -C31:1	0.00	0.00	0.00	0.00	0.00	0.00	0.00
<i>n</i> -C31	0.00	0.00	0.00	0.00	0.00	0.00	0.00
<i>n</i> -C32:1	0.00	0.00	0.00	0.00	0.00	0.00	0.00
<i>n</i> -C32	0.00	0.00	0.00	0.00	0.00	0.00	0.00
<i>n</i> -C33:1	0.00	0.00	0.00	0.00	0.00	0.00	0.00
<i>n</i> -C33	0.00	0.00	0.00	0.00	0.00	0.00	0.00
<i>n</i> -C34:1	0.00	0.00	0.00	0.00	0.00	0.00	0.00
<i>n</i> -C34	0.00	0.00	0.00	0.00	0.00	0.00	0.00
<i>n</i> -C35:1	0.00	0.00	0.00	0.00	0.00	0.00	0.00
<i>n</i> -C35	0.00	0.00	0.00	0.00	0.00	0.00	0.00
<i>n</i> -C36:1	0.00	0.00	0.00	0.00	0.00	0.00	0.00
<i>n</i> -C36	0.00	0.00	0.00	0.00	0.00	0.00	0.00
<i>n</i> -C37:1	0.00	0.00	0.00	0.00	0.00	0.00	0.00
<i>n</i> -C37	0.00	0.00	0.00	0.00	0.00	0.00	0.00
<i>n</i> -C38:1	0.00	0.00	0.00	0.00	0.00	0.00	0.00
<i>n</i> -C38	0.00	0.00	0.00	0.00	0.00	0.00	0.00
<i>n</i> -C39:1	0.00	0.00	0.00	0.00	0.00	0.00	0.00
<i>n</i> -C39	0.00	0.00	0.00	0.00	0.00	0.00	0.00

Table A 5 continued: Spekk Fm. ample G001955

Table A 6: stepwise closed-system (MSSV)-pyrolysis

Table A 6: stepwise closed-system (MSSV)-pyrolysis

Formation/Basin	Are Fm. G001965											
GFZ Code	1965AA	1965AB	1965AC	1965AD	1965AE/M	1965AF/N	1965AG	1965AH	1965AI	1965AK	1965AL	
File	200-300	200-350	200-400	200-450	200-500	200-550	200-601.1	200-653.1	200-700.9	200-740.1	200-780	
Temperature [°C]	1 K/min	1 K/min	1 K/min	1 K/min	1 K/min	1 K/min	1 K/min	1 K/min	1 K/min	1 K/min	1 K/min	
Rate	1 K/min	1 K/min	1 K/min	1 K/min	1 K/min	1 K/min	1 K/min	1 K/min	1 K/min	1 K/min	1 K/min	
Totals	mg/g sample	mg/g sample	mg/g sample	mg/g sample	mg/g sample	mg/g sample	mg/g sample	mg/g sample	mg/g sample	mg/g sample	mg/g sample	mg/g sample
C1+ (-blank)	6.84	11.30	26.26	39.09	48.40	48.22	46.48	49.99	51.28	52.80	46.70	
C1-5	0.40	1.22	4.80	14.26	32.38	38.74	41.23	47.24	50.74	52.62	46.33	
C2-5	0.31	0.90	3.44	8.94	17.61	10.66	3.60	0.58	0.24	0.15	0.38	
C6-14 (-blank)	2.73	4.74	11.98	18.98	13.12	8.34	4.84	2.65	0.42	0.05	0.05	
C6-14 Hump	1.24	1.84	3.56	3.14	1.33	0.83	0.15	0.14	0.00	0.00	0.00	
C6-14 Resolved	1.49	2.90	8.43	15.84	11.79	7.51	4.70	2.51	0.42	0.05	0.05	
C15+ (-blank)	3.71	5.34	9.47	5.85	2.90	1.14	0.40	0.09	0.12	0.14	0.32	
C15+ Hump	3.26	4.21	7.05	3.68	1.96	0.86	0.00	0.09	0.12	0.14	0.32	
C15+ Resolved	0.45	1.12	2.42	2.17	0.94	0.28	0.40	0.01	0.00	0.00	0.00	
GOR	0.06	0.12	0.22	0.57	2.02	4.09	7.86	17.21	94.12	286.49	124.48	
Gas Wetness (C <sub>2-5</sub> /C <sub>1-5</sub> )	0.79	0.74	0.72	0.63	0.54	0.28	0.09	0.01	0.00	0.00	0.01	
Compound	mg/g sample	mg/g sample	mg/g sample	mg/g sample	mg/g sample	mg/g sample	mg/g sample	mg/g sample	mg/g sample	mg/g sample	mg/g sample	mg/g sample
Methane	0.08	0.32	1.37	5.32	14.77	28.09	37.63	46.67	50.50	52.47	45.94	
Ethane	0.02	0.09	0.63	3.01	6.77	8.07	3.51	0.50	0.17	0.09	0.11	
Propane	0.03	0.14	0.70	2.52	5.56	2.14	0.03	0.00	0.00	0.00	0.00	
i-Butane	0.00	0.00	0.10	0.00	1.05	0.11	0.00	0.00	0.00	0.00	0.00	
n-Butane	0.00	0.00	0.19	0.00	1.61	0.03	0.00	0.00	0.00	0.00	0.00	
i-Pentane	0.06	0.29	0.67	1.19	0.57	0.01	0.00	0.00	0.00	0.00	0.00	
n-Pentane	0.00	0.02	0.13	0.66	0.32	0.00	0.00	0.00	0.00	0.00	0.00	
Cyclopentane	0.00	0.00	0.03	0.11	0.11	0.00	0.00	0.00	0.00	0.00	0.00	
2-Methylpentane	0.00	0.01	0.07	0.24	0.01	0.00	0.00	0.00	0.00	0.00	0.00	
3-Methylpentane	0.00	0.01	0.02	0.08	0.02	0.00	0.00	0.00	0.00	0.00	0.00	
n-Hexane	0.00	0.01	0.08	0.41	0.11	0.00	0.00	0.00	0.00	0.00	0.00	
Methylcyclopentane	0.00	0.00	0.05	0.20	0.18	0.00	0.00	0.00	0.00	0.00	0.00	
Benzene	0.01	0.02	0.06	0.16	0.46	1.02	2.80	2.34	0.35	0.04	0.02	
Thiophene	0.00	0.01	0.03	0.02	0.02	0.00	0.00	0.00	0.00	0.00	0.00	
Cyclohexane	0.00	0.00	0.02	0.03	0.03	0.00	0.00	0.00	0.00	0.00	0.00	
2-Methylhexane	0.01	0.02	0.08	0.05	0.01	0.00	0.00	0.00	0.00	0.00	0.00	
2,3-Dimethylpentane	0.00	0.00	0.01	0.03	0.00	0.00	0.00	0.00	0.00	0.00	0.00	
1,1-Dimethylpentane	0.00	0.00	0.00	0.01	0.01	0.00	0.00	0.00	0.00	0.00	0.00	
3-Methylhexane	0.00	0.01	0.03	0.09	0.01	0.00	0.00	0.00	0.00	0.00	0.00	
n-Heptane	0.01	0.02	0.11	0.40	0.03	0.00	0.00	0.00	0.00	0.00	0.00	
Methyl-Cyclohexane	0.01	0.01	0.03	0.05	0.05	0.01	0.00	0.00	0.00	0.00	0.00	
Ethylcyclopentane	0.00	0.00	0.01	0.06	0.02	0.00	0.00	0.00	0.00	0.00	0.00	
2,5-Dimethylhexane	0.00	0.01	0.02	0.03	0.01	0.00	0.00	0.00	0.00	0.00	0.00	
2,4-Dimethylhexane	0.00	0.00	0.00	0.00	0.00	0.00	0.00	0.00	0.00	0.00	0.00	
3,3-Dimethylhexane	0.00	0.00	0.00	0.00	0.00	0.00	0.00	0.00	0.00	0.00	0.00	
2,3,4-Trimethylpentane	0.00	0.01	0.04	0.05	0.01	0.00	0.00	0.00	0.00	0.00	0.00	
Toluene	0.01	0.05	0.22	0.66	1.49	2.08	0.98	0.02	0.00	0.00	0.00	
2-Methylthiophene	0.01	0.02	0.05	0.07	0.05	0.01	0.00	0.00	0.00	0.00	0.00	
3-Methylthiophene	0.00	0.01	0.02	0.03	0.03	0.01	0.00	0.00	0.00	0.00	0.00	
n-Octane	0.00	0.01	0.07	0.28	0.01	0.00	0.00	0.00	0.00	0.00	0.00	
Ethylbenzene	0.01	0.02	0.08	0.21	0.32	0.15	0.01	0.00	0.00	0.00	0.00	
Ethylthiophene	0.00	0.01	0.02	0.03	0.01	0.00	0.00	0.00	0.00	0.00	0.00	
2,5-Dimethylthiophene	0.00	0.00	0.02	0.03	0.01	0.00	0.00	0.00	0.00	0.00	0.00	
m/p-Xylene	0.01	0.05	0.18	0.53	1.01	0.97	0.07	0.00	0.00	0.00	0.00	
2,4-Dimethylthiophene	0.00	0.02	0.03	0.04	0.03	0.03	0.00	0.00	0.00	0.00	0.00	
2,3-Dimethylthiophene	0.00	0.01	0.04	0.04	0.02	0.00	0.00	0.00	0.00	0.00	0.00	
Styrene	0.00	0.00	0.00	0.00	0.00	0.00	0.00	0.00	0.00	0.00	0.00	
o-Xylene	0.00	0.02	0.08	0.26	0.41	0.21	0.01	0.00	0.00	0.00	0.00	
n-Nonane	0.00	0.01	0.05	0.20	0.00	0.00	0.00	0.00	0.00	0.00	0.00	
2-Propylthiophene	0.00	0.01	0.02	0.07	0.04	0.01	0.00	0.00	0.00	0.00	0.00	
Propylbenzene	0.00	0.01	0.03	0.02	0.00	0.00	0.00	0.00	0.00	0.00	0.00	
2-Ethyl-5-Methylthiophene	0.00	0.01	0.02	0.03	0.02	0.03	0.00	0.00	0.00	0.00	0.00	
(?)-Benzene	0.01	0.02	0.09	0.26	0.38	0.14	0.01	0.00	0.00	0.00	0.00	
1,3,5-Trimethylbenzene	0.02	0.03	0.05	0.22	0.22	0.13	0.01	0.00	0.00	0.00	0.00	
Phenol	0.03	0.20	0.57	0.71	1.27	0.77	0.08	0.00	0.00	0.00	0.00	
1-Ethyl-2-Methylbenzene	0.00	0.01	0.04	0.09	0.11	0.03	0.01	0.00	0.00	0.00	0.00	
2,3,5-Trimethylthiophene	0.00	0.00	0.00	0.03	0.01	0.00	0.00	0.00	0.00	0.00	0.00	
1,2,4-Trimethylbenzene	0.01	0.02	0.07	0.19	0.27	0.11	0.01	0.00	0.00	0.00	0.00	
n-Decane	0.01	0.01	0.05	0.18	0.01	0.00	0.00	0.00	0.00	0.00	0.00	
1,2,3-Trimethylbenzene	0.01	0.04	0.10	0.19	0.16	0.04	0.00	0.00	0.00	0.00	0.00	
o-Cresol	0.01	0.05	0.33	0.69	0.60	0.06	0.00	0.00	0.00	0.00	0.00	
m/p-Cresol	0.02	0.11	0.50	0.89	1.02	0.17	0.00	0.00	0.00	0.00	0.00	
Dimethylphenol	0.00	0.01	0.05	0.13	0.07	0.00	0.00	0.00	0.00	0.00	0.00	
n-Undecane	0.01	0.01	0.05	0.17	0.00	0.00	0.00	0.00	0.00	0.00	0.00	
1,2,3,4-Tetramethylbenzene	0.00	0.03	0.17	0.16	0.07	0.01	0.00	0.00	0.00	0.00	0.00	
Naphthalene	0.00	0.01	0.01	0.03	0.09	0.50	0.42	0.01	0.00	0.00	0.00	
n-Dodecane	0.01	0.02	0.08	0.21	0.02	0.00	0.00	0.00	0.00	0.00	0.00	
2-Methylnaphthalene	0.01	0.02	0.07	0.17	0.43	0.33	0.03	0.00	0.00	0.00	0.00	
1-Methylnaphthalene	0.01	0.02	0.07	0.14	0.23	0.09	0.02	0.00	0.00	0.00	0.00	
n-Tridecane	0.02	0.02	0.06	0.13	0.01	0.00	0.00	0.00	0.00	0.00	0.00	
n-Tetradecane	0.03	0.04	0.07	0.12	0.01	0.00	0.00	0.00	0.00	0.00	0.00	
Dimethylnaphthalene	0.06	0.09	0.17	0.28	0.35	0.06	0.02	0.00	0.00	0.00	0.00	
n-Pentadecane	0.03	0.04	0.08	0.12	0.01	0.00	0.00	0.00	0.00	0.00	0.00	
Trimethylnaphthalene	0.01	0.02	0.03	0.00	0.00	0.00	0.00	0.00	0.00	0.00	0.00	
Trimethylnaphthalene	0.02	0.05	0.06	0.04	0.03	0.00	0.00	0.00	0.00	0.00	0.00	
Trimethylnaphthalene	0.00	0.00	0.00	0.07	0.05	0.00	0.00	0.00	0.00	0.00	0.00	
n-Hexadecane	0.02	0.03	0.08	0.08	0.01	0.00	0.00	0.00	0.00	0.00	0.00	
Isopropylidimethylnaphthalene	0.00	0.00	0.00	0.01	0.00	0.00	0.00	0.00	0.00	0.00	0.00	
n-Heptadecane	0.01	0.02	0.05	0.07	0.00	0.00	0.00	0.00	0.00	0.00	0.00	
Pristane	0.01	0.01	0.05	0.02	0.00	0.00	0.00	0.00	0.00	0.00	0.00	
Prist-1-ene	0.01	0.01	0.04	0.01	0.01	0.00	0.00	0.00	0.00	0.00	0.00	
n-Octadecane	0.01	0.01	0.04	0.06	0.00	0.00	0.00	0.00	0.00	0.00	0.00	
Phytane	0.00	0.00	0.02	0.01	0.01	0.00	0.00	0.00	0.00	0.00	0.00	
n-Nonadecane	0.00	0.01	0.04	0.05	0.00	0.00	0.00	0.00	0.00	0.00	0.00	
n-Icosane	0.00	0.01	0.04	0.04	0.01	0.00	0.00	0.00	0.00	0.00	0.00	
n-Henicosane	0.00	0.01	0.03	0.03	0.00	0.00	0.00	0.00	0.00	0.00	0.00	
n-Docosane	0.00	0.01	0.03	0.02	0.00	0.00	0.00	0.00	0.00	0.00	0.00	
n-Tricosane	0.00	0.01	0.03	0.02	0.00	0.00	0.00	0.00	0.00	0.00	0.00	
n-Tetracosane	0.00	0.01	0.03	0.01	0.00	0.00	0.00	0.00	0.00	0.00	0.00	
n-Pentacosane	0.00	0.01	0.02	0.01	0.00	0.00	0.00	0.00	0.00	0.00	0.00	
n-Hexacosane	0.00	0.00	0.02	0.01	0.00	0.00	0.00	0.00	0.00	0.00	0.00	
n-Heptacosane	0.00	0.00	0.01	0.00	0.00	0.00	0.00	0.00	0.00	0.00	0.00	
n-Octacosane	0.00	0.00	0.01	0.00	0.00	0.00	0.00	0.00	0.00	0.00	0.00	
n-Nonacosane	0.00	0.00	0.01	0.00	0.00	0.00	0.00	0.00	0.00	0.00	0.00	
n-Triacontane	0.00	0.00										

Table A 6: stepwise closed-system (MSSV)-pyrolysis

Company										
Formation/Basin		Are Fm.								
GFZ Code		G001965								
File	1965JA	1965JB	1965JC	1965JD	1965GA	1965JE	1965JF	1965JG	1965JI	
Temperature [°C]	500	525	550	575	600.5	620	640	660	700	
Rate	0.1 K/min	0.1 K/min	0.1 K/min	0.1 K/min	0.1 K/min	0.1 K/min	0.1 K/min	0.1 K/min	0.1 K/min	
Totals	mg/g sample	mg/g sample	mg/g sample	mg/g sample	mg/g sample	mg/g sample	mg/g sample	mg/g sample	mg/g sample	
C1+ (-blank)	43.72	43.65	44.68	45.80	48.17	49.23	48.90	49.66	36.85	
C1-5	38.56	40.60	42.07	44.12	47.34	48.95	48.82	49.63	36.84	
C2-5	12.46	6.27	3.75	0.84	1.01	0.59	0.52	0.61	0.70	
C6-14 (-blank)	4.36	3.05	2.60	1.69	0.83	0.29	0.08	0.03	0.01	
C6-14Hump	0.02	0.00	0.00	0.02	0.14	0.00	0.00	0.00	0.00	
C6-14 Resolved	4.34	3.05	2.60	1.66	0.70	0.29	0.08	0.03	0.01	
C15+ (-blank)	0.80	0.00	0.00	0.00	0.00	0.00	0.00	0.00	0.00	
C15+ Hump	0.75	0.00	0.00	0.00	0.00	0.00	0.00	0.00	0.00	
C15+ Resolved	0.06	0.00	0.00	0.00	0.00	0.00	0.00	0.00	0.00	
GOR	7.46	13.29	16.15	26.18	56.96	171.66	578.28	1544.41	3688.67	
Gas Wetness (C <sub>2</sub> -C <sub>14</sub> )	0.32	0.15	0.09	0.02	0.02	0.01	0.01	0.01	0.02	
Compound	mg/g sample	mg/g sample	mg/g sample	mg/g sample	mg/g sample	mg/g sample	mg/g sample	mg/g sample	mg/g sample	
Methane	26.10	34.32	38.32	43.28	46.34	48.36	48.29	49.02	36.14	
Ethane	7.99	4.08	1.90	0.26	0.23	0.17	0.12	0.36	0.48	
Propane	2.92	0.84	0.81	0.33	0.00	0.00	0.00	0.03	0.00	
i-Butane	0.24	0.12	0.00	0.00	0.00	0.00	0.00	0.00	0.00	
n-Butane	0.02	0.00	0.00	0.00	0.00	0.00	0.00	0.00	0.00	
i-Pentane	0.00	0.00	0.00	0.00	0.00	0.00	0.00	0.00	0.00	
n-Pentane	0.00	0.00	0.00	0.00	0.00	0.00	0.00	0.00	0.00	
Cyclopentane	0.00	0.00	0.00	0.00	0.00	0.00	0.00	0.00	0.00	
2-Methylpentane	0.00	0.00	0.00	0.00	0.00	0.00	0.00	0.00	0.00	
3-Methylpentane	0.00	0.00	0.00	0.00	0.00	0.00	0.00	0.00	0.00	
n-Hexane	0.00	0.00	0.00	0.00	0.00	0.00	0.00	0.00	0.00	
Methylcyclopentane	0.00	0.00	0.00	0.00	0.00	0.00	0.00	0.00	0.00	
Benzene	0.95	1.54	1.96	1.51	0.58	0.23	0.06	0.02	0.01	
Thiophene	0.00	0.00	0.00	0.00	0.00	0.00	0.00	0.00	0.00	
Cyclohexane	0.00	0.00	0.00	0.00	0.00	0.00	0.00	0.00	0.00	
2-Methylhexane	0.00	0.00	0.00	0.00	0.00	0.00	0.00	0.00	0.00	
2,3-Dimethylpentane	0.00	0.00	0.00	0.00	0.00	0.00	0.00	0.00	0.00	
1,1-Dimethylpentane	0.00	0.00	0.00	0.00	0.00	0.00	0.00	0.00	0.00	
3-Methylhexane	0.00	0.00	0.00	0.00	0.00	0.00	0.00	0.00	0.00	
n-Heptane	0.00	0.00	0.00	0.00	0.00	0.00	0.00	0.00	0.00	
Methyl-Cyclohexane	0.00	0.00	0.00	0.00	0.00	0.00	0.00	0.00	0.00	
Ethylcyclopentane	0.00	0.00	0.00	0.00	0.00	0.00	0.00	0.00	0.00	
2,5-Dimethylhexane	0.00	0.00	0.00	0.00	0.00	0.00	0.00	0.00	0.00	
2,4-Dimethylhexane	0.00	0.00	0.00	0.00	0.00	0.00	0.00	0.00	0.00	
3,3-Dimethylhexane	0.00	0.00	0.00	0.00	0.00	0.00	0.00	0.00	0.00	
2,3,4-Trimethylpentane	0.00	0.00	0.00	0.00	0.00	0.00	0.00	0.00	0.00	
Toluene	1.79	0.99	0.41	0.02	0.01	0.00	0.00	0.00	0.00	
2-Methylthiophene	0.00	0.00	0.00	0.00	0.00	0.00	0.00	0.00	0.00	
3-Methylthiophene	0.00	0.00	0.00	0.00	0.00	0.00	0.00	0.00	0.00	
n-Octane	0.00	0.00	0.00	0.00	0.00	0.00	0.00	0.00	0.00	
Ethylbenzene	0.03	0.00	0.00	0.00	0.00	0.00	0.00	0.00	0.00	
Ethylthiophene	0.00	0.00	0.00	0.00	0.00	0.00	0.00	0.00	0.00	
2,5-Dimethylthiophene	0.00	0.00	0.00	0.00	0.00	0.00	0.00	0.00	0.00	
m/p-Xylene	0.57	0.05	0.00	0.00	0.00	0.00	0.00	0.00	0.00	
2,4-Dimethylthiophene	0.00	0.00	0.00	0.00	0.00	0.00	0.00	0.00	0.00	
2,3-Dimethylthiophene	0.00	0.00	0.00	0.00	0.00	0.00	0.00	0.00	0.00	
Styrene	0.00	0.00	0.00	0.00	0.00	0.00	0.00	0.00	0.00	
o-Xylene	0.10	0.01	0.00	0.00	0.00	0.00	0.00	0.00	0.00	
n-Nonane	0.00	0.00	0.00	0.00	0.00	0.00	0.00	0.00	0.00	
2-Propylthiophene	0.00	0.00	0.00	0.00	0.00	0.00	0.00	0.00	0.00	
Propylbenzene	0.00	0.00	0.00	0.00	0.00	0.00	0.00	0.00	0.00	
2-Ethyl-5-Methylthiophene	0.00	0.00	0.00	0.00	0.00	0.00	0.00	0.00	0.00	
(?) -Benzene	0.01	0.00	0.00	0.00	0.00	0.00	0.00	0.00	0.00	
1,3,5-Trimethylbenzene	0.04	0.00	0.00	0.00	0.00	0.00	0.00	0.00	0.00	
Phenol	0.00	0.00	0.00	0.00	0.00	0.00	0.00	0.00	0.00	
1-Ethyl-2-Methylbenzene	0.00	0.00	0.00	0.00	0.00	0.00	0.00	0.00	0.00	
2,3,5-Trimethylthiophene	0.00	0.00	0.00	0.00	0.00	0.00	0.00	0.00	0.00	
1,2,4-Trimethylbenzene	0.02	0.00	0.00	0.00	0.00	0.00	0.00	0.00	0.00	
n-Decane	0.00	0.00	0.00	0.00	0.00	0.00	0.00	0.00	0.00	
1,2,3-Trimethylbenzene	0.00	0.00	0.00	0.00	0.00	0.00	0.00	0.00	0.00	
o-Cresol	0.00	0.00	0.00	0.00	0.00	0.00	0.00	0.00	0.00	
m/p-Cresol	0.00	0.00	0.00	0.00	0.00	0.00	0.00	0.00	0.00	
Dimethylphenol	0.00	0.00	0.00	0.00	0.00	0.00	0.00	0.00	0.00	
n-Undecane	0.00	0.00	0.00	0.00	0.00	0.00	0.00	0.00	0.00	
1,2,3,4-Tetramethylbenzene	0.00	0.00	0.00	0.00	0.00	0.00	0.00	0.00	0.00	
Naphthalene	0.40	0.30	0.17	0.02	0.01	0.00	0.00	0.00	0.00	
n-Dodecane	0.00	0.00	0.00	0.00	0.00	0.00	0.00	0.00	0.00	
2-Methylnaphthalene	0.02	0.00	0.00	0.00	0.00	0.00	0.00	0.00	0.00	
1-Methylnaphthalene	0.02	0.00	0.00	0.00	0.00	0.00	0.00	0.00	0.00	
n-Tridecane	0.00	0.00	0.00	0.00	0.00	0.00	0.00	0.00	0.00	
n-Tetradecane	0.00	0.00	0.00	0.00	0.00	0.00	0.00	0.00	0.00	
Dimethylnaphthalene	0.00	0.00	0.00	0.00	0.00	0.00	0.00	0.00	0.00	
n-Pentadecane	0.00	0.00	0.00	0.00	0.00	0.00	0.00	0.00	0.00	
Trimethylnaphthalene	0.00	0.00	0.00	0.00	0.00	0.00	0.00	0.00	0.00	
Trimethylnaphthalene	0.00	0.00	0.00	0.00	0.00	0.00	0.00	0.00	0.00	
Trimethylnaphthalene	0.00	0.00	0.00	0.00	0.00	0.00	0.00	0.00	0.00	
n-Hexadecane	0.00	0.00	0.00	0.00	0.00	0.00	0.00	0.00	0.00	
Isopropylidimethylnaphthalene	0.00	0.00	0.00	0.00	0.00	0.00	0.00	0.00	0.00	
n-Heptadecane	0.00	0.00	0.00	0.00	0.00	0.00	0.00	0.00	0.00	
Pristane	0.00	0.00	0.00	0.00	0.00	0.00	0.00	0.00	0.00	
Prist.-1-ene	0.00	0.00	0.00	0.00	0.00	0.00	0.00	0.00	0.00	
n-Octadecane	0.00	0.00	0.00	0.00	0.00	0.00	0.00	0.00	0.00	
Phytane	0.00	0.00	0.00	0.00	0.00	0.00	0.00	0.00	0.00	
n-Nonadecane	0.00	0.00	0.00	0.00	0.00	0.00	0.00	0.00	0.00	
n-Icosane	0.00	0.00	0.00	0.00	0.00	0.00	0.00	0.00	0.00	
n-Henicosane	0.00	0.00	0.00	0.00	0.00	0.00	0.00	0.00	0.00	
n-Docosane	0.00	0.00	0.00	0.00	0.00	0.00	0.00	0.00	0.00	
n-Tricosane	0.00	0.00	0.00	0.00	0.00	0.00	0.00	0.00	0.00	
n-Tetracosane	0.00	0.00	0.00	0.00	0.00	0.00	0.00	0.00	0.00	
n-Pentacosane	0.00	0.00	0.00	0.00	0.00	0.00	0.00	0.00	0.00	
n-Hexacosane	0.00	0.00	0.00	0.00	0.00	0.00	0.00	0.00	0.00	
n-Heptacosane	0.00	0.00	0.00	0.00	0.00	0.00	0.00	0.00	0.00	
n-Octacosane	0.00	0.00	0.00	0.00	0.00	0.00	0.00	0.00	0.00	
n-Nonacosane	0.00	0.00	0.00	0.00	0.00	0.00	0.00	0.00	0.00	
n-Triacontane	0.00	0.00	0.00	0.00	0.00	0.00	0.00	0.00	0.00	
Summations	mg/g sample	mg/g sample	mg/g sample	mg/g sample	mg/g sample	mg/g sample	mg/g sample	mg/g sample	mg/g sample	
n-C <sub>6-14</sub>	0.00	0.00	0.00	0.00	0.00	0.00	0.00	0.00	0.00	
n-C <sub>15+</sub>	0.00	0.00	0.00	0.00	0.00	0.00	0.00	0.00	0.00	
Mono-aromatic Compounds	3.50	2.59	2.37	1.53	0.60	0.24	0.06	0.02	0.01	
Di-aromatic Compounds	0.43	0.30	0.17	0.02	0.01	0.00	0.00	0.00	0.00	
Phenolic Compounds	0.00	0.00	0.00	0.00	0.00	0.00	0.00	0.00	0.00	
Thiophenic Compounds	0.00	0.00	0.00	0.00	0.00	0.00	0.00	0.00	0.00	

Table A 6 continued: Are Fm. sample G001965 at 0.1°C/min

Table A 6 continued: Åre Fm. sample G001965 at 0.7°C/min

Formation/Basin		Spekk Fm. G001955													
GFZ Code	File	1955DA	1955DB	1955DC	1955DD	1955DE	1955DF	1955DG	1955DH	1955DI	1955DK	1955DM	1955DN	1955EH	
Temperature [°C]	Rate	200-300 1 K/min	200-351.6 1 K/min	200-400 1 K/min	200-425 1 K/min	200-450 1 K/min	200-475.1 1 K/min	200-500 1 K/min	200-550 1 K/min	200-600 1 K/min	200-650.6 1 K/min	200-700.5 1 K/min	200-740 1 K/min	200-780 1 K/min	
Totals		mg/g sample	mg/g sample	mg/g sample	mg/g sample	mg/g sample	mg/g sample	mg/g sample	mg/g sample	mg/g sample	mg/g sample	mg/g sample	mg/g sample	mg/g sample	
C1+ (-blank)		2.93	6.11	12.99	17.15	18.66	20.56	18.99	17.41	15.76	14.72	12.85	10.26	8.50	
C1-5		0.15	0.46	1.58	3.24	6.00	11.01	13.39	14.07	13.66	12.41	10.20	8.50	8.50	
C2-5		0.11	0.36	1.22	2.52	4.64	8.49	9.39	6.22	2.40	0.24	0.02	0.03	0.04	
C6-14 (-blank)		1.38	2.56	6.18	8.91	9.98	8.03	4.97	3.14	1.87	1.05	0.24	0.07	0.00	
C6-14Hump		0.62	1.06	2.00	2.18	1.50	0.51	0.13	0.03	0.01	0.04	0.00	0.00	0.00	
C6-14 Resolved		0.76	1.50	4.19	6.74	8.48	7.52	4.84	3.11	1.86	1.01	0.24	0.07	0.00	
C15+ (-blank)		1.41	3.09	5.23	5.00	2.68	1.52	0.63	0.20	0.03	0.00	0.00	0.00	0.00	
C15+ Hump		0.34	0.53	1.00	1.25	1.00	0.72	0.44	0.13	0.03	0.00	0.00	0.00	0.00	
C15+ Resolved		1.07	2.56	4.23	3.75	1.69	0.81	0.19	0.07	0.00	0.00	0.00	0.00	0.00	
GOR		0.05	0.08	0.14	0.23	0.47	1.15	2.39	4.21	7.31	12.98	51.44	140.43	#DIV/0!	
Gas Wetness (C <sub>2+2</sub> /C <sub>1+5</sub> )		0.79	0.79	0.77	0.78	0.77	0.77	0.70	0.44	0.17	0.02	0.00	0.00	0.00	
Compound		mg/g sample	mg/g sample	mg/g sample	mg/g sample	mg/g sample	mg/g sample	mg/g sample	mg/g sample	mg/g sample	mg/g sample	mg/g sample	mg/g sample	mg/g sample	
Methane		0.03	0.09	0.36	0.72	1.36	2.52	4.00	7.85	11.46	13.42	12.38	10.18	8.46	
Ethane		0.01	0.04	0.22	0.63	1.20	1.94	2.84	3.88	2.35	0.21	0.01	0.01	0.01	
Propane		0.01	0.05	0.28	0.67	1.36	2.29	3.26	2.09	0.02	0.00	0.00	0.00	0.00	
i-Butane		0.00	0.01	0.00	0.00	0.00	0.43	0.63	0.16	0.00	0.00	0.00	0.00	0.00	
n-Butane		0.01	0.03	0.00	0.00	0.00	1.22	1.37	0.01	0.00	0.00	0.00	0.00	0.00	
i-Pentane		0.01	0.06	0.15	0.24	0.40	0.52	0.29	0.01	0.00	0.00	0.00	0.00	0.00	
n-Pentane		0.00	0.01	0.10	0.24	0.40	0.71	0.45	0.00	0.00	0.00	0.00	0.00	0.00	
Cyclopentane		0.00	0.00	0.01	0.03	0.06	0.09	0.10	0.00	0.00	0.00	0.00	0.00	0.00	
2-Methylpentane		0.00	0.01	0.04	0.09	0.16	0.13	0.01	0.00	0.00	0.00	0.00	0.00	0.00	
3-Methylpentane		0.00	0.00	0.01	0.03	0.06	0.07	0.01	0.00	0.00	0.00	0.00	0.00	0.00	
n-Hexane		0.00	0.01	0.07	0.17	0.33	0.40	0.07	0.00	0.00	0.00	0.00	0.00	0.00	
Methylcyclopentane		0.00	0.00	0.03	0.07	0.14	0.23	0.16	0.00	0.00	0.00	0.00	0.00	0.00	
Benzene		0.00	0.01	0.03	0.05	0.07	0.08	0.21	0.39	1.13	0.94	0.22	0.06	0.01	
Thiophene		0.00	0.01	0.01	0.02	0.03	0.04	0.05	0.02	0.00	0.00	0.00	0.00	0.00	
Cyclohexane		0.00	0.00	0											

306

Table A 6: stepwise closed-system (MSSV)-pyrolysis

Formation/Basin	Green River Shale											
GFZ Code	G004750											
File	4750AA	4750AB	4750AC	4750AD	4750AE	4750AF	4750AG	4750AI	4750AJ	4750AL	4750AN	
Temperature [°C]	200-300	200-350	200-400	200-450	200-500	200-550	200-601.3	200-650.2	200-700	200-740	200-780	
Rate	1 K/min	1 K/min	1 K/min	1 K/min	1 K/min	1 K/min	1 K/min	1 K/min	1 K/min	1 K/min	1 K/min	
Totals	mg/g sample	mg/g sample	mg/g sample	mg/g sample	mg/g sample	mg/g sample	mg/g sample	mg/g sample	mg/g sample	mg/g sample	mg/g sample	mg/g sample
C1+ (-blank)	3.05	9.69	33.92	96.36	87.58	73.32	59.52	54.22	48.71	41.50	33.16	
C1-5	0.11	0.47	3.09	20.37	53.29	53.11	46.87	46.82	45.01	41.10	33.07	
C2-5	0.09	0.39	2.55	17.57	42.88	29.75	15.34	4.11	0.27	0.16	0.15	
C6-14 (-blank)	1.14	3.40	11.80	45.46	27.22	17.31	11.45	7.25	3.68	0.40	0.08	
C6-14Hump	0.46	1.39	3.21	5.92	0.90	0.24	0.25	0.05	0.00	0.01	0.04	
C6-14 Resolved	0.68	2.01	8.59	39.54	26.32	17.06	11.20	7.20	3.68	0.39	0.04	
C15+ (-blank)	1.80	5.82	19.03	30.53	7.07	2.90	1.20	0.15	0.02	0.00	0.00	
C15+ Hump	1.09	3.69	12.84	17.82	2.53	0.61	0.41	0.07	0.00	0.00	0.00	
C15+ Resolved	0.71	2.13	6.19	12.71	4.54	2.30	0.79	0.09	0.02	0.00	0.00	
GOR	0.04	0.05	0.10	0.27	1.55	2.63	3.70	6.33	12.15	101.95	377.61	
Gas Wetness (C <sub>2</sub> g/C <sub>1</sub> g)	0.81	0.83	0.83	0.86	0.80	0.56	0.33	0.09	0.01	0.00	0.00	
Compound	mg/g sample	mg/g sample	mg/g sample	mg/g sample	mg/g sample	mg/g sample	mg/g sample	mg/g sample	mg/g sample	mg/g sample	mg/g sample	mg/g sample
Methane	0.02	0.08	0.54	2.80	10.42	23.36	31.52	42.71	44.74	40.94	32.93	
Ethane	0.01	0.02	0.33	2.64	11.20	18.10	15.03	3.93	0.18	0.08	0.08	
Propane	0.00	0.05	0.51	4.04	14.29	9.76	0.12	0.06	0.01	0.03	0.02	
i-Butane	0.00	0.01	0.08	0.52	1.96	0.69	0.00	0.00	0.00	0.00	0.00	
n-Butane	0.00	0.02	0.19	2.04	6.37	0.20	0.00	0.00	0.00	0.00	0.00	
i-Pentane	0.00	0.03	0.11	0.63	0.95	0.04	0.00	0.00	0.00	0.00	0.00	
n-Pentane	0.00	0.01	0.16	1.70	1.79	0.03	0.00	0.00	0.00	0.00	0.00	
Cyclopentane	0.00	0.00	0.01	0.17	0.84	0.04	0.00	0.00	0.00	0.00	0.00	
2-Methylpentane	0.00	0.01	0.09	0.43	0.12	0.01	0.00	0.00	0.00	0.00	0.00	
3-Methylpentane	0.00	0.00	0.02	0.14	0.07	0.00	0.00	0.00	0.00	0.00	0.00	
n-Hexane	0.00	0.01	0.14	1.52	0.41	0.00	0.00	0.00	0.00	0.00	0.00	
Methylcyclopentane	0.00	0.00	0.03	0.43	1.57	0.01	0.00	0.00	0.00	0.00	0.00	
Benzene	0.00	0.02	0.08	0.56	0.69	1.75	4.12	5.74	2.97	0.22	0.00	
Thiophene	0.00	0.00	0.01	0.06	0.10	0.15	0.09	0.00	0.00	0.00	0.00	
Cyclohexane	0.00	0.00	0.02	0.11	0.20	0.00	0.00	0.00	0.00	0.00	0.00	
2-Methylhexane	0.00	0.01	0.03	0.13	0.03	0.00	0.00	0.00	0.00	0.00	0.00	
2,3-Dimethylpentane	0.00	0.00	0.02	0.03	0.01	0.00	0.00	0.00	0.00	0.00	0.00	
1,1-Dimethylpentane	0.00	0.00	0.00	0.02	0.06	0.00	0.00	0.00	0.00	0.00	0.00	
3-Methylhexane	0.00	0.00	0.02	0.14	0.02	0.00	0.00	0.00	0.00	0.00	0.00	
n-Heptane	0.00	0.01	0.18	1.69	0.14	0.00	0.00	0.00	0.00	0.00	0.00	
Methyl-Cyclohexane	0.00	0.01	0.03	0.27	0.33	0.00	0.00	0.00	0.00	0.00	0.00	
Ethylcyclopentane	0.00	0.00	0.01	0.26	0.15	0.00	0.00	0.00	0.00	0.00	0.00	
2,5-Dimethylhexane	0.00	0.01	0.03	0.10	0.03	0.00	0.00	0.00	0.00	0.00	0.00	
2,4-Dimethylhexane	0.00	0.00	0.00	0.00	0.01	0.00	0.00	0.00	0.00	0.00	0.00	
3,3-Dimethylhexane	0.00	0.00	0.00	0.01	0.01	0.00	0.00	0.00	0.00	0.00	0.00	
2,3,4-Trimethylpentane	0.00	0.02	0.07	0.30	0.07	0.00	0.00	0.00	0.00	0.00	0.00	
Toluene	0.00	0.01	0.07	0.62	3.02	4.01	3.46	0.08	0.00	0.00	0.00	
2-Methylthiophene	0.00	0.01	0.07	0.23	0.20	0.05	0.00	0.00	0.00	0.00	0.00	
3-Methylthiophene	0.00	0.00	0.02	0.12	0.12	0.11	0.01	0.01	0.00	0.00	0.00	
n-Octane	0.01	0.02	0.18	1.38	0.05	0.00	0.00	0.00	0.00	0.00	0.00	
Ethylbenzene	0.00	0.01	0.03	0.26	0.85	0.95	0.13	0.01	0.00	0.00	0.00	
Ethylthiophene	0.01	0.01	0.05	0.14	0.10	0.00	0.00	0.00	0.00	0.00	0.00	
2,5-Dimethylthiophene	0.00	0.00	0.02	0.08	0.02	0.00	0.00	0.00	0.00	0.00	0.00	
m/p-Xylene	0.02	0.07	0.25	0.76	1.80	1.87	0.48	0.00	0.00	0.00	0.00	
2,4-Dimethylthiophene	0.00	0.01	0.04	0.12	0.16	0.04	0.00	0.00	0.00	0.00	0.00	
2,3-Dimethylthiophene	0.01	0.01	0.04	0.09	0.07	0.01	0.00	0.00	0.00	0.00	0.00	
Styrene	0.00	0.00	0.00	0.00	0.00	0.00	0.00	0.00	0.00	0.00	0.00	
o-Xylene	0.00	0.01	0.05	0.39	0.94	0.73	0.07	0.00	0.00	0.00	0.00	
n-Nonane	0.01	0.03	0.16	1.25	0.06	0.00	0.00	0.00	0.00	0.00	0.00	
2-Propylthiophene	0.00	0.01	0.03	0.15	0.11	0.02	0.00	0.00	0.00	0.00	0.00	
Propylbenzene	0.00	0.01	0.05	0.07	0.02	0.01	0.00	0.00	0.00	0.00	0.00	
2-Ethyl-5-Methylthiophene	0.00	0.01	0.05	0.15	0.03	0.00	0.00	0.00	0.00	0.00	0.00	
(?)-Benzene	0.00	0.02	0.08	0.41	1.01	0.89	0.03	0.00	0.00	0.00	0.00	
1,3,5-Trimethylbenzene	0.00	0.00	0.03	0.11	0.19	0.14	0.01	0.00	0.00	0.00	0.00	
Phenol	0.00	0.00	0.01	0.05	0.00	0.01	0.00	0.00	0.00	0.00	0.00	
1-Ethyl-2-Methylbenzene	0.00	0.01	0.04	0.23	0.39	0.12	0.00	0.00	0.00	0.00	0.00	
2,3,5-Trimethylthiophene	0.00	0.00	0.00	0.00	0.00	0.00	0.00	0.00	0.00	0.00	0.00	
1,2,4-Trimethylbenzene	0.01	0.02	0.08	0.41	0.69	0.38	0.01	0.00	0.00	0.00	0.00	
n-Decane	0.01	0.03	0.15	1.19	0.02	0.00	0.00	0.00	0.00	0.00	0.00	
1,2,3-Trimethylbenzene	0.01	0.04	0.14	0.34	0.37	0.13	0.00	0.00	0.00	0.00	0.00	
o-Cresol	0.00	0.00	0.02	0.11	0.03	0.01	0.00	0.00	0.00	0.00	0.00	
m/p-Cresol	0.00	0.00	0.01	0.12	0.08	0.01	0.00	0.00	0.00	0.00	0.00	
Dimethylphenol	0.00	0.00	0.01	0.14	0.01	0.00	0.00	0.00	0.00	0.00	0.00	
n-Undecane	0.01	0.03	0.16	1.22	0.05	0.01	0.00	0.00	0.00	0.00	0.00	
1,2,3,4-Tetramethylbenzene	0.00	0.02	0.06	0.16	0.16	0.03	0.00	0.00	0.00	0.00	0.00	
Naphthalene	0.00	0.00	0.01	0.03	0.44	1.31	1.95	0.79	0.00	0.00	0.00	
n-Dodecane	0.01	0.04	0.18	1.01	0.02	0.00	0.00	0.00	0.00	0.00	0.00	
2-Methylnaphthalene	0.00	0.00	0.01	0.04	0.60	1.09	0.15	0.00	0.00	0.00	0.00	
1-Methylnaphthalene	0.00	0.00	0.01	0.02	0.46	0.38	0.00	0.00	0.00	0.00	0.00	
n-Tridecane	0.02	0.05	0.21	0.92	0.00	0.00	0.00	0.00	0.00	0.00	0.00	
n-Tetradecane	0.02	0.06	0.20	0.95	0.03	0.02	0.00	0.00	0.00	0.00	0.00	
Dimethylnaphthalene	0.01	0.02	0.08	0.20	0.54	0.20	0.00	0.00	0.00	0.00	0.00	
n-Pentadecane	0.03	0.07	0.21	0.81	0.05	0.01	0.00	0.00	0.00	0.00	0.00	
Trimethylnaphthalene	0.00	0.00	0.02	0.07	0.07	0.00	0.00	0.00	0.00	0.00	0.00	
Trimethylnaphthalene	0.01	0.02	0.03	0.15	0.09	0.01	0.00	0.00	0.00	0.00	0.00	
Trimethylnaphthalene	0.00	0.00	0.00	0.00	0.00	0.00	0.00	0.00	0.00	0.00	0.00	
n-Hexadecane	0.04	0.08	0.24	0.80	0.06	0.02	0.00	0.00	0.00	0.00	0.00	
Isopropylidimethylnaphthalene	0.00	0.01	0.02	0.03	0.00	0.00	0.00	0.00	0.00	0.00	0.00	
n-Heptadecane	0.04	0.09	0.25	0.72	0.03	0.02	0.00	0.00	0.00	0.00	0.00	
Pristane	0.02	0.03	0.07	0.04	0.02	0.01	0.00	0.00	0.00	0.00	0.00	
Prist-1-ene	0.00	0.01	0.01	0.02	0.02	0.00	0.00	0.00	0.00	0.00	0.00	
n-Octadecane	0.02	0.06	0.17	0.57	0.02	0.03	0.00	0.00	0.00	0.00	0.00	
Phytane	0.07	0.09	0.10	0.04	0.04	0.01	0.00	0.00	0.00	0.00	0.00	
n-Nonadecane	0.02	0.05	0.17	0.52	0.03	0.01	0.00	0.00	0.00	0.00	0.00	
n-Icosane	0.02	0.05	0.16	0.45	0.04	0.01	0.00	0.00	0.00	0.00	0.00	
n-Henicosane	0.01	0.05	0.16	0.38	0.03	0.01	0.00	0.00	0.00	0.00	0.00	
n-Docosane	0.01	0.04	0.15	0.34	0.02	0.01	0.00	0.00	0.00	0.00	0.00	
n-Tricosane	0.01	0.04	0.16	0.31	0.01	0.00	0.00	0.00	0.00	0.00	0.00	
n-Tetracosane	0.01	0.03	0.13	0.26	0.00	0.00	0.00	0.00	0.00	0.00	0.00	
n-Pentacosane	0.01	0.04	0.15	0.24	0.01	0.00	0.00	0.00	0.00	0.00	0.00	
n-Hexacosane	0.00	0.03	0.13	0.20	0.01	0.00	0.00	0.00	0.00	0.00	0.00	
n-Heptacosane	0.01	0.03	0.16	0.19	0.00	0.00	0.00	0.00	0.00	0.00	0.00	
n-Octacosane	0.00	0.02	0.12	0.14	0.00	0.00	0.00	0.00	0.00	0.00	0.00	
n-Nonacosane	0.00	0.02	0.13	0.11	0.00	0.00	0.00	0.00	0.00	0.00	0.00	
n-Triacontane	0.01	0.02	0.09	0.08	0.00	0.00	0.00	0.00	0.00	0.00	0.00	
Summations	mg/g sample	mg/g sample</										

Table A 6: stepwise closed-system (MSSV)-pyrolysis

Formation/Basin	synthetic Mix I/II G0047501965											
GFZ Code	4750BA	4750BB	4750BC	4750BD	4750BE	4750BF	4750BG	4750BI	4750BJ	4750BL	4750BN	
File	200-300	200-350	200-400	200-450	200-500	200-550	200-600	200-650.4	200-700	200-740	200-780	
Temperature [°C]	1 K/min	1 K/min	1 K/min	1 K/min	1 K/min	1 K/min	1 K/min	1 K/min	1 K/min	1 K/min	1 K/min	
Rate	1 K/min	1 K/min	1 K/min	1 K/min	1 K/min	1 K/min	1 K/min	1 K/min	1 K/min	1 K/min	1 K/min	
Totals	mg/g sample	mg/g sample	mg/g sample	mg/g sample	mg/g sample	mg/g sample	mg/g sample	mg/g sample	mg/g sample	mg/g sample	mg/g sample	mg/g sample
C1+ (-blank)	6.12	9.06	35.39	75.16	71.00	63.61	58.29	55.63	54.31	54.27	44.04	
C1-5	0.37	1.04	5.07	24.09	45.68	47.70	50.50	50.44	53.29	54.25	44.04	
C2-5	0.31	0.80	3.83	18.48	31.06	19.46	8.80	1.72	0.27	0.19	0.17	
C6-14 (-blank)	2.46	3.93	14.10	37.86	21.14	13.99	7.46	4.86	1.01	0.01	0.00	
C6-14Hump	1.19	1.49	3.85	5.02	0.91	0.52	0.46	0.29	0.03	0.00	0.00	
C6-14 Resolved	1.27	2.43	10.25	32.84	20.23	13.47	7.00	4.57	0.98	0.01	0.00	
C15+ (-blank)	3.30	4.10	16.22	13.20	4.18	1.92	0.32	0.33	0.00	0.00	0.00	
C15+ Hump	2.48	2.98	11.33	7.21	1.92	0.88	0.17	0.30	0.00	0.00	0.00	
C15+ Resolved	0.82	1.12	4.89	5.99	2.26	1.03	0.16	0.03	0.00	0.00	0.00	
GOR	0.06	0.13	0.17	0.47	1.80	3.00	6.49	9.71	52.69	3690.61	#DIV/0!	
Gas Wetness (C <sub>2-5</sub> /C <sub>1-5</sub> )	0.84	0.77	0.76	0.77	0.68	0.41	0.17	0.03	0.01	0.00	0.00	
Compound	mg/g sample	mg/g sample	mg/g sample	mg/g sample	mg/g sample	mg/g sample	mg/g sample	mg/g sample	mg/g sample	mg/g sample	mg/g sample	mg/g sample
Methane	0.06	0.24	1.24	5.62	14.62	28.24	41.70	48.72	53.03	54.06	43.87	
Ethane	0.02	0.08	0.66	3.94	9.73	13.33	8.60	1.60	0.18	0.10	0.08	
Propane	0.03	0.12	0.78	4.48	10.93	5.39	0.07	0.02	0.02	0.02	0.04	
i-Butane	0.00	0.01	0.12	0.78	1.62	0.13	0.00	0.00	0.00	0.00	0.00	
n-Butane	0.02	0.04	0.27	2.34	3.88	0.05	0.00	0.00	0.00	0.00	0.00	
i-Pentane	0.07	0.15	0.44	1.23	0.77	0.03	0.00	0.00	0.00	0.00	0.00	
n-Pentane	0.01	0.02	0.20	1.67	0.85	0.01	0.00	0.00	0.00	0.00	0.00	
Cyclopentane	0.00	0.00	0.03	0.19	0.37	0.01	0.00	0.00	0.00	0.00	0.00	
2-Methylpentane	0.00	0.01	0.10	0.44	0.04	0.00	0.00	0.00	0.00	0.00	0.00	
3-Methylpentane	0.00	0.01	0.03	0.16	0.03	0.00	0.00	0.00	0.00	0.00	0.00	
n-Hexane	0.00	0.01	0.15	1.29	0.14	0.00	0.00	0.00	0.00	0.00	0.00	
Methylcyclopentane	0.00	0.00	0.05	0.43	0.55	0.00	0.00	0.00	0.00	0.00	0.00	
Benzene	0.01	0.02	0.05	0.18	0.77	1.42	3.83	3.91	0.70	0.01	0.00	
Thiophene	0.00	0.01	0.03	0.05	0.08	0.08	0.00	0.00	0.00	0.00	0.00	
Cyclohexane	0.00	0.00	0.02	0.08	0.09	0.00	0.00	0.00	0.00	0.00	0.00	
2-Methylhexane	0.00	0.01	0.06	0.18	0.01	0.00	0.00	0.00	0.00	0.00	0.00	
2,3-Dimethylpentane	0.01	0.01	0.02	0.03	0.00	0.00	0.00	0.00	0.00	0.00	0.00	
1,1-Dimethylpentane	0.00	0.00	0.00	0.02	0.02	0.00	0.00	0.00	0.00	0.00	0.00	
3-Methylhexane	0.00	0.00	0.02	0.12	0.00	0.00	0.00	0.00	0.00	0.00	0.00	
n-Heptane	0.01	0.03	0.19	1.32	0.04	0.00	0.00	0.00	0.00	0.00	0.00	
Methyl-Cyclohexane	0.00	0.01	0.02	0.16	0.11	0.00	0.00	0.00	0.00	0.00	0.00	
Ethylcyclopentane	0.00	0.00	0.02	0.19	0.04	0.00	0.00	0.00	0.00	0.00	0.00	
2,5-Dimethylhexane	0.00	0.01	0.03	0.07	0.01	0.00	0.00	0.00	0.00	0.00	0.00	
2,4-Dimethylhexane	0.00	0.00	0.00	0.00	0.00	0.00	0.00	0.00	0.00	0.00	0.00	
3,3-Dimethylhexane	0.00	0.00	0.00	0.01	0.00	0.00	0.00	0.00	0.00	0.00	0.00	
2,3,4-Trimethylpentane	0.00	0.01	0.06	0.15	0.02	0.00	0.00	0.00	0.00	0.00	0.00	
Toluene	0.01	0.04	0.18	0.87	2.45	3.32	1.72	0.02	0.00	0.00	0.00	
2-Methylthiophene	0.00	0.02	0.08	0.15	0.18	0.05	0.01	0.00	0.00	0.00	0.00	
3-Methylthiophene	0.00	0.01	0.04	0.05	0.09	0.07	0.00	0.00	0.00	0.00	0.00	
n-Octane	0.01	0.02	0.16	1.03	0.01	0.01	0.00	0.00	0.00	0.00	0.00	
Ethylbenzene	0.01	0.01	0.07	0.34	0.72	0.44	0.02	0.00	0.00	0.00	0.00	
Ethylthiophene	0.00	0.01	0.04	0.06	0.06	0.00	0.00	0.00	0.00	0.00	0.00	
2,5-Dimethylthiophene	0.00	0.00	0.02	0.05	0.01	0.00	0.00	0.00	0.00	0.00	0.00	
m/p-Xylene	0.02	0.06	0.27	0.81	1.50	1.59	0.15	0.00	0.00	0.00	0.00	
2,4-Dimethylthiophene	0.00	0.01	0.06	0.10	0.12	0.01	0.00	0.00	0.00	0.00	0.00	
2,3-Dimethylthiophene	0.00	0.01	0.04	0.07	0.06	0.01	0.00	0.00	0.00	0.00	0.00	
Styrene	0.00	0.00	0.00	0.00	0.00	0.00	0.00	0.00	0.00	0.00	0.00	
o-Xylene	0.01	0.02	0.09	0.42	0.76	0.51	0.01	0.00	0.00	0.00	0.00	
n-Nonane	0.01	0.02	0.14	0.86	0.00	0.00	0.00	0.00	0.00	0.00	0.00	
2-Propylthiophene	0.00	0.01	0.03	0.16	0.05	0.00	0.00	0.00	0.00	0.00	0.00	
Propylbenzene	0.00	0.01	0.05	0.02	0.00	0.00	0.00	0.00	0.00	0.00	0.00	
2-Ethyl-5-Methylthiophene	0.00	0.01	0.05	0.08	0.02	0.00	0.00	0.00	0.00	0.00	0.00	
(?)-Benzene	0.01	0.02	0.10	0.41	0.74	0.41	0.00	0.00	0.00	0.00	0.00	
1,3,5-Trimethylbenzene	0.00	0.01	0.03	0.11	0.17	0.13	0.00	0.00	0.00	0.00	0.00	
Phenol	0.01	0.06	0.28	0.69	0.83	0.83	0.00	0.00	0.00	0.00	0.00	
1-Ethyl-2-Methylbenzene	0.01	0.01	0.06	0.18	0.31	0.09	0.00	0.00	0.00	0.00	0.00	
2,3,5-Trimethylthiophene	0.00	0.00	0.00	0.00	0.00	0.00	0.00	0.00	0.00	0.00	0.00	
1,2,4-Trimethylbenzene	0.01	0.02	0.09	0.33	0.53	0.26	0.00	0.00	0.00	0.00	0.00	
n-Decane	0.01	0.02	0.14	0.78	0.00	0.00	0.00	0.00	0.00	0.00	0.00	
1,2,3-Trimethylbenzene	0.02	0.05	0.16	0.33	0.30	0.09	0.00	0.00	0.00	0.00	0.00	
o-Cresol	0.00	0.02	0.18	0.59	0.45	0.08	0.00	0.00	0.00	0.00	0.00	
m/p-Cresol	0.02	0.04	0.28	0.80	0.75	0.23	0.00	0.00	0.00	0.00	0.00	
Dimethylphenol	0.00	0.00	0.03	0.17	0.06	0.00	0.00	0.00	0.00	0.00	0.00	
n-Undecane	0.01	0.02	0.13	0.75	0.00	0.00	0.00	0.00	0.00	0.00	0.00	
1,2,3,4-Tetramethylbenzene	0.00	0.01	0.05	0.06	0.04	0.00	0.00	0.00	0.00	0.00	0.00	
Naphthalene	0.01	0.01	0.03	0.12	0.36	0.89	0.58	0.06	0.00	0.00	0.00	
n-Dodecane	0.02	0.03	0.15	0.85	0.00	0.00	0.00	0.00	0.00	0.00	0.00	
2-Methylnaphthalene	0.01	0.00	0.05	0.26	0.65	0.70	0.00	0.00	0.00	0.00	0.00	
1-Methylnaphthalene	0.01	0.01	0.05	0.22	0.42	0.24	0.01	0.00	0.00	0.00	0.00	
n-Tridecane	0.02	0.03	0.17	0.73	0.01	0.00	0.00	0.00	0.00	0.00	0.00	
n-Tetradecane	0.03	0.04	0.18	0.59	0.02	0.00	0.00	0.00	0.00	0.00	0.00	
Dimethylnaphthalene	0.05	0.06	0.14	0.31	0.52	0.16	0.00	0.00	0.00	0.00	0.00	
n-Pentadecane	0.04	0.05	0.17	0.44	0.03	0.05	0.00	0.00	0.00	0.00	0.00	
Trimethylnaphthalene	0.01	0.01	0.04	0.06	0.05	0.01	0.00	0.00	0.00	0.00	0.00	
Trimethylnaphthalene	0.01	0.01	0.04	0.10	0.06	0.00	0.00	0.00	0.00	0.00	0.00	
Trimethylnaphthalene	0.00	0.00	0.00	0.00	0.00	0.00	0.00	0.00	0.00	0.00	0.00	
n-Hexadecane	0.05	0.05	0.17	0.41	0.00	0.00	0.00	0.00	0.00	0.00	0.00	
Isopropylidimethylnaphthalene	0.00	0.00	0.00	0.00	0.00	0.00	0.00	0.00	0.00	0.00	0.00	
n-Heptadecane	0.03	0.04	0.17	0.37	0.03	0.01	0.00	0.00	0.00	0.00	0.00	
Pristane	0.02	0.02	0.07	0.01	0.00	0.00	0.00	0.00	0.00	0.00	0.00	
Prist-1-ene	0.01	0.01	0.01	0.01	0.01	0.02	0.00	0.00	0.00	0.00	0.00	
n-Octadecane	0.02	0.03	0.12	0.27	0.01	0.00	0.00	0.00	0.00	0.00	0.00	
Phytane	0.04	0.04	0.07	0.03	0.02	0.01	0.00	0.00	0.00	0.00	0.00	
n-Nonadecane	0.01	0.02	0.12	0.24	0.01	0.01	0.00	0.00	0.00	0.00	0.00	
n-Icosane	0.01	0.02	0.11	0.19	0.00	0.01	0.00	0.00	0.00	0.00	0.00	
n-Henicosane	0.01	0.01	0.12	0.15	0.02	0.02	0.00	0.00	0.00	0.00	0.00	
n-Docosane	0.01	0.01	0.12	0.12	0.01	0.01	0.00	0.00	0.00	0.00	0.00	
n-Tricosane	0.01	0.01	0.12	0.08	0.01	0.00	0.00	0.00	0.00	0.00	0.00	
n-Tetracosane	0.00	0.01	0.10	0.07	0.01	0.00	0.00	0.00	0.00	0.00	0.00	
n-Pentacosane	0.00	0.01	0.10	0.06	0.01	0.00	0.00	0.00	0.00	0.00	0.00	
n-Hexacosane	0.00	0.00	0.09	0.04	0.00	0.00	0.00	0.00	0.00	0.00	0.00	
n-Heptacosane	0.00	0.01	0.09	0.03	0.00	0.00	0.00	0.00	0.00	0.00	0.00	
n-Octacosane	0.00	0.00	0.07	0.02	0.00	0.00	0.00	0.00	0.00	0.00	0.00	
n-Nonacosane	0.00	0.00	0.07	0.02	0.00	0.00	0.00	0.00	0.00	0.00	0.00	
n-Triacontane	0.00	0.00	0.05	0.01	0.00	0.00	0.00	0.00	0.00	0.00	0.00	
Summations	mg/g sample	mg/g sample	mg/g sample									



Table A 7: Late Gas Potential Screening (immature samples)

Table A 7: Late Gas Potential Screening (immature samples)

Company	Shell			Silurian Hot Shale			Silurian Hot Shale			Silurian Hot Shale			Silurian Hot Shale		
Formation/Basin	Akata Shale			Silurian Hot Shale			Silurian Hot Shale			Silurian Hot Shale			Silurian Hot Shale		
GFZ Code	G005935			G005936			G005937			G006948			G006949		
File	G005935AE	G005935AB	G005935AC	G005936AA	G005936AB	G005936AC	G005937AA	G005937AB	G005937AC	G005937AA	G005937AB	G005937AC	G006948A	G006948B	G006948C
Temperature [°C]	200-460	200-560	200-700	200-460	200-560	200-700	200-460	200-560	200-700	200-460	200-560	200-700	200-460	200-560	200-700
Rate	2K/min	2K/min	2K/min	2K/min	2K/min	2K/min	2K/min	2K/min	2K/min	2K/min	2K/min	2K/min	2K/min	2K/min	2K/min
Totals	mg/g TOC	mg/g TOC	mg/g TOC	mg/g TOC	mg/g TOC	mg/g TOC	mg/g TOC	mg/g TOC	mg/g TOC	mg/g TOC	mg/g TOC	mg/g TOC	mg/g TOC	mg/g TOC	mg/g TOC
Total C1+ (-blank)	335.70	194.13	204.38	28.32	19.08	30.45	3.22	6.65	31.54	18.13	36.52	26.30	51.06	26.30	51.06
Total C1-5	95.56	145.51	193.56	14.54	0.20	5.20	0.99	3.36	24.45	4.92	19.34	15.88	38.85	15.88	38.85
Total C2-5	79.22	62.08	1.80	8.64	0.18	1.08	0.61	0.05	0.10	1.42	0.12	2.23	3.05	2.23	3.05
Total C <sub>6-14</sub> (-blank)	173.91	39.67	5.44	3.84	0.00	0.00	0.34	0.14	0.00	5.52	2.83	6.61	3.45	6.61	3.45
Total C <sub>15+</sub> (-blank)	66.23	8.96	5.39	9.94	18.88	25.25	1.88	3.15	7.09	7.69	14.35	3.81	8.76	3.81	8.76
Total C <sub>25+</sub> (-blank)	240.14	48.63	10.83	13.78	18.88	25.25	2.23	3.29	7.09	13.21	17.18	10.42	12.21	10.42	12.21
GOR	0.40	2.99	17.88	1.06	0.01	0.21	0.44	1.02	3.45	0.37	1.13	1.52	3.18	1.52	3.18
Gas Wetness (C <sub>2</sub> /C <sub>1+</sub> )	0.83	0.43	0.01	0.59	0.92	0.21	0.62	0.02	0.00	0.29	0.01	0.14	0.08	0.29	0.01
Compound	mg/g TOC	mg/g TOC	mg/g TOC	mg/g TOC	mg/g TOC	mg/g TOC	mg/g TOC	mg/g TOC	mg/g TOC	mg/g TOC	mg/g TOC	mg/g TOC	mg/g TOC	mg/g TOC	mg/g TOC
Methane	16.34	83.43	191.76	5.90	0.02	4.11	0.38	3.30	24.35	3.50	19.22	13.65	35.80	3.50	19.22
Ethane	14.57	40.33	1.39	2.49	0.02	0.35	0.16	0.00	0.00	1.04	0.01	1.25	1.94	1.04	0.01
Propane	18.50	19.42	0.08	2.44	0.01	0.08	0.16	0.00	0.00	0.00	0.00	0.00	0.00	0.00	0.00
i-Butane	2.74	1.27	0.00	0.37	0.01	0.04	0.02	0.00	0.00	0.00	0.00	0.00	0.00	0.00	0.00
n-Butane	7.03	0.15	0.00	0.91	0.00	0.00	0.05	0.00	0.00	0.00	0.00	0.00	0.00	0.00	0.00
i-Pentane	2.39	0.02	0.00	0.15	0.00	0.00	0.01	0.00	0.00	0.00	0.00	0.00	0.00	0.00	0.00
n-Pentane	4.91	0.03	0.00	0.35	0.00	0.00	0.01	0.00	0.00	0.00	0.00	0.00	0.00	0.00	0.00
Cyclopentane	0.47	0.02	0.00	0.00	0.00	0.00	0.00	0.00	0.00	0.00	0.00	0.00	0.00	0.00	0.00
2-Methylpentane	2.01	0.01	0.00	0.00	0.00	0.00	0.00	0.00	0.00	0.00	0.00	0.00	0.00	0.00	0.00
3-Methylpentane	0.95	0.01	0.00	0.00	0.00	0.00	0.00	0.00	0.00	0.00	0.00	0.00	0.00	0.00	0.00
n-Hexane	4.34	0.01	0.00	0.13	0.00	0.00	0.02	0.00	0.00	0.00	0.00	0.00	0.00	0.00	0.00
Methylcyclopentane	1.78	0.00	0.00	0.01	0.00	0.00	0.00	0.00	0.00	0.00	0.00	0.00	0.00	0.00	0.00
Benzene	0.93	5.62	5.50	1.84	0.00	1.75	0.46	0.51	0.37	5.14	2.43	5.49	2.89	5.14	2.43
Thiophene	0.39	0.59	0.00	0.23	0.00	0.00	0.00	0.00	0.00	0.00	0.00	0.00	0.00	0.00	0.00
Cyclohexane	0.35	0.00	0.00	0.00	0.00	0.00	0.00	0.00	0.00	0.00	0.00	0.00	0.00	0.00	0.00
2-Methylhexane	0.57	0.00	0.00	0.00	0.00	0.00	0.00	0.00	0.00	0.00	0.00	0.00	0.00	0.00	0.00
2,3-Dimethylpentane	0.42	0.00	0.00	0.00	0.00	0.00	0.00	0.00	0.00	0.00	0.00	0.00	0.00	0.00	0.00
1,1-Dimethylpentane	0.00	0.00	0.00	0.00	0.00	0.00	0.00	0.00	0.00	0.00	0.00	0.00	0.00	0.00	0.00
3-Methylhexane	0.64	0.00	0.00	0.00	0.00	0.00	0.00	0.00	0.00	0.00	0.00	0.00	0.00	0.00	0.00
n-Heptane	4.75	0.00	0.00	0.00	0.00	0.00	0.00	0.00	0.00	0.00	0.00	0.00	0.00	0.00	0.00
Methyl-Cyclohexane	0.70	0.00	0.00	0.00	0.00	0.00	0.00	0.00	0.00	0.00	0.00	0.00	0.00	0.00	0.00
Ethylcyclopentane	0.80	0.00	0.00	0.00	0.00	0.00	0.00	0.00	0.00	0.00	0.00	0.00	0.00	0.00	0.00
2,5-Dimethylhexane	0.08	0.00	0.00	0.00	0.00	0.00	0.00	0.00	0.00	0.00	0.00	0.00	0.00	0.00	0.00
2,4-Dimethylhexane	0.02	0.00	0.00	0.00	0.00	0.00	0.00	0.00	0.00	0.00	0.00	0.00	0.00	0.00	0.00
3,3-Dimethylhexane	0.03	0.00	0.00	0.00	0.00	0.00	0.00	0.00	0.00	0.00	0.00	0.00	0.00	0.00	0.00
2,3,4-Trimethylpentane	0.92	0.00	0.00	0.00	0.00	0.00	0.00	0.00	0.00	0.00	0.00	0.00	0.00	0.00	0.00
Toluene	4.00	11.86	0.08	1.13	0.00	0.00	0.00	0.00	0.00	0.01	0.00	0.01	0.01	0.01	0.01
2-Methylthiophene	0.87	0.20	0.00	0.00	0.00	0.00	0.00	0.00	0.00	0.00	0.00	0.00	0.00	0.00	0.00
3-Methylthiophene	0.24	0.25	0.00	0.00	0.00	0.00	0.00	0.00	0.00	0.00	0.00	0.00	0.00	0.00	0.00
n-Octane	3.82	0.00	0.00	0.00	0.00	0.00	0.00	0.00	0.00	0.00	0.00	0.00	0.00	0.00	0.00
Ethylbenzene	1.54	1.01	0.00	0.00	0.00	0.00	0.00	0.00	0.00	0.00	0.00	0.00	0.00	0.00	0.00
Ethylthiophene	0.47	0.00	0.00	0.00	0.00	0.00	0.00	0.00	0.00	0.00	0.00	0.00	0.00	0.00	0.00
2,5-Dimethylthiophene	0.26	0.00	0.00	0.00	0.00	0.00	0.00	0.00	0.00	0.00	0.00	0.00	0.00	0.00	0.00
m/p-Xylene	4.22	4.92	0.00	0.00	0.00	0.00	0.00	0.00	0.00	0.00	0.00	0.00	0.00	0.00	0.00
2,4-Dimethylthiophene	0.64	0.00	0.00	0.00	0.00	0.00	0.00	0.00	0.00	0.00	0.00	0.00	0.00	0.00	0.00
2,3-Dimethylthiophene	0.62	0.00	0.00	0.00	0.00	0.00	0.00	0.00	0.00	0.00	0.00	0.00	0.00	0.00	0.00
Styrene	0.45	0.00	0.00	0.00	0.00	0.00	0.00	0.00	0.00	0.00	0.00	0.00	0.00	0.00	0.00
o-Xylene	2.03	1.52	0.00	0.00	0.00	0.00	0.00	0.00	0.00	0.00	0.00	0.00	0.00	0.00	0.00
n-Nonane	3.00	0.00	0.00	0.00	0.00	0.00	0.00	0.00	0.00	0.00	0.00	0.00	0.00	0.00	0.00
2-Propylthiophene	0.80	0.00	0.00	0.00	0.00	0.00	0.00	0.00	0.00	0.00	0.00	0.00	0.00	0.00	0.00
Propylbenzene	0.08	0.00	0.00	0.00	0.00	0.00	0.00	0.00	0.00	0.00	0.00	0.00	0.00	0.00	0.00
2-Ethyl-5-Methylthiophene	0.39	0.00	0.00	0.00	0.00	0.00	0.00	0.00	0.00	0.00	0.00	0.00	0.00	0.00	0.00
(?) - Benzene	1.97	0.69	0.00	0.00	0.00	0.00	0.00	0.00	0.00	0.00	0.00	0.00	0.00	0.00	0.00
2-Ethyl-4-Methylthiophene	0.33	0.00	0.00	0.00	0.00	0.00	0.00	0.00	0.00	0.00	0.00	0.00	0.00	0.00	0.00
1,3,5-Trimethylbenzene	0.54	0.39	0.00	0.00	0.00	0.00	0.00	0.00	0.00	0.00	0.00	0.00	0.00	0.00	0.00
Phenol	1.14	0.65	0.00	0.00	0.00	0.00	0.00	0.00	0.00	0.00	0.00	0.00	0.00	0.00	0.00
1-Ethyl-2-Methylbenzene	1.24	0.37	0.00	0.00	0.00	0.00	0.00	0.00	0.00	0.00	0.00	0.00	0.00	0.00	0.00
2,3,5-Trimethylthiophene	0.44	0.00	0.00	0.00	0.00	0.00	0.00	0.00	0.00	0.00	0.00	0.00	0.00	0.00	0.00
1,2,4-Trimethylbenzene	1.90	0.56	0.00	0.00	0.00	0.00	0.00	0.00	0.00	0.00	0.00	0.00	0.00	0.00	0.00
n-Decane	2.78	0.00	0.00	0.00	0.00	0.00	0.00	0.00	0.00	0.00	0.00	0.00	0.00	0.00	0.00
1,2,3-Trimethylbenzene	1.64	0.19	0.00	0.00	0.00	0.00	0.00	0.00	0.00	0.00	0.00	0.00	0.00	0.00	0.00
o-Cresol	1.54	0.00	0.00	0.00	0.00	0.00	0.00	0.00	0.00	0.00	0.00	0.00	0.00	0.00	0.00
m/p-Cresol	1.58	0.00	0.00	0.00	0.00	0.00	0.00	0.00	0.00	0.00	0.00	0.00	0.00	0.00	0.00
Dimethylphenol	0.62	0.00	0.00	0.00	0.00	0.00	0.00	0.00	0.00	0.00	0.00	0.00	0.00	0.00	0.00
n-Undecane	2.77	0.00	0.00	0.00											

**Table A 7 continued: samples provided by Total**

Table A 7: Late Gas Potential Screening (immature samples)

Company	Total			Petrobras			ENI		
Formation/Basin	Toarcian Shale			Irati Fm.			Hekkingen Fm.		
GFZ Code	G006209			G005812			G005762		
File	G006209AA	G006209AB	G006209AC	G005812AA	G005812AB	G005812AC	G005762AA	G005762AB	G005762AC
Temperature [°C]	200-460	200-560	200-700	200-480	200-580	200-690	200-480	200-580	200-690
Rate	2K/min	2K/min	2K/min	5K/min	5K/min	5K/min	5K/min	5K/min	5K/min
Totals	mg/g TOC	mg/g TOC	mg/g TOC	mg/g TOC	mg/g TOC	mg/g TOC	mg/g TOC	mg/g TOC	mg/g TOC
Total C1+ (-blank)	484.44	410.97	332.25	421.18	365.54	278.92	134.16	128.57	122.62
Total C1-5	137.37	283.80	280.04	141.13	273.72	244.74	55.07	104.22	113.23
Total C2-5	118.87	149.59	4.08	119.71	142.63	18.15	43.36	36.89	2.66
Total C <sub>6-14</sub> (-blank)	238.60	94.50	19.52	209.47	80.09	34.18	66.48	24.35	9.39
Total C <sub>15+</sub> (-blank)	108.47	32.67	32.69	70.57	11.73	0.00	12.60	0.00	0.00
Total C <sub>6+</sub> (-blank)	347.07	127.17	52.21	280.05	91.82	34.18	79.08	24.35	9.39
GOR	0.40	2.23	5.36	0.50	2.98	7.16	0.70	4.28	12.06
Gas Wetness (C <sub>2-5</sub> /C <sub>1-5</sub> )	0.87	0.53	0.01	0.85	0.52	0.07	0.79	0.35	0.02
Compound	mg/g TOC	mg/g TOC	mg/g TOC	mg/g TOC	mg/g TOC	mg/g TOC	mg/g TOC	mg/g TOC	mg/g TOC
Methane	0.00	0.00	0.00	21.42	131.09	226.58	11.71	67.33	110.57
Ethane	0.00	0.00	0.00	18.37	82.64	17.20	9.79	25.69	1.47
Propane	0.00	0.00	0.00	27.16	49.17	0.21	10.43	9.85	0.25
i-Butane	0.00	0.00	0.00	6.24	5.48	0.00	1.40	0.63	0.00
n-Butane	0.00	0.00	0.00	11.64	1.18	0.00	4.07	0.10	0.00
i-Pentane	0.00	0.00	0.00	7.16	0.24	0.00	2.19	0.01	0.00
n-Pentane	0.00	0.00	0.00	8.15	0.26	0.00	2.61	0.02	0.00
Cyclopentane	0.00	0.00	0.00	0.59	0.21	0.00	0.29	0.01	0.00
2-Methylpentane	0.00	0.00	0.00	5.28	0.07	0.00	0.86	0.00	0.00
3-Methylpentane	0.00	0.00	0.00	1.70	0.01	0.00	0.32	0.00	0.00
n-Hexane	0.00	0.00	0.00	5.39	0.04	0.00	1.74	0.01	0.00
Methylcyclopentane	0.00	0.00	0.00	2.19	0.04	0.00	0.68	0.00	0.00
Benzene	0.00	0.00	0.00	0.50	5.61	27.88	0.71	3.49	9.10
Thiophene	0.00	0.00	0.00	0.26	0.88	0.33	0.29	0.47	0.00
Cyclohexane	0.00	0.00	0.00	0.42	0.00	0.00	0.17	0.00	0.00
2-Methylhexane	0.00	0.00	0.00	1.29	0.00	0.00	0.16	0.00	0.00
2,3-Dimethylpentane	0.00	0.00	0.00	0.35	0.00	0.00	0.21	0.00	0.00
1,1-Dimethylpentane	0.00	0.00	0.00	0.00	0.00	0.00	0.00	0.00	0.00
3-Methylhexane	0.00	0.00	0.00	1.54	0.00	0.00	0.22	0.00	0.00
n-Heptane	0.00	0.00	0.00	6.61	0.00	0.00	1.71	0.00	0.00
Methyl-Cyclohexane	0.00	0.00	0.00	1.06	0.00	0.00	0.31	0.00	0.00
Ethylcyclopentane	0.00	0.00	0.00	0.84	0.00	0.00	0.29	0.00	0.00
2,5-Dimethylhexane	0.00	0.00	0.00	0.32	0.00	0.00	0.05	0.00	0.00
2,4-Dimethylhexane	0.00	0.00	0.00	0.03	0.00	0.00	0.02	0.00	0.00
3,3-Dimethylhexane	0.00	0.00	0.00	0.06	0.00	0.00	0.01	0.00	0.00
2,3,4-Trimethylpentane	0.00	0.00	0.00	1.53	0.00	0.00	0.35	0.00	0.00
Toluene	0.00	0.00	0.00	2.70	14.40	0.99	2.73	6.94	0.15
2-Methylthiophene	0.00	0.00	0.00	0.85	0.52	0.00	1.02	0.25	0.00
3-Methylthiophene	0.00	0.00	0.00	0.28	0.77	0.00	0.27	0.25	0.00
n-Octane	0.00	0.00	0.00	4.70	0.00	0.00	1.21	0.00	0.00
Ethylbenzene	0.00	0.00	0.00	1.15	2.77	0.00	0.86	0.58	0.00
Ethylthiophene	0.00	0.00	0.00	0.47	0.10	0.00	0.44	0.00	0.00
2,5-Dimethylthiophene	0.00	0.00	0.00	0.17	0.00	0.00	0.47	0.00	0.00
m/p-Xylene	0.00	0.00	0.00	5.61	10.87	0.00	2.11	3.02	0.00
2,4-Dimethylthiophene	0.00	0.00	0.00	0.59	0.14	0.00	0.47	0.00	0.00
2,3-Dimethylthiophene	0.00	0.00	0.00	0.59	0.11	0.00	0.55	0.00	0.00
Styrene	0.00	0.00	0.00	1.37	0.03	0.00	0.02	0.00	0.00
o-Xylene	0.00	0.00	0.00	1.81	3.24	0.00	1.12	0.85	0.00
n-Nonane	0.00	0.00	0.00	3.14	0.00	0.00	0.85	0.00	0.00
2-Propylthiophene	0.00	0.00	0.00	0.69	0.08	0.00	0.39	0.00	0.00
Propylbenzene	0.00	0.00	0.00	0.09	0.00	0.00	0.02	0.01	0.00
2-Ethyl-5-Methylthiophene	0.00	0.00	0.00	0.50	0.01	0.00	0.50	0.00	0.00
(?) -Benzene	0.00	0.00	0.00	2.45	4.34	0.00	0.97	0.45	0.00
2-Ethyl-4-Methylthiophene	0.00	0.00	0.00	0.78	0.00	0.00	0.27	0.00	0.00
1,3,5-Trimethylbenzene	0.00	0.00	0.00	0.66	1.13	0.00	0.27	0.25	0.00
Phenol	0.00	0.00	0.00	0.50	0.00	0.00	0.64	0.47	0.00
1-Ethyl-2-Methylbenzene	0.00	0.00	0.00	1.08	0.60	0.00	0.60	0.18	0.00
2,3,5-Trimethylthiophene	0.00	0.00	0.00	0.71	0.00	0.00	0.39	0.00	0.00
1,2,4-Trimethylbenzene	0.00	0.00	0.00	2.78	2.73	0.00	0.73	0.34	0.00
n-Decane	0.00	0.00	0.00	2.42	0.00	0.00	0.67	0.00	0.00
1,2,3-Trimethylbenzene	0.00	0.00	0.00	3.08	1.29	0.00	0.62	0.09	0.00
o-Cresol	0.00	0.00	0.00	0.25	0.00	0.00	0.62	0.06	0.00
m/p-Cresol	0.00	0.00	0.00	0.26	0.00	0.00	0.72	0.15	0.00
Dimethylphenol	0.00	0.00	0.00	0.00	0.00	0.00	0.00	0.00	0.00
n-Undecane	0.00	0.00	0.00	2.26	0.00	0.00	0.64	0.00	0.00
1,2,3,4-Tetramethylbenzene	0.00	0.00	0.00	1.01	0.00	0.00	0.28	0.00	0.00
Naphthalene	0.00	0.00	0.00	0.55	4.15	3.96	0.40	1.83	0.24
n-Dodecane	0.00	0.00	0.00	1.85	0.00	0.00	0.59	0.00	0.00
2-Methylnaphthalene	0.00	0.00	0.00	0.84	5.39	0.08	0.50	0.85	0.00
1-Methylnaphthalene	0.00	0.00	0.00	0.65	2.62	0.06	0.48	0.39	0.00
n-Tridecane	0.00	0.00	0.00	1.67	0.00	0.00	0.49	0.00	0.00
n-Tetradecane	0.00	0.00	0.00	1.28	0.00	0.00	0.36	0.00	0.00
Dimethylnaphthalene	0.00	0.00	0.00	2.17	2.32	0.00	0.75	0.14	0.00
n-Pentadecane	0.00	0.00	0.00	1.22	0.12	0.00	0.34	0.00	0.00
Trimethylnaphthalene	0.00	0.00	0.00	0.48	0.14	0.00	0.12	0.00	0.00
Trimethylnaphthalene	0.00	0.00	0.00	0.66	0.15	0.00	0.14	0.00	0.00
Trimethylnaphthalene	0.00	0.00	0.00	0.63	0.00	0.00	0.22	0.00	0.00
n-Hexadecane	0.00	0.00	0.00	0.73	0.00	0.00	0.22	0.00	0.00
Isopropylidimethylnaphthalene	0.00	0.00	0.00	0.14	0.00	0.00	0.06	0.00	0.00
n-Heptadecane	0.00	0.00	0.00	0.73	0.00	0.00	0.13	0.00	0.00
Pristane	0.00	0.00	0.00	0.45	0.00	0.00	0.03	0.00	0.00
Prist-1-ene	0.00	0.00	0.00	0.07	0.00	0.00	0.01	0.00	0.00
n-Octadecane	0.00	0.00	0.00	0.32	0.00	0.00	0.11	0.00	0.00
Phytane	0.00	0.00	0.00	0.09	0.00	0.00	0.02	0.00	0.00
n-Nonadecane	0.00	0.00	0.00	0.36	0.00	0.00	0.12	0.00	0.00
n-Icosane	0.00	0.00	0.00	0.20	0.00	0.00	0.06	0.00	0.00
n-Henicosane	0.00	0.00	0.00	0.15	0.00	0.00	0.04	0.00	0.00
n-Docosane	0.00	0.00	0.00	0.11	0.00	0.00	0.02	0.00	0.00
n-Tricosane	0.00	0.00	0.00	0.08	0.00	0.00	0.01	0.00	0.00
n-Tetracosane	0.00	0.00	0.00	0.07	0.00	0.00	0.01	0.00	0.00
n-Pentacosane	0.00	0.00	0.00	0.03	0.00	0.00	0.00	0.00	0.00
n-Hexacosane	0.00	0.00	0.00	0.02	0.00	0.00	0.00	0.00	0.00
n-Heptacosane	0.00	0.00	0.00	0.00	0.00	0.00	0.00	0.00	0.00
n-Octacosane	0.00	0.00	0.00	0.00	0.00	0.00	0.00	0.00	0.00
n-Nonacosane	0.00	0.00	0.00	0.00	0.00	0.00	0.00	0.00	0.00
n-Triacontane	0.00	0.00	0.00	0.00	0.00	0.00	0.00	0.00	0.00
Summations	mg/g TOC	mg/g TOC	mg/g TOC	mg/g TOC	mg/g TOC	mg/g TOC	mg/g TOC	mg/g TOC	mg/g TOC
n-C <sub>6-14</sub>	0.00	0.00	0.00	29.32	0.04	0.00	8.26	0.01	0.00
n-C <sub>15+</sub>	0.00	0.00	0.00	4.02	0.12	0.00	1.06	0.00	0.00
Mono-aromatic Compounds	0.00	0.00	0.00	21.91	46.98	28.87	10.73	16.21	9.25
Di-aromatic Compounds	0.00	0.00	0.00	5.97	14.78	4.09	2.61	3.20	0.24
Phenolic Compounds	0.00	0.00	0.00	1.01	0.00	0.00	1.98	0.68	0.00
Thiophenic Compounds	0.00	0.00	0.00	5.88	2.62	0.33	5.06	0.97	0.00

Table A 7 continued: samples provided by Total, Petrobras, and ENI

Table A 7: Late Gas Potential Screening (immature samples)

Company	ENI									
Formation/Basin	Domanik Fm.			Murzuq Basin			G007160		Ghadames Basin	
GFZ Code	G004563			G004564			G007160		G007161	
File	G004563BA	G004563BB	G004563BC	G004564BA	G004564BB	G004564BC	G007160AB	G007160AC	G007161AB	G007161AC
Temperature [°C]	200-480	200-580	200-690	200-480	200-580	200-690	200-560	200-700	200-560	200-700
Rate	5K/min	5K/min	5K/min	5K/min	5K/min	5K/min	2K/min	2K/min	2K/min	2K/min
Totals	mg/g TOC	mg/g TOC	mg/g TOC	mg/g TOC	mg/g TOC	mg/g TOC	mg/g TOC	mg/g TOC	mg/g TOC	mg/g TOC
Total C1+ (-blank)	462.54	405.68	307.29	122.80	125.37	144.64	266.84	229.72	44.93	68.04
Total C1-5	149.84	298.18	264.75	68.51	104.23	132.68	212.90	220.27	36.41	60.52
Total C2-5	126.14	157.02	13.94	52.83	35.77	2.29	93.64	4.46	12.00	8.25
Total C <sub>6-14</sub> (-blank)	227.24	87.79	36.78	50.78	19.19	7.85	50.64	9.12	5.35	2.16
Total C <sub>15+</sub> (-blank)	85.46	19.72	5.77	3.51	1.95	4.11	3.30	0.33	3.17	5.36
Total C <sub>6+</sub> (-blank)	312.70	107.51	42.55	54.30	21.14	11.96	53.94	9.45	8.52	7.52
GOR	0.48	2.77	6.22	1.26	4.93	11.09	3.95	23.31	4.27	8.05
Gas Wetness (C <sub>2+</sub> /C <sub>1-5</sub> )	0.84	0.53	0.05	0.77	0.34	0.02	0.44	0.02	0.33	0.14
Compound	mg/g TOC	mg/g TOC	mg/g TOC	mg/g TOC	mg/g TOC	mg/g TOC	mg/g TOC	mg/g TOC	mg/g TOC	mg/g TOC
Methane	23.69	141.16	250.80	15.68	68.46	130.40	119.25	215.81	24.41	52.27
Ethane	25.25	95.20	13.19	11.67	26.04	0.82	60.79	1.36	4.24	1.45
Propane	28.30	50.69	0.21	13.18	8.37	1.35	25.71	0.00	0.19	0.00
i-Butane	4.77	4.88	0.00	2.40	0.37	0.00	1.89	0.00	0.00	0.00
n-Butane	14.53	1.47	0.00	7.03	0.08	0.00	0.17	0.00	0.00	0.00
i-Pentane	6.09	0.29	0.00	3.08	0.01	0.00	0.03	0.00	0.00	0.00
n-Pentane	9.73	0.31	0.00	4.31	0.02	0.00	0.04	0.00	0.00	0.00
Cyclopentane	1.30	0.25	0.00	0.23	0.00	0.00	0.01	0.00	0.00	0.00
2-Methylpentane	4.24	0.08	0.00	1.17	0.00	0.00	0.01	0.00	0.00	0.00
3-Methylpentane	1.70	0.00	0.00	0.60	0.00	0.00	0.00	0.00	0.00	0.00
n-Hexane	6.59	0.05	0.00	2.50	0.00	0.00	0.01	0.00	0.00	0.00
Methylcyclopentane	3.38	0.05	0.00	0.50	0.00	0.00	0.00	0.00	0.00	0.00
Benzene	0.35	6.79	29.83	0.82	3.03	7.38	4.87	6.09	3.04	1.51
Thiophene	0.32	1.21	0.30	0.14	0.33	0.00	0.45	0.00	0.42	0.00
Cyclohexane	0.57	0.00	0.00	0.16	0.00	0.00	0.00	0.00	0.00	0.00
2-Methylhexane	1.14	0.00	0.00	0.37	0.00	0.00	0.00	0.00	0.00	0.00
2,3-Dimethylpentane	0.32	0.00	0.00	0.14	0.00	0.00	0.00	0.00	0.00	0.00
1,1-Dimethylpentane	0.00	0.00	0.00	0.00	0.00	0.00	0.00	0.00	0.00	0.00
3-Methylhexane	1.62	0.00	0.00	0.40	0.00	0.00	0.00	0.00	0.00	0.00
n-Heptane	7.50	0.00	0.00	1.88	0.00	0.00	0.00	0.00	0.00	0.00
Methyl-Cyclohexane	1.44	0.00	0.00	0.33	0.00	0.00	0.00	0.00	0.00	0.00
Ethylcyclopentane	1.39	0.00	0.00	0.23	0.00	0.00	0.00	0.00	0.00	0.00
2,5-Dimethylhexane	0.25	0.00	0.00	0.04	0.00	0.00	0.00	0.00	0.00	0.00
2,4-Dimethylhexane	0.02	0.00	0.00	0.01	0.00	0.00	0.00	0.00	0.00	0.00
3,3-Dimethylhexane	0.04	0.00	0.00	0.00	0.00	0.00	0.00	0.00	0.00	0.00
2,3,4-Trimethylpentane	1.68	0.00	0.00	0.15	0.00	0.00	0.00	0.00	0.00	0.00
Toluene	2.72	16.23	1.04	3.51	6.71	0.13	13.07	0.09	0.59	0.02
2-Methylthiophene	1.58	0.87	0.00	0.22	0.21	0.00	0.00	0.00	0.00	0.00
3-Methylthiophene	0.36	1.48	0.00	0.11	0.10	0.00	0.23	0.00	0.00	0.00
n-Octane	4.99	0.00	0.00	1.13	0.00	0.00	0.00	0.00	0.00	0.00
Ethylbenzene	1.10	3.39	0.00	1.00	0.45	0.00	1.13	0.00	0.00	0.00
Ethylthiophene	1.18	0.00	0.00	0.03	0.00	0.00	0.00	0.00	0.00	0.00
2,5-Dimethylthiophene	0.81	0.00	0.00	0.03	0.00	0.00	0.00	0.00	0.00	0.00
m/p-Xylene	4.56	10.37	0.00	3.04	3.44	0.00	7.94	0.00	0.00	0.00
2,4-Dimethylthiophene	1.38	0.34	0.00	0.10	0.00	0.00	0.00	0.00	0.00	0.00
2,3-Dimethylthiophene	1.71	0.29	0.00	0.07	0.00	0.00	0.00	0.00	0.00	0.00
Styrene	0.88	0.05	0.00	0.22	0.00	0.00	0.00	0.00	0.00	0.00
o-Xylene	1.82	3.21	0.00	1.43	0.93	0.00	2.07	0.00	0.00	0.00
n-Nonane	3.50	0.00	0.00	0.62	0.00	0.00	0.00	0.00	0.00	0.00
2-Propylthiophene	0.93	0.11	0.00	0.33	0.00	0.00	0.00	0.00	0.00	0.00
Propylbenzene	0.11	0.00	0.00	0.01	0.01	0.00	0.00	0.00	0.00	0.00
2-Ethyl-5-Methylthiophene	1.30	0.03	0.00	0.04	0.00	0.00	0.00	0.00	0.00	0.00
(?)-Benzene	2.03	4.19	0.00	1.46	0.39	0.00	1.35	0.00	0.00	0.00
2-Ethyl-4-Methylthiophene	1.17	0.00	0.00	0.04	0.00	0.00	0.00	0.00	0.00	0.00
1,3,5-Trimethylbenzene	0.70	1.12	0.00	0.41	0.30	0.00	0.78	0.00	0.00	0.00
Phenol	0.48	0.20	0.00	0.05	0.00	0.00	0.00	0.00	0.00	0.00
1-Ethyl-2-Methylbenzene	1.12	0.66	0.00	0.62	0.00	0.00	0.12	0.00	0.00	0.00
2,3,5-Trimethylthiophene	1.69	0.00	0.00	0.07	0.00	0.00	0.00	0.00	0.00	0.00
1,2,4-Trimethylbenzene	2.12	2.46	0.00	1.47	0.47	0.00	1.26	0.00	0.00	0.00
n-Decane	2.57	0.00	0.00	0.41	0.00	0.00	0.00	0.00	0.00	0.00
1,2,3-Trimethylbenzene	2.07	1.05	0.00	0.90	0.13	0.00	0.31	0.00	0.00	0.00
o-Cresol	0.46	0.00	0.00	0.02	0.00	0.00	0.00	0.00	0.00	0.00
m/p-Cresol	0.33	0.00	0.00	0.18	0.00	0.00	0.00	0.00	0.00	0.00
Dimethylphenol	0.00	0.00	0.00	0.00	0.00	0.00	0.00	0.00	0.00	0.00
n-Undecane	2.14	0.00	0.00	0.30	0.00	0.00	0.00	0.00	0.00	0.00
1,2,3,4-Tetramethylbenzene	0.00	0.00	0.00	0.00	0.00	0.00	0.00	0.00	0.00	0.00
Naphthalene	0.46	4.49	3.08	0.26	0.80	0.16	6.11	0.07	0.47	0.03
n-Dodecane	1.68	0.00	0.00	0.00	0.00	0.00	0.00	0.00	0.00	0.00
2-Methylnaphthalene	0.81	4.78	0.00	0.47	0.16	0.00	3.28	0.00	0.00	0.00
1-Methylnaphthalene	0.50	2.40	0.00	0.41	0.13	0.00	1.07	0.00	0.00	0.00
n-Tridecane	1.44	0.00	0.00	0.16	0.00	0.00	0.00	0.00	0.00	0.00
n-Tetradecane	1.11	0.10	0.00	0.08	0.00	0.00	0.00	0.00	0.00	0.00
Dimethylnaphthalene	1.76	2.01	0.00	0.61	0.00	0.00	0.41	0.00	0.00	0.00
n-Pentadecane	0.95	0.16	0.00	0.05	0.00	0.00	0.00	0.00	0.00	0.00
Trimethylnaphthalene	0.35	0.00	0.00	0.11	0.00	0.00	0.00	0.00	0.00	0.00
Trimethylnaphthalene	0.32	0.00	0.00	0.06	0.00	0.00	0.00	0.00	0.00	0.00
Trimethylnaphthalene	0.46	0.00	0.00	0.04	0.00	0.00	0.00	0.00	0.00	0.00
n-Hexadecane	0.67	0.00	0.00	0.02	0.00	0.00	0.00	0.00	0.00	0.00
Isopropylidimethylnaphthalene	0.00	0.00	0.00	0.01	0.00	0.00	0.00	0.00	0.00	0.00
n-Heptadecane	0.65	0.00	0.00	0.02	0.00	0.00	0.00	0.00	0.00	0.00
Pristane	0.15	0.00	0.00	0.01	0.00	0.00	0.00	0.00	0.00	0.00
Prist-1-ene	0.05	0.00	0.00	0.01	0.00	0.00	0.00	0.00	0.00	0.00
n-Octadecane	0.36	0.00	0.00	0.00	0.00	0.00	0.00	0.00	0.00	0.00
Phytane	0.06	0.00	0.00	0.00	0.00	0.00	0.00	0.00	0.00	0.00
n-Nonadecane	0.39	0.00	0.00	0.00	0.00	0.00	0.00	0.00	0.00	0.00
n-Icosane	0.27	0.00	0.00	0.00	0.00	0.00	0.00	0.00	0.00	0.00
n-Henicosane	0.19	0.00	0.00	0.00	0.00	0.00	0.00	0.00	0.00	0.00
n-Docosane	0.12	0.00	0.00	0.00	0.00	0.00	0.00	0.00	0.00	0.00
n-Tricosane	0.09	0.00	0.00	0.00	0.00	0.00	0.00	0.00	0.00	0.00
n-Tetracosane	0.08	0.00	0.00	0.00	0.00	0.00	0.00	0.00	0.00	0.00
n-Pentacosane	0.06	0.00	0.00	0.00	0.00	0.00	0.00	0.00	0.00	0.00
n-Hexacosane	0.04	0.00	0.00	0.00	0.00	0.00	0.00	0.00	0.00	0.00
n-Heptacosane	0.04	0.00	0.00	0.00	0.00	0.00	0.00	0.00	0.00	0.00
n-Octacosane	0.02	0.00	0.00	0.00	0.00	0.00	0.00	0.00	0.00	0.00
n-Nonacosane	0.02	0.00	0.00	0.00	0.00	0.00	0.00	0.00	0.00	0.00
n-Triacontane	0.01	0.00	0.00	0.00	0.00	0.00	0.00	0.00	0.00	0.00
Summations	mg/g TOC	mg/g TOC	mg/g TOC	mg/g TOC	mg/g TOC	mg/g TOC	mg/g TOC	mg/g TOC	mg/g TOC	mg/g TOC
n-C <sub>6-14</sub>	31.52	0.15	0.00	7.10	0.00	0.00	0.01	0.00	0.00	0.00
n-C <sub>15+</sub>	3.96	0.16	0.00	0.09	0.00	0.00	0.00	0.00	0.00	0.00
Mono-aromatic Compounds	18.72	49.46	30.87	14.66	15.85	7.51	32.91	6.18	3.64	1.53
Di-aromatic Compounds	4.66	13.68	3.08	1.97	1.08	0.16	10.86	0.07	0.47	0.03
Phenolic Compounds	1.28	0.20	0.00	0.25	0.00	0.00	0.00	0.00	0.00	0.00
Thiophenic Compounds	12.42	4.33	0.30	1.19	0.63	0.00	0.68	0.00	0.42	0.00

Table A 7 continued: samples provided by ENI

**Table A 7 continued: samples provided by Devon**

Table A 7: Late Gas Potential Screening (immature samples)

Company Formation/Basin GFZ Code File Temperature [°C] Rate	Wintershall																							
	Rheden-18-SP-845				Rheden-19-SP-870				Rheden-19-SP-890				Rheden-19-SP-955				Rheden-29-SP-865				Bahrenborstel-Z-2-SP-285			
	G006533				G006536				G006538				G006540				G006548				G006552			
	G006533AB		G006533AC		G006536AB		G006536AC		G006538AB		G006538AC		G006540AB		G006540AC		G006548AB		G006548AC		G006552AB		G006552AC	
	200-560 2K/min	200-700 2K/min	200-560 2K/min	200-700 2K/min	200-560 2K/min	200-700 2K/min	200-560 2K/min	200-700 2K/min	200-560 2K/min	200-700 2K/min	200-560 2K/min	200-700 2K/min	200-560 2K/min	200-700 2K/min	200-560 2K/min	200-700 2K/min	200-560 2K/min	200-700 2K/min	200-560 2K/min	200-700 2K/min	200-560 2K/min	200-700 2K/min	200-560 2K/min	200-700 2K/min
Totals	mg/g TOC	mg/g TOC	mg/g TOC	mg/g TOC	mg/g TOC	mg/g TOC	mg/g TOC	mg/g TOC	mg/g TOC	mg/g TOC	mg/g TOC	mg/g TOC	mg/g TOC	mg/g TOC	mg/g TOC	mg/g TOC	mg/g TOC	mg/g TOC	mg/g TOC	mg/g TOC	mg/g TOC	mg/g TOC	mg/g TOC	mg/g TOC
Total C1+ (-blank)	136.51	143.97	490.58	389.23	120.82	132.32	353.24	285.21	109.40	116.48	53.53	83.14												
Total C1-5	111.06	141.45	360.35	343.40	100.37	126.61	273.58	254.42	89.61	114.17	46.96	80.39												
Total C2-5	44.79	2.04	216.25	11.28	39.08	1.75	157.94	7.45	33.69	1.55	12.52	1.18												
Total C <sub>6-14</sub> (-blank)	23.33	2.41	113.33	43.70	17.52	5.19	69.77	25.73	17.83	1.60	5.33	0.98												
Total C <sub>15+</sub> (-blank)	2.12	0.11	16.90	2.12	2.93	0.53	9.89	5.06	1.96	0.72	1.23	1.77												
Total C <sub>20+</sub> (-blank)	25.45	2.51	130.23	45.83	20.45	5.71	79.66	30.79	19.79	2.31	6.56	2.75												
GOR	4.36	56.27	2.77	7.49	4.91	22.17	3.43	8.26	4.53	49.33	7.16	29.24												
Gas Wetness (C <sub>2</sub> ∕C <sub>1+2</sub> )	0.40	0.01	0.60	0.03	0.39	0.01	0.58	0.03	0.38	0.01	0.27	0.01												
Compound	mg/g TOC	mg/g TOC	mg/g TOC	mg/g TOC	mg/g TOC	mg/g TOC	mg/g TOC	mg/g TOC	mg/g TOC	mg/g TOC	mg/g TOC	mg/g TOC	mg/g TOC	mg/g TOC	mg/g TOC	mg/g TOC	mg/g TOC	mg/g TOC	mg/g TOC	mg/g TOC	mg/g TOC	mg/g TOC	mg/g TOC	mg/g TOC
Methane	66.27	139.41	144.09	332.12	61.29	124.86	115.64	246.97	55.93	112.62	34.45	79.21												
Ethane	28.10	1.09	128.28	6.47	24.38	0.88	96.93	2.37	21.86	0.47	8.92	0.51												
Propane	13.35	0.16	69.78	1.69	11.66	0.26	45.82	0.91	9.55	0.14	2.10	0.08												
i-Butane	1.17	0.00	4.44	0.00	1.08	0.00	2.80	0.00	0.84	0.00	0.23	0.00												
n-Butane	0.18	0.00	1.64	0.00	0.20	0.00	0.63	0.00	0.14	0.00	0.03	0.00												
i-Pentane	0.05	0.00	0.23	0.00	0.03	0.00	0.06	0.00	0.02	0.00	0.00	0.00												
n-Pentane	0.03	0.00	0.20	0.00	0.02	0.00	0.07	0.00	0.02	0.00	0.00	0.00												
Cyclopentane	0.02	0.00	0.36	0.00	0.03	0.00	0.07	0.00	0.01	0.00	0.00	0.00												
2-Methylpentane	0.01	0.00	0.05	0.00	0.01	0.00	0.02	0.00	0.00	0.00	0.00	0.00												
3-Methylpentane	0.00	0.00	0.01	0.00	0.00	0.00	0.01	0.00	0.00	0.00	0.00	0.00												
n-Hexane	0.00	0.00	0.03	0.00	0.00	0.00	0.01	0.00	0.00	0.00	0.00	0.00												
Methylcyclopentane	0.00	0.00	0.05	0.00	0.01	0.00	0.01	0.00	0.00	0.00	0.00	0.00												
Benzene	3.02	2.12	13.65	38.68	2.07	4.45	7.04	22.62	2.41	1.41	0.82	0.78												
Thiophene	0.00	0.00	0.90	0.00	0.00	0.00	0.54	0.00	0.00	0.00	0.00	0.00												
Cyclohexane	0.00	0.00	0.00	0.00	0.00	0.00	0.00	0.00	0.00	0.00	0.00	0.00												
2-Methylhexane	0.00	0.00	0.00	0.00	0.00	0.00	0.00	0.00	0.00	0.00	0.00	0.00												
2,3-Dimethylpentane	0.00	0.00	0.00	0.00	0.00	0.00	0.00	0.00	0.00	0.00	0.00	0.00												
1,1-Dimethylpentane	0.00	0.00	0.00	0.00	0.00	0.00	0.00	0.00	0.00	0.00	0.00	0.00												
3-Methylhexane	0.00	0.00	0.00	0.00	0.00	0.00	0.00	0.00	0.00	0.00	0.00	0.00												
n-Heptane	0.00	0.00	0.00	0.00	0.00	0.00	0.00	0.00	0.00	0.00	0.00	0.00												
Methyl-Cyclohexane	0.00	0.00	0.00	0.00	0.00	0.00	0.00	0.00	0.00	0.00	0.00	0.00												
Ethylcyclopentane	0.00	0.00	0.00	0.00	0.00	0.00	0.00	0.00	0.00	0.00	0.00	0.00												
2,5-Dimethylhexane	0.00	0.00	0.00	0.00	0.00	0.00	0.00	0.00	0.00	0.00	0.00	0.00												
2,4-Dimethylhexane	0.00	0.00	0.00	0.00	0.00	0.00	0.00	0.00	0.00	0.00	0.00	0.00												
3,3-Dimethylhexane	0.00	0.00	0.00	0.00	0.00	0.00	0.00	0.00	0.00	0.00	0.00	0.00												
2,3,4-Trimethylpentane	0.00	0.00	0.00	0.00	0.00	0.00	0.00	0.00	0.00	0.00	0.00	0.00												
Toluene	6.66	0.08	29.51	1.21	4.29	0.18	19.66	0.46	5.07	0.04	1.72	0.02												
2-Methylthiophene	0.00	0.00	0.00	0.00	0.00	0.00	0.12	0.00	0.00	0.00	0.00	0.00												
3-Methylthiophene	0.01	0.00	0.28	0.00	0.00	0.00	0.00	0.00	0.00	0.00	0.00	0.00												
n-Octane	0.00	0.00	0.00	0.00	0.00	0.00	0.00	0.00	0.00	0.00	0.00	0.00												
Ethylbenzene	0.67	0.00	7.50	0.00	0.53	0.00	4.02	0.00	0.45	0.00	0.10	0.00												
Ethylthiophene	0.00	0.00	0.00	0.00	0.00	0.00	0.00	0.00	0.00	0.00	0.00	0.00												
2,5-Dimethylthiophene	0.00	0.00	0.00	0.00	0.00	0.00	0.00	0.00	0.00	0.00	0.00	0.00												
m/p-Xylene	3.09	0.00	11.71	0.00	2.12	0.00	10.06	0.00	2.31	0.00	0.77	0.00												
2,4-Dimethylthiophene	0.00	0.00	0.08	0.00	0.00	0.00	0.00	0.00	0.00	0.00	0.00	0.00												
2,3-Dimethylthiophene	0.00	0.00	0.10	0.00	0.00	0.00	0.00	0.00	0.00	0.00	0.00	0.00												
Styrene	0.00	0.00	0.00	0.00	0.00	0.00	0.00	0.00	0.00	0.00	0.00	0.00												
o-Xylene	0.87	0.00	5.30	0.00	0.63	0.00	3.48	0.00	0.62	0.00	0.18	0.00												
n-Nonane	0.00	0.00	0.00	0.00	0.00	0.00	0.00	0.00	0.00	0.00	0.00	0.00												
2-Propylthiophene	0.00	0.00	0.00	0.00	0.00	0.00	0.00	0.00	0.00	0.00	0.00	0.00												
Propylbenzene	0.00	0.00	0.00	0.00	0.00	0.00	0.00	0.00	0.00	0.00	0.00	0.00												
2-Ethyl-5-Methylthiophene	0.00	0.00	0.00	0.00	0.00	0.00	0.00	0.00	0.00	0.00	0.00	0.00												
(?) - Benzene	0.63	0.00	6.15	0.00	0.58	0.00	3.54	0.00	0.40	0.00	0.09	0.00												
2-Ethyl-4-Methylthiophene	0.00	0.00	0.00	0.00	0.00	0.00	0.00	0.00	0.00	0.00	0.00	0.00												
1,3,5-Trimethylbenzene	0.28	0.00	0.76	0.00	0.24	0.00	0.68	0.00	0.21	0.00	0.08	0.00												
Phenol	1.05	0.00	0.00	0.00	0.42	0.00	0.00	0.00	0.82	0.00	0.04	0.00												
1-Ethyl-2-Methylbenzene	0.13	0.00	1.00	0.00	0.14	0.00	0.33	0.00	0.08	0.00	0.02	0.00												
2,3,5-Trimethylthiophene	0.00	0.00	0.00	0.00	0.00	0.00	0.00	0.00	0.00	0.00	0.00	0.00												

Table A 7 continued: samples provided by Maersk

Table A 7: Late Gas Potential Screening (immature samples)

Company	GFZ											
Formation/Basin GFZ Code File Temperature [°C] Rate	Kugmallit Fm. G000206			Talang Akar Coal G000670			Botneheia Shale G000689			Woodford Shale G000690		
	G00206ED	G00206EB	G00206EC	G00670AA	G00670AB	G00670AC	G00689AA	G00689AB	G00689AC	G00690AA	G00690AB	G00690AC
	200-480	200-580	200-690	200-460	200-560	200-700	200-460	200-560	200-700	200-460	200-560	200-700
	5K/min	5K/min	5K/min	2K/min	2K/min	2K/min	2K/min	2K/min	2K/min	2K/min	2K/min	2K/min
Totals	mg/g TOC	mg/g TOC	mg/g TOC	mg/g TOC	mg/g TOC	mg/g TOC	mg/g TOC	mg/g TOC	mg/g TOC	mg/g TOC	mg/g TOC	mg/g TOC
Total C1+ (-blank)	57.18	79.96	101.08	96.84	110.99	124.21	209.09	209.85	216.56	168.58	158.39	136.40
Total C1-5	36.12	64.37	92.82	30.36	82.74	114.58	58.28	154.14	162.73	55.99	114.51	117.88
Total C2-5	17.32	11.36	1.54	23.02	38.17	1.24	51.30	78.08	0.19	46.71	58.53	1.16
Total C <sub>6-14</sub> (-blank)	19.14	13.33	6.38	43.57	23.27	7.50	108.81	36.46	6.05	82.53	35.86	6.47
Total C <sub>15+</sub> (-blank)	1.93	2.25	1.88	22.90	4.98	2.13	41.99	19.25	47.78	30.06	8.01	12.05
Total C <sub>6+</sub> (-blank)	21.06	15.58	8.26	66.48	28.25	9.63	150.80	55.71	53.83	112.59	43.88	18.52
GOR	1.71	4.13	11.24	0.46	2.93	11.90	0.39	2.77	3.02	0.50	2.61	6.37
Gas Wetness (C <sub>2-6</sub> /C <sub>1-6</sub> )	0.48	0.18	0.02	0.76	0.46	0.01	0.88	0.51	0.00	0.83	0.51	0.01
Compound	mg/g TOC	mg/g TOC	mg/g TOC	mg/g TOC	mg/g TOC	mg/g TOC	mg/g TOC	mg/g TOC	mg/g TOC	mg/g TOC	mg/g TOC	mg/g TOC
Methane	18.79	53.01	91.27	7.35	44.57	113.34	6.98	76.06	162.54	9.28	55.99	116.72
Ethane	5.25	8.88	1.11	4.84	20.28	0.93	7.57	42.56	0.00	8.86	35.85	0.97
Propane	2.47	1.64	0.05	6.03	13.66	0.04	11.44	25.74	0.00	11.45	19.68	0.07
i-Butane	0.43	0.11	0.00	1.48	2.19	0.00	1.50	2.22	0.00	1.13	1.44	0.00
n-Butane	2.23	0.04	0.00	2.23	0.50	0.00	4.88	1.06	0.00	4.98	0.40	0.00
i-Pentane	0.43	0.04	0.00	1.65	0.08	0.00	1.38	0.00	0.00	1.48	0.03	0.00
n-Pentane	0.31	0.01	0.00	1.47	0.03	0.00	3.56	0.00	0.00	3.48	0.03	0.00
Cyclopentane	0.06	0.00	0.00	0.22	0.08	0.00	0.35	0.00	0.00	0.36	0.07	0.00
2-Methylpentane	0.12	0.00	0.00	0.87	0.01	0.00	0.69	0.00	0.00	0.85	0.00	0.00
3-Methylpentane	0.07	0.00	0.00	0.31	0.00	0.00	0.54	0.00	0.00	0.34	0.00	0.00
n-Hexane	0.11	0.00	0.00	1.11	0.00	0.00	2.79	0.00	0.00	2.45	0.00	0.00
Methylcyclopentane	0.10	0.00	0.00	0.59	0.02	0.00	0.90	0.00	0.00	0.76	0.01	0.00
Benzene	0.14	1.44	5.74	0.30	1.87	6.70	0.44	3.41	6.95	0.41	2.76	6.25
Thiophene	0.06	0.00	0.00	0.02	0.02	0.00	0.12	0.00	0.00	0.20	0.96	0.00
Cyclohexane	0.01	0.00	0.00	0.20	0.01	0.00	0.47	0.00	0.00	0.20	0.00	0.00
2-Methylhexane	0.02	0.00	0.00	0.26	0.00	0.00	0.45	0.00	0.00	0.19	0.00	0.00
2,3-Dimethylpentane	0.09	0.00	0.00	0.04	0.00	0.00	0.07	0.00	0.00	0.05	0.00	0.00
1,1-Dimethylpentane	0.00	0.00	0.00	0.00	0.00	0.00	0.00	0.00	0.00	0.00	0.00	0.00
3-Methylhexane	0.03	0.00	0.00	0.22	0.00	0.00	0.48	0.00	0.00	0.29	0.00	0.00
n-Heptane	0.08	0.00	0.00	1.26	0.00	0.00	3.25	0.00	0.00	2.53	0.00	0.00
Methyl-Cyclohexane	0.01	0.00	0.00	0.52	0.00	0.00	0.97	0.00	0.00	0.35	0.00	0.00
Ethylcyclopentane	0.02	0.00	0.00	0.16	0.00	0.00	0.35	0.00	0.00	0.40	0.00	0.00
2,5-Dimethylhexane	0.02	0.00	0.00	0.03	0.00	0.00	0.17	0.00	0.00	0.05	0.00	0.00
2,4-Dimethylhexane	0.01	0.00	0.00	0.00	0.00	0.00	0.04	0.00	0.00	0.01	0.00	0.00
3,3-Dimethylhexane	0.00	0.00	0.00	0.01	0.00	0.00	0.02	0.00	0.00	0.02	0.00	0.00
2,3,4-Trimethylpentane	0.03	0.00	0.00	0.16	0.00	0.00	0.88	0.00	0.00	0.58	0.00	0.00
Toluene	0.67	2.84	0.11	1.12	4.34	0.09	1.44	9.10	0.00	1.94	7.06	0.00
2-Methylthiophene	0.12	0.11	0.00	0.02	0.00	0.00	0.20	0.00	0.00	0.88	0.78	0.00
3-Methylthiophene	0.06	0.05	0.00	0.02	0.00	0.00	0.07	0.00	0.00	0.19	0.82	0.00
n-Octane	0.05	0.00	0.00	1.02	0.00	0.00	2.84	0.00	0.00	1.82	0.00	0.00
Ethylbenzene	0.15	0.15	0.00	0.32	0.65	0.00	0.86	1.44	0.00	0.77	1.31	0.00
Ethylthiophene	0.03	0.00	0.00	0.02	0.00	0.00	0.20	0.00	0.00	0.46	0.14	0.00
2,5-Dimethylthiophene	0.03	0.00	0.00	0.00	0.00	0.00	0.03	0.00	0.00	0.36	0.00	0.00
m/p-Xylene	0.71	1.58	0.00	1.24	2.80	0.00	2.13	6.12	0.00	1.93	4.36	0.00
2,4-Dimethylthiophene	0.04	0.00	0.00	0.07	0.00	0.00	0.13	0.00	0.00	0.42	0.10	0.00
2,3-Dimethylthiophene	0.04	0.00	0.00	0.01	0.00	0.00	0.09	0.00	0.00	0.55	0.08	0.00
Styrene	0.01	0.00	0.00	0.14	0.00	0.00	0.45	0.00	0.00	0.08	0.00	0.00
o-Xylene	0.25	0.32	0.00	0.46	0.86	0.00	1.11	2.07	0.00	1.09	1.68	0.00
n-Nonane	0.04	0.00	0.00	0.81	0.00	0.00	2.14	0.00	0.00	1.26	0.00	0.00
2-Propylthiophene	0.03	0.00	0.00	0.12	0.00	0.00	0.35	0.00	0.00	0.49	0.00	0.00
Propylbenzene	0.06	0.00	0.00	0.05	0.00	0.00	0.15	0.00	0.00	0.07	0.00	0.00
2-Ethyl-5-Methylthiophene	0.02	0.00	0.00	0.03	0.00	0.00	0.04	0.00	0.00	0.42	0.00	0.00
(?)-Benzene	0.26	0.19	0.00	0.51	0.88	0.00	1.26	1.62	0.00	1.15	1.56	0.00
2-Ethyl-4-Methylthiophene	0.00	0.00	0.00	0.00	0.00	0.00	0.00	0.00	0.00	0.00	0.00	0.00
1,3,5-Trimethylbenzene	0.09	0.12	0.00	0.22	0.38	0.00	0.42	0.77	0.00	0.32	0.48	0.00
Phenol	0.72	1.47	0.00	0.50	0.90	0.00	0.21	0.00	0.00	0.07	0.00	0.00
1-Ethyl-2-Methylbenzene	0.36	0.05	0.00	0.24	0.31	0.00	0.58	0.19	0.00	0.59	0.20	0.00
2,3,5-Trimethylthiophene	0.07	0.00	0.00	0.00	0.00	0.00	0.13	0.00	0.00	0.38	0.00	0.00
1,2,4-Trimethylbenzene	0.28	0.24	0.00	0.52	0.71	0.00	1.16	1.57	0.00	0.99	1.12	0.00
n-Decane	0.06	0.00	0.00	0.75	0.00	0.00	1.83	0.00	0.00	1.00	0.00	0.00
1,2,3-Trimethylbenzene	0.17	0.05	0.00	0.25	0.19	0.00	0.42	0.26	0.00	0.00	0.35	0.00
o-Cresol	1.48	0.23	0.00	0.65	0.28	0.00	0.16	0.00	0.00	0.09	0.00	0.00
m/p-Cresol	1.49	0.48	0.00	0.73	0.55	0.00	0.19	0.00	0.00	0.22	0.00	0.00
Dimethylphenol	0.00	0.00	0.00	0.17	0.08	0.00	0.00	0.00	0.00	0.12	0.00	0.00
n-Undecane	0.02	0.00	0.00	0.79	0.00	0.00	1.61	0.00	0.00	0.82	0.00	0.00
1,2,3,4-Tetramethylbenzene	0.72	0.00	0.00	0.12	0.00	0.00	0.00	0.00	0.00	0.57	0.00	0.00
Naphthalene	0.06	0.57	0.14	0.35	1.00	0.45	0.29	1.53	0.00	0.29	1.59	0.00
n-Dodecane	0.08	0.00	0.00	0.77	0.00	0.00	1.36	0.00	0.00	0.66	0.00	0.00
2-Methylnaphthalene	0.13	0.38	0.00	0.65	1.44	0.00	0.64	1.35	0.00	0.44	1.89	0.00
1-Methylnaphthalene	0.13	0.15	0.00	0.49	0.62	0.00	0.50	1.07	0.00	0.37	0.85	0.00
n-Tridecane	0.04	0.00	0.00	0.70	0.00	0.00	1.22	0.00	0.00	0.58	0.00	0.00
n-Tetradecane	0.01	0.00	0.00	0.62	0.00	0.00	0.98	0.06	0.00	0.41	0.00	0.00
Dimethylnaphthalene	0.20	0.12	0.00	1.54	0.79	0.00	0.88	0.72	0.00	0.73	0.00	0.00
n-Pentadecane	0.01	0.00	0.00	0.73	0.08	0.00	0.80	0.00	0.00	0.39	0.00	0.00
Trimethylnaphthalene	0.03	0.01	0.00	0.17	0.00	0.00	0.15	0.00	0.00	0.16	0.00	0.00
Trimethylnaphthalene	0.02	0.01	0.00	0.24	0.00	0.00	0.17	0.00	0.00	0.19	0.00	0.00
Trimethylnaphthalene	0.07	0.02	0.00	0.16	0.00	0.00	0.05	0.00	0.00	0.09	0.00	0.00
n-Hexadecane	0.01	0.00	0.00	0.55	0.00	0.00	0.64	0.00	0.00	0.27	0.00	0.00
Isopropylidimethylnaphthalene	0.00	0.00	0.00	0.13	0.00	0.00	0.00	0.00	0.00	0.00	0.00	0.00
n-Heptadecane	0.01	0.00	0.00	0.75	0.00	0.00	0.48	0.00	0.00	0.27	0.00	0.00
Pristane	0.00	0.00	0.00	0.17	0.00	0.00	0.04	0.00	0.00	0.04	0.00	0.00



Table A 7: Late Gas Potential Screening (immature samples)

Company												
Formation/Basin GFZ Code File Temperature [°C] Rate	Chatanooga Shale G000692			Alaskan Tasmantite G000693			Jet Rock G000696			Boghead Coal G000697		
	G00692AA 200-460 2K/min	G00692AB 200-560 2K/min	G00692AC 200-700 2K/min	G00693AA 200-460 2K/min	G00693AB 200-560 2K/min	G00693AC 200-700 2K/min	G00696AA 200-460 2K/min	G00696AB 200-560 2K/min	G00696AC 200-700 2K/min	G00697AA 200-460 2K/min	G00697AB 200-560 2K/min	G00697AC 200-700 2K/min
	mg/g TOC	mg/g TOC	mg/g TOC	mg/g TOC	mg/g TOC	mg/g TOC	mg/g TOC	mg/g TOC	mg/g TOC	mg/g TOC	mg/g TOC	mg/g TOC
	mg/g TOC	mg/g TOC	mg/g TOC	mg/g TOC	mg/g TOC	mg/g TOC	mg/g TOC	mg/g TOC	mg/g TOC	mg/g TOC	mg/g TOC	mg/g TOC
Total C1+ (-blank)	235.89	199.39	189.65	687.26	597.76	422.76	1387.88	1295.99	925.89	428.32	457.81	343.33
Total C1-5	95.54	148.14	169.06	123.17	414.52	367.92	265.73	688.71	779.26	90.65	322.44	299.71
Total C2-5	79.67	66.59	2.50	111.18	275.78	10.09	210.43	341.45	8.39	75.45	190.04	9.07
Total C <sub>6-14</sub> (-blank)	116.46	41.43	4.15	287.07	145.22	46.11	718.24	495.40	109.65	180.22	96.63	39.94
Total C <sub>15+</sub> (-blank)	23.89	9.82	16.45	277.02	38.02	8.74	403.91	111.88	36.96	157.45	38.73	3.67
Total C <sub>6+</sub> (-blank)	140.35	51.25	20.60	564.10	183.24	54.85	1122.15	607.28	146.62	337.66	135.37	43.61
GOR	0.68	2.89	8.21	0.22	2.26	6.71	0.24	1.13	5.31	0.27	2.38	6.87
Gas Wetness (C <sub>2</sub> g/C <sub>1g</sub> )	0.83	0.45	0.01	0.90	0.67	0.03	0.79	0.50	0.01	0.83	0.59	0.03
Compound	mg/g TOC	mg/g TOC	mg/g TOC	mg/g TOC	mg/g TOC	mg/g TOC	mg/g TOC	mg/g TOC	mg/g TOC	mg/g TOC	mg/g TOC	mg/g TOC
Methane	15.86	81.56	166.56	11.99	138.74	357.83	55.30	347.26	770.87	15.21	132.40	290.84
Ethane	14.98	44.37	1.83	18.39	128.93	9.24	50.97	193.06	7.57	14.12	100.40	8.62
Propane	18.28	19.69	0.16	26.30	114.46	0.14	54.86	122.04	0.16	18.02	73.08	0.14
i-Butane	2.79	1.23	0.00	1.12	10.60	0.00	10.05	13.92	0.00	1.84	5.76	0.00
n-Butane	8.65	0.28	0.00	14.42	7.28	0.00	24.71	2.91	0.00	10.30	2.39	0.00
i-Pentane	3.34	0.00	0.00	2.19	1.92	0.00	12.49	0.87	0.00	3.98	1.11	0.00
n-Pentane	5.93	0.00	0.00	12.78	0.93	0.00	15.49	0.44	0.00	8.54	0.48	0.00
Cyclopentane	0.65	0.00	0.00	1.46	1.67	0.00	5.39	1.64	0.00	0.96	0.80	0.00
2-Methylpentane	1.89	0.00	0.00	0.90	0.23	0.00	7.41	0.11	0.00	1.52	0.12	0.00
3-Methylpentane	0.99	0.00	0.00	0.44	0.08	0.00	3.18	0.00	0.00	0.54	0.03	0.00
n-Hexane	3.89	0.00	0.00	12.65	0.17	0.00	9.92	0.05	0.00	8.56	0.09	0.00
Methylcyclopentane	1.86	0.00	0.00	2.46	0.58	0.00	13.94	0.16	0.00	1.97	0.18	0.00
Benzene	0.86	4.09	5.46	1.05	16.53	38.38	1.94	23.33	91.21	0.56	12.09	34.54
Thiophene	0.19	1.45	0.00	0.12	0.20	0.00	0.28	0.84	0.00	0.10	0.28	0.00
Cyclohexane	0.61	0.00	0.00	1.02	0.11	0.00	4.81	0.05	0.00	0.49	0.00	0.00
2-Methylhexane	0.69	0.00	0.00	1.02	0.00	0.00	3.19	0.00	0.00	0.46	0.00	0.00
2,3-Dimethylpentane	0.29	0.00	0.00	0.08	0.00	0.00	0.86	0.00	0.00	0.06	0.00	0.00
1,1-Dimethylpentane	0.00	0.00	0.00	0.00	0.00	0.00	0.00	0.00	0.00	0.00	0.00	0.00
3-Methylhexane	0.86	0.00	0.00	0.44	0.00	0.00	2.92	0.00	0.00	0.45	0.00	0.00
n-Heptane	3.51	0.00	0.00	9.51	0.00	0.00	9.28	0.00	0.00	9.04	0.00	0.00
Methyl-Cyclohexane	1.15	0.00	0.00	1.99	0.00	0.00	8.58	0.00	0.00	1.12	0.00	0.00
Ethylcyclopentane	0.69	0.00	0.00	1.50	0.00	0.00	4.05	0.00	0.00	1.00	0.00	0.00
2,5-Dimethylhexane	0.11	0.00	0.00	0.51	0.00	0.00	0.54	0.00	0.00	0.12	0.00	0.00
2,4-Dimethylhexane	0.02	0.00	0.00	0.04	0.00	0.00	0.14	0.00	0.00	0.03	0.00	0.00
3,3-Dimethylhexane	0.02	0.00	0.00	0.05	0.00	0.00	0.05	0.00	0.00	0.08	0.00	0.00
2,3,4-Trimethylpentane	0.75	0.00	0.00	1.37	0.00	0.00	1.67	0.00	0.00	0.66	0.00	0.00
Toluene	3.97	9.94	0.00	3.89	31.76	2.85	10.90	59.00	4.32	2.26	23.19	1.68
2-Methylthiophene	0.76	1.16	0.00	0.39	0.17	0.00	0.89	0.00	0.00	0.36	0.00	0.00
3-Methylthiophene	0.14	0.71	0.00	0.08	0.00	0.00	0.66	0.00	0.00	0.33	0.00	0.00
n-Octane	2.33	0.00	0.00	11.83	0.00	0.00	6.95	0.00	0.00	7.77	0.00	0.00
Ethylbenzene	1.57	1.18	0.00	2.07	7.98	0.00	4.95	11.06	0.03	0.94	5.43	0.00
Ethylthiophene	0.29	0.00	0.00	0.10	0.00	0.00	0.32	0.00	0.00	0.18	0.00	0.00
2,5-Dimethylthiophene	0.21	0.00	0.00	0.11	0.00	0.00	0.17	0.00	0.00	0.17	0.00	0.00
m/p-Xylene	3.74	5.93	0.00	2.59	13.83	0.00	13.51	42.79	0.10	1.79	8.55	0.00
2,4-Dimethylthiophene	0.25	0.00	0.00	0.40	0.00	0.00	1.54	0.00	0.00	0.24	0.00	0.00
2,3-Dimethylthiophene	0.59	0.00	0.00	0.50	0.00	0.00	1.11	0.00	0.00	0.22	0.00	0.00
Styrene	0.10	0.00	0.00	0.67	0.00	0.00	1.07	0.00	0.00	0.37	0.00	0.00
o-Xylene	1.82	2.02	0.00	1.98	5.97	0.00	4.93	8.90	0.02	1.19	3.82	0.00
n-Nonane	1.41	0.00	0.00	9.63	0.00	0.00	4.52	0.00	0.00	7.40	0.00	0.00
2-Propylthiophene	0.68	0.00	0.00	0.86	0.00	0.00	2.45	0.00	0.00	0.42	0.00	0.00
Propylbenzene	0.07	0.00	0.00	0.32	0.00	0.00	0.15	0.25	0.00	0.21	0.12	0.00
2-Ethyl-5-Methylthiophene	0.23	0.00	0.00	0.15	0.00	0.00	0.46	0.00	0.00	0.28	0.00	0.00
(?) -Benzene	2.16	1.19	0.00	2.28	8.66	0.00	6.30	15.38	1.06	1.00	4.03	0.00
2-Ethyl-4-Methylthiophene	0.00	0.00	0.00	0.00	0.00	0.00	0.00	0.00	0.00	0.00	0.00	0.00
1,3,5-Trimethylbenzene	0.60	0.61	0.00	0.29	1.06	0.00	2.78	8.08	0.03	0.24	0.60	0.00
Phenol	0.15	0.00	0.00	0.16	0.00	0.00	42.21	96.98	0.98	0.19	1.17	0.00
1-Ethyl-2-Methylbenzene	0.91	0.00	0.00	1.61	2.12	0.00	0.00	0.00	0.00	0.60	1.18	0.00
2,3,5-Trimethylthiophene	0.23	0.00	0.00	0.30	0.00	0.00	0.00	0.00	0.00	0.00	0.00	0.00
1,2,4-Trimethylbenzene	2.07	1.40	0.00	1.66	4.10	0.00	6.35	7.41	0.00	0.75	1.75	0.00
n-Decane	0.98	0.00	0.00	8.85	0.00	0.00	3.41	0.00	0.00	7.39	0.00	0.00
1,2,3-Trimethylbenzene	1.11	0.45	0.00	0.54	0.82	0.00	2.77	1.76	0.00	0.70	0.53	0.00
o-Cresol	0.14	0.00	0.00	0.99	0.00	0.00	36.64	40.88	0.38	0.99	0.44	0.00
m/p-Cresol	0.28	0.00	0.00	0.63	0.00	0.00	69.74	41.15	0.44	1.05	1.00	0.00
Dimethylphenol	0.00	0.00	0.00	0.00	0.00	0.00	0.00	0.00	0.00	0.44	0.00	0.00
n-Undecane	0.73	0.00	0.00	7.51	0.00	0.00	2.80	0.58	0.00	7.14	0.00	0.00
1,2,3,4-Tetramethylbenzene	0.00	0.00	0.00	0.00	0.00	0.00	13.57	4.16	0.00	0.46	0.00	0.00
Naphthalene	0.47	2.31	0.00	1.04	5.80	3.22	1.84	14.98	2.64	0.42	3.68	2.58
n-Dodecane	0.56	0.00	0.00	5.68	0.00	0.00	4.01	1.09	0.00	6.46	0.00	0.00
2-Methylnaphthalene	0.85	1.75	0.00	1.18	5.97	0.00	4.30	16.94	0.40	0.50	3.21	0.00
1-Methylnaphthalene	0.69	0.87	0.00	1.46	3.56	0.00	4.14	7.25	0.18	0.74	2.10	0.00
n-Tridecane	0.46	0.00	0.00	4.48	0.00	0.00	4.84	0.14	0.00	5.96	0.00	0.00
n-Tetradecane	0.27	0.00	0.00	3.62	0.00	0.00	2.36	0.08	0.00	5.96	0.07	0.00
Dimethylnaphthalene	1.23	0.56	0.00	1.20	2.78	0.00	6.17	6.84	0.18	0.75	1.53	0.00
n-Pentadecane	0.21	0.00	0.00	3.22	0.30	0.00	2.35	1.45	0.00	5.52	0.29	0.00
Trimethylnaphthalene	0.26	0.00	0.00	0.12	0.00	0.00	0.00	0.00	0.00	0.00	0.00	0.00
Trimethylnaphthalene	0.30	0.00	0.00	0.64	0.00	0.00	0.00	0.00	0.00	0.00	0.00	0.00
Trimethylnaphthalene	0.11	0.00	0.00	0.15	0.00	0.00	0.00	0.00	0.00	0.00	0.00	0.00
n-Hexadecane	0.12	0.00	0.00	2.71	0.00	0.00	0.00	0.00	0.00	5.21	0.24	0.00
Isopropylidimethylnaphthalene	0.00	0.00	0.00	0.00	0.00	0.00	0.00	0.00	0.00	0.00	0.00	0.00
n-Heptadecane	0.13	0.00	0.00	2.66	0.00	0.00	0.00	0.00	0.00	4.97	0.37	0.00
Pristane	0.04	0.00	0.00	0.17	0.00	0.00	0.00	0.00	0.00	0.13	0.00	0.00
Prist-1-ene	0.02	0.00	0.00	0.13	0.00	0.00	0.00	0.00	0.00	0.05	0.00	0.00
n-Octadecane	0.04	0.00	0.00	2.03	0.00	0.00	0.00	0.00	0.00	4.17	0.37	0.00
Phytane	0.02	0.00	0.00	0.15	0.00	0.00	0.00	0.00	0.00	0.14	0.00	0.00
n-Nonadecane	0.04	0.00	0.00	1.85	0.00	0.00	0.00	0.00	0.00	3.62	0.53	0.00
n-Icosane	0.02	0.00	0.00	1.40	0.00	0.00	0.00	0.00	0.00	2.96	0.44	0.00
n-Henicosane	0.01	0.00	0.00	1.10	0.00	0.00	0.00	0.00	0.00	2.68	0.46	0.00
n-Docosane	0.00	0.00	0.00	0.87	0.00	0.00	0.00	0.00	0.00	2.46	0.63	0.00
n-Tricosane	0.00	0.00	0.00	0.67	0.00	0.00	0.00	0.00	0.00	2.44	0.63	0.00
n-Tetracosane	0.00	0.00	0.00	0.57	0.00	0.00	0.00	0.00	0.00	2.40	0.57	0.00
n-Pentacosane	0.00	0.00	0.00	0.44	0.00	0.00	0.00	0.00	0.00	2.33	0.48	0.00

Table A 7: Late Gas Potential Screening (immature samples)

Company	GFZ																	
Formation/Basin	Cannel Coal			Talang Akar Coal			Brown Limestone			Alum Shale								
GFZ Code	G000698			G000726			G000731			G000753								
File	G00698AA	G00698AB	G00698AC	G00726AA	G00726AB	G00726AC	G00731AA	G00731AB	G00731AC	G00753AA	G00753AB	G00753AC						
Temperature [°C]	200-460	200-560	200-700	200-460	200-560	200-700	200-460	200-560	200-700	200-460	200-560	200-700						
Rate	2K/min	2K/min	2K/min	2K/min	2K/min	2K/min	2K/min	2K/min	2K/min	2K/min	2K/min	2K/min						
Totals	mg/g TOC	mg/g TOC	mg/g TOC	mg/g TOC	mg/g TOC	mg/g TOC	mg/g TOC	mg/g TOC	mg/g TOC	mg/g TOC	mg/g TOC	mg/g TOC	mg/g TOC	mg/g TOC	mg/g TOC			
Total C1+ (-blank)	92.66	109.02	114.43	83.24	94.85	100.24	2336.42	2075.50	1546.59	255.84	272.67	258.66						
Total C1-5	33.76	79.18	109.17	29.13	67.48	95.19	647.77	1337.92	1412.78	130.25	212.05	247.32						
Total C2-5	25.17	29.40	0.91	22.00	27.49	0.66	552.29	718.21	14.26	98.95	81.47	1.79						
Total C <sub>6-14</sub> (-blank)	42.85	21.71	2.21	40.66	21.15	3.74	1212.23	599.70	125.68	99.52	46.88	5.26						
Total C <sub>15+</sub> (-blank)	16.05	8.13	3.05	13.45	6.22	1.31	476.42	137.89	8.14	26.07	13.74	6.07						
Total C <sub>6+</sub> (-blank)	58.90	29.83	5.26	54.11	27.37	5.05	1688.65	737.59	133.82	125.59	60.62	11.34						
GOR	0.57	2.65	20.74	0.54	2.47	18.84	0.38	1.81	10.56	1.04	3.50	21.81						
Gas Wetness (C <sub>2-5</sub> /C <sub>1-5</sub> )	0.75	0.37	0.01	0.76	0.41	0.01	0.85	0.54	0.01	0.76	0.38	0.01						
Compound	mg/g TOC	mg/g TOC	mg/g TOC	mg/g TOC	mg/g TOC	mg/g TOC	mg/g TOC	mg/g TOC	mg/g TOC	mg/g TOC	mg/g TOC	mg/g TOC	mg/g TOC	mg/g TOC	mg/g TOC			
Methane	8.59	49.79	108.26	7.14	39.99	94.53	95.48	619.71	1398.52	31.29	130.58	245.53						
Ethane	6.33	19.37	0.61	4.85	16.52	0.50	98.16	430.49	12.69	26.26	55.18	1.19						
Propane	6.63	8.75	0.07	6.21	9.15	0.04	136.47	239.44	0.33	25.59	22.57	0.20						
i-Butane	0.82	0.68	0.00	1.28	0.94	0.00	23.87	20.26	0.00	3.88	1.57	0.00						
n-Butane	2.97	0.09	0.00	2.05	0.12	0.00	60.76	5.10	0.00	11.51	0.21	0.00						
i-Pentane	1.03	0.01	0.00	1.55	0.09	0.00	26.08	1.16	0.00	6.51	0.23	0.00						
n-Pentane	1.97	0.01	0.00	1.22	0.02	0.00	49.23	1.21	0.00	6.05	0.06	0.00						
Cyclopentane	0.42	0.02	0.00	0.21	0.03	0.00	5.29	1.09	0.00	0.49	0.00	0.00						
2-Methylpentane	0.47	0.00	0.00	0.77	0.00	0.00	24.27	0.28	0.00	1.86	0.00	0.00						
3-Methylpentane	0.20	0.00	0.00	0.24	0.00	0.00	5.21	0.07	0.00	1.22	0.00	0.00						
n-Hexane	1.27	0.00	0.00	0.77	0.00	0.00	30.62	0.14	0.00	3.23	0.00	0.00						
Methylcyclopentane	0.60	0.00	0.00	0.61	0.00	0.00	11.89	0.22	0.00	1.05	0.00	0.00						
Benzene	0.33	2.14	1.81	0.33	1.73	3.69	2.79	36.40	112.12	0.80	3.76	5.76						
Thiophene	0.04	0.08	0.00	0.03	0.07	0.00	5.90	34.95	0.00	0.28	0.51	0.00						
Cyclohexane	0.14	0.00	0.00	0.14	0.00	0.00	0.00	0.00	0.00	0.17	0.00	0.00						
2-Methylhexane	0.13	0.00	0.00	0.18	0.00	0.00	6.17	0.00	0.00	0.71	0.00	0.00						
2,3-Dimethylpentane	0.03	0.00	0.00	0.03	0.00	0.00	0.57	0.00	0.00	0.09	0.00	0.00						
1,1-Dimethylpentane	0.00	0.00	0.00	0.00	0.00	0.00	0.00	0.00	0.00	0.00	0.00	0.00						
3-Methylhexane	0.13	0.00	0.00	0.15	0.00	0.00	5.01	0.00	0.00	0.83	0.00	0.00						
n-Heptane	1.18	0.00	0.00	0.80	0.00	0.00	31.17	0.00	0.00	2.00	0.00	0.00						
Methyl-Cyclohexane	0.22	0.00	0.00	0.34	0.00	0.00	5.30	0.00	0.00	0.38	0.00	0.00						
Ethylcyclopentane	0.23	0.00	0.00	0.15	0.00	0.00	5.64	0.00	0.00	0.39	0.00	0.00						
2,5-Dimethylhexane	0.02	0.00	0.00	0.02	0.00	0.00	1.10	0.00	0.00	0.11	0.00	0.00						
2,4-Dimethylhexane	0.00	0.00	0.00	0.01	0.00	0.00	0.09	0.00	0.00	0.02	0.00	0.00						
3,3-Dimethylhexane	0.01	0.00	0.00	0.01	0.00	0.00	0.19	0.00	0.00	0.01	0.00	0.00						
2,3,4-Trimethylpentane	0.15	0.00	0.00	0.16	0.00	0.00	7.75	0.00	0.00	0.39	0.00	0.00						
Toluene	1.71	5.04	0.00	1.22	4.11	0.04	18.22	91.83	5.54	4.53	10.73	0.00						
2-Methylthiophene	0.12	0.08	0.00	0.07	0.08	0.00	24.00	26.23	0.00	0.53	0.56	0.00						
3-Methylthiophene	0.05	0.03	0.00	0.03	0.06	0.00	6.23	28.51	0.00	0.25	0.41	0.00						
n-Octane	0.91	0.00	0.00	0.64	0.00	0.00	21.72	0.00	0.00	1.12	0.00	0.00						
Ethylbenzene	0.57	0.55	0.00	0.37	0.49	0.00	3.02	18.71	0.00	1.71	1.19	0.00						
Ethylthiophene	0.04	0.00	0.00	0.02	0.00	0.00	17.68	6.56	0.00	0.13	0.00	0.00						
2,5-Dimethylthiophene	0.04	0.00	0.00	0.02	0.00	0.00	37.07	1.38	0.00	0.14	0.00	0.00						
m/p-Xylene	1.13	2.49	0.00	1.18	2.51	0.00	16.25	50.26	0.00	4.89	8.09	0.00						
2,4-Dimethylthiophene	0.03	0.00	0.00	0.05	0.00	0.00	18.26	7.18	0.00	0.33	0.00	0.00						
2,3-Dimethylthiophene	0.12	0.00	0.00	0.06	0.00	0.00	12.89	5.91	0.00	0.37	0.00	0.00						
Styrene	0.03	0.00	0.00	0.09	0.00	0.00	4.18	0.67	0.00	0.19	0.00	0.00						
o-Xylene	0.68	0.81	0.00	0.47	0.68	0.00	9.17	16.89	0.00	2.05	2.06	0.00						
n-Nonane	0.65	0.00	0.00	0.46	0.00	0.00	16.95	0.00	0.00	0.53	0.00	0.00						
2-Propylthiophene	0.20	0.00	0.00	0.13	0.00	0.00	8.66	0.87	0.00	0.63	0.00	0.00						
Propylbenzene	0.03	0.00	0.00	0.02	0.01	0.00	0.00	0.00	0.00	0.03	0.00	0.00						
2-Ethyl-5-Methylthiophene	0.04	0.00	0.00	0.03	0.00	0.00	32.51	1.50	0.00	0.14	0.00	0.00						
(?)-Benzene	0.57	0.51	0.00	0.55	0.60	0.00	4.45	19.42	0.00	2.97	1.51	0.00						
2-Ethyl-4-Methylthiophene	0.00	0.00	0.00	0.00	0.00	0.00	9.90	2.29	0.00	0.16	0.00	0.00						
1,3,5-Trimethylbenzene	0.14	0.25	0.00	0.14	0.26	0.00	6.02	5.72	0.00	0.75	0.97	0.00						
Phenol	0.33	1.15	0.00	0.69	1.54	0.00	0.66	1.37	0.00	0.06	0.00	0.00						
1-Ethyl-2-Methylbenzene	0.75	0.24	0.00	0.40	0.19	0.00	3.96	2.97	0.00	1.08	0.37	0.00						
2,3,5-Trimethylthiophene	0.00	0.00	0.00	0.00	0.00	0.00	23.59	1.05	0.00	0.29	0.00	0.00						
1,2,4-Trimethylbenzene	0.45	0.43	0.00	0.50	0.49	0.00	9.31	11.17	0.00	2.51	1.73	0.00						
n-Decane	0.55	0.00	0.00	0.42	0.00	0.00	14.71	0.00	0.00	0.28	0.00	0.00						
1,2,3-Trimethylbenzene	0.21	0.00	0.00	0.29	0.14	0.00	12.51	5.21	0.00	0.90	0.37	0.00						
o-Cresol	0.85	0.09	0.00	0.88	0.23	0.00	2.05	0.00	0.00	0.41	0.00	0.00						
m/p-Cresol	0.97	0.33	0.00	1.12	0.58	0.00	2.09	0.00	0.00	0.35	0.00	0.00						
Dimethylphenol	0.22	0.00	0.00	0.21	0.00	0.00	0.00	0.00	0.00	0.00	0.00	0.00						
n-Undecane	0.50	0.00	0.00	0.41	0.00	0.00	12.54	0.00	0.00	0.21	0.00	0.00						
1,2,3,4-Tetramethylbenzene	0.14	0.00	0.00	0.14	0.00	0.00	5.95	0.00	0.00	0.00	0.00	0.00						
Naphthalene	0.28	1.25	0.00	0.36	1.20	0.09	2.12	21.97	3.83	0.48	2.78	0.00						
n-Dodecane	0.48	0.00	0.00	0.39	0.00	0.00	9.75	0.00	0.00	0.17	0.00	0.00						
2-Methylnaphthalene	0.49	0.95	0.00	0.64	1.38	0.00	2.38	22.92	0.00	1.18	2.65	0.00						
1-Methylnaphthalene	0.45	0.37	0.00	0.54	0.53	0.00	2.00	13.32	0.00	0.92	1.01	0.00						
n-Tridecane	0.39	0.00	0.00	0.41	0.00	0.00	9.59	0.00	0.00	0.15	0.00	0.00						
n-Tetradecane	0.28	0.00	0.00	0.34	0.01	0.00	7.37	1.61	0.00	0.06	0.00	0.00						
Dimethylnaphthalene	0.55	0.29	0.00	1.78	0.59	0.00	8.19	11.11	0.00	1.67	0.72	0.00						
n-Pentadecane	0.29	0.00	0.00	0.36	0.09	0.00	8.15	1.33	0.00	0.15	0.00	0.00						
Trimethylnaphthalene	0.06	0.02	0.00	0.15	0.00	0.00	0.70	0.00	0.00	0.40	0.00	0.00						
Trimethylnaphthalene	0.09	0.02	0.00	0.22	0.00	0.00	2.38	0.00	0.00	0.38	0.00	0.00						
Trimethylnaphthalene	0.14	0.04	0.00	0.18	0.00	0.00	0.82	0.00	0.00	0.13	0.00	0.00						
n-Hexadecane	0.21	0.01	0.00	0.26	0.01	0.00	6.87	0.43	0.00	0.03	0.00	0.00						
Isopropylidimethylnaphthalene	0.00	0.02	0.00	0.27	0.04	0.00	0.00	0.00	0.00	0.15	0.00	0.00						
n-Heptadecane	0.23	0.02	0.00	0.29	0.02	0.00	6.29	0.85	0.00	0.05	0.00	0.00						
Pristane	0.04	0.00	0.00	0.06	0.00	0.00	0.80	0.00	0.00	0.04	0.00	0.00						
Prist-1-ene	0.01	0.00	0.00	0.02	0.00	0.00	0.32	0.00	0.00	0.01	0.00	0.00						
n-Octadecane	0.16	0.03	0.00	0.20	0.02	0.00	4.26	0.93	0.00	0.01	0.00	0.00						
Phytane	0.02	0.00	0.00	0.02	0.01	0.00	0.26	0.00	0.00	0.04	0.00	0.00						
n-Nonadecane	0.20	0.03	0.00	0.21	0.03	0.00	4.17	2.37	0.00	0.04	0.00	0.00						
n-Icosane	0.13	0.02	0.00	0.14	0.03	0.00	3.21	0.78	0.00	0.02	0.00	0.00						
n-Henicosane	0.09	0.02	0.00	0.09	0.03	0.00	2.48	0.28	0.00	0.01	0.00	0.00						
n-Docosane	0.07	0.02	0.00	0.06	0.06	0.00	1.81	0.38	0.00	0.00	0.00	0.00						
n-Tricosane	0.06	0.02	0.00	0.05	0.08	0.00	1.54	0.00	0.00	0.00	0.00	0.00						
n-Tetracosane	0.04																	

Table A 7: Late Gas Potential Screening (immature samples)

Company	GFZ											
Formation/Basin GFZ Code File Temperature [°C] Rate	Alum Shale G000758			Messel Oil Shale G000859			Autun Oil Shale G000883			Talang Akar Coal G000899		
	G00758AA	G00758AB	G00758AC	G00859AA	G00859AB	G00859AC	G00883AA	G00883AB	G00883AC	G00899AA	G00899AB	G00899AC
	200-460	200-560	200-700	200-460	200-560	200-700	200-460	200-560	200-700	200-460	200-560	200-700
	2K/min	2K/min	2K/min	2K/min	2K/min	2K/min	2K/min	2K/min	2K/min	2K/min	2K/min	2K/min
	Rate	2K/min	2K/min	2K/min	2K/min	2K/min	2K/min	2K/min	2K/min	2K/min	2K/min	2K/min
Totals	mg/g TOC	mg/g TOC	mg/g TOC	mg/g TOC	mg/g TOC	mg/g TOC	mg/g TOC	mg/g TOC	mg/g TOC	mg/g TOC	mg/g TOC	mg/g TOC
Total C1+ (-blank)	173.21	178.45	161.84	367.68	382.63	311.07	295.36	273.39	219.01	133.71	157.72	166.25
Total C1-5	81.69	140.44	150.76	102.10	267.27	289.90	81.02	199.52	190.90	57.60	119.22	160.57
Total C2-5	64.18	57.44	1.16	82.97	144.16	3.72	68.84	117.22	5.21	41.37	39.32	1.49
Total C <sub>6-14</sub> (-blank)	71.81	33.16	4.08	172.98	86.21	15.32	136.42	59.70	14.64	58.56	33.79	5.29
Total C <sub>15+</sub> (-blank)	19.71	4.85	7.00	92.59	29.14	5.84	77.92	14.16	13.47	17.55	4.71	0.39
Total C <sub>6+</sub> (-blank)	91.52	38.01	11.08	265.58	115.35	21.17	214.34	73.87	28.11	76.11	38.50	5.68
GOR	0.89	3.69	13.60	0.38	2.32	13.70	0.38	2.70	6.79	0.76	3.10	28.26
Gas Wetness (C <sub>2,g</sub> /C <sub>1,g</sub> )	0.79	0.41	0.01	0.81	0.54	0.01	0.85	0.59	0.03	0.72	0.33	0.01
Compound	mg/g TOC	mg/g TOC	mg/g TOC	mg/g TOC	mg/g TOC	mg/g TOC	mg/g TOC	mg/g TOC	mg/g TOC	mg/g TOC	mg/g TOC	mg/g TOC
Methane	17.51	83.01	149.59	19.14	123.12	286.18	12.18	82.30	185.70	16.23	79.89	159.08
Ethane	15.97	36.19	0.66	15.54	75.88	3.10	10.73	50.71	4.02	8.70	25.67	1.11
Propane	15.82	17.30	0.08	18.88	56.05	0.19	15.56	41.83	1.03	9.49	10.97	0.11
i-Butane	2.41	1.68	0.00	3.98	5.49	0.00	3.10	9.67	0.00	2.98	1.13	0.00
n-Butane	7.47	0.23	0.00	9.52	1.35	0.00	5.80	4.77	0.00	4.22	0.21	0.00
i-Pentane	3.83	0.30	0.00	6.64	1.02	0.00	2.71	0.59	0.00	5.45	0.35	0.00
n-Pentane	3.87	0.03	0.00	6.84	0.22	0.00	4.12	0.58	0.00	2.19	0.03	0.00
Cyclopentane	0.29	0.00	0.00	0.86	0.49	0.00	0.42	0.23	0.00	0.35	0.00	0.00
2-Methylpentane	1.13	0.00	0.00	2.29	0.04	0.00	1.62	0.06	0.00	1.16	0.00	0.00
3-Methylpentane	0.68	0.00	0.00	0.86	0.02	0.00	0.67	0.03	0.00	0.32	0.00	0.00
n-Hexane	2.25	0.00	0.00	5.33	0.03	0.00	3.09	0.10	0.00	1.24	0.00	0.00
Methylcyclopentane	0.63	0.00	0.00	2.03	0.07	0.00	0.97	0.10	0.00	0.76	0.00	0.00
Benzene	0.69	3.07	4.08	0.52	7.33	14.20	1.08	4.67	15.06	0.39	3.13	4.94
Thiophene	0.22	0.30	0.00	0.20	0.32	0.00	0.12	0.00	0.00	0.09	0.12	0.00
Cyclohexane	0.16	0.00	0.00	0.39	0.00	0.00	0.23	0.00	0.00	0.07	0.00	0.00
2-Methylhexane	0.59	0.00	0.00	0.37	0.00	0.00	0.58	0.00	0.00	0.41	0.00	0.00
2,3-Dimethylpentane	0.07	0.00	0.00	0.08	0.00	0.00	0.06	0.00	0.00	0.04	0.00	0.00
1,1-Dimethylpentane	0.00	0.00	0.00	0.00	0.00	0.00	0.00	0.00	0.00	0.00	0.00	0.00
3-Methylhexane	0.51	0.00	0.00	0.69	0.00	0.00	0.57	0.00	0.00	0.23	0.00	0.00
n-Heptane	1.57	0.00	0.00	5.92	0.00	0.00	3.48	0.00	0.00	1.23	0.00	0.00
Methyl-Cyclohexane	0.28	0.00	0.00	0.74	0.00	0.00	0.56	0.00	0.00	0.15	0.00	0.00
Ethylcyclopentane	0.24	0.00	0.00	0.79	0.00	0.00	0.32	0.00	0.00	0.22	0.00	0.00
2,5-Dimethylhexane	0.11	0.00	0.00	0.15	0.00	0.00	0.18	0.00	0.00	0.11	0.00	0.00
2,4-Dimethylhexane	0.02	0.00	0.00	0.03	0.00	0.00	0.03	0.00	0.00	0.01	0.00	0.00
3,3-Dimethylhexane	0.02	0.00	0.00	0.03	0.00	0.00	0.04	0.00	0.00	0.01	0.00	0.00
2,3,4-Trimethylpentane	0.32	0.00	0.00	0.72	0.00	0.00	0.85	0.00	0.00	0.18	0.00	0.00
Toluene	2.95	7.61	0.00	2.84	16.59	0.41	1.87	10.80	0.00	1.90	7.42	0.07
2-Methylthiophene	0.42	0.35	0.00	0.59	0.25	0.00	0.36	0.00	0.00	0.12	0.11	0.00
3-Methylthiophene	0.17	0.24	0.00	0.28	0.27	0.00	0.41	0.00	0.00	0.00	0.12	0.00
n-Octane	0.98	0.00	0.00	4.84	0.00	0.00	2.93	0.00	0.00	0.88	0.00	0.00
Ethylbenzene	1.14	1.08	0.00	1.21	3.89	0.00	1.07	2.42	0.00	0.62	0.76	0.00
Ethylthiophene	0.15	0.00	0.00	0.24	0.00	0.00	0.15	0.00	0.00	0.10	0.00	0.00
2,5-Dimethylthiophene	0.09	0.00	0.00	0.22	0.00	0.00	0.08	0.00	0.00	0.08	0.00	0.00
m/p-Xylene	2.91	5.31	0.00	2.95	8.39	0.00	2.86	8.05	0.00	1.78	4.21	0.00
2,4-Dimethylthiophene	0.21	0.00	0.00	0.57	0.00	0.00	0.37	0.00	0.00	0.22	0.00	0.00
2,3-Dimethylthiophene	0.24	0.00	0.00	0.48	0.00	0.00	0.44	0.00	0.00	0.26	0.00	0.00
Styrene	0.24	0.00	0.00	0.17	0.00	0.00	0.15	0.00	0.00	0.05	0.00	0.00
o-Xylene	1.31	1.51	0.00	1.48	3.46	0.00	1.38	3.52	0.00	0.61	0.85	0.00
n-Nonane	0.51	0.00	0.00	4.15	0.00	0.00	2.12	0.00	0.00	0.66	0.00	0.00
2-Propylthiophene	0.43	0.00	0.00	0.49	0.00	0.00	0.35	0.00	0.00	0.25	0.00	0.00
Propylbenzene	0.01	0.00	0.00	0.17	0.00	0.00	0.13	0.00	0.00	0.02	0.00	0.00
2-Ethyl-5-Methylthiophene	0.09	0.00	0.00	0.34	0.00	0.00	0.06	0.00	0.00	0.10	0.00	0.00
(?) -Benzene	1.83	1.39	0.00	1.63	3.87	0.00	1.58	3.14	0.00	0.90	0.87	0.00
2-Ethyl-4-Methylthiophene	0.11	0.00	0.00	0.30	0.00	0.00	0.00	0.00	0.00	0.00	0.00	0.00
1,3,5-Trimethylbenzene	0.45	0.65	0.00	0.36	0.74	0.00	0.44	0.99	0.00	0.27	0.38	0.00
Phenol	0.07	0.00	0.00	0.19	1.23	0.00	0.19	0.00	0.00	1.82	4.01	0.00
1-Ethyl-2-Methylbenzene	0.71	0.15	0.00	1.89	1.61	0.00	0.76	0.66	0.00	0.65	0.22	0.00
2,3,5-Trimethylthiophene	0.21	0.00	0.00	0.41	0.00	0.00	0.00	0.00	0.00	0.00	0.00	0.00
1,2,4-Trimethylbenzene	1.43	1.32	0.00	1.50	2.29	0.00	1.78	3.18	0.00	0.68	0.57	0.00
n-Decane	0.36	0.00	0.00	3.87	0.00	0.00	1.88	0.00	0.00	0.58	0.00	0.00
1,2,3-Trimethylbenzene	0.61	0.29	0.00	1.83	0.96	0.00	1.37	0.81	0.00	0.52	0.16	0.00
o-Cresol	0.28	0.00	0.00	1.10	0.50	0.00	0.15	0.00	0.00	2.21	0.52	0.00
m/p-Cresol	0.20	0.00	0.00	1.44	1.49	0.00	0.23	0.00	0.00	1.85	1.13	0.00
Dimethylphenol	0.00	0.00	0.00	0.00	0.00	0.00	0.00	0.00	0.00	0.49	0.00	0.00
n-Undecane	0.31	0.00	0.00	4.05	0.00	0.00	1.81	0.00	0.00	0.61	0.00	0.00
1,2,3,4-Tetramethylbenzene	0.00	0.00	0.00	0.00	0.00	0.00	0.00	0.00	0.00	0.18	0.00	0.00
Naphthalene	0.37	1.56	0.00	0.51	3.57	0.28	0.46	2.17	0.00	0.22	1.53	0.07
n-Dodecane	0.27	0.00	0.00	3.77	0.00	0.00	1.66	0.00	0.00	0.67	0.00	0.00
2-Methylnaphthalene	0.68	1.72	0.00	0.64	3.98	0.00	0.69	2.89	0.00	0.44	1.48	0.00
1-Methylnaphthalene	0.58	0.67	0.00	0.82	1.92	0.00	0.59	1.66	0.00	0.46	0.48	0.00
n-Tridecane	0.24	0.00	0.00	3.55	0.00	0.00	1.86	0.00	0.00	0.51	0.00	0.00
n-Tetradecane	0.11	0.00	0.00	2.92	0.00	0.00	1.41	0.00	0.00	0.37	0.01	0.00
Dimethylnaphthalene	0.90	0.53	0.00	1.43	1.72	0.00	1.42	1.89	0.00	1.41	0.54	0.00
n-Pentadecane	0.26	0.00	0.00	2.76	0.00	0.00	1.44	0.00	0.00	0.39	0.14	0.00
Trimethylnaphthalene	0.20	0.00	0.00	0.00	0.00	0.00	0.28	0.00	0.00	0.10	0.00	0.00
Trimethylnaphthalene	0.19	0.00	0.00	0.00	0.00	0.00	0.41	0.00	0.00	0.12	0.00	0.00
Trimethylnaphthalene	0.08	0.00	0.00	0.00	0.00	0.00	0.29	0.00	0.00	0.24	0.00	0.00
n-Hexadecane	0.05	0.00	0.00	2.41	0.07	0.00	1.10	0.00	0.00	0.33	0.00	0.00
Is												

Table A 7: Late Gas Potential Screening (immature samples)

Company	GFZ											
Formation/Basin	Arang Coal			Spekk Fm.			Are Fm.			Fischschiefer		
GFZ Code	G00950AA	G00950AB	G00950AC	G001955DE	G001955EH	G001955DM	G001955AD	G001955AN	G001955AI	G004070AA	G004070AB	G004070AC
File	200-460	200-560	200-700	200-450	200-550	200-700	200-450	200-550	200-700	200-460	200-560	200-700
Temperature [°C]	2K/min	2K/min	2K/min	1K/min	1K/min	1K/min	1K/min	1K/min	1K/min	2K/min	2K/min	2K/min
Rate	mg/g TOC	mg/g TOC	mg/g TOC	mg/g TOC	mg/g TOC	mg/g TOC	mg/g TOC	mg/g TOC	mg/g TOC	mg/g TOC	mg/g TOC	mg/g TOC
Totals	mg/g TOC	mg/g TOC	mg/g TOC	mg/g TOC	mg/g TOC	mg/g TOC	mg/g TOC	mg/g TOC	mg/g TOC	mg/g TOC	mg/g TOC	mg/g TOC
Total C1+ (-blank)	111.80	143.57	156.24	259.59	242.18	175.41	99.32	122.52	130.26	445.69	402.64	307.45
Total C1-5	44.99	113.63	148.21	83.40	195.74	172.56	36.23	98.43	128.91	124.12	286.39	274.38
Total C2-5	31.32	36.06	0.93	64.49	86.51	0.34	22.71	27.02	0.60	102.95	161.17	4.08
Total C <sub>6-14</sub> (-blank)	50.42	26.49	3.86	138.85	43.70	2.85	48.23	21.19	1.05	225.34	94.58	25.28
Total C <sub>15+</sub> (-blank)	16.38	3.45	4.17	37.33	2.75	0.00	14.86	2.90	0.30	96.23	21.66	7.79
Total C <sub>p</sub> (-blank)	66.80	29.94	8.03	176.19	46.44	2.85	63.09	24.09	1.34	321.56	116.25	33.07
GOR	0.67	3.80	18.45	0.47	4.21	60.52	0.57	4.09	95.93	0.39	2.46	8.30
Gas Wetness (C <sub>2</sub> /C <sub>1+5</sub> )	0.70	0.32	0.01	0.77	0.44	0.00	0.63	0.27	0.00	0.83	0.56	0.01
Compound	mg/g TOC	mg/g TOC	mg/g TOC	mg/g TOC	mg/g TOC	mg/g TOC	mg/g TOC	mg/g TOC	mg/g TOC	mg/g TOC	mg/g TOC	mg/g TOC
Methane	13.67	77.57	147.28	18.90	109.19	172.23	13.52	71.36	128.31	21.17	125.22	270.30
Ethane	7.26	23.56	0.71	16.72	53.90	0.14	7.65	20.49	0.44	19.08	90.82	3.20
Propane	7.71	10.41	0.07	18.89	29.07	0.00	6.40	5.45	0.00	23.63	60.13	0.17
i-Butane	1.75	1.00	0.00	0.00	2.18	0.00	0.00	0.27	0.00	4.20	5.57	0.00
n-Butane	3.99	0.21	0.00	0.00	0.20	0.00	0.00	0.07	0.00	11.15	1.05	0.00
i-Pentane	3.31	0.20	0.00	5.58	0.09	0.00	3.03	0.02	0.00	5.97	0.14	0.00
n-Pentane	2.12	0.02	0.00	6.64	0.04	0.00	1.69	0.01	0.00	8.10	0.04	0.00
Cyclopentane	0.21	0.00	0.00	0.77	0.02	0.00	0.28	0.00	0.00	0.95	0.36	0.00
2-Methylpentane	0.85	0.00	0.00	2.22	0.01	0.00	0.61	0.00	0.00	3.67	0.03	0.00
3-Methylpentane	0.23	0.00	0.00	0.84	0.00	0.00	0.21	0.00	0.00	1.40	0.00	0.00
n-Hexane	1.51	0.00	0.00	4.60	0.01	0.00	1.05	0.00	0.00	5.85	0.02	0.00
Methylcyclopentane	0.40	0.00	0.00	1.96	0.00	0.00	0.52	0.00	0.00	2.73	0.03	0.00
Benzene	0.50	3.08	2.52	0.94	5.37	3.11	0.41	2.58	0.89	1.62	7.24	23.97
Thiophene	0.03	0.08	0.00	0.06	0.33	0.00	0.05	0.05	0.00	0.57	1.40	0.00
Cyclohexane	0.06	0.00	0.00	0.34	0.01	0.00	0.09	0.00	0.00	0.55	0.00	0.00
2-Methylhexane	0.21	0.00	0.00	0.70	0.00	0.00	0.14	0.00	0.00	0.44	0.00	0.00
2,3-Dimethylpentane	0.02	0.00	0.00	0.19	0.00	0.00	0.07	0.00	0.00	1.05	0.00	0.00
1,1-Dimethylpentane	0.00	0.00	0.00	0.06	0.00	0.00	0.02	0.00	0.00	0.00	0.00	0.00
3-Methylhexane	0.17	0.00	0.00	1.00	0.00	0.00	0.23	0.00	0.00	1.16	0.00	0.00
n-Heptane	1.52	0.00	0.00	4.65	0.00	0.00	1.02	0.00	0.00	6.54	0.00	0.00
Methyl-Cyclohexane	0.12	0.00	0.00	0.73	0.00	0.00	0.14	0.03	0.00	0.99	0.00	0.00
Ethylcyclopentane	0.14	0.00	0.00	0.82	0.00	0.00	0.16	0.00	0.00	1.14	0.00	0.00
2,5-Dimethylhexane	0.03	0.00	0.00	0.25	0.00	0.00	0.09	0.00	0.00	0.18	0.00	0.00
2,4-Dimethylhexane	0.01	0.00	0.00	0.01	0.00	0.00	0.01	0.00	0.00	0.02	0.00	0.00
3,3-Dimethylhexane	0.00	0.00	0.00	0.02	0.00	0.00	0.01	0.00	0.00	0.03	0.00	0.00
2,3,4-Trimethylpentane	0.10	0.00	0.00	0.70	0.00	0.00	0.12	0.00	0.00	1.45	0.00	0.00
Toluene	1.85	6.86	0.09	3.31	12.39	0.04	1.67	5.28	0.00	3.08	18.04	0.36
2-Methylthiophene	0.10	0.05	0.00	1.71	0.13	0.00	0.17	0.03	0.00	1.65	0.87	0.00
3-Methylthiophene	0.05	0.04	0.00	0.42	0.25	0.00	0.08	0.04	0.00	0.46	1.23	0.00
n-Octane	1.28	0.00	0.00	3.28	0.00	0.00	0.70	0.00	0.00	5.29	0.00	0.00
Ethylbenzene	0.56	0.54	0.00	1.30	1.45	0.00	0.53	0.37	0.00	1.35	3.83	0.00
Ethylthiophene	0.02	0.00	0.00	0.77	0.00	0.00	0.07	0.00	0.00	0.77	0.00	0.00
2,5-Dimethylthiophene	0.02	0.00	0.00	0.94	0.00	0.00	0.07	0.00	0.00	0.69	0.00	0.00
m/p-Xylene	1.49	3.34	0.00	3.03	5.85	0.00	1.33	2.46	0.00	4.59	10.59	0.00
2,4-Dimethylthiophene	0.08	0.00	0.00	0.83	0.04	0.00	0.10	0.06	0.00	0.78	0.22	0.00
2,3-Dimethylthiophene	0.08	0.00	0.00	1.14	0.02	0.00	0.10	0.01	0.00	1.07	0.16	0.00
Styrene	0.01	0.00	0.00	0.00	0.00	0.00	0.00	0.00	0.00	0.90	0.04	0.00
o-Xylene	0.64	0.78	0.00	1.64	1.84	0.00	0.66	0.53	0.00	2.03	4.22	0.00
n-Nonane	1.05	0.00	0.00	2.55	0.00	0.00	0.52	0.00	0.00	4.22	0.00	0.00
2-Propylthiophene	0.15	0.00	0.00	0.72	0.03	0.00	0.19	0.01	0.00	0.83	0.00	0.00
Propylbenzene	0.02	0.00	0.00	0.31	0.00	0.00	0.05	0.00	0.00	0.21	0.05	0.00
2-Ethyl-5-Methylthiophene	0.02	0.00	0.00	1.18	0.12	0.00	0.07	0.07	0.00	0.96	0.00	0.00
(?)-Benzene	0.70	0.57	0.00	1.66	1.29	0.00	0.65	0.35	0.00	2.29	4.09	0.00
2-Ethyl-4-Methylthiophene	0.00	0.00	0.00	0.00	0.00	0.00	0.07	0.00	0.00	0.70	0.00	0.00
1,3,5-Trimethylbenzene	0.16	0.31	0.00	1.15	0.90	0.00	0.55	0.34	0.00	0.72	1.00	0.00
Phenol	1.84	2.71	0.00	0.31	0.00	0.00	1.81	1.94	0.00	0.33	0.42	0.00
1-Ethyl-2-Methylbenzene	0.37	0.00	0.00	1.04	0.17	0.00	0.23	0.06	0.00	1.37	1.17	0.00
2,3,5-Trimethylthiophene	0.00	0.00	0.00	0.78	0.00	0.00	0.07	0.00	0.00	0.95	0.00	0.00
1,2,4-Trimethylbenzene	0.54	0.45	0.00	1.33	0.75	0.00	0.48	0.27	0.00	2.25	2.60	0.00
n-Decane	0.95	0.00	0.00	2.18	0.00	0.00	0.47	0.00	0.00	3.95	0.00	0.00
1,2,3-Trimethylbenzene	0.42	0.11	0.00	1.12	0.24	0.00	0.49	0.09	0.00	2.57	1.12	0.00
o-Cresol	1.64	0.28	0.00	0.00	0.00	0.00	1.76	0.15	0.00	0.57	0.00	0.00
m/p-Cresol	1.77	0.67	0.00	0.00	0.00	0.00	2.25	0.42	0.00	0.68	0.00	0.00
Dimethylphenol	0.33	0.00	0.00	0.00	0.00	0.00	0.33	0.01	0.00	0.00	0.00	0.00
n-Undecane	0.99	0.00	0.00	2.01	0.00	0.00	0.42	0.00	0.00	3.89	0.00	0.00
1,2,3,4-Tetramethylbenzene	0.15	0.00	0.00	0.70	0.00	0.00	0.41	0.02	0.00	0.00	0.00	0.00
Naphthalene	0.20	1.08	0.14	0.45	4.28	0.01	0.07	1.26	0.00	0.60	5.94	0.96
n-Dodecane	0.99	0.00	0.00	1.83	0.00	0.00	0.53	0.01	0.00	3.55	0.00	0.00
2-Methylnaphthalene	0.37	0.94	0.12	0.80	2.35	0.00	0.44	0.83	0.00	1.06	6.69	0.00
1-Methylnaphthalene	0.39	0.32	0.15	0.74	0.59	0.00	0.35	0.23	0.00	0.94	2.87	0.00
n-Tridecane	0.82	0.00	0.00	1.54	0.00	0.00	0.34	0.00	0.00	3.41	0.00	0.00
n-Tetradecane	0.67	0.00	0.00	1.83	0.02	0.00	0.31	0.00	0.00	2.77	0.07	0.00
Dimethylnaphthalene	1.15	0.29	0.00	1.28	0.26	0.00	0.71	0.16	0.00	2.06	2.08	0.00
n-Pentadecane	0.60	0.09	0.00	1.30	0.01	0.00	0.31	0.01	0.00	2.65	0.15	0.00
Trimethylnaphthalene	0.12	0.00	0.00	0.21	0.00	0.00	0.00	0.00	0.00	0.38	0.08	0.00
Trimethylnaphthalene	0.28	0.00	0.00	0.32	0.01	0.00	0.10	0.01	0.00	0.91	0.08	0.00
Trimethylnaphthalene	0.24	0.00	0.00	0.21	0.00	0.00	0.17	0.01	0.00	1.46	0.07	0.00
n-Hexadecane	0.50	0.01	0.00	0.95	0.00	0.00	0.21	0.00	0.00	2.35	0.03	0.00
Isopropylidimethylnaphthalene	0.38	0.00	0.00	0.05	0.00	0.00	0.03	0.00	0.00	0.00	0.00	0.00
n-Heptadecane	0.49	0.01	0.01	0.63	0.01	0.00	0.17	0.00	0.00	2.38	0.09	0.00
Pristane	0.05	0.00	0.00	0.12	0.00	0.00	0.05	0.01	0.00	0.48	0.00	0.00
Prist-1-ene	0.03	0.00	0.00	0.00	0.00	0.00	0.03	0.01	0.00	0.08	0.00	0.00
n-Octadecane	0.41	0.01	0.02	0.44	0.00	0.00	0.15	0.00	0.00	1.84	0.07	0.00
Phytane	0.02	0.00	0.00	0.05	0.00	0.00	0.03	0.00	0.00	0.15	0.00	0.00
n-Nonadecane	0.38	0.02	0.02	0.37	0.00	0.00	0.13	0.00	0.00	1.75	0.20	0.00
n-Icosane	0.31	0.01	0.04	0.26	0.00	0.00	0.11	0.00	0.00	1.35	0.17	0.00
n-Henicosane	0.25	0.02	0.05	0.15	0.00	0.00	0.08	0.00	0.00	1.05	0.08	0.00
n-Docosane	0.21	0.02	0.05	0.09	0.00	0.00	0.06	0.00	0.00	0.73	0.11	0.00
n-Tricosane	0.17	0.01	0.04	0.05	0.00	0.00	0.04	0.00	0.00	0.61	0.17	0.00
n-Tetracosane	0.13	0.01	0.02	0.03	0.00	0.00	0.03	0.00	0.00	0.50	0.18	0.00
n-Pentacosane	0.10	0.01	0.01	0.01	0.00	0.00	0.02	0.00	0.00	0.41	0.13	0.00
n-Hexacosane	0.08	0.00										

Table A 7: Late Gas Potential Screening (immature samples)

Company	GFZ											
Formation/Basin	Fischschiefer			Fischschiefer			Green River Shale			Mix type I/II		
GFZ Code	G004071AA	G004071AB	G004071AC	G004072AC	G004072AA	G004072AB	G004750AD	G004750AF	G004750AJ	G004750BD	G004750BF	G004750BJ
File	200-460	200-560	200-700	200-460	200-560	200-700	200-450	200-550	200-700	200-450	200-550	200-700
Temperature [°C]	2K/min	2K/min	2K/min	2K/min	2K/min	2K/min	1K/min	1K/min	1K/min	1K/min	1K/min	1K/min
Rate	mg/g TOC	mg/g TOC	mg/g TOC	mg/g TOC	mg/g TOC	mg/g TOC	mg/g TOC	mg/g TOC	mg/g TOC	mg/g TOC	mg/g TOC	mg/g TOC
Totals	mg/g TOC	mg/g TOC	mg/g TOC	mg/g TOC	mg/g TOC	mg/g TOC	mg/g TOC	mg/g TOC	mg/g TOC	mg/g TOC	mg/g TOC	mg/g TOC
Total C1+ (-blank)	431.15	398.49	324.33	354.73	316.55	262.64	751.65	571.95	376.88	240.11	203.23	173.50
Total C1-5	132.36	294.67	298.00	109.07	232.30	238.80	158.90	414.29	351.07	76.98	152.40	170.27
Total C2-5	109.11	162.14	4.21	89.94	123.05	2.88	137.08	232.06	2.06	59.03	62.18	0.85
Total C <sub>6-14</sub> (-blank)	226.19	92.99	23.25	178.98	72.99	14.88	354.61	135.00	26.81	120.97	44.71	3.23
Total C <sub>15+</sub> (-blank)	72.60	10.83	3.08	66.67	11.27	8.96	238.15	22.66	-1.00	42.16	6.12	0.00
Total C <sub>6+</sub> (-blank)	298.80	103.82	26.33	245.66	84.25	23.84	592.75	157.66	25.81	163.14	50.83	3.23
GOR	0.44	2.84	11.32	0.44	2.76	10.02	0.27	2.63	13.60	0.47	3.00	52.69
Gas Wetness (C <sub>2+</sub> /C <sub>1+</sub> )	0.82	0.55	0.01	0.82	0.53	0.01	0.86	0.56	0.01	0.77	0.41	0.00
Compound	mg/g TOC	mg/g TOC	mg/g TOC	mg/g TOC	mg/g TOC	mg/g TOC	mg/g TOC	mg/g TOC	mg/g TOC	mg/g TOC	mg/g TOC	mg/g TOC
Methane	23.25	132.53	293.79	12.18	82.30	185.70	21.84	182.22	348.96	17.94	90.22	169.41
Ethane	20.27	91.28	3.17	10.73	50.71	4.02	20.58	141.21	1.39	12.60	42.58	0.57
Propane	25.52	59.72	0.25	15.56	41.83	1.03	31.51	76.10	0.11	14.32	17.21	1.06
i-Butane	4.37	5.69	0.00	3.10	9.67	0.00	4.04	5.36	0.00	2.49	0.43	0.00
n-Butane	11.62	1.13	0.00	5.80	4.77	0.00	15.93	1.59	0.00	7.48	0.16	0.01
i-Pentane	6.52	0.14	0.00	2.71	0.59	0.00	4.91	0.32	0.00	3.95	0.08	0.00
n-Pentane	8.40	0.14	0.00	4.12	0.58	0.00	13.23	0.27	0.00	5.32	0.03	0.00
Cyclopentane	0.97	0.41	0.00	0.42	0.23	0.00	1.30	0.34	0.00	0.62	0.02	0.00
2-Methylpentane	4.12	0.03	0.00	1.62	0.06	0.00	3.35	0.05	0.00	1.42	0.00	0.00
3-Methylpentane	1.54	0.00	0.00	0.67	0.03	0.00	1.13	0.02	0.00	0.51	0.00	0.00
n-Hexane	6.01	0.02	0.00	3.09	0.10	0.00	11.82	0.04	0.00	4.12	0.00	0.00
Methylcyclopentane	2.85	0.03	0.00	0.97	0.10	0.00	3.33	0.05	0.00	1.39	0.00	0.00
Benzene	0.46	7.61	22.39	1.08	4.67	15.06	4.36	13.87	23.16	0.57	4.55	2.22
Thiophene	0.46	1.49	0.00	0.12	0.00	0.00	0.44	1.17	0.00	0.15	0.27	0.00
Cyclohexane	0.50	0.00	0.00	0.29	0.00	0.00	0.85	0.00	0.00	0.25	0.00	0.00
2-Methylhexane	1.08	0.00	0.00	0.58	0.00	0.00	1.03	0.00	0.00	0.59	0.00	0.00
2,3-Dimethylpentane	0.09	0.00	0.00	0.06	0.00	0.00	0.24	0.00	0.00	0.11	0.00	0.00
1,1-Dimethylpentane	0.00	0.00	0.00	0.00	0.00	0.00	0.13	0.00	0.00	0.05	0.00	0.00
3-Methylhexane	1.32	0.00	0.00	0.57	0.00	0.00	1.11	0.00	0.00	0.38	0.00	0.00
n-Heptane	6.80	0.00	0.00	3.48	0.00	0.00	13.22	0.00	0.00	4.22	0.00	0.00
Methyl-Cyclohexane	1.07	0.00	0.00	0.56	0.00	0.00	2.11	0.00	0.00	0.52	0.00	0.00
Ethylcyclopentane	1.19	0.00	0.00	0.32	0.00	0.00	2.01	0.00	0.00	0.60	0.00	0.00
2,5-Dimethylhexane	0.23	0.00	0.00	0.18	0.00	0.00	0.80	0.00	0.00	0.22	0.00	0.00
2,4-Dimethylhexane	0.02	0.00	0.00	0.03	0.00	0.00	0.03	0.00	0.00	0.01	0.00	0.00
3,3-Dimethylhexane	0.03	0.00	0.00	0.04	0.00	0.00	0.08	0.00	0.00	0.02	0.00	0.00
2,3,4-Trimethylpentane	1.60	0.00	0.00	0.85	0.00	0.00	2.30	0.00	0.00	0.47	0.00	0.00
Toluene	2.96	17.57	0.53	1.87	10.80	0.00	4.84	31.29	0.00	2.78	10.62	0.00
2-Methylthiophene	1.57	1.07	0.00	0.36	0.00	0.00	1.82	0.42	0.00	0.48	0.15	0.00
3-Methylthiophene	0.43	1.32	0.00	0.41	0.00	0.00	0.95	0.86	0.00	0.15	0.21	0.00
n-Octane	5.20	0.00	0.00	2.93	0.00	0.00	10.75	0.00	0.00	3.29	0.02	0.00
Ethylbenzene	1.43	3.80	0.00	1.07	2.42	0.00	2.01	7.44	0.00	1.08	1.41	52.69
Ethylthiophene	0.75	0.00	0.00	0.15	0.00	0.00	1.07	0.00	0.00	0.19	0.00	0.00
2,5-Dimethylthiophene	0.80	0.00	0.00	0.08	0.00	0.00	0.61	0.00	0.00	0.16	0.00	0.00
m/p-Xylene	4.84	10.85	0.00	2.86	8.05	0.00	5.91	14.62	0.00	2.59	5.08	0.00
2,4-Dimethylthiophene	0.86	0.30	0.00	0.37	0.00	0.00	0.94	0.34	0.00	0.33	0.03	0.00
2,3-Dimethylthiophene	1.02	0.19	0.00	0.44	0.00	0.00	0.69	0.05	0.00	0.22	0.02	0.00
Styrene	0.89	0.04	0.00	0.15	0.00	0.00	0.00	0.00	0.00	0.00	0.00	0.00
o-Xylene	1.98	4.22	0.00	1.38	3.52	0.00	3.05	5.71	0.00	1.35	1.63	0.00
n-Nonane	4.05	0.00	0.00	2.12	0.00	0.00	9.74	0.00	0.00	2.76	0.00	0.00
2-Propylthiophene	0.89	0.00	0.00	0.35	0.00	0.00	1.18	0.12	0.00	0.51	0.01	0.00
Propylbenzene	0.23	0.05	0.00	0.13	0.00	0.00	0.52	0.09	0.00	0.07	0.00	0.00
2-Ethyl-5-Methylthiophene	0.95	0.00	0.00	0.06	0.00	0.00	1.15	0.00	0.00	0.27	0.00	0.00
(?)-Benzene	2.26	4.24	0.00	1.58	3.14	0.00	3.21	6.95	0.00	1.32	1.32	0.00
2-Ethyl-4-Methylthiophene	0.80	0.00	0.00	0.00	0.00	0.00	0.00	0.00	0.00	0.21	0.00	0.00
1,3,5-Trimethylbenzene	0.62	1.02	0.00	0.44	0.99	0.00	0.83	1.09	0.00	0.34	0.42	0.00
Phenol	0.35	0.00	0.00	0.19	0.00	0.00	0.35	0.11	0.00	2.19	2.64	0.00
1-Ethyl-2-Methylbenzene	1.18	0.93	0.00	0.76	0.66	0.00	1.82	0.97	0.00	0.57	0.29	0.00
2,3,5-Trimethylthiophene	0.97	0.00	0.00	0.00	0.00	0.00	0.00	0.00	0.00	0.00	0.00	0.00
1,2,4-Trimethylbenzene	2.17	2.83	0.00	1.78	3.18	0.00	3.17	2.96	0.00	1.05	0.83	0.00
n-Decane	3.65	0.00	0.00	1.88	0.00	0.00	9.30	0.02	0.00	2.51	0.00	0.00
1,2,3-Trimethylbenzene	2.73	1.31	0.00	1.37	0.81	0.00	2.63	0.98	0.00	1.05	0.29	0.00
o-Cresol	0.42	0.00	0.00	0.15	0.00	0.00	0.82	0.04	0.00	1.90	0.27	0.00
m/p-Cresol	0.30	0.00	0.00	0.23	0.00	0.00	0.90	0.12	0.00	2.55	0.73	0.00
Dimethylphenol	0.00	0.00	0.00	0.00	0.00	0.00	1.07	0.00	0.00	0.53	0.01	0.00
n-Undecane	3.45	0.00	0.00	1.81	0.00	0.00	9.55	0.09	0.00	2.40	0.00	0.00
1,2,3,4-Tetramethylbenzene	0.00	0.00	0.00	0.00	0.00	0.00	1.25	0.21	0.00	0.19	0.01	0.00
Naphthalene	0.57	5.36	0.76	0.46	2.17	0.00	0.25	10.24	0.00	0.39	2.85	0.00
n-Dodecane	3.14	0.00	0.00	1.66	0.00	0.00	7.90	0.00	0.00	2.72	0.00	0.00
2-Methylnaphthalene	0.98	6.24	0.00	0.69	2.89	0.00	0.33	8.52	0.00	0.83	2.25	0.00
1-Methylnaphthalene	0.87	3.03	0.00	0.59	1.66	0.00	0.18	3.00	0.00	0.72	0.77	0.00
n-Tridecane	2.98	0.00	0.00	1.86	0.00	0.00	7.16	0.00	0.00	2.33	0.01	0.00
n-Tetradecane	2.45	0.07	0.00	1.41	0.00	0.00	7.40	0.13	0.00	1.89	0.01	0.00
Dimethylnaphthalene	2.23	2.45	0.00	1.42	1.89	0.00	1.54	1.52	0.00	0.98	0.50	0.00
n-Pentadecane	2.32	0.16	0.00	1.44	0.00	0.00	6.35	0.08	0.00	1.41	0.17	0.00
Trimethylnaphthalene	0.38	0.00	0.00	0.28	0.00	0.00	0.54	0.04	0.00	0.20	0.02	0.00
Trimethylnaphthalene	0.82	0.00	0.00	0.41	0.00	0.00	1.14	0.10	0.00	0.31	0.01	0.00
Trimethylnaphthalene	1.62	0.00	0.00	0.29	0.00	0.00	0.00	0.00	0.00	0.00	0.00	0.00
n-Hexadecane	1.87	0.00	0.00	1.10	0.00	0.00	6.25	0.14	0.00	1.31	0.01	0.00
Isopropylidimethylnaphthalene	0.00	0.00	0.00	0.00	0.00	0.00	0.20	0.00	0.00	0.00	0.00	0.00
n-Heptadecane	1.81	0.00	0.00	1.22	0.00	0.00	5.63	0.18	0.00	1.18	0.02	0.00
Pristane	0.48	0.00	0.00	0.27	0.00	0.00	0.28	0.05	0.00	0.05	0.00	0.00
PrisL-1-ene	0.07	0.00	0.00	0.07	0.00	0.00	0.14	0.00	0.00	0.02	0.05	0.00
n-Octadecane	1.24	0.00	0.00	0.96	0.00	0.00	4.45	0.20	0.00	0.88	0.01	0.00
Phytane	0.10	0.00	0.00	0.13	0.00	0.00	0.33	0.11	0.00	0.09	0.02	0.00
n-Nonadecane	0.92	0.00	0.00	0.88	0.00	0.00	4.09	0.10	0.00	0.76	0.05	0.00
n-Icosane	0.54	0.00	0.00	0.76	0.00	0.00	3.47	0.05	0.00	0.62	0.02	0.00
n-Henicosane	0.32	0.00	0.00	0.60	0.00	0.00	2.99	1.11	0.00	0.49	0.07	0.00
n-Docosane	0.19	0.00	0.00	0.48	0.00	0.00	2.67	0.06	0.00	0.38	0.03	0.00
n-Tricosane	0.13	0.00	0.00	0.36	0.00	0.00	2.43	0.01	0.00	0.27	0.01	0.00
n-Tetracosane	0.11	0.00	0.00	0.28	0.00	0.00	2.04	0.01	0.00	0.21	0.01	0.00
n-Pentacosane	0.07	0.00	0.00	0.22	0.00	0.00	1.88	0.02	0.00	0.18	0.	

Table A 7: Late Gas Potential Screening (immature samples)

Company	GFZ					
Formation/Basin	Bakken Shale			Taglu Fm.		
GFZ Code	G005298			SN6750		
File	G005298CA	G005298CB	G005298CC	SN6750II	SN6750IS	SN6750IO
Temperature [°C]	200-460	200-560	200-700	200-460	200-550	200-700
Rate	2K/min	2K/min	2K/min	1K/min	1K/min	1K/min
Totals	mg/g TOC	mg/g TOC	mg/g TOC	mg/g TOC	mg/g TOC	mg/g TOC
Total C1+ (-blank)	322.56	232.30	224.13	126.12	130.69	142.09
Total C1-5	113.86	170.64	203.09	53.35	103.58	140.82
Total C2-5	93.54	85.79	1.88	34.67	34.41	0.21
Total C <sub>6-14</sub> (-blank)	162.74	52.84	12.22	55.28	20.33	1.26
Total C <sub>15+</sub> (-blank)	45.97	8.82	8.82	17.48	6.78	0.00
Total C <sub>6+</sub> (-blank)	208.71	61.66	21.04	72.76	27.12	1.26
GOR	0.55	2.77	9.65	0.73	3.82	111.64
Gas Wetness (C <sub>2-5</sub> /C <sub>1-5</sub> )	0.82	0.50	0.01	0.65	0.33	0.00
Compound	mg/g TOC	mg/g TOC	mg/g TOC	mg/g TOC	mg/g TOC	mg/g TOC
Methane	20.32	84.84	201.21	18.68	69.13	140.60
Ethane	19.17	51.18	1.13	10.39	21.93	0.14
Propane	21.63	29.48	0.26	8.97	9.91	0.00
i-Butane	3.63	2.40	0.00	1.68	1.33	0.00
n-Butane	9.19	0.35	0.00	3.79	0.21	0.00
i-Pentane	5.00	0.05	0.00	2.67	0.05	0.00
n-Pentane	6.56	0.05	0.00	2.07	0.02	0.00
Cyclopentane	0.72	0.09	0.00	0.29	0.01	0.00
2-Methylpentane	2.75	0.01	0.00	0.71	0.00	0.00
3-Methylpentane	0.91	0.00	0.00	0.23	0.00	0.00
n-Hexane	4.51	0.01	0.00	1.44	0.00	0.00
Methylcyclopentane	1.87	0.01	0.00	0.51	0.00	0.00
Benzene	0.53	3.77	12.09	0.42	2.66	1.07
Thiophene	0.33	1.27	0.00	0.02	0.00	0.00
Cyclohexane	0.33	0.00	0.00	0.11	0.00	0.00
2-Methylhexane	0.79	0.00	0.00	0.33	0.00	0.00
2,3-Dimethylpentane	0.34	0.00	0.00	0.10	0.00	0.00
1,1-Dimethylpentane	0.00	0.00	0.00	0.02	0.00	0.00
3-Methylhexane	0.71	0.00	0.00	0.07	0.00	0.00
n-Heptane	4.69	0.00	0.00	1.30	0.00	0.00
Methyl-Cyclohexane	0.73	0.00	0.00	0.25	0.00	0.00
Ethylcyclopentane	0.80	0.00	0.00	0.16	0.00	0.00
2,5-Dimethylhexane	0.20	0.00	0.00	0.10	0.00	0.00
2,4-Dimethylhexane	0.04	0.00	0.00	0.01	0.00	0.00
3,3-Dimethylhexane	0.04	0.00	0.00	0.01	0.00	0.00
2,3,4-Trimethylpentane	0.99	0.00	0.00	0.10	0.00	0.00
Toluene	2.54	8.96	0.18	1.78	5.55	0.02
2-Methylthiophene	1.71	1.32	0.00	0.00	0.00	0.00
3-Methylthiophene	0.42	1.13	0.00	0.00	0.00	0.00
n-Octane	3.41	0.00	0.00	1.05	0.00	0.00
Ethylbenzene	1.01	1.54	0.00	0.54	0.44	0.00
Ethylthiophene	0.89	0.21	0.00	0.01	0.00	0.00
2,5-Dimethylthiophene	1.01	0.05	0.00	0.01	0.00	0.00
m/p-Xylene	3.41	5.96	0.00	1.60	2.88	0.00
2,4-Dimethylthiophene	1.06	0.33	0.00	0.06	0.00	0.00
2,3-Dimethylthiophene	1.11	0.19	0.00	0.00	0.00	0.00
Styrene	0.41	0.02	0.00	0.00	0.00	0.00
o-Xylene	1.51	2.32	0.00	0.64	0.66	0.00
n-Nonane	2.53	0.00	0.00	0.81	0.00	0.00
2-Propylthiophene	0.69	0.02	0.00	0.20	0.00	0.00
Propylbenzene	0.15	0.00	0.00	0.17	0.00	0.00
2-Ethyl-5-Methylthiophene	1.25	0.02	0.00	0.07	0.00	0.00
(?)-Benzene	1.65	1.83	0.00	0.77	0.44	0.00
2-Ethyl-4-Methylthiophene	0.63	0.00	0.00	0.00	0.00	0.00
1,3,5-Trimethylbenzene	0.67	0.74	0.00	0.23	0.43	0.00
Phenol	0.20	0.00	0.00	3.41	1.61	0.00
1-Ethyl-2-Methylbenzene	0.83	0.21	0.00	0.20	0.09	0.00
2,3,5-Trimethylthiophene	1.07	0.00	0.00	0.00	0.00	0.00
1,2,4-Trimethylbenzene	1.76	1.96	0.00	0.57	0.35	0.00
n-Decane	2.14	0.00	0.00	0.80	0.00	0.00
1,2,3-Trimethylbenzene	1.78	1.02	0.00	0.77	0.16	0.00
o-Cresol	0.42	0.00	0.00	2.60	0.10	0.00
m/p-Cresol	0.21	0.00	0.00	3.13	0.27	0.00
Dimethylphenol	0.00	0.00	0.00	0.46	0.00	0.00
n-Undecane	1.79	0.00	0.00	0.75	0.00	0.00
1,2,3,4-Tetramethylbenzene	0.00	0.00	0.00	0.30	0.00	0.00
Naphthalene	0.41	2.37	0.26	0.22	0.97	0.04
n-Dodecane	1.63	0.00	0.00	0.82	0.00	0.00
2-Methylnaphthalene	0.70	2.63	0.00	0.38	0.67	0.00
1-Methylnaphthalene	0.62	1.18	0.00	0.39	0.21	0.00
n-Tridecane	1.46	0.00	0.00	0.63	0.00	0.00
n-Tetradecane	1.11	0.05	0.00	0.56	0.00	0.00
Dimethylnaphthalene	1.40	0.93	0.00	0.90	0.14	0.00
n-Pentadecane	1.01	0.00	0.00	0.51	0.00	0.00
Trimethylnaphthalene	0.35	0.00	0.00	0.13	0.01	0.00
Trimethylnaphthalene	0.44	0.00	0.00	0.39	0.00	0.00
Trimethylnaphthalene	0.32	0.00	0.00	0.61	0.00	0.00
n-Hexadecane	0.72	0.00	0.00	0.40	0.00	0.00
Isopropylidimethylnaphthalene	0.09	0.00	0.00	0.07	0.00	0.00
n-Heptadecane	0.60	0.00	0.00	0.40	0.00	0.00
Pristane	0.11	0.00	0.00	0.08	0.00	0.00
Prist-1-ene	0.04	0.00	0.00	0.01	0.00	0.00
n-Octadecane	0.39	0.00	0.00	0.34	0.00	0.00
Phytane	0.05	0.00	0.00	0.03	0.00	0.00
n-Nonadecane	0.40	0.00	0.00	0.32	0.00	0.00
n-Icosane	0.28	0.00	0.00	0.23	0.00	0.00
n-Henicosane	0.19	0.00	0.00	0.18	0.00	0.00
n-Docosane	0.14	0.00	0.00	0.14	0.00	0.00
n-Tricosane	0.10	0.00	0.00	0.12	0.00	0.00
n-Tetracosane	0.07	0.00	0.00	0.08	0.00	0.00
n-Pentacosane	0.03	0.00	0.00	0.07	0.00	0.00
n-Hexacosane	0.02	0.00	0.00	0.03	0.00	0.00
n-Heptacosane	0.01	0.00	0.00	0.02	0.00	0.00
n-Octacosane	0.00	0.00	0.00	0.01	0.00	0.00
n-Nonacosane	0.00	0.00	0.00	0.01	0.00	0.00
n-Triacontane	0.00	0.00	0.00	0.00	0.00	0.00
Summations	mg/g TOC	mg/g TOC	mg/g TOC	mg/g TOC	mg/g TOC	mg/g TOC
n-C <sub>6-14</sub>	23.25	0.06	0.00	8.15	0.00	0.00
n-C <sub>15+</sub>	3.96	0.00	0.00	2.87	0.00	0.00
Mono-aromatic Compounds	15.84	28.31	12.27	7.68	13.65	1.09
Di-aromatic Compounds	4.24	7.10	0.26	3.03	2.00	0.04
Phenolic Compounds	0.82	0.00	0.00	9.60	1.98	0.00
Thiophenic Compounds	10.17	4.54	0.00	0.37	0.00	0.00

Table A 7 continued: samples provided by GFZ

Table A 8: Late Gas Potential Screening (maturity series)

Table A 8: Late Gas Potential Screening (maturity series)

Company	Shell							
Formation/Basin	Exshaw Fm.							
GFZ Code	G006384		G006385		G006386		G006387	
File	G006384AB	G006384AC	G006385AB	G006385AC	G006386AB	G006386AC	G006387AB	G006387AC
Temperature [°C]	200-560	200-700	200-560	200-700	200-560	200-700	200-560	200-700
Rate	2K/min	2K/min	2K/min	2K/min	2K/min	2K/min	2K/min	2K/min
Totals	mg/g TOC	mg/g TOC	mg/g TOC	mg/g TOC	mg/g TOC	mg/g TOC	mg/g TOC	mg/g TOC
Total C1+ (-blank)	29.60	51.24	201.10	220.01	20.03	56.04	177.88	177.82
Total C1-5	19.39	41.61	160.75	215.76	13.55	49.32	135.58	165.93
Total C2-5	2.69	2.57	64.69	1.91	0.66	1.24	61.13	1.90
Total C <sub>6-14</sub> (-blank)	3.00	1.55	36.80	2.18	2.22	1.46	32.13	3.21
Total C <sub>15+</sub> (-blank)	7.21	8.08	3.55	2.07	4.26	5.25	10.17	8.67
Total C <sub>6+</sub> (-blank)	10.21	9.63	40.35	4.24	6.48	6.71	42.30	11.89
GOR	1.90	4.32	3.98	50.83	2.09	7.35	3.21	13.96
Gas Wetness (C <sub>2-5</sub> /C <sub>1-5</sub> )	0.14	0.06	0.40	0.01	0.05	0.03	0.45	0.01
Compound	mg/g TOC	mg/g TOC	mg/g TOC	mg/g TOC	mg/g TOC	mg/g TOC	mg/g TOC	mg/g TOC
Methane	16.70	39.04	96.05	213.85	12.89	48.09	74.45	164.03
Ethane	1.27	0.52	43.72	1.02	0.26	0.68	40.28	0.92
Propane	0.16	0.00	17.35	0.32	0.04	0.00	16.52	0.15
i-Butane	0.00	0.00	1.03	0.00	0.00	0.00	0.76	0.00
n-Butane	0.00	0.00	0.14	0.00	0.00	0.00	0.24	0.00
i-Pentane	0.00	0.00	0.03	0.00	0.00	0.00	0.02	0.00
n-Pentane	0.00	0.00	0.03	0.00	0.00	0.00	0.02	0.00
Cyclopentane	0.00	0.00	0.01	0.00	0.00	0.00	0.02	0.00
2-Methylpentane	0.00	0.00	0.01	0.00	0.00	0.00	0.00	0.00
3-Methylpentane	0.00	0.00	0.00	0.00	0.00	0.00	0.00	0.00
n-Hexane	0.00	0.00	0.00	0.00	0.00	0.00	0.00	0.00
Methylcyclopentane	0.00	0.00	0.00	0.00	0.00	0.00	0.00	0.00
Benzene	2.18	1.27	4.56	1.80	1.56	1.26	3.57	2.64
Thiophene	0.00	0.00	0.16	0.00	0.00	0.00	0.31	0.00
Cyclohexane	0.00	0.00	0.00	0.00	0.00	0.00	0.00	0.00
2-Methylhexane	0.00	0.00	0.00	0.00	0.00	0.00	0.00	0.00
2,3-Dimethylpentane	0.00	0.00	0.00	0.00	0.00	0.00	0.00	0.00
1,1-Dimethylpentane	0.00	0.00	0.00	0.00	0.00	0.00	0.00	0.00
3-Methylhexane	0.00	0.00	0.00	0.00	0.00	0.00	0.00	0.00
n-Heptane	0.00	0.00	0.00	0.00	0.00	0.00	0.00	0.00
Methyl-Cyclohexane	0.00	0.00	0.00	0.00	0.00	0.00	0.00	0.00
Ethylcyclopentane	0.00	0.00	0.00	0.00	0.00	0.00	0.00	0.00
2,5-Dimethylhexane	0.00	0.00	0.00	0.00	0.00	0.00	0.00	0.00
2,4-Dimethylhexane	0.00	0.00	0.00	0.00	0.00	0.00	0.00	0.00
3,3-Dimethylhexane	0.00	0.00	0.00	0.00	0.00	0.00	0.00	0.00
2,3,4-Trimethylpentane	0.00	0.00	0.00	0.00	0.00	0.00	0.00	0.00
Toluene	0.09	0.01	11.12	0.13	0.05	0.02	9.09	0.09
2-Methylthiophene	0.00	0.00	0.00	0.00	0.00	0.00	0.00	0.00
3-Methylthiophene	0.00	0.00	0.10	0.00	0.00	0.00	0.06	0.00
n-Octane	0.00	0.00	0.00	0.00	0.00	0.00	0.00	0.00
Ethylbenzene	0.00	0.00	0.91	0.00	0.00	0.00	1.18	0.00
Ethylthiophene	0.00	0.00	0.00	0.00	0.00	0.00	0.00	0.00
2,5-Dimethylthiophene	0.00	0.00	0.00	0.00	0.00	0.00	0.00	0.00
m/p-Xylene	0.00	0.00	6.13	0.00	0.01	0.00	5.44	0.00
2,4-Dimethylthiophene	0.00	0.00	0.01	0.00	0.00	0.00	0.00	0.00
2,3-Dimethylthiophene	0.00	0.00	0.01	0.00	0.00	0.00	0.00	0.00
Styrene	0.00	0.00	0.00	0.00	0.00	0.00	0.00	0.00
o-Xylene	0.00	0.00	1.40	0.00	0.00	0.00	1.51	0.00
n-Nonane	0.00	0.00	0.00	0.00	0.00	0.00	0.00	0.00
2-Propylthiophene	0.00	0.00	0.00	0.00	0.00	0.00	0.00	0.00
Propylbenzene	0.00	0.00	0.00	0.00	0.00	0.00	0.00	0.00
2-Ethyl-5-Methylthiophene	0.00	0.00	0.00	0.00	0.00	0.00	0.00	0.00
(?) -Benzene	0.00	0.00	1.05	0.00	0.00	0.00	1.21	0.00
2-Ethyl-4-Methylthiophene	0.00	0.00	0.00	0.00	0.00	0.00	0.00	0.00
1,3,5-Trimethylbenzene	0.00	0.00	0.56	0.00	0.00	0.00	0.53	0.00
Phenol	0.00	0.00	0.00	0.00	0.00	0.00	0.00	0.00
1-Ethyl-2-Methylbenzene	0.00	0.00	0.09	0.00	0.00	0.00	0.08	0.00
2,3,5-Trimethylthiophene	0.00	0.00	0.00	0.00	0.00	0.00	0.00	0.00
1,2,4-Trimethylbenzene	0.00	0.00	0.80	0.00	0.00	0.00	0.93	0.00
n-Decane	0.00	0.00	0.00	0.00	0.00	0.00	0.00	0.00
1,2,3-Trimethylbenzene	0.00	0.00	0.20	0.00	0.00	0.00	0.22	0.00
o-Cresol	0.00	0.00	0.00	0.00	0.00	0.00	0.00	0.00
m/p-Cresol	0.00	0.00	0.00	0.00	0.00	0.00	0.00	0.00
Dimethylphenol	0.00	0.00	0.00	0.00	0.00	0.00	0.00	0.00
n-Undecane	0.00	0.00	0.00	0.00	0.00	0.00	0.00	0.00
1,2,3,4-Tetramethylbenzene	0.00	0.00	0.00	0.00	0.00	0.00	0.00	0.00
Naphthalene	0.18	0.03	3.61	0.02	0.08	0.02	2.19	0.03
n-Dodecane	0.00	0.00	0.00	0.00	0.00	0.00	0.00	0.00
2-Methylnaphthalene	0.00	0.00	1.86	0.01	0.00	0.00	1.56	0.00
1-Methylnaphthalene	0.00	0.00	0.61	0.00	0.00	0.00	0.62	0.00
n-Tridecane	0.00	0.00	0.00	0.00	0.00	0.00	0.00	0.00
n-Tetradecane	0.00	0.00	0.00	0.00	0.00	0.00	0.00	0.00
Dimethylnaphthalene	0.00	0.00	0.26	0.00	0.00	0.00	0.34	0.00
n-Pentadecane	0.00	0.00	0.00	0.00	0.00	0.00	0.00	0.00
Trimethylnaphthalene	0.00	0.00	0.00	0.00	0.00	0.00	0.00	0.00
Trimethylnaphthalene	0.00	0.00	0.00	0.00	0.00	0.00	0.00	0.00
Trimethylnaphthalene	0.00	0.00	0.00	0.00	0.00	0.00	0.00	0.00
n-Hexadecane	0.00	0.00	0.00	0.00	0.00	0.00	0.00	0.00
Isopropylidimethylnaphthalene	0.00	0.00	0.00	0.00	0.00	0.00	0.00	0.00
n-Heptadecane	0.00	0.00	0.00	0.00	0.00	0.00	0.00	0.00
Pristane	0.00	0.00	0.00	0.00	0.00	0.00	0.00	0.00
Prist-1-ene	0.00	0.00	0.00	0.00	0.00	0.00	0.00	0.00
n-Octadecane	0.00	0.00	0.00	0.00	0.00	0.00	0.00	0.00
Phytane	0.00	0.00	0.00	0.00	0.00	0.00	0.00	0.00
n-Nonadecane	0.00	0.00	0.00	0.00	0.00	0.00	0.00	0.00
n-Icosane	0.00	0.00	0.00	0.00	0.00	0.00	0.00	0.00
n-Henicosane	0.00	0.00	0.00	0.00	0.00	0.00	0.00	0.00
n-Docosane	0.00	0.00	0.00	0.00	0.00	0.00	0.00	0.00
n-Tricosane	0.00	0.00	0.00	0.00	0.00	0.00	0.00	0.00
n-Tetracosane	0.00	0.00	0.00	0.00	0.00	0.00	0.00	0.00
n-Pentacosane	0.00	0.00	0.00	0.00	0.00	0.00	0.00	0.00
n-Hexacosane	0.00	0.00	0.00	0.00	0.00	0.00	0.00	0.00
n-Heptacosane	0.00	0.00	0.00	0.00	0.00	0.00	0.00	0.00
n-Octacosane	0.00	0.00	0.00	0.00	0.00	0.00	0.00	0.00
n-Nonacosane	0.00	0.00	0.00	0.00	0.00	0.00	0.00	0.00
n-Triacontane	0.00	0.00	0.00	0.00	0.00	0.00	0.00	0.00
Summations	mg/g TOC	mg/g TOC	mg/g TOC	mg/g TOC	mg/g TOC	mg/g TOC	mg/g TOC	mg/g TOC
n-C <sub>14</sub>	0.00	0.00	0.00	0.00	0.00	0.00	0.00	0.00
n-C <sub>15+</sub>	0.00	0.00	0.00	0.00	0.00	0.00	0.00	0.00
Mono-aromatic Compounds	2.27	1.28	26.81	1.94	1.62	1.28	23.76	2.72
Di-aromatic Compounds	0.18	0.03	6.35	0.03	0.09	0.02	4.71	0.03
Phenolic Compounds	0.00	0.00	0.00	0.00	0.00	0.00	0.00	0.00
Thiophenic Compounds	0.00	0.00	0.28	0.00	0.00	0.00	0.38	0.00

Table A 8: Exshaw Fm. samples provided by Shell

Company														
GFZ German Carboniferous Coals														
Formation/Basin		Sandbochum1			Wlstedde		Dickebank-2		Verden-1		Siedenburg Z-1		Granterath-1	
GFZ Code		G00721			G001088		G001083		G001086		G001092		G001096	
File		G00721AA			G001088AB		G001083AB		G001086AB		G001092AB		G001096AB	
Temperature [°C]		200-460			200-560		200-560		200-560		200-560		200-560	
Rate		2K/min			2K/min		2K/min		2K/min		2K/min		2K/min	
Totals		mg/g TOC	mg/g TOC	mg/g TOC	mg/g TOC	mg/g TOC	mg/g TOC	mg/g TOC	mg/g TOC	mg/g TOC	mg/g TOC	mg/g TOC	mg/g TOC	mg/g TOC
Total C1+ (-blank)		87.74	117.42	136.97	78.68	110.17	87.50	125.24	55.73	92.32	16.25	57.47	6.10	36.60
Total C1-5		33.75	91.55	113.57	67.95	107.23	74.56	123.00	48.21	90.79	14.78	56.95	5.43	36.03
Total C2-5		23.94	32.38	1.41	18.88	5.04	20.22	7.06	10.75	5.39	2.92	5.80	1.90	4.46
Total C6-14 (-blank)		40.42	20.91	2.43	10.43	2.94	12.93	2.25	7.52	1.53	1.47	0.52	0.67	0.58
Total C15+ (-blank)		13.57	4.97	20.97	0.31	0.00	0.00	0.00	0.00	0.00	0.00	0.00	0.00	0.00
Total C6+ (-blank)		53.98	25.88	23.40	10.74	2.94	12.93	2.25	7.52	1.53	1.47	0.52	0.67	0.58
GOR		0.63	3.54	4.85	6.33	36.52	5.76	54.70	6.41	59.49	10.05	110.00	8.15	62.58
Gas Wetness (C2+2/C1+5)		0.71	0.35	0.01	0.28	0.05	0.27	0.06	0.22	0.06	0.20	0.10	0.35	0.12
Compound		mg/g TOC	mg/g TOC	mg/g TOC	mg/g TOC	mg/g TOC	mg/g TOC	mg/g TOC	mg/g TOC	mg/g TOC	mg/g TOC	mg/g TOC	mg/g TOC	mg/g TOC
Methane		9.91	59.16	112.16	49.07	102.20	54.34	115.94	37.45	85.40	11.86	51.15	3.53	31.53
Ethane		6.81	21.01	1.25	11.78	2.06	11.01	3.37	6.76	3.20	1.56	3.91	0.78	2.86
Propane		6.42	9.67	0.00	3.60	0.53	1.70	0.60	1.07	0.38	0.57	0.26	0.24	0.21
i-Butane		0.89	0.93	0.00	0.22	0.00	0.64	0.00	0.28	0.00	0.08	0.00	0.05	0.00
n-Butane		3.24	0.23	0.00	0.06	0.00	0.35	0.00	0.12	0.00	0.00	0.00	0.00	0.00
i-Pentane		1.01	0.02	0.00	0.01	0.00	0.04	0.00	0.01	0.00	0.00	0.00	0.00	0.00
n-Pentane		2.12	0.02	0.00	0.00	0.00	0.04	0.00	0.01	0.00	0.00	0.00	0.00	0.00
Cyclopentane		0.44	0.05	0.00	0.00	0.00	0.01	0.00	0.01	0.00	0.00	0.00	0.00	0.00
2-Methylpentane		0.50	0.01	0.00	0.00	0.00	0.00	0.00	0.00	0.00	0.00	0.00	0.00	0.00
3-Methylpentane		0.20	0.00	0.00	0.00	0.00	0.00	0.00	0.00	0.00	0.00	0.00	0.00	0.00
n-Hexane		1.58	0.00	0.00	0.00	0.00	0.01	0.00	0.00	0.00	0.00	0.00	0.00	0.00
Methylcyclopentane		0.66	0.01	0.00	0.00	0.00	0.01	0.00	0.00	0.00	0.00	0.00	0.00	0.00
Benzene		0.33	2.03	1.94	1.63	1.87	2.54	1.90	1.65	1.04	0.63	0.40	0.40	0.40
Thiophene		0.01	0.03	0.00	0.00	0.00	0.00	0.00	0.00	0.00	0.00	0.00	0.00	0.00
Cyclohexane		0.19	0.03	0.00	0.00	0.00	0.00	0.00	0.00	0.00	0.00	0.00	0.00	0.00
2-Methylhexane		0.09	0.00	0.00	0.00	0.00	0.00	0.00	0.00	0.00	0.00	0.00	0.00	0.00
2,3-Dimethylpentane		0.02												



Table A 8: Late Gas Potential Screening (maturity series)

Company	New Zealand Coals unextracted									
Formation/Basin GFZ Code File Temperature [°C] Rate	NZ-Coal unextracted									
	G001983			G001982		G001984		G001981		
	G001983AA	G001983AD	G001983AC	G001982AB	G001982AC	G001984AB	G001984AC	G001981AB	G001981AC	
	200-460 2K/min	200-560 2K/min	200-700 2K/min	200-560 2K/min	200-700 2K/min	200-560 2K/min	200-700 2K/min	200-560 2K/min	200-700 2K/min	
Totals	mg/g TOC	mg/g TOC	mg/g TOC	mg/g TOC	mg/g TOC	mg/g TOC	mg/g TOC	mg/g TOC	mg/g TOC	
Total C1+ (-blank)	123.77	156.65	163.13	134.16	151.71	121.13	134.44	122.22	144.57	
Total C1-5	52.42	109.14	152.98	107.67	148.14	99.90	131.64	103.41	141.88	
Total C2-5	36.33	39.08	1.52	35.23	7.25	30.21	6.09	31.63	5.89	
Total C <sub>6-14</sub> (-blank)	53.20	32.58	7.49	22.81	3.58	19.30	2.80	18.50	2.69	
Total C <sub>15+</sub> (-blank)	18.15	14.93	2.66	3.69	0.00	1.93	0.00	0.31	0.00	
Total C <sub>6+</sub> (-blank)	71.35	47.51	10.15	26.50	3.58	21.23	2.80	18.81	2.69	
GOR	0.73	2.30	15.07	4.06	41.40	4.70	47.07	5.50	52.66	
Gas Wetness (C <sub>2</sub> g/C <sub>1</sub> g)	0.69	0.36	0.01	0.33	0.05	0.30	0.05	0.31	0.04	
Compound	mg/g TOC	mg/g TOC	mg/g TOC	mg/g TOC	mg/g TOC	mg/g TOC	mg/g TOC	mg/g TOC	mg/g TOC	
Methane	16.09	70.06	151.46	72.44	140.88	69.69	125.55	71.78	135.99	
Ethane	7.17	23.07	1.20	23.43	3.27	20.40	2.58	20.62	3.59	
Propane	7.65	12.23	0.08	8.83	0.90	7.18	0.82	7.78	0.93	
i-Butane	1.90	1.92	0.00	0.93	0.00	0.81	0.00	0.88	0.00	
n-Butane	4.30	0.63	0.00	0.11	0.00	0.09	0.00	0.20	0.00	
i-Pentane	2.47	0.14	0.00	0.05	0.00	0.04	0.00	0.06	0.00	
n-Pentane	2.08	0.04	0.00	0.02	0.00	0.01	0.00	0.02	0.00	
Cyclopentane	0.25	0.04	0.00	0.01	0.00	0.01	0.00	0.01	0.00	
2-Methylpentane	0.71	0.00	0.00	0.00	0.00	0.00	0.00	0.00	0.00	
3-Methylpentane	1.65	0.00	0.00	0.00	0.00	0.00	0.00	0.00	0.00	
n-Hexane	1.41	0.00	0.00	0.00	0.00	0.00	0.00	0.00	0.00	
Methylcyclopentane	0.52	0.01	0.00	0.00	0.00	0.00	0.00	0.00	0.00	
Benzene	0.36	2.72	6.87	2.82	3.07	2.81	2.29	2.62	2.21	
Thiophene	0.02	0.00	0.00	0.00	0.00	0.00	0.00	0.00	0.00	
Cyclohexane	0.07	0.00	0.00	0.00	0.00	0.00	0.00	0.00	0.00	
2-Methylhexane	0.33	0.00	0.00	0.00	0.00	0.00	0.00	0.00	0.00	
2,3-Dimethylpentane	0.03	0.00	0.00	0.00	0.00	0.00	0.00	0.00	0.00	
1,1-Dimethylpentane	0.00	0.00	0.00	0.00	0.00	0.00	0.00	0.00	0.00	
3-Methylhexane	0.15	0.00	0.00	0.00	0.00	0.00	0.00	0.00	0.00	
n-Heptane	1.33	0.00	0.00	0.00	0.00	0.00	0.00	0.00	0.00	
Methyl-Cyclohexane	0.14	0.00	0.00	0.00	0.00	0.00	0.00	0.00	0.00	
Ethylcyclopentane	0.15	0.00	0.00	0.00	0.00	0.00	0.00	0.00	0.00	
2,5-Dimethylhexane	0.02	0.00	0.00	0.00	0.00	0.00	0.00	0.00	0.00	
2,4-Dimethylhexane	0.14	0.00	0.00	0.00	0.00	0.00	0.00	0.00	0.00	
3,3-Dimethylhexane	0.00	0.00	0.00	0.00	0.00	0.00	0.00	0.00	0.00	
2,3,4-Trimethylpentane	0.13	0.00	0.00	0.00	0.00	0.00	0.00	0.00	0.00	
Toluene	1.83	6.80	0.12	6.34	0.10	5.89	0.08	5.80	0.08	
2-Methylthiophene	0.05	0.00	0.00	0.00	0.00	0.00	0.00	0.00	0.00	
3-Methylthiophene	0.02	0.00	0.00	0.00	0.00	0.00	0.00	0.00	0.00	
n-Octane	0.99	0.00	0.00	0.00	0.00	0.00	0.00	0.00	0.00	
Ethylbenzene	0.54	0.82	0.00	0.58	0.00	0.41	0.00	0.43	0.00	
Ethylthiophene	0.02	0.00	0.00	0.00	0.00	0.00	0.00	0.00	0.00	
2,5-Dimethylthiophene	0.01	0.00	0.00	0.00	0.00	0.00	0.00	0.00	0.00	
m/p-Xylene	1.50	3.97	0.00	3.13	0.00	2.72	0.00	2.57	0.00	
2,4-Dimethylthiophene	0.05	0.00	0.00	0.00	0.00	0.00	0.00	0.00	0.00	
2,3-Dimethylthiophene	0.08	0.00	0.00	0.00	0.00	0.00	0.00	0.00	0.00	
Styrene	0.10	0.00	0.00	0.00	0.00	0.00	0.00	0.00	0.00	
o-Xylene	0.63	1.20	0.00	0.87	0.00	0.64	0.00	0.61	0.00	
n-Nonane	0.80	0.00	0.00	0.00	0.00	0.00	0.00	0.00	0.00	
2-Propylthiophene	0.13	0.00	0.00	0.00	0.00	0.00	0.00	0.00	0.00	
Propylbenzene	0.03	0.00	0.00	0.00	0.00	0.00	0.00	0.00	0.00	
2-Ethyl-5-Methylthiophene	0.01	0.00	0.00	0.00	0.00	0.00	0.00	0.00	0.00	
(?)-Benzene	0.70	0.87	0.00	0.50	0.00	0.33	0.00	0.36	0.00	
2-Ethyl-4-Methylthiophene	0.00	0.00	0.00	0.00	0.00	0.00	0.00	0.00	0.00	
1,3,5-Trimethylbenzene	0.18	0.36	0.00	0.28	0.00	0.23	0.00	0.29	0.00	
Phenol	1.61	3.36	0.00	1.35	0.00	1.20	0.00	0.92	0.00	
1-Ethyl-2-Methylbenzene	0.21	0.00	0.00	0.12	0.00	0.08	0.00	0.08	0.00	
2,3,5-Trimethylthiophene	0.00	0.00	0.00	0.00	0.00	0.00	0.00	0.00	0.00	
1,2,4-Trimethylbenzene	0.78	0.83	0.00	0.49	0.00	0.36	0.00	0.34	0.00	
n-Decane	0.69	0.00	0.00	0.00	0.00	0.00	0.00	0.00	0.00	
1,2,3-Trimethylbenzene	0.71	0.32	0.00	0.21	0.00	0.12	0.00	0.10	0.00	
o-Cresol	1.74	0.50	0.00	0.02	0.00	0.01	0.00	0.01	0.00	
m/p-Cresol	1.60	1.10	0.00	0.00	0.00	0.00	0.00	0.00	0.00	
Dimethylphenol	0.41	0.00	0.00	0.00	0.00	0.00	0.00	0.00	0.00	
n-Undecane	0.71	0.00	0.00	0.00	0.00	0.00	0.00	0.00	0.00	
1,2,3,4-Tetramethylbenzene	0.38	0.00	0.00	0.03	0.00	0.03	0.00	0.04	0.00	
Naphthalene	0.14	1.30	0.06	1.31	0.07	1.05	0.05	0.93	0.05	
n-Dodecane	0.78	0.00	0.00	0.00	0.00	0.00	0.00	0.00	0.00	
2-Methylnaphthalene	0.33	1.72	0.00	1.15	0.00	0.69	0.00	0.64	0.00	
1-Methylnaphthalene	0.38	0.57	0.00	0.37	0.00	0.23	0.00	0.20	0.00	
n-Tridecane	0.59	0.00	0.00	0.00	0.00	0.00	0.00	0.00	0.00	
n-Tetradecane	0.46	0.00	0.00	0.00	0.00	0.00	0.00	0.00	0.00	
Dimethylnaphthalene	0.82	0.35	0.00	0.27	0.00	0.14	0.00	0.15	0.00	
n-Pentadecane	0.45	0.06	0.00	0.00	0.00	0.00	0.00	0.00	0.00	
Trimethylnaphthalene	0.12	0.17	0.00	0.00	0.00	0.00	0.00	0.00	0.00	
Trimethylnaphthalene	0.55	0.03	0.00	0.00	0.00	0.00	0.00	0.00	0.00	
Trimethylnaphthalene	0.91	0.03	0.00	0.00	0.00	0.00	0.00	0.00	0.00	
n-Hexadecane	0.38	0.02	0.00	0.00	0.00	0.00	0.00	0.00	0.00	
Isopropylidimethylnaphthalene	0.04	0.04	0.00	0.00	0.00	0.00	0.00	0.00	0.00	
n-Heptadecane	0.42	0.10	0.00	0.00	0.00	0.00	0.00	0.00	0.00	
Pristane	0.05	0.00	0.00	0.00	0.00	0.00	0.00	0.00	0.00	
Prist-1-ene	0.03	0.00	0.00	0.00	0.00	0.00	0.00	0.00	0.00	
n-Octadecane	0.29	0.10	0.01	0.00	0.00	0.00	0.00	0.00	0.00	
Phytane	0.03	0.02	0.00	0.00	0.00	0.00	0.00	0.00	0.00	
n-Nonadecane	0.31	0.09	0.01	0.00	0.00	0.00	0.00	0.00	0.00	
n-Icosane	0.21	0.08	0.01	0.00	0.00	0.00	0.00	0.00	0.00	
n-Henicosane	0.16	0.07	0.01	0.00	0.00	0.00	0.00	0.00	0.00	
n-Docosane	0.13	0.08	0.01	0.00	0.00	0.00	0.00	0.00	0.00	
n-Tricosane	0.10	0.09	0.01	0.00	0.00	0.00	0.00	0.00	0.00	
n-Tetracosane	0.08	0.07	0.00	0.00	0.00	0.00	0.00	0.00	0.00	
n-Pentacosane	0.07	0.06	0.00	0.00	0.00	0.00	0.00	0.00	0.00	
n-Hexacosane	0.04	0.05	0.00	0.00	0.00	0.00	0.00	0.00	0.00	
n-Heptacosane	0.04	0.03	0.00	0.00	0.00	0.00	0.00	0.00	0.00	
n-Octacosane	0.02	0.02	0.00	0.00	0.00	0.00	0.00	0.00	0.00	
n-Nonacosane	0.02	0.02	0.00	0.00	0.00	0.00	0.00	0.00	0.00	
n-Triacontane	0.01	0.01	0.00	0.00	0.00	0.00	0.00	0.00	0.00	
Summations	mg/g TOC	mg/g TOC	mg/g TOC	mg/g TOC	mg/g TOC	mg/g TOC	mg/g TOC	mg/g TOC	mg/g TOC	
n-C <sub>6-14</sub>	7.76	0.00	0.00	0.00	0.00	0.00	0.00	0.00	0.00	
n-C <sub>15+</sub>	2.73	0.94	0.05	0.00	0.00	0.00	0.00	0.00	0.00	
Mono-aromatic Compounds	7.49	17.90	6.99	15.32	3.18	13.59	2.38	13.20	2.29	
Di-aromatic Compounds	3.25	4.16	0.07	3.10	0.07	2.12	0.05	1.92	0.05	
Phenolic Compounds	5.36	4.96	0.00	1.37	0.00	1.21	0.00	0.94	0.00	
Thiophenic Compounds	0.38	0.00	0.00	0.00	0.00	0.00	0.00	0.00	0.00	

Table A 8: unextracted New Zealand Coals provided by GFZ

[illegible]

Table A 8: unextracted New Zealand Coals provided by GFZ

Table A 8: Late Gas Potential Screening (maturity series)

Company	New Zealand Coals extracted							
Formation/Basin	NZ-Coal extracted							
GFZ Code	G001983K		G001982K		G001984K		G001981K	
File	G001983BB	G001983BC	G001982BB	G001982BC	G001984BB	G001984BC	G001981BB	G001981BC
Temperature [°C]	200-560	200-700	200-560	200-700	200-560	200-700	200-560	200-700
Rate	2K/min	2K/min	2K/min	2K/min	2K/min	2K/min	2K/min	2K/min
Totals	mg/g TOC	mg/g TOC	mg/g TOC	mg/g TOC	mg/g TOC	mg/g TOC	mg/g TOC	mg/g TOC
Total C1+ (-blank)	133.97	191.57	122.63	144.19	112.62	134.81	115.05	133.63
Total C1-5	113.12	187.90	103.05	141.50	94.54	132.55	97.85	131.08
Total C2-5	34.02	6.32	31.07	6.99	26.86	5.70	28.94	4.57
Total C <sub>6-14</sub> (-blank)	20.10	2.87	18.37	2.69	17.19	2.26	16.23	2.03
Total C <sub>15+</sub> (-blank)	0.75	0.80	1.21	0.00	0.89	0.00	0.97	0.52
Total C <sub>6+</sub> (-blank)	20.85	3.67	19.58	2.69	18.08	2.26	17.20	2.55
GOR	5.42	51.21	5.26	52.61	5.23	58.70	5.69	51.30
Gas Wetness (C <sub>2</sub> /C <sub>1-5</sub> )	0.30	0.03	0.30	0.05	0.28	0.04	0.30	0.03
Compound	mg/g TOC	mg/g TOC	mg/g TOC	mg/g TOC	mg/g TOC	mg/g TOC	mg/g TOC	mg/g TOC
Methane	79.10	181.58	71.98	134.51	67.69	126.85	68.91	126.51
Ethane	21.94	2.62	20.78	2.72	18.25	2.35	17.89	1.93
Propane	8.01	0.59	7.29	0.52	5.99	0.44	7.43	0.62
i-Butane	1.05	0.00	0.78	0.00	0.78	0.00	1.11	0.00
n-Butane	0.05	0.00	0.08	0.00	0.06	0.00	0.09	0.00
i-Pentane	0.01	0.00	0.05	0.00	0.04	0.00	0.01	0.00
n-Pentane	0.01	0.00	0.01	0.00	0.02	0.00	0.01	0.00
Cyclopentane	0.01	0.00	0.01	0.00	0.01	0.00	0.00	0.00
2-Methylpentane	0.00	0.00	0.00	0.00	0.00	0.00	0.00	0.00
3-Methylpentane	0.00	0.00	0.00	0.00	0.00	0.00	0.00	0.00
n-Hexane	0.00	0.00	0.00	0.00	0.00	0.00	0.00	0.00
Methylcyclopentane	0.00	0.00	0.00	0.00	0.00	0.00	0.00	0.00
Benzene	2.87	2.59	2.48	2.34	2.42	1.95	2.38	1.55
Thiophene	0.00	0.00	0.00	0.00	0.00	0.00	0.00	0.00
Cyclohexane	0.00	0.00	0.00	0.00	0.00	0.00	0.00	0.00
2-Methylhexane	0.00	0.00	0.00	0.00	0.00	0.00	0.00	0.00
2,3-Dimethylpentane	0.00	0.00	0.00	0.00	0.00	0.00	0.00	0.00
1,1-Dimethylpentane	0.00	0.00	0.00	0.00	0.00	0.00	0.00	0.00
3-Methylhexane	0.00	0.00	0.00	0.00	0.00	0.00	0.00	0.00
n-Heptane	0.00	0.00	0.00	0.00	0.00	0.00	0.00	0.00
Methyl-Cyclohexane	0.00	0.00	0.00	0.00	0.00	0.00	0.00	0.00
Ethylcyclopentane	0.00	0.00	0.00	0.00	0.00	0.00	0.00	0.00
2,5-Dimethylhexane	0.00	0.00	0.00	0.00	0.00	0.00	0.00	0.00
2,4-Dimethylhexane	0.00	0.00	0.00	0.00	0.00	0.00	0.00	0.00
3,3-Dimethylhexane	0.00	0.00	0.00	0.00	0.00	0.00	0.00	0.00
2,3,4-Trimethylpentane	0.00	0.00	0.00	0.00	0.00	0.00	0.00	0.00
Toluene	6.31	0.09	5.42	0.07	5.31	0.07	5.23	0.07
2-Methylthiophene	0.00	0.00	0.00	0.00	0.00	0.00	0.00	0.00
3-Methylthiophene	0.00	0.00	0.00	0.00	0.00	0.00	0.00	0.00
n-Octane	0.00	0.00	0.00	0.00	0.00	0.00	0.00	0.00
Ethylbenzene	0.48	0.00	0.42	0.00	0.35	0.00	0.37	0.00
Ethylthiophene	0.00	0.00	0.00	0.00	0.00	0.00	0.00	0.00
2,5-Dimethylthiophene	0.00	0.00	0.00	0.00	0.00	0.00	0.00	0.00
m/p-Xylene	3.12	0.00	2.56	0.00	2.41	0.00	2.44	0.00
2,4-Dimethylthiophene	0.00	0.00	0.00	0.00	0.00	0.00	0.00	0.00
2,3-Dimethylthiophene	0.00	0.00	0.00	0.00	0.00	0.00	0.00	0.00
Styrene	0.00	0.00	0.00	0.00	0.00	0.00	0.00	0.00
o-Xylene	0.72	0.00	0.64	0.00	0.54	0.00	0.58	0.00
n-Nonane	0.00	0.00	0.00	0.00	0.00	0.00	0.00	0.00
2-Propylthiophene	0.00	0.00	0.00	0.00	0.00	0.00	0.00	0.00
Propylbenzene	0.00	0.00	0.00	0.00	0.00	0.00	0.00	0.00
2-Ethyl-5-Methylthiophene	0.00	0.00	0.00	0.00	0.00	0.00	0.00	0.00
(?)-Benzene	0.41	0.00	0.36	0.00	0.29	0.00	0.29	0.00
2-Ethyl-4-Methylthiophene	0.00	0.00	0.00	0.00	0.00	0.00	0.00	0.00
1,3,5-Trimethylbenzene	0.28	0.00	0.23	0.00	0.19	0.00	0.34	0.00
Phenol	0.96	0.00	1.01	0.00	1.24	0.00	0.61	0.00
1-Ethyl-2-Methylbenzene	0.09	0.00	0.09	0.00	0.06	0.00	0.07	0.00
2,3,5-Trimethylthiophene	0.00	0.00	0.00	0.00	0.00	0.00	0.00	0.00
1,2,4-Trimethylbenzene	0.41	0.00	0.33	0.00	0.29	0.00	0.29	0.00
n-Decane	0.00	0.00	0.00	0.00	0.00	0.00	0.00	0.00
1,2,3-Trimethylbenzene	0.12	0.00	0.13	0.00	0.09	0.00	0.08	0.00
o-Cresol	0.01	0.00	0.01	0.00	0.01	0.00	0.01	0.00
m/p-Cresol	0.00	0.00	0.00	0.00	0.00	0.00	0.00	0.00
Dimethylphenol	0.00	0.00	0.00	0.00	0.00	0.00	0.00	0.00
n-Undecane	0.00	0.00	0.00	0.00	0.00	0.00	0.00	0.00
1,2,3,4-Tetramethylbenzene	0.02	0.00	0.04	0.00	0.02	0.00	0.01	0.00
Naphthalene	1.06	0.03	1.00	0.05	0.93	0.03	0.90	0.05
n-Dodecane	0.00	0.00	0.00	0.00	0.00	0.00	0.00	0.00
2-Methylnaphthalene	0.57	0.00	0.68	0.00	0.52	0.00	0.47	0.00
1-Methylnaphthalene	0.20	0.00	0.25	0.00	0.18	0.00	0.16	0.00
n-Tridecane	0.00	0.00	0.00	0.00	0.00	0.00	0.00	0.00
n-Tetradecane	0.00	0.00	0.00	0.00	0.00	0.00	0.00	0.00
Dimethylnaphthalene	0.12	0.00	0.17	0.00	0.11	0.00	0.10	0.00
n-Pentadecane	0.00	0.00	0.00	0.00	0.00	0.00	0.00	0.00
Trimethylnaphthalene	0.00	0.00	0.00	0.00	0.00	0.00	0.00	0.00
Trimethylnaphthalene	0.00	0.00	0.00	0.00	0.00	0.00	0.00	0.00
Trimethylnaphthalene	0.00	0.00	0.00	0.00	0.00	0.00	0.00	0.00
n-Hexadecane	0.00	0.00	0.00	0.00	0.00	0.00	0.00	0.00
Isopropylidimethylnaphthalene	0.00	0.00	0.00	0.00	0.00	0.00	0.00	0.00
n-Heptadecane	0.00	0.00	0.00	0.00	0.00	0.00	0.00	0.00
Pristane	0.00	0.00	0.00	0.00	0.00	0.00	0.00	0.00
Prist-1-ene	0.00	0.00	0.00	0.00	0.00	0.00	0.00	0.00
n-Octadecane	0.00	0.00	0.00	0.00	0.00	0.00	0.00	0.00
Phytane	0.00	0.00	0.00	0.00	0.00	0.00	0.00	0.00
n-Nonadecane	0.00	0.00	0.00	0.00	0.00	0.00	0.00	0.00
n-Icosane	0.00	0.00	0.00	0.00	0.00	0.00	0.00	0.00
n-Henicosane	0.00	0.00	0.00	0.00	0.00	0.00	0.00	0.00
n-Docosane	0.00	0.00	0.00	0.00	0.00	0.00	0.00	0.00
n-Tricosane	0.00	0.00	0.00	0.00	0.00	0.00	0.00	0.00
n-Tetracosane	0.00	0.00	0.00	0.00	0.00	0.00	0.00	0.00
n-Pentacosane	0.00	0.00	0.00	0.00	0.00	0.00	0.00	0.00
n-Hexacosane	0.00	0.00	0.00	0.00	0.00	0.00	0.00	0.00
n-Heptacosane	0.00	0.00	0.00	0.00	0.00	0.00	0.00	0.00
n-Octacosane	0.00	0.00	0.00	0.00	0.00	0.00	0.00	0.00
n-Nonacosane	0.00	0.00	0.00	0.00	0.00	0.00	0.00	0.00
n-Triacontane	0.00	0.00	0.00	0.00	0.00	0.00	0.00	0.00
Summations	mg/g TOC	mg/g TOC	mg/g TOC	mg/g TOC	mg/g TOC	mg/g TOC	mg/g TOC	mg/g TOC
n-C <sub>6-14</sub>	0.00	0.00	0.00	0.00	0.00	0.00	0.00	0.00
n-C <sub>15+</sub>	0.00	0.00	0.00	0.00	0.00	0.00	0.00	0.00
Mono-aromatic Compounds	14.82	2.68	12.65	2.41	11.93	2.01	12.06	1.62
Di-aromatic Compounds	1.95	0.03	2.11	0.05	1.74	0.03	1.63	0.05
Phenolic Compounds	0.97	0.00	1.03	0.00	1.25	0.00	0.62	0.00
Thiophenic Compounds	0.00	0.00	0.00	0.00	0.00	0.00	0.00	0.00

Table A 8: extracted New Zealand Coals provided by GFZ



Table A 8: Late Gas Potential Screening (maturity series)

Company	GFZ Barnett Shale									
Formation/Basin	Barnett Shale									
GFZ Code	G007219		G007247		G007249		G007250		G007257	
File	7219AA	7219AB	7247AA	7247AB	7249AA	7249AB	7250AA	7250AB	7257AA	7257AB
Temperature [°C]	200-560	200-700	200-560	200-700	200-560	200-700	200-560	200-700	200-560	200-700
Rate	2K/min	2K/min	2K/min	2K/min	2K/min	2K/min	2K/min	2K/min	2K/min	2K/min
Totals	mg/g TOC	mg/g TOC	mg/g TOC	mg/g TOC	mg/g TOC	mg/g TOC	mg/g TOC	mg/g TOC	mg/g TOC	mg/g TOC
Total C1+ (-blank)	17.98	44.03	100.80	79.57	326.34	272.29	71.52	101.22	29.41	69.22
Total C1-5	16.35	42.58	81.72	77.39	252.03	264.83	60.93	101.22	26.71	69.22
Total C2-5	2.32	1.27	36.69	3.78	115.82	3.13	17.21	1.51	3.96	1.74
Total C <sub>6-14</sub> (-blank)	1.63	1.29	19.08	2.17	61.05	7.46	9.03	0.00	2.70	0.00
Total C <sub>15+</sub> (-blank)	0.00	0.16	-0.01	0.00	13.26	0.00	1.56	0.00	0.00	0.00
Total C <sub>6+</sub> (-blank)	1.63	1.45	19.08	2.17	74.31	7.46	10.59	0.00	2.70	0.00
GOR	10.04	29.44	4.28	35.62	3.39	35.50	5.75	-	9.89	-
Gas Wetness (C <sub>2-5</sub> /C <sub>1-5</sub> )	0.14	0.03	0.45	0.05	0.46	0.01	0.28	0.01	0.15	0.03
Compound	mg/g TOC	mg/g TOC	mg/g TOC	mg/g TOC	mg/g TOC	mg/g TOC	mg/g TOC	mg/g TOC	mg/g TOC	mg/g TOC
Methane	14.04	41.32	45.03	73.61	136.22	261.70	43.71	99.71	22.75	67.48
Ethane	1.49	0.86	24.29	2.94	76.55	2.26	12.71	0.50	2.89	0.84
Propane	0.13	0.19	9.08	0.00	32.80	0.00	3.32	0.12	0.27	0.00
i-Butane	0.00	0.00	0.50	0.00	2.23	0.00	0.14	0.00	0.00	0.00
n-Butane	0.00	0.00	0.24	0.00	0.48	0.00	0.05	0.00	0.00	0.00
i-Pentane	0.00	0.00	0.01	0.00	0.07	0.00	0.01	0.00	0.00	0.00
n-Pentane	0.00	0.00	0.01	0.00	0.07	0.00	0.01	0.00	0.00	0.00
Cyclopentane	0.00	0.00	0.01	0.00	0.08	0.00	0.00	0.00	0.00	0.00
2-Methylpentane	0.00	0.00	0.00	0.00	0.02	0.00	0.00	0.00	0.00	0.00
3-Methylpentane	0.00	0.00	0.00	0.00	0.00	0.00	0.00	0.00	0.00	0.00
n-Hexane	0.00	0.00	0.00	0.00	0.01	0.00	0.00	0.00	0.00	0.00
Methylcyclopentane	0.00	0.00	0.00	0.00	0.01	0.00	0.00	0.00	0.00	0.00
Benzene	0.47	0.52	1.83	0.00	4.47	4.69	1.38	0.92	1.17	0.12
Thiophene	0.00	0.00	0.22	0.00	0.93	0.34	0.08	0.00	0.05	0.00
Cyclohexane	0.00	0.00	0.00	0.00	0.00	0.00	0.00	0.00	0.00	0.00
2-Methylhexane	0.00	0.00	0.00	0.00	0.00	0.00	0.00	0.00	0.00	0.00
2,3-Dimethylpentane	0.00	0.00	0.00	0.00	0.00	0.00	0.00	0.00	0.00	0.00
1,1-Dimethylpentane	0.00	0.00	0.00	0.00	0.00	0.00	0.00	0.00	0.00	0.00
3-Methylhexane	0.00	0.00	0.00	0.00	0.00	0.00	0.00	0.00	0.00	0.00
n-Heptane	0.00	0.00	0.00	0.00	0.00	0.00	0.00	0.00	0.00	0.00
Methyl-Cyclohexane	0.00	0.00	0.00	0.00	0.00	0.00	0.00	0.00	0.00	0.00
Ethylcyclopentane	0.00	0.00	0.00	0.00	0.00	0.00	0.00	0.00	0.00	0.00
2,5-Dimethylhexane	0.00	0.00	0.00	0.00	0.00	0.00	0.00	0.00	0.00	0.00
2,4-Dimethylhexane	0.00	0.00	0.00	0.00	0.00	0.00	0.00	0.00	0.00	0.00
3,3-Dimethylhexane	0.00	0.00	0.00	0.00	0.00	0.00	0.00	0.00	0.00	0.00
2,3,4-Trimethylpentane	0.00	0.00	0.00	0.00	0.00	0.00	0.00	0.00	0.00	0.00
Toluene	0.00	0.00	3.73	0.00	10.65	0.00	2.07	0.00	0.36	0.00
2-Methylthiophene	0.00	0.00	0.27	0.00	0.69	0.00	0.00	0.00	0.00	0.00
3-Methylthiophene	0.00	0.00	0.08	0.00	0.96	0.00	0.00	0.00	0.00	0.00
n-Octane	0.00	0.00	0.00	0.00	0.00	0.00	0.00	0.00	0.00	0.00
Ethylbenzene	0.00	0.00	0.46	0.00	1.69	0.00	0.02	0.00	0.00	0.00
Ethylthiophene	0.00	0.00	0.00	0.00	0.00	0.00	0.00	0.00	0.00	0.00
2,5-Dimethylthiophene	0.00	0.00	0.00	0.00	0.00	0.00	0.00	0.00	0.00	0.00
m/p-Xylene	0.00	0.00	2.34	0.00	6.63	0.00	0.49	0.00	0.00	0.00
2,4-Dimethylthiophene	0.00	0.00	0.00	0.00	0.14	0.00	0.00	0.00	0.00	0.00
2,3-Dimethylthiophene	0.00	0.00	0.00	0.00	0.11	0.00	0.00	0.00	0.00	0.00
Styrene	0.00	0.00	0.00	0.00	0.02	0.00	0.00	0.00	0.00	0.00
o-Xylene	0.00	0.00	0.83	0.00	2.20	0.00	0.07	0.00	0.00	0.00
n-Nonane	0.00	0.00	0.00	0.00	0.00	0.00	0.00	0.00	0.00	0.00
2-Propylthiophene	0.00	0.00	0.00	0.00	0.00	0.00	0.00	0.00	0.00	0.00
Propylbenzene	0.00	0.00	0.00	0.00	0.00	0.00	0.00	0.00	0.00	0.00
2-Ethyl-5-Methylthiophene	0.00	0.00	0.00	0.00	0.00	0.00	0.00	0.00	0.00	0.00
(?)-Benzene	0.00	0.00	0.00	0.00	2.19	0.00	0.00	0.00	0.00	0.00
2-Ethyl-4-Methylthiophene	0.00	0.00	0.00	0.00	0.00	0.00	0.00	0.00	0.00	0.00
1,3,5-Trimethylbenzene	0.00	0.00	0.00	0.00	0.75	0.00	0.00	0.00	0.00	0.00
Phenol	0.00	0.00	0.00	0.00	0.00	0.00	0.00	0.00	0.00	0.00
1-Ethyl-2-Methylbenzene	0.00	0.00	0.00	0.00	0.38	0.00	0.00	0.00	0.00	0.00
2,3,5-Trimethylthiophene	0.00	0.00	0.00	0.00	0.00	0.00	0.00	0.00	0.00	0.00
1,2,4-Trimethylbenzene	0.00	0.00	0.00	0.00	1.42	0.00	0.00	0.00	0.00	0.00
n-Decane	0.00	0.00	0.00	0.00	0.00	0.00	0.00	0.00	0.00	0.00
1,2,3-Trimethylbenzene	0.00	0.00	0.00	0.00	0.47	0.00	0.00	0.00	0.00	0.00
o-Cresol	0.00	0.00	0.00	0.00	0.00	0.00	0.00	0.00	0.00	0.00
m/p-Cresol	0.00	0.00	0.00	0.00	0.00	0.00	0.00	0.00	0.00	0.00
Dimethylphenol	0.00	0.00	0.00	0.00	0.00	0.00	0.00	0.00	0.00	0.00
n-Undecane	0.00	0.00	0.00	0.00	0.00	0.00	0.00	0.00	0.00	0.00
1,2,3,4-Tetramethylbenzene	0.00	0.00	0.00	0.00	0.00	0.00	0.00	0.00	0.00	0.00
Naphthalene	0.00	0.00	0.68	0.00	3.37	0.00	0.32	0.00	0.11	0.00
n-Dodecane	0.00	0.00	0.00	0.00	0.00	0.00	0.00	0.00	0.00	0.00
2-Methylnaphthalene	0.00	0.00	0.00	0.00	3.37	0.00	0.00	0.00	0.00	0.00
1-Methylnaphthalene	0.00	0.00	0.00	0.00	1.28	0.00	0.00	0.00	0.00	0.00
n-Tridecane	0.00	0.00	0.00	0.00	0.00	0.00	0.00	0.00	0.00	0.00
n-Tetradecane	0.00	0.00	0.00	0.00	0.00	0.00	0.00	0.00	0.00	0.00
Dimethylnaphthalene	0.00	0.00	0.00	0.00	0.82	0.00	0.00	0.00	0.00	0.00
n-Pentadecane	0.00	0.00	0.00	0.00	0.00	0.00	0.00	0.00	0.00	0.00
Trimethylnaphthalene	0.00	0.00	0.00	0.00	0.00	0.00	0.00	0.00	0.00	0.00
Trimethylnaphthalene	0.00	0.00	0.00	0.00	0.00	0.00	0.00	0.00	0.00	0.00
Trimethylnaphthalene	0.00	0.00	0.00	0.00	0.00	0.00	0.00	0.00	0.00	0.00
n-Hexadecane	0.00	0.00	0.00	0.00	0.00	0.00	0.00	0.00	0.00	0.00
Isopropylidimethylnaphthalene	0.00	0.00	0.00	0.00	0.00	0.00	0.00	0.00	0.00	0.00
n-Heptadecane	0.00	0.00	0.00	0.00	0.00	0.00	0.00	0.00	0.00	0.00
Pristane	0.00	0.00	0.00	0.00	0.00	0.00	0.00	0.00	0.00	0.00
Prist-1-ene	0.00	0.00	0.00	0.00	0.00	0.00	0.00	0.00	0.00	0.00
n-Octadecane	0.00	0.00	0.00	0.00	0.00	0.00	0.00	0.00	0.00	0.00
Phytane	0.00	0.00	0.00	0.00	0.00	0.00	0.00	0.00	0.00	0.00
n-Nonadecane	0.00	0.00	0.00	0.00	0.00	0.00	0.00	0.00	0.00	0.00
n-Icosane	0.00	0.00	0.00	0.00	0.00	0.00	0.00	0.00	0.00	0.00
n-Henicosane	0.00	0.00	0.00	0.00	0.00	0.00	0.00	0.00	0.00	0.00
n-Docosane	0.00	0.00	0.00	0.00	0.00	0.00	0.00	0.00	0.00	0.00
n-Tricosane	0.00	0.00	0.00	0.00	0.00	0.00	0.00	0.00	0.00	0.00
n-Tetracosane	0.00	0.00	0.00	0.00	0.00	0.00	0.00	0.00	0.00	0.00
n-Pentacosane	0.00	0.00	0.00	0.00	0.00	0.00	0.00	0.00	0.00	0.00
n-Hexacosane	0.00	0.00	0.00	0.00	0.00	0.00	0.00	0.00	0.00	0.00
n-Heptacosane	0.00	0.00	0.00	0.00	0.00	0.00	0.00	0.00	0.00	0.00
n-Octacosane	0.00	0.00	0.00	0.00	0.00	0.00	0.00	0.00	0.00	0.00
n-Nonacosane	0.00	0.00	0.00	0.00	0.00	0.00	0.00	0.00	0.00	0.00
n-Triacontane	0.00	0.00	0.00	0.00	0.00	0.00	0.00	0.00	0.00	0.00
Summations	mg/g TOC	mg/g TOC	mg/g TOC	mg/g TOC	mg/g TOC	mg/g TOC	mg/g TOC	mg/g TOC	mg/g TOC	mg/g TOC
n-C <sub>6-14</sub>	0.00	0.00	0.00	0.00	0.01	0.00	0.00	0.00	0.00	0.00
n-C <sub>15+</sub>	0.00	0.00	0.00	0.00	0.00	0.00	0.00	0.00	0.00	0.00
Mono-aromatic Compounds	0.47	0.52	9.19	0.00	30.86	4.69	4.03	0.92	1.53	0.12
Di-aromatic Compounds	0.00	0.00	0.68	0.00	8.83	0.00	0.32	0.00	0.11	0.00
Phenolic Compounds	0.00	0.00	0.00	0.00	0.00	0.00	0.00	0.00	0.00	0.00

Table A 8: Barnett Shales provided by GFZ

Table A 9: Open-system pyrolysis GC-FID of residues prepared by MSSV-pyrolysis

Table A 9: Open-system pyrolysis GC-FID of residues prepared by MSSV-pyrolysis

Formation/Basin	Are Fm.					
Residue Temperature [°C]	300	350	400	450	500	550
GFZ Code	G001965	G001965	G001965	G001965	G001965	G001965
File	G001965CB	G001965CC	G001965CD	G001965CE	G001965CF	G001965CG
Temperature [°C]	300-600	300-600	300-600	300-600	300-600	300-600
Rate	60K/min	60K/min	60K/min	60K/min	60K/min	60K/min
Totals	mg/g sample	mg/g sample	mg/g sample	mg/g sample	mg/g sample	mg/g sample
C <sub>1+</sub> (-blank)	66.09	79.09	51.86	23.43	8.87	3.36
C <sub>1-5</sub>	18.94	24.56	20.87	11.29	3.20	0.55
C <sub>2-5</sub>	10.76	13.48	10.52	3.75	0.82	0.26
C <sub>6-14</sub> (-blank)	23.91	27.39	15.33	6.31	3.98	2.35
C <sub>6-14</sub> Hump	6.10	6.83	3.14	0.84	0.07	0.00
C <sub>6-14</sub> Resolved	17.81	20.56	12.19	5.47	3.91	2.35
C <sub>15+</sub> (-blank)	23.24	27.14	15.66	5.83	1.69	0.46
C <sub>15+</sub> Hump	18.72	21.40	11.97	3.19	0.21	0.00
C <sub>15+</sub> Resolved	4.52	5.74	3.69	2.64	1.48	0.46
GOR	0.40	0.45	0.67	0.93	0.56	0.20
Gas Wetness (C2-5/C1-5)	0.57	0.55	0.50	0.33	0.26	0.46
Compounds Summation	mg/g sample	mg/g sample	mg/g sample	mg/g sample	mg/g sample	mg/g sample
n-C <sub>6-14</sub>	2.31	2.92	2.01	0.33	0.15	0.01
n-C <sub>15+</sub>	1.36	1.69	1.00	0.31	0.09	0.00
Mono-aromatic Compounds	2.67	3.14	2.09	1.13	1.01	1.12
Di-aromatic Compounds	0.83	1.01	0.69	0.62	0.67	0.58
Phenolic Compounds	3.31	3.96	1.80	1.13	0.88	0.30
Thiophenic Compounds	0.44	0.44	0.21	0.07	0.06	0.02
Single Compounds	mg/g sample	mg/g sample	mg/g sample	mg/g sample	mg/g sample	mg/g sample
Methane	8.18	11.08	10.35	7.54	2.38	0.30
Ethene	1.13	1.26	1.09	0.58	0.08	0.06
Ethane	2.78	3.72	3.30	1.56	0.31	0.05
Propane	2.65	3.44	2.59	0.77	0.10	0.05
i-Butane	0.09	0.12	0.09	0.03	0.02	0.01
1-Butene	0.74	0.93	0.66	0.14	0.03	0.01
n-Butane	0.45	0.58	0.42	0.08	0.06	0.01
i-Pentane	0.42	0.45	0.22	0.07	0.01	0.00
Pentene	0.24	0.30	0.24	0.04	0.01	0.00
n-Pentane	0.25	0.33	0.23	0.04	0.03	0.00
Cyclopentane	0.02	0.03	0.02	0.00	0.01	0.00
2-Methylpentane	0.09	0.11	0.06	0.01	0.00	0.00
3-Methylpentane	0.02	0.02	0.02	0.01	0.00	0.00
1-Hexene	0.22	0.28	0.21	0.03	0.01	0.00
n-Hexane	0.18	0.24	0.17	0.02	0.01	0.00
Methylcyclopentane	0.03	0.04	0.03	0.00	0.01	0.00
Benzene	0.32	0.36	0.24	0.17	0.13	0.19
Thiophene	0.05	0.04	0.02	0.01	0.01	0.01
Cyclohexane	0.02	0.03	0.01	0.00	0.00	0.00
2-Methylhexane	0.04	0.07	0.03	0.00	0.00	0.00
2,3-Dimethylpentane	0.02	0.03	0.01	0.00	0.00	0.00
1,1-Dimethylpentane	0.00	0.00	0.00	0.00	0.00	0.00
3-Methylhexane	0.02	0.02	0.01	0.00	0.00	0.00
1-Heptene	0.15	0.20	0.15	0.02	0.00	0.00
n-Heptane	0.18	0.25	0.17	0.02	0.01	0.00
Methyl-Cyclohexane	0.03	0.03	0.02	0.00	0.00	0.00
Ethylcyclopentane	0.02	0.03	0.02	0.00	0.00	0.00
2,5-Dimethylhexane	0.07	0.07	0.03	0.01	0.00	0.00
2,4-Dimethylhexane	0.01	0.03	0.01	0.00	0.00	0.00
3,3-Dimethylhexane	0.04	0.04	0.02	0.00	0.00	0.00
2,3,4-Trimethylpentane	0.07	0.08	0.03	0.00	0.00	0.00
Toluene	0.83	0.98	0.68	0.37	0.28	0.49
2-Methylthiophene	0.10	0.09	0.04	0.02	0.02	0.00
3-Methylthiophene	0.05	0.05	0.02	0.01	0.01	0.00
1-Octene	0.13	0.16	0.12	0.02	0.00	0.00
n-Octane	0.17	0.21	0.14	0.02	0.00	0.00
Ethylbenzene	0.16	0.20	0.13	0.05	0.05	0.01
Ethylthiophene	0.04	0.04	0.03	0.01	0.00	0.00
2,5-Dimethylthiophene	0.04	0.03	0.02	0.00	0.00	0.00
m/p-Xylene	0.57	0.67	0.45	0.24	0.23	0.27
2,4-Dimethylthiophene	0.04	0.05	0.02	0.01	0.01	0.00
2,3-Dimethylthiophene	0.03	0.03	0.01	0.01	0.01	0.00
Styrene	0.09	0.08	0.04	0.03	0.02	0.02
o-Xylene	0.21	0.25	0.16	0.07	0.08	0.06
1-Nonene	0.10	0.14	0.09	0.01	0.00	0.00
n-Nonane	0.12	0.15	0.11	0.02	0.00	0.00
2-Propylthiophene	0.05	0.07	0.04	0.01	0.01	0.00
Propylbenzene	0.08	0.05	0.02	0.00	0.00	0.00
2-Ethyl-5-Methylthiophene	0.06	0.04	0.01	0.00	0.00	0.00
(?)-Benzene	0.18	0.27	0.17	0.08	0.07	0.02
1,3,5-Trimethylbenzene	0.04	0.06	0.05	0.03	0.03	0.02
Phenol	1.38	1.66	0.67	0.40	0.39	0.23
1-Ethyl-2-Methylbenzene	0.03	0.00	0.02	0.03	0.04	0.02
2,3,5-Trimethylthiophene	0.00	0.00	0.00	0.00	0.00	0.00

Table A 9: Open-system pyrolysis GC-FID of residues prepared by MSSV-pyrolysis

Formation/Basin	Are Fm.					
Residue Temperature [°C]	300	350	400	450	500	550
1,2,4-Trimethylbenzene	0.13	0.18	0.12	0.06	0.07	0.03
1-Decene	0.08	0.10	0.08	0.01	0.00	0.00
<i>n</i> -Decane	0.10	0.13	0.10	0.01	0.00	0.00
1,2,3-Trimethylbenzene	0.11	0.12	0.06	0.03	0.04	0.01
<i>o</i> -Cresol	0.45	0.64	0.38	0.27	0.16	0.01
<i>m/p</i> -Cresol	1.43	1.62	0.74	0.45	0.31	0.05
Dimethylphenol	0.05	0.03	0.02	0.01	0.01	0.00
1-Undecene	0.13	0.15	0.10	0.02	0.02	0.00
<i>n</i> -Undecane	0.09	0.11	0.08	0.01	0.00	0.00
1,2,3,4-Tetramethylbenzene	0.11	0.17	0.06	0.03	0.00	0.00
Naphthalene	0.11	0.14	0.10	0.08	0.11	0.30
1-Dodecene	0.10	0.11	0.07	0.01	0.01	0.00
<i>n</i> -Dodecane	0.09	0.11	0.08	0.02	0.00	0.00
2-Methylnaphthalene	0.22	0.26	0.18	0.14	0.21	0.19
1-Tridecene	0.09	0.11	0.07	0.01	0.00	0.00
1-Methylnaphthalene	0.13	0.18	0.11	0.10	0.13	0.06
<i>n</i> -Tridecane	0.10	0.13	0.08	0.02	0.01	0.00
1-Tetradecene	0.20	0.21	0.09	0.04	0.06	0.00
<i>n</i> -Tetradecane	0.10	0.15	0.08	0.02	0.01	0.00
Dimethylnaphthalene	0.25	0.26	0.18	0.20	0.19	0.03
1-Pentadecene	0.11	0.13	0.08	0.03	0.01	0.00
<i>n</i> -Pentadecane	0.10	0.11	0.07	0.02	0.01	0.00
Trimethylnaphthalene	0.04	0.05	0.03	0.03	0.02	0.00
Trimethylnaphthalene	0.02	0.03	0.01	0.01	0.00	0.00
Trimethylnaphthalene	0.06	0.09	0.07	0.06	0.01	0.00
1-Hexadecene	0.07	0.10	0.06	0.02	0.01	0.00
<i>n</i> -Hexadecane	0.07	0.08	0.06	0.02	0.00	0.00
Isopropylidimethylnaphthalene	0.01	0.02	0.01	0.00	0.00	0.00
1-Heptadecene	0.06	0.07	0.04	0.03	0.02	0.00
<i>n</i> -Heptadecane	0.07	0.10	0.06	0.01	0.01	0.00
Pristane	0.02	0.02	0.01	0.01	0.00	0.00
Prist.-1-ene	0.08	0.06	0.01	0.01	0.01	0.00
1-Octadecene	0.04	0.05	0.03	0.00	0.00	0.00
<i>n</i> -Octadecane	0.07	0.09	0.07	0.02	0.01	0.00
Phytane	0.02	0.04	0.02	0.02	0.01	0.00
1-Nonadecene	0.04	0.05	0.03	0.00	0.00	0.00
<i>n</i> -Nonadecane	0.07	0.09	0.06	0.03	0.01	0.00
1-Icosene	0.04	0.05	0.03	0.01	0.00	0.00
<i>n</i> -Icosane	0.05	0.06	0.05	0.02	0.01	0.00
1-Henicosene	0.03	0.03	0.02	0.00	0.00	0.00
<i>n</i> -Henicosane	0.05	0.06	0.04	0.01	0.00	0.00
1-Docosene	0.03	0.04	0.02	0.00	0.00	0.00
<i>n</i> -Docosane	0.05	0.06	0.04	0.01	0.00	0.00
1-Tricosene	0.03	0.04	0.02	0.00	0.00	0.00
<i>n</i> -Tricosane	0.05	0.06	0.04	0.01	0.00	0.00
1-Tetracosene	0.03	0.03	0.02	0.00	0.00	0.00
<i>n</i> -Tetracosane	0.05	0.06	0.04	0.01	0.00	0.00
1-Pentacosene	0.03	0.03	0.01	0.00	0.00	0.00
<i>n</i> -Pentacosane	0.04	0.06	0.03	0.01	0.00	0.00
1-Hexacosene	0.02	0.03	0.01	0.00	0.00	0.00
<i>n</i> -Hexacosane	0.04	0.05	0.03	0.01	0.00	0.00
1-Heptacosene	0.02	0.02	0.01	0.00	0.00	0.00
<i>n</i> -Heptacosane	0.03	0.04	0.02	0.01	0.00	0.00
1-Octacosene	0.01	0.02	0.01	0.00	0.00	0.00
<i>n</i> -Octacosane	0.03	0.03	0.02	0.00	0.00	0.00
1-Nonacosene	0.01	0.01	0.00	0.00	0.00	0.00
<i>n</i> -Nonacosane	0.02	0.03	0.02	0.00	0.00	0.00
1-Triacontene	0.00	0.00	0.00	0.00	0.00	0.00
<i>n</i> -Triacontane	0.00	0.00	0.00	0.00	0.00	0.00
<i>n</i> -C31:1	0.00	0.00	0.00	0.00	0.00	0.00
<i>n</i> -C31	0.00	0.00	0.00	0.00	0.00	0.00
<i>n</i> -C32:1	0.00	0.00	0.00	0.00	0.00	0.00
<i>n</i> -C32	0.00	0.00	0.00	0.00	0.00	0.00
<i>n</i> -C33:1	0.00	0.00	0.00	0.00	0.00	0.00
<i>n</i> -C33	0.00	0.00	0.00	0.00	0.00	0.00
<i>n</i> -C34:1	0.00	0.00	0.00	0.00	0.00	0.00
<i>n</i> -C34	0.00	0.00	0.00	0.00	0.00	0.00
<i>n</i> -C35:1	0.00	0.00	0.00	0.00	0.00	0.00
<i>n</i> -C35	0.00	0.00	0.00	0.00	0.00	0.00
<i>n</i> -C36:1	0.00	0.00	0.00	0.00	0.00	0.00
<i>n</i> -C36	0.00	0.00	0.00	0.00	0.00	0.00
<i>n</i> -C37:1	0.00	0.00	0.00	0.00	0.00	0.00
<i>n</i> -C37	0.00	0.00	0.00	0.00	0.00	0.00
<i>n</i> -C38:1	0.00	0.00	0.00	0.00	0.00	0.00
<i>n</i> -C38	0.00	0.00	0.00	0.00	0.00	0.00
<i>n</i> -C39:1	0.00	0.00	0.00	0.00	0.00	0.00
<i>n</i> -C39	0.00	0.00	0.00	0.00	0.00	0.00

Table A 9 continued: Are Fm. sample G001965

Table A 9: Open-system pyrolysis GC-FID of residues prepared by MSSV-pyrolysis

Formation/Basin	Mix type I/II				GRS			
Residue Temperature [°C]	350	400	450	500	350	400	450	500
GFZ Code					G004750	G004750	G004750	G004750
File	G004750EB	G004750EC	G004750ED	G004750EE	G004750FB	G004750FD	G004750FE	G004750FF
Temperature [°C]	300-600	300-600	300-600	300-600	300-600	300-600	300-600	300-600
Rate	60K/min	60K/min	60K/min	60K/min	60K/min	60K/min	60K/min	60K/min
Totals	mg/g sample	mg/g sample	mg/g sample	mg/g sample	mg/g sample	mg/g sample	mg/g sample	mg/g sample
C <sub>1+</sub> (-blank)	92.31	60.71	16.93	4.89	115.58	81.42	10.36	1.15
C <sub>1-5</sub>	18.30	16.15	6.71	1.81	15.18	12.23	2.25	0.37
C <sub>2-5</sub>	12.26	10.15	2.66	0.46	13.08	10.26	1.29	0.15
C <sub>6-14</sub> (-blank)	27.58	17.16	3.06	1.60	33.25	22.58	1.68	0.19
C <sub>6-14</sub> Hump	7.49	3.91	0.71	0.09	8.59	5.28	0.45	0.00
C <sub>6-14</sub> Resolved	20.09	13.25	2.35	1.51	24.66	17.31	1.23	0.19
C <sub>15+</sub> (-blank)	46.43	27.40	7.16	1.47	67.14	46.61	6.44	0.59
C <sub>15+</sub> Hump	37.02	21.79	5.45	0.45	53.77	36.90	5.75	0.46
C <sub>15+</sub> Resolved	9.40	5.61	1.71	1.02	13.37	9.71	0.69	0.13
GOR	0.25	0.36	0.66	0.59	0.15	0.18	0.28	0.47
Gas Wetness (C2-5/C1-5)	0.67	0.63	0.40	0.25	0.86	0.84	0.57	0.40
Compounds Summation	mg/g sample	mg/g sample	mg/g sample	mg/g sample	mg/g sample	mg/g sample	mg/g sample	mg/g sample
n-C <sub>6-14</sub>	6.62	5.03	0.37	0.05	11.56	8.88	0.49	0.01
n-C <sub>15+</sub>	5.55	3.32	0.43	0.04	9.27	6.84	0.37	0.00
Mono-aromatic Compounds	2.15	1.55	0.46	0.34	1.66	1.11	0.15	0.03
Di-aromatic Compounds	0.50	0.38	0.23	0.33	0.20	0.15	0.04	0.02
Phenolic Compounds	1.37	0.59	0.18	0.16	0.15	0.09	0.00	0.00
Thiophenic Compounds	0.45	0.23	0.04	0.03	0.51	0.27	0.02	0.00
Single Compounds	mg/g sample	mg/g sample	mg/g sample	mg/g sample	mg/g sample	mg/g sample	mg/g sample	mg/g sample
Methane	6.03	6.00	4.05	1.36	2.11	1.97	0.96	0.22
Ethene	1.02	1.03	0.36	0.05	1.07	0.89	0.10	0.05
Ethane	2.76	2.52	1.06	0.21	1.91	1.71	0.38	0.01
Propane	2.98	2.50	0.57	0.06	3.19	2.48	0.29	0.03
i-Butane	0.10	0.08	0.02	0.01	0.09	0.06	0.01	0.00
1-Butene	0.99	0.79	0.10	0.01	1.40	0.98	0.07	0.00
n-Butane	0.71	0.58	0.07	0.01	0.93	0.75	0.07	0.01
i-Pentane	0.26	0.10	0.01	0.00	0.14	0.07	0.01	0.00
Pentene	0.50	0.44	0.05	0.00	0.85	0.70	0.05	0.00
n-Pentane	0.44	0.34	0.04	0.01	0.60	0.44	0.04	0.00
Cyclopentane	0.04	0.03	0.00	0.00	0.05	0.04	0.00	0.00
2-Methylpentane	0.09	0.05	0.00	0.00	0.08	0.04	0.00	0.00
3-Methylpentane	0.02	0.01	0.00	0.00	0.02	0.02	0.00	0.00
1-Hexene	0.70	0.55	0.04	0.00	1.38	1.11	0.06	0.00
n-Hexane	0.36	0.29	0.02	0.00	0.52	0.39	0.03	0.00
Methylcyclopentane	0.06	0.04	0.01	0.01	0.11	0.07	0.00	0.00
Benzene	0.24	0.21	0.07	0.04	0.18	0.16	0.04	0.01
Thiophene	0.03	0.01	0.01	0.00	0.03	0.02	0.00	0.00
Cyclohexane	0.04	0.02	0.00	0.00	0.06	0.04	0.00	0.00
2-Methylhexane	0.04	0.02	0.00	0.00	0.04	0.03	0.00	0.00
2,3-Dimethylpentane	0.02	0.01	0.00	0.00	0.02	0.01	0.00	0.00
1,1-Dimethylpentane	0.00	0.00	0.00	0.00	0.00	0.00	0.00	0.00
3-Methylhexane	0.02	0.02	0.00	0.00	0.03	0.02	0.00	0.00
1-Heptene	0.50	0.40	0.03	0.00	0.96	0.77	0.04	0.00
n-Heptane	0.39	0.29	0.02	0.00	0.58	0.42	0.03	0.00
Methyl-Cyclohexane	0.08	0.04	0.01	0.00	0.13	0.09	0.01	0.00
Ethylcyclopentane	0.04	0.03	0.00	0.00	0.06	0.04	0.00	0.00
2,5-Dimethylhexane	0.08	0.03	0.00	0.00	0.10	0.05	0.00	0.00
2,4-Dimethylhexane	0.02	0.01	0.00	0.00	0.02	0.01	0.00	0.00
3,3-Dimethylhexane	0.05	0.02	0.00	0.00	0.05	0.03	0.00	0.00
2,3,4-Trimethylpentane	0.08	0.05	0.01	0.00	0.09	0.05	0.00	0.00
Toluene	0.54	0.43	0.13	0.07	0.33	0.25	0.03	0.01
2-Methylthiophene	0.11	0.05	0.02	0.01	0.12	0.06	0.01	0.00
3-Methylthiophene	0.03	0.01	0.00	0.00	0.02	0.00	0.00	0.00
1-Octene	0.44	0.36	0.03	0.00	0.81	0.66	0.04	0.00
n-Octane	0.37	0.28	0.02	0.00	0.56	0.41	0.02	0.00
Ethylbenzene	0.14	0.11	0.02	0.02	0.11	0.08	0.01	0.00
Ethylthiophene	0.06	0.03	0.00	0.00	0.09	0.05	0.00	0.00
2,5-Dimethylthiophene	0.04	0.03	0.00	0.00	0.05	0.04	0.00	0.00
m/p-Xylene	0.45	0.28	0.10	0.07	0.36	0.18	0.02	0.00
2,4-Dimethylthiophene	0.03	0.02	0.00	0.00	0.04	0.02	0.00	0.00
2,3-Dimethylthiophene	0.04	0.02	0.00	0.00	0.05	0.03	0.00	0.00
Styrene	0.11	0.07	0.01	0.00	0.11	0.08	0.00	0.00
o-Xylene	0.19	0.14	0.03	0.03	0.19	0.14	0.01	0.00
1-Nonene	0.37	0.31	0.02	0.00	0.72	0.57	0.03	0.00
n-Nonane	0.33	0.25	0.02	0.00	0.50	0.37	0.02	0.00
2-Propylthiophene	0.04	0.03	0.01	0.00	0.04	0.03	0.00	0.00
Propylbenzene	0.04	0.02	0.00	0.00	0.06	0.04	0.00	0.00
2-Ethyl-5-Methylthiophene	0.05	0.02	0.00	0.00	0.05	0.03	0.00	0.00
(?)-Benzene	0.15	0.11	0.03	0.03	0.11	0.07	0.01	0.00
1,3,5-Trimethylbenzene	0.05	0.03	0.01	0.01	0.03	0.02	0.00	0.00
Phenol	0.49	0.18	0.05	0.06	0.01	0.01	0.00	0.00
1-Ethyl-2-Methylbenzene	0.08	0.07	0.02	0.02	0.07	0.05	0.00	0.00
2,3,5-Trimethylthiophene	0.00	0.00	0.00	0.00	0.00	0.00	0.00	0.00

Table A 9 continued: synthetic mixture I-III and Green River Shale sample G004750



Table A 9: Open-system pyrolysis GC-FID of residues prepared by MSSV-pyrolysis

Formation/Basin	Mix type I/III				GRS			
Residue Temperature [°C]	350	400	450	500	350	400	450	500
1,2,4-Trimethylbenzene	0.14	0.09	0.03	0.03	0.11	0.07	0.01	0.00
1-Decene	0.40	0.30	0.02	0.00	0.80	0.62	0.03	0.00
<i>n</i> -Decane	0.30	0.22	0.02	0.00	0.48	0.35	0.02	0.00
1,2,3-Trimethylbenzene	0.13	0.06	0.02	0.02	0.10	0.05	0.00	0.00
<i>o</i> -Cresol	0.24	0.12	0.05	0.03	0.00	0.00	0.00	0.00
<i>m/p</i> -Cresol	0.59	0.28	0.08	0.07	0.07	0.04	0.00	0.00
Dimethylphenol	0.04	0.02	0.00	0.00	0.07	0.04	0.00	0.00
1-Undecene	0.38	0.28	0.02	0.01	0.72	0.55	0.03	0.00
<i>n</i> -Undecane	0.29	0.21	0.02	0.00	0.48	0.35	0.02	0.00
1,2,3,4-Tetramethylbenzene	0.07	0.03	0.00	0.00	0.00	0.00	0.00	0.00
Naphthalene	0.08	0.06	0.03	0.05	0.04	0.03	0.01	0.00
1-Dodecene	0.34	0.25	0.01	0.00	0.62	0.49	0.03	0.00
<i>n</i> -Dodecane	0.28	0.20	0.02	0.00	0.49	0.36	0.02	0.00
2-Methylnaphthalene	0.13	0.10	0.05	0.10	0.07	0.04	0.01	0.01
1-Tridecene	0.31	0.23	0.01	0.00	0.54	0.42	0.02	0.00
1-Methylnaphthalene	0.07	0.05	0.04	0.06	0.00	0.02	0.01	0.01
<i>n</i> -Tridecane	0.31	0.21	0.02	0.00	0.44	0.32	0.02	0.00
1-Tetradecene	0.30	0.22	0.02	0.02	0.48	0.39	0.02	0.00
<i>n</i> -Tetradecane	0.27	0.17	0.02	0.00	0.44	0.32	0.02	0.00
Dimethylnaphthalene	0.13	0.10	0.07	0.10	0.04	0.02	0.01	0.01
1-Pentadecene	0.28	0.20	0.03	0.00	0.49	0.36	0.02	0.00
<i>n</i> -Pentadecane	0.25	0.17	0.02	0.00	0.40	0.28	0.02	0.00
Trimethylnaphthalene	0.03	0.02	0.01	0.01	0.01	0.01	0.00	0.00
Trimethylnaphthalene	0.02	0.02	0.01	0.01	0.03	0.02	0.00	0.00
Trimethylnaphthalene	0.04	0.03	0.02	0.01	0.01	0.01	0.00	0.00
1-Hexadecene	0.25	0.17	0.01	0.00	0.43	0.33	0.02	0.00
<i>n</i> -Hexadecane	0.26	0.16	0.02	0.00	0.41	0.28	0.01	0.00
Isopropylidimethylnaphthalene	0.00	0.00	0.00	0.00	0.01	0.00	0.00	0.00
1-Heptadecene	0.22	0.15	0.01	0.00	0.38	0.29	0.01	0.00
<i>n</i> -Heptadecane	0.24	0.15	0.02	0.00	0.38	0.26	0.01	0.00
Pristane	0.02	0.01	0.00	0.00	0.01	0.00	0.00	0.00
Prist.-1-ene	0.09	0.01	0.00	0.00	0.11	0.02	0.00	0.00
1-Octadecene	0.18	0.12	0.01	0.00	0.33	0.25	0.01	0.00
<i>n</i> -Octadecane	0.20	0.13	0.02	0.01	0.30	0.23	0.01	0.00
Phytane	0.03	0.02	0.01	0.01	0.03	0.02	0.00	0.00
1-Nonadecene	0.16	0.11	0.01	0.01	0.28	0.22	0.01	0.00
<i>n</i> -Nonadecane	0.20	0.13	0.02	0.00	0.30	0.23	0.01	0.00
1-Icosene	0.15	0.10	0.01	0.00	0.27	0.21	0.01	0.00
<i>n</i> -Icosane	0.17	0.12	0.02	0.01	0.28	0.20	0.01	0.00
1-Henicosene	0.13	0.08	0.00	0.00	0.25	0.18	0.00	0.00
<i>n</i> -Henicosane	0.18	0.11	0.01	0.00	0.29	0.20	0.01	0.00
1-Docosene	0.15	0.09	0.01	0.00	0.26	0.20	0.01	0.00
<i>n</i> -Docosane	0.17	0.10	0.02	0.00	0.26	0.18	0.01	0.00
1-Tricosene	0.14	0.08	0.00	0.00	0.23	0.17	0.01	0.00
<i>n</i> -Tricosane	0.18	0.10	0.02	0.00	0.28	0.19	0.01	0.00
1-Tetracosene	0.13	0.07	0.00	0.00	0.23	0.16	0.00	0.00
<i>n</i> -Tetracosane	0.16	0.09	0.02	0.00	0.24	0.17	0.01	0.00
1-Pentacosene	0.12	0.06	0.01	0.00	0.20	0.14	0.00	0.00
<i>n</i> -Pentacosane	0.17	0.09	0.02	0.00	0.26	0.17	0.01	0.00
1-Hexacosene	0.11	0.06	0.00	0.00	0.21	0.15	0.00	0.00
<i>n</i> -Hexacosane	0.15	0.08	0.02	0.00	0.24	0.16	0.00	0.00
1-Heptacosene	0.09	0.04	0.00	0.00	0.17	0.11	0.00	0.00
<i>n</i> -Heptacosane	0.15	0.07	0.02	0.00	0.25	0.17	0.01	0.00
1-Octacosene	0.09	0.04	0.00	0.00	0.15	0.11	0.00	0.00
<i>n</i> -Octacosane	0.12	0.06	0.02	0.00	0.21	0.15	0.01	0.00
1-Nonacosene	0.06	0.03	0.00	0.00	0.12	0.08	0.00	0.00
<i>n</i> -Nonacosane	0.11	0.05	0.01	0.00	0.20	0.14	0.01	0.00
1-Triacontene	0.07	0.03	0.00	0.00	0.11	0.07	0.00	0.00
<i>n</i> -Triacontane	0.08	0.04	0.01	0.00	0.14	0.11	0.01	0.00
<i>n</i> -C31:1	0.06	0.02	0.00	0.00	0.10	0.05	0.00	0.00
<i>n</i> -C31	0.09	0.04	0.01	0.00	0.15	0.12	0.01	0.00
<i>n</i> -C32:1	0.02	0.02	0.00	0.00	0.04	0.05	0.00	0.00
<i>n</i> -C32	0.05	0.02	0.00	0.00	0.08	0.08	0.01	0.00
<i>n</i> -C33:1	0.01	0.01	0.00	0.00	0.02	0.02	0.00	0.00
<i>n</i> -C33	0.04	0.02	0.00	0.00	0.07	0.07	0.01	0.00
<i>n</i> -C34:1	0.01	0.01	0.00	0.00	0.02	0.02	0.00	0.00
<i>n</i> -C34	0.02	0.01	0.00	0.00	0.05	0.05	0.01	0.00
<i>n</i> -C35:1	0.01	0.00	0.00	0.00	0.01	0.01	0.00	0.00
<i>n</i> -C35	0.02	0.01	0.00	0.00	0.04	0.04	0.01	0.00
<i>n</i> -C36:1	0.01	0.00	0.00	0.00	0.02	0.01	0.00	0.00
<i>n</i> -C36	0.02	0.01	0.00	0.00	0.03	0.03	0.01	0.00
<i>n</i> -C37:1	0.01	0.00	0.00	0.00	0.01	0.01	0.00	0.00
<i>n</i> -C37	0.02	0.01	0.00	0.00	0.03	0.04	0.00	0.00
<i>n</i> -C38:1	0.01	0.00	0.00	0.00	0.01	0.01	0.00	0.00
<i>n</i> -C38	0.01	0.01	0.00	0.00	0.02	0.03	0.01	0.00
<i>n</i> -C39:1	0.00	0.00	0.00	0.00	0.01	0.00	0.00	0.00
<i>n</i> -C39	0.01	0.01	0.00	0.00	0.02	0.03	0.00	0.00

Table A 9 continued: synthetic mixture I-III and Green River Shale sample G004750

Table A 9: Open-system pyrolysis GC-FID of residues prepared by MSSV-pyrolysis

Formation/Basin	Spekk Fm.				Westphalian Coal		
Residue Temperature [°C]	350	400	450	500	400	450	500
GFZ Code	G001955	G001955	G001955	G001955	G000721	G000721	G000721
File	G001955GB	G001955GC	G001955GD	G001955GE	G00721CA	G00721CB	G00721CC
Temperature [°C]	300-600	300-600	300-600	300-600	300-600	300-600	300-600
Rate	60K/min	60K/min	60K/min	60K/min	60K/min	60K/min	60K/min
Totals	mg/g sample	mg/g sample	mg/g sample	mg/g sample	mg/g sample	mg/g sample	mg/g sample
C <sub>1+</sub> (-blank)	26.90	13.45	2.10	0.53	102.25	50.09	11.49
C <sub>1-5</sub>	5.81	3.94	1.15	0.26	32.68	19.23	5.02
C <sub>2-5</sub>	4.36	2.74	0.49	0.08	16.26	6.53	0.86
C <sub>6-14</sub> (-blank)	8.48	3.91	0.39	0.17	26.25	9.70	3.25
C <sub>6-14</sub> Hump	2.55	1.00	0.08	0.00	3.22	1.21	0.03
C <sub>6-14</sub> Resolved	5.94	2.91	0.32	0.17	23.03	8.49	3.22
C <sub>15+</sub> (-blank)	12.61	5.60	0.56	0.11	43.31	21.16	3.22
C <sub>15+</sub> Hump	11.27	4.89	0.36	0.00	38.67	15.51	0.78
C <sub>15+</sub> Resolved	1.33	0.71	0.20	0.11	4.64	5.65	2.43
GOR	0.28	0.41	1.21	0.92	0.47	0.62	0.78
Gas Wetness (C2-5/C1-5)	0.75	0.70	0.42	0.30	0.50	0.34	0.17
Compounds Summation	mg/g sample	mg/g sample	mg/g sample	mg/g sample	mg/g sample	mg/g sample	mg/g sample
n-C <sub>6-14</sub>	1.55	1.01	0.04	0.00	4.03	0.77	0.04
n-C <sub>15+</sub>	0.55	0.34	0.04	0.00	1.85	0.34	0.01
Mono-aromatic Compounds	0.72	0.36	0.08	0.04	3.42	1.87	0.95
Di-aromatic Compounds	0.13	0.07	0.02	0.03	1.22	0.82	0.70
Phenolic Compounds	0.06	0.02	0.00	0.00	3.44	1.89	0.81
Thiophenic Compounds	0.35	0.10	0.02	0.01	0.13	0.04	0.02
Single Compounds	mg/g sample	mg/g sample	mg/g sample	mg/g sample	mg/g sample	mg/g sample	mg/g sample
Methane	1.45	1.20	0.66	0.18	16.42	12.70	4.16
Ethane	0.32	0.20	0.06	0.01	1.35	0.87	0.13
Ethane	0.96	0.66	0.18	0.03	5.49	2.79	0.46
Propane	1.07	0.68	0.10	0.01	4.28	1.54	0.12
i-Butane	0.04	0.02	0.00	0.00	0.14	0.05	0.01
1-Butene	0.38	0.23	0.02	0.00	1.05	0.29	0.02
n-Butane	0.26	0.17	0.01	0.00	0.91	0.20	0.03
i-Pentane	0.09	0.02	0.02	0.00	0.20	0.06	0.01
Pentene	0.17	0.12	0.00	0.00	0.43	0.09	0.00
n-Pentane	0.16	0.10	0.01	0.00	0.55	0.10	0.01
Cyclopentane	0.01	0.01	0.00	0.00	0.09	0.02	0.01
2-Methylpentane	0.04	0.02	0.00	0.00	0.09	0.02	0.00
3-Methylpentane	0.01	0.01	0.00	0.00	0.03	0.01	0.00
1-Hexene	0.19	0.13	0.01	0.00	0.39	0.07	0.00
n-Hexane	0.12	0.07	0.00	0.00	0.42	0.07	0.01
Methylcyclopentane	0.02	0.01	0.00	0.00	0.09	0.03	0.01
Benzene	0.09	0.05	0.02	0.01	0.26	0.19	0.12
Thiophene	0.02	0.01	0.00	0.00	0.00	0.00	0.00
Cyclohexane	0.01	0.01	0.00	0.00	0.04	0.01	0.00
2-Methylhexane	0.02	0.01	0.00	0.00	0.03	0.01	0.00
2,3-Dimethylpentane	0.01	0.00	0.00	0.00	0.01	0.00	0.00
1,1-Dimethylpentane	0.00	0.00	0.00	0.00	0.00	0.00	0.00
3-Methylhexane	0.01	0.01	0.00	0.00	0.03	0.00	0.00
1-Heptene	0.13	0.09	0.00	0.00	0.22	0.04	0.00
n-Heptane	0.12	0.07	0.00	0.00	0.37	0.06	0.00
Methyl-Cyclohexane	0.02	0.01	0.00	0.00	0.05	0.01	0.00
Ethylcyclopentane	0.01	0.01	0.00	0.00	0.04	0.01	0.00
2,5-Dimethylhexane	0.03	0.01	0.00	0.00	0.06	0.02	0.00
2,4-Dimethylhexane	0.01	0.00	0.00	0.00	0.01	0.00	0.00
3,3-Dimethylhexane	0.02	0.01	0.00	0.00	0.02	0.01	0.00
2,3,4-Trimethylpentane	0.03	0.01	0.00	0.00	0.07	0.01	0.00
Toluene	0.18	0.10	0.02	0.01	1.07	0.62	0.33
2-Methylthiophene	0.09	0.02	0.01	0.00	0.02	0.00	0.00
3-Methylthiophene	0.01	0.00	0.00	0.00	0.01	0.00	0.00
1-Octene	0.11	0.08	0.00	0.00	0.23	0.04	0.00
n-Octane	0.10	0.06	0.00	0.00	0.29	0.05	0.00
Ethylbenzene	0.05	0.03	0.01	0.00	0.22	0.09	0.03
Ethylthiophene	0.04	0.01	0.00	0.00	0.00	0.00	0.00
2,5-Dimethylthiophene	0.06	0.02	0.00	0.00	0.00	0.00	0.00
m/p-Xylene	0.13	0.06	0.01	0.01	0.81	0.47	0.24
2,4-Dimethylthiophene	0.03	0.01	0.00	0.00	0.01	0.00	0.00
2,3-Dimethylthiophene	0.02	0.01	0.00	0.00	0.01	0.00	0.00
Styrene	0.04	0.02	0.02	0.00	0.05	0.01	0.01
o-Xylene	0.07	0.04	0.01	0.00	0.24	0.10	0.06
1-Nonene	0.08	0.06	0.00	0.00	0.17	0.02	0.00
n-Nonane	0.08	0.05	0.00	0.00	0.22	0.04	0.00
2-Propylthiophene	0.02	0.01	0.00	0.00	0.04	0.02	0.00
Propylbenzene	0.01	0.00	0.00	0.00	0.04	0.00	0.00
2-Ethyl-5-Methylthiophene	0.06	0.01	0.00	0.00	0.03	0.01	0.01
(?)-Benzene	0.05	0.03	0.00	0.00	0.28	0.14	0.05
1,3,5-Trimethylbenzene	0.01	0.01	0.00	0.00	0.14	0.08	0.03
Phenol	0.01	0.00	0.00	0.00	0.99	0.58	0.35
1-Ethyl-2-Methylbenzene	0.04	0.02	0.00	0.00	0.10	0.03	0.01
2,3,5-Trimethylthiophene	0.00	0.00	0.00	0.00	0.02	0.01	0.01

Table A 9 continued: Spekk Fm. sample G004750 and Westphalian Coal sample G000721

Table A 9: Open-system pyrolysis GC-FID of residues prepared by MSSV-pyrolysis

Formation/Basin	Spekk Fm.				Westphalian Coal		
Residue Temperature [°C]	350	400	450	500	400	450	500
1,2,4-Trimethylbenzene	0.04	0.02	0.00	0.00	0.22	0.11	0.06
1-Decene	0.08	0.05	0.00	0.00	0.14	0.02	0.00
<i>n</i> -Decane	0.06	0.04	0.00	0.00	0.19	0.04	0.00
1,2,3-Trimethylbenzene	0.03	0.01	0.00	0.00	0.05	0.03	0.02
<i>o</i> -Cresol	0.02	0.00	0.00	0.00	0.99	0.53	0.16
<i>m/p</i> -Cresol	0.03	0.01	0.00	0.00	1.25	0.69	0.28
Dimethylphenol	0.01	0.00	0.00	0.00	0.21	0.10	0.02
1-Undecene	0.08	0.05	0.00	0.00	0.14	0.02	0.01
<i>n</i> -Undecane	0.06	0.04	0.00	0.00	0.18	0.04	0.00
1,2,3,4-Tetramethylbenzene	0.02	0.01	0.00	0.00	0.15	0.07	0.01
Naphthalene	0.02	0.01	0.00	0.01	0.16	0.12	0.16
1-Dodecene	0.06	0.04	0.00	0.00	0.14	0.01	0.00
<i>n</i> -Dodecane	0.06	0.03	0.00	0.00	0.21	0.04	0.00
2-Methylnaphthalene	0.03	0.02	0.01	0.01	0.27	0.19	0.25
1-Tridecene	0.05	0.04	0.00	0.00	0.21	0.06	0.00
1-Methylnaphthalene	0.02	0.01	0.00	0.01	0.21	0.13	0.11
<i>n</i> -Tridecane	0.06	0.03	0.00	0.00	0.21	0.05	0.00
1-Tetradecene	0.05	0.04	0.00	0.00	0.15	0.04	0.00
<i>n</i> -Tetradecane	0.05	0.03	0.00	0.00	0.16	0.05	0.00
Dimethylnaphthalene	0.03	0.02	0.01	0.01	0.35	0.23	0.15
1-Pentadecene	0.06	0.03	0.00	0.00	0.08	0.01	0.00
<i>n</i> -Pentadecane	0.04	0.03	0.00	0.00	0.14	0.02	0.00
Trimethylnaphthalene	0.01	0.00	0.00	0.00	0.09	0.05	0.01
Trimethylnaphthalene	0.01	0.00	0.00	0.00	0.08	0.04	0.01
Trimethylnaphthalene	0.00	0.00	0.00	0.00	0.07	0.05	0.00
1-Hexadecene	0.03	0.02	0.00	0.00	0.09	0.02	0.00
<i>n</i> -Hexadecane	0.04	0.02	0.00	0.00	0.11	0.02	0.00
Isopropylidimethylnaphthalene	0.00	0.00	0.00	0.00	0.01	0.01	0.00
1-Heptadecene	0.03	0.02	0.00	0.00	0.14	0.03	0.00
<i>n</i> -Heptadecane	0.03	0.02	0.00	0.00	0.13	0.04	0.00
Pristane	0.00	0.00	0.00	0.00	0.03	0.01	0.00
Prist.-1-ene	0.02	0.00	0.00	0.00	0.01	0.01	0.00
1-Octadecene	0.02	0.01	0.00	0.00	0.06	0.03	0.00
<i>n</i> -Octadecane	0.03	0.02	0.00	0.00	0.11	0.02	0.00
Phytane	0.00	0.00	0.00	0.00	0.03	0.00	0.00
1-Nonadecene	0.02	0.01	0.00	0.00	0.06	0.02	0.00
<i>n</i> -Nonadecane	0.03	0.01	0.01	0.00	0.14	0.06	0.00
1-Icosene	0.02	0.01	0.00	0.00	0.04	0.01	0.00
<i>n</i> -Icosane	0.02	0.01	0.00	0.00	0.07	0.02	0.00
1-Henicosene	0.01	0.01	0.00	0.00	0.04	0.00	0.00
<i>n</i> -Henicosane	0.02	0.01	0.00	0.00	0.09	0.04	0.00
1-Docosene	0.01	0.01	0.00	0.00	0.03	0.00	0.00
<i>n</i> -Docosane	0.01	0.01	0.00	0.00	0.08	0.00	0.00
1-Tricosene	0.01	0.01	0.00	0.00	0.04	0.00	0.00
<i>n</i> -Tricosane	0.01	0.01	0.00	0.00	0.06	0.00	0.00
1-Tetracosene	0.01	0.00	0.00	0.00	0.03	0.00	0.00
<i>n</i> -Tetracosane	0.01	0.01	0.00	0.00	0.06	0.00	0.00
1-Pentacosene	0.01	0.00	0.00	0.00	0.03	0.00	0.00
<i>n</i> -Pentacosane	0.01	0.01	0.00	0.00	0.05	0.00	0.00
1-Hexacosene	0.01	0.00	0.00	0.00	0.02	0.00	0.00
<i>n</i> -Hexacosane	0.01	0.00	0.00	0.00	0.04	0.00	0.00
1-Heptacosene	0.00	0.00	0.00	0.00	0.01	0.00	0.00
<i>n</i> -Heptacosane	0.01	0.00	0.00	0.00	0.04	0.00	0.00
1-Octacosene	0.00	0.00	0.00	0.00	0.01	0.00	0.00
<i>n</i> -Octacosane	0.01	0.00	0.00	0.00	0.02	0.00	0.00
1-Nonacosene	0.00	0.00	0.00	0.00	0.01	0.00	0.00
<i>n</i> -Nonacosane	0.01	0.00	0.00	0.00	0.02	0.00	0.00
1-Triacontene	0.00	0.00	0.00	0.00	0.00	0.00	0.00
<i>n</i> -Triacontane	0.00	0.00	0.00	0.00	0.00	0.00	0.00
<i>n</i> -C31:1	0.00	0.00	0.00	0.00	0.00	0.00	0.00
<i>n</i> -C31	0.01	0.00	0.00	0.00	0.00	0.00	0.00
<i>n</i> -C32:1	0.00	0.00	0.00	0.00	0.00	0.00	0.00
<i>n</i> -C32	0.00	0.00	0.00	0.00	0.00	0.00	0.00
<i>n</i> -C33:1	0.00	0.00	0.00	0.00	0.00	0.00	0.00
<i>n</i> -C33	0.00	0.00	0.00	0.00	0.00	0.00	0.00
<i>n</i> -C34:1	0.00	0.00	0.00	0.00	0.00	0.00	0.00
<i>n</i> -C34	0.00	0.00	0.00	0.00	0.00	0.00	0.00
<i>n</i> -C35:1	0.00	0.00	0.00	0.00	0.00	0.00	0.00
<i>n</i> -C35	0.00	0.00	0.00	0.00	0.00	0.00	0.00
<i>n</i> -C36:1	0.00	0.00	0.00	0.00	0.00	0.00	0.00
<i>n</i> -C36	0.00	0.00	0.00	0.00	0.00	0.00	0.00
<i>n</i> -C37:1	0.00	0.00	0.00	0.00	0.00	0.00	0.00
<i>n</i> -C37	0.00	0.00	0.00	0.00	0.00	0.00	0.00
<i>n</i> -C38:1	0.00	0.00	0.00	0.00	0.00	0.00	0.00
<i>n</i> -C38	0.00	0.00	0.00	0.00	0.00	0.00	0.00
<i>n</i> -C39:1	0.00	0.00	0.00	0.00	0.00	0.00	0.00
<i>n</i> -C39	0.00	0.00	0.00	0.00	0.00	0.00	0.00

Table A 9 continued: Spekk Fm. sample G004750 and Westphalian Coal sample G000721

Table A 10: Late Gas Potential Screening of residues prepared by MSSV-pyrolysis

Table A 10: Late Gas Potential Screening of residues prepared by MSSV-pyrolysis

Formation/Basin Residue Temperature [°C] File Temperature [°C] Rate	Are Fm.							
	400		450		500		550	
	1965FA 200-560 2K/min	1965FB 200-700 2K/min	1965DG 200-560 2K/min	1965DH 200-700 2K/min	1965EA 200-560 2K/min	1965DA 200-700 2K/min	1965EB 200-560 2K/min	1965DB 200-700 2K/min
	mg/g rock	mg/g rock	mg/g rock	mg/g rock	mg/g rock	mg/g rock	mg/g rock	mg/g rock
Totals	mg/g rock	mg/g rock	mg/g rock	mg/g rock	mg/g rock	mg/g rock	mg/g rock	mg/g rock
Total C1+ (-blank)	33.30	51.13	21.11	39.70	11.84	35.60	5.01	24.94
Total C1-5	29.57	49.84	18.20	38.27	8.23	35.29	0.20	24.70
Total C2-5	6.47	0.57	2.30	0.82	1.04	0.95	0.19	0.37
Total C <sub>6-14</sub> (-blank)	3.43	0.59	2.28	0.36	3.25	0.31	4.71	0.21
Total C <sub>15+</sub> (-blank)	0.30	0.70	0.64	1.06	0.36	0.01	0.11	0.04
Total C <sub>6+</sub> (-blank)	3.73	1.29	2.91	1.43	3.61	0.31	4.82	0.24
GOR	7.93	38.62	6.24	26.81	2.28	113.47	0.04	101.27
Gas Wetness (C <sub>2,g</sub> /C <sub>1,g</sub> )	0.22	0.01	0.13	0.02	0.13	0.03	0.99	0.01
Compound	mg/g rock	mg/g rock	mg/g rock	mg/g rock	mg/g rock	mg/g rock	mg/g rock	mg/g rock
Methane	23.10	49.27	15.89	37.45	7.19	34.34	0.00	24.33
Ethane	4.30	0.16	1.71	0.35	0.62	0.37	0.00	0.20
Propane	0.74	0.23	0.16	0.00	0.18	0.20	0.03	0.13
i-Butane	0.18	0.00	0.01	0.00	0.01	0.00	0.02	0.00
n-Butane	0.04	0.00	0.00	0.00	0.01	0.00	0.00	0.00
i-Pentane	0.00	0.00	0.00	0.00	0.00	0.00	0.00	0.00
n-Pentane	0.00	0.00	0.00	0.00	0.00	0.00	0.00	0.00
Cyclopentane	0.00	0.00	0.00	0.00	0.00	0.00	0.00	0.00
2-Methylpentane	0.00	0.00	0.00	0.00	0.00	0.00	0.00	0.00
3-Methylpentane	0.00	0.00	0.00	0.00	0.00	0.00	0.00	0.00
n-Hexane	0.00	0.00	0.00	0.00	0.00	0.00	0.00	0.00
Methylcyclopentane	0.00	0.00	0.00	0.00	0.00	0.00	0.00	0.00
Benzene	0.79	0.31	0.63	0.20	0.66	0.24	0.20	0.16
Thiophene	0.00	0.00	0.00	0.00	0.00	0.00	0.00	0.00
Cyclohexane	0.00	0.00	0.00	0.00	0.00	0.00	0.00	0.00
2-Methylhexane	0.00	0.00	0.00	0.00	0.00	0.00	0.00	0.00
2,3-Dimethylpentane	0.00	0.00	0.00	0.00	0.00	0.00	0.00	0.00
1,1-Dimethylpentane	0.00	0.00	0.00	0.00	0.00	0.00	0.00	0.00
3-Methylhexane	0.00	0.00	0.00	0.00	0.00	0.00	0.00	0.00
n-Heptane	0.00	0.00	0.00	0.00	0.00	0.00	0.00	0.00
Methyl-Cyclohexane	0.00	0.00	0.00	0.00	0.00	0.00	0.00	0.00
Ethylcyclopentane	0.00	0.00	0.00	0.00	0.00	0.00	0.00	0.00
2,5-Dimethylhexane	0.00	0.00	0.00	0.00	0.00	0.00	0.00	0.00
2,4-Dimethylhexane	0.00	0.00	0.00	0.00	0.00	0.00	0.00	0.00
3,3-Dimethylhexane	0.00	0.00	0.00	0.00	0.00	0.00	0.00	0.00
2,3,4-Trimethylpentane	0.00	0.00	0.00	0.00	0.00	0.00	0.00	0.00
Toluene	1.17	0.01	0.87	0.01	1.12	0.01	0.22	0.00
2-Methylthiophene	0.00	0.00	0.00	0.00	0.00	0.00	0.00	0.00
3-Methylthiophene	0.00	0.00	0.00	0.00	0.00	0.00	0.00	0.00
n-Octane	0.00	0.00	0.00	0.00	0.00	0.00	0.00	0.00
Ethylbenzene	0.02	0.00	0.01	0.00	0.01	0.00	0.01	0.00
Ethylthiophene	0.00	0.00	0.00	0.00	0.00	0.00	0.00	0.00
2,5-Dimethylthiophene	0.00	0.00	0.00	0.00	0.00	0.00	0.00	0.00
m/p-Xylene	0.34	0.00	0.16	0.00	0.32	0.00	0.63	0.00
2,4-Dimethylthiophene	0.00	0.00	0.00	0.00	0.00	0.00	0.00	0.00
2,3-Dimethylthiophene	0.00	0.00	0.00	0.00	0.00	0.00	0.00	0.00
Styrene	0.00	0.00	0.00	0.00	0.00	0.00	0.00	0.00
o-Xylene	0.06	0.00	0.02	0.00	0.07	0.00	0.06	0.00
n-Nonane	0.00	0.00	0.00	0.00	0.00	0.00	0.00	0.00
2-Propylthiophene	0.00	0.00	0.00	0.00	0.00	0.00	0.00	0.00
Propylbenzene	0.00	0.00	0.00	0.00	0.00	0.00	0.00	0.00
2-Ethyl-5-Methylthiophene	0.00	0.00	0.00	0.00	0.00	0.00	0.00	0.00
(?) -Benzene	0.01	0.00	0.00	0.00	0.00	0.00	0.04	0.00
1,3,5-Trimethylbenzene	0.02	0.00	0.01	0.00	0.02	0.00	0.05	0.00
Phenol	0.00	0.00	0.00	0.00	0.00	0.00	0.01	0.00
1-Ethyl-2-Methylbenzene	0.00	0.00	0.00	0.00	0.00	0.00	0.01	0.00
2,3,5-Trimethylthiophene	0.00	0.00	0.00	0.00	0.00	0.00	0.00	0.00
1,2,4-Trimethylbenzene	0.02	0.00	0.00	0.00	0.02	0.00	0.06	0.00
n-Decane	0.00	0.00	0.00	0.00	0.00	0.00	0.00	0.00
1,2,3-Trimethylbenzene	0.00	0.00	0.00	0.00	0.01	0.00	0.02	0.00
o-Cresol	0.00	0.00	0.00	0.00	0.00	0.00	0.00	0.00
m/p-Cresol	0.00	0.00	0.00	0.00	0.00	0.00	0.00	0.00
Dimethylphenol	0.00	0.00	0.00	0.00	0.00	0.00	0.00	0.00
n-Undecane	0.00	0.00	0.00	0.00	0.00	0.00	0.00	0.00
1,2,3,4-Tetramethylbenzene	0.00	0.00	0.00	0.00	0.00	0.00	0.00	0.00
Naphthalene	0.25	0.03	0.13	0.02	0.26	0.00	0.37	0.00
n-Dodecane	0.00	0.00	0.00	0.00	0.00	0.00	0.00	0.00
2-Methylnaphthalene	0.03	0.00	0.01	0.00	0.02	0.00	0.05	0.00
1-Methylnaphthalene	0.01	0.00	0.01	0.00	0.02	0.00	0.03	0.00
n-Tridecane	0.00	0.00	0.00	0.00	0.00	0.00	0.00	0.00
n-Tetradecane	0.00	0.00	0.00	0.00	0.00	0.00	0.00	0.00
Dimethylnaphthalene	0.00	0.00	0.00	0.00	0.00	0.00	0.00	0.00
n-Pentadecane	0.00	0.00	0.00	0.00	0.00	0.00	0.00	0.00
Trimethylnaphthalene	0.00	0.00	0.00	0.00	0.00	0.00	0.00	0.00
Trimethylnaphthalene	0.00	0.00	0.00	0.00	0.00	0.00	0.00	0.00
Trimethylnaphthalene	0.00	0.00	0.00	0.00	0.00	0.00	0.00	0.00
n-Hexadecane	0.00	0.00	0.00	0.00	0.00	0.00	0.00	0.00
Isopropylidimethylnaphthalene	0.00	0.00	0.00	0.00	0.00	0.00	0.00	0.00
n-Heptadecane	0.00	0.00	0.00	0.00	0.00	0.00	0.00	0.00
Pristane	0.00	0.00	0.00	0.00	0.00	0.00	0.00	0.00
Prist-1-ene	0.00	0.00	0.00	0.00	0.00	0.00	0.00	0.00
n-Octadecane	0.00	0.00	0.00	0.00	0.00	0.00	0.00	0.00
Phytane	0.00	0.00	0.00	0.00	0.00	0.00	0.00	0.00
n-Nonadecane	0.00	0.00	0.00	0.00	0.00	0.00	0.00	0.00
n-Icosane	0.00	0.00	0.00	0.00	0.00	0.00	0.00	0.00
n-Henicosane	0.00	0.00	0.00	0.00	0.00	0.00	0.00	0.00
n-Docosane	0.00	0.00	0.00	0.00	0.00	0.00	0.00	0.00
n-Tricosane	0.00	0.00	0.00	0.00	0.00	0.00	0.00	0.00
n-Tetracosane	0.00	0.00	0.00	0.00	0.00	0.00	0.00	0.00
n-Pentacosane	0.00	0.00	0.00	0.00	0.00	0.00	0.00	0.00
n-Hexacosane	0.00	0.00	0.00	0.00	0.00	0.00	0.00	0.00
n-Heptacosane	0.00	0.00	0.00	0.00	0.00	0.00	0.00	0.00
n-Octacosane	0.00	0.00	0.00	0.00	0.00	0.00	0.00	0.00
n-Nonacosane	0.00	0.00	0.00	0.00	0.00	0.00	0.00	0.00
n-Triacontane	0.00	0.00	0.00	0.00	0.00	0.00	0.00	0.00
Summations	mg/g rock	mg/g rock	mg/g rock	mg/g rock	mg/g rock	mg/g rock	mg/g rock	mg/g rock
n-C <sub>6-14</sub>	0.00	0.00	0.00	0.00	0.00	0.00	0.00	0.00
n-C <sub>15+</sub>	0.00	0.00	0.00	0.00	0.00	0.00	0.00	0.00
Mono-aromatic Compounds	2.44	0.32	1.71	0.21	2.23	0.25	1.28	0.17
Di-aromatic Compounds	0.29	0.03	0.15	0.02	0.29	0.00	0.45	0.00
Phenolic Compounds	0.00	0.00	0.00	0.00	0.00	0.00	0.01	0.00
Thiophenic Compounds	0.00	0.00	0.00	0.00	0.00	0.00	0.00	0.00

Table A10: Are Fm. sample G001965

[illegible]

337

Table A 10: Late Gas Potential Screening of residues prepared by MSSV-pyrolysis

Formation/Basin	Westphalian Coal					
Residue Temperature [°C]	400		450		500	
File	721EA	721EB	721EC	721ED	721EE	721EF
Temperature [°C]	560	700	560	700	560	700
Rate	2K/min	2K/min	2K/min	2K/min	2K/min	2K/min
Totals	mg/g rock	mg/g rock	mg/g rock	mg/g rock	mg/g rock	mg/g rock
Total C1+ (-blank)	69.97	84.94	40.69	65.94	21.84	49.11
Total C1-5	58.06	82.88	34.75	64.77	19.04	48.46
Total C2-5	16.18	0.48	5.96	0.36	1.46	0.27
Total C <sub>6-14</sub> (-blank)	10.63	0.82	5.41	0.48	2.59	0.30
Total C <sub>15+</sub> (-blank)	1.27	1.24	0.53	0.69	0.22	0.35
Total C <sub>6+</sub> (-blank)	11.90	2.06	5.94	1.17	2.80	0.65
GOR	4.88	40.22	5.85	55.44	6.80	74.13
Gas Wetness (C <sub>2-5</sub> /C <sub>1-5</sub> )	0.28	0.01	0.17	0.01	0.08	0.01
Compound	mg/g rock	mg/g rock	mg/g rock	mg/g rock	mg/g rock	mg/g rock
Methane	41.88	82.41	28.79	64.40	14.78	47.53
Ethane	11.97	0.41	4.92	0.30	1.25	0.22
Propane	3.71	0.03	0.90	0.03	0.11	0.02
i-Butane	0.27	0.00	0.05	0.00	0.01	0.00
n-Butane	0.04	0.00	0.01	0.00	0.00	0.00
i-Pentane	0.01	0.00	0.00	0.00	0.00	0.00
n-Pentane	0.00	0.00	0.00	0.00	0.00	0.00
Cyclopentane	0.00	0.00	0.00	0.00	0.00	0.00
2-Methylpentane	0.00	0.00	0.00	0.00	0.00	0.00
3-Methylpentane	0.00	0.00	0.00	0.00	0.00	0.00
n-Hexane	0.00	0.00	0.00	0.00	0.00	0.00
Methylcyclopentane	0.00	0.00	0.00	0.00	0.00	0.00
Benzene	1.57	0.57	1.09	0.34	0.85	0.24
Thiophene	0.00	0.00	0.00	0.00	0.00	0.00
Cyclohexane	0.00	0.00	0.00	0.00	0.00	0.00
2-Methylhexane	0.00	0.00	0.00	0.00	0.00	0.00
2,3-Dimethylpentane	0.00	0.00	0.00	0.00	0.00	0.00
1,1-Dimethylpentane	0.00	0.00	0.00	0.00	0.00	0.00
3-Methylhexane	0.00	0.00	0.00	0.00	0.00	0.00
n-Heptane	0.00	0.00	0.00	0.00	0.00	0.00
Methyl-Cyclohexane	0.00	0.00	0.00	0.00	0.00	0.00
Ethylcyclopentane	0.00	0.00	0.00	0.00	0.00	0.00
2,5-Dimethylhexane	0.00	0.00	0.00	0.00	0.00	0.00
2,4-Dimethylhexane	0.00	0.00	0.00	0.00	0.00	0.00
3,3-Dimethylhexane	0.00	0.00	0.00	0.00	0.00	0.00
2,3,4-Trimethylpentane	0.00	0.00	0.00	0.00	0.00	0.00
Toluene	3.08	0.03	1.76	0.02	0.96	0.01
2-Methylthiophene	0.00	0.00	0.00	0.00	0.00	0.00
3-Methylthiophene	0.00	0.00	0.00	0.00	0.00	0.00
n-Octane	0.00	0.00	0.00	0.00	0.00	0.00
Ethylbenzene	0.16	0.00	0.05	0.00	0.01	0.00
Ethylthiophene	0.00	0.00	0.00	0.00	0.00	0.00
2,5-Dimethylthiophene	0.00	0.00	0.00	0.00	0.00	0.00
m/p-Xylene	1.31	0.01	0.63	0.01	0.21	0.00
2,4-Dimethylthiophene	0.00	0.00	0.00	0.00	0.00	0.00
2,3-Dimethylthiophene	0.00	0.00	0.00	0.00	0.00	0.00
Styrene	0.00	0.00	0.00	0.00	0.00	0.00
o-Xylene	0.24	0.00	0.09	0.00	0.02	0.00
n-Nonane	0.00	0.00	0.00	0.00	0.00	0.00
2-Propylthiophene	0.00	0.00	0.00	0.00	0.00	0.00
Propylbenzene	0.00	0.00	0.00	0.00	0.00	0.00
2-Ethyl-5-Methylthiophene	0.00	0.00	0.00	0.00	0.00	0.00
(?)-Benzene	0.14	0.00	0.04	0.00	0.00	0.00
1,3,5-Trimethylbenzene	0.15	0.00	0.05	0.00	0.01	0.00
Phenol	1.13	0.01	0.42	0.00	0.02	0.00
1-Ethyl-2-Methylbenzene	0.02	0.00	0.01	0.00	0.00	0.00
2,3,5-Trimethylthiophene	0.00	0.00	0.00	0.00	0.00	0.00
1,2,4-Trimethylbenzene	0.12	0.00	0.04	0.00	0.01	0.00
n-Decane	0.00	0.00	0.00	0.00	0.00	0.00
1,2,3-Trimethylbenzene	0.02	0.00	0.01	0.00	0.00	0.00
o-Cresol	0.09	0.00	0.02	0.00	0.00	0.00
m/p-Cresol	0.23	0.00	0.04	0.00	0.00	0.00
Dimethylphenol	0.00	0.00	0.00	0.00	0.00	0.00
n-Undecane	0.00	0.00	0.00	0.00	0.00	0.00
1,2,3,4-Tetramethylbenzene	0.00	0.00	0.00	0.00	0.00	0.00
Naphthalene	0.73	0.03	0.42	0.02	0.19	0.01
n-Dodecane	0.00	0.00	0.00	0.00	0.00	0.00
2-Methylnaphthalene	0.45	0.01	0.17	0.01	0.03	0.00
1-Methylnaphthalene	0.11	0.00	0.05	0.00	0.01	0.00
n-Tridecane	0.00	0.00	0.00	0.00	0.00	0.00
n-Tetradecane	0.00	0.00	0.00	0.00	0.00	0.00
Dimethylnaphthalene	0.06	0.00	0.02	0.00	0.00	0.00
n-Pentadecane	0.00	0.00	0.00	0.00	0.00	0.00
Trimethylnaphthalene	0.00	0.00	0.00	0.00	0.00	0.00
Trimethylnaphthalene	0.00	0.00	0.00	0.00	0.00	0.00
Trimethylnaphthalene	0.00	0.00	0.00	0.00	0.00	0.00
n-Hexadecane	0.00	0.00	0.00	0.00	0.00	0.00
Isopropylidimethylnaphthalene	0.00	0.00	0.00	0.00	0.00	0.00
n-Heptadecane	0.00	0.00	0.00	0.00	0.00	0.00
Pristane	0.00	0.00	0.00	0.00	0.00	0.00
Prist-1-ene	0.00	0.00	0.00	0.00	0.00	0.00
n-Octadecane	0.00	0.00	0.00	0.00	0.00	0.00
Phytane	0.00	0.00	0.00	0.00	0.00	0.00
n-Nonadecane	0.00	0.00	0.00	0.00	0.00	0.00
n-Icosane	0.00	0.00	0.00	0.00	0.00	0.00
n-Henicosane	0.00	0.00	0.00	0.00	0.00	0.00
n-Docosane	0.00	0.00	0.00	0.00	0.00	0.00
n-Tricosane	0.00	0.00	0.00	0.00	0.00	0.00
n-Tetracosane	0.00	0.00	0.00	0.00	0.00	0.00
n-Pentacosane	0.00	0.00	0.00	0.00	0.00	0.00
n-Hexacosane	0.00	0.00	0.00	0.00	0.00	0.00
n-Heptacosane	0.00	0.00	0.00	0.00	0.00	0.00
n-Octacosane	0.00	0.00	0.00	0.00	0.00	0.00
n-Nonacosane	0.00	0.00	0.00	0.00	0.00	0.00
n-Triacontane	0.00	0.00	0.00	0.00	0.00	0.00
Summations	mg/g rock	mg/g rock	mg/g rock	mg/g rock	mg/g rock	mg/g rock
n-C <sub>6-14</sub>	0.00	0.00	0.00	0.00	0.00	0.00
n-C <sub>15+</sub>	0.00	0.00	0.00	0.00	0.00	0.00
Mono-aromatic Compounds	6.83	0.62	3.76	0.37	2.08	0.25
Di-aromatic Compounds	1.35	0.05	0.65	0.03	0.24	0.01
Phenolic Compounds	1.46	0.01	0.49	0.00	0.02	0.00
Thiophenic Compounds	0.00	0.00	0.00	0.00	0.00	0.00

Table A 10 continued: Westphalian Coal sample G000721

Table A 11: Open-system Pyrolysis GC-FID of residues prepared by open-system pyrolysis (SRA)

Table A 11: Open-system Pyrolysis GC-FID of residues prepared by open-system pyrolysis (SRA)

Formation/Basin	Are Fm.			Westphalian Coal		
Residue Temperature [°C]	400	450	500	400	450	500
GFZ Code	G001965	G001965	G001965	G000721	G000721	G000721
File	G01965KA	G01965KB	G01965KC	G00721BA	G00721BB	G00721BC
Temperature [°C]	300-600	300-600	300-600	300-600	300-600	300-600
Rate	60K/min	60K/min	60K/min	60K/min	60K/min	60K/min
Totals	mg/g sample	mg/g sample	mg/g sample	mg/g sample	mg/g sample	mg/g sample
C <sub>1+</sub> (-blank)	20.33	7.32	2.28	93.01	40.19	8.86
C <sub>1-5</sub>	11.73	5.65	1.76	34.08	23.31	7.43
C <sub>2-5</sub>	5.52	1.77	1.24	17.13	8.84	1.28
C <sub>6-14</sub> (-blank)	7.15	1.13	0.21	26.61	10.27	1.44
C <sub>6-14</sub> Hump	1.16	0.14	0.01	4.99	0.90	0.02
C <sub>6-14</sub> Resolved	6.00	0.99	0.20	21.62	9.38	1.41
C <sub>15+</sub> (-blank)	1.45	0.55	0.32	32.32	6.60	0.00
C <sub>15+</sub> Hump	1.03	0.49	0.31	27.26	4.17	0.28
C <sub>15+</sub> Resolved	0.43	0.06	0.01	5.06	2.43	0.28
GOR	1.36	3.36	3.33	0.58	1.38	5.18
Gas Wetness (C2-5/C1-5)	0.47	0.31	0.71	0.50	0.38	0.17
Compounds Summation	mg/g sample	mg/g sample	mg/g sample	mg/g sample	mg/g sample	mg/g sample
n-C <sub>6-14</sub>	0.93	0.04	0.00	4.15	1.10	0.02
n-C <sub>15+</sub>	0.09	0.00	0.00	1.52	0.18	0.01
Mono-aromatic Compounds	1.49	0.45	0.13	3.83	2.53	0.65
Di-aromatic Compounds	0.28	0.08	0.02	1.18	0.71	0.16
Phenolic Compounds	0.95	0.10	0.00	3.24	1.94	0.34
Thiophenic Compounds	0.13	0.02	0.00	0.18	0.07	0.01
Single Compounds	mg/g sample	mg/g sample	mg/g sample	mg/g sample	mg/g sample	mg/g sample
Methane	6.21	3.88	0.52	16.95	14.47	6.15
Ethene	0.61	0.00	0.00	1.64	1.07	0.23
Ethane	1.09	0.83	0.06	5.40	3.47	0.75
Propane	0.98	0.22	0.00	4.51	2.17	0.17
i-Butane	0.03	0.01	0.00	0.14	0.07	0.00
1-Butene	0.18	0.01	0.00	1.14	0.45	0.02
n-Butane	0.26	0.03	0.00	0.94	0.35	0.01
i-Pentane	0.15	0.02	0.00	0.22	0.09	0.01
Pentene	0.13	0.02	0.00	0.47	0.15	0.00
n-Pentane	0.12	0.02	0.01	0.56	0.19	0.00
Cyclopentane	0.01	0.00	0.00	0.09	0.02	0.00
2-Methylpentane	0.02	0.00	0.00	0.10	0.03	0.00
3-Methylpentane	0.01	0.00	0.00	0.03	0.01	0.00
1-Hexene	0.10	0.01	0.00	0.41	0.11	0.00
n-Hexane	0.08	0.01	0.00	0.43	0.13	0.00
Methylcyclopentane	0.01	0.00	0.00	0.09	0.03	0.00
Benzene	0.22	0.08	0.07	0.32	0.36	0.14
Thiophene	0.02	0.02	0.00	0.00	0.00	0.00
Cyclohexane	0.01	0.00	0.00	0.04	0.01	0.00
2-Methylhexane	0.01	0.00	0.00	0.03	0.01	0.00
2,3-Dimethylpentane	0.01	0.00	0.00	0.02	0.00	0.00
1,1-Dimethylpentane	0.00	0.00	0.00	0.00	0.00	0.00
3-Methylhexane	0.01	0.00	0.00	0.03	0.01	0.00
1-Heptene	0.08	0.00	0.00	0.31	0.08	0.00
n-Heptane	0.09	0.00	0.00	0.39	0.11	0.00
Methyl-Cyclohexane	0.01	0.00	0.00	0.07	0.02	0.00
Ethylcyclopentane	0.01	0.00	0.00	0.04	0.01	0.00
2,5-Dimethylhexane	0.01	0.00	0.00	0.07	0.02	0.00
2,4-Dimethylhexane	0.01	0.00	0.00	0.01	0.00	0.00
3,3-Dimethylhexane	0.01	0.00	0.00	0.03	0.01	0.00
2,3,4-Trimethylpentane	0.01	0.00	0.00	0.06	0.01	0.00
Toluene	0.53	0.22	0.05	1.26	0.87	0.28
2-Methylthiophene	0.04	0.00	0.00	0.02	0.01	0.00
3-Methylthiophene	0.01	0.01	0.00	0.02	0.00	0.00
1-Octene	0.06	0.00	0.00	0.24	0.06	0.00
n-Octane	0.07	0.00	0.00	0.30	0.09	0.00
Ethylbenzene	0.10	0.01	0.00	0.24	0.13	0.01
Ethylthiophene	0.00	0.00	0.00	0.01	0.00	0.00
2,5-Dimethylthiophene	0.00	0.00	0.00	0.01	0.00	0.00
m/p-Xylene	0.29	0.08	0.01	0.88	0.61	0.15
2,4-Dimethylthiophene	0.01	0.00	0.00	0.01	0.01	0.00
2,3-Dimethylthiophene	0.02	0.00	0.00	0.01	0.00	0.00
Styrene	0.02	0.00	0.00	0.06	0.02	0.00
o-Xylene	0.11	0.02	0.00	0.27	0.13	0.02
1-Nonene	0.04	0.00	0.00	0.17	0.04	0.00
n-Nonane	0.05	0.00	0.00	0.22	0.06	0.00
2-Propylthiophene	0.02	0.00	0.00	0.05	0.02	0.00
Propylbenzene	0.01	0.00	0.00	0.04	0.00	0.00
2-Ethyl-5-Methylthiophene	0.00	0.00	0.00	0.02	0.01	0.01
(?)-Benzene	0.08	0.01	0.00	0.28	0.15	0.01
1,3,5-Trimethylbenzene	0.02	0.01	0.00	0.14	0.10	0.01
Phenol	0.51	0.07	0.00	0.95	0.64	0.16
1-Ethyl-2-Methylbenzene	0.04	0.01	0.00	0.11	0.04	0.00
2,3,5-Trimethylthiophene	0.00	0.00	0.00	0.03	0.02	0.01

Table A 11: Open-system Pyrolysis GC-FID of residues prepared by open-system pyrolysis (SRA)

Formation/Basin	Are Fm.			Westphalian Coal		
Residue Temperature [°C]	400	450	500	400	450	500
1,2,4-Trimethylbenzene	0.06	0.01	0.00	0.23	0.12	0.01
1-Decene	0.04	0.00	0.00	0.14	0.03	0.00
<i>n</i> -Decane	0.05	0.00	0.00	0.21	0.06	0.00
1,2,3-Trimethylbenzene	0.03	0.00	0.00	0.07	0.02	0.00
<i>o</i> -Cresol	0.14	0.01	0.00	0.90	0.49	0.06
<i>m/p</i> -Cresol	0.29	0.02	0.00	1.19	0.72	0.11
Dimethylphenol	0.01	0.00	0.00	0.20	0.09	0.01
1-Undecene	0.03	0.01	0.00	0.15	0.04	0.00
<i>n</i> -Undecane	0.04	0.00	0.00	0.17	0.04	0.00
1,2,3,4-Tetramethylbenzene	0.03	0.00	0.00	0.17	0.06	0.00
Naphthalene	0.08	0.04	0.01	0.19	0.14	0.06
1-Dodecene	0.03	0.00	0.00	0.14	0.02	0.00
<i>n</i> -Dodecane	0.06	0.00	0.00	0.18	0.04	0.00
2-Methylnaphthalene	0.08	0.02	0.00	0.28	0.20	0.05
1-Tridecene	0.03	0.00	0.00	0.20	0.05	0.00
1-Methylnaphthalene	0.06	0.01	0.00	0.22	0.12	0.02
<i>n</i> -Tridecane	0.04	0.00	0.00	0.22	0.05	0.00
1-Tetradecene	0.02	0.00	0.00	0.12	0.05	0.00
<i>n</i> -Tetradecane	0.02	0.00	0.00	0.16	0.04	0.00
Dimethylnaphthalene	0.06	0.01	0.00	0.32	0.16	0.02
1-Pentadecene	0.01	0.00	0.00	0.07	0.01	0.00
<i>n</i> -Pentadecane	0.02	0.00	0.00	0.13	0.02	0.00
Trimethylnaphthalene	0.00	0.00	0.00	0.09	0.03	0.00
Trimethylnaphthalene	0.00	0.00	0.00	0.07	0.02	0.00
Trimethylnaphthalene	0.00	0.00	0.00	0.02	0.03	0.00
1-Hexadecene	0.01	0.00	0.00	0.08	0.02	0.00
<i>n</i> -Hexadecane	0.01	0.00	0.00	0.09	0.02	0.00
Isopropyldimethylnaphthalene	0.00	0.00	0.00	0.01	0.01	0.00
1-Heptadecene	0.01	0.00	0.00	0.10	0.02	0.00
<i>n</i> -Heptadecane	0.00	0.00	0.00	0.12	0.02	0.00
Pristane	0.00	0.00	0.00	0.01	0.00	0.00
Prist.-1-ene	0.00	0.00	0.00	0.00	0.00	0.00
1-Octadecene	0.01	0.00	0.00	0.05	0.00	0.00
<i>n</i> -Octadecane	0.00	0.00	0.00	0.09	0.02	0.00
Phytane	0.00	0.00	0.00	0.01	0.00	0.00
1-Nonadecene	0.00	0.00	0.00	0.06	0.01	0.00
<i>n</i> -Nonadecane	0.00	0.00	0.00	0.12	0.01	0.00
1-Icosene	0.00	0.00	0.00	0.04	0.01	0.00
<i>n</i> -Icosane	0.00	0.00	0.00	0.06	0.01	0.00
1-Henicosene	0.00	0.00	0.00	0.03	0.00	0.00
<i>n</i> -Henicosane	0.00	0.00	0.00	0.06	0.00	0.00
1-Docosene	0.00	0.00	0.00	0.03	0.00	0.00
<i>n</i> -Docosane	0.00	0.00	0.00	0.07	0.00	0.00
1-Tricosene	0.00	0.00	0.00	0.04	0.00	0.00
<i>n</i> -Tricosane	0.00	0.00	0.00	0.05	0.00	0.00
1-Tetracosene	0.00	0.00	0.00	0.02	0.00	0.00
<i>n</i> -Tetracosane	0.00	0.00	0.00	0.04	0.00	0.00
1-Pentacosene	0.00	0.00	0.00	0.02	0.00	0.00
<i>n</i> -Pentacosane	0.00	0.00	0.00	0.04	0.00	0.00
1-Hexacosene	0.00	0.00	0.00	0.01	0.00	0.00
<i>n</i> -Hexacosane	0.00	0.00	0.00	0.02	0.00	0.00
1-Heptacosene	0.00	0.00	0.00	0.01	0.00	0.00
<i>n</i> -Heptacosane	0.00	0.00	0.00	0.03	0.00	0.00
1-Octacosene	0.00	0.00	0.00	0.01	0.00	0.00
<i>n</i> -Octacosane	0.00	0.00	0.00	0.02	0.00	0.00
1-Nonacosene	0.00	0.00	0.00	0.01	0.00	0.00
<i>n</i> -Nonacosane	0.00	0.00	0.00	0.01	0.00	0.00
1-Triacontene	0.00	0.00	0.00	0.00	0.00	0.00
<i>n</i> -Triacontane	0.00	0.00	0.00	0.00	0.00	0.00
<i>n</i> -C31:1	0.00	0.00	0.00	0.00	0.00	0.00
<i>n</i> -C31	0.00	0.00	0.00	0.00	0.00	0.00
<i>n</i> -C32:1	0.00	0.00	0.00	0.00	0.00	0.00
<i>n</i> -C32	0.00	0.00	0.00	0.00	0.00	0.00
<i>n</i> -C33:1	0.00	0.00	0.00	0.00	0.00	0.00
<i>n</i> -C33	0.00	0.00	0.00	0.00	0.00	0.00
<i>n</i> -C34:1	0.00	0.00	0.00	0.00	0.00	0.00
<i>n</i> -C34	0.00	0.00	0.00	0.00	0.00	0.00
<i>n</i> -C35:1	0.00	0.00	0.00	0.00	0.00	0.00
<i>n</i> -C35	0.00	0.00	0.00	0.00	0.00	0.00
<i>n</i> -C36:1	0.00	0.00	0.00	0.00	0.00	0.00
<i>n</i> -C36	0.00	0.00	0.00	0.00	0.00	0.00
<i>n</i> -C37:1	0.00	0.00	0.00	0.00	0.00	0.00
<i>n</i> -C37	0.00	0.00	0.00	0.00	0.00	0.00
<i>n</i> -C38:1	0.00	0.00	0.00	0.00	0.00	0.00
<i>n</i> -C38	0.00	0.00	0.00	0.00	0.00	0.00
<i>n</i> -C39:1	0.00	0.00	0.00	0.00	0.00	0.00
<i>n</i> -C39	0.00	0.00	0.00	0.00	0.00	0.00

Table A 11 continued: Åre Fm. sample G001965 and Westphalian Coal sample G000721



**Table A 12: Late Gas Potential Screening of residues prepared by open-system pyrolysis (SRA)**

**Table A 12: Åre Fm. sample G001965 and Westphalian Coal sample G000721**

Table A 13:  $\delta^{13}\text{C}$  composition of  $\text{C}_{1-4}$  gases at different MSSV-pyrolysis end temperaturesTable A 13:  $\delta^{13}\text{C}$  composition of  $\text{C}_{1-4}$  gases at different MSSV-pyrolysis end temperatures

Sample-ID	Heat. Rate	Temp.	Methane	Ethylene	Ethane	Propene	Propane	Butane
	$^{\circ}\text{C}/\text{min}$	$[^{\circ}\text{C}]$	$\delta^{13}\text{C} [‰]$					
G001965 Are Fm.	1	250 - 300	-34.4	--	-28.6	-24.0	-27.8	--
	1	250 - 350	-34.8	-17.1	-29.8	-23.6	-28.5	-28.5
	1	250 - 400	-36.1	-18.5	-30.9	-23.7	-28.9	-28.4
	1	250 - 450	-36.4	--	-29.8	-22.2	-28.6	-28.2
	1	250 - 500	-34.3	--	-28.5	--	-26.5	-19.9
	1	250 - 550	-30.7	--	-24.9	--	-9.2	--
	1	250 - 600	-29.4	--	-14.3	--	--	--
	1	250 - 650	-27.5	--	--	--	--	--
	1	250 - 700	-25.5	--	--	--	--	--
	1	250 - 740	-24.0	--	--	--	--	--
	1	250 - 780	-22.6	--	--	--	--	--
G004750 1965 I/III Mix	1	250 - 300	-35.8	--	-29.6	--	-28.6	--
	1	250 - 350	-37.1	-15.8	-31.0	-24.7	-29.8	-30.2
	1	250 - 400	-38.7	-19.9	-32.8	-27.6	-31.6	-31.4
	1	250 - 450	-40.1	-22.5	-32.8	-27.4	-31.9	-31.7
	1	250 - 500	-37.5	--	-32.4	-22.7	-30.0	-24.0
	1	250 - 550	-34.3	--	-28.6	--	-12.4	--
	1	250 - 600	-31.4	--	-19.9	--	--	--
	1	250 - 650	-30.4	--	--	--	--	--
	1	250 - 700	-28.4	--	--	--	--	--
	1	250 - 740	-24.9	--	--	--	--	--
	1	250 - 780	-23.9	--	--	--	--	--
G004750 GRS	1	250 - 300	-42.8	--	--	-34.7	--	--
	1	250 - 350	-44.5	-31.8	-36.0	-34.7	-36.3	-34.0
	1	250 - 400	-46.3	-30.6	-38.1	-35.2	-37.2	-35.0
	1	250 - 450	-46.9	-30.8	-39.0	-33.5	-36.9	-34.5
	1	250 - 500	-45.9	-25.3	-36.8	-24.0	-32.6	-26.1
	1	250 - 550	-42.2	--	-31.7	-17.4	-16.8	--
	1	250 - 600	-37.3	--	-22.9	--	--	--
	1	250 - 650	-34.8	--	-12.7	--	--	--
	1	250 - 700	-33.0	--	--	--	--	--
	1	250 - 740	-30.8	--	--	--	--	--
	1	250 - 780	-28.1	--	--	--	--	--
G001955 Spekk	1	250 - 300	-42.4	--	--	--	--	--
	1	250 - 350	-42.6	-30.3	-36.0	-33.9	-36.1	-34.0
	1	250 - 400	-43.2	-29.0	-37.4	-33.8	-36.4	-34.5
	1	250 - 450	-44.6	-27.3	-36.9	-31.1	-35.9	-33.9
	1	250 - 500	-44.3	--	-36.1	-25.4	-33.3	-26.4
	1	250 - 550	-40.1	--	-32.8	--	-17.8	--
	1	250 - 600	-36.9	--	-23.4	--	--	--
	1	250 - 650	-33.2	--	--	--	--	--
	1	250 - 700	-30.2	--	--	--	--	--
	1	250 - 750	-26.5	--	--	--	--	--
	1	250 - 780	-24.3	--	--	--	--	--
G005935 Akata Shale	2	200 - 460	-39.35	-21.51	-32.93	-28.58	-31.41	-30.17
	2	200 - 560	-34.90	--	-27.73	--	-11.02	--
	2	200 - 700	-28.42	--	--	--	--	--
G006207 Mahakam Delta	2	200 - 460	-39.19	--	-32.50	-28.17	-31.33	-30.54
	2	200 - 560	-34.59	--	-27.38	--	-12.83	--
	2	200 - 700	-27.58	--	--	--	--	--
G005812 Iratí Fm.	5	200 - 480	-33.06	-17.54	-27.51	-22.46	-26.25	-22.88
	5	200 - 580	-29.15	--	-21.03	-7.54	-3.57	--
	5	200 - 690	-23.89	--	0.30	--	--	--
G005763 Hekkingen Fm.	5	200 - 480	-38.06	-21.61	-31.80	-27.45	-30.68	-29.09
	5	200 - 580	-33.88	--	-26.87	--	-7.93	--
	5	200 - 690	-28.94	--	-6.49	--	--	--
G004564 Murzuq Basin	5	200 - 480	-38.13	-21.84	-34.33	-26.72	-31.98	-29.81
	5	200 - 580	-33.92	--	-27.82	--	-11.11	--
	5	200 - 690	-29.76	--	--	--	--	--
G006208 Toarcian Shale	2	200 - 460	-42.34	-26.81	-35.36	-31.03	-33.39	-31.64
	2	200 - 560	-38.75	--	-30.10	-15.12	-16.09	--
	2	200 - 700	-30.92	--	--	--	--	--
G006156 New Albany Shale	2	200 - 460	-42.13	-24.20	-36.17	-28.51	-33.53	-31.11
	2	200 - 560	-36.79	--	-29.45	--	-14.69	--
	2	200 - 700	-29.52	--	--	--	--	--
G006155 Caney Shale	2	200 - 460	-43.29	-29.11	-37.89	-33.02	-35.88	-33.53
	2	200 - 560	-39.52	--	-33.55	-16.14	-18.34	--
	2	200 - 700	-32.21	--	--	--	--	--
G005298 Bakken Shale	2	200 - 460	-41.11	-24.17	-35.14	-29.91	-33.98	-32.11
	2	200 - 560	-37.39	--	-30.94	--	-15.49	--
	2	200 - 700	-30.78	--	--	--	--	--
G004070 Schönebeck Fm.	2	200 - 460	-42.59	-25.01	-35.19	-30.13	-34.13	-31.80
	2	200 - 560	-38.58	--	-29.98	-15.09	-15.48	--
	2	200 - 700	-31.16	--	--	--	--	--